

Birla Central Library

PILANI (Jaipur State)

Engg College Branch

Class No :- 621.38415

Book No :- H916P

Accession No :- 31675

Acc No

ISSUE LABEL

Not later than the latest date stamped below.

--	--	--	--

INTERNATIONAL SERIES IN PHYSICS

LEE A. DuBRIDGE, CONSULTING EDITOR

**PHENOMENA IN
HIGH-FREQUENCY SYSTEMS**

*The quality of the materials used in the manufacture
of this book is governed by continued postwar shortages.*

INTERNATIONAL SERIES IN PURE AND APPLIED PHYSICS

G. P. HARNWELL, *Consulting Editor*

BACHER AND GOUDSMIT—ATOMIC ENERGY STATES
BITTER—INTRODUCTION TO FERROMAGNETISM
BRILLOUIN—WAVE PROPAGATION IN PERIODIC STRUCTURES
CADY—PIEZOELECTRICITY
CLARK—APPLIED X-RAYS
CURTIS—ELECTRICAL MEASUREMENTS
DAVEY—CRYSTAL STRUCTURE AND ITS APPLICATIONS
EDWARDS—ANALYTIC AND VECTOR MECHANICS
HARDY AND PERRIN—THE PRINCIPLES OF OPTICS
HARNWELL—ELECTRICITY AND ELECTROMAGNETISM
HARNWELL AND LIVINGOOD—EXPERIMENTAL ATOMIC PHYSICS
HOUSTON—PRINCIPLES OF MATHEMATICAL PHYSICS
HUGHES AND DUBRIDGE—PHOTOELECTRIC PHENOMENA
HUND—HIGH-FREQUENCY MEASUREMENTS
PHENOMENA IN HIGH-FREQUENCY SYSTEMS
KEMBLE—PRINCIPLES OF QUANTUM MECHANICS
KENNARD—KINETIC THEORY OF GASES
KOLLER—THE PHYSICS OF ELECTRON TUBES
MORSE—VIBRATION AND SOUND
PAULING AND GOUDSMIT—THE STRUCTURE OF LINE SPECTRA
RICHTMYER AND KENNARD—INTRODUCTION TO MODERN PHYSICS
RUARK AND UREY—ATOMS, MOLECULES AND QUANTA
SEITZ—THE MODERN THEORY OF SOLIDS
SLATER—INTRODUCTION TO CHEMICAL PHYSICS
MICROWAVE TRANSMISSION
SLATER AND FRANK—ELECTROMAGNETISM
INTRODUCTION TO THEORETICAL PHYSICS
MECHANICS
SMYTHE—STATIC AND DYNAMIC ELECTRICITY
STRATTON—ELECTROMAGNETIC THEORY
WHITE—INTRODUCTION TO ATOMIC SPECTRA
WILLIAMS—MAGNETIC PHENOMENA

Dr. Lee A. DuBridge was consulting editor of the series from 1939 to 1946.

PHENOMENA IN HIGH-FREQUENCY SYSTEMS

BY
AUGUST HUND
*Consulting Engineer, Fellow of the American Physical
Society, Fellow of the Institute of Radio Engineers,
Fellow of the American Association for the
Advancement of Science*

FIRST EDITION
SEVENTH IMPRESSION

McGRAW-HILL BOOK COMPANY, Inc.
NEW YORK AND LONDON
1936

COPYRIGHT, 1936, BY THE
MCGRAW-HILL BOOK COMPANY, INC.

PRINTED IN THE UNITED STATES OF AMERICA

*All rights reserved. This book, or
part thereof, may not be reproduced
in any form without permission of
the publishers.*

*In gratitude to the Institution
where Maxwellian Reasonings
were verified by Hertzian Waves.*

PREFACE

Faraday's experimental investigations on electricity and magnetism and Clerk-Maxwell's electromagnetic theory were the basis of the classical experiments of Heinrich Hertz. Strange as it may seem, Faraday, without being a mathematician, was responsible for some of the crowning assumptions used for the derivations of the Maxwellian field equations, and Maxwell, without being an experimenter, laid the foundation for the successful laboratory demonstrations of his predictions at Karlsruhe. Hertz was both a philosophical experimenter and a mathematical thinker—an unusual combination, which brought about the discovery of electromagnetic waves. Additional mathematical speculations by H. Hertz, and especially by H. A. Lorentz, gave the Maxwellian electromagnetic theory the reputation which it still holds today, in spite of the many radical changes with respect to concepts in modern physics. Thus, A. Sommerfeld, by means of Maxwellian thinking, could create a theory which tells us how to distinguish between space and surface waves. It also gives us the Sommerfeldian numerical distance by means of which it is possible, for instance, to compute attenuation losses of electromagnetic waves sent out from broadcast stations. By means of the Lorentzian modification of Maxwell's theory, it is possible to explain wave propagation through the ionized layer of the upper atmosphere. It is also possible to account for certain oscillations in vacuum tubes. An almost forgotten classical theory by W. Voigt on static piezoelectricity recently arose again into prominence, when quartz and other crystals found application in the high- as well as in the audio-frequency field. Here also experimenters, namely, the Curie brothers, laid the foundation for the extended theoretical speculations of W. Voigt and his associates. It is the law of evaporation which was basic to the theoretical contributions of O. W. Richardson, which play such an important part in applied electronics of the high-frequency field. The experiments of Hertz, Hallwachs, and Geitel give us the photoelectric devices of today, and the contribution of A. Einstein gives us the well-known law for photoelectric effects, utilizing Planck's quantum. It was H. A. Lorentz as well as A. Einstein who applied relativistic views to electron motions, which play an important part in electron tubes excited at high voltages.—In short, the cooperation between experimenters and theoretical thinkers led to most of the invaluable devices used in high-frequency systems today, and it will probably be the same combination of workers that will lead on in

the field. A book combining both experimental and theoretical reasonings should, therefore, be in order.

Inasmuch as the title of this book is "Phenomena in High-frequency Systems," not only high-frequency phenomena are dealt with, but also phenomena within parts of apparatus and systems which are used in the radio-frequency as well as in the communication field. It was the aim to give a thorough up-to-date discussion of phenomena occurring in high-frequency systems with many applications to problems arising in communication engineering. Phenomena and actions in tubes are discussed with respect to basic principles, without too much stress on tube design, which may change from time to time. Phenomena in filament—as well as filament-less—tubes are dealt with in detail. A discussion of piezoelectric phenomena correlating the pioneer work of Voigt with present-day findings and applications is presented. Ionic and electronic oscillations within tubes as well as in the ionized regions of the upper atmosphere are discussed in detail. A brief review of classical experience and theory precedes many of the discussions so that it should not be necessary to consult other texts in order to understand difficult descriptions given in this book. Inasmuch as phenomena dealing with modulation are dealt with in detail in the book "High-frequency Measurements," the subject is omitted in this publication.

As in the author's book "High-frequency Measurements," the nomenclature recognized by the Standardization Committee of the Institute of Radio Engineers is followed. Since many branches of science are here dealt with, duplication of symbols occurs in some cases. However, duplication is never found in any one formula. Thus, with magnetic phenomena, μ is the conventional symbol for the magnetic permeability, and with electron tubes the same letter is found for the conventional amplification factor. Since the letter e is used to denote the instantaneous value of a voltage, it could not be employed to express the charge of an electron; therefore q is used. ϵ , a large script epsilon, is used for the electric-field intensity so that it will not be confused with the voltage E which corresponds to it. There should be no confusion between e used for the base of the natural logarithm and the quantity ϵ . Since ϵ is used for 2.7183, the letter κ is employed for the dielectric constant. κ_e is used for the effective dielectric constant, since in some cases, for instance for the ionized layer of the upper atmosphere and the earth crust, one has to deal with a complex value of the effective dielectric constant. The symbol κ is also used for the coupling factor. In a similar way T is used with oscillators and the like for the period of oscillation, and in places dealing with physics for the absolute temperature.

The author has attempted to give references to reliable papers published in various countries and to present the subject matter in combina-

tion with his experience. Most of the references given in the footnotes are added to enable the reader to refer to other details. For this reason the author of each article referred to is listed in the Index with a brief description of the contents of the article.

The author is much indebted to his wife and to Miss Eunice LeMelle for their assistance in the preparation of the manuscript and in proof-reading. He is also indebted to Mr. J. W. McRae of the California Institute of Technology, who was kind enough to read the entire manuscript with respect to exposition.

The author welcomes any corrections or suggestions for improvement.

AUGUST HUND.

LOS ANGELES, CALIF.,
December, 1935.

CONTENTS

PREFACE	Page vii
--------------------------	---------------------------

CHAPTER I

ACTIONS AND EFFECTS IN SPACE-DISCHARGE DEVICES	1
Thermionic Emission—Richardson, Space Charge (Child, Langmuir and Schottky) and Emission Current Equation for Very Low Positive and Negative Cold-electrode Potentials—Losses in Thermionic Tubes—Anode Effect on the Hot Cathode—Emission Ability and Electron Affinity—Customary Cathode Materials—Emission in Three-element Thermionic Tubes—Electronic and Ionic Oscillations, and Ionic To-and-fro Motions in Thermionic Tubes—Secondary Emission in Three-electrode Thermionic Tubes—Thermionic Emission in Double-plate Tubes—Thermionic Emission in Double-grid Tubes—Action in a Triple-grid Tube. (Pentode)—Effect of a Magnetic Field on Electrons in Thermionic Tubes—Magnetron Effect in Thermionic Tubes—Thermionic Tubes with Positive Ionization—Ionization in Cold-electrode Tubes—Spark and Arc—The Paschen Law—Hertz, Hallwachs, Elster and Geitel Effects, Photoelectric Tubes and Kerr Cell.	

CHAPTER II

HIGH-FREQUENCY GENERATORS	56
Frequency Spectrum—Notes on the Generation of Commercial High-frequency Currents—Notes on Alternators—Notes on Electron-tube Oscillators—Building up of Self-excited Tube Oscillations—Important Tube Relations for Three-element Electron Tubes—The Loaded Plate Circuit of a Three-element Tube—Theory of the Tuned-grid Oscillator—Theory of the A. Meissner Oscillator—Theory of the Tuned-plate Oscillator—Vector Diagram of a Tuned-plate Oscillator—Amplitude and Phase of Oscillations in a Tuned-plate Generator—Efficiency of the Tuned-plate Oscillator—Oscillation Characteristics—Effect of the Load in the External Plate Circuit on the Internal Impedance across the Grid and Filament—Tube Oscillator with Interelectrode Back Feed—Theory of the Hartley Oscillator—Effect of Grid Current in Tube Oscillators—Stability of Frequency in Tube Generators—Gradual and Abrupt Frequency Changes in Tube Oscillators—Synchronization of Tube Generators—Notes on Harmonics in Tube Generators—Notes on Tube Generators of Great Frequency Constancy—Piezo-electric Oscillator—Magnetostriction Oscillator—Dynatron Oscillator—Special Tube Generators—Tube Oscillators for Very High Voltages and Oscillators for Very Large Currents—Oscillators for Very High Frequency.	

CHAPTER III

VOLTAGE AND CURRENT CHANGERS	141
Tesla's Transformer for Obtaining High Voltages of Discrete Wave Trains—Resonance Transformer for Obtaining High Voltages of Sustained High-frequency Currents—Current Changers Using Shunts.	

CHAPTER IV

PHASE CHANGERS. 143

Phase Changers by means of Reactance and Resistance—The Revolving-field Phase Changer and Phase Multiplier—Phase Changers and Phase Multipliers by Means of Out-of-phase Currents—Phase Changers by Means of a Recurrent Network—Phase Changers by Means of Tube Circuits—Phase and Corresponding Frequency Change.

CHAPTER V

FREQUENCY CHANGERS. 150

Triple Frequency by Means of the Alternating-current Arc (Zenneck)—Double Frequency by Means of Unsymmetrical Magnetization (Arco)—Triple Frequency by Means of Transformers Which Are Magnetized to a Different Degree (Epstein, Joly)—Double Frequency by Means of Rectified Half Waves—Frequency Multiplier by K. Schmidt—Six-fold Frequency by Means of a Full-wave Kenotron Rectifier Which Employs Temperature and Space-charge Effects—Frequency Multiplication by Means of Current Impulses—Two-element Tubes as Frequency Multiplier—Three-element Tube as a Frequency Multiplier—Magnetron as Frequency Doubler—Cathode-ray Tube for Frequency Multiplication—Temperature Effect of a Hot Cathode as Frequency Doubler.

CHAPTER VI

RECTIFICATION AND INVERSION OF CURRENTS. 159

Basic Characteristics of Rectifiers—Form Factor, Peak (Amplitude) Factor, and Useful Portion of a Rectified Current—Direct-current Reading in Comparison with the Effective Value of the Second Harmonic—Voltage, Current, and Power in a Rectified Circuit—Derivation of the Rectification Law—Notes on the Application of Rectifier and Inverter Circuits—Practical Rectifiers—Electrolytic and Contact Rectifiers—Electrostatic Relay as a Rectifier—Cuprox Rectifier—The Two-electrode (Anode and Hot-cathode) Thermionic Rectifier—Mercury-arc Rectifier—Hot-cathode Mercury-vapor Rectifier—The Tungar Rectifier—Rectification Action in an Ordinary Three-element Thermionic Tube When Used as a Demodulator—Rectification by Means of Cold-electrode Tubes—Rectifiers for Obtaining B and Other Voltages for Tube Circuits.

CHAPTER VII

VOLTAGE, CURRENT, AND POWER AMPLIFIERS. 185

Magnetic Amplifiers—The Ordinary Triode as an Amplifier—Special Remarks on Voltage and Power Amplification—Estimation of Power Output and Amount of Second-harmonic Distortion—Plate-current Grid-voltage Characteristic and Grid Bias for Loaded Plate Circuits—Uses of Lumped Characteristics—Effect of Interelectrode Capacitance and Grid Resistance on the Amplification—Resistance- and Resistance-capacitance-coupled Amplifiers—Supply Voltages for Resistance-coupled Amplifiers—Effect of Capacitance-resistance Coupling and Grid-plate Interelectrode Capacitance on the Frequency Characteristic of an Amplifier—Special Remarks on the Design of Resistance-capacitance-coupled Amplifiers—Design Formulas for

Resistance-coupled Amplifiers and Width of Pass Band—The Transformer-coupled Amplifier—Remarks on the Design of Transformer-coupled Amplifiers—Tuned Amplifier—The Amplifier with Choke-capacitance Coupling—Regenerative Amplifiers—Notes on Practical Regenerative Amplifiers—Superregenerative Circuits—Self-oscillations in Cascade Amplifiers and Their Prevention—Notes on Frequency Limitation and Tube and Other Noises in Amplifiers—Notes on Push-pull Amplifiers—Notes on Amplifiers Using Tubes with Several Grids—Amplifiers Utilizing Devices with Negative Resistance—Notes on Special Grid Tubes—Glow-tube Amplifiers—Trigger Circuits—Thermal Amplifiers—Notes on Telephone Receivers and Their Amplification Action.

CHAPTER VIII

THEORY OF ELECTROSTRICTION WITH SPECIAL REFERENCE TO PIEZO ELECTRICITY IN QUARTZ.	284
Experimental Evidence—Relation of Curie and Lippmann Effects to the Ny Tsi Ze Saturation Phenomenon—Static Theory of Piezo Electricity—Notes on Dynamic Piezo Electricity—Design Formulas for Curie-cut Quartz Elements Producing Longitudinal Vibrations—Design Formulas for the 30-deg.-cut Crystal—Temperature Coefficients of Curie-cut and 30-deg.-cut Quartz Elements—Air-gap and Pressure Effect on Frequency—Total Values of Polarization, Displacement Current, and Charge for Mounted Quartz Elements—Theory of the Vibrating Quartz Rod and Its Equivalent Electric Circuit—Longitudinal, Transverse, and Torsional Quartz Oscillations—Surface and Space Charges.	

CHAPTER IX

ELECTROMAGNETIC THEORY.	324
Gauss' Theorem—Application of Poisson's Equation—Ampere's Law—Maxwell's Displacement Current—First Field Equation for the Ionized Medium—Faraday's Induction Law—Field Equations for the Dielectric and for Conductors (Stationary Bodies)—Application of the Field Equations to the Case of Penetration into a Conductor—Propagation of Electromagnetic Waves—Scalar and Vector Potentials—Spherical, Cylindrical and Beam Wave Propagation—Magnitude and Direction of the Electric and Magnetic Field of a Current Element and Radiation Resistance—Radiation Resistance of Commercial Antennas—Derivation of the Formulas for the Electric- and Magnetic-field Intensity Due to a Sender Antenna (Induction and Radiation Fields, and Received Current)—Notes on Wave Propagation with Respect to Wave Length and Distance—Sommerfeld's Surface and Space Waves and Numerical Distance.	

CHAPTER X

THEORY OF THE IONIZED LAYER (HEAVISIDE-KENNELLY LAYER)	367
Causes of Abnormal Field Intensities and the Ionization of the Upper Atmosphere—Direct and Indirect Rays, Their Phase Difference and Dead Zones—Effective Dielectric Constant of the Ionized Medium—Phase Velocity, Group Velocity of Propagation, Index of Refraction, and Critical Frequency—Dispersive Properties of the Ionized Layer—Notes on the Physics of the Atmosphere and Selective Absorption—Bending and Path	

of the Rays—Effect of the Earth's Magnetic Field on the Path of Transmission and Selective Absorption Due to Electron Motions—Polarization of the Received Electromagnetic Waves and Fading—Long-time-interval Echo Effects.

CHAPTER XI

LINES OF LONG AND SHORT ELECTRICAL LENGTH WITH SPECIAL REFERENCE TO ANTENNA PROBLEMS. 406

Formation of Progressive and Standing Waves along an Electrical Line and Impedance at the Generator End—Time and Space Functions, Velocity of Propagation, and Propagation Constant—Current and Voltage Distributions along Lines and Antennas and Possible Modes—Effective Antenna Reactance for the Loaded and Unloaded Antenna—Apparent Effective and True Effective Antenna Constants—Transmission-line and High-frequency Equation—Theory for the Experimental Determination of the Propagation Constant and Surge Impedance of a Line—Theory of the Lecher System When Excited with a Harmonic E.M.F.

CHAPTER XII

DIRECTIVE SYSTEMS. 454

Theory of the Wave Antenna (Beverage Antenna)—Sommerfeld-Pfrang Reciprocity Theorem, the Carson Theorem, the Lorentz Theorem, and Ballantine's Combined Lorentz-Carson Theorem—The Theory of the Loop Antenna as a Receiver with Special Reference to Field-intensity Measurements and the Determination of Effective Height—The Loop Aerial as Transmitter and Its Radiation Energy Compared with That of an Open Antenna—Directional Effects of Linear and Coil Antennas—Antenna Effect, Width Effect, and One-sided Loop System—Space Characteristics of Antennas and Loops and Effective Height in Any Direction—Application to Airplane and Airship Guiding—The Goniometer (Inclined Double-loop Antenna)—Theory of the Double-loop and the Adcock System—Direct and Indirect Waves, Bearing Error with Loops, and Goniometer Systems—Day and Night Effects on Vertical Antennas and Loops When Used as a Receiver and Austin's Barrage Circuit Method—Directive Antenna Arrays—Elementary and Group Characteristics—Space Radiation by Means of Higher Modes of Distributions along Aerials.

CHAPTER XIII

THEORY OF RECURRENT NETWORKS. 531

Artificial Lines—Application of Artificial Lines for the Determination of Amplification and the Measurement of Small Currents (Theory of the Attenuation Box)—Theory of Filters with T and π Sections—Recurrent Network in a Circuit—Equations for any Alternating-current Network—Filter Impedance and Effective Voltages at the End of a Recurrent Network—Propagation Constant and Characteristic (Surge) Impedance of a Recurrent Network—Action of Parallel and Series Impedances in Networks—Theory of the Low-pass Filter with Inductance along and Capacitance across the Section—Design of a Low-pass Filter—Design of a Low-pass Filter Which Also Completely Suppresses Currents of a Definite Frequency—Theory of the High-pass Filter with Capacitance along and Inductance

CONTENTS

XV
PAGE

across the Section—Notes on Symmetrical Recurrent Networks Which Use Capacitance and Inductance Combinations along and across a Section (Band-pass and Band-suppression Filters)—Theory and Design Formulas of Uniform Band-pass Filters—The Coupled-circuit Filter—Characteristic Impedance of Coupled-circuit Filter—Filter Impedance and Effective Voltages at the End of a Coupled-circuit Filter—Design of a Band-pass Filter Consisting of Coupled Circuits—Notes on a Coupled-circuit Filter with Coil Losses—Filters with Unequal Sections (Composite Networks)—Theory of Zobel's Composite Filters—Design Formulas for Derived-type Filter Sections—Notes on Coils and Condensers Used in Filter Circuits—Transformer as a Matching Device in Filter Circuits—The Three-element Electron Tube as an Unsymmetrical Network—Notes on Coupling Devices Employing Recurrent Networks.

APPENDIX

USEFUL RELATIONS AND TABLES	595
INDEX	611

PHENOMENA IN HIGH-FREQUENCY SYSTEMS

Foundation of present-day physics has mostly to do with electrical phenomena. Many of these phenomena play an important part in high-frequency systems. A thorough understanding of physical principles and a mastery of theoretical speculations were what led Heinrich Hertz to his far-reaching discoveries. The applied field is still an open territory, and a thorough knowledge of underlying principles and theoretical analysis no doubt will give rise to further progress.

CHAPTER I

ACTIONS AND EFFECTS IN SPACE-DISCHARGE DEVICES

In vacuum tubes, the electrons can be conveniently produced by means of thermionic emission for which comparatively low positive potentials are sufficient to cause a current flow toward the anode. The current can then be readily varied within certain limits by changing the temperature of the cathode, the anode potential, or both.

There are also tubes where the cathode emission is produced by bombardment of the cathode with positive ions. Much higher voltages are then needed in order to pull the electrons out of the cathode surface and the current flow cannot be varied as smoothly and readily as in the case of thermionic tubes. The original Braun cathode-ray tube is an example. On the other hand, when the pressure and the kind of gas are properly chosen, discharges of this type can take place for comparatively low voltages. The glow-discharge tubes used as rectifiers, voltage regulators, and recently also as amplifiers are examples.

When both the thermionic effect and the effect due to positive ionization are combined, considerable space currents can be obtained for relatively low anode potentials since the positive ionization neutralizes the electron space charge and thus reduces the anode potential necessary for a given space current. The tungar and mercury-vapor rectifiers are examples.

Space currents can also be produced by exposing an electrode to light as in the case of photoelectric cells.

1. Thermionic Emission.—The simplest kind of thermionic tube consists of two electrodes, one more or less incandescent, as shown in

Fig. 1. When the vacuum is very high, a pure electron current i_e flows between the electrodes when the hot electrode is at a negative potential with respect to the cold electrode. When a negative potential (except for comparatively low values) is applied to the cold electrode with respect to the other electrode, there is no current flow.

This effect was noticed by Thomas A. Edison in 1883 while he was working with his carbon-filament lamps, and it was at first investigated by J. A. Fleming,¹ J. J. Thomson, and A. Wehnelt. It was J. A. Fleming

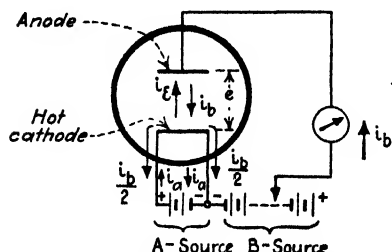


FIG. 1.—Showing that the negative side of the filament carries more current than the positive side.

who applied the Edison effect to an apparatus for rectifying high-frequency currents (Fleming valve). Other important developments are the three-element tube, invented by Lee De Forest (1907) who interposed a third electrode between the hot cathode and the anode, and the double-grid tube (four electrodes).² With the three-element tube it is possible to rectify, amplify, and generate currents. It is possible to check space

charge and to reduce internal tube capacities with the double grid.

The tubes of Fleming, De Forest, and Wehnelt originally operated not as a result of pure electron discharge but as a result of both electron emission and positive ionization. Credit is due I. Langmuir³ for the introduction of tubes in which there existed a pure electron discharge. Pure electron emission is also used in the Coolidge X-ray tube.

Electrons attracted to the positive electrode maintained at a potential of e volts with respect to the cathode attain a velocity v cm/sec, according to

$$qe = 0.5m[v^2 - v_0^2] \quad (1)$$

¹ FLEMING, J. A., *Phil. Mag.*, **42**, 52, 1896; *Proc. Roy. Soc. (London)*, **47**, 118, 1890; **14**, 187, 1896; **74**, 475, 1905; *London Electrician*, **55**, 303, 1905; *Electrician*, **61**, 843, 1908; *Jahrb. dr. Tel.*, **1**, 95, 1908; J. J. THOMSON, *Phil. Mag.*, **48**, 1899; A. WEHNELT, *Physik. Z.*, **5**, 680, 1904; *Ann. Physik*, **14**, 425, 1904; *Ann. Physik*, **19**, 138, 1906.

² SCHOTTKY, W., *Arch. Elektrotech.*, **8**, 299, 1919; A. W. HULL and N. H. WILLIAMS, *Phys. Rev.*, **27**, 433, 1926. I. Langmuir seems to be the first one to suggest a special grid to remove space charge (1913) and W. Schottky to suggest a special grid for screening; I. LANGMUIR, *Phys. Rev.*, **2**, 450, 1913; *Physik. Z.*, **15**, 348, 1914; W. SCHOTTKY, *Physik. Z.*, **12**, 872, 1914; **15**, 526, 624, 1914; **20**, 220, 1919.

³ LANGMUIR, I., *Phys. Rev.*, **34**, 401, 1913; *Physik. Z.*, **15**, 348, 516, 1914; W. SCHOTTKY, *Physik. Z.*, **15**, 526, 624, 1914; *Ann. Physik*, **44**, 1011, 1914; *Z. f. Physik*, **14**, 63, 1923.

where

$$q = 1.592 \times 10^{-19} \text{ coulomb}$$

$$m = 0.902 \times 10^{-27} \text{ gram}$$

and v_0 is the initial velocity of the electrons.

For the normal components of these initial velocities, the Maxwellian velocity-distribution law holds. The electrons leave the hot cathode with a mean velocity v_0 which for tungsten is about as great as though they had already passed through a distance corresponding to $\frac{1}{5}$ volt. For oxide cathodes, the volt velocity is somewhat smaller. This explains why a small current still flows toward the cold electrode for $e = 0$ and for small negative values of e (Fig. 3). When the positive potential e of the cold electrode is kept constant (Fig. 1), and the absolute tempera-

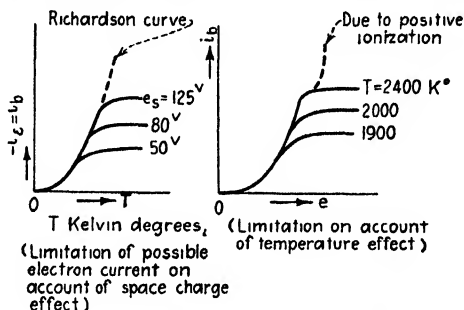


FIG. 2.—Space-current curves.

ture ($T = 273^\circ +$ centigrade temperature) is gradually raised, curves as shown in Fig. 2 are obtained. When the temperature is kept constant and the positive potential e of the cold electrode is varied, we have the other set of curves shown in this figure. In each case the electron current i_a passing toward the anode is compensated by an equal and opposite current i_b (Fig. 1) taken from the B battery which supplies the positive potential to pull the electrons toward the cold electrode. This current passes back to the B source through the filament. That is, one side of the filament carries a current $\left(i_a - \frac{i_b}{2}\right)$ and the other side a current $\left(i_a + \frac{i_b}{2}\right)$. In most tubes i_a is much larger than the emission current so that the difference is hardly noticeable, but in certain circuits precautions must be taken so that the negative end of the filament which gives off more electrons will not become dangerously overloaded. Therefore a *filament meter* should always be inserted at the *negative end* of the filament in order to indicate the maximum current flow.

From the constant-voltage and constant-temperature characteristics of Fig. 2, it can be seen that saturation due either to *space charge* or to

temperature effect can take place. The first kind of current limitation is due to the fact that the electrons that escape from the surface of the hot cathode do not all pass toward the anode. A portion of the emitted electrons forms an electron cloud around the cathode and repels new electrons. Many of the electric lines of force coming from the anode will then end on electrons in space and some of the electrons close to the filament are even pulled back to the less negative surface of the cathode because of the image effect. In other words, a *potential minimum* exists somewhere between the hot cathode and the anode, and only electrons with sufficient initial velocity can overcome this potential minimum and reach the anode. When $e \geq e_s$, that is, when the anode potential e is at least equal to the saturation potential e_s , the potential minimum has withdrawn to the surface of the hot cathode and all the emitted electrons, even the slowest, reach the anode. For values of e smaller than e_s , the potential minimum moves out into the space between the cathode and the anode, and for a certain negative value $-e_{\min}$ reaches the cold electrode.¹

As to the temperature limitation of the anode current (Fig. 2), the number of electrons emitted from the hot cathode depends upon its temperature and the electron affinity² of its emitting surface. This affinity has been found to depend upon the material of the cathode. For materials with smaller electron affinity the electrons can be pulled out more easily.

Alkali oxides on the surface of platinum (Wehnelt) produce a pronounced space current even though the cathode is heated only to a dull red, whereas, for tungsten and molybdenum cathodes, higher temperatures are needed in order to free sufficient electrons. For a given filament material the temperature of the hot cathode determines the life of the tube. The temperature is usually chosen so that the life can be guaranteed from 1000 to 2000 working hours. At normal operating temperatures, 1 watt of power expended in heating the cathode gives a total emission current from 2 to about 5 ma for tungsten filament, 10 to 40 ma for thoriated tungsten, and 20 to 80 ma for oxide filaments.

For a cathode of a given material and at a certain temperature, only a definite number of electrons are emitted and can reach the anode.

¹ This is the small negative potential which must be applied to the anode of a tube to just make the anode space current vanish (Fig. 3). When a tube is to be used as a rectifier, as an indicator of small high-frequency currents, or as a two-electrode tube voltmeter, it is necessary that no space current should flow before the high-frequency potential is applied. The steady anode potential must therefore be made equal to $-e_{\min}$. This is usually done by means of a potentiometer connected across the filament supply (Fig. 118 on p. 175).

² A. Wehnelt (*loc. cit.*) appears to have investigated electron affinity first. See also O. W. Richardson, "The Emission of Electricity from Hot Bodies," Longmans, Green & Company, London. P. Debije (*Ann. Physik*, **32**, 1910) shows that an electron cannot detach itself so readily from a smooth surface as from sharp edges and corners of irregular surfaces.

If, then, the saturation potential ($e = e_s$) is applied to the anode, all the electrons are brought to the anode by means of the electric field. A still higher anode potential can then give an increase in space current only when the temperature of the cathode is increased.

2. Richardson, Space-charge (Child, Langmuir, and Schottky) and Current Equation for Very Low Positive and Negative Cold-electrode Potentials.—Richardson's original¹ equation

$$i_s = aS\sqrt{T}\epsilon^{-\frac{b}{T}} \quad \text{milliamperes} \quad (2)$$

gives an expression for the saturation space current i_s . The quantity T denotes the absolute temperature in Kelvin degrees and S the area of the cathode in square centimeters. The quantities a and b depend upon the material of the cathode and have values as given in Table I. Equation (2) is based on the laws of the kinetic gas theory (electron

TABLE I

Material of hot cathode	a	b
Tungsten... ..	2.36×10^{10}	5.25×10^4
Molybdenum.....	2.1×10^{10}	5×10^4
Thorium.....	20×10^{10}	3.8×10^4
Oxide.	2 to 24×10^7	1.9 to 2.4×10^4

evaporation) and utilizes the Clausius-Clapeyron formula for the rate of evaporation of a liquid. W. Schottky² gives a more accurate emission formula and, if the modifications of Dushman and von Raschevsky³ are employed, we have for the saturation current in milliamperes

$$i_s = SAT^2\epsilon^{-\frac{q\phi}{kT}} \quad (\text{modified Richardson equation}) \quad (3)$$

where S denotes the area of the cathode in square centimeters, A a factor,⁴ equal to 60,200 ma/(cm deg)², T the absolute temperature, ϵ the base of the system of natural logarithms. The other factors denote the electronic charge $q = 1.592 \times 10^{-19}$ coulomb, the Boltzmann

¹ *Camb. Phil. Proc.*, **11**, 286, 1901; *Phil. Trans.*, **201**, 516, 1903; *Phil. Mag.*, **18**, 695, 1909; **23**, 633, 1914; *Proc. Roy. Soc. (London)*, **A91**, 530, 1915.

² SCHOTTKY, W., *Verh. Phys. Ges.*, **21**, 529, 1919. This formula is based upon the M. von Laue law for electron evaporation (*Jahrb. Radioakt., Elektronik*, **15**, 257, 1918).

³ DUSHMAN, S., *Phys. Rev.*, **20**, 109, 1922; **21**, 623, 1923; **23**, 156, 1924; S. DUSHMAN, H. N. ROWE, J. EWALD, and C. A. KIDNER, *Phys. Rev.*, **25**, 338, 1926; N. VON RASCHEVSKY, *Z. Physik*, **32**, 746; **33**, 606, 1925; **35**, 905; **36**, 628, 1926.

⁴ Above value holds for carbon, calcium, molybdenum, platinum, tantalum, thorium, and tungsten. It is, however, 162,000 for caesium; 26,800 for nickel and generally much lower for oxides coated on platinum, for instance 16,200 for As_2O_3 and only 570 for ThO_2 .

constant $k = 1.372 \times 10^{-16}$ erg/deg, and $\Phi = 8.62 \times 10^{-5}$ B volt is the volt equivalent of the work necessary to free an electron from the cathode. The quantity B is known as the "electron affinity" of the cathode material. The quantity Φ is also known as "Richardson's work function" and as a rule its value is smaller the larger the atomic number, as can be seen from Table II.

TABLE II

Material of hot cathode	Electron affinity B	Richardson's work function Φ , volts
Tungsten.....	52.6×10^3	4.53
Molybdenum.....	50×10^3	4.31
Thorium.....	34.1×10^3	2.94
Platinum.....	62.7×10^3	5.4

For anode potentials e which are smaller than the value e_s , which just produces the saturation current i_s , the space charge due to the cloud of electrons limits the electron current i_e flowing to the anode. This space current, according to Child,¹ Langmuir, and Schottky, follows a three-halves-power law which may be written in the form

$$i = k_1 e^{1.5} \quad \text{milliamperes (theoretical space-charge current)} \quad (4)$$

which is true for electrodes of any form. The voltage e between the cathode and the anode is expressed in volts and k_1 is the geometrical form factor of the electrodes. This relation assumes that the electrons have no initial velocity. The derivation for plane electrodes is given on page 326 and the current for each square centimeter of surface is, then,

$$i = 2.33 \times 10^{-3} \frac{e^{1.5}}{d^2} \quad \text{milliamperes (Langmuir)} \quad (5)$$

if d is the distance in centimeters between the electrodes. The theoretical formula

$$i = 29.3 \times 10^{-3} \frac{l}{d} e^{1.5} \quad \text{milliamperes (Langmuir)} \quad (6)$$

holds for a cylindrical anode of length l and diameter d , with the hot cathode a straight filament stretched along the axis of the cylinder.

The current-voltage curves of customary electron tubes approximate the shape indicated in Fig. 2. There are portions which are more or less

¹ CHILD, C. D., *Phys. Rev.*, **32**, 492, 1911; I. LANGMUIR, *Phys. Rev.*, **2**, 450, 1913; W. SCHOTTKY, *Physik. Z.*, **15**, 526, 624, 1914; P. S. EFSTEIN, *Verh. Phys. Ges.*, **21**, 85, 1919.

curved, and portions for which Ohm's law holds, that is, for which linearity exists. The formula

$$i = Ke^n \quad (7)$$

expresses, therefore, the characteristic for any portion. The quantity n is about 2 for the lower portion and is unity for the straight middle portion. For the upper portion of the characteristic of certain tubes $n = 1.5$, if the effect of the saturation is neglected. The internal static resistance R_p of a tube for a certain voltage e is

$$R_p = \frac{e}{i} \quad (8)$$

and for a variable anode potential e the dynamic resistance r_p becomes

$$r_p = \frac{de}{di} = \frac{e}{ni} = \frac{R_p}{n} \quad (9)$$

since

$$\frac{de}{di} = \frac{1}{Kne^{(n-1)}} \quad \text{and} \quad R_p = \frac{e}{i} = \frac{1}{Ke^{(n-1)}}$$

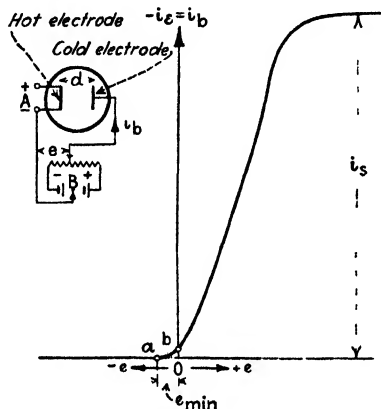


FIG. 3.—Current due to electron pressure for region ab .

The dynamic resistance is therefore

smaller than the static (direct-current) resistance as long as $n > 1$.

From Fig. 3, an experimental curve, it can be seen that for the potential ($e = 0$) at the cold electrode a small space current still flows, and that a small space current exists even for small negative potentials (curve ab). The reason for this is that the electron evaporation from the surface of the hot cathode follows the Maxwellian velocity-distribution law. Hence electrons with a temperature velocity greater than the velocity $v = \sqrt{\frac{2q}{m}(-e)}$ due to the applied electric field $-e/d$ reach the cold electrode and constitute a space current $i_e = -i$. The current for the branch ab then follows the equation

$$i = i_0 e^{-\frac{qe}{kT}} = i_0 e^{-\frac{e}{8.6 \times 10^{-5} T}} \quad \text{milliamperes} \quad (10)$$

(emission current for a negative potential e on the cold electrode)

In this equation, $q = 1.592 \times 10^{-19}$ coulomb and the Boltzmann constant $k = 1.372 \times 10^{-16}$ erg/deg $= 1.372 \times 10^{-16} \times 10^{-7}$ watt. The quantity i_0 denotes the current for zero plate potential in milliamperes, and T is the absolute temperature. The absolute temperature for hot

cathodes of tungsten is about $T = 2300^\circ\text{K}$. Hence $e^{-\frac{8.6 \times 10^{-5} \times 2300}{e}}$ is the decay term for negative plate potentials of e volts and (10) yields

$$i = i_0 \left[\frac{1}{1 + e} \right]^e \quad (10a)$$

If the total emission current is 22.5 ma, then for a negative plate potential $e = 2$ volts, this relation shows that

$$i = \frac{22.5}{150^2} = 10^{-3} \text{ milliamperes}$$

or 1 μa of space current. From this it is evident that only small negative cold-electrode potentials can produce a measurable current. This relation also holds in some measure for very small positive anode potentials, since then the electron motion is mostly due to the temperature velocity. This is true for positive potentials lower than 1 volt. The space-charge law [Eq. (4)] no longer holds. Since, for tungsten, the electrons leave the cathode with a mean velocity corresponding to $\frac{1}{2}$ volt, a cylindrical anode of diameter d and length l such that $l/d = 3.4$ gives, according to (6), for zero anode potential ($e = 0$), a space current

$$i_0 = 29.3 \times 10^{-3} \times 3.4 \times (0.2)^{1.5} = 10^{-1} (0.2)^{1.5} \text{ milliamperes}$$

which shows that for a cylindrical thermionic tube of the foregoing dimensions the space current is very small.

3. Losses in Thermionic Tubes.—The foregoing consideration of Eq. (10) shows that a thermionic tube passes practically no current for negative potentials on the cold electrode. The two-element thermionic tube is therefore a rectifier. When pure electron discharge prevails and e denotes the positive potential effective at the cold electrode and i_b the corresponding current delivered by the B battery (Fig. 1), practically all the power lost within the tube due to this current is that due to the kinetic energy $N(\frac{1}{2}mv^2)$ given up at the anode when the electrons are suddenly stopped at this electrode. With N denoting the number of electrons emitted by the hot cathode per unit time and unit area, the anode loss is

$$W_a = N(\frac{1}{2})mv^2 = Nqe = ei_b = Ke^{n+1} \quad (11)$$

since, according to (7), $i_b = Ke^n$, which for the case of a kenotron rectifier, for $n = 1.5$, gives

$$W_a = Ke^{2.5} \quad (12)$$

The energy lost in heating the cathode is

$$W_c = i_a^2 R \quad (13)$$

if R denotes the effective resistance of the cathode. This loss can also be found from the relation

$$W_e = k_1 h S [T^4 - T_1^4] = 12.54 \left[\frac{T}{1703} \right]^{4.74} S \text{ watts/cm}^2 \quad (13a)$$

where T denotes the absolute temperature of the cathode and T_1 that of the neighboring space. The first part is the Stefan-Boltzmann approximation expression for the radiation energy per second. The most exact total radiation energy is $5.7 \times 10^{-5} (T^4 - T_1^4)$ erg/cm²/sec. The factor k_1 stands for the radiated energy of a black body per square centimeter for $T = 1$ Kelvin degree, where T_1 is equal to absolute zero. The quantity h is Planck's constant and S the area in square centimeters. The last relation in (13a) is of greatest importance and, according to Langmuir,¹ holds for tungsten.

The percentage efficiency of the thermionic rectifier is therefore

$$\eta = \frac{\text{input} - [W_a + W_e]}{\text{input}} 100 \quad (14)$$

The following is an application of this expression using data furnished by experiments of S. Dushman.² A high-voltage rectifier (kenotron) was connected through a load resistance so that the saturation current I_s existed. The voltage drop in the tube was $E = 145$ volts in comparison with the total voltage of 15,000 volts applied to the series combination of thermionic tube and load resistance. All other data and calculations are as follows:

Anode: Molybdenum cylinder 7.62 cm long, diameter 2.54 cm.

Cathode: Axial tungsten filament (10 mil).

Temperature of filament: 2550°K.

Maximum thermionic current: About $I = 400$ ma.

Voltage drop in tube: $E = \left[\frac{400}{29.3} \frac{2.54}{2} \frac{10^3}{10} \right]^{3/4} = 145$ volts.

Anode loss [Eq. (11)]: $W_a = EI = 145 \times 0.4 = 58$ watts.

Cathode loss: $W_e = 72$ watts.

Total loss: $W_a + W_e = 0.13$ kw.

Rectified energy: Input = 15,000 \times 0.4 = 6 kw.

Efficiency [Eq. (14)]: $\eta = \frac{5.87}{6} 100 = 97.8\%$.

4. Anode Effect on the Hot Cathode.—The heat developed in the anode also radiates against the hot cathode and increases the electron emission. This becomes more true as the anode potential is chosen higher, since then the electrons bombard the anode with greater velocity. Normally, for receiver tubes, this effect is of small importance, since the back radiation on the cathode occurs, according to Eq. (13a), with

¹ *Phys. Rev.*, **34**, 1912.

² *Gen. Elec. Rev.*, March, 1915.

the fourth power of the absolute temperature, and the anode operates at quite a low temperature. But when the heat developed in the anode is appreciable (overloaded kenotrons, transmitter tubes, etc.), the radiation effect on the cathode may give rise to the disintegration of the filament used as the hot cathode. For tungsten electrodes, an anode temperature of 1000° produces about 3.5 per cent increase of the temperature of the hot cathode, which increases the emission current by about one-fifth. Since hot oxide cathodes are dull emitters, it takes much less temperature increase at the anode (about 150°) to produce the same percentage increase in temperature of the hot cathode. It sometimes happens that for a constant anode potential the emission current keeps on increasing and in the end burns out the filament.

With respect to the emission current, it has been brought out that the negative end of the filament carries more emission current and therefore heats up more than the positive end (Fig. 1). When a high resistance is inserted in the negative end of the cathode source, the B-battery current flows through the positive end and thus reduces the filament-heating current. When the cathode is heated by alternating current, this unequal heating, due to the space current, is avoided. In any case, when the tube is not worked with full saturation current ($i_e = i_s$), little difficulty arises. This is true for many amplifier and oscillator circuits, since the average value of the space current is only about $i_s/2$.

5. Emission Ability and Electron Affinity.—The modified Richardson equation (3), for the total emission per square centimeter of a hot cathode, becomes, when written in the logarithmic form,

$$\log_{10} i_s = \log_{10} A + 2 \log_{10} T - 0.4343 \frac{q\Phi}{kT}$$

and since $\frac{q\Phi}{kT} = 11,600 \frac{\Phi}{T}$, where T denotes again the absolute temperature of the hot cathode and Φ Richardson's work function in volts (Table II on page 6), we have

$$\log_{10} i_s = \log_{10} A + 2 \log_{10} T - 5040 \frac{\Phi}{T} \quad (15)$$

which can be solved graphically by plotting the sloping T lines for a fixed absolute temperature against the work function (given in Table II) since, for certain conditions, $A = 60.2$ amp/cm² deg² and $\log A = 1.7792$.

For tungsten filaments, the total emission current $i_s = -i_e$ for normal filament temperatures, $T = 2300, 2400, 2500$, and 2600°K , is about 138, 365, 891, and 2044 ma/cm² of the cathode surface. In this range, an increase of 5 per cent in the filament current about doubles the

emission current. The emission below 2100°K is very small (only about 4.2 ma/cm² at 2000°) and of no practical value. At a temperature of 2800°K the melting point of tungsten is reached. For oxide filaments the emission is about 0.8, 38, and 588 ma/cm² for $T = 1000, 1200,$ and 1400°K, respectively.

From Table II it can be seen that thorium requires the least work for emitting the electrons, that is, the lowest temperature, while a platinum cathode requires a high temperature for the same emission. The constant B in the table is known as the *electron affinity* and is likewise smaller for a better thermionic emitter since

$$B = 11,600\Phi \text{ Kelvin degrees} \quad (16)$$

According to L. R. Koller and K. H. Kingdon,¹ the constant A in Eq. (15) does not have the value $A = 60,200 \text{ ma/cm}^2 \text{ deg}^2$ for oxide, but for a mixture of barium oxide and strontium oxide while burning $A = 1.07$. For a thoriated tungsten cathode it is $A = 7000 \text{ ma/cm}^2 \text{ deg}^2$. The electron affinity B of these two cases is 12,100 and 31,200°K.

It is not easy to measure the temperature of the hot cathode. Therefore, it is customary to express the watt input of a filament in terms of the corresponding total emission current which is also known as the "saturation current."

6. Customary Cathode Materials.—The values given above for B show that oxide-coated filaments at about 1300°K are good emitters. This had already been found years ago by Wehnelt who experimented with calcium oxide and found that wires covered with it liberated electrons freely at comparatively low temperatures. Today barium oxide and strontium oxide are more often used. A mixture of these oxides, with paraffin as a binder, is brushed on platinum iridium or other wire. The paraffin is then burned off, leaving the oxide coating behind.

Another type of low-temperature emitter can be secured by mixing thorium oxide with tungsten and drawing the mixture to form a wire. When such a wire filament is heated, oxygen is given off and, after continued heating, thorium evaporation toward the surface of the wire causes a monatomic layer of thorium to form on the surface.² This kind of filament is a generous emitter.

If the vacuum is not sufficiently good, the emission becomes much smaller. For this reason a "getter" of magnesium is provided inside the bulb of the tube. On being raised to a high temperature, the magnesium burns and takes up the remaining gases, at the same time absorbing the oxygen of the original thorium oxide. If too many electrons are drawn

¹ KOLLER, L. R., *Phys. Rev.*, **25**, 246, 671, 1925; K. H. KINGDON, *Phys. Rev.*, **23**, 774, 1924; **24**, 510, 1924.

² LANGMUIR, 1914.

from the filament, the emission practically disappears since all the thorium will be evaporated from the surface of the filament. The filament can then be reactivated by raising the filament temperature above normal without drawing off any electrons (zero anode potential). Monatomic thorium is thus forced to the surface of the filament. A reactivation of this kind is, of course, only possible as long as traces of thorium oxide are still contained within the filament. Two reactivations are as a rule about all that can be expected. It is therefore essential not to overload such tubes. Their life is then prolonged. Tantalum, calcium, and caesium with work functions as low as 4.12, 2.24, and 1.38 volts are likewise good emitters.

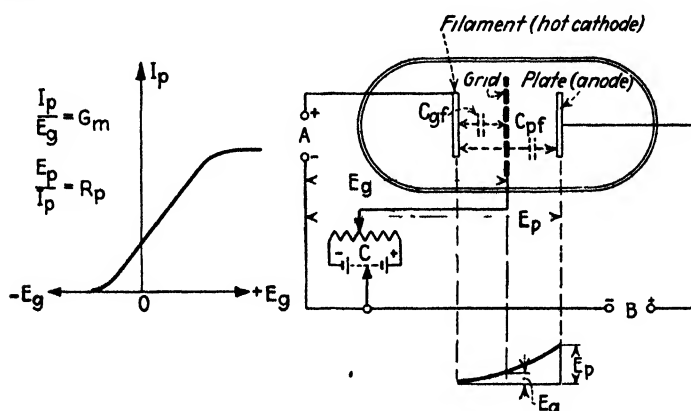


FIG. 4.—Display in a three-element thermionic tube.

7. Emission in Three-element Thermionic Tubes.—The ordinary three-element tube is as shown in Fig. 4. The Lee DeForest grid is interposed between a hot cathode which emits electrons and an anode called the “plate” which receives them.

1. When a grid is added to a two-element tube without a potential impressed on it, the current I_p passing to the plate will be somewhat smaller than without a grid. The reason for this is that the insulated grid attracts some of the electrons and becomes negatively charged. It then reduces the field in the neighborhood of the filament. In other words, the grid acts as a screen, and the space current flowing between the plate and filament is reduced.

2. If a negative potential E_g , with respect to the negative end of the hot cathode, is impressed on the grid, the effect just mentioned is still more pronounced and for a proper choice of the negative potential the plate current I_p can be stopped altogether. This means that all the electrons emitted at the hot cathode turn around in the immediate neighborhood of the grid and return to the cathode.

3. A certain positive potential $+E_g$ applied to the grid neutralizes the negative charge of the floating grid and causes a current flow as though the grid did not exist.

4. When a larger positive potential $+E_g$ is applied, the electron current is increased, provided that a sufficient number of electrons are available at the hot cathode.

The purpose of the grid is, therefore, to change the field distribution between the cathode and the plate, that is, to change the space-charge distribution. It will be most effective when mounted close to the filament, since the emission current depends upon the magnitude of the potential minimum (near the cathode) which is due to the space-charge effect, and also on how great an effect the positive plate potential E_p has on the electric field near the surface of the hot cathode. Further, the finer the grid mesh, the greater will be its effect. The effect of the grid potential can be determined by the interelectrode capacities indicated in Fig. 4. A charge Q exists on the cathode which is

$$\begin{aligned} Q &= C_{pf}E_p + C_{gf}E_g \\ &= C_{gf}\left[E_g + \frac{C_{pf}}{C_{gf}}E_p\right] \\ &= C\left\{\frac{C_{gf}}{C}\left[E_g + \frac{C_{pf}}{C_{gf}}E_p\right]\right\} \\ &= CE \end{aligned}$$

where C denotes the equivalent capacitance. If the potentials E_p and E_g are increased or decreased simultaneously by a small amount δE , then E is changed by this amount or

$$\begin{aligned} E + \delta E &= \frac{C_{gf}}{C}\left\{[E_g + \delta E] + \frac{C_{pf}}{C_{gf}}[E_p + \delta E]\right\} \\ &= \frac{C_{gf}}{C}\left\{\left[E_g + \frac{C_{pf}}{C_{gf}}E_p\right] + \left[\delta E + \frac{C_{pf}}{C_{gf}}\delta E\right]\right\} \end{aligned}$$

Subtracting from this

$$E = \frac{C_{gf}}{C}\left[E_g + \frac{C_{pf}}{C_{gf}}E_p\right]$$

yields

$$\delta E = \frac{C_{gf}}{C}\left[1 + \frac{C_{pf}}{C_{gf}}\right]\delta E$$

or

$$\frac{C}{C_{gf}} = 1 + \frac{C_{pf}}{C_{gf}}$$

Putting $C_{gf}/C_{pf} = \mu$, we have

$$E = \frac{1}{1 + \frac{1}{\mu}}\left[\frac{E_p}{\mu} + E_g\right] \quad (16a)$$

where μ is known as the "amplification factor" of a three-element tube; from this it can be seen that for a large amplification factor

$$E \cong \left[\frac{E_p}{\mu} + E_g\right] \quad (16b)$$

From this result it is evident that the grid does not completely screen off all lines of force due to the positive plate potential E_p . The resultant or lumped potential E acting at the plane of the grid is partly due to the actual grid potential E_g plus the portion E_p/μ of the plate potential E_p which grips through the grid meshes. The through grip is expressed by the reciprocal of the amplification factor which is discussed in detail in the chapter on amplifiers. Since, according to (16a), the three-element tube acts as though a potential E attracted the electrons from the hot cathode, the space-charge relation of Eq. (7) gives for the total electron current ($-i_e = I_g + I_p$)

$$\begin{aligned} I_g + I_p &= kE^n = k\left[\frac{E_p}{\mu} + E_g\right]^n \\ &= K[\mu E_g + E_p]^n \end{aligned} \quad (17)$$

where $K = k/\mu^n$ is the lumped conductivity of the tube. For negligible grid current,¹ the basic equation for the amplifier becomes

$$I_p = \frac{1}{R_p}[\mu E_g + E_p]^n = \frac{1}{R_p}E_i^n \quad (18)$$

where I_p is the current delivered by the B battery, E_i the lumped plate voltage, and R_p the static internal plate resistance of the tube. This resistance depends upon the material and dimensions of the hot cathode, its temperature, and the location of the grid with respect to the hot cathode and the plate. The exponent n depends upon the portion of the characteristic. It is usually about 2 near the zero value of I_p , becomes about 1 for the middle portion, and for the upper knee, not including the saturation region, is about 1.5. When variable potentials act on the electrodes, the dynamic resistance r_p of the plate is given by

$$\frac{\partial e_p}{\partial i_p} = r_p \quad (19)$$

if e_p and i_p stand for the variable plate potential and current, respectively. If e_g denotes the variable grid potential producing the variations i_p and e_p , respectively, the dynamic mutual conductance over the grid (*mutual plate conductance*) is

$$g_m = \frac{\partial i_p}{\partial e_g} \quad (20)$$

¹ The grid current disappears for tungsten cathodes for about $E_g = -1.5$ volts, for thorium filaments at about $-\frac{1}{2}$ volt, and for oxide filaments at about $+2$ volts. The concept of lumped voltage $E_i = \mu E_g + E_p$ was introduced by W. H. Eccles ("Continuous Wave Wireless Telegraphy I," Wireless Press, Ltd., London, 1921).

while its static value according to Fig. 4 is

$$G_m = \frac{I_p}{E_g} \quad (21)$$

From (19) and (20) we obtain

$$g_m r_p = \mu \quad (22)$$

which is a *basic relation for amplifier measurements*. The quantity g_m denotes the steepness of the dynamic grid-potential plate-current characteristic, and the amplification factor μ , according to (22), is that quantity which when multiplied by the change in grid potential produces the same effect in the plate current i_p as the corresponding change in the plate

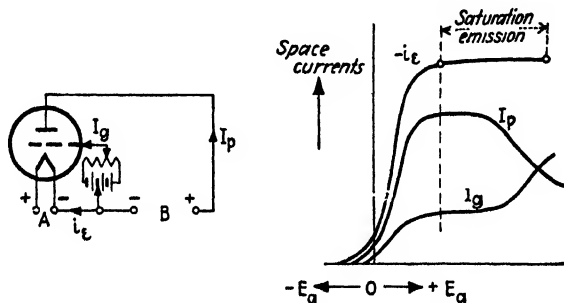


FIG. 5.—Space currents in a three-element tube.

voltage. This can also be seen from Eq. (18), holding for the static characteristic shown in Fig. 4. Putting $I_p = 0$ yields

$$\mu = -\frac{E_p}{E_g}$$

The negative sign indicates that the corresponding variation in the plate potential is of opposite polarity to that in the grid potential. For no reactive external plate load, the plate-current variation is therefore in phase with the potential variation on the grid causing it.

When a grid current flows, the total emission current, according to Fig. 5, is

$$-i_e = I_g + I_p \quad (23)$$

The flat portion of the total space current i_e indicates that all electrons liberated at the hot cathode constitute the resultant current flow. When the grid becomes too positive, it will attract enough electrons to diminish the actual anode (plate) current. Use of this is made in certain sensitive tube galvanometers.¹ For most work, the grid current should be kept

¹ "High Frequency Measurements," McGraw-Hill Book Company, Inc., New York, 1933.

as small as possible, since the steepness of the grid-potential plate-current characteristic will decrease if grid currents flow at the expense of the plate current. Also a current flow in the grid circuit uses energy and may decrease the voltage to be amplified.

According to (6) and (16a) for a cylindrical anode, a coaxial grid, and a filament along the axis of the cylinders, the total space current is

$$i_s = \frac{29.3 \times 10^{-3}}{\rho^2} \frac{l}{d} E^{1.5} \quad \text{milliamperes} \quad (24)$$

for $E = \frac{1}{1 + \frac{1}{\mu}} \left[\frac{E_p}{\mu} + E_g \right]$. The quantity d now denotes the diameter of

the grid cylinder since the resultant potential $\frac{E_p}{\mu} + E_g$ acts at this electrode. The quantity ρ^2 depends upon the ratio of the diameter of the filament to d and for thin filaments is about unity. This expression does not hold in the saturation region and assumes, as in the Child space-change relation, that the initial velocity of the electrons is negligible.

8. Electronic and Ionic Oscillations and Ionic to-and-fro Motions in Thermionic Tubes.—In the theory of the ionized layer (Chap. X), it is shown that electromagnetic waves passing through an ionized space cause ions to vibrate according to the frequency of the exciting current which produces the waves. If the effect of the earth's magnetic or any other magnetic field is neglected, the effective dielectric constant κ_e of an ionized layer is smaller than for a perfect vacuum. If $\omega/2\pi$ is the frequency of the exciting current producing the electromagnetic waves, N the number of ions per cubic centimeter, q the charge, and m the mass of an ion, for the effective dielectric constant in the e.s.c.g.s. system, we obtain

$$\kappa_e = 1 - \frac{4\pi Nq^2}{m\omega^2} \quad (25)$$

if no collisions take place. If the ions collide ν times per second, this constant becomes

$$\kappa_e' = 1 - \frac{4\pi Nq^2}{m\omega\sqrt{\omega^2 + \nu^2}} \quad (26)$$

if all collisions are assumed inelastic. In the same chapter it is proved that the group velocity with which the energy of the wave is transmitted through an ionized gas is

$$c^{11} = c\sqrt{\text{effective dielectric constant}} \quad (27)$$

which means that it becomes zero when the value of the effective dielectric constant vanishes. The quantity $c = 3 \times 10^{10}$ cm/sec is the velocity of

electromagnetic waves in free space. For $\kappa_e = 0$, the ionized gas will not transmit the electromagnetic wave, since the ions are excited with their natural frequency and attain maximum amplitude of vibration. Under such conditions they will collide with molecules and give up the energy obtained from the electromagnetic wave.

Since the electrons are much lighter than other ions, it will be permissible to assume that they vibrate, leaving the heavier ions at rest. Then, if there are no collisions, we find that for $\kappa_e = 0$ the resonance frequency is

$$f_0 = q\sqrt{\frac{N}{m\pi}} = 8980\sqrt{N} \text{ cycles/sec} \quad (28)$$

which for $N = 10^5$ electrons/cc gives 2840 kc/sec. This is the same formula as that found by Tonks and Langmuir (page 21) for plasma-electron oscillations in tubes. From this formula, when the frequency f_0 has been found by means of the selective absorption of the corresponding electromagnetic wave, the number of electrons per cubic centimeter can be computed. When a magnetic field of H gauss also acts, assuming that the magnetic field of the wave is negligible in comparison with it, the resonance frequency is

$$f_0 = 53 \times 10^{-16} H \frac{q}{m} \text{ kc/sec} \quad (29)$$

where the charge q of the ion is expressed in e.s.c.g.s. units and its mass in grams. For an electromagnetic wave passing through an ionized gas of hydrogen ions and a field strength of $H = 0.5$ gauss, this would correspond to a resonance frequency of the ions of only 775 cycles/sec and, for electrons having a mass about 1800 times lighter, to 1.395×10^3 kc/sec.

In dealing with motions of electrons in vacuum tubes, conditions may occur at very high frequencies f for which the time of transit of electrons from the hot cathode to the anode is no longer negligible with the duration of the period $1/f$ of the variable electrode potentials. This will give rise to phase effects¹ and electron lags.² Both play a part in amplifiers and oscillators operating in the range of very high frequencies, since only those electrons and ions which have time to pass from the cathode to the anode during half the period ($= 0.5/f$) can contribute to the alternating component of the plate current. The phase effect can become so pronounced that energy regeneration (feedback), and therefore self-oscillation due to external circuit elements, is impossible, the phase relation between the alternating potentials of grid and plate being no longer cor-

¹ See p. 66 under footnote 1.

² For details see "High-frequency Measurements," McGraw-Hill Book Company, Inc., New York, 1933, p. 32.

rect. It can then happen that, for *positive* grid potentials and negative or zero plate potentials, electronic and ionic oscillations can occur within the tube, with frequencies determined by the electrode spacing and the potential distribution between the electrodes.

If a tube with oscillating ions within it is connected to a suitable resonator system, it may happen that variable potentials may be reflected back on the electrodes and produce regeneration within the tube. Such regeneration can be of two kinds. One may increase the power of the oscillating ions, that is, increase the amplitude of vibration. This occurs

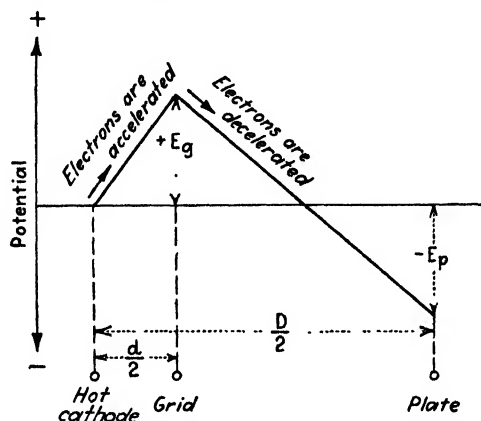


FIG. 6.—Electron display in a tube with cylindrical electrodes for Barkhausen-Kurz oscillations.

only to a small degree in the ultrahigh-frequency range. The other is a regeneration of the frequency and is made noticeable by an increase of the frequency of the original ionic oscillation.

The Barkhausen-Kurz generator (page 132) due to “electron dance,” the Whiddington, and the Gill and Morrell ionic generators are examples.¹ In the Barkhausen-Kurz circuit, a thermionic tube with cylindrical anode and grid and axial filament are used. The grid is at a positive potential E_g and the plate at a negative potential ($-E_p$) which is normally smaller in magnitude than E_g . Both potentials are with respect to the hot cathode as indicated in Fig. 6. Assuming the outer cylinder and the hot cathode to be at the same negative potential, the electrons that are emitted at the hot cathode and fall through the mesh of the grid vibrate between the cathode and the outside cylinder of diameter D . If the electrons move with the velocity $c = 3 \times 10^{10}$ cm/sec, the wave length

¹ BARKHAUSEN, H., and K. KURZ, *Physik. Z.*, **21**, 1, 1920; R. W. WHIDDINGTON, *Radio Rev.*, **1**, 53, 1919; E. W. B. GILL and J. H. MORRELL, *Phil. Mag.*, **6**, 44, 161, 1922; W. H. MOORE, *Proc. I.R.E.*, **22**, 1021, 1934, describes electron oscillations without tuned circuits; F. HAMBURGER, *Proc. I.R.E.*, **22**, 79, 1934 (electron oscillations with a triple-grid tube).

would be about equal to D since this is about the path of the electron for a complete to-and-fro vibration (strictly, twice the distance of cylinder to surface of cathode). But the velocity is actually smaller and equal to

$$v = \sqrt{\frac{2q}{m} E_g} = 6 \times 10^7 \sqrt{E_g^{(\text{volts})}} \text{ cm/sec} \quad (30)$$

The wave length must be larger, according to the ratio c/v_1 , because one must take the average velocity v_1 of the vibrating electron. Since the electron reverses its direction at the surface of the filament and at the inner surface of the exterior cylinder, and since maximum velocity occurs at the grid, we have $v_1 = v/2$. Hence

$$\lambda^{(\text{cm})} = \frac{2c}{v}$$

and from $\lambda f = c$

$$f = \frac{v}{2D} = \frac{3 \times 10^4 \sqrt{E_g^{(\text{volts})}}}{D^{(\text{cm})}} \text{ kc/sec} \quad (31)$$

When plate and cathode potential are unequal, for instance, where E_p is negative with respect to the negative end of the hot cathode, and the grid is at a positive potential, we have for the diameters D and d of the plate and grid cylinders (Fig. 6) the accelerating electric field

$$\varepsilon_1 = \frac{E_g}{d/2}$$

between cathode and grid, and between grid and plate the decelerating field.

$$\varepsilon_2 = -\frac{E_g - E_p}{D/2 - d/2}$$

An electron emitted at the surface of the hot cathode experiences therefore the constant acceleration

$$a_1 = \frac{\varepsilon_1 q}{m} = \frac{2E_g \cdot q}{m \cdot d}$$

and reaches the grid, when starting with zero velocity, after

$$T_1 = \frac{v}{a_1} = \frac{\sqrt{\frac{2q}{m} E_g}}{\frac{2E_g \cdot q}{m \cdot d}} = \frac{d}{\sqrt{2}} \sqrt{\frac{m}{q E_g}} \text{ seconds}$$

The electron after falling through the grid plane experiences a negative acceleration

$$-a_2 = -\frac{\varepsilon_2 q}{m} = \frac{2[E_o - E_p]q}{[D - d]m}$$

and comes to rest after

$$T_2 = \frac{v}{a_2} = \frac{[D - d]E_o}{[E_o - E_p]\sqrt{2}} \sqrt{\frac{m}{q \cdot E_o}} \text{ seconds}$$

The time $T_1 + T_2$ corresponds to one-half the period of the electronic to-and-fro oscillation between the filament and the place near the plate where the electron turns around. Then $\frac{1}{2[T_1 + T_2]}$ is the frequency, which gives

$$f = \frac{\sqrt{\frac{2q}{m}E_o}}{2} \frac{E_o - E_p}{D \cdot E_o - d \cdot E_p} = 3 \times 10^4 \sqrt{E_o} \frac{E_o - E_p}{D \cdot E_o - d \cdot E_p} \text{ kc/sec} \quad (32)$$

where the potentials are again expressed in volts and the respective diameters in centimeters.

When ionic oscillations are produced, the circuit is as shown in Fig. 7.

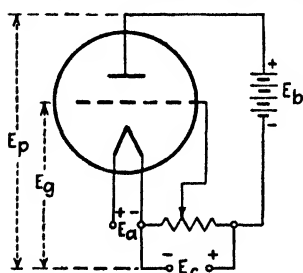


FIG. 7.—Circuit for ionic oscillations.

The tube then contains small traces of mercury vapor, hydrogen, or other gases. The grid is a fine mesh and acts more or less as a screen, taking most of the electric lines of force coming from the positive plate and terminating them on it. The frequency is again for practical purposes dependent only on the grid potential E_g and on the relative location of the electrodes. The positive grid potential in the Whiddington experiments was about 1 volt.

If the initial velocity of the electrons is neglected, they will arrive at the grid with a speed of $v = 6 \times 10^7$ cm/sec, while ions of charge q and mass m will arrive with a velocity $v = \sqrt{2q/m}$ cm/sec, for unity positive grid potential. The electrons that have fallen through the meshes of the grid will be greatly accelerated because of the positive plate potential E_p , which now acts on them, and they will collide with molecules, thus producing positive and negative ions which pass back to the filament and on to the plate, respectively. The positive ions, arriving at spots of powerful electronic emission, will give rise to a new excessive electron emission and sustain the oscillation. For a grid cylinder 6 mm in diameter, monatomic hydrogen ions give a frequency of 1×10^7 cycles/sec, and monatomic mercury ions 6.6×10^5 cycles/sec, since $q/m = 10,000$ and 50, respectively. For multiatomic mercury ions the frequency of singly charged ions consisting of 2, 3, and 4 atoms, respectively, is then $1/\sqrt{2}$, $1/\sqrt{3}$, and $1/\sqrt{4}$ times 6.6×10^5 cycles/sec.

Both electronic (Barkhausen) and ionic (Whiddington) oscillations give a frequency which is proportional to the square root of the grid potential.

In some cases very high-frequency currents obtained from thermionic tubes can also be explained by means of the ordinary Thomson formula $T = 2\pi\sqrt{CL}$ where L denotes the inductance of the short external connection, and C the capacitance of the grid-plate condenser. The capacitance is smaller than that expected from the dimensions, since the effective dielectric constant is less than unity, because of the ionization.

According to L. Tonks and I. Langmuir,¹ plasma-electron and plasma-ion oscillations can take place in ionized gases. For instance, in one tube the pressure of the mercury vapor could be varied by means of the temperature. Two hot electrodes were used in the tube in order to change the number of electrons per cubic centimeter. By means of different voltages between the hot electrodes and the cold anode, the velocity of the electrons could be varied. It was found that oscillations existed between 10^3 and 10^6 kc/sec.

In the case of plasma-electron oscillations, a certain impact sets the electrons into such rapid vibration that the positive ions with their large mass cannot follow their motion and can be considered to be at rest. If the equilibrium is disturbed along the X direction, the disturbance being the same everywhere in the YZ plane, we need consider one dimension only, and we obtain for the displacement of the electron and the electron concentration N (number of electrons per cubic centimeter)

$$\delta N = N \frac{\partial \xi}{\partial x}$$

If \mathcal{E} denotes the electric-field intensity due to the displacement of the electrons, $\mathcal{E} = 0$ before the displacement took place, and, according to the Poisson equation,

$$\frac{\partial \mathcal{E}}{\partial x} = 4\pi q \delta N$$

where q is the charge of one electron. Eliminating δN gives

$$\frac{\partial \mathcal{E}}{\partial x} = 4\pi q N \frac{\partial \xi}{\partial x}$$

or

$$\mathcal{E} = 4\pi q N \xi$$

From the equation of motion, we have

¹ *Phys. Rev.*, **23**, 195, 1929.

$$\begin{aligned} m \frac{\partial^2 \xi}{\partial t^2} &= -q\mathcal{E} \\ &= -4\pi q^2 N \xi \end{aligned}$$

where m is the mass of one electron.

Hence the frequency of plasma-electron oscillation becomes

$$f = q \sqrt{\frac{N}{\pi m}}$$

which is the same expression as that found in connection with the ionized layer of the atmosphere [page 382, and formula (28) on page 17]. In the experiments mentioned above, $N = 10^{10}$ electrons/cc, and $f = 9 \times 10^5$ kc/sec. It is to be understood, however, that only *slow* electrons, which remain during at least one period in the space of the oscillations, contribute to the electron density N . Hence the effective electron concentration N depends on the frequency of the oscillations; but the latter is also dependent on N . The explanation is therefore not quite so simple as indicated above and the oscillation cannot be propagated from the place of disturbance directly in form of waves since we do not obtain the equation for a progressive wave.

As far as the plasma-ion oscillations are concerned, they must occur at a considerably lower frequency, since the mass of a positive ion is comparatively large. Hence for the rapidly movable electrons each phase of this oscillation may be considered a condition of equilibrium. Now, according to the Boltzmann equation, with the Boltzmann constant k , we have for the electrons

$$\delta N = N \left[e^{\frac{qE}{kT}} - 1 \right]$$

if E is the potential of the electric field and T the absolute temperature corresponding to the average kinetic energy of the electrons. Now, if N' denotes the number of positive ions per cubic centimeter and m' the mass of one positive ion, according to Poisson's equation, we have

$$\frac{\partial^2 E}{\partial x^2} = -4\pi q [\delta N' - \delta N]$$

and the equation of motion becomes

$$q \frac{\partial E}{\partial x} = -m' \frac{\partial^2 \xi}{\partial t^2}$$

For the case $qE/kT \ll 1$

$$\frac{\partial^2 E}{\partial x^2} = 4\pi N q \left[\frac{\partial \xi}{\partial x} + \frac{qE}{kT} \right]$$

If a plane wave of form $\xi = \epsilon^{2\pi j \left(\mu - \frac{x}{\lambda} \right)}$ is found to be the solution of this equation, then the frequency becomes

$$f = \sqrt{\frac{q^2 N}{\pi m' + q^2 N m' \frac{\lambda^2}{kT}}}.$$

For rapid oscillations $q^2 N \lambda^2 / \pi k T \ll 1$ which for the limiting cases gives

$$f = q \sqrt{\frac{N}{\pi m'}}$$

For mercury ions, the limiting frequency is about 600 times smaller than for electron oscillations; that is, $f_{\min} = 1.5 \times 10^3$ kc/sec.

For slow oscillations we have about the case which corresponds to sound waves in gases. Since $q^2 N \lambda^2 / \pi k T \gg 1$ we have, for the limiting case, a velocity of propagation

$$c' = \sqrt{\frac{kT}{m'}} = 3.9 \times 10^5 \sqrt{T \frac{m}{m'}}$$

If $T = 10^4$ deg, $c' = 6.5 \times 10^4$ cm/sec since for mercury $\sqrt{m/m'} = 1/600$.

Now let us consider the case of a simple glow tube, that is, a tube with two plane parallel electrodes perpendicular to the x -axis. In this case both electrons and positive ions exist. Suppose a high-frequency field $\mathcal{E} \sin \omega t$ acts. Then an ion of mass m and charge q will vibrate along the direction of the \mathcal{E} field—along the x direction—and we have the equation of motion

$$m \frac{d^2 x}{dt^2} = q \mathcal{E} \sin \omega t$$

The ion has, therefore, the velocity

$$v = \frac{dx}{dt} = \frac{q \mathcal{E}}{\omega m} [1 - \cos \omega t] + C$$

where the integration constant C represents the velocity of the ion along the x direction when the electric-field intensity is just passing through zero. Consequently, the displacement x of the ion from the point where it was when the field intensity just passed through its zero value is

$$x = \underbrace{\left[\frac{q \mathcal{E}}{\omega m} + C \right] t}_{\text{uniform drift of mid-point of oscillation}} - \underbrace{\frac{q \mathcal{E}}{\omega^2 m} \sin \omega t}_{\text{to-and-fro oscillation about mid-point}}$$

Since the uniform velocity of the mid-point about which the ion oscillates decreases with increasing m , and since there is also a decrease in the amplitude of the oscillation with an increase of the mass of the ion, it may be assumed that the much lighter free electrons transfer most of the power due to the exciting field $\mathcal{E} \sin \omega t$. This was borne out recently when it was found to be possible to use such tubes for amplifier and oscillator work even though comparatively high gas pressures were used.

From the foregoing it is also clear why it is easier to excite glows with high-frequency fields. *Even with internal electrodes* it may happen that no electrons will be collected by the electrodes, although there may exist a sort of convection current somewhere between the electrodes due to the vibrating ions. Such a condition will exist if the distance traveled by the much lighter electrons, during one-half cycle of the oscillating field $\mathcal{E} \sin 2\pi ft$, is not sufficient to take the oscillating electrons to one of the electrodes. No charge can then be given to the electrodes. The electrons remain in the space between the electrodes and cause more ionization due to collision. If the frequency is sufficiently high, there can be no permanent separation of the charges, just as many electrons vibrating in one direction as in the other. There can then be no effective space charge to destroy the field. Instead, we have a neutral cloud consisting of both types of charges. For this reason, only a low potential is required to cause glow excitation when high-frequency fields excite the ions.

9. Secondary Emission in Three-electrode Thermionic Tubes.—

An electron bombarding a metal surface with sufficient energy can produce secondary-electron emission. The minimum volt energy needed for such an action on customary electrode materials is above 10 volts. Secondary emission is more easily produced when the exciting electrons arrive at the electrode surface with a large tangential component of velocity. For a perpendicular arrival they usually pierce their way into the electrode and simply produce heat. The average emission velocity of the secondary electrons is smaller than the velocity of the exciting primary electrons. It is about 10 volts for a positive plate potential of 500 volts.

Secondary-electron emission does not play a great part in ordinary two-element¹ tubes but is of importance in three-element thermionic

¹ When electrons hit a target with very great speed, they produce X-rays, an electromagnetic radiation, just as successive bullets hitting a target send off sound waves from the target, that is, an entirely different form of energy. X-rays can also be produced by the impact of positively charged ions, or atoms that have lost an electron, on a metal target. This was proved by W. M. Coates and E. O. Lawrence, who stepped up mercury positive ions to 1,000,000 volts and, on having them strike targets of various elements, observed that X-rays are given off. The process is, of course, not very efficient since a 1,000,000-volt positive ion will produce only about the same quantity of X-rays as a 10,000-volt electron. It takes too much voltage

tubes. In the latter case, secondary emission from the grid may also take place. Then the static characteristic curves are as shown in Fig. 8, if it is assumed that the grid does not attain any appreciable temperature and thus acts as an emitter of primary electrons, and that the vacuum is

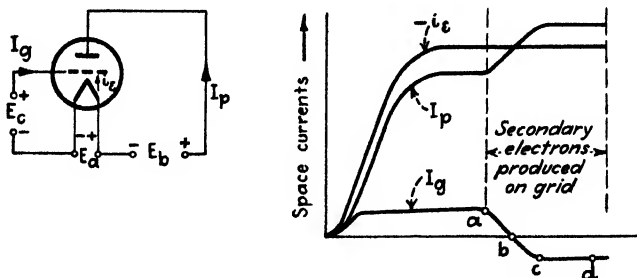


FIG. 8.—Showing condition for which secondary electrons are generated.

very high, no gases being driven out at the plate by electronic bombardment. The shape of the portion *bcd* of the characteristic is a desirable feature since it shows that any positive grid currents are counteracted. This characteristic can be used to advantage in amplifiers. Also, the negative characteristic *abc* can be used to produce oscillations of very high frequency. A still more desirable form of operation is that obtained when the plate of a three-element thermionic tube is made to emit secondary electrons. Then the characteristics are those of a tube known as "Hull's dynatron."¹ In this apparatus the grid is a perforated plate

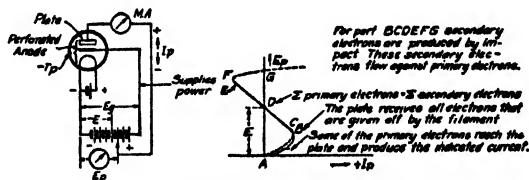


FIG. 9.—Explaining dynatron action.

so that high-speed electrons can fall through it and bombard the other plate, which, for normal operation, is at a smaller positive potential than that of the grid, both potentials being measured from the negative end of the hot cathode. Figure 9 shows the display. The electrons that fall

to bombard the heavy masses associated with positive ions as compared with the very small mass of an electron.

¹ HULL, A. W., *Proc. I.R.E.*, 6, 5, 1918; O. AUSTIN and H. STARKE, Sekundäre Elektronenemission (Secondary Electron Emission), *Ann. Physik*, 9, 271, 1902; H. STARKE and M. BALTRUSCHAT, *Physik. Z.*, 23, 403, 1922; H. LANGE, *Z. Hochfreq.*, 26, 38, 1925 (with many references). For applications of the dynatron effect see "High-frequency Measurements," McGraw-Hill Book Company, Inc., New York, 1933, pp. 28, 174, 175, 328-329.

through the grid produce, by impact at the plate, secondary electrons which move backward toward the more positive grid. The current due to the secondary electrons is to be subtracted from the plate current I_p and added to the grid current I_g . The number of the secondary electrons depends upon the number and velocity of the arriving primary electrons, their angle of incidence, and the work function of the material of the plate. The number of the primary electrons depends upon E_g and the temperature of the hot cathode. The superimposed weaker potential E_p has little effect on the emission of the primary electrons, as long as $E_p < E_g$. When E_p is comparatively small, corresponding to portion AB of the typical dynatron characteristic only a small number of primary electrons pass through the openings of the grid. They come from the most negative portion of the hot cathode and have comparatively small velocities when arriving at the plate. The current ($-I_p$) compensating the arriving electron flow is then as for any ordinary three-electrode tube. But, as the potential E_p is increased, many primary electrons arrive with sufficient speed to produce secondary electrons. This effect can be so pronounced that one primary electron gives rise to as many as 20 secondary electrons which then flow backward toward the more positive grid. An inverse current flow ($-I_p$) sets in since

$$\Sigma \text{ primary electrons} + \Sigma \text{ secondary electrons}$$

becomes a negative quantity. At point D this sum is exactly zero.

It is evident that, for a considerable region, such an apparatus has a falling volt-ampere characteristic; that is, it acts as a negative resistance ($-r$) and we have

$$I_p = \frac{E_p}{(-r)} + K \quad (33)$$

where the constant K may be made zero by the application of the proper fixed positive potential E to the plate. In such a circuit the grid branch only supplies the energy; that is, it accelerates the primary and receives the secondary electrons. Only the differential effect gives an energy flow in the exterior plate branch.

10. Thermionic Emission in Double-plate Tubes.—The arrangement indicated in Fig. 10 leads to another apparatus which acts as a negative resistance and is known as the "negatron."¹ The anode potentials E_{p_1} and E_{p_2} are chosen so that the total space current I for the significant portion of the characteristic (for negative resistance) is equivalent to all of the available electrons given off at the hot cathode. The plate P_1 acts as a deflection anode while P_2 acts in the usual way. The negative

¹ SCOTT-TAGGART, I., *Radio Rev.*, **2**, 598, 1921; *London Electrician*, **87**, 386, 1921,

resistance ($-r$) is then produced by the plate resistance of anode P_1 with respect to the hot cathode.

11. Thermionic Emission in Double-grid Tubes.—Double-grid tubes can be used either in the *space-charge connection* or in the *shield-grid connection*. In the former, the space charge near the filament is partially or entirely removed and a steep work characteristic is secured, while in the latter the effective capacitance between plate and control grid is adjusted to a negligible amount (cut down to about 1 per cent of the geometrical value).

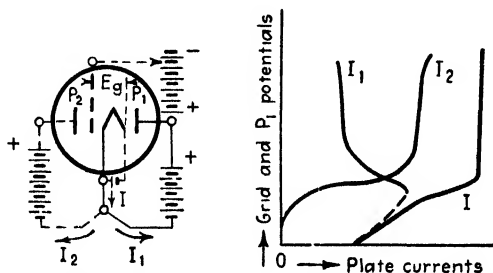


FIG. 10.—Four-element tube with P_1 as deflection anode, P_2 as customary anode, and grid between P_2 and hot cathode.

Consider first a single-grid tube (Fig. 5), in which the plate potential E_p is assumed to be zero and the grid potential E_g is made positive to several volts, for example, to 20 volts. Then the electrons emitted by the hot cathode pass with a comparatively low velocity toward the grid. Some of them fall through the grid openings into the space between the grid and the plate, and some of these return again to the grid. Therefore, the negative space charge in the neighborhood of the hot cathode is greatly reduced, and only a comparatively low positive plate potential is needed to attract the accelerated electrons to it. Thus, when the positive grid potential is not high enough to give rise to grid current at the expense of the plate current, the tube characteristic is steeper. However, this three-electrode arrangement is not desirable, since, for an effective removal of the space charge, the grid, which also acts as the control grid, must draw appreciable current and thus loses the character of a true potential device. An additional grid is therefore necessary.

Figure 11 shows the circuit of a double-grid tube in the space-charge connection. The grid next to the hot cathode is brought to a positive potential of about $E_{g1} = 20$ volts so that a saturation emission current flows. It serves as a space-charge "transplanter" since it acts like the grid of a single-grid tube with such a positive potential. The mesh of the first grid is usually rather open so that a comparatively small plate potential E_p is sufficient to attract the electrons. The control grid, which is to be a potential device rather than a current-absorbing electrode,

is inserted between the space-charge grid and the plate. The space-charge grid may be regarded as the source of electrons, since, for the particular case shown in the figure, electrons fall through its openings with an average velocity of $v = 6 \times 10^7 \sqrt{22.5} = 2850$ km/sec, which, for a negative potential $E_{c_1} = -1.5$ volt on the control grid, becomes zero at places close to this grid. Any positive control-grid variations will then effectively pass on the electrons toward the positive plate. The control grid, which generally has a fine mesh, therefore acts exactly as in the single-grid tube and the law given in Eq. (16a) can be applied when the amplification factor μ_2 is introduced to account for the action

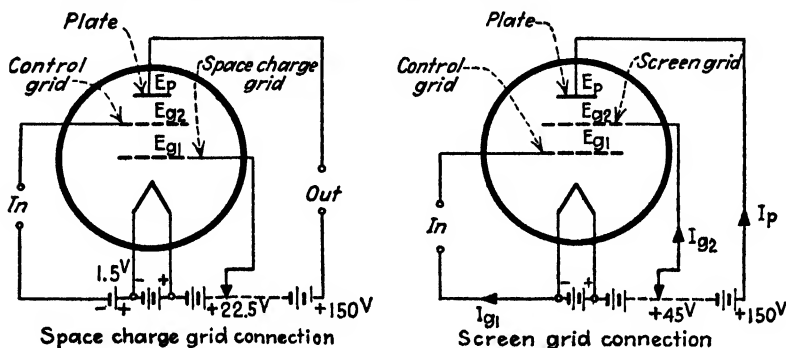


FIG. 11.—Double-grid tubes.

of the control grid of potential E_{c_1} . The tube can be imagined as though no plate and hot cathode existed at all, but only a space-charge grid which apparently emits the electrons and a fictitious plate at the plane of the control grid, with a potential

$$E_2 = \frac{E_p}{\mu_2} + E_{c_1} \quad (34)$$

The part E_p/μ_2 is the portion of the actual plate potential E_p which acts through the control grid on the electrons flying through the space-charge grid. Hence, for zero and negative values of the resultant potential E_2 , no electrons are attracted either to the control grid or to the plate and the space-charge grid takes up the entire emission current (Fig. 12). But for positive values of E_2 the resultant current $I_p + I_{q_1}$ increases rapidly at the expense of the space-grid current I_{q_1} . The $I_p + I_{q_1}$ curve is now the *characteristic curve of the tube* and, with a properly designed space-charge circuit, is *much steeper* than the space-charge curve $I = KE^{1.5}$ of an ordinary single-grid tube.¹

The quantity e_2 is about the maximum resultant positive-voltage swing that the tube can handle without distortion. The smaller this

¹ E denotes the equivalent anode voltage ($\mu E_c + E_p$); compare Eq. (17) on p. 14.

value is, the steeper the effective characteristic of $I_p + I_{g_1}$, and the more amplification is obtained. It is about

$$e_2 = 1.5 + \text{voltage drop along the hot cathode} \quad (35)$$

where 1.5 volts is the voltage against which the electrons can just not pass. For an *indirectly heated cathode* the *steepness* of the characteristic is *increased* since the second portion of (35) disappears. If *all* electrons should start out with zero velocity, the steepness would become infinite. The increased steepness of the characteristic with space-charge tubes means that the plate current I_p also varies according to a steep curve, since the control grid is usually at a negative potential and should not draw appreciable current. The term E_p/μ_2 for a steep characteristic

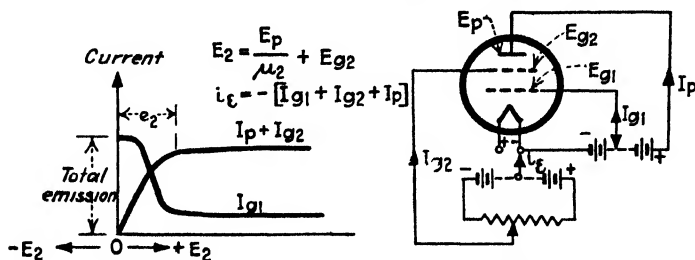


FIG. 12.—Illustrates space-charge action and no-distortion condition.

is small compared with the value E_p/μ of a single-grid tube. Hence, for one and the same positive plate potential E_p the amplification factor of the double-grid tube is higher. Therefore, if only amplifications of the same order as those obtained with single-grid tubes are required, the anode potential E_p can be chosen much lower for space-charge tubes. Unlike that for single-grid tubes, the characteristic is all the steeper the higher the saturation current, that is, the higher the temperature of the hot cathode, since then the saturation potential E_{g_1} is smaller.

The screen-grid connection shown in Fig. 11 employs the grid next to the hot cathode as the control grid. The purpose of the fine-mesh grid next to the plate is merely to cause most of the lines of electric force, originating at the more positive plate, to terminate on it, so that no appreciable displacement currents, resulting from variations in plate potentials, can take place between the plate and the control electrode. On the other hand, the control grid has a fairly open mesh; consequently the plate current I_p and steepness of the characteristic are both high. The screening effect due to the screen-grid potential E_s is particularly important in connection with amplifiers, where it is desirable to reduce the effect on the control-grid circuit of variations occurring in the plate circuit. These can be made negligible by means of the effect of the screen grid, even though the amplification factor of the tube is relatively large.

As in the case of the space-charge tube, the grid next to the plate can be imagined as having a potential

$$E_2 = \frac{E_p}{\mu_2} + E_{g_2}$$

With this substitution, the screen-grid tube consists of a hot cathode, a control grid, and a fictitious plate of potential E_2 in the plane of the screen grid of the actual tube. Applying again the results of Eq. (16a) to this fictitious tube, and calling μ_1 the amplification factor due to the actual control grid, we have a fictitious two-element tube, consisting of the actual cathode and a plate of potential

$$E_1 = \frac{E_2}{\mu_1} + E_{g_1} \quad (36)$$

in the plane of the control grid of the actual tube. Substituting the value of E_2 , we have¹

$$E_1 = \frac{E_p}{\mu_1\mu_2} + \frac{E_{g_2}}{\mu_1} + E_{g_1} \quad (36a)$$

showing that the effective potential at the control grid includes, in addition to the applied potential E_{g_1} of this grid, a portion of the plate potential and a portion of the screen-grid potential. The resultant current $I_{g_1} + I_{g_2} + I_p$ which is equal and opposite to the space electron emission ($-i_e$) flowing away from the hot cathode is therefore a function of the effective potential E_1 . If this function is $i_e = kE_1^n$ and if $R = [\mu_1\mu_2]^n/k$, we obtain the relation

$$\begin{aligned} i_e &= \frac{1}{R}[\mu_1\mu_2 E_{g_1} + \mu_2 E_{g_2} + E_p]^n \\ &= \frac{E_1^n}{R} \end{aligned} \quad (37)$$

where E_1 denotes the effective lumped plate potential imagined in the plane of the control grid and R the fictitious static internal plate resistance. Since (36a) can also be written in the form

$$E_1 = \frac{1}{\mu_1} \left[\frac{E_p}{\mu_2} + E_{g_2} \right] + E_{g_1} = \frac{1}{\mu_1} E_2 + E_{g_1} \quad (36b)$$

we see that, for $R_p' = \mu_1^n/k$, (37) can be expressed by

$$i_e = \frac{1}{R_p'} [\mu_1 E_{g_1} + E_2]^n \quad (37a)$$

¹ Eq. 36a requires that $\mu_1 \gg 1$ and $\mu_2 \gg 1$. The first condition is seldom fulfilled since most screen tubes have values of μ_1 between 2 and 10. The exact formula is:

$$E_1 = \frac{\mu_1}{1 + \mu_1} \left[\frac{\mu_2}{1 + \mu_2} \frac{E_p}{\mu_1\mu_2} + \frac{\mu_2}{1 + \mu_2} \frac{E_{g_2}}{\mu_1} + E_{g_1} \right]$$

This expression is similar to that of a single-grid tube with the amplification factor μ_1 and plate potential E_s . The displacement of the characteristic is therefore given by the factor $\mu_1 E_{s_1}$. The back action on the grid circuit, due to the plate potential, is given by the term $E_p/\mu_1\mu_2$, which can be made small without making the displacement potential small, since it depends mostly upon E_{s_1} and μ_1 . Since the control grid has a rather open mesh, μ_1 is not high; it may be equal to 3. Then the screen-grid potential E_{s_1} need not be so high. The fine mesh of the screen grid produces a high amplification factor, about 25. According to Eq. (37), the amplification factor of the control grid over the entire electrode system is then $\mu_1\mu_2 = 75$, even though only normal plate potentials are employed. The screen grid takes current since E_{s_1} is positive. This current effect is made less pronounced when E_p is chosen correspondingly high. The screen-grid arrangement gives high amplification with plate potentials between 120 and 150 volts. To obtain the same degree of amplification, a single-grid tube would require at least 500 volts. Because of the shielding effect of the screen grid, the emission current is kept constant, while for single-grid tubes the fictitious plate potential $[(E_p/\mu) + E_i]$ at the plane of the actual grid affects the plate potential which in turn acts back on I_p .

A disadvantage of the shield-grid tube is its high internal plate resistance. This can be understood from the following derivation. Any current variation δi_e in the emission current flowing partially to the plate and partially to the screen grid produces corresponding potential variations δE_{s_1} and δE_p which, for a straight portion ($n = 1$) of the equivalent characteristic Eq. (37) having a steepness $k = \mu_1\mu_2/R$, yields

$$\begin{aligned}\delta i_e &= k \left[\delta E_{s_1} + \frac{\delta E_p}{\mu_1\mu_2} \right] \\ &= k \delta E_{s_1} + \frac{k}{\mu_1\mu_2} \delta E_p \\ &= k \delta E_{s_1} + \frac{\delta E_p}{r_p}\end{aligned}\tag{38}$$

where

$$r_p = \frac{\mu_1\mu_2}{k}\tag{39}$$

represents the internal plate resistance of the tube. Equation (39) when written as

$$kr_p = \mu_1\mu_2 = \mu\tag{39a}$$

has the same form as Eq. (22) for single-grid tubes, since k is actually the mutual conductance of the equivalent three-element tube. Hence, for equal mutual conductance, the internal plate resistance is increased

as the amplification factor $\mu = \mu_1\mu_2$ becomes larger, and is therefore much higher for a screen-grid tube than for a single-grid tube, since $\mu_1\mu_2$ is high.

Another type of double-grid tube is due to N. E. Wunderlich's work. The second grid is wound between the meshes of the customary grid. By means of such a tube, it is possible to obtain full-wave grid rectification in a balanced circuit in which negligible high-frequency current flows in the plate branch. This tube was developed for grid-leak power detection. The modulated high-frequency voltage is applied between the two grids with a center tap to the cathode through a grid-leak and grid-condenser arrangement.

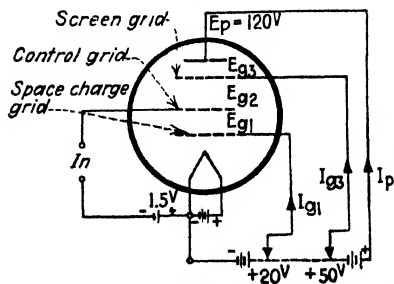


FIG. 13.—Triple-grid tube.

12. Action in a Triple-grid Tube (Pentode).—If the current flowing through a properly adjusted control grid of the triple-grid tube indicated in Fig. 13 is neglected, the total emission current is equal to $I_p + I_{g_1} + I_{g_2}$. The first grid again acts as space-charge transplanter and the third grid as a screen grid. Therefore a tube of this type combines the features

of the space-charge and the shield-grid types; that is, it has a high amplification factor with comparatively low plate potentials. The internal resistance of the pentode is comparatively low as in the case for single-grid tubes.

13. Effect of a Magnetic Field on Electrons in Thermionic Tubes.—

It can be shown¹ that a magnetic field H causes a projected charged particle to move along an orbit which is a helix. The radius of curvature of the helix is $\rho = mv/Hq \sin\theta$, if the charged particle of mass m and charge q is projected with a velocity v at an angle θ with respect to H .

¹ "High-frequency Measurements," McGraw-Hill Book Company, Inc., New York, 1933, p. 30. The general action of magnetic and electric forces on charged particles has been treated by G. Stokes, *Phil. Mag.*, **2**, 359, 1876, and by J. J. Thomson in his book "Conduction of Electricity through Gases," Cambridge University Press, 1903, p. 81. The application to thermionic tubes is due to H. Gerdien, *D.R.P.*, 276528, 1910; O. W. Richardson, *Proc. Roy. Soc. (London)*, **90**, 174, 1914; A. W. Hull (1913) through his well-known magnetron, *Phys. Rev.*, **17**, 539, 1921; **18**, 31, 1921; *J. A.I.E.E.*, **40**, 715, 1921. Other early experimenters were P. C. Hewitt, F. K. Vreeland, and R. von Lieben. E. Habann, *Jah. b. dr. Tel.*, **24**, 115, 135, 1924, developed a short-wave generator based on a negative resistance (see p. 138). A generator of this kind was also used by H. Yagi, *Proc. I.R.E.*, **16**, 715, 1922, and K. Okabe, *Proc. I.R.E.*, **17**, 652, 1929. For rectification where a magnetic field produces ionization in cold-electrode tubes, V. Push and C. G. Smith, *Proc. I.R.E.*, **10**, 41, 1922. Leigh Page, *Phys. Rev.*, **18**, 58, 1921, gives the theory of motion of electrons between coaxial cylinders which takes into account the variation of mass with velocity.

The axis of the cylindrical helix is parallel to the lines of magnetic force. Hence, if the particle is projected in a direction perpendicular to the lines of force, the helix shrinks into a circle of radius mv/Hq .

Suppose we have two plane parallel electrodes as shown in Fig. 14. The cathode gives off electrons. The magnetic field of the heating current of the cathode will be at first neglected. The lines of magnetic force act along the X direction and a homogeneous electric field $\mathcal{E} = E/d$ acts along the Z direction. The path of an electron in the ZY plane is then as indicated. When no magnetic field is applied, the electron travels along OA , which is a line of electric force; but when a certain

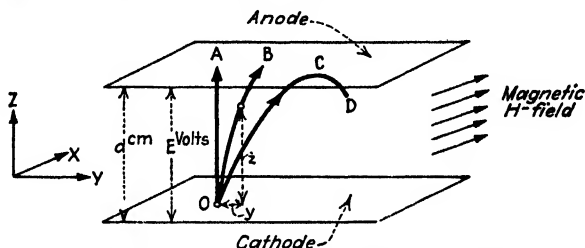


FIG. 14.—Electron path when electric field E/d and magnetic field H act for plane parallel electrodes.

magnetic field intensity H is applied, the path of the electron will be curved, as indicated by OB , which is a part of a cycloid. When the magnetic field H has a certain critical value H_c , the path OCD just touches the anode. If the field H is less than H_c , then for a very large anode the space current from the hot cathode to the anode would be the same after the stationary state is reached, although the time of travel from O to C is longer than for the direct path OA . In fact, the only change introduced by a field of strength $H \leq H_c$ would be an increase in the time taken to reach the steady-state condition, after a constant anode potential has been suddenly applied. But for fields larger than H_c the electrons miss the anode and no space current is possible, unless other conditions such as oscillations are produced in a capacity-inductance circuit connected between the cathode and the anode (Habann generator, Fig. 15). The magnetic field $H > H_c$ is then a magnetic space-charge transplanter, since electron clouds will be produced near the anode and cathode.

For the combined action of the electric field $\mathcal{E} = E/d$ and magnetic field H on one electron of mass m and charge q , we obtain

$$\begin{aligned} m \frac{d^2 z}{dt^2} &= q\mathcal{E} - Hq \frac{dy}{dt} \\ m \frac{d^2 y}{dt^2} &= Hq \frac{dz}{dt} \end{aligned} \quad (40)$$

showing that the electron travels along a cycloid. Integrating the second

expression we obtain

$$Hqz = m \frac{dy}{dt} = mv \quad (41)$$

Hence, for the critical field H_c which produces the tangential path OCD , we find from the energy relation for an electron of zero initial velocity that

$$\frac{1}{2} mv^2 = qE$$

Combining this with (41) we obtain, for $z = d$,

$$H_c = \frac{\sqrt{2E}}{d} \sqrt{q/m}$$

or

$$H_c = \frac{3.35}{d} \sqrt{E} \quad (\text{critical magnetic field for two plane parallel electrodes}) \quad (42)$$

where H_c is in gauss, E in volts, and d in centimeters.

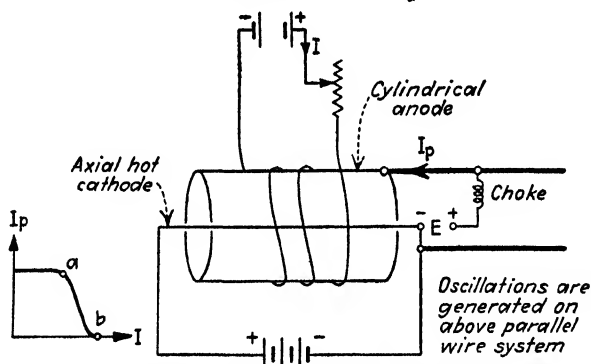


FIG. 15.—Habann generator (ab corresponds to region for which oscillations occur).

The anode in practical tubes is usually cylindrical, as in Figs. 15 and 16. The path of the electron is then somewhat different, since the electric lines of force are radii and the field is no longer uniform as in the case of Figs. 14 and 17. The equations given in Fig. 17 are the solution of Eq. (40). From the relation

$$z = \rho[1 - \cos \theta]$$

it can be seen that in case of $z = d$ for which the electron just hits the anode and gives up its charge, $d = 2\rho = 2m\varepsilon/qH_c^2$ confirms solution (42) since the circle producing the cycloid path is tangent to either the cathode or the anode plane. According to the assumptions made, the application of the critical field H_c should cause a sudden cessation of the space cur-

rent. Actually, since the electrons have various initial velocities, this is not exactly true.

The operation of tubes with cylindrical electrodes is essentially the same as that with the plane parallel electrodes, but the electric field is no longer uniform. When the magnetizing current $I = 0$, the electrons will be projected along radii, that is, along paths as OA . For small magnetizing currents, the path becomes bent as indicated by OB ; for the

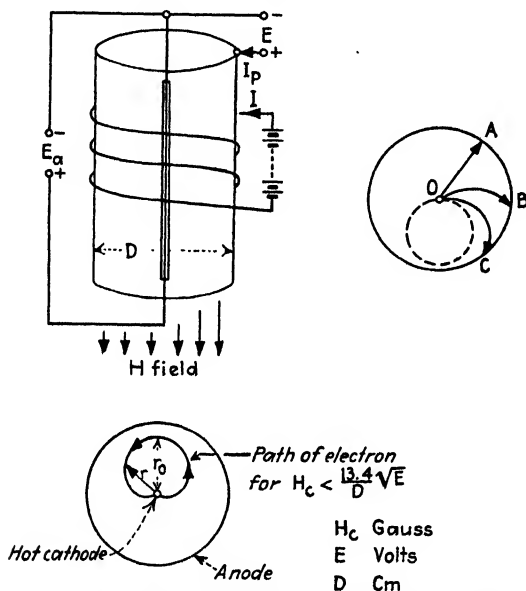


FIG. 16.—Electron path for cylindrical electrodes.

critical magnetization, the electron just hits the anode in a tangential direction as shown by OC ; and for fields much stronger than this the electron turns completely around, as indicated by the heart-shaped orbit. For magnetic-field strengths near the critical value and above it, where quite a rapid decrease in the plate current I_p is noted, the characteristic curves are as indicated in Fig. 18. This portion is useful for amplification and oscillator work as is described on page 138.

It can be seen from the electron path of the cylindrical electrodes (Fig. 16) or the plane parallel electrodes (Fig. 14) that something similar to the Barkhausen-Kurz electron oscillations must take place with magnetic fields just a little stronger than those required to produce the electron path OC , which is tangential to the anode surface. In this case, the electron will turn around near the anode and sweep back again toward the hot cathode from which it came. At points where this reversal occurs (Fig. 16 for end of radius vector r_0), there must be zero velocity along the direction r_0 , and, with fields just slightly greater H_c , vector r_0 is almost

equal to the radius $D/2$ of the anode cylinder. It can be assumed that there must be a dense negative space charge near this electrode. Also there must be a similar space charge near the hot cathode, for in this region new electrons are being given off constantly, and others are return-

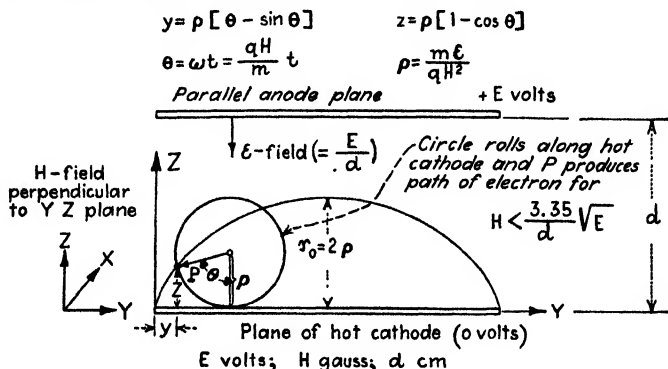


FIG. 17.—Cycloid electron path.

ing along the dotted path (Fig. 16). Hence, if there were charge collectors at these places, electronic oscillations would occur. Since the time t_0 taken by the electron to pass from the hot cathode toward its maximum displacement near the anode corresponds to about half a period, the frequency is

$$f_0 = \frac{1}{2t_0} \text{ cycles/sec} \quad (43)$$

if t_0 is expressed in seconds. The frequency of oscillation therefore de-

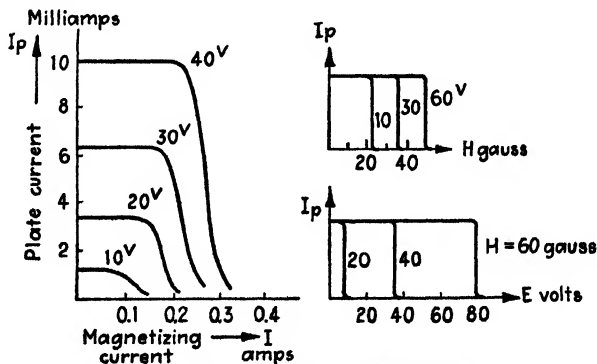


FIG. 18.—Magnetron characteristics.

pends upon the strength of the magnetic field H , since this field determines the length of the path and consequently the time taken to traverse it.

If the diameter of the filament is neglected in comparison with the radius $D/2$ of the anode cylinder in Fig. 16, the path of the electron that

comes from the hot cathode is affected by both the electric field \mathcal{E} and the magnetic field H . The electric field \mathcal{E} due to the positive potential E on the cylindrical anode has a tendency to pull the electron along a radius to the anode, while the magnetic force which acts perpendicular to such a radius has a tendency to whirl the electron around the radius. The two fields, acting together, produce the resultant path, the projections of which on the plane of the paper are curved lines OB , OC , etc. We have, therefore, for the *radial* component

$$\underbrace{m \frac{d^2 r}{dt^2}}_{\text{mass times acceleration}} - \underbrace{mr\omega^2}_{\text{centrifugal force}} = \underbrace{q\mathcal{E}}_{\text{mechanical force due to potential } E \text{ producing electric field } \mathcal{E}} + \underbrace{r\omega Hq}_{\text{mechanical force due to magnetic field } H} \quad (44)$$

The energy relation $\frac{1}{2}mv^2 = qE$ consists of the velocity contribution along the electric field, that is, the velocity dr/dt and the contribution parallel to the anode surface which is $r\omega$. Hence the energy relation gives

$$\frac{1}{2}m \left[\frac{dr}{dt} \right]^2 + \frac{1}{2}mr^2\omega^2 = qE \quad (45)$$

which, for the velocity contribution due to the electric field, gives

$$\frac{dr}{dt} = \sqrt{\frac{2qE}{m} - r^2\omega^2} \quad (46)$$

This portion, because it is along the radius, becomes zero at points where the electron just begins to turn around (corresponding to the extremity of radius vector r_0 in Fig. 16), that is, for $r = r_0$. Hence

$$r_0\omega = \sqrt{\frac{2qE}{m}} \quad (47)$$

is the remaining velocity component at places of maximum electronic displacement from the hot cathode for applied magnetic-field intensities H equal to and smaller than the critical value H_c for which the electron orbit just touches the anode. Also

$$r_0 = \frac{\sqrt{2qE/m}}{\omega} = \frac{6 \times 10^7 \sqrt{E}}{\omega} = 956 \times 10^4 T \sqrt{E} \quad (48)$$

denotes the radius vector bringing the electron nearest to the anode while describing any closed path in T sec. The quantity E is in volts and r_0 in centimeters. The value of ω can be found from the *tangential* components of the equation of electronic motion, which gives

$$\omega = -\frac{qH}{2m} \quad (49)$$

for cylindrical electrodes or half of the value obtained for two plane parallel electrodes (Fig. 14). This may be demonstrated as follows: Upon differentiation of the first expression in (40) and by substituting the value of d^2y/dt^2 from the second equation, we have

$$m \frac{d^3z}{dt^3} = -Hq \frac{d^2y}{dt^2} = -\frac{H^2q^2}{m} \frac{dz}{dt}$$

or

$$m \frac{d^3z}{dt^3} + \frac{H^2q^2}{m} \frac{dz}{dt} = 0$$

which has a solution

$$\frac{dz}{dt} = v_z = Z e^{j\omega t}$$

for the velocity v_z along a line of electric force \mathcal{E} , where $Z = z_{\max} e^{j\varphi}$ denotes the complex amplitude which contains both amplitude z_{\max} and phase φ . Hence the acceleration $d^2z/dt^2 = j\omega v_z$, and $d^3z/dt^3 = -\omega^2 v_z$ give when introduced in the foregoing result

$$-m\omega^2 v_z + \frac{H^2q^2}{m} v_z = 0$$

or

$$\omega = \frac{qH}{m} \quad (50)$$

for plane parallel electrodes.

Substituting the value $\omega = qH/2m$ in (48) gives

$$r_0 = \frac{\sqrt{8mE/q}}{H} = \frac{6.7\sqrt{E}}{H} \quad (\text{for cylindrical electrodes}) \quad (51)$$

where r_0 is in centimeters, E in volts, and H in gauss. The critical magnetic-field strength $H = H_c$ will cause the electron orbit just to touch the anode, and r_0 becomes equal to the radius $D/2$ of the anode cylinder. Hence

$$H_c = \frac{13.4\sqrt{E}}{D} \quad (\text{critical magnetic-field strength for cylindrical electrodes}) \quad (52)$$

By comparing this result with that for plane parallel electrodes (Eq. 42), it is noted that thermionic tubes with cylindrical electrodes require *twice* as strong a magnetic field for the same anode-potential and anode-cathode spacing in order that the electron following its curved orbit may just miss the anode and pass back again toward the hot cathode.

Now, the magnetron (Habann generator, page 34) consists either of a lumped or of a distributed (parallel-wire system) tank circuit connected between the anode and the hot cathode. Oscillations are observed in the

external resonator system when the anode current is about to fall off to a zero value (theoretically when the anode current suddenly stops), that is, when the critical magnetic-field intensity is applied. According to Eq. (46), we have

$$\frac{dt}{dr} = \frac{1}{\sqrt{A - r^2\omega^2}} \quad (53)$$

for $A = 2qE/m$. Hence the time t in seconds to move an electron along the curved path to a position corresponding to the extremity of radius vector r becomes

$$t = \int \frac{dr}{\sqrt{A - r^2\omega^2}} = \frac{1}{\omega} \sin^{-1} \frac{\omega \cdot r}{\sqrt{A}} \quad (54)$$

since $\int \frac{dr}{\sqrt{a^2 - r^2}} = \sin^{-1} \frac{r}{a}$; $a = \frac{\sqrt{A}}{\omega}$ and

$$\int \frac{dr}{\sqrt{A - (r\omega)^2}} = \frac{1}{\omega} \int \frac{dr}{\sqrt{a^2 - r^2}}$$

Inserting the value for ω from Eq. (49), we have

$$t_0^{(\text{sec})} = \frac{2m}{qH} \sin^{-1} \frac{r}{r_0} = \frac{1132 \times 10^{-10}}{H^{(\text{gauss})}} \sin^{-1} \frac{r}{r_0} \quad (55)$$

Hence the time elapsed to bring the electron to a position of maximum displacement from the cathode, that is, nearest to the anode, becomes, since $r = r_0$,

$$t_0^{\text{sec}} = \frac{m\pi}{qH} = \frac{178 \times 10^{-9}}{H^{(\text{gauss})}} \quad (56)$$

Twice this time, or $T = 2t_0$, represents approximately the full period of the oscillations observed in the exterior resonator circuit, because t_0 is the time taken by the electrons to bring their negative charges nearest to the anode. The theoretical frequency of oscillation is

$$f_0 = \frac{1}{2t_0} = 2.81H^{(\text{gauss})} \text{ megacycles/sec} \quad (57)$$

The energy of the negative space-charge oscillations is greatest when H is in the neighborhood of the critical intensity H_c since then electrons sweep very close to the surface of the anode. According to measurements by K. Okabe,¹ the experimental wave-length formula is

$$\lambda_0^{(\text{cm})} = \frac{13 \times 10^3}{H^{(\text{gauss})}} \quad (58)$$

¹ *Loc. cit.*

which would correspond to a constant 2.3 instead of the value 2.81 in the theoretical frequency formula.

14. Magnetron Effect in Thermionic Tubes.—A. W. Hull¹ shows that there is a limit to the diameter of filament in thermionic tubes because of the deflection of electrons by the magnetic field of the filament current I_a , which also tends to carry the electrons along spiral orbits instead of along lines of electric forces. Hence for any filament current there must be a certain anode potential below which the electrons cannot reach the anode. According to A. W. Hull, the electrons only reach a

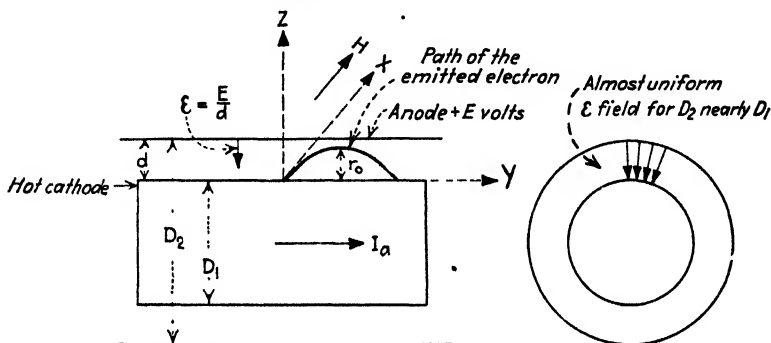


FIG. 19.—Magnetron effect for a large cylindrical hot cathode.

cylindrical anode of diameter D_2 when the anode potential E is equal to or greater than the critical value

$$\begin{aligned} E_c (\text{volts}) &= \frac{2q}{m} I_a^2 \left[\log_e \frac{D_2}{D_1} \right]^2 \\ &= 188 \times 10^{-4} I_a^2 \left[\log_{10} \frac{D_2}{D_1} \right]^2 \end{aligned} \quad (59)$$

where I_a denotes the heating current of the cylindrical cathode, of diameter D_1 , in amperes. For a tungsten filament operating at a temperature of 2500°K and for the diameters expressed in centimeters the critical voltage is

$$E_c (\text{volts}) = 441 \times 10^2 D_2^3 \left[\log_{10} \frac{D_2}{D_1} \right]^2 \quad (59a)$$

With an anode diameter $D_2 = 5$ cm and a cathode diameter $D_1 = 0.0025$ cm, the critical voltage would be very low, namely, 0.0075 volt, while for $D_1 = 2.5$ cm the tube would have to operate above $E_c = 62,300$ volts to produce a space current. For tungsten filaments operating at 2500°K appreciable magnetron effects occur for cathode currents of 50 amp and higher. The simplified theory is briefly as follows: Assume in the diagram of Fig. 19 that the spacing $(D_2 - D_1)/2 = d$ is *small* compared

¹ *Loc. cit.*

with either diameter. Then the electric-field strength along the Z -axis can be taken as homogeneous and equal to E/d . The magnetic lines of flux are circles around the cathode since the current I_a flows along the cylinder and H acts along the X -axis. Hence Eqs. (40) are again the expressions for the electron motion. Using the derivation leading to Eq. (50), we find for the change in acceleration along the electric vector

$$\frac{d^2 v_z}{dt^2} = - \left[\frac{qH}{m} \right]^2 v_z \quad (60)$$

with a solution

$$v_z = A_1 \sin \omega t + A_2 \cos \omega t$$

Introducing the value of ω obtained in Eq. (50) gives

$$v_z = A_1 \frac{Hq}{m} t + A_2 \cos \frac{Hq}{m} t \quad (61)$$

Differentiating the second equation of (40) and substituting the value $d^2 z/dt^2$ from the first equation gives for the rate of change of the acceleration along the Y -axis

$$\frac{d^2 v_y}{dt^2} = \frac{q^2}{m} H \varepsilon - \frac{q^2}{m} H^2 v_y \quad (62)$$

with a solution

$$v_y = -A_1 \cos \frac{Hq}{m} t + A_2 \sin \frac{Hq}{m} t + \frac{\varepsilon}{H} \quad (63)$$

when the initial velocity of the electrons is neglected. Hence, for time $t = 0$, $v_y = v_z = 0$, we find that $A_1 = -\varepsilon/H$ and $A_2 = 0$, also,

$$v_z = -\frac{\varepsilon}{H} \sin \frac{qH}{m} t$$

$$v_y = -\frac{\varepsilon}{H} \left[1 - \cos \frac{qH}{m} t \right]$$

which gives for the z - and y -components of the orbit of the electron

$$\left. \begin{aligned} z &= \int_0^t v_z dt = \frac{m\varepsilon}{qH^2} \left[1 - \cos \frac{qH}{m} t \right] \\ y &= \int_0^t v_y dt = \frac{m\varepsilon}{qH^2} \left[\frac{qH}{m} t - \sin \frac{qH}{m} t \right] \end{aligned} \right\} \quad (64)$$

the same results as previously given in the equations of Fig. 17. The coordinate system of Fig. 19 is chosen so that the cycloid of Fig. 17 shows the path of the electron for the effect on the magnetic field H of the filament current. Hence the electron orbit will just strike the anode when $r_0 = 2\rho = d = (D_2 - D_1)/2$. But $\rho = m\varepsilon/qH^2$. Hence

$$d = \frac{2m\varepsilon}{qH^2} \quad (65)$$

is the condition for which space current can just flow across the tube and for $d > 2m\varepsilon/qH^2$ theoretically no current is possible. Since $\varepsilon = E/d$ and for an average diameter $(D_1 + D_2)/2 = D$, the magnetic intensity $H = I_a/\pi D$, the critical anode potential, below which no thermionic space current toward the anode can flow, is

$$E_c = K \left[\frac{d \cdot I_a}{D} \right]^2 \quad (66)$$

15. Thermionic Tubes with Positive Ionization.—The original thermionic tubes (DeForest, von Lieben) as well as the tungar rectifier and the thyratron are devices whose operation is partially due to positive ionization. For tubes with pure electron emission, the negative space charge limits the current flow, unless a sufficiently high anode potential is applied. But when a certain number of gas molecules are introduced into the tube, so that the mean free path is less than the distance between the electrodes, a *larger* space current can be obtained for a given anode potential. Some of the electrons given off at the hot cathode will then collide with these molecules and produce positive ions and electrons through collision. The positive ions will partially or entirely neutralize the negative space charges and therefore increase the current flow toward the anode. At the same time, the positive ions move toward the hot cathode and may, because of their speed and comparatively large mass (*mv*-momentum) give rise to a disintegration of this electrode. However, if the anode potential is not too high, and if the pressure of the gas is properly chosen (1 to 10 mm of mercury), the momentum can be made small enough so that the cathode will have a long life. Argon gas is one of the few gases which is suitable for this class of work.

16. Ionization in Cold-electrode Tubes.—Geissler tubes, neon, helium, and similar tubes (Fig. 20) are representatives of this class. The cold electrodes are situated in a gaseous mixture such as helium and neon at about 1 to 20 mm mercury pressure. The negative glow is responsible for a portion of the luminosity noted in such tubes. When the pressure is decreased, the layer of this glow becomes thicker until for still lower pressures it disappears altogether. For commercial tubes the pressure is so chosen that the luminous layer at the cathode is about 2 mm thick. Though many other gases give rise to ionization, neon is preferred because the cathode drop of potential for metals is then low. This means that a comparatively low voltage (about 90 volts) is sufficient to start ionization. After the gas becomes ionized, a smaller voltage can sustain a flow of current. Thus one can distinguish between a lower and higher critical voltage. The higher voltage is that for which the internal resistance of the tube suddenly changes from an infinite to a finite value and space current suddenly begins to flow. The lower voltage is that below which

no ionization is possible under any condition. Experiments show that, for any gas in a tube, the potential necessary to start a current flow depends upon the gas, its pressure and the shape and the material of the electrodes.

The distribution of ionization between two electrodes depends on the pressure of the gas. At atmospheric pressure the mean free path is exceedingly small and the degree of ionization is about the same in the vicinity of either electrode. But as the pressure is decreased the degree

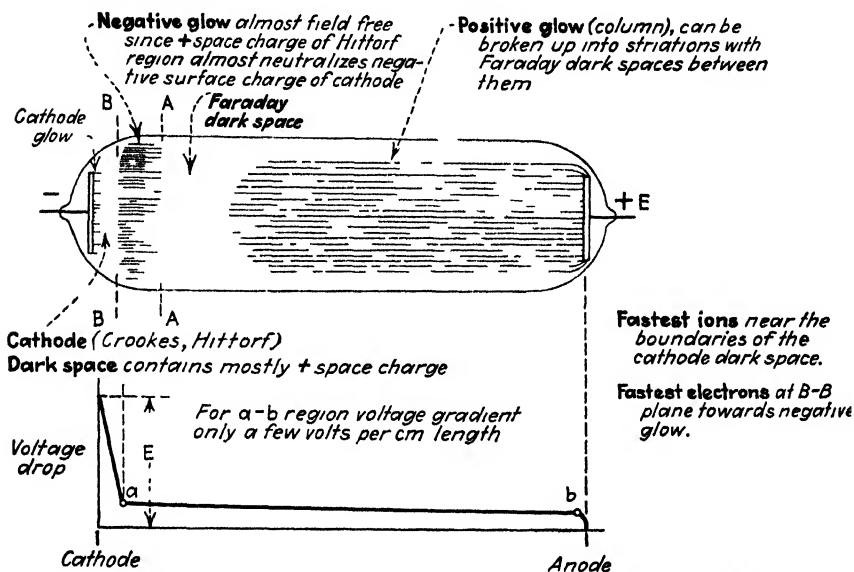


Fig. 20.—Glow discharge for about 1 mm of mercury column (for small anodes there may exist also an anode glow)

of ionization becomes more pronounced near the positive electrode, since some of the electrons repelled at the cathode, and accelerated toward the anode, reach the space near the anode with sufficient velocity to produce increased ionization near the anode. This is why the gas becomes more conducting for decreased pressure, as long as the electrode distance is larger than the mean free path.

With reference to Fig. 20 it can be seen that *most of the voltage drop* within the tube occurs *within Crookes' dark space* (also known as the "Hittorf space"), that is, near the cathode. In a properly designed glow-discharge tube it can be made as high as nine-tenths of the total voltage applied to the tube. It is possible to shorten the tube considerably by moving the anode right next to the negative glow (AA in Fig. 20) and working, so to speak, without any positive column and Faraday dark space. This is due to the fact that for any gas pressure

the positions of the negative glow, the Faraday dark space, and the convex front of the positive column are fixed with respect to the cathode. Hence, if the anode is moved, these portions do not change. But if, on the other hand, the cathode is moved, these boundaries move with it. Consequently, if the distance between the anode and cathode is chosen short enough, the anode may be within the Faraday dark space and no positive column can exist. This is very important in the *design of glow tubes* for which the positive glow is of no importance. Moreover, if the gas pressure is lowered, these *distances from the cathode* all increase approximately inversely proportionally with the pressure. Hence, with a fixed cathode-anode distance, the cathode dark space increases until it reaches the anode as the pressure is lowered. On the other hand, at higher pressures the cathode dark space and the Faraday dark space move so much toward the cathode that they are no longer distinguishable, and the entire cathode-anode distance as well as the inside of the tube is filled with the positive column. For still higher pressures, the positive column gradually withdraws from the glass walls of the tube and a streamer-like discharge takes place between the two electrodes. Generally it can be said that for the same applied voltage E , with all conditions the same except that the distance from cathode to anode is longer than shown in Fig. 20, the conditions in the Faraday dark space hardly change. The positive glow simply becomes longer in order to *complete* the circuit. The discharge characteristic from cathode to plane AA remains practically the same. This is a very important feature of such tubes and is used in the design of glow-discharge tubes with and without an intervening electrode. The latter can be made to amplify and generate oscillations like thermionic tubes.

Ionization is brought about in cold-electrode tubes through the presence of electrons and ions. These exist in all gases, even in atmospheric air, since, because of radioactive disintegration in the earth's crust, about half a dozen ions are present in each cubic centimeter. Also, electrons are given off from hot metals and flames and may be due to ultraviolet radiation. Of course, the number of ions present depends upon the degree of recombination. Therefore, when electrodes are surrounded by a gas of reduced pressure, an electric field existing between the electrodes will move the positive ions and electrons to the respective electrodes of opposite polarity. When the speed of these becomes sufficiently high to ionize, new ions are being formed and the space current is increased.

The mass of a positive neon ion is about 2×10^4 times as large as the mass of an electron under similar conditions. Hence for the same temperature we see that because of the equality of the average kinetic energy $\frac{1}{2}mv^2$ for one electron of mass m and velocity v_1 and one positive

neon ion of mass ($2 \times 10^4 m$) and velocity v_2 the velocity of the electron must be $10^2 \sqrt{2} = 141$ times greater than that of a neon ion. Therefore, it is evident that an auxiliary electrode inserted between the cathode and the anode will receive 141 times *more electrons than ions* and will become negatively charged.

A glow-discharge tube with a grid forms a very sensitive relay.¹ However, it differs in many ways from the ordinary tube in which the grid is submerged in the path of a pure electron discharge from a hot cathode. Instead, the space is filled with both positive and negative ions. When a negative potential is applied to the grid, some of the positive ions are attracted to it and form a positively charged sheath about its conductors. Thus the charge placed on the grid is exactly neutralized and therefore the grid in a glow-discharge tube has no effect after a discharge takes place. But the grid can be used to change the conditions of the breakdown voltage of the tube, that is, to change the critical voltage at which the discharge just begins. The relation between the spacing of the electrodes and the breakdown voltages between them is given by the Paschen law (Sec. 18). In such grid-glow tubes, which give only "threshold" amplification,² the anode-grid spacing is chosen short with respect to the anode-cathode spacing. If neon gas corresponding to a few millimeters of the mercury column is used, the breakdown voltage between anode and grid is much higher than for the longer grid-to-cathode gap. Suppose these voltages are 1200 and 300 volts. For such a case a direct-current source of 1200 volts is connected through a protective resistance to the anode and the cathode. Across the source is a potentiometer and the grid is connected through another protective resistance to a suitable point on the potentiometer. If the tap is so chosen that the voltage between the grid and the cathode is less than 300 volts, no discharge can set in, since the remaining 900 volts is not sufficient to initiate a discharge. But as soon as some superimposed auxiliary potential produces the required voltage of 300 volts between the grid and the cathode, a breakdown will take place between these electrodes, and on account of the strong field between the grid and the anode the glow discharge will spread to the anode. The glow discharge will then be maintained by the anode-cathode potential.

17. Spark and Arc.—Similar effects can also take place at atmospheric and other higher pressures. They were investigated in 1903 by Townsend. The mean free path is, at these pressures, exceedingly short (see Table XV, page 384), and the electron can travel only a very small distance before colliding with a molecule. Hence, in order to

¹ KNOWLES, D. D., *Elec. J.*, **27**, 116, 1930; I. LANGMUIR, *Gen. Elec. Rev.*, **26**, 731, 1923.

² Relay or trigger actions. For details see Sec. 110, p. 264.

attain sufficient speed to cause ionization, the electrons must be accelerated by an intense electric field, which means that a high voltage must be applied between the two electrodes in order to liberate sufficient electrons through collisions.

When N_1 electrons/sq cm exist in the immediate plane of the cathode ($x = 0$) and when N additional electrons are produced by collision when N_1 electrons pass through a distance of x cm, we have, in the plane $x = x$, $N_x = N_1 + N$ electrons/sq cm. Now, if each electron moving through a distance of 1 cm can create n new electrons by collision, the number of electrons gained for a distance dx is $dN_x = nN_x dx$, which upon integration yields

$$N_x = A\epsilon^{nx}$$

But, at the cathode $x = 0$, $N_x = N_1$; that is, $N_1 = A$; and at the anode where $x = d$, we have $N_x = N_2$ and

$$N_2 = N_1\epsilon^{nd} \quad (67)$$

which gives the number of electrons per square centimeter arriving at the positive electrode. This relation shows that the more electrons arrive at the anode, the longer the distance d between the electrodes, while for high-vacuum thermionic tubes the total number of electrons attracted by an anode of sufficiently high potential to receive all the available electrons is independent of the distance d . In fact, when space charge is present (emission current less than saturation current) in thermionic tubes, the emission current decreases with an increase of d .

From (67) we note that, when the vacuum is not very good, the space current is given by

$$I = I_s\epsilon^{nd} \quad (68)$$

when I_s stands for the saturation current.

When the anode potential is chosen sufficiently high, the positive ions gain enough speed to dislodge electrons from neutral atoms. If n_1 and n_2 denote the number of negative and positive ions per unit distance produced by collision with gas molecules of electrons and positive ions, respectively, the number of negative ions arriving at the anode will be

$$N_2 = N_1 \frac{[n_1 - n_2]\epsilon^{[n_1 - n_2]d}}{n_1 - n_2\epsilon^{[n_1 - n_2]d}} \quad (69)$$

where N_2/N_1 is again equal to I/I_s for each square centimeter electrode surface. The space current I can assume considerable values. The derivation of this formula is as follows: When $N_{(-)}$ is the number of negative ions generated between the cathode and the plane $x = x$, then

$$N_x = N_1 + N_{(-)}$$

negative ions must pass through each square centimeter of this plane. Now, when $N_{(+)}$ is the number of positive ions dislodged between the anode and plane $x + dx$, then the pairs of ions dislodged between plane x and plane $[x + dx]$ is

$$[N_1 + N_{(-)}]n_1dx + N_{(+)}n_2dx$$

that is,

$$\frac{dN_{(-)}}{dx} = [N_1 + N_{(-)}]n_1 + N_{(+)}n_2 \quad (70)$$

Hence, when $N_2 = N_1 + N_{(-)} + N_{(+)}$ ions arrive at plane $x = d$, we have

$$N_{(+)} = N_2 - [N_1 + N_{(-)}] \quad (71)$$

Combining (70) and (71) gives

$$\frac{dN_{(-)}}{dx} = [N_1 + N_{(-)}][n_1 - n_2] + n_2N_2 \quad (72)$$

with a solution

$$N_1 + N_{(-)} = A\epsilon^{[n_1-n_2]x} - \frac{N_2 \cdot n_2}{n_1 - n_2} \quad (73)$$

At the cathode where $x = 0$ and $N_{(-)} = 0$, and the constant A becomes

$$A = N_1 + \frac{N_2 \cdot n_2}{n_1 - n_2} \quad (74)$$

and at the anode where $x = d$ and $N_2 = N_1 + N_{(-)}$ for $N_{(+)} = 0$

$$N_2 = A\epsilon^{[n_1-n_2]d} - \frac{N_2 \cdot n_2}{n_1 - n_2} \quad (75)$$

Introducing the value of A from (74) and solving give the solution found in Eq. (69). Such ionization will cause the electrons in the atoms to become excited, resulting in the production of light. Thus a tube containing mercury will glow with the characteristic *blue glow*.

When the pressure on the tube is increased, say to atmospheric pressure, high voltages across the electrodes are necessary in order to produce ionization. The gas remains practically nonconducting until the critical voltage is reached, when a *spark* occurs. Then the gas becomes highly ionized, and the resistance of the gap drops to a very low value. In other words, the denominator in (69) must practically vanish, so that

$$n_1 = n_2\epsilon^{[n_1-n_2]d} \quad (76)$$

gives the state of affairs when a *spark* occurs. The number of ions formed is then very large.

If the degree of ionization becomes so pronounced that the heavy ions bombarding the cathode produce incandescence at the cathode, this

electrode will give off metal vapor, some of which will pass into the electrode gap and produce an arc. The neutral atoms of the vapor will be broken up in the arc into positive and negative ions and the ultraviolet rays produced by the arc will cause additional ionization. An arc requires at least one electron-emitting "cathode spot." The mercury-arc rectifier is an example. In it the vapor is due to the mercury of the cathode. A low pressure is used and the arc is started by an auxiliary electrode and can be drawn out to about 100 cm length even though the anode potential is as low as 100 volts.

Over a good portion of the operating range, an arc often has the characteristics of a negative resistance, and this is used to advantage for the production of electromagnetic oscillations, as in the Poulsen arc. A similar negative-resistance action can be obtained from the arc in a tungar rectifier, when a heavy space current is produced and the filament supply is cut off after the arc has been started.

As far as arc discharges at different and atmospheric pressures are concerned, reference is made to the work of J. J. Thomson, J. S. Townsend, and G. Mie,¹ K. T. Compton, I. Langmuir and Mott Smith, and J. Slepian. The distribution of space charge is especially complicated for atmospheric pressure, as is brought out in the publications of J. Slepian, who finds for certain assumptions that the maximum voltage gradient in the space charge for N ions per cubic centimeter is

$$\left(\frac{\partial E}{\partial x}\right)_{\max} = 1.89 \times 10^{-3} \sqrt{NE}$$

Assuming, as a first approximation, that the electrical breakdown will occur if the maximum electrical gradient at normal atmospheric pressure and temperature is about 30,000 volts/cm, we find that

$$\left(\frac{\partial E}{\partial x}\right)_{\max} = 30,000 = 1.89 \times 10^{-3} \sqrt{NE^{\text{volts}}}$$

or

$$E = \frac{2.52 \times 10^{14}}{N} - \text{volts}$$

which means that the breakdown voltage varies inversely as the density of ionization. If the gas is at $t^{\circ}\text{C.}$, the breakdown voltage for N ion pairs per cubic centimeter becomes

$$E = \frac{2.52 \times 10^{14}}{N} \left[\frac{273}{273 + t} \right]^2$$

¹ GEIGER, H., and K. SCHEEL, "Handbuch der Physik," Julius Springer, Berlin, Vol. XIV; J. S. TOWNSEND, "Electricity in Gases," Oxford University Press, London, 1913; K. T. COMPTON, *Phys. Rev.*, **21**, 269, 1923; *Proc. A.I.E.E.*, **46**, 868, 1927; I. LANGMUIR and MOTT SMITH, *Gen. Elec. Rev.*, **27**, 449, 538, 616, 762, 810, 1924; J. SLEPIAN, *Proc. A.I.E.E.*, **47**, 706, 1928; **48**, 661, 1929.

18. The Paschen Law.—Paschen's discharge law states that the breakdown voltage producing a discharge (not exactly true for cylindrical electrodes) depends only upon the product of the pressure and the distance between the electrodes. This is equivalent to saying that it depends only upon the mass of the gas between the unit surfaces of the electrodes. Hence when the spacing between electrodes is fixed and the pressure of the gas surrounding the electrodes is gradually lowered, a definite pressure exists for which the discharge may be initiated with a minimum anode potential. The values of pressure and spacing which require a minimum anode potential to start the discharge are characteristic for the design of glow-discharge tubes.

19. Hertz, Hallwachs, Elster, and Geitel Effects, Photoelectric Tubes.—In 1887 H. Hertz found that the ultraviolet rays from a spark gap affected the action of another spark gap. Hallwachs (1888) showed that a negative charge on a body is lost when ultraviolet light falls on it, and that this is not true for positive charges. Elster and Geitel (1889) discovered that electropositive bodies, such as sodium and potassium, show photoelectric effects for ordinary light. Rubidium, which is even more electropositive, loses negative charges if affected only by the rays coming from a glass rod which is heated just to redness. It is the discovery of Elster and Geitel that is utilized in modern photoelectric cells. They are of two types, in one of which there is very good vacuum, and in the other a gas under low pressure. In the original Elster and Geitel tubes the pressure was a few millimeters of mercury, so that at about 150 volts anode potential a glow discharge took place. For gas-filled tubes the characteristic is as indicated in Fig. 21. Illumination of the photoelectric cathode liberates electrons which, for sufficient anode potential, ionize the space between both electrodes, and the number N_2 of negative ions arriving at the anode follow approximately the expression given in Eq. (69), where d denotes the distance in centimeters between the electrodes. When a highly evacuated cell is used, saturation takes place just as in ordinary thermionic tubes. Figure 22 gives the characteristics of a commercial gas-filled photoelectric cell, from which it can be seen that excessive anode potentials and excessive illumination must be avoided in order not to have abnormal plate currents. If this is not done, the ionization can become so pronounced that a self-sustaining glow discharge occurs and changes the characteristic of the tube. The lumen

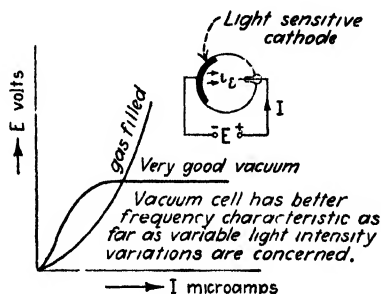


FIG. 21.—Showing difference in characteristics for high-vacuum and gaseous photoelectric cell.

used in these graphs is the unit of luminous flux which is equal to the flux emitted in a unit solid angle by a source with an average candle power throughout the unit solid angle of one candle. When the candle power

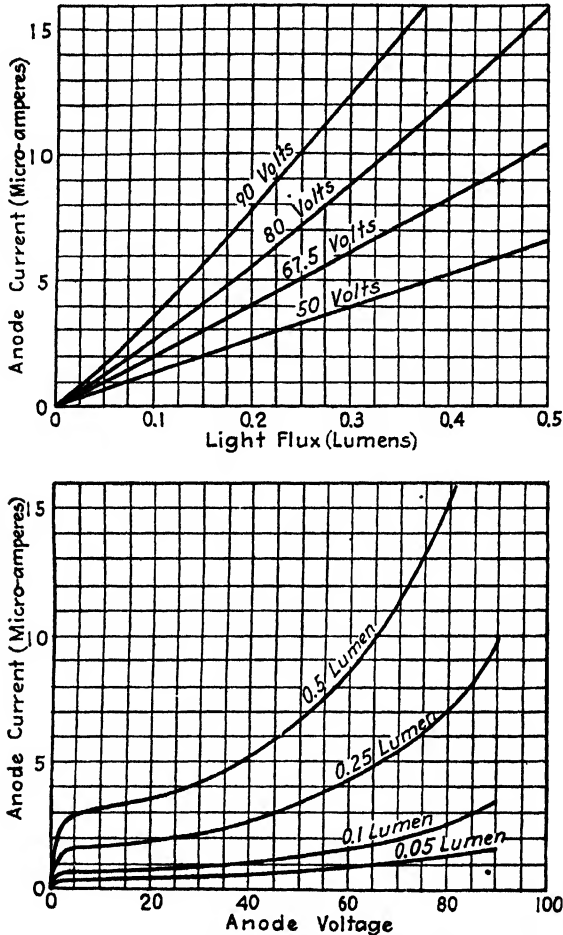


FIG. 22.—Characteristics of commercial photoelectric cells.

(cp) is known, the light flux Φ_l in lumens falling upon a given area A , at a distance d , is given by

$$\Phi_l = (\text{cp}) \frac{A}{d^2} \quad (77)$$

∴ We must distinguish between static and dynamic effects. The dynamic sensitivity is generally expressed in microamperes per lumen.

The energy required for the emission of photoelectrons is obtained by the absorption of energy from the incident light.

Photoelectric cells do not work equally well for the entire frequency band of light and infra- and ultraviolet frequencies (Fig. 23). There are, for instance, cells (H. C. Rentschler) with active material sensitive only to that portion of spectrum with wave lengths between 0.00031 to 0.00029 mm (31×10^2 to $29 \times 10^2 \text{ \AA}$), while for other cells (for instance, UX-868) the active cathode gives a large response to red and infrared light.

From the foregoing discussion, it will be evident that the photoelectric current increases with the intensity of illumination, and an almost linear

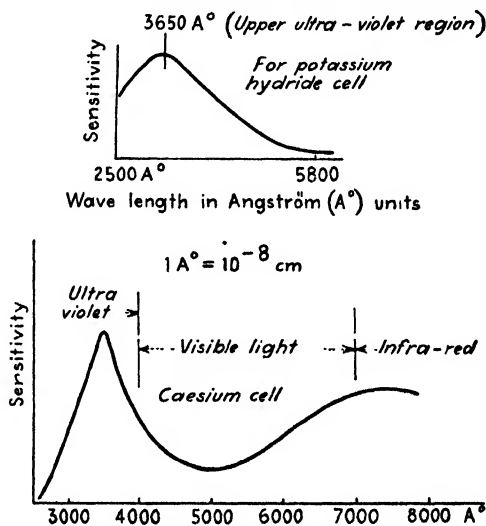


FIG. 23.—Photoelectric sensitivity curves.

relation exists for a wide range between photoelectric space current and intensity of illumination.

The energy equation $E = \frac{1}{2}mv^2$ forms the second basic relation of a photoelectric cell, if v denotes the maximum velocity of the liberated electrons. This velocity does not depend on the *intensity* of the incident light but on its *frequency*, since, according to the Einstein law,

$$qE + \Phi = hf \quad (78)$$

a linear relation exists where $h = 6.55 \times 10^{-27}$ denotes the Planck constant and Φ the *photoelectric* work function, that is, the energy required to liberate an electron from the light-sensitive cathode. Hence the portion hf of the energy of the incident light is transferred to each electron and is sufficient to force it out of the metal with the energy qE . The critical frequency f_c , for which the energy of the incident light is just *not* enough to eject an electron, corresponds to the photoelectric low-frequency limit. This limit is usually expressed by the wave length $\lambda_c = c/f_c$ where c is the velocity of light. For tungsten it is 2600 \AA ; for zinc, copper, and

platinum, 3720, 2955, and 1962 Å, respectively. For sodium and potassium the critical frequencies lie in the red part of the spectrum while, according to the foregoing figures, zinc requires much higher frequencies—those of ultraviolet rays. The *photoelectric* work function Φ for tungsten is 4.58 compared with 4.52 volts which is the *thermionic* work function. The photoelectric work function Φ is also slightly higher for platinum, namely, 6.3 volts, instead of 6.27 volts as in the case of thermionic emission. The photoelectric work function for zinc is 3.57 and for copper 4.1 to 4.5 volts. From relation (78) it is seen that the energy is greater the shorter the wave length of the incident illumination. This is the reason that, for Roentgen rays, the work function Φ , that is, the energy required for ejecting an electron from the light-sensitive metal, is very small compared with the energy qE , and Eq. (78) is practically

$$hf = qE \quad (79)$$

Photoelectric effects of gases and nonmetals, such as carbon, are considerably smaller and all require exciting frequencies that are at least in the ultraviolet spectrum. Phosphorescent substances are likewise photoelectric.

The *photoelectric* as well as the *Compton* and *Raman* effects, as far as the frequency is concerned, can be explained in terms of the light-quantum idea, since the momentum as well as the energy of the light quantum plays a part. In each effect, energy in amounts of hf is absorbed from radiation of frequency f , not slowly, as might be expected from waves, but suddenly, since each corpuscle upon impact brings with it the energy hf and the corresponding momentum hf/c , which explains the radiation pressure. In the Compton effect, the quantum undergoes an impact with an essentially free electron with which it exchanges energy and momentum according to ordinary laws of elastic collision. In the case of the Raman effect, the quantum preserves its identity after an impact with a molecule to which it transfers only a portion of its energy. The question arises "What are electrons?" Are they really discrete particles or are they waves? Light has been thrown on this subject by the classic experiments of C. J. Davisson and L. H. Germer¹ by means of which it is suggested that *electrons are particles which behave like waves*. This was also the conviction of Louis de Broglie² who assumed that every microscopic mechanical phenomenon is to a certain extent a wave phenomenon and that every problem in microscopic mechanics is in a way a problem in optics. After Schrödinger's paper, this idea was taken up by leading physicists. It is known as "wave mechanics." De Broglie assumed that a sort of wave motion is associated with the moving particles of momentum mv such that its wave length is equal to Planck's constant divided by the momentum of the particle. Hence

¹ *J. Franklin Inst.*, **205**, 597, 1928; *Proc. Nat. Acad. Sci.*, **14**, 317, 1928; *J. Chem. Education*, **5**, 1041, 1928; *Nature*, **119**, 558, 1927; *Phys. Rev.*, **30**, 705, 1927; C. ECKART, *Proc. Nat. Acad. Sci.*, **13**, 460, 1927; *J. Optical Soc. Am.*, **18**, 193, 1929; K. K. DARROW, *Bell System Tech. J.*, **9**, 163, 1930.

² *Phil. Mag.*, **47**, 446, 1924; *Ann. phys.*, **3**, 22, 1925; E. SCHRÖDINGER, *Ann. Physik*, **79**, 361, 489, 1926; *Phys. Rev.*, **28**, 1049, 1926.

$$\lambda = \frac{h}{mv} \quad (80)$$

Now for electrons of speeds as occurring in thermionic tubes

$$\frac{1}{2}mv^2 = \frac{Eq}{300} \quad (81)$$

if q is expressed in e.s.u. and the bombarding potential E in volts. Combining (80) and (81) gives the wave length of the *de Broglie phase wave*

$$\lambda = h \sqrt{\frac{150}{mqE}} \text{ cm}$$

Since h/\sqrt{mq} is about 10^{-8}

$$\lambda = \frac{12.25}{\sqrt{E}} 10^{-8} \text{ cm} = \frac{12.25}{\sqrt{E(\text{volts})}} \text{ \AA} \quad (82)$$

This relation has been confirmed by the experiments of Davisson and Germer. They found, for instance, the value h/mv for electrons which were accelerated from rest through a potential difference of 54 volts, a wave length of 1.65 \AA which is in good agreement with the theoretical value $12.25/\sqrt{54} = 1.67 \text{ \AA}$. Therefore the electrons have waves which, so to speak, guide them and supply the laws of motion.

In addition to the Broglie phase wave, the *X-ray wave* is also associated with an electron of given velocity. This wave of length λ' is produced when the entire kinetic energy of the electron is converted into radiation. It is inversely proportional to the energy of the electrons while the wave length λ of the Broglie phase wave is inversely proportional to the momentum of the electron (Eq. 80), the factor of proportionality being, for λ , simply Planck's constant h and, for λ' , hc . Hence

$$\lambda' = \frac{hc}{\frac{1}{2}mv^2} = \frac{300h}{qE} = \frac{12,350}{E(\text{volts})} \text{ \AA} \quad (83)$$

The X-ray wave length expressed in terms of the wave length of the Broglie phase wave is

$$\lambda' = \frac{1010}{\sqrt{E}} \lambda \quad (84)$$

The Broglie phase waves which are accelerated with about 100 volts are then of the order of wave lengths as found with moderately hard X-rays.

Therefore, the corpuscles associated with the waves expressed by Eqs. (82) and (84) move with a speed which is equal to the group velocity of the associated wave. According to the derivation in Sec. 146 on pages 379-381, for the group velocity we have

$$c'' = c' - \lambda \frac{dc'}{d\lambda} \quad (85)$$

if c' stands for the phase velocity of the Broglie or X-ray wave, respectively. Now, according to the quantum and wave mechanics, the energy of a corpuscle of radiation is

$$W = hf = \frac{hc'}{\lambda} \quad (86)$$

and the momentum of the elementary corpuscle moving with velocity v is

$$mv = \frac{h}{\lambda} \quad (87)$$

Employing again the energy relation

$$W = \frac{1}{2}mv^2 \quad (88)$$

for sufficiently low-speed electrons, we can again use the constant mass m of the electron instead of the effective mass

$$m_e = \frac{m}{\sqrt{1 - [v/c]^2}}$$

which holds for the electron moving at any speed v . Combining (87) and (88) yields

$$W' = \frac{[mv]^2}{2m} \quad (89)$$

Equation (85), for the *group velocity* of the wave train associated with the corpuscles, gives

$$c'' = f\lambda - \lambda \frac{d[f\lambda]}{d\lambda} = -\lambda^2 \frac{df}{d\lambda} = -\frac{\lambda^2}{h} \frac{dW}{d\lambda} = -\frac{\lambda^2}{h} \frac{dW}{d(mv)} \frac{d(mv)}{d\lambda}$$

But, $dW/d(mv) = v$ and $d(mv)/d\lambda = -h/\lambda^2$; hence

$$c'' = v \quad (90)$$

The Kerr cell (Karolus type)¹ consists of two condenser plates whose dielectric is either carbon disulphide or, preferably, nitrobenzene. When a beam of light, polarized in a plane making an angle of 45 deg with the electric field, is obtained from a Nicol prism and passed through the cell, the charged condenser breaks up the beam into two component beams, whose planes of polarization are, respectively, parallel to and perpendicular to the electric field (ordinary and extraordinary beam). Therefore the two beams are polarized in planes perpendicular to each other and are propagated with different velocities. On emerging from the cell, the resultant beam is passed through an analyzer to a photoelectric cell. In the transmission plane of the analyzer the two component beams interfere with each other and the resultant intensity in this plane therefore varies between zero and a maximum. Hence, when the two Nicols are crossed, no light is passed on to the photoelectric cell when the condenser has no charge (no voltage across it), while a certain voltage E produces increasing light intensity in the transmission plane for each wave length until the path difference $\lambda/2$ is reached. For larger path differences the intensity falls off again until for a path difference of 1λ darkness exists again. Hence, for $\lambda/2$, $(3/2)\lambda$, $(5/2)\lambda$, etc., we have light maxima, and for λ , 2λ , 3λ , etc., light minima, for the case of monochromatic light. When d_λ denotes the path difference of the two rays in wave lengths, \mathcal{E} the electric-field strength due to the Kerr condenser, K the Kerr constant, and l the length of the light path in the field expressed in centimeters, we have the expression

$$d_\lambda = K \cdot l \cdot \mathcal{E}^2 \quad (91)$$

¹ SCHROETER, F., *Z. tech. Physik*, 7, 422, 1926.

The transmitted light is therefore proportional to the square of the voltage $E = a\mathcal{E}$ applied to the Kerr condenser (a is equal to the distance between the condenser plates). A steady voltage E superimposed on a variable voltage coming from an amplifier or some other source makes the small variations all the more effective on the photoelectric cell. According to Karolus, a steady voltage source of about 300 volts and variable control voltages up to 200 volts amplitude value produce negligible conduction currents in the Kerr condenser. The Kerr condenser is about 3 mm deep and the spacing of the condenser plates can be made a fractional part of 1 mm. The aperture is still sufficient to transmit enough light into a photoelectric cell. The inertia effect of the cell is practically negligible up to the highest frequencies used in high-frequency work. Modulations up to 100 kc/sec and higher have been carried on with such cells. Such cells also play an important part in television work.

CHAPTER II

HIGH-FREQUENCY GENERATORS

Modern high-frequency generators produce sustained oscillating currents with a wave shape more or less sinusoidal. On the other hand, the generators of the days of H. Hertz, and commonly used until about 1913, produced discrete damped wave trains (spark-gap and buzzer oscillators) and, if sustained (Poulsen and other arcs), were sinusoidal only under certain conditions. Alternators that are available produce only currents of the lower high-frequency band. It was with the advent of tube oscillators that high-frequency currents could be readily and economically produced. Work in high-frequency laboratories then became much simplified and a great field for further investigation and development was opened up.

20. Frequency Spectrum.—If we include all possible frequencies for which electromagnetic waves may exist, we can include all the cases corresponding to the lowest commercial frequency up to the range of the rays coming from interstellar regions. According to modern views of wave propagation, we may distinguish electromagnetic waves which are essentially surface waves, others with a propagation partially due to the existence of the ionized layer of the atmosphere, and, third, waves which have more or less optical properties as far as their propagation is concerned. The dividing line is by no means sharp but it may be assumed from the theory of the ionized layer that for waves below 10 m in length (above 30 megacycles/sec) the sky wave passing toward this layer will never be returned. Electromagnetic waves corresponding to frequencies higher than 3×10^7 cycles/sec can be treated like light rays;¹ obstacles large compared with the wave length produce shadow effects, and the amplitude decreases in the region of direct wave propagation as the square of the distance from the source. Short radio waves below 8 meters can be

¹ HAHNEMANN, W., *Die Wellengruppen der Radiotechnik* (The Wave Groups of the Radio Technique), pamphlet of the Lorenz Co., Berlin, Tempelhof; F. GERTH and W. SCHEPPMANN, *Z. Hochfreq.*, **33**, 3, 1929, gives a report of the work of A. Esau and the authors with waves below 10 m in length (frequencies higher than 3×10^7 cycles/sec); F. SCHROETER, *E.N.T.*, **7**, 1, 1930 (describes transmission with short Hertzian and infrared waves); H. E. HOLLMANN, *Ann. Physik*, **86**, 129, 1928, and K. KOHL, *Ann. Physik*, **85**, 1, 1928 (describe experiments with electron tubes of the Barkhausen, Gill and Morrell, and Whiddington type); W. H. MOORE, *Proc. I.R.E.*, **22**, 1021, 1934; H. N. KOZANOWSKI, *Proc. I.R.E.*, **20**, 957, 1932; E. KARPLUS, *Proc. I.R.E.*, **19**, 1715, 1931; F. B. LEWELLYN, *Proc. I.R.E.*, **21**, 1532, 1933.

transmitted over somewhat longer distances (about 10 to 15 per cent more) than the horizon of vision because the path of propagation is somewhat curved instead of geometrically straight. This is due to successive refractions caused by the atmosphere. The density of the atmosphere is increased during night hours and a longer transmission path exists during hours of darkness. Short Hertzian waves produced with Barkhausen-Kurz and magnetron¹ generators (Habann generators), however, have decidedly different properties from *actual* optical waves when the intervening medium is fog and smoke. They pass through fog and smoke just as well as through optically clear atmosphere. As far as electromagnetic waves with *apparent* optical propagation properties are concerned, reference is made to earlier workers using spark gaps and recent workers using electron tubes and other devices.² Oscillations having wave lengths between 3 cm and 10 m in length are produced either by small spark-gap oscillators or by means of electron oscillations due to electric-field effects or both electric- and magnetic-field effects in vacuum tubes. A parallel-wire system or Hertzian mirrors are used for detecting the ultrashort wave. Small dipoles are then used at the focus of a receiving parabolic mirror. The short waves between 3 and 0.18 cm can be produced by a method due to Mrs. Glagolewa-Arkadiewa,³ where exceedingly small sparks occur between small iron filings. The fundamental oscillations are in this region and the harmonics reach into the infrared region corresponding to a wave length of 0.03 mm in length. Another method of generation is the well-known method of Nichols and Tear.³ In the range from 3 down to 0.003 cm, the waves have to be detected by means of heat effects, or the wave length must be determined by means of the interferometer. The waves between 400 and 0.7μ where $\mu = 0.001$ mm are given off by mercury-vapor lamps and the gas-mantle burner and are detected by means of the light effects on selenium and molybdenum (Coblentz).

¹ YAGI, H. *Proc. I.R.E.*, **16**, 715, 1928; K. OKABE, *Proc. I.R.E.*, **17**, 652, 1929.

² HERTZ, H., "Gesammelte Werke," II, 3d ed., 1914 ("Electric Waves," translated by D. E. Jones, 1900); P. DRUDE, *Ann. Physik*, **55**, 633, 1895; **58**, 1, 1896; **59**, 17, 1896; **61**, 466, 1897; A. COLLEY, *Physik. Z.*, **10**, 239, 1909; A. LAMPA, *Wiener Ber.*, **105**, 587, 1896; P. LEBEDEV, *Wied. Ann.*, **56**, 1, 1895; W. MOEBIUS, *Ann. Physik*, **62**, 293, 1920; E. F. NICHOLS and I. D. TEAR, *Phys. Rev.*, **21**, 587, 1923; A. GLAGOLEWA-ARKADIEWA, *Z. Physik*, **24**, 153, 1924; H. BARKHAUSEN and K. KURZ, *Physik. Z.*, **21**, 1, 1920; J. S. TOWNSEND and J. H. MORRELL, *Phil. Mag.*, **42**, 265, 1921; A. MARCUS, *Phys. Rev.*, **27**, 250, 1926; F. HOLBORN, *Z. Physik*, **6**, 328, 1921; W. H. ECCLES and F. W. JORDAN, *Electrician*, **83**, 299, 1919; W. C. HUXFORD, *Phys. Rev.*, **25**, 686, 1925; G. C. SOUTHWORTH, *Radio Rev.*, **1**, 577, 1919; GUTTON and TOULY, *Compt. rend.*, **168**, 271, 1919; GUTTON and PIERRET, *Compt. rend.*, **180**, 1910, 1925; L. NETTELTON, *Proc. Nat. Acad. Sci.*, **8**, 353, 1922; A. SCHEIBE, *Ann. Physik*, **73**, 54, 1924; M. T. GRECHOWA, *Z. Physik*, **35**, 50, 1925.

³ *Loc. cit.*

21. Notes on the Generation of Commercial High-frequency Currents. For the generation of commercial high-frequency currents, reference is made to Table III.

TABLE III

Wave shape	Kind of excitation		Practical applications
Damped discrete current trains	Ordinary spark-gap oscillator. The frequency can be computed from the circuit constants. There are two frequencies if a resonator is coupled to the oscillator. The two frequencies exist simultaneously		All oscillators which use ordinary spark gaps
Feebly damped current trains	Excitation of impact. The frequency depends on the circuit constants which are excited by a coupled spark-gap circuit by means of impact. Hence single periodicity exists	<ol style="list-style-type: none"> 1. Quenched spark gap. The gap quenches the spark automatically by cooling and deionization 2. Quenching tubes interrupt the spark 3. Mechanical interruption of the spark 	<ol style="list-style-type: none"> 1. Wien's quenched spark, Peuckert, Lepel, Chaffee, and Poulsen arc gaps. (For pronounced second type of arc oscillations.) 2. Wien's quenching tubes 3. Rotating spark gaps for an appropriate speed of revolution (not synchronous gaps). Buzzer interrupters (G. Eichhorn and L. W. Austin exciters) 4. A high resistance is inserted in the oscillator circuit and a slightly damped resonator is used (E. Nesper). The high resistance interrupts the spark and the secondary current swings out without returning energy to the primary circuit
Sustained oscillating currents	Revolving generators (alternators). The frequency depends either directly or indirectly upon the number of revolutions per second of the alternator and the number of equal poles		<ol style="list-style-type: none"> 1. R. Goldschmidt (utilizes reflection principle in the alternator) 2. Alexanderson-Fessenden (inductor alternator). K. Schmidt (inductor alternator with frequency multiplier) 3. M. Latour (cascade alternator)
	Stationary generators. The frequency can be calculated from circuit constants (with the exception of certain types of arc oscillators) or it depends upon dimensions of the tube (electronic oscillators) or can be calculated from the dimensions of a control element (which is either piezoelectric or magnetostrictive)		<ol style="list-style-type: none"> 1. All kinds of electron-tube oscillators, Poulsen arc, Lepel, Peuckert, Chaffee oscillators, dynatron oscillator 2. Magnetron generator. Barkhausen and Kurs oscillator, (Whiddington, Morrell and Gill). Piezo oscillator. Magnetostriction oscillator

22. Notes on Alternators.¹—The fundamental frequency of customary alternators depends on the number of poles and the speed of rotation. The highest frequency obtainable is therefore limited, since a machine with a small diameter can contain only a certain number of magnetic

¹ For details on alternators and arc and spark-gap oscillators, reference is made to "Hochfrequenz-messtechnik," 2d ed., Julius Springer, Berlin, 1928, pp. 1-16.

poles, although it may rotate at a high speed. On the other hand, a machine with a large diameter has space for many poles but is limited as to its speed-of rotation.

An alternator can be of the alternate or of the equal-pole type. When t denotes the number of teeth of the rotor and n the number of revolutions per second, for the fundamental frequency in cycles per second, we have

$$\left. \begin{aligned} f &= \frac{n \cdot t}{2} \text{ (for the alternate-pole type)} \\ f &= n \cdot t \text{ (for the equal-pole type)} \end{aligned} \right\} \quad (1)$$

Hence the equal-pole type of alternator gives twice the frequency for the same number of revolutions and the same number of pole teeth and is consequently preferred for high-frequency work. The alternating-current winding for an equal-pole-type machine is laid in slots in the laminated iron core. The number of stator teeth of such a generator has nothing to do with the frequency.

For the ordinary *inductor* type of alternator (Alexanderson-Fessenden), the total magnetic flux from stator to rotor is nearly constant since it merely shifts back and forth from one stator tooth to the next as the rotor revolves. In the *reactor* type of alternator, the magnetic reluctance between the stator and motor varies (minimum when rotor teeth face stator teeth, maximum when the teeth of either stator or rotor, respectively, face the slots of the other). It is to be noted that the reactance type of alternator requires only half as many stator slots as does the inductor type. The same winding serves for both the direct-current excitation and the high-frequency current. Although the reactance type of an alternator is economical as to the number of stator teeth, little winding space is left when many teeth are provided in order to obtain a high frequency. But, since the frequency depends only upon the number of rotor teeth and the speed of the rotor, sections of the stator can be cut out, without affecting the frequency in any way.

A very ingenious alternator, devised by R. Goldschmidt, is based on the reflection principle, by means of which the frequency is greatly increased above that which would otherwise be expected from the number of equal poles and revolutions per second. The alternator uses alternating-current windings in both the rotor and the stator. Reflections take place between these two windings because of their relative speed.

Another ingenious alternator is due to M. Latour. It consists of several generators in cascade. S_1, S_2, S_3 , and S_4 are stators, and R_1, R_2, R_3 , and R_4 are the corresponding rotors of the four machines. The first machine is excited by a direct current and delivers a two-phase current of frequency f , which is determined by the number of equal poles and the

speed of the rotor. The revolving field produced by the two-phase winding in the second machine is arranged so that it turns in opposition to the direction of rotation of the rotor R_2 . Hence a two-phase current of frequency $2f$ is induced in the stator S_2 . The revolving field due to this current in the third machine produces a current $3f$ in R_3 since the direction of rotation of R_3 is again arranged in opposition. In a similar way, a high-frequency current of frequency $4f$ is delivered by the fourth machine. Slip rings are avoided since each stator connects to the next stator, or rotor to the next rotor. Condensers are inserted between the machines in order to compensate for the leakage reactance.

The alternator of the Société Française Radio-électrique is likewise of equal-pole type. The stator contains a zigzag high-frequency winding and the number of rotor teeth to stator teeth is in the ratio of 3:2. Hence three voltage waves which are 120 deg out of phase are induced in the stator winding. The rotor teeth are shaped in such a way that the wave shape is distorted. The corresponding fundamental currents give zero effect in the external circuit, while the effects of the third, ninth, and fifteenth harmonic are additive.

23. Notes on Electron-tube Oscillators.—The action of tube oscillators commonly used depends upon the amplification property of the three-element electron tube. Dynatron and Magnetron oscillators employing secondary emission of electrons and a magnetic field, respectively, depend upon *negative-resistance* action. In some ways, oscillations in ordinary three-element tubes can also be considered to be due to a negative-resistance action, since the feedback of energy into the grid branch causes resistance neutralization when oscillations take place. Two-element tubes having only a hot cathode and an anode can produce low-frequency oscillations because of the effect of the temperature of the hot cathode on the thermionic emission.

Figure 24 shows basic electron-tube oscillators. One of these oscillators, invented by A. Meissner, uses a separate oscillating circuit which takes its energy from the plate circuit and sustains the oscillations by the back feed into the grid branch and by the amplification of the tube back into the plate circuit. The three other fundamental circuits include the resonant circuit, in either the grid or plate branch, or use either the entire external grid-plate inductive reactance or a portion of it in the actual oscillator circuit. For the sake of simplicity, the condensers for by-passing the high-frequency currents around the batteries are not shown. In practical work it is of advantage to insert the B supply in the low side, that is, next to the filament. The plate potential can be supplied by series-plate feed as in Fig. 24. On the other hand, it is often of advantage to use a parallel plate supply as shown in the modified Hartley circuit of Fig. 25. The choke L_0 prevents the high-frequency current

from passing through the power-supply branch and the condenser C_0 keeps the direct-current component out of the high-frequency circuit. Such feeds are of especial advantage when working in the range of very

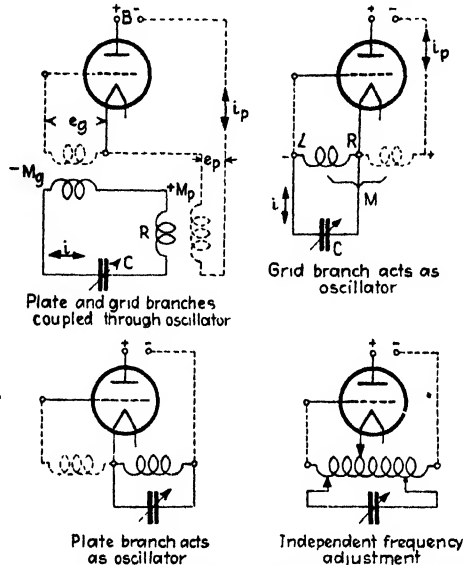


FIG. 24.—Basic oscillator circuits with series plate feed (parallel plate feed through high-frequency chokes used in higher frequency range).

high frequencies, since then even air coils having a comparatively few turns are sufficient to prevent the high-frequency current from flowing through the B battery. It is also of advantage when resistance- and

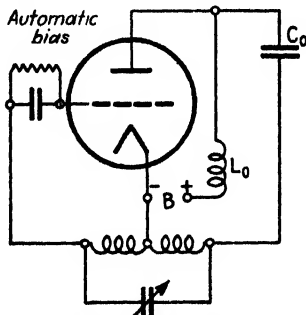


FIG. 25.—Useful oscillator with parallel plate feed.

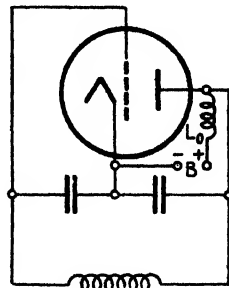


FIG. 26.—Colpitt oscillator.

resistance-capacitance-coupled amplifiers (page 206) are used, since no portion of the supply voltage is used up in the coupling resistances.

Figure 26 shows the Colpitt oscillator which requires a parallel plate feed. It is similar to the Hartley circuit except that an external capacity

coupling is used instead of a magnetic coupling. Of course, an internal coupling due to the interelectrode capacity also exists in each circuit. The grid current might be checked by a C battery instead of a grid condenser with a leak as in Fig. 25. The action of these devices is explained in detail on pages 177 to 180. Figure 27 shows an oscillator

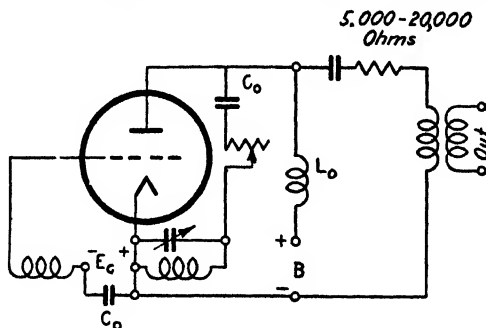


FIG. 27.—Parallel plate feed and parallel output (C_0 such that almost zero reactance for operating frequency, L_0 high-frequency choke)

which uses a parallel plate feed as well as a parallel output branch. Figure 28 gives basic short-wave generators. In some cases the high-frequency choke is replaced by a tank circuit (condenser in parallel with an inductance).

24. Building Up of Self-excited Tube Oscillations.—On account of the amplification action in thermionic tubes, variable grid potentials produce increased potential variations on the plate. Hence, as soon as the circuit of a tube oscillator (Fig. 29) is closed, a transient current

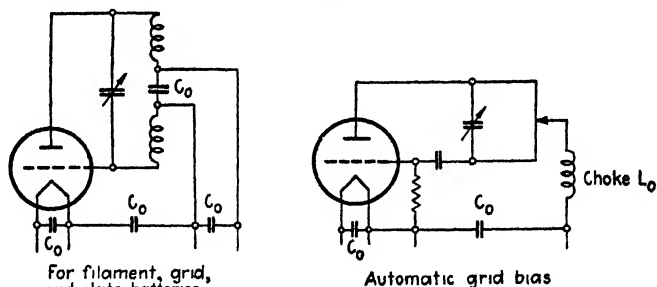


FIG. 28.—Typical oscillators for frequencies above 30 megacycles/sec, C_0 by-pass condensers.

flows and the condenser begins to charge or discharge according to the natural period of the oscillating circuit. During this process resultant grid and plate potentials may be established so that the CL circuit is kept in a state of oscillation (Fig. 30). This takes place with a proper relative arrangement of the grid and plate windings, the voltages e ,

and e_p being of opposite polarity at any instant. Pure sinusoidal oscillations are obtained when the variations take place along the straight portion of the dynamic characteristic of the entire circuit. Such oscillations may be recognized by the absence of harmonics. Harmonics are present when the variations extend to the curved portion of the grid-voltage plate-current characteristic, or when the coupling between the anode and grid coils is so close that at times large negative grid potentials stop the plate current I_p altogether. When the oscillations are stopped, the reading I_p of the average plate current decreases. This is not true with pure sinusoidal oscillations.

25. Important Tube Relations for Three-element Electron Tubes.—

The basic relation of such tubes was derived in Sec. 7 and is given by Eq. (18) on page 14. If it is compared with the expressions given by pioneer contributors to the theory of tubes, we have, for the static plate-current lumped-anode potential characteristic

$$\begin{aligned}
 I_p &= A[E_p + \mu E_g]^{1.5} \text{ (Langmuir)} \\
 &= \alpha \left[\frac{E_p}{\mu} + E_g + m \right]^2 \text{ (Van der Bijl)} \\
 &= \varphi[E_g + DE_p] \text{ (Barkhausen)} \\
 &= b \left[E_p + \frac{a}{b} E_g + \frac{c}{b} \right] \text{ (Vallauri)} \\
 &= \frac{1}{R_p} [E_p + \mu E_g - X] \text{ (Gutton)} \\
 &= \frac{1}{R_p} [E_p + \mu E_g + m]^n = \frac{E_p^n}{R_p} \text{ (universal formula)} \quad (2)
 \end{aligned}$$

where R_p denotes the internal static resistance of the tube (from cathode to anode), and the exponent n is different for different portions of the characteristic and may be partly considered a dimension quantity of the tube. It is equal to unity for the straight portion of the characteristic, about equal to 2 for the lower portion, and about equal to 1.5 for the upper portion of certain tubes when the portion of saturation is not taken into account. The quantity m denotes here that portion which produces the emission current if both the grid and the plate are connected

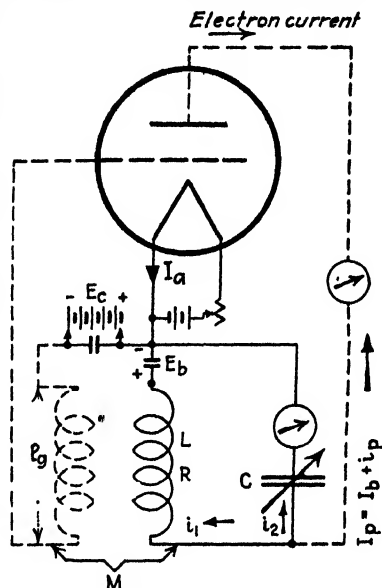


FIG. 29. Tube generator for performance of Fig. 30.

to the negative end of the hot cathode without the use of a battery in this branch. It is a negligible quantity when the tube is operated at normal plate potentials. Typical curves showing the shape of the static characteristic are shown in Fig. 32.

In many cases, G. Gutton and G. Vallauri assume that the tube works along an almost flat surface of $I_p = bE_p + aE_g + c$. The quantity μ is known as the *amplification factor*. It is proportional to the distance between cathode and plate, inversely proportional to the distance between cathode and grid, and inversely proportional to the width of the

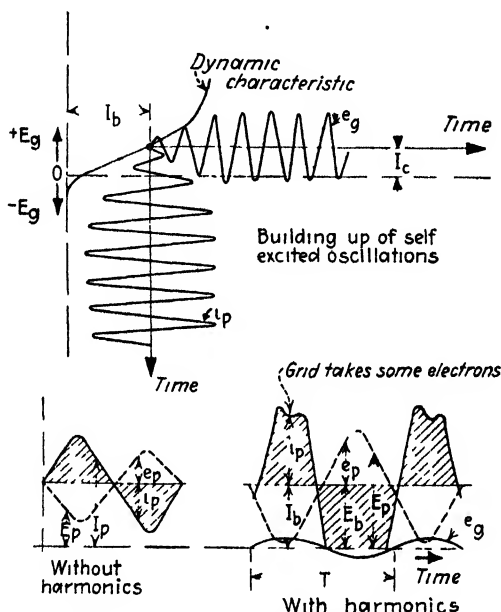


FIG. 30.—Self-excited tube oscillations.

grid mesh (distance between grid wires). It is seen that in Vallauri's formula $a/b = \mu$, where a stands for the steepness of the grid-potential plate-current characteristic [equal to quantity $G_m = I_p/E_g$ of Eq. (21) on page 15], b denotes the steepness of the static plate-potential plate-current characteristic (equal to $I_p/E_p = 1/R_p$), that is, equal to the static cathode-plate conductivity within the tube since R_p stands for the static resistance. This quantity changes with grid and anode potentials and depends besides on the temperature of the cathode and the distribution of the space charge. For measurements, the temperature effect on R_p is an important one, since by changing the filament current the internal plate current can be changed over wide limits. Use of this temperature effect is made in the time-axis apparatus used to produce a linear deflection in the cathode-ray tube. Such a cathode temperature is then used

that a full saturation current flows to the plate, and the space current through the tube is the same for a wide variation of the voltage applied to it. The quantity E_l is known as the lumped-anode potential and in many cases it is convenient to deal with it instead of the components μE_g and E_p . In formulas (19), (20), and (22) in Sec. 7, it has been proved that the *dynamic* internal plate resistance r_p , mutual conductance g_m over grid, and amplification factor are

$$r_p = \frac{\partial e_p}{\partial i_p}; \quad g_m = \frac{\partial i_p}{\partial e_g}; \quad \mu = \frac{\partial e_p}{\partial e_g} \quad \bullet \quad (3)$$

where

$$\frac{g_m \cdot r_p}{\mu} = 1 \quad (4)$$

Equation (4) is an important relation¹ since, when any two of these quantities are determined from measurements, the other one is fixed. The internal resistance of receiving tubes varies from about 3000 to 100,000 ohms. The first limit corresponds to low- μ three-element tubes, and the other to high- μ tubes. The amplification factor varies usually from about 2.5 to 30, and the mutual conductance from 0.2 to 0.6 ma/volt. The change in the plate current which depends on the grid potential is greatest for the middle portion of the characteristic. The steepness of the main tube characteristic, according to Eq. (2), is equal to $\partial I_p / \partial E_l$ and $E_l = I_p + \mu E_g$, since $m \cong 0$. The first relation of Eq. (3) holds for constant grid potential, the second one for constant plate potential, and the third relation for constant plate current. When, therefore, the plate current is varied from a value I_p to a somewhat larger value I_p' by increasing the plate potential from a value E_p to a value E_p' , the original plate current I_p can be obtained again by decreasing the grid

¹ Unless especially mentioned, small letters stand for dynamic and capitals for static values. The sources connected in the filament, grid, and plate branch are known as A, C, and B batteries, respectively. The corresponding voltages and currents, on account of being steady, are then E_a , E_c , E_b , and I_a , I_b . The grid current I_c is not mentioned since in a properly adjusted three-element tube it is very small. The instantaneous variable (oscillating) voltages and currents are e_p , e_g , and i_p , respectively. Their maximum values are for simplicity's sake denoted by e_p' , e_g' , and i_p' since formulas seem to look confusing when the suffix m or some other suffix is added to p or g . Such an exception is made only in this particular case of tubes. Since we have also to deal with resultant tube potentials and currents, we call these *pulsating* values $E_p = E_b + e_p$, $E_g = E_c + e_g$, and $I_p = I_b + i_p$. To simplify formulas further, E_g and E_p are used as the effective values for alternating grid and plate potentials and I_p denotes the effective value of the alternating current flowing in the plate circuit. R_p and r_p denote the static and dynamic tube resistance and g_m the dynamic mutual conductance over the grid. The filament^{*} battery is omitted in many figures. The small condenser indicated across B and C batteries is a by-pass condenser.

potential E_g to a certain value E_g' . According to the foregoing definition, the amplification factor is then

$$\mu = \frac{E_p' - E_p}{E_g - E_g'} \quad (5)$$

When the almost straight portion of the characteristic is considered, for which $n = 1$ and $R_p = r_p$, Eq. (2) reads

$$I_p = \frac{1}{r_p}[E_p + \mu E_g] = \frac{\partial i_p}{\partial e_p} E_p + \frac{\partial i_p}{\partial e_g} E_g \quad (6)$$

and, when current variations i_p exist, we have

$$I_p + i_p = \frac{\partial i_p}{\partial e_p}[E_p + e_p] + \frac{\partial i_p}{\partial e_g}[E_g + e_g] \quad (7)$$

Subtracting (6) from (7) gives

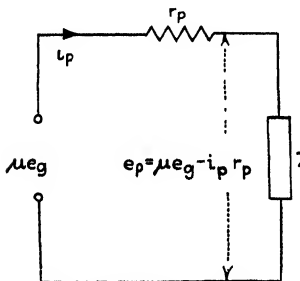


FIG. 31.—Equivalent network for impedance loaded three-element tube.

$$\begin{aligned} i_p &= \frac{\partial i_p}{\partial e_p} e_p + \frac{\partial i_p}{\partial e_g} e_g \\ &= \frac{e_p + \mu e_g}{r_p} \end{aligned} \quad (8)$$

where it is assumed that the grid current is negligible.

26. The Loaded Plate Circuit of a Three-element Tube.—As far as *variable* currents i_p are concerned, if the tube is closed through an external impedance Z , we have the equivalent circuit¹ shown in Fig. 31. It is as though a variable voltage μe_g were impressed on a series combination made up of the dynamic plate resistance r_p of the tube and the external plate impedance Z , since the internal-tube capacities can in many cases be neglected. The correctness of this equivalent circuit is evident from Eq. (8), when we substitute $e_p = -Zi_p$. The latter relation is an expression of the fact that a rise in plate current produces a drop of plate

¹ Relations (8) and (8a) hold well within the customary high-frequency range. This is, however, not true when the time of electron flight from the hot cathode to the anode becomes a noticeable fraction of the period $1/f$ of the high-frequency current of frequency f . For instance, if it takes an electron exactly the full period $1/f$ sec. of the high-frequency current to cross the hot cathode-anode distance, the current has a phase angle of 360 deg. and correspondingly less for other noticeable ratios of passage time to period of oscillation. This means the fictitious driving voltage μe_g is complex since μ has a real and a reactive component of the form $\mu_1 \pm j\mu_2$. The same is true for the dynamic plate resistance r_p and the current i_p since they are in the very high-frequency range of the form

$$r_p = r_1 \pm jr_2 \quad \text{and} \quad i_p = i_1 \pm ji_2$$

potential equal to the voltage consumed in the external impedance. Hence

$$[Z + r_p]i_p = \mu e_g \quad (8a)$$

Also, for $Z = \infty$, no plate current flows and

$$\mu = \frac{e_p}{e_g}$$

that is, the voltage amplification is equal to the amplification factor.

We must distinguish between static and dynamic tube characteristics, and characteristics which hold for the tube only or for a tube with an external anode branch. The latter is of importance, since a tube must deliver energy. Figure 32 gives the various static characteristics. The

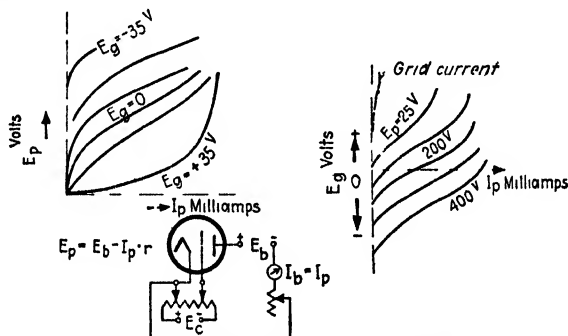


FIG 32—Static tube characteristics.

internal effective plate resistance of the tube is r_p which, in the case of variations along the straight portion of the characteristic, is equal to the static resistance R_p . For other portions of the characteristic it is

$$r_p = \frac{\partial[E_p + \mu E_g]}{\partial I_p} \cong \frac{R_p}{n}$$

According to Eq. (18) on page 14, we have for any grid voltage, whether variable or not, and for negligible grid current

$$I_p = \frac{E_l^n}{R_p}$$

where R_p denotes again the direct-current resistance and the lumped-triode voltage is $E_l = \mu E_g + E_p$. The quantity R_p can be found from the characteristic for which I_p is plotted against E_l (Fig. 134). It depends on the operating point. For many purposes it seems more convenient to express the triode action by

$$I_p = K \left[\frac{E_p}{\mu} - E_g \right]^n$$

The minus sign enters since the plate potential decreases when E_g and I_p increase. The factor K is again determined by the operating point on the plate-current grid-voltage characteristic. It denotes the steepness at that point. The dynamic plate conductance then is

$$g_p = \frac{\partial I_p}{\partial E_p} = n \frac{K}{\mu} \left[\frac{E_p}{\mu} - E_g \right]^{(n-1)}$$

leading to the dynamic plate resistance of the triode at any point on the characteristic

$$r_p = \frac{\mu}{nK} \left[\frac{E_p}{\mu} - E_g \right]^{(1-n)}$$

which for three-halves-power law gives $n = \frac{3}{2}$ and

$$r_p = \frac{2}{3} \frac{\mu}{K} \left[\frac{E_p}{\mu} - E_g \right]^{-\frac{1}{2}}$$

Moreover, one group of characteristics (Fig. 32) represents the anode current I_p which depends on the plate potential E_p , holding for a particu-

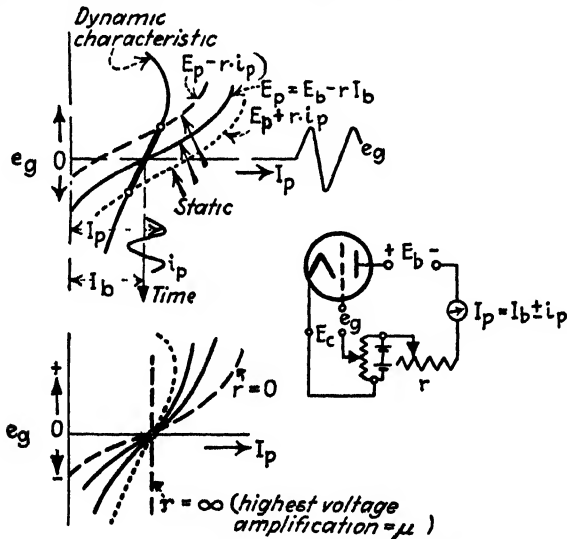


FIG. 33.—Dynamic tube characteristics.

lar fixed grid potential E_g . The other group gives the plate current which depends on the grid potential, each curve holding for a particular plate potential. Figure 33 gives the corresponding dynamic characteristic for the case of an external resistance load. The resultant potentials and currents are then $E_g = E_c + e_g$; $E_p = E_b + e_p$; $I_p = I_b + i_p$. It is seen that, because of the potential variations e_g on the grid, the dynamic

characteristic is a characteristic turned into the position of the heavy curve which for small variations is almost linear. Now, according to Eq. (8a) and Fig. 31, a pure resistance load ($Z = R$) in the external plate circuit is the simplest case and a single-valued characteristic is obtained. A tuned plate circuit (current resonance) acts, under certain conditions, as a pure resistance load and is used in some tube oscillators as well as with certain types of amplifiers. Hence, for a tuned plate circuit as in Fig. 29, the external load is

$$Z = \frac{L}{CR} \quad (9)$$

which is a pure resistance if the effective resistance R of the oscillatory circuit is small. Otherwise, we have for the effective external plate impedance

$$Z = \frac{\omega_0^2 L^2}{R} - j\omega_0 L \quad (9a)$$

where $\omega_0/(2\pi)$ denotes the resonance frequency of the tuned plate circuit. A tube circuit delivers energy to some other circuit such as an antenna. Hence the effective resistance R is increased and is usually not negligible so that (9a) rather than (9) is the expression for Z . Therefore, it is evident that the plate current i_p does not vary quite in phase with the grid voltage e_g . The dynamic characteristic is then no longer a more or less straight single-valued curve as for pure resistance load, but a closed path of oval shape as indicated in Fig. 34, since the impedance

$$Z = R \pm jX,$$

together with the tube resistance r_p , produces a phase angle

$$\varphi = \tan^{-1} \{ \pm X/(R + r_p) \}.$$

It is seen that we have to deal with a vector triangle of sides μe_g , $r_p i_p$, and $Z \cdot i_p$ instead of a term $R \cdot i_p$ for the drop $-e_p = \mu e_g$ for a pure resistance load $Z = R$. The effect of the external plate impedance gives characteristics which resemble an ellipse with a wattless area for a pure inductive or a pure capacity load, respectively, since the driving voltage μe_g works over a series combination $r_p + j\omega L$ or $r_p - j/(\omega C)$. The main axis of this oval-shaped characteristic is almost a straight line when $Z \geq r_p$. For $Z = r_p$ in the vector diagram, we have $\varphi = 45^\circ$. This angle determines the shape of the characteristic¹ area and with a decrease of φ the oval becomes narrower.

¹ An application of a reactive load to an amplifier is given on pp. 194, 196-198.

27. Theory of the Tuned-grid Oscillator.—The actual oscillator is the heavily drawn branch of Fig. 24. Using, for the sake of simplicity, the generalized symbolic method where n denotes the generalized angular

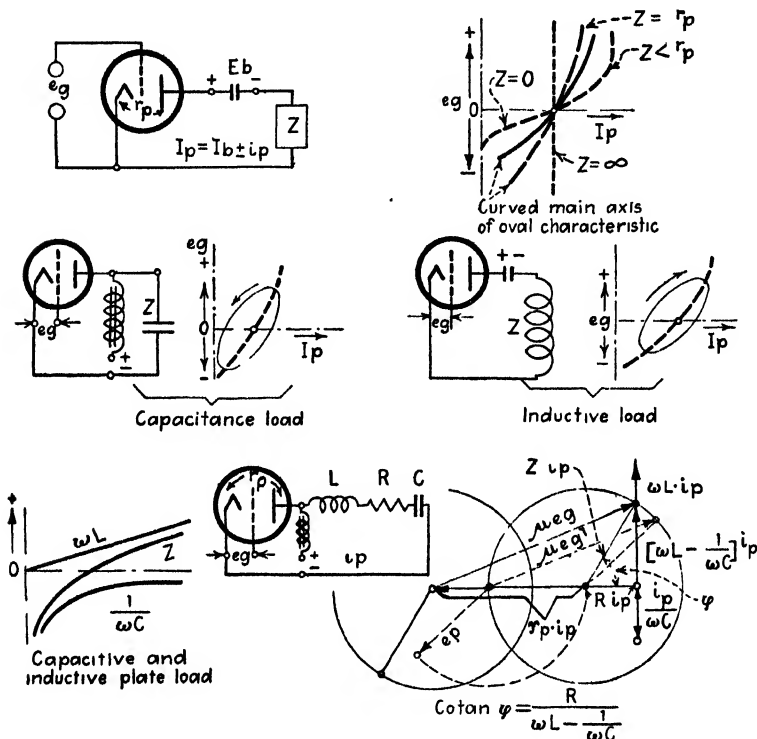


FIG. 34.—Reactive plate load.

velocity $n = \alpha + j\omega$, for the sum of the voltages around the heavily drawn oscillator, we have for the amplitude values i' and i_p' of i and i_p

$$\underbrace{i' \left[R + nL + \frac{1}{nC} \right]}_{\text{voltage due to the oscillator alone}} + \underbrace{i_p' nM}_{\text{voltage coming from the plate circuit}} = 0 \quad (10)$$

According to Fig. 35 and Eq. (3) for negligible grid current, we have

$$\frac{\partial i_p}{\partial e_g} = g_m \cong \frac{i_p'}{e_g'}$$

that is, equal to the steepness of the grid-potential plate-current characteristic. The approximation holds for the straight portion of the characteristic—otherwise for small variations only. It is the quantity

which L. A. Hazeltine calls "mutual conductance" over the grid to plate in his derivation.¹ Hence

$$i_p' = g_m \cdot e_g' = g_m \frac{i'}{nC} \quad (11)$$

Eliminating i_p' in (10) by means of (11) gives

$$R + nL + \frac{1}{nC} + \frac{g_m M}{C} = 0$$

or the quadratic equation

$$n^2 L + n \left[R + \frac{g_m M}{C} \right] + \frac{1}{C} = 0 \quad (12)$$

which, for the case of oscillation, gives

$$\begin{aligned} n &= \alpha \pm j\omega \\ &= -\frac{1}{2L} \left[R + \frac{g_m M}{C} \right] \pm j \sqrt{\frac{1}{CL} - \left[\frac{1}{2L} \left(R + \frac{g_m M}{C} \right) \right]^2} \end{aligned} \quad (13)$$

But for sustained oscillations the damping factor α must vanish ($\alpha = 0$), which means

$$g_m^{(\text{mbos})} = \frac{C^{(dd)} R^{(\Omega)}}{[-M]^{(\text{henry})}} \quad \text{and} \quad f = \frac{1}{2\pi \sqrt{C^{(dd)} L^{(\text{henry})}}} \text{ cycles/sec} \quad (14)$$

The negative sign necessarily belongs to the mutual inductance M and expresses the fact that the windings in the plate branch must *oppose* the windings in the grid branch. The expressions in Eq. (14) refer to the condition for which sustained oscillations are just possible. In this case the effective oscillation voltage is just equal to μe_g . For the case where μe_g is smaller than the oscillation voltage required, a damped wave train is produced which dies out before being observed, while, for μe larger than the oscillation voltage, growing oscillations are established until the energy balance, as well as tube characteristic, limits a further growth of the oscillating current. Since the internal tube resistance, according to Eq. (4), is equal to μ/g_m , we find by means of the value of g_m found in Eq. (14) that

$$r_p = - \left[\frac{\mu M}{R \cdot C} \right] \quad (15)$$

indicating that for a condition of sustained oscillations the tube offers a *negative* resistance action. The expression for g_m in Eq. (14) indicates how the circuit constants have to be related for the existence of sustained

¹ For the theory by L. A. Hazeltine see *Proc. I.R.E.*, 6, 63, 1918.

oscillations. For $g_m < CR/M$, a small oscillation cannot be self-sustained; and if $g_m > CR/M$ any oscillation, however small, will increase in amplitude up to an equilibrium value at which the losses in the tube circuit are equal to the power supplied from the B battery. Figure 35 shows that the steepness of the grid-potential plate-current characteristic varies, that is, $g_m = \partial i_p / \partial e_g$, and passes through a maximum (corresponding to the mid-point of the straight portion of I_p function (E_g) curve. Now, for a fixed steady plate potential, and circuit constants C ,

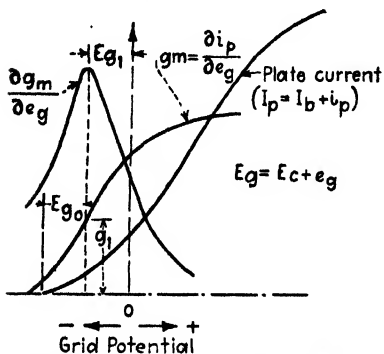


Fig. 35.—Optimum condition for starting oscillations.

R , and L , sustained oscillations just set in for a certain steepness g_m of the ($I_p - E_g$) characteristic, for instance, corresponding to a fixed grid bias ($-E_{g0}$) volts. However, the “falling in” of oscillations for such a position is not so critical as for points of some less negative grid potentials. The most sensitive falling in occurs when $\partial g_m / \partial e_g$ becomes a maximum corresponding to a fixed negative grid potential which is ($-E_{g1}$). The steepness then varies most rapidly.

The steepness g_m corresponding to this optimum condition can be satisfied by changing the mutual inductance M between the tuned grid circuit and the plate circuit. This property has been used by L. B. Turner to obtain a very sensitive trigger relay (page 277).

28. Theory of the A. Meissner Oscillator.—The power dissipated in the oscillator circuit must be continually supplied in order to maintain the oscillation. Therefore, it is possible to derive the oscillator relations by means of this principle. In the heavily drawn oscillator circuit of total inductance L (Fig. 24) the oscillation of angular velocity $\omega = 1/\sqrt{CL}$ can be sustained when the power supplied to it is sufficient to cover the losses. The induced amplitude voltages in the grid and plate coils are

$$\left. \begin{aligned} e_g' &= j\omega M_g i' \\ e_p' &= j\omega M_p i' \end{aligned} \right\} \quad (16)$$

and, since the losses are to be supplied by the B battery in the anode branch, for the energy compensation we have

$$\underbrace{\frac{e_p' \cdot i_p'}{2}}_{\text{energy delivered by plate coil}} = \underbrace{\frac{i'^2 \cdot R}{2}}_{\text{energy dissipated in oscillator branch}} \quad (17)$$

since the effective value is equal to twice the amplitude value. But $e_p' = g_m \cdot e_g'$; hence

$$i'^2 \cdot R = g_m e_g' \cdot i_p' = -g_m \omega^2 M_g M_p i'^2 \quad (18)$$

and the conditions for which sustained oscillations are just possible are

$$g_m (\text{mhos}) = \frac{R}{\omega^2 [+M_g][-M_p]} = \frac{C^{(fd)} L^{(\text{henry})} R^{(\Omega)}}{[+M_g^{(\text{henry})}][-M_p^{(\text{henry})}]} \quad (19)$$

since

$$\omega = \frac{1}{\sqrt{CL}} \quad (20)$$

Grid and plate windings have therefore to act again in opposition so that either M_g is positive and M_p is negative or vice versa. The apparent resistance reaction is

$$r_p = -\mu \frac{\omega^2 M_g M_p}{R} \quad (21)$$

and is *negative* which accounts for the existence of self-excited oscillations.

29. Theory of the Tuned-plate Oscillator.

The oscillator shown in Fig. 29 can, as far as the variable-current display alone is concerned, be considered as an equivalent circuit, as indicated in Fig. 31. The external plate impedance Z then consists of the plate coil (L , R) in parallel with its tuning condenser C (Fig. 36). The instantaneous value of the plate current is

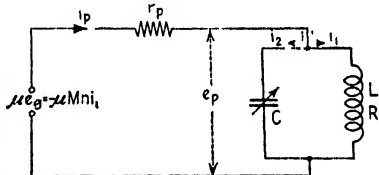


FIG. 36.—Equivalent tuned-plate oscillator.

$$i_p = i_1 + i_2$$

and the driving voltage

$$\mu e_g = \mu(-M)ni_1$$

since the current i_1 induces the voltage e_g in the grid coil and the grid windings must be in opposition to the plate windings. Since the voltage across the coil is the same as that across the condenser, we have

$$\left. \begin{aligned} -\mu Mni_1 &= r_p[i_1 + i_2] + [R + nL]i_1 \\ \frac{i_2}{nC} &= [R + nL]i_1 \end{aligned} \right\} \quad (22)$$

Eliminating i_2 in the first equation by means of $i_2 = nC[R + nL]i_1$ from the second equation, we find

$$r_p CLn^2 + [L + r_p RC + \mu M]n + [r_p + R] = 0 \quad (23)$$

that is, a quadratic equation for n with the solution

$$n = \alpha \pm j\omega$$

where

$$\left. \begin{aligned} \alpha &= -\frac{1}{2} \left[\frac{1}{r_p C} + \frac{R}{L} + \frac{\mu M}{r_p C L} \right] \\ \omega &= \sqrt{1 + \frac{(R/r_p)}{C L} - \alpha^2} \end{aligned} \right\} \quad (24)$$

For sustained oscillations $\alpha = 0$, and

$$f = \frac{1}{2\pi} \sqrt{1 + \frac{(R/r_p)}{C L}} = f_0 \sqrt{1 + \frac{R}{r_p}}; \quad r_p = \frac{-\mu M - L}{RC} \quad (25)$$

when the frequency is in cycles per second, and all other quantities in practical units, that is, in farads, henries, and ohms, respectively. Hence the critical coupling for which sustained oscillations just exist is

$$-M = RC \frac{r_p}{\mu} + \frac{L}{\mu} = \frac{RC}{g_m} + \frac{L}{\mu} \quad (25a)$$

It can be seen that, for negligible effective resistance R , the ordinary frequency formula $f_0 = 1/(2\pi\sqrt{C\bar{L}})$ is obtained. But for a *loaded* tube circuit the frequency is different. The foregoing results can also be checked by means of Eqs. (3) and (8) for plate-current variations since

$$\begin{aligned} i_p &= \frac{\partial i_p}{\partial e_p} e_p + \frac{\partial i_p}{\partial e_g} e_g = \frac{e_p}{r_p} + g_m e_g \\ &= \frac{e_p + \mu e_g}{r_p} \end{aligned} \quad (26)$$

30. Vector Diagram of a Tuned-plate Oscillator.—If I_p , I_1 , I_2 , E_g , and E_p , in this particular case, are the effective values of the variable currents and voltages in the oscillator shown in Fig. 37, we have the indicated vector diagram. The driving e.m.f. is practically equal to the effective, alternating plate potential E_p , but out of phase by the angle γ , since the plate coil has a watt component $R I_1$ and a wattless component $\omega L I_1$. The effective grid potential E_g and plate potential E_p are not exactly in antiphase but differ from 180 deg by this small angle γ . The condenser current I_2 leads E_p by 90 deg and the coil current I_1 is only approximately in antiphase with I_2 . The resultant effective plate current I_p is therefore equal to the geometrical addition of I_1 and I_2 . If $R = 0$, it would be in phase with the effective grid potential E_g , since for such a condition I_1 would be the true combination of I_2 for the current

circulation around the LC branch. Introducing the corresponding vector values written with a dot below, we have, according to (26),

$$\begin{aligned} I_P = I_1 + I_2 &= \frac{1}{r_p} [E_P + \mu E_G] = \frac{1}{r_p} \{ - [R + nL]I_1 + \mu M n I_1 \} \\ &= \frac{1}{r_p} \{ n[\mu M - L]I_1 - R I_1 \} \end{aligned} \quad (27)$$

But for sustained oscillations $\alpha = 0$ and $n = j\omega$; hence

$$\tan \delta = \frac{R}{\omega(\mu M - L)} \quad (28)$$

and for the corresponding effective values

$$I_P = \frac{I_1}{r_p} \sqrt{R^2 + \omega^2(\mu M - L)^2} \quad (29)$$

Hence the combination acts as though a coil of resistance R and inductance $(\mu M - L)$ were in the external plate branch.

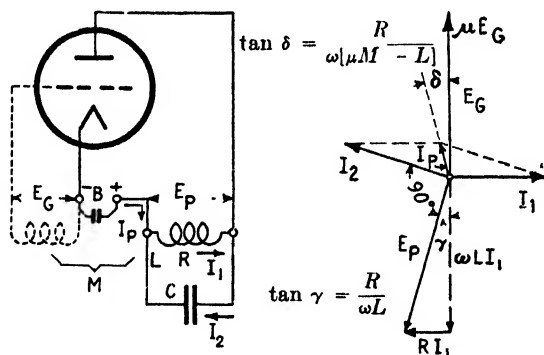


FIG. 37.—Vector diagram of a tube oscillator.

31. Amplitude and Phase of Oscillations in a Tuned-plate Generator.

In order to sustain the oscillations in the tube generator shown in Fig. 38, the induced voltage e_g across the grid coil must have the same amplitude and the same phase as the original voltage, since the grid voltage produces a variable plate current; this in turn produces the oscillatory current, and this again, by means of a back feed, the grid voltage. If the phase of the e.m.f. fed back into the grid circuit were somewhat behind the original phase, the phase of the plate current produced by it would also be behind with respect to the original anode current; and the *frequency of oscillation would become lower*. Hence, for sustained oscillations of fixed frequency, the maintenance of the same phase is just as important as that of the amplitude.

grid bias E_g , current pulses only will be produced in the plate circuit as in Fig. 40. The same can be used for frequency multiplication (Sec. 64, page 153).

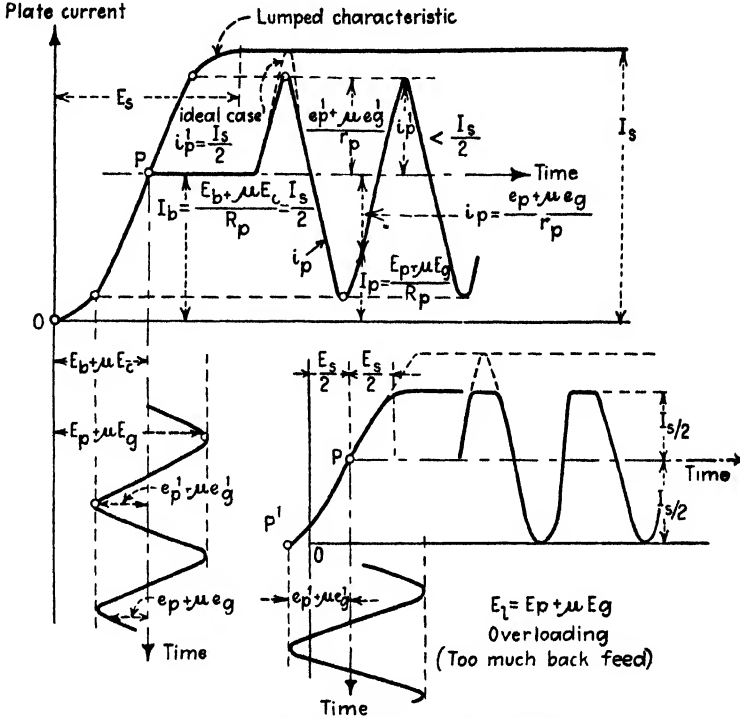


FIG. 39.—Undistorted and distorted oscillations.

Since, for resonance, the external plate impedance of Fig. 38 is about

$$Z = \frac{L}{CR} = \frac{\omega^2 L^2}{R} \quad (33)$$

that is, an ohmic resistance, we have for the maximum value of the oscillating plate potential

$$e_p' = \frac{L}{CR} i_p' \quad (34)$$

which, for normal oscillations (undistorted case of Fig. 39) must be

$$e_p' \leq \frac{LI_s}{2CR} \quad (35)$$

But the resultant voltage (pulsating plate potential) between the hot cathode and the plate is

$$E_p = E_b - \frac{L}{CR} i_p' \sin \omega t \quad (36)$$

and

$$E_p' = E_b - \frac{L}{CR} i_p' \geq 0 \quad (37)$$

since the resultant plate potential never falls below a zero value. Since the maximum value of i_p' is at most $I_s/2$, we have

$$\frac{L}{CR} \leq \frac{2E_b}{I_s} \quad (38)$$

According to Eq. (29), the amplitude value of the oscillating current passing through the plate coil is

$$i_1' = \frac{r_p \cdot i_p'}{\sqrt{R^2 + [\omega(L + \mu M)]^2}} \quad (39)$$

But, according to Eq. (25a),

$$L + \mu M = -r_p RC$$

and, in addition, introducing the substitution $\omega = 1/\sqrt{CL}$ in Eq. (39), we have

$$i_1' = \frac{i_p'}{R\sqrt{C/L + 1/r_p^2}} \cong \frac{i_p' \sqrt{L/C}}{R} \leq \frac{I_s \sqrt{L/C}}{2R} \quad (40)$$

But the current i_2 through the condenser is, for resonance, practically the continuation of the sinusoidal coil current i_1 , and the amplitude of the oscillating current in the CL branch, according to Eq. (40), can then never be greater than $(I_s/2R)\sqrt{L/C}$, where L is in henries, C in farads, R in ohms, and the saturation current I_s in amperes. Since the negative grid bias E_c can be so adjusted as to bring the operating point P (Fig. 39) in the middle of the characteristic, the steady B-battery current is then $I_b = I_s/2$ and the optimum amplitude value of the oscillatory current is

$$i_1' = \frac{I_b}{R} \sqrt{\frac{L}{C}} \quad (41)$$

An optimum is also obtained when

$$i_1' = E_b \sqrt{\frac{C}{L}} \quad (42)$$

since, according to Eq. (38), for maximum output we have

$$I_b = \frac{I_s}{2} = \frac{E_b CR}{L}$$

Equations (41) and (42) give

$$\frac{E_b}{I_b} = \frac{L}{CR} \quad (43)$$

Hence the ratio of L/C should be so chosen as to make it equal to $2RE_b/I_s$, since then the amplitude of the oscillatory current

$$i_1' = \sqrt{\frac{E_b I_s}{2R}} \quad (44)$$

32. Efficiency of the Tuned-plate Oscillator.—For *optimum* alternating-current output the efficiency, as far as the plate input only is concerned, is

$$\eta = 100 \frac{[i_1'/\sqrt{2}]^2 R}{E_b I_b} = 100 \frac{E_b I_s/4}{E_b (I_s/2)} = 50\% \quad (45)$$

Therefore the alternating-current output can be increased by choosing a larger supply voltage E_b . With increasing plate voltage, the electrons

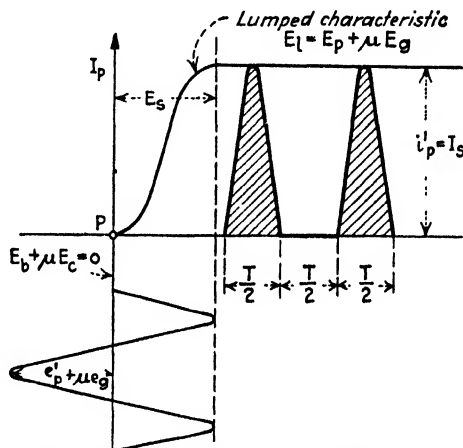


FIG. 40.—Most efficient operation at the expense of output power.

emitted at the hot cathode strike the positive plate with increased speed and heat it up by electronic bombardment. An oscillator operating with a dull-red anode is a common occurrence with power oscillators and shows that much oscillating energy is being supplied. But, for still higher supply voltages, the plate must be artificially cooled (water cooled, for example) in order to give increased output without injury to the tube. For small tube oscillators, the filament supply ($E_a \cdot I_a$) is considerable in comparison with the power ($E_b I_b$) delivered by the B battery and the over-all efficiency is much lower than 50 per cent.

The plate efficiency given by Eq. (45) is low because the oscillations take place about the mid-point of the characteristic and only maximum output is delivered for such an adjustment. For tube oscillations with this adjustment, the B battery supplies the power $E_b I_b = E_b I_s/2$.

In case of oscillations the power $E_b I_b/2 = E_b I_s/4$ is dissipated in the plate in the form of heat. In this case the battery current does not change as oscillations set in. This is true because the power delivered by the B battery to the oscillating tube circuit is

$$\begin{aligned} W &= \frac{1}{T} \int_0^T E_b [I_b + i_p] dt \\ &= E_b I_b - \frac{e_p' \cdot i_p'}{2} = E_b \frac{I_b}{2} \end{aligned} \quad (46)$$

since

$$\begin{aligned} e_p &= e_p' \sin \left(\omega t - \frac{\pi}{2} - \varphi_1 \right) \cong e_p' \sin \left(\omega t - \frac{\pi}{2} \right) \\ i_p &= i_p' \sin \left(\omega t + \frac{\pi}{2} + \varphi_2 \right) \cong i_p' \sin \left(\omega t + \frac{\pi}{2} \right) \end{aligned}$$

and for maximum output $e_p' = E_b$ and $i_p' = I_b$. The supply voltage E_b is fixed. Hence, for this case of maximum output, the plate current must sink to half of its original value. This is the reason a plate-current dip is noted in properly adjusted tube oscillators when the oscillations set in. The efficiency can be increased when there are periods during each cycle of the oscillation for which no plate current flows. This occurs, for instance, when the negative grid bias E_c is so chosen that $-\mu E_c = E_b$; that is, no plate current ($I_b = 0$) exists. We then have the case indicated in Fig. 40, in which the plate can heat up only during every other half cycle. The power supplied by the B battery is only

$$W_1 = \frac{e_p' i_p'}{\pi} \quad (47)$$

The power delivered by the tube to the oscillator is

$$W_2 = \frac{[i_p' / \sqrt{2}]^2 L / (CR)}{2} = \frac{i_p'^2}{4} \frac{L}{CR} = \frac{e_p' i_p'}{4} \quad (48)$$

with an efficiency of

$$\eta = \frac{100 W_2}{W_1} = 78.5\% \quad (49)$$

The output of the tube, however, is lower. Therefore, it is evident that the efficiency varies from 50 to about 78 per cent depending on whether the oscillations take place about the mid-point of the characteristic or some point corresponding to a negative grid bias E_c which makes $[E_b - \mu E_c] < E_s/2$ and not smaller than 0. The efficiency is then usually increased at the expense of distortion.

33. Oscillation Characteristics.—The average power in the oscillating plate circuit shown in Fig. 38 is

$$W = \frac{1}{2} e_p' i_p' = \frac{L}{CR} (i_p')^2$$

For small oscillations, which occur over only a limited portion of the grid-potential plate-current characteristic, the plate current is given by

$$i_p = g_m \cdot e_g \quad (50)$$

but if the amplitudes i_p' are considerable, the curvature of the characteristic must be taken into account. The instantaneous value of the alternating plate current is then a function of both the variable grid potential and the plate potential, and the equations are no longer linear. For this reason, according to H. G. Moeller,¹ it is convenient to use oscillation characteristics as indicated in Fig. 41, where the calculation is based on the amplitudes of the sinusoidal potentials and currents. The relation between i_p , e_g , e_p over the oscillation circuit and back feed is then again linear, since in

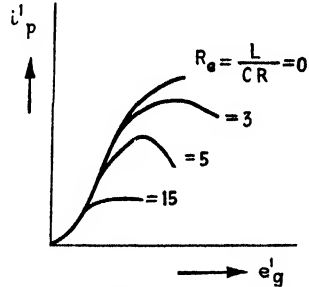


FIG. 41.—Oscillation characteristics.

$$i_p' = \frac{CR}{M} e_g' = \frac{L}{MR_e} e_g' \quad (51)$$

L/MR_e may be considered a constant because the tuned-plate circuit acts externally like an effective resistance

$$R_e = \frac{L}{CR} \quad (51a)$$

This can also be seen from the energy relation

$$\frac{1}{2} e_p' i_p' = \frac{1}{T} \int_0^T e_p i_p dt = \frac{1}{T} \int_0^T e_p F(e_g, e_p) dt = \frac{1}{2} e_p' e_g' \bar{g}_m \quad (52)$$

where \bar{g} denotes the mean steepness of the corresponding grid-voltage plate-current characteristic. Hence Eq. (50) can be brought into the form

$$i_p' = \bar{g}_m e_g' \quad (53)$$

where \bar{g}_m may be called the mean conductance over the grid to plate of the characteristic oscillation curve. The oscillation characteristic given by (53) can be constructed by means of Eq. (52) or be obtained

¹ MOELLER, H. G., "Die Elektronenröhren," 2d ed., p. 78, Vieweg, Braunschweig, Germany, 1922; also third edition, p. 54; also *Jahrb. d. drahtl.*, **14**, 326, 1919.

experimentally by means of the cathode-ray oscillograph. In a similar way, the lumped oscillation characteristic

$$i_p' = F(e_i') \quad (54)$$

can be used when the lumped amplitude

$$e_i' = \mu e_a' - e_p' \quad (55)$$

The negative sign enters since the alternating component of the grid potential increases when the corresponding anode potential decreases. Equation (51) is derived as follows: The induced maximum voltage across the grid coil (Fig. 38) is

$$e_a' = \omega M i_1' = \frac{M i_1'}{\sqrt{CL}}$$

Combining this with the approximation of Eq. (40) which is

$$i_1' = \frac{i_p' \sqrt{L/C}}{R} \quad (56)$$

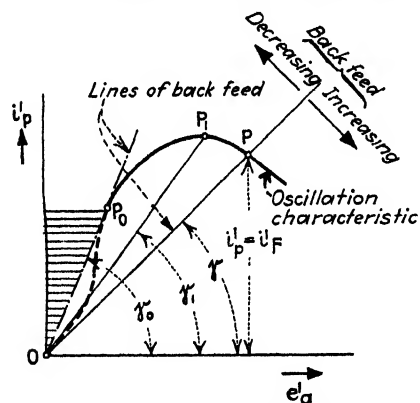


FIG. 42.—Back-feed diagram (i_p' is final amplitude).

we find, upon elimination of i_1' , the expression of Eq. (51). From Eq. (51) it is evident that for self-excitation of tube oscillations the dependence of e_a' on i_p' is dependent not only on the oscillation characteristic (Fig. 42) but also on the inclination γ of the line OP , since

$$\gamma = \tan^{-1} \frac{CR}{M} \quad (57)$$

Hence, if this line does not intersect the oscillation characteristic, no oscillations are possible. The shaded region corresponds to a condition of this kind. Therefore, the steepness

$$\bar{g}_m = \frac{CR}{M} = \frac{L}{MR_s} \quad (58)$$

corresponds to the mean mutual conductance over grid to plate. Self-excited oscillations are impossible for large values of \bar{g}_m . This happens if either the coupling M is too loose or the product CR is too large. If the \bar{g}_m line just produces a tangent at P_0 on the oscillation characteristic, the oscillation, if existing at all, is apt to cease at any time. Oscillations for steepness OP_1 cannot begin to build up on their own account. The line

OP_1 of back coupling is not tangent to the oscillation characteristic at the origin and the steepness γ_1 is greater than the steepness γ required by the tangent at O . A somewhat closer coupling must be chosen in order to make the line of back coupling just tangent to the curvature of the oscillation characteristic near the origin. The intersection P then lies on a stable portion (drawn in full line) of the oscillation characteristic. The oscillations can then build up to the point P . Hereafter, the coupling can be loosened up somewhat, for instance, corresponding to a feedback line OP_1 without in any way disturbing the stability of the oscillations. If the mean steepness \bar{g}_m is reduced just beyond that corresponding to an angle γ_0 , the oscillations suddenly cease. This is why it is necessary at times to tighten up the coupling of a tube oscillator in order to start the oscillations. After this the coupling can again be loosened. The starting up of self-excited oscillations can also be accomplished by changing the oscillation characteristic. This is done by choosing a proper grid bias. The starting of oscillations can then be made very critical and is used, for example, in the trigger relay (page 277). This effect of the grid bias, however, can be disadvantageous since for certain systems using grid modulation the oscillation may suddenly stop when a certain grid potential is exceeded. When the lumped oscillation characteristic [Eqs. (54) and (55)] is used, the graphical solution for the final oscillation amplitude is as follows. According to Fig. 38 and Eq. (55), we have

$$e_i' = \mu e_g' - e_p' = \mu \omega M i_1' - \omega L i_1' = \frac{[\mu M - L] i_1'}{\sqrt{CL}} \quad (59)$$

Combining this result with Eq. (56), the lumped amplitude becomes

$$e_i' = \frac{\mu M - L}{CR} i_p' = \mu e_g' - e_p' \quad (60)$$

if $(\mu M - L)/CR$ denotes the feedback factor and is again a slanting line at the angle

$$\delta = \tan^{-1} \frac{\mu M - L}{CR} \quad (61)$$

The construction is shown in Fig. 43. Draw the feedback line OP at the angle δ . The intersection with the lumped oscillation characteristic at P determines the final amplitude $i_p' = i_F'$ of the oscillating plate current, and OA gives the lumped oscillating amplitude potential $\mu e_g' - e_p'$. The amplitude of the alternating current $i_1 = i_1' \sin \omega t$ can

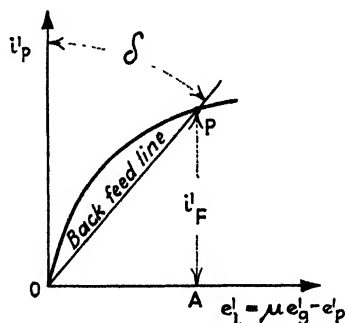


FIG. 43.—Lumped back-feed characteristic.

then be calculated by means of Eq. (56), since i_p' is found from this construction.

34. Effect of the Load in the External Plate Circuit on the Internal Impedance between Grid and Filament.—Because of the interelectrode capacitances, especially the grid-plate capacitance, the input characteristic between grid and filament is different with different kinds of plate loads and degree of loading.¹ Assuming a proper negative grid bias so that the grid current can be neglected, for an impedance input $Z_1 = R_1 \pm jX_1$ and a plate output $Z_2 = R_2 \pm jX_2$, we have the circuit indicated in Fig. 44, where all currents and voltages denote the maximum instantaneous alternating values due to a sinusoidal impressed voltage $e_g = e_g' \sin \omega t$. This voltage is due to the voltage drop across the external

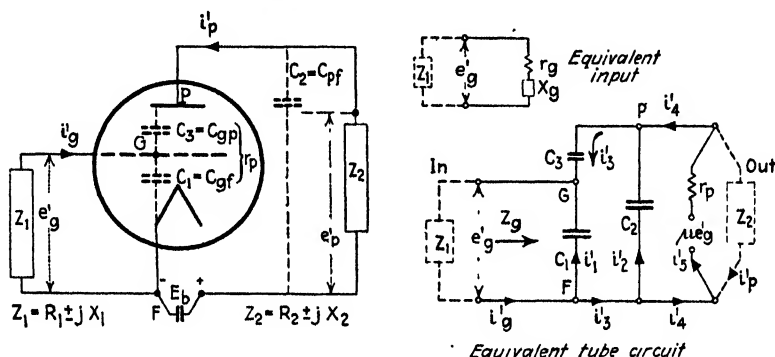


FIG. 44.—Equivalent tube circuit with impedance input and output.

input impedance Z_1 . As will be shown, even for a properly biased grid for which no grid convection current flows, an *effective* grid impedance

$$Z_g = r_g \pm jX_g \quad (62)$$

exists with an active loss or *gain* component r_g depending upon whether the effective resistance r_g has a positive or a negative value. For a negative value, regeneration takes place, since the reflection of the actions in the external plate branch Z_2 in virtue of the plate-grid capacitance increases the original grid voltage e_g . When

$$R_1 + r_g \leq 0 \quad (63)$$

sustained oscillations take place, since a negative resistance action is effective in the entire input circuit. Therefore, oscillations can also be produced through internal feedback. This is a desirable feature in

¹ NICHOLS, H. W., *Phys. Rev.*, **13**, 440, 1919; J. M. MILLER, *Bur. Standards, Sci. Paper* 351; A. S. BLATTERMANN, *Radio Rev.*, **1**, 633, 1920; S. BALLANTINE, *Proc. I.R.E.*, **7**, 129, 1919; J. H. MORECROFT, *Proc. I.R.E.*, **8**, 239, 1920.

certain circuits and the cause of trouble in amplifiers that are not properly designed.

The derivation is briefly as follows. According to Helmholtz's (generalized Kirchhoff's) laws, for the abbreviation $n = j\omega$, we have

$$\begin{aligned} \mu e_g' &= i_b' r_p + Z_2 i_p' & i_g' &= i_1' + i_3' \\ Z_2 i_p' &= -\frac{i_2'}{nC_2} & i_3' &= i_2' + i_4' \\ \frac{i_1'}{nC_1} &= \frac{i_2'}{nC_2} + \frac{i_3'}{nC_3} & i_b' &= i_p' + i_4' \\ e_g' &= \frac{i_1'}{nC_1} = i_g' Z_g \end{aligned}$$

which upon elimination of all the currents leads to Eq. (62), since

$$r_g = \frac{ac + bd}{c^2 + d^2} \quad \text{and} \quad X_g = \frac{bc - ad}{c^2 + d^2} \quad (64)$$

for

$$\left. \begin{aligned} a &= AR_2 + \frac{X_2}{\omega r_p} \\ b &= AX_2 - \frac{R_2}{\omega r_p} - \frac{1}{\omega} \\ c &= \frac{R_2}{r_p} [\mu C_3 + B] + B - \omega X_2 D \\ d &= \frac{X_2}{r_p} [\mu C_3 + B] + \omega R_2 D \\ A &= C_2 + C_3; \quad B = C_1 + C_3; \quad D = C_1 C_2 + C_1 C_3 + C_2 C_3 \end{aligned} \right\} \quad (65)$$

The effective impedance Z_g , when the filament-grid gap is considered, is then

$$Z_g = \frac{r_p A - (j/\omega)[1 + (r_p/Z_2)]}{\mu C_3 + B + (r_p/Z_2)B + j\omega r_p D} \quad (66)$$

and the power dissipated in this gap becomes

$$W_g = \frac{i_g'^2}{2} r_g = \left[\frac{e_g'}{Z_g} \right]^2 \frac{r_g}{2} = \frac{1}{2} \frac{e_g'^2 r_g}{r_g^2 + X_g^2} \quad (67)$$

Case A. The External Plate Load Is a Pure Resistance R_2 .—Then $Z_2 = R_2$, and

$$Z_g = \frac{\alpha\gamma + \beta\delta}{\gamma^2 + \omega^2\delta^2} + \frac{1}{j\omega \frac{\gamma^2 + \omega^2\delta^2}{\beta\gamma + \alpha\delta\omega^2}} = r_g + \frac{1}{j\omega C_g} = r_g - jX_g \quad (68)$$

for

$$\alpha = r_p A; \quad \beta = 1 + \frac{r_p}{R_2}; \quad \gamma = \mu C_3 + B\beta; \quad \delta = r_p D \quad (68a)$$

The internal grid-filament gap acts as a resistance r_o in series with a condenser C_o . The effective grid resistance is positive since the numerator $[\alpha\gamma + \beta\delta]$ is always positive and the grid circuit, even for a proper negative bias, dissipates the energy $0.5 \frac{r_o}{r_o^2 + X_o^2} e_o'^2$. In the low-frequency range (frequency below about 150 kc/sec) Eq. (68) can be written to a fair degree of approximation as

$$Z_o = \frac{\alpha\gamma + \beta\delta}{\gamma^2} + \frac{1}{j\omega(\gamma/\beta)} = r_o + \frac{1}{\omega C_o} \quad (68b)$$

The effective series capacitance C_o then becomes

$$C_o = \frac{\gamma}{\beta} = \underbrace{C_1 + C_3}_{\text{geometrical grid capacitance}} + \underbrace{\left(\frac{\mu R_2}{R_2 + r_p} \right) C_3}_{\text{increase of capacitance}} \quad (69)$$

According to this result and Fig. 44, it can be seen that the true grid capacitance $C_1 + C_3$, because of the back action of the external plate load R_2 , is increased to an effective value C_o , which becomes greater as the amplification factor of the tube, the load resistance R_2 , and the grid-plate capacitance become greater. For a load resistance R_2 that is very large in comparison with the internal tube resistance r_p , the increase is proportional to μC_3 , that is, to the grid-plate capacitance. Therefore, the effective input capacitance can be several times the geometrical value $C_1 + C_3$. When the external plate circuit is short-circuited ($R_2 = 0$), the remaining term $C_o = C_1 + C_3$ confirms the true grid capacitance. For very high frequencies, the terms of Eq. (68) with the factor ω^2 become significant and

$$C_o \cong \frac{\delta}{\alpha} = \frac{D}{A} = \frac{C_1 C_2 + C_1 C_3 + C_2 C_3}{C_2 + C_3} \quad (70)$$

The effective grid resistance r_o is then practically equal to zero.

Case B. The External Plate Load Is Inductive ($Z_2 = R_2 + j\omega L_2$).—The numerator $ac + bd$ of Eq. (64) for a positive value gives a positive and for a negative value a negative input resistance r_p . The latter condition produces regeneration, for which the back action of the external plate branch produces a certain voltage in phase with the original grid voltage. Since, for a positive reactance,

$$ac + bd = R_2 C_3^2 + \frac{F}{r_p} [R_2^2 + X_2^2] - \frac{X_2}{\omega r_p} \mu C_3 \quad (71)$$

for

$$F = C_3 [C_2 + \mu (C_2 + C_3)] \quad (71a)$$

The input resistance r_g is negative for $ac + bd < 0$; that is

$$\frac{\mu X_2}{\omega} > H[R_2^2 + X_2^2] + r_p R_2 C_3 \quad (72)$$

for

$$H = C_3 + \mu[C_2 + C_3] \quad (72a)$$

Hence, for $X_2 = \omega L_2$, we have

$$\mu L_2 > H[R_2^2 + \omega^2 L_2^2] + r_p R_2 C_3 \quad (73)$$

For an efficient coil loading for which $R_2^2 \ll \omega^2 L_2^2$ since $R_2 \cong 0$

$$1 > \frac{\omega^2 L_2}{H}$$

or

$$\omega < \frac{1}{\sqrt{[C_2 + C_3(1 + \frac{1}{\mu})]L_2}} \quad (74)$$

The quantity $f_0 = \omega/2\pi = 1/(2\pi\sqrt{C'L_2})$ would be the critical frequency of the variations in the tube circuit for which the resulting tube capacitance ($C' = C_2 + C_3[1 + 1/\mu]$), together with the loading L_2 , would just produce a zero input resistance r_g , while for a negative value of r_g the total reactance due to C' and L_2 , according to Eq. (74), must be *inductive*. Therefore regeneration takes place for frequencies lower than f_0 and self-oscillations for which $R_1 + r_g = 0$ can be produced only for frequencies lower than this critical value. For low frequencies, the condition required by Eq. (74) is usually satisfied; and since R_2 is small compared with ωL_2 and $R_2 \ll r_p$, the effective grid resistance r_g and input capacitance become, to a good degree of approximation,

$$\left. \begin{aligned} r_g &= -\mu \frac{L_2}{r_p} \frac{C_3}{[C_1 + C_3]^2} \\ C_g &= C_1 + C_3 \end{aligned} \right\} \quad (75)$$

If, however, the resistance R_2 is large, the value of r_g will be positive. The property of negative resistance reaction of an inductive plate load on the grid circuit is utilized in the piezo oscillator where, for the crystal connected between the grid and the filament, oscillations can exist only when the equivalent reactance of the tank circuit (Fig. 63) is inductive. As soon as the tank circuit is tuned and tends to become capacitive, the oscillations will stop. When, however, the crystal is connected between the grid and the plate and the feedback occurs through the grid-filament interelectrode capacitance, only a capacitive plate load can support oscillations.

Case C. The External Plate Load Is Capacitive ($Z_2 = R_2 - \frac{j}{\omega C_2}$).—

Since for this case $Z_2 = R_2 - jX_2$, for $ac + bd$, Eq. (64) gives positive terms which will numerically outbalance the negative terms, and r_u is always positive. A certain amount of energy will be subtracted by the grid from the source supplying the grid potential.

Case D. External Grid and External Plate Impedances.—For the circuit shown in Fig. 44, not only a reaction of the actions in the external plate branch on the grid circuit exists but also a reaction of the actions in the grid branch on the plate circuit, since

$$\left. \begin{aligned} i_u' &= j\omega C_1 e_u' + j\omega C_3 e_u' - j\omega C_3 e_p' \\ i_s' &= j\omega C_2 e_p' + \frac{e_p'}{Z_2} + j\omega C_3 e_p' - j\omega C_3 e_u' \end{aligned} \right\} \quad (76)$$

Considering the plate reaction on the grid e.m.f., we have the circuit indicated in Fig. 45, where the indicated voltages and current again denote the maximum instantaneous values. The original grid voltage e_u' then produces a potential change $\mu e_u'$ on the plate and a variable plate current $i_p = i_p' \sin \omega t$ with an amplitude given by

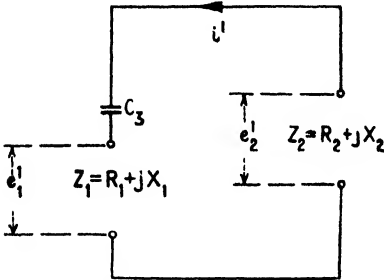


FIG. 45.—Plate reaction on grid potential.

producing a reaction voltage

$$e_2' = -Z_2 i_p' = -\frac{Z_2}{Z_2 + r_p} \mu e_u'$$

This voltage forces a current

$$i' = -\frac{e_2'}{Z_1 + \frac{1}{j\omega C_3}} = \frac{-Z_2}{[Z_2 + r_p] \left[Z_1 - \frac{j}{\omega C_3} \right]} \mu e_u'$$

back into the external grid impedance Z_1 which gives rise to a superimposed grid voltage

$$\begin{aligned} e_1' &= Z_1 i' = -\frac{Z_1 Z_2}{[Z_2 + r_p] \left[Z_1 - \frac{j}{\omega C_3} \right]} \mu e_u' \\ &= \frac{-[R_1 \pm jX_1][R_2 \pm jX_2]}{[R_2 + r_p \pm jX_2] \left[R_1 + j \left(\pm X_1 - \frac{1}{\omega C_3} \right) \right]} \mu e_u' \\ &= -[P - jQ] \mu e_u' \end{aligned} \quad (77)$$

showing again that an active component $\mu e_g' P$, which is either in phase or in antiphase with the original grid voltage e_g' , and a quadrature component $\mu e_g' Q$ are produced. Regeneration takes place when the real part is negative. The resultant grid voltage e_r' becomes

$$e_r' = e_g' + e_1' = [1 \pm \mu P] e_g' \quad (78)$$

Figure 46 shows the case where the external grid and plate impedances are coils ($Z_1 = R_1 + j\omega L_1$ and $Z_2 = R_2 + j\omega L_2$). The maximum instantaneous value e_g' again denotes the original grid voltage causing the maximum current i_g' through the grid coil which, because of the resistance R_1 , lags e_g' by somewhat less than 90 deg. The corresponding change

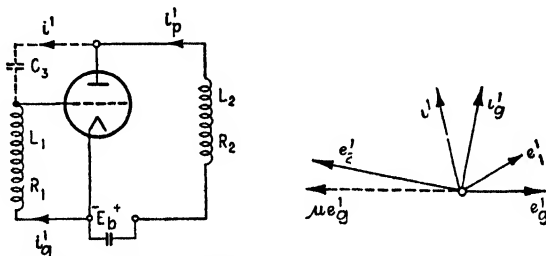


FIG. 46.—Vector diagram for coil input and coil output.

in the plate potential is $-\mu e_g'$ for no-reactance load in the external plate circuit. Hence, for a coil load ($R_2 + jX_2$), the potential e_p' is more than 180 deg out of phase and will react through the grid-plate capacitance C_3 and produce a leading current i' which has a component in phase with the original grid current. The corresponding feedback voltage e_1' shows likewise that, as a rule, a large component in phase with the original grid voltage e_g' exists, which accounts for regeneration. When the vector diagrams are drawn for either Z_1 or Z_2 or both, capacitive, no inphase components are reflected from the external plate circuit.

35. Tube Oscillator with Interelectrode Back Feed.—The circuit is the one indicated in Fig. 46. When the grid bias is sufficiently negative, $i' = i_g'$ and $i_p' = i' + i_g'$ and

$$\begin{aligned} e_p' &= e_g' - \frac{i'}{j\omega C_3}; & e_g' &= [R_1 + j\omega L_1] i_g' \\ [R_2 + j\omega L_2] i_p' &= \left[R_1 + j \left(\omega L_1 - \frac{1}{\omega C_3} \right) \right] i' \end{aligned} \quad (79)$$

But, according to Eqs. (4) and (8),

$$i_p' = g_m e_g' + \frac{e_p'}{r_p} \quad (80)$$

Combining these relations and neglecting terms which are small compared with unity, the frequency of oscillation is found to be

$$f = \frac{1}{2\pi\sqrt{[L_1 + L_2]C_3}} \quad (81)$$

Oscillations are possible for

$$[L_1 + L_2]C_3 < -\frac{L_1L_2[1 + \mu]}{[R_1 + R_2]r_p + \frac{L_2}{C_3}} \quad (82)$$

since $g_m \cdot r_p = \mu$. This relation brings out the important fact that oscillations cease to exist when the coupling capacity C_3 increases beyond a critical value.

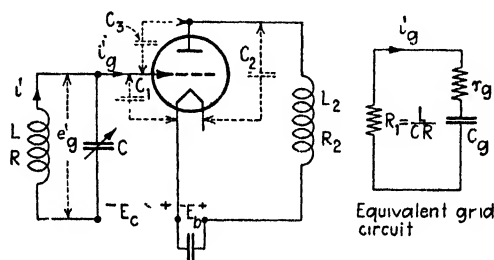


FIG. 47.—Equivalent grid circuit for tuned input and inductive plate load.

The tuned-grid circuit shown in Fig. 47, for an inductive plate load $Z_2 = R_2 + j\omega L_2$, will behave like the indicated equivalent circuit and give rise to oscillations when the negative resistance action r_p is numerically equal to L/CR or larger. For low values of L_2 or at low frequencies, Eq. (75) can be applied, and the condition for oscillation is

$$\frac{L}{CR} \leq \frac{L_2}{r_p} \frac{\mu G_3}{[C_1 + C_3]^2} \quad (83)$$

Since the reactance $1/(\omega C_g)$ of the effective grid capacitance C_g is generally very large compared with the effective grid resistance r_g ,

$$i_g' \cong \frac{C_g}{C + C_g} i'$$

and the power fed back by the plate reactance into the grid gap is

$$W_2 = \left[\frac{i_g'}{\sqrt{2}} \right]^2 r_g = \left[\frac{C_g}{C + C_g} \right]^2 \frac{r_g i'^2}{2}$$

while the power dissipated in the grid coil is

$$W_1 = \left[\frac{i'}{\sqrt{2}} \right]^2 R$$

The total power taken from the source producing the original grid voltage e_g' is therefore

$$W = W_1 - W_2 = 0.5i'^2 \left[R - \left(\frac{C_g}{C + C_g} \right)^2 r_g \right] \quad (84)$$

The criterion for the existence of oscillations, for any condition, is

$$R \leq \left(\frac{C_g}{C + C_g} \right)^2 r_g \quad (85)$$

Again making the assumption made in Eq. (83)

$$R \leq \frac{\mu L_2 C_3}{\bar{r}_p [C + C_1 + C_3]^2} \quad (86)$$

Figure 48 gives the Lorenz and the Kuehn-Huth generators based on interelectrode back coupling. Such a generator is especially good for very high frequencies and radio amateurs call it the "TNT oscillator."

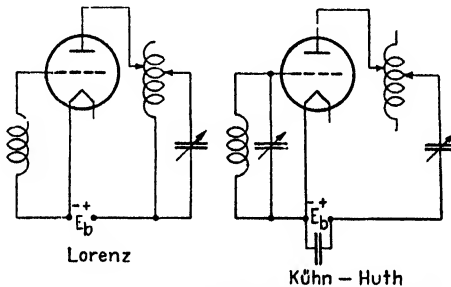


FIG. 48.—Internal feedback generators.

With all circuits which apply parallel resonance it must be remembered that for a coil (L , R) in parallel with a condenser (C) we must distinguish between three critical frequencies. The one

$$f_1 = \frac{1}{2\pi\sqrt{CL}}$$

is due to the simplified relation $\omega_1 L = 1/\omega_1 C$ for which the resistance R of the coil is assumed equal to zero and the tank circuit is not supposed to transfer any power at all to another branch. In reality the parallel combination has an effective resistance

$$R_e = \frac{1}{\omega^2 C^2 R} \cong \frac{L}{CR}$$

in series with an effective reactance $X_e = 1/(j\omega C)$ and this combination gives the pure resistance at a frequency f_2 which is slightly higher than f_1 since, for $X_e = 0$, $R_e = RL^2/(\omega^2 C^2 L^2 R^2 + R^4 C^2)$ and

$$f_2 = \frac{1}{2\pi} \sqrt{\frac{1}{CL} + \left[\frac{R}{L}\right]^2}$$

The third frequency is the isochronous frequency

$$f_3 = \frac{1}{2\pi} \sqrt{\frac{1}{CL} - \left[\frac{R}{2L}\right]^2}$$

In the case of oscillations depending on interelectrode back feed, we have several coupled oscillating circuits. There are at least two possible natural fundamental periods. As a rule, only one of the corresponding oscillations is properly fed back into the grid branch in order to be sustained. But, when the frequency of the oscillator is varied over a wide range, it may happen that the oscillation suddenly jumps to another frequency which then becomes possible. This case is discussed in detail in Sec. 39.

36. Theory of the Hartley Oscillator.—The oscillator shown in Fig. 49 is dependent partly on magnetic feedback (M) and partly on capacity

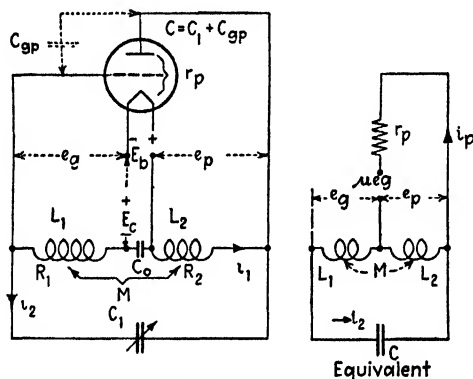


FIG. 49.—Equivalent Hartley oscillator.

feedback, the coupling capacity being $C = C_1 + C_{gp}$. It should be noted that the latter is partially due to the interelectrode capacitance between the grid and the plate. The capacitance C_0 is a large by-pass condenser for the B and C batteries. The grid is again at such a negative potential that the grid current can be neglected. The indicated voltages and currents are the instantaneous alternating-current values. According to Eq. (8) and for $n = d/dt$ and $n^2 = d^2/dt^2$, we have

$$r_p i_p = \underbrace{e_p + \mu e_g}_{\text{lumped tube voltage}} = r_p [i_1 + i_2] \quad (87)$$

where

$$\left. \begin{aligned} e_p &= -\underbrace{[R_2 + nL_2]i_1}_{\text{voltage drop across plate coil}} + \underbrace{nMi_2}_{\text{due to grid coil}} \\ e_g &= -\underbrace{[R_1 + nL_1]i_2}_{\text{voltage drop across grid coil}} + \underbrace{nMi_1}_{\text{due to plate coil}} \end{aligned} \right\} \quad (88)$$

Hence

$$r_p[i_1 + i_2] + n[L_2 + \mu M]i_1 + n[\mu L_1 + M]i_2 + R_2i_1 + \mu R_1i_2 = 0$$

or

$$\frac{i_1}{i_2} = -\frac{[r_p + \mu R_1] + n[\mu L_1 + M]}{[r_p + R_2] + n[L_2 + \mu M]} \quad (89)$$

Neglecting the drop across the biasing condenser C_0 of the batteries and realizing that grid and plate potentials are at any instant in opposition, we have

$$e_p - e_g = -\frac{i_2}{nC}$$

or

$$-R_2i_1 - nL_2i_1 - nMi_2 + R_1i_2 + nL_1i_2 + nMi_1 = -\frac{i_2}{nC}$$

Multiplying this expression symbolically by $(-n)$ yields

$$i_1[L_2 - M]n^2 + n[R_2i_1 - R_1i_2] = i_2[L_1 - M]n^2 + \frac{i_2}{C}$$

or

$$\frac{i_1}{i_2} = \frac{[L_1 - M]n^2 + nR_1 + \frac{1}{C}}{[L_2 - M]n^2 + nR_2} \quad (90)$$

By eliminating the current ratio i_1/i_2 by means of (89) and (90), putting $n = j\omega$, and realizing that R_2/r_p as well as $\mu R_1/r_p$ are negligibly small compared with unity, oscillations of frequency

$$f = \frac{1}{2\pi\sqrt{[L_1 + L_2 + 2M]C}} \quad (91)$$

occur, which, for no magnetic coupling ($M = 0$), become

$$f = \frac{1}{2\pi\sqrt{[L_1 + L_2]C}} \quad (92)$$

The condition for maintenance of oscillations is

$$\mu \geq \frac{r_p[R_1 + R_2][L_1 + L_2 + 2M]C}{[L_1 - M][L_2 + M]} + \frac{L_2 + M}{L_1 + M} \quad (93)$$

37. Effect of Grid Current in Tube Oscillators.—So far, it has been assumed that no grid current exists. But, as a matter of fact, even with a grid condenser and grid leak, a certain grid current flows. It has an effect on the constancy¹ of the frequency.

When the grid, as well as the plate, takes a convection current, we have for the resultant quantities

$$E_p = E_b + e_p$$

$$E_g = E_c + e_g$$

$$I_p = I_b + i_p$$

$$I_g = I_c + i_g$$

the two functions

$$I_p = \varphi(E_g, E_p)$$

$$I_g = \Psi(E_g, E_p)$$

When the resultant grid and plate potentials vary in such a manner that the plate current I_p remains constant, we have

$$\begin{aligned} \frac{dI_p}{dE_g} &= \frac{\partial I_p}{\partial E_g} + \frac{\partial I_p}{\partial E_p} \frac{dE_p}{dE_g} \\ &= g_m + \frac{1}{r_p}[-\mu] = g_m - \frac{\mu}{r_p} = 0 \end{aligned} \quad (94)$$

since

$$\mu = \frac{\partial I_p / \partial E_g}{\partial I_p / \partial E_p} = -\frac{dE_p}{dE_g} = g_m \cdot r_p$$

When the resultant grid current I_g is kept constant,

$$\begin{aligned} \frac{dI_g}{dE_p} &= \frac{\partial I_g}{\partial E_p} + \frac{\partial I_g}{\partial E_g} \frac{dE_g}{dE_p} \\ &= g_n + \frac{1}{r_g}[-\mu_n] = g_n - \frac{g_n \cdot r_g}{r_g} = 0 \end{aligned} \quad (95)$$

Since for constant I_g the inverse amplification factor

$$\mu_n = \frac{\partial I_g / \partial E_p}{\partial I_g / \partial E_g} = -\frac{dE_g}{dE_p} = \frac{g_n}{1/r_g}$$

¹ Martyn, D. F., *Exptl. Wireless*, **7**, 13, 1930, gives a good review of this case. Other references are J. Bethenod, *Lumière élec.*, p. 225, Dec. 18, 1916; M. Latour, *Electrician*, **45**, 280, 1916; G. VALLAURI, *L'Elettrotecnica*, **3**, 4, 1917; L. A. Hazeltine, *Proc. I.R.E.*, **6**, 63, 1918; W. H. Eccles, *Proc. Phys. Soc. London*, **32**, 92, 1920; R. A. Heising, *Proc. A.I.E.E.*, **39**, 365, 1920; I. H. Vincent, *Proc. Roy. Soc. (London) (A)*, **97**, 191, 1920; J. Edgeworth, *Jour. I.E.E.*, **64**, 349, 1926; F. B. Llewellyn, *Bell System Tech. J.*, **V**, July, 1926; K. B. Eller, *Proc. I.R.E.*, **16**, 1706, 1928. With respect to frequency constancy for variations of line voltage and temperature effects see: F. B. Llewellyn, *Proc. I.R.E.*, **19**, 2063, 1931; J. B. Dow, *Proc. I.R.E.*, **19**, 2069, 1931.

because g_n stands for the inverse mutual conductance, that is, the mutual grid conductance and r_g the internal grid resistance. Therefore, we have for the variable terms e_p , e_g , i_p , and i_g

$$i_p \cdot r_p = e_p + \mu e_g \quad (94a)$$

since a variable grid voltage e_g is equivalent to a variable voltage μe_g in the plate circuit, and

$$i_g \cdot r_g = e_g + \mu_n e_p \quad (95a)$$

since a variable voltage e_p in the plate circuit is equivalent to a voltage $\mu_n \cdot e_p$ in the grid circuit. Applying these relations in the form

$$\left. \begin{aligned} i_p &= \frac{e_p}{r_p} + \frac{\mu e_g}{r_p} = a \cdot e_p + b \cdot e_g \\ i_g &= \frac{e_g}{r_g} + \frac{\mu_n e_p}{r_g} = c \cdot e_p + d \cdot e_g \end{aligned} \right\} \quad (96)$$

to the tuned-plate oscillator indicated in Fig. 50, for $n = d/dt$, $n^2 = d^2/dt^2$, and $n^3 = d^3/dt^3$, we have

$$\left. \begin{aligned} e_g &= \underbrace{nM i_1}_{\text{voltage induced in grid coil}} - \underbrace{nL_1 i_g}_{\text{voltage drop in grid coil}} \\ e_p &= \underbrace{nM i_g}_{\text{voltage induced in plate coil}} - \underbrace{nL_2 i_1}_{\text{voltage drop in plate coil}} \end{aligned} \right\} \quad (97)$$

Eliminating i_g and i_p from (96) and (97) gives

$$cC[L_1 L_2 - M^2]n^3 i_1 + [(L_1 L_2 - M^2)(ac - bd) + L_2 C]n^2 i_1 + [aL_2 + cL_1 - M(b + d)]n i_1 + i_1 = 0 \quad (98)$$

By neglecting d in comparison with c , since the effect of the plate voltage on grid current is small, and putting

$$i_1 = i_1' \sin \omega t$$

that is, $n = j\omega$, the frequency of oscillation becomes

$$f = \frac{1}{2\pi \sqrt{CL_2 + (L_1 L_2 - M^2)/r_p \cdot r_g}} \quad (99)$$

The frequency generated, therefore, is always less than that given by the simplified relation $f_0 = 1/(2\pi \sqrt{CL_2})$ since $L_1 L_2$ is always greater than M^2 . Oscillations for small variations in the frequency are obtained when

$$M = \sqrt{\frac{r_g}{r_p} L_2 [\mu M - L_2]} \quad (100)$$

If the resistance R_1 and R_2 of the grid and plate coils are taken into consideration, the frequency of the tuned-plate oscillator becomes for $A = L_2R_1 + L_1R_2$ and $B = L_1L_2 - M^2$

$$f = \frac{1}{2\pi\sqrt{C[L_2 + (A/r_g)] + B[(1 - \mu\mu_n)/r_g \cdot r_p]}} \quad (101)$$

For a tuned-grid oscillator, we have

$$f = \frac{1}{2\pi\sqrt{C[L_1 + (A/r_p)] + B[(1 - \mu\mu_n)/r_g \cdot r_p]}} \quad (102)$$

since the condenser C is now across the grid coil L_1R_1 .

38. Stability of Frequency in Tube Generators.—Stable tube oscillations can exist only when amplitude as well as phase equilibrium prevails,

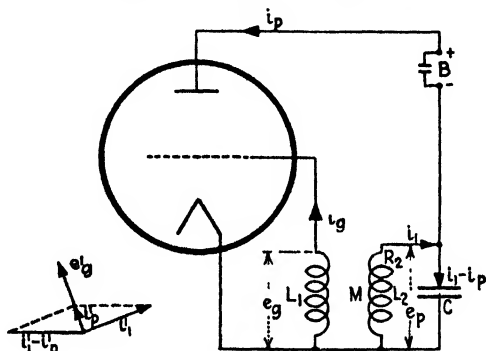


FIG. 50.—Tuned-plate oscillator (for negligible i_g).

since the amplitude of the sustained oscillations is determined by the energy (amplitude) equilibrium, and the frequency by phase equilibrium. If, for instance, the variable plate current set up by the back coupling and the resulting effect of the grid potential is out of phase with the original alternating plate current, the frequency cannot be constant. For a lagging current, returned to the plate branch, each succeeding oscillation would fall somewhat behind the preceding oscillation which would produce a lowering of the frequency. For too loose a back coupling, less amplitude would be returned than required by the previous oscillation and the variations would gradually die out, while for too much back feed growing oscillations are produced until, for reasons of saturation and energy balance, a constant amplitude equilibrium is attained. For properly designed tube oscillators, a frequency constancy of a high order can be obtained.¹ The frequency for certain cases can be constant

¹ HORTON, J. W., *Bell System Tech. J.*, 3, July, 1925; E. FROMY, *L'onde élec.*, 4, 433, 1925; J. EDGEWORTH, *loc. cit.*; K. B. ELLER, *loc. cit.*; W. LAZAREF, *Z. Hochfreq.*, 33, 55, 1929; D. F. MARTYN, *loc. cit.*; H. G. MÖLLER, "Die Elektronenröhren," Vieweg, Braunschweig, Germany, 1929; J. B. DOW, *loc. cit.*

to as close as 0.01 per cent. For the tube generator indicated in Fig. 50, the conditions for great frequency constancy are

1. The grid current as small as possible (negative bias on grid sufficiently large).
2. The filament current as low as possible.
3. The coupling between plate and grid coils not too loose.
4. The grid inductance small.
5. The supply voltage delivered by the B battery as high as the tube can stand.

The method of adjustment is, first, to produce oscillations with a certain negative grid bias and high B-battery voltage and a coupling which is not too loose. The filament current is decreased until the oscillations break off. The grid bias is then gradually changed until oscillations set in again. Hereafter the filament is again somewhat decreased.

The phase and amplitude equilibrium can be readily understood by considering a tank circuit for which a coil (L , R) and a condenser (C) are connected in parallel and the combination traversed by a variable current of instantaneous value i . Since the voltage drop around the circuit must vanish, for $n = d/dt$ and $1/n = \int dt$, we have

$$[R + nL]i + \frac{i}{nC} = 0$$

When such a combination is inserted in the external plate branch of a tube, a voltage which is proportional to i under certain conditions can be fed back and we have

$$[R + nL]i + \frac{i}{nC} = ki$$

or

$$[R - k] + \left[nL + \frac{1}{nC} \right] = 0$$

which for $k \geq R$ produces sustained oscillations whose ideal frequency $\omega_0/2\pi$ is

$$f_0 = \frac{1}{2\pi\sqrt{CL}}$$

The two equilibrium conditions then require that the voltage of reaction $e = ki$ at any instant is proportional to i and has the same frequency; that is, the amplitude must be proportional to i and e must be in phase with i . The latter condition is affected by the different branches of the tube circuit. Taking a phase difference into account, we have

$$e = \underbrace{k_1 i}_{\text{active}} + \underbrace{k_2 ni}_{\text{reactive}}$$

where k_1 is always positive and k_2 is either positive or negative depending on whether the voltage e is leading or lagging i . We then obtain

$$[R + nL]i + \frac{i}{nC} = [k_1 + nk_2]i$$

or

$$n[L - k_2] + [R - k_1] + \frac{1}{nC} = 0$$

giving a sustained oscillation of frequency

$$f = \frac{1}{2\pi\sqrt{[L - k_2]C}} \quad (103)$$

for $k_1 \geq R$. Hence, for a leading reaction voltage e , the frequency f is greater than f_0 . For e in phase with i we have, as above, $f = f_0$ and for a

lagging e.m.f. k_2 negative and $f < f_0$. Since amplitude as well as phase affects k_2 , both will influence the frequency. Therefore it can be seen that filament current (changes plate resistance r_p), B-battery voltage, coupling, resistance of coils, and grid current must have an effect on the frequency. A fairly constant frequency oscillator can therefore be obtained with the modified Meissner circuit shown in Fig. 51 for which the foregoing conditions

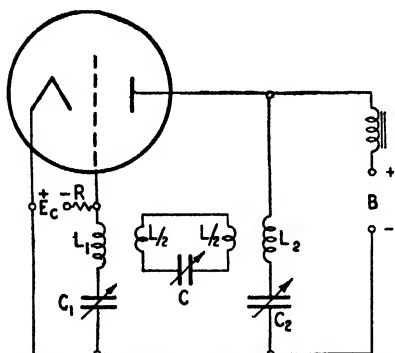


FIG. 51.—Modified A. Meissner oscillator with good frequency constancy.

are satisfied when $C_1L_1 = C_2L_2 = CL$.

The frequency is then $1/(2\pi\sqrt{CL})$. Figure 52 gives a circuit for which the oscillation frequency is also independent of the resistance since e_p and i_p are in phase.

The ideal resonance frequency of the tube oscillator shown in Fig. 50 is

$$f_0 = \frac{\omega_0}{2\pi} = \frac{1}{2\pi\sqrt{CL_2}}$$

a. First, if only the effect of the plate-coil resistance R_2 is considered and the grid current neglected, a frequency shift $\Delta f = f - f_0$ will take place, since the condition of the phase equilibrium requires a change Δf in frequency. For the maximum values of voltages and currents, we find for $n = j\omega = j2\pi f$

$$\begin{aligned} e_p' &= nMi_1' \\ e_p' &= [R_2 + nL_2]i_1' \end{aligned}$$

According to Eq. (55), the maximum value of the lumped alternating tube voltage

$$e_i' = \mu e_g' - e_p'$$

The feedback factor is then

$$Z_B = \frac{e_i'}{i_p'} = \left[\mu \frac{e_g'}{e_p'} - 1 \right] \frac{e_p'}{i_p'} = \left[\mu \frac{e_g'}{e_p'} - 1 \right] Z_2 \quad (105)$$

The effect of the grid current is at present neglected and the entire emission current is equal to the plate current. But the condition of phase equilibrium requires that e_i' be in phase with i_p' ; that is, Z_B must be a real quantity. Since

$$\frac{e_g'}{e_p'} = \frac{nM}{R_2 + j\omega L_2} = \frac{j\omega M}{R_2 + j\omega L_2}$$

Z_2 given by Eq. (104) gives upon substitution in (105)

$$Z_B = \left[\frac{j\omega M}{R_2 + j\omega L_2} - 1 \right] \frac{[R_2 + j\omega L_2]/(j\omega C)}{2L_2[\alpha + j\Delta\omega]} = \frac{j\omega[\mu M - L_2] - R_2}{j2\omega CL_2[\alpha + j\Delta\omega]} = \frac{a + jb}{2C[\alpha + j\Delta\omega]} \quad (105a)$$

for

$$a = \mu \frac{M}{L_2} - 1; \quad b = \frac{R_2}{\omega L_2} \quad (105b)$$

Hence

$$Z_B = \frac{A + jB}{2C[\alpha^2 + \Delta\omega^2]} \quad (106)$$

for

$$A = \alpha a + (\Delta\omega)b; \quad B = \alpha b - (\Delta\omega)a \quad (106a)$$

But Z_B because of the phase equilibrium must be a real quantity, which means that the imaginary term of Z_B must vanish. This happens for $B = 0$ or the shift

$$\Delta\omega = \frac{\alpha b}{a} = \frac{\alpha R_2}{\omega[\mu M - L_2]} \quad (107)$$

in the angular velocity $\omega = 2\pi f$. Since $\Delta\omega = \Delta f/(2\pi)$, the frequency deviation Δf from the ideal value $f_0 = 1/(2\pi\sqrt{CL_2})$ due to phase equilibrium is

$$\Delta f = \frac{\alpha R_2}{f[\mu M - L_2]} = \frac{R_2 \cdot \delta}{\mu M - L_2} \quad (108)$$

where δ stands for the logarithmic decrement $\delta = R_2/(2fL_2)$ of the oscillatory circuit CL_2 in the external plate circuit (Fig. 50).

b. When the effect of grid currents is taken into account, a frequency deviation Δf exists even for a tube oscillator (Fig. 52) for which phase equilibrium in the external circuit is provided. The reason for this is that, for instance, in the tuned-plate oscillator of Fig. 50 we deal with an effective grid resistance $r = e_g'/i_g'$ and the full feedback voltage nMi_1' no longer acts across the grid and the filament but only the portion

$$e_g' = \frac{r_g}{r_g + j\omega L_1} nMi_1' \quad (109)$$

Again we have an oscillation frequency $f = f_0 + \Delta f$, instead of the ideal frequency $\omega_0/(2\pi) = f_0 = 1/(2\pi\sqrt{CL_2})$. Since the grid current depends on the filament current, supply voltage of the B battery, and M , it can be minimized. The voltage $j\omega Mi_1'$ induced across the grid coil lags the current i_1' by 90 deg and for a pure ohmic grid resistance r_g is in phase with the grid current i_g' . This alternating current reacts on the plate current, which in turn affects the damping factor $\alpha = R_2/(2L_2)$ of the oscillating branch. The result is the production of a phase angle between i_p' and e_g' . Owing to phase equilibrium this angle is compensated by the change Δf in f_0 producing the frequency f .

According to Eq. (40),

$$i_1' = \frac{\sqrt{L_2/C}}{R_2} i_p'$$

and (109) becomes

$$e_g' = \frac{r_g M}{CR_2[r_g + j\omega L_1]} i_p' = \frac{M}{CR_2 \left[1 + \frac{j\omega L_1}{r_g} \right]} i_p' \quad (109a)$$

Utilizing the value of Z_2 from Eq. (104a) for $K = \frac{M}{CR_2} i_p'$ we obtain the back-feed factor

$$Z_B = \frac{K}{\left[1 + \frac{j\omega L_1}{r_g} \right] \left[1 + j\frac{\Delta\omega}{\alpha} \right]} = \frac{K}{\left[1 - \frac{\omega L_1}{r_g} \frac{\Delta\omega}{\alpha} \right] + j \left[\frac{\omega L_1}{r_g} + \frac{\Delta\omega}{\alpha} \right]} \quad (110)$$

Again the phase equilibrium requires that Z_B be a real quantity, that is, contain no imaginary terms; hence from

$$\frac{\omega L_1}{r_g} + \frac{\Delta\omega}{\alpha} = 0$$

we find the deviation Δf from the ideal frequency f_0

$$\Delta f = -\frac{\alpha f L_1}{r_g} \quad (111)$$

The percentage frequency shift is therefore

$$F\% = \frac{\Delta f}{f} 100 = -\frac{R_2 L_1}{2r_g L_2} 100 \quad (112)$$

since the damping term $\alpha = R_2/(2L_2)$. When the logarithmic decrement $\delta = \alpha/f$ is introduced, we obtain for frequency deviation the expression

$$\Delta f = -\frac{L_1}{r_g} f^2 \delta \quad (113)$$

Therefore when the effective grid resistance is $r_g = 2 \times 10^3$ ohms, $R_2 = 1$ ohm, and $L_1 = L_2 = 5 \times 10^{-3}$ henry, the percentage frequency deviation from the ideal frequency is

$$F = -\frac{10^2}{4 \times 10^3} = -0.025\%$$

For a low-frequency generator, the effective resistance R_2 is usually of much higher order on account of the required high inductance L_2 , and the percentage frequency decrease may be considerable. It is quite possible that the audio frequency is off by a large fraction of an octave. Since the grid as well as the plate resistance can be readily changed by means of the filament current, the pitch of a low-frequency generator can be easily varied by means of the filament. The frequency decreases when either the filament current is increased or the inductance M between the grid and plate coil is increased.

The effect of the alternating current in the grid branch on the decrement of tuned-plate reactance (Fig. 50), for $n = j\omega$, is determined thus

$$\left. \begin{aligned} -e_p' &= [nL_2 + R_2]i_1' - nMi_g' \\ i_g' &= \frac{e_g'}{r_g} = \frac{nMi_1'}{r_g} \end{aligned} \right\}$$

hence

$$-e_p' = \left\{ nL_2 + \left[R_2 - \frac{n^2 M^2}{r_g} \right] \right\} i_1' = \left\{ j\omega L_2 + \left[R_2 + \frac{\omega^2 M^2}{r_g} \right] \right\} i_1' \quad (114)$$

Therefore, the resistance of the plate coil, because of the grid current, is increased by the amount $\omega^2 M^2/r_g$. Hence when

$$\delta_1 = \frac{\alpha_1}{f} = \frac{R_2}{2fL_2} \quad (115)$$

denotes the logarithmic decrement per cycle when no grid current flows ($r_g = \infty$), the additional decrement δ_2 due to the energy absorbed by the grid is

$$\delta_2 = \frac{\alpha_2}{f} = \frac{\omega^2 M^2/r_g}{2fL_2} \quad (116)$$

The total effective decrement in the tuned-plate circuit when grid current is allowed to flow then becomes

$$\delta_e = \delta_1 + \delta_2 = \frac{\pi}{L_2} \left[\frac{R_2}{\omega} + \frac{\omega M^2}{r_g} \right] \quad (117)$$

If the conditions around the tuned-plate circuit are now considered, we have, for the effective resistance $R_e = R_2 + \omega^2 M^2 / r_g$ and inductance L_2 , the effective damping factor

$$\alpha = \frac{R_e}{2L_2} = \alpha_1 + \alpha_2 \quad (118)$$

Now, the ideal frequency $\omega_0 / (2\pi)$ is given by

$$\omega_0 = \sqrt{\frac{1}{CL_2}}$$

and the actual frequency $\omega / (2\pi)$ by

$$\omega = \sqrt{\frac{1}{CL_2} - \alpha^2}$$

Hence

$$\omega^2 - \omega_0^2 = -\alpha^2$$

or

$$-\alpha^2 = (\omega + \omega_0)(\omega - \omega_0) \cong 2\omega\Delta\omega$$

that is,

$$\frac{\Delta\omega}{\omega} = -\frac{1}{2} \left(\frac{\alpha}{\omega} \right)^2 = -\frac{1}{2} \left[\frac{f \cdot \delta_e}{\omega} \right]^2 = -\frac{1}{8\pi^2} \delta_e^2$$

and the percentage frequency decrease due to the total effective decrement δ_e becomes

$$F\% = 100 \frac{\Delta f}{f} = 1.27 \delta_e^2 \quad (119)$$

which shows that the frequency deviation is appreciable for larger decrements since it is proportional to δ_e^2 .

A circuit with great frequency constancy utilizes electron coupling between the oscillation generating portion of the circuit and the work circuit.¹ Such a coupling isolates the work circuit from the frequency determining portion of the tube oscillator.

39. Gradual and Abrupt Frequency Changes in Tube Oscillators.—

Even though we deal normally with sustained oscillations, the effect of coupling and tuning² plays a part in the stability and frequency of the

¹ Dow, J. B., *Proc. I.R.E.*, **19**, 2095, 1931; F. B. LEWELLYN, *Proc. I.R.E.*, **19**, 2063, 1931.

² MÖLLER, H. G., *Jahrb. drahtl.*, **16**, 402, 1920; F. HARMS, *Jahrb. drahtl.*, **15**, 442, 1920; J. S. TOWNSEND, *Rad. Rev.*, **1**, 367, 1920; H. PAULI, *Ann. Physik*, **65**, 274, 1921; W. GRÖSSER, *Arch. Elektrotech.*, **10**, 317, 1921; W. ROGOWSKI, *Arch. Elektrotech.*, **10**, 1, 15, 209, 1921; *Z. Physik.*, **3**, 135, 1922; K. HEEGNER, *Arch. Elektrotech.*, **11**, 239, 1922; **12**, 211, 1923; W. RUNGE, *Jahrb. drahtl.*, **23**, 1, 1924; *Arch. Elektrotech.*, **13**, 34, 1924; W. ALBERSHEIM, *Arch. Elektrotech.*, **14**, 23, 1924 (with many references).

oscillations. Figure 53 gives the case of a tuned-plate oscillator to which is coupled a secondary system either tuned to the natural frequency $f_1 = 1/(2\pi\sqrt{C_1L_1})$ of the plate circuit or out of tune. Then, according to the theory of coupled circuits, we have to deal with three distinctly

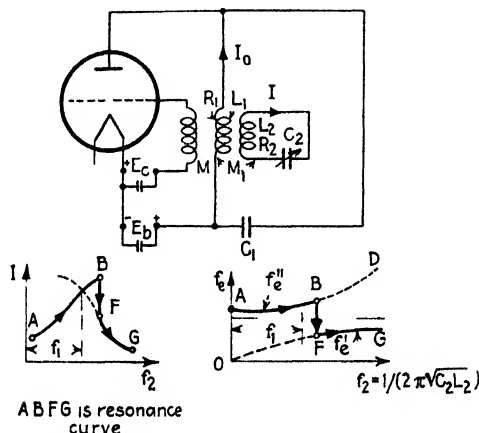


FIG 53 — f_e is effective frequency of oscillator, f_1 natural frequency of C_1L_1 and f_e of C_2L_2 (capacitance C_2 is decreased)

different frequencies even in the case of equal oscillation constants $C_1L_1 = C_2L_2$. They are

$$f_1 = \frac{1}{2\pi\sqrt{C_1L_1}} \quad \text{(natural frequency of plate circuit when oscillating alone)}$$

$$f_2 = \frac{1}{2\pi\sqrt{C_2L_2}} \quad \text{(natural frequency of coupled circuit when oscillating alone)}$$

and an effective frequency f_e when the circuits are coupled to each other. For sustained oscillations, two effective frequencies f_e' and f_e'' are possible, since for negligible resistances and $\kappa = M/\sqrt{L_1L_2}$

$$f_e = \pm \sqrt{\frac{f_1^2 + f_2^2 \pm \sqrt{[f_1^2 - f_2^2]^2 + 4\kappa^2 f_1^2 f_2^2}}{2[1 - \kappa^2]}} \quad (119a)$$

For equal oscillation constants $C_1L_1 = C_2L_2$ the two possible frequencies would be $f_e'' = f_1/\sqrt{1 - \kappa}$ and $f_e' = f_1/\sqrt{1 + \kappa}$, respectively. Therefore, when the natural frequency f_2 of the circuit carrying the effective current I is increased by gradually decreasing the setting of condenser C_2 , the effective frequency either is f_e' and varies along OFG or is equal to f_e'' varying along ABD . What actually happens for a certain degree of coupling κ is that the frequency which is measured with a loosely coupled frequency meter at first follows the heavily drawn AB curve; that is, f_e' does not exist at all. Then at B the oscillation suddenly jumps to the

frequency curve f_e' and varies with a further decrease of setting C_2 along FG . This is an essential difference between an oscillator of this type and a spark-gap oscillator-resonator system for which both coupling frequencies exist simultaneously. For such a tight coupling, the resonance curve registered by the effective current I against the setting C_2 (when plotted against decreasing values, that is, against increasing natural frequency f_2) no longer is of the normal shape but is as indicated in Fig. 53 and along $ABFG$. The frequency f_1 which corresponds to the ideal frequency of the undisturbed oscillator then corresponds no longer to a maximum current indication, but to a frequency corresponding to points B and F which is greater than f_1 . A similar but not identical

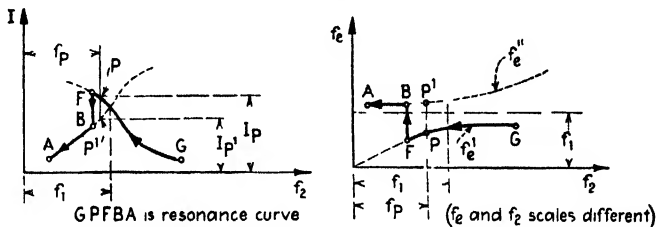


FIG. 54.—Condition when C_2 of Fig. 53 is increased

action takes place when the natural frequency f_2 is decreased from some higher value as is shown in Fig. 54. The effects indicated in Figs. 53 and 54 are experimental facts. Since at B the frequency jumps abruptly to the other possible coupled-circuit frequency, an unstable condition must exist. This is especially noted when, for a certain natural frequency $f_2 = f_P$ (Fig. 54) obtained by increasing the condenser capacity C_2 to a value which produces a natural frequency $f_P < f_1$, the circuit is opened and closed again. With the closing of the circuit, the oscillator current will not be I_P as before, but only I_P' . The reason is that the effective frequency f_e' corresponding to point P is not stable but obtained only by "drawing or pulling along" the oscillation produced by the tube. Hence, after the oscillation is keyed or interrupted, the more stable frequency f_e'' will exist in this particular case. Inasmuch as the experiment shows that either the effective frequency f_e' (before keying) or f_e'' (after keying) is in this particular case possible, the condition of the coupled-circuit system

$$\left. \begin{aligned} g_m &\geq C_e R_e + \frac{L_e}{r_p} \\ M &\geq C_e \frac{r_p}{\mu} \left[R_e + \frac{L_e}{r_p C_e} \right] \end{aligned} \right\} \quad (120)$$

must be satisfied. Herein M denotes the mutual inductance between grid and plate coils of proper polarity and R_e , C_e , L_e the effective constants

of the external plate circuit C_1L_1 . For such a condition the damping factor of Eq. (24) on page 74 vanishes. The negative resistance reaction

$$\frac{L_e + \mu M}{r_p C_e}$$

fed back into the external plate circuit either neutralizes or outbalances the positive resistance R_e . By means of the generalized¹ impedance

$$Z_e = R_1 + nL_1 + \frac{1}{nC_1} + \frac{[nM_1]^2}{nL_2 + 1/(nC_2)}$$

around the external plate branch C_1, L_1, R_1 when supplying energy to the coupled circuit C_2, L_2, R_2 , it can be shown that, for sustained oscillations ($n = j\omega$), the effective equivalent-circuit constants are

$$\left. \begin{aligned} R_e &= R_1 + AR_2 \\ L_e &= L_1 - AL_2 \\ C_e &= \frac{C_1 C_2}{C_2 - AC_1} \end{aligned} \right\} \quad (121)$$

for

$$A = \frac{[\omega_r M]^2}{[\omega L_2 - 1/(\omega C_2)]^2 + R_2^2} \quad (121a)$$

The external plate circuit $C_1L_1R_1$ and its coupled circuit $C_2L_2R_2$ have an equivalent circuit which can be thought of as made up of an effective resistance R_e and an effective inductance L_e' for which

$$\left. \begin{aligned} R_e &= R_1 + AR_2 \\ L_e' &= [L_1 - 1/(\omega^2 C_1)] - A[L_2 - 1/(\omega^2 C_2)] \end{aligned} \right\} \quad (122)$$

For resonance ($\omega/(2\pi) = \omega_r/(2\pi) = f_r$) the reactance $\omega_e L_e'$ must vanish. From Eqs. (121) and (122) it is evident that for $f_2 > f_1$ the effect on the C_1L_1 circuit is as though an inductance were added and the effective frequency f_e made smaller than f_1 . The opposite happens for $f_2 < f_1$. This can also be understood from the following reasoning. When the secondary circuit C_2L_2 is tuned, it acts like an ohmic resistance. But when C_2 is somewhat decreased, the natural frequency f_2 becomes higher and the circuit acts like a condenser. Therefore the current I leads the resonance current, and the voltage ωMI induced in the external plate circuit must also lead. But this means the current produced by it lags behind this voltage and the effect is as though an inductance were inserted in the C_1L_1 circuit. In the same way it is evident that for condenser settings C_2 which make $f_2 < f_1$ the effect on the external plate circuit is as though a small capacitance ΔC were inserted in series with

¹For details: Hochfrequenzmesstechnik, 2d ed., Chap. XXV, Springer, Berlin, 1928.

the condenser C_1 . Hence the effective frequency f_e is no longer equal to f_1 but $f_e > f_1$ since $C_e' = (C_1 \cdot \Delta C)/(C_1 + \Delta C)$; that is, $C_e' L_1 < C_1 L_1$.

The effect of circuit C_2, L_2, R_2 on the natural frequency f_1 of the C_1, L_1, R_1 circuit (Fig. 53) can therefore be calculated. If I_0 and I denote the effective currents flowing through coils L_1 and L_2 , respectively, and I_0 and I their vectors, the voltage induced across L_2 is $E = j\omega_e M_1 I_0$. The current flowing in the coupled circuit is

$$I = \frac{E}{2L_2[\alpha_2 + j\Delta\omega]}$$

where $\alpha_2 = R_2/(2L_2)$ and $\Delta\omega = \omega_e - \omega_2$. This current reacts again on the primary coil L_1 inducing the back voltage $E_1 = -j\omega_e M_1 I$. The impedance reflected back into the primary circuit then becomes

$$Z_B = \frac{E_1}{I_0} = \frac{\omega_e^2 M_1^2}{2L_2[\alpha_2 + j\Delta\omega]} = \frac{\omega_e^2 M_1^2}{2L_2[\alpha_2^2 + \Delta\omega^2]} \alpha_2 - j \frac{\omega_e^2 M_1^2}{2L_2[\alpha_2^2 + \Delta\omega^2]} \Delta\omega = \frac{\Delta R_1 + j\omega \Delta L_1}{\alpha_2^2 + \Delta\omega^2} \quad (123)$$

This equation expresses in a more convenient form the result of Eq. (122). For resonance $\Delta\omega$ must vanish and the impedance reflected back into the primary circuit becomes the pure resistance $\Delta R_1' = \omega_e^2 M_1^2 / R_2$. The inductance reflected back into the $C_1 L_1$ circuit for any other condition is

$$\Delta L_1 = - \frac{\omega_e M_1^2}{2L_2[\alpha_2^2 + \Delta\omega^2]} \Delta\omega \quad (124)$$

and the effective frequency becomes

$$f_e = \frac{1}{2\pi\sqrt{C_1[L_1 + \Delta L_1]}} \quad (125)$$

We have, for different degrees of coupling between the $C_1 L_1$ and $C_2 L_2$ circuit, the resonance curves indicated in Fig. 55. The upper representation (a) gives the true resonance curve and the current maximum corresponds to $f_e = f_e' = f_e'' = f_1$. For representations b, c, and d, the mutual inductance M_1 (Fig. 53) increases for each successive illustration; mutual inductance M between grid and plate coil is of such a magnitude as to keep the circuit in a state of oscillation at all times. For case b, the maximum current setting is much sharper and still indicates the actual frequency $f_e = f_e' = f_e'' = f_1$ since only the side portions of the resonance curve are, it might be said, curved in because of the interaction of the circuits. This curve could not be used to read off values in order to determine the logarithmic decrement. With M_1 still more increased as for c and d, the left and right branches of the original resonance curve are unequally distorted and either cut through each other or give an overlap without intersection, respectively. The circuits then can be made to drag the

oscillations along (pulling or drawing effect) beyond the natural frequency f_1 of the tube oscillator for decreasing C_2 settings and below the value f_1 for increasing C_2 settings. This "drawing" of the oscillation can be carried on only until a critical setting of C_2 is obtained, since then the

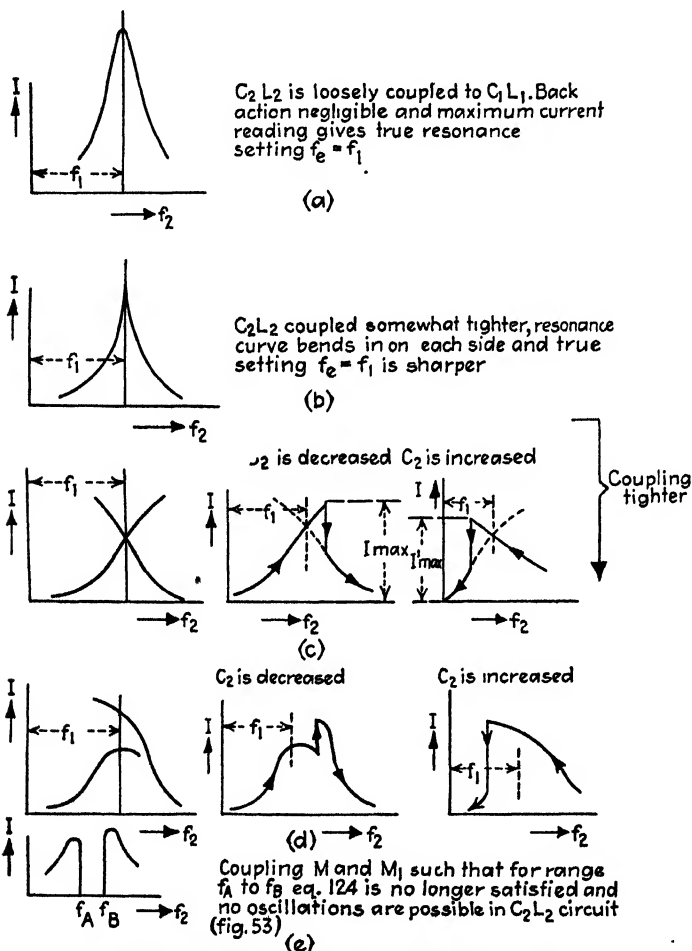


FIG. 55.—Resonance curves for coupled-tube generator.

oscillation suddenly jumps on to one of the other possible coupling frequencies. The critical setting of C_2 for which an abrupt change in the effective current takes place is by no means the same for increasing C_2 as for decreasing C_2 settings. As a rule, the maximum settings I'_{\max} and I_{\max} have not the same value and under no circumstances indicate circuit resonance. This is again entirely different from the case with damped oscillations in coupled circuits for which the two current maxima indicate

the actual resonance conditions for the two coupling frequencies which occur simultaneously. Case *d* with a still tighter coupling M_1 gives two different maxima for decreasing C_2 settings and another different maximum setting for increasing values of C_2 . Case *e* illustrates the condition for which the two critical settings of C_2 , corresponding to frequencies f_A and f_B , are determined by the limiting condition of Eq. (120). There exists quite a range of C_2 settings for which the tube refuses to oscillate. By varying the coupling M , the range $f_B - f_A$ can as a rule be decreased to zero and even be driven so far beyond this point as to obtain phenomenon as indicated in *d* and *c*. From this it is evident that cases *c*, *d*, and *e* are of no use when measuring the actual frequency of a tube generator. They explain, however, many difficulties experienced with step-over resonators, and the tuned-plate, tuned-grid tube generators. It is of interest now to find out, for instance, why for decreasing values of C_2 (Fig. 53) the frequency f_e varies along the f_e'' curve and then suddenly at *B* jumps over to point *F* in order to proceed along the f_e' curve. Equation (119a) gives

$$[1 - \kappa^2]f_e^4 - [f_1^2 + f_2^2]f_e^2 + f_1^2f_2^2 = 0$$

or

$$\left[1 - \frac{f_1^2}{f_e^2}\right] \left[1 - \frac{f_2^2}{f_e^2}\right] = \kappa^2 = \frac{M^2}{L_1L_2} \quad (126)$$

When plotting (Fig. 56) f_e^2 against the square of the natural frequency f_2 of the secondary circuit, we obtain a hyperbola with the asymptotes

$$1 - \frac{f_1^2}{f_e^2} = 0 \quad \text{and} \quad 1 - \frac{f_2^2}{f_e^2} = 0 \quad (126a)$$

The first parentheses gives $f_e^2 = f_1^2$, an asymptotical line which is parallel with the $f_2^2 =$ axis, while the other parenthesis yields the equation of the other asymptote which, since $f_e^2/f_2^2 = 1$, must make an angle of 45 deg with both the f_e^2 - and the f_2^2 -axis. The upper branch *AA'* of the hyperbola starts closest to the line $f_e^2 = f_1^2$ corresponding to the natural frequency of the tube oscillator when not coupled to C_2L_2 . Oscillations with gradually increasing settings of f_2 must therefore start along this branch since then the lowest impedance is offered. The opposite is true when the resonance setting C_2 of circuit C_2L_2 makes the secondary circuit capacitive and the frequency f_2 is gradually lowered since the lower branch *B'B* is the path along which the frequency f_e^2 varies. For any frequency $f_2^2 = OP$, the ordinates *PA* and *PB* are proportional to squares of possible frequencies f_e'' and f_e' , while *Pa* and *Pb* are the values for $M_1 = 0$.

If both (f_e' and f_e'') are possible according to Eq. (120), for possible values which are relatively close together, the stable frequency is the one

that produces the smallest amplitude. It is the one that will be obtained after keying the circuit, that is, after interrupting the oscillation that was "drawn along" and closing the circuit again. However, if the two possible frequencies f_e' and f_e'' differ greatly from each other, the most stable oscillation is that which builds up to the final amplitude most rapidly. The reason why the secondary current I suddenly jumps from B to F (Figs. 53 and 54) is that the natural impedances of C_1L_1 and C_2L_2 are quite different from that of C_2L_2 . Consequently the instability becomes so pronounced that the oscillation changes suddenly so that it can build up the more stable oscillation.

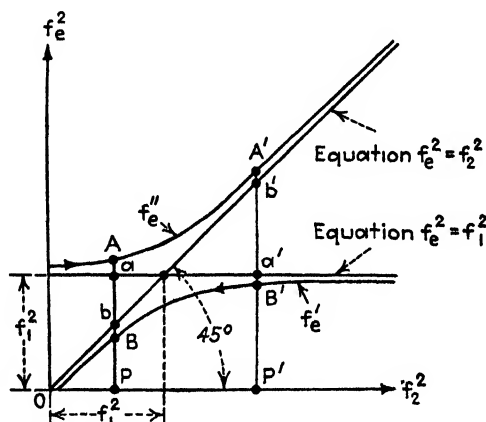


FIG. 56.—Theoretical explanation of the experimental phenomena of Figs. 53 and 54.

The equation of the so-called "resonance curve," according to Fig. 53, is

$$I = \frac{\omega_e M_1 I_0}{\sqrt{R_2^2 + \left[\omega_e L_2 - \frac{1}{\omega_e C_2} \right]^2}} \quad (127)$$

if I_0 and I denote the effective values of current which flow through coils L_1 and L_2 , respectively. It can be seen that, for mutual inductances M_1 which transfer considerable energy to the secondary (C_2L_2), the back action of current I changes the impressed angular velocity ω_e as well as I_0 . Therefore the plot of I against C_2 cannot give the shape of the ordinary resonance curve. For such work it is convenient to plot (as in Fig. 57) the ratio $(I/I_0)^2$ against the ratio of the change in frequency $\Delta f = f_e - f_2$ to the damping factor $\alpha_2 = R_2/(2L_2)$ of the secondary circuit since, from Eq. (127), we find

$$\left[\frac{I}{I_0} \right]^2 = \frac{\omega_e^2 M_1^2}{R_2^2 + [\omega_e L_2 - 1/(\omega_e C_2)]^2} = \frac{L_1}{L_2} \frac{[\kappa/\alpha_2]^2}{1 + [\Delta\omega/\alpha_2]^2} \quad (128)$$

where κ denotes the coupling factor $M_1/\sqrt{L_1L_2}$. In Fig. 57, curve 1-A-1 indicates the case of a very loose coupling and curve 2-A-2 the critical condition for somewhat tighter coupling, when actual resonance is still indicated by a sharp maximum value. Curves 3-A'-B give the case of much tighter coupling for which the two branches of the apparent resonance curve cross each other at A'. Here the maximum readings corresponding to points B indicate only the conditions for which the oscillation ceases in order to jump suddenly to an oscillation at the more stable coupling frequency. These conditions can also be understood from frequency curves of Fig. 56.

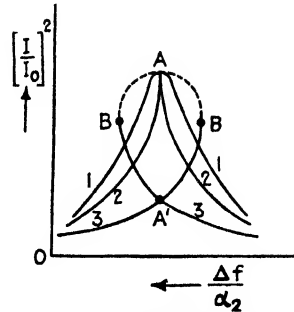


FIG. 57.—Substitute resonance curves for coupling effect to tube oscillators.

Since the resistance reflected back into the C_1L_1 circuit, according to (121), is

$$\Delta R_1 = \frac{\omega_e^2 M_1^2}{[\omega_e L_2 - 1/(\omega_e C_2)]^2} R_2$$

if R_2^2 is neglected and, according to (126),

$$[C_1 L_1 \omega_e^2 - 1][C_2 L_2 \omega_e^2 - 1] = M_1^2 C_1 C_2 \omega_e^4$$

we obtain

$$\Delta R_1 = \frac{\omega_e^4 M_1^2 C_2^2}{[C_2 L_2 \omega_e^2 - 1]^2} R_2 = \frac{C_2 C_1 L_1 \omega_e^2 - 1}{C_1 C_2 L_2 \omega_e^2 - 1} R_2 = \frac{L_1 f_e'^2 - f_1^2}{L_2 f_e'^2 - f_2^2} R_2 = \frac{L_1 Aa}{L_2 Ab} R_2 \quad (129)$$

because, for the f_e'' branch of the hyperbola of Fig. 56, we have $f_e'^2 = PA$; $f_1^2 = Pa$; $f_2^2 = Pb$; $PA - Pa = Aa$; and $PA - Pb = Ab$. Hence ΔR_1 is comparatively small when the natural frequency f_2 of the secondary circuit is smaller than the natural frequency f_1 of the C_1L_1 circuit ($f_2^2 < f_1^2$ in the figure) since Aa/Ab is small. Hence the increase of primary resistance cannot be very large. But, for f_2 much larger than f_1 the ratio Aa/Ab is no longer a small fraction and the effective resistance $R_e = R_1 + \Delta R_1$ can become large enough so that the condition of Eq. (120) is no longer satisfied. Then the oscillation of frequency f_e'' will cease and jump to an oscillation of frequency f_e' , since the corresponding ratio $B'a'/B'b'$ is again a small quantity.

40. Synchronization of Tube Generators.—Unlike alternators, tube generators give rise to automatic¹ synchronization. The reason for this

¹ VINCENT, I. H., *Proc. Phys. Soc. London*, **32**, Part 2, 84, 1919; H. G. MÖLLER, *Jahrb. drahtl.*, **17**, 256, 1921; E. V. APPLETON, *Proc. Cambridge Phil. Soc.*, **21**, Part 3, 231, 1922; J. GOLZ, *Jahrb. drahtl.*, **19**, 281, 1922; F. ROSSMANN and J. ZENNECK, *Jahrb. drahtl.*, **23**, 47, 1924; B. VAN DER POL, *Phil. Mag.*, **3**, 65, 1927.

is that the maintenance of oscillations depends upon a certain relation connecting the circuit constants. These constants are greatly affected when a tube oscillator is influenced by oscillations of another source near resonance. Thus one tube can be operated so that its frequency is controlled, through a certain range of variation of its own circuit constants, by the output of another oscillator. The first oscillator is then said to be operating in the "zero-beat note" or silent region and variations of its capacitance, or inductance can, within this region, produce only a 180-deg phase shift. The (frequency) width of the silent region depends on the relative amplitude of the oscillations due to each of the two tube generators. Such automatic synchronization plays a part in autodyne

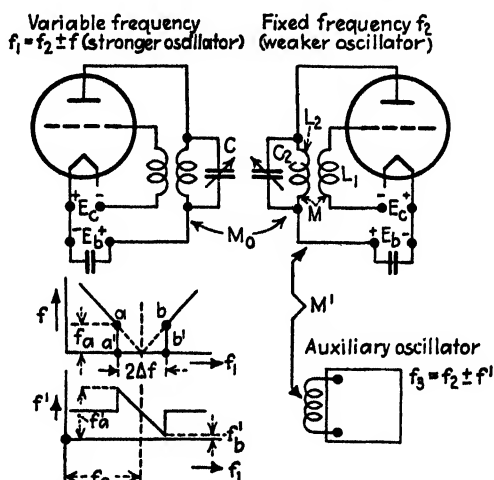


FIG. 58.—Automatic synchronization ($2\Delta f$ silent region, f_0 true resonance).

reception for which the detector acts as a generator. Near the zero-beat region, the detector will be controlled by the frequency of the other generator. A silent region exists whether the weaker oscillator is affected by an induced external e.m.f. in the grid coil L_1 or an induced e.m.f. in the plate coil L_2 (Fig. 58). Also, the phase shift of the current in the weaker circuit with respect to that of the strong oscillator which takes place when C_2 is varied within the silent region is about 180 deg for either case. But true resonance (f_0) takes place in case of pick-up by means of the grid coil at 0 deg, and in case of pick-up by means of the plate coil at 90 deg. What happens can be readily understood from the arrangement shown in Fig. 58. When the frequency f_1 of the stronger oscillator is varied, by means of the setting of the condenser C , in the neighborhood of the fixed frequency f_2 of the weaker oscillator, a beat tone of frequency $f = f_1 - f_2$ will be noticed in a telephone receiver inserted at a suitable place in the circuit of the weaker oscillator. But there is

complete silence for a region $2\Delta f$ since the weaker oscillator is completely controlled by the frequency f_1 and, so to speak, acts like an amplifier. That this is true can be checked by an auxiliary oscillator of fixed frequency f_3 which produces a beat tone $f' = f_3 - f_2$ of unchanged frequency in a telephone receiver inserted in the auxiliary circuit for all C settings of the stronger oscillator which do not correspond to the silent region $2\Delta f$. The frequency f_3 must be chosen so high that no synchronizing effect exists between the weaker oscillator and the auxiliary oscillator.

Now, as soon as the weaker oscillator produces a beat note $f = f_a$ near the point a of the characteristic, the tone is apt to disappear suddenly since for point a the frequency jumps to the position a' . At the same time the pitch of the tone observed in the receiver in the auxiliary oscillator changes to a value $f' = f'_a$, indicating that another frequency now exists in the weaker circuit. Upon changing the setting C further, the beat frequency f' varies almost linearly to a value f'_b until suddenly the weaker circuit, which acts as an amplifier for region $2\Delta f$, again starts to build up oscillations corresponding to its own circuit constants. The silent region corresponding to the range $2\Delta f$ becomes wider the looser the coupling M between L_1 and L_2 and the larger the amplitude of the induced voltage due to the other oscillator.

The nonexistence of self-excited oscillations in the C_2L_2 branch can be explained by means of the dynamic grid-voltage plate-current characteristic indicated in Fig. 59. When the oscillator C_2L_2 produces self-oscillations (beyond range $2\Delta f$), the steepness AB satisfies the condition [Eq. (120)] for sustained oscillations since the effective circuit constants give

$$g_m = C_e R_e + \frac{L_e}{r_p}$$

The effect of the forced oscillations due to the generator of frequency f_1 is of little importance since only a small amplitude effect occurs when f_1 is very different from f_2 . But as f_1 approaches the frequency f_2 , the circuit C_2L_2 is more nearly tuned to the forced frequency and the self-oscillation becomes modulated and as such reacts on the grid e.m.f., giving, in addition to the component e_2 , which is only due to self-oscillations, also a component e_1 which is due to the stronger oscillator. The

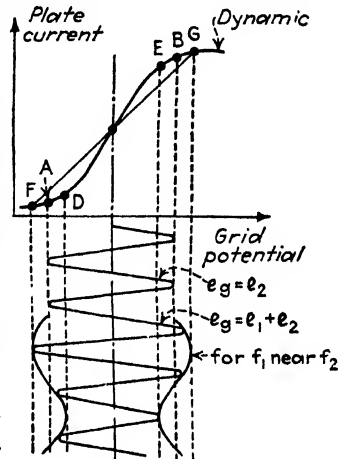


FIG. 59.—Grid swing for automatic synchronization.

average mutual conductance \bar{g}_m corresponds to a slope somewhere between DE and FG , that is, a smaller steepness than g_m . But g_m is that steepness given by AB for which sustained oscillations are just possible; hence the

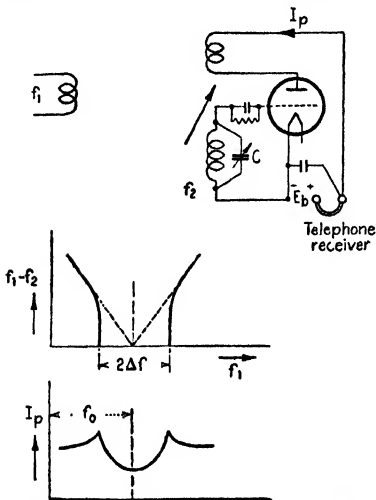


FIG. 60.—Autodyne reception utilizing synchronization.

circuit stops producing self-oscillations and amplifies the forced oscillations due to the other oscillator only. When C_2 is varied corresponding to range $2\Delta f$, the frequency is not affected, but only the phase of the induced oscillation with respect to the phase of the current in the stronger oscillator undergoes a change. This explanation has a direct bearing upon autodyne reception where e_1 is directly impressed on a receiving tube which acts as a rectifier and oscillator. The circuit is then as in Fig. 60. From the foregoing explanations it will be evident that the law of superposition does not hold if a tube is affected, in addition to its self-oscillation, by a forced

oscillation, since the effective decrement undergoes a change.

In Fig. 61, ψ denotes the phase displacement between the oscillation of a generator of frequency f_1 and the oscillation in a circuit C_2L_2 which

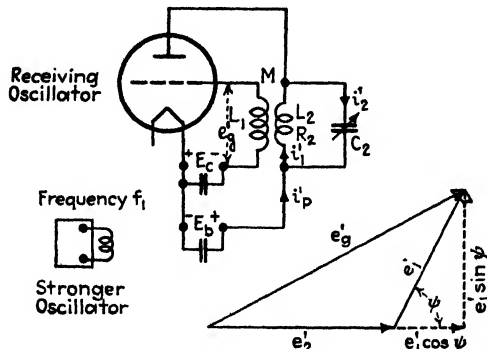


FIG. 61.—Phase angle ψ for detuning $f_1 - f_2$.

is detuned so that $\Delta f = f_1 - f_2$. All voltages and currents in this figure again denote the maximum alternating values. The quantity e_v' denotes the resultant grid voltage due to the back feed which is

$$e_v' = j\omega_1 M i_1'$$

and is due to the voltage e_1' induced across the grid coil by the oscillator

of frequency f_1 . The greatest detuning Δf for which the receiving circuit is still controlled by the stronger oscillator occurs for $\sin \psi = 1$ and this detuning corresponds in Figs. 58 and 60 to half the silent region. Therefore it is only necessary to obtain an expression for $\sin \psi$ which connects the circuit constants of the receiver with the amplitudes of the impressed external voltage and the e.m.f. fed back by means of M . We have

$$\begin{aligned} i_p' &= i_1' + i_2' \\ i_1'[R_2 + j\omega_1 L_2] &= \frac{i_2'}{j\omega_1 C_2} \end{aligned}$$

and, upon elimination of i_2' ,

$$i_1' = \frac{i_p'}{j\omega_1 C_2 [R_2 + j\omega_1 L_2] + 1} = \frac{i_p'}{j\omega_1 C_2 R_2 [1 + j(\Delta\omega/\alpha)]} \quad (130)$$

for $\Delta\omega = \omega_1 - \omega_2$ and $\alpha = R_2/(2L_2)$, since

$$\begin{aligned} j\omega_1 C_2 [R_2 + j\omega_1 L_2] + 1 &= j\omega_1 C_2 R_2 \left\{ 1 + \frac{1}{R_2} \left[j\omega_1 L_2 + \frac{1}{j\omega_1 C_2} \right] \right\} \\ &= j\omega_1 C_2 R_2 \left\{ 1 + j \frac{\omega_1 L_2}{R_2} \left[1 - \frac{1}{\omega_1^2 C_2 L_2} \right] \right\} \\ &= j\omega_1 C_2 R_2 \left\{ 1 + j \frac{\omega L_2}{R_2} \left[1 - \frac{\omega_2^2}{\omega_1^2} \right] \right\} \\ &= j\omega_1 C_2 R_2 \left\{ 1 + j \frac{\omega L_2}{R_2} \left[\frac{[\omega_1 + \omega_2][\omega_1 - \omega_2]}{\omega_1^2} \right] \right\} \\ &\cong j\omega_1 C_2 R_2 \left\{ 1 + j \frac{\omega_1 L_2}{R_2} \left[\frac{2\omega_1 \cdot \Delta\omega}{\omega_1^2} \right] \right\} \\ &= j\omega_1 C_2 R_2 \left\{ 1 + j \frac{2L_2}{R_2} \Delta\omega \right\} \end{aligned}$$

Hence

$$e_u' = e_1' + e_2' = e_1' [\cos \Psi + j \sin \Psi] + \frac{M i_p'}{C_2 R_2 [1 + j(\Delta\omega/\alpha)]} = a + j b \quad (131)$$

for

$$\begin{cases} a = e_1' \cos \Psi + \frac{M i_p'}{c} \\ b = e_1' \sin \Psi - \Delta\omega \frac{M i_p'}{\alpha \cdot c} \\ c = C_2 R_2 \left[1 + \left(\frac{\Delta\omega}{\alpha} \right)^2 \right] \end{cases} \quad (131a)$$

The phase displacement θ between the resultant grid voltage e_u' and the plate current is then, according to (131),

$$\theta = \tan^{-1} \frac{b}{a} \quad (132)$$

But the alternating plate current i_p' must be in phase with the resultant grid voltage e_g' ; that is, θ must vanish. This occurs when $b = 0$, or

$$\sin \Psi = \frac{\Delta\omega \cdot M \cdot i_p'}{\alpha \cdot c \cdot e_1'} \quad (133)$$

which is the relation for the phase shift Ψ in the silent region. Since this region, for properly adjusted receivers, is small, $[\Delta\omega/\alpha]^2$ can be neglected in comparison with unity and

$$\sin \Psi \cong 2\pi \frac{\Delta f \cdot M \cdot i_p'}{\alpha C_2 R_2 e_1'} \quad (133a)$$

The angle $\Psi = 90^\circ$ is the angle for which the source of frequency f_1 just controls the frequency of the weaker oscillator. For $\sin \Psi = 1$ this gives the amount of detuning Δf

$$\Delta f = \frac{\alpha \cdot C_2 \cdot R_2 \cdot e_1'}{2\pi M \cdot i_p'} \quad (134)$$

from the position of true resonance. $2\Delta f$ or

$$S = \frac{\alpha C_2 R_2 e_1'}{\pi M i_p'} \quad (135)$$

corresponds to the entire silent region for which the receiver is completely controlled by the oscillator of frequency f_1 . It is noted that the width of this region is proportional to the induced grid voltage due to the external stronger oscillator and inversely proportional to the amplitude of the plate current. The width is also directly proportional to the damping factor $\alpha = R_2/(2L_2)$ and inversely proportional to the mutual inductance M between the grid and the plate coil. Since, for resonance, the plate circuit acts like a resistance $L_2/(C_2 R_2)$ and $e_p' = [L_2/(C_2 R_2)]i_p'$, for small silent regions we have the approximate formula

$$S \cong \frac{R_2 \cdot e_1'}{2\pi M e_p'} \quad (135a)$$

41. Notes on Harmonics in Tube Generators.—Considering the tuned-plate oscillator shown in Fig. 37, for the vector values of the alternating currents we have

$$I_p = I_1 + I_2$$

and from

$$I_1[R + j\omega L] = \frac{I_2}{j\omega C}$$

the relation for the coil current in the plate circuit

$$I_1 = \frac{I_p}{1 + j\omega C[R + j\omega L]}$$

which for the logarithmic decrement $\delta = 2R/(fL)$ and $\omega^2 CL = f^2/f_0^2 = \rho$ leads to

$$I_1 = \frac{I_p}{1 - \rho + j(\delta/\pi)\rho} \quad (136)$$

since $f_0 = 1/(2\pi\sqrt{CL})$ and $\omega CR = \rho\delta/\pi$. Calling $f = pf_0$ the frequency of any harmonic ($p = 1, 2, 3, 4, 5$, etc.) of the distorted current of fundamental frequency f_0 , we find the ratio

$$\frac{I_p'}{I_1} = 1 - p^2 + j\frac{p^2\delta}{\pi} \quad (137)$$

If the decrement of the CL circuit is neglected, the ratio of the corresponding effective values becomes

$$\frac{I_p}{I_1} = 1 - p^2 \quad (138)$$

Hence, if all harmonic components in the plate current I_p had the same intensity, for the double-frequency term ($p = 2$) we should have a coil current of only ${}_2I_1 = I_p/3$, for the triple frequency ${}_3I_1 = I_p/8$, for the fourth harmonic ${}_4I_1 = I_p/15$. However, the harmonic components in the plate current do not have the same intensities but have amplitudes which become smaller as the order of the harmonic increases. Hence, if the amplitude of the fundamental current in I_p has an amplitude equal to unity, that of the second 30 per cent of it, that of the third 20 per cent, and that of the fourth 5 per cent of the fundamental, we see that for the double-frequency term the coil current is only ${}_2I_1 = I_p/6$, for the triple frequency ${}_3I_1 = I_p/24$, and for the fourth harmonic ${}_4I_1 = I_p/300$, while the fundamental component for such an ideal case ($\delta = 0$) would produce an infinite current through the coil since $1 - p^2 = 0$. But because of the finite decrement δ of the CL circuit, such a fundamental current is never obtained through L since, according to Eq. (137), the ratio becomes

$$\frac{I_p}{I_1} = \sqrt{[1 - p^2]^2 + \left[\frac{p^2\delta}{\pi}\right]^2} \quad (139)$$

If the ratio δ/π is $\frac{1}{20}$, the fundamental coil current becomes

$$I_1 = \frac{I_p}{(\delta/\pi)p^2} = 20I_p$$

since $p = 1$. Hence, if the intensity of the second harmonic in I_p is as strong as 50 per cent, that is, $I_p/2$, the current of the second harmonic through L , according to Eq. (139), is only

$${}_2I_1 = \frac{I_p}{\sqrt{[1 - p^2]^2 + \left[\frac{\delta}{\pi}p^2\right]^2}} = \frac{I_p}{\sqrt{[1 - 4]^2 + \left[\frac{1}{20^4}\right]^2}} = \frac{I_p}{\sqrt{9.04}} \cong \frac{I_p}{3}$$

which still shows that, even with such a large decrement $\delta = \pi/20$, the effect of the second harmonic is small. For smaller decrements the harmonic content in I_1 is still more suppressed. When the plate current I_p is of rectangular form, only odd harmonics are possible and the equation for the plate current is expressed by

$$\frac{I_s}{2} + \frac{2}{\pi} I_s \sin \omega t - \frac{2}{3\pi} I_s \sin 3\omega t + \frac{2}{5\pi} I_s \sin 5\omega t \quad (140)$$

if I_s denotes the saturation current. The amplitudes of the fundamental, third, fifth, seventh, etc., harmonic current in I_p are then in the ratio $1:\frac{1}{3}:\frac{1}{5}:\frac{1}{7}$, etc. The amplitude of the third harmonic of the coil current is only one seven-hundred-fiftieth and that of the fifth only one three-thousand-two-hundred-fiftieth of the amplitude of the fundamental if a decrement $\delta = 0.04\pi$ is assumed. The effect of the harmonic content is therefore less than 1 per cent. If more accuracy is required, a step-over resonator should be used and in such a way that no drawing or pulling effect exists.

42. Notes on Tube Generators of Great Frequency Constancy.—As has been pointed out in Secs. 27, 28, 29, and 33, the frequency of ordinary tube oscillators depends upon the oscillation characteristic of the tube. The frequency is affected by any changes in the dynamic plate resistance, the load, the grid current, etc. Even with the most careful precautions it is hardly possible to obtain tube generators that have a frequency constancy which at best is better than one part in ten thousand. Although this accuracy is more than sufficient for ordinary laboratory work, it is not sufficient for precision measurements when calibrating frequency meters, etc.

With the advent of the piezo resonator (W. G. Cady) and the piezo oscillator (C. W. Pierce, W. G. Cady, J. M. Miller)¹ as well as the mag-

¹ CADY, W. G., *Proc. I.R.E.*, **10**, 83, 1922; G. W. PIERCE, *Proc. Am. Acad. Arts Sci.*, **59**, 81, 1923; D. W. DYE, *Proc. Phys. Soc. London*, **38**, 399, 457, 1926; E. GIEBE and A. SCHEIBE, *Z. Physik*, **33**, 335, 1925; *Elektrotech. Z.*, **47**, 380, 1926; R. JOUAUST, *L'onde élec.*, November and December, 1927; A. MEISSNER, *Z. tech. Physik*, **7**, 585, 1926; A. W. HULL, *Phys. Rev.*, **27**, 439, 1926; **8**, 74, 1927; *E.N.T.*, **3**, 401, 1926, *Z. Hochfreq.*, **29**, 20, 1927; *Proc. I.R.E.*, **15**, 281, 1927; *Physik. Z.*, **28**, 621, 1927; K. S. VAN DYKE, *Phys. Rev.*, **25**, 895, 1925; **31**, 303, 1928; *Proc. I.R.E.*, **16**, 742, 1928; E. M. TERRY, *Phys. Rev.*, **29**, 366, 1927; *Proc. I.R.E.*, **16**, 1486, 1928; G. W. N. COBOLD and A. E. UNDERDOWN, *J.I.E.E.*, **66**, 855, 1928; R. H. WORRALL and R. B. OWENS, *Proc. I.R.E.*, **16**, 778, 1928; Y. WATANABE, *J.I.E.E. (Japan)*, No. 466, 529, 1927; A. CROSSLEY, *Proc. I.R.E.*, **15**, 9, 1927; J. R. HARRISON, *Proc. I.R.E.*, **15**, 1040, 1927; **16**, 1455, 1928; **18**, 95, 1930; C. W. GOYDER, *Exptl. Wireless*, **3**, 94, 165, 1926; R. C. HITCHCOCK, *Elec. J.*, **24**, 430, 1927; J. W. WRIGHT, *Proc. I.R.E.*, **17**, 127, 1929; for other details and references see Chap. VIII.

netostriiction oscillator (G. W. Pierce),¹ it became possible to attain great frequency constancy. In this respect, the piezo-electric oscillator is particularly valuable since, with a properly designed crystal holder and temperature control, a constancy of a few parts in one million and better can be obtained.²

43. Piezo-electric Oscillator.—In the piezo-electric oscillator, a properly cut element of crystal quartz, as explained in detail in Chap. VIII, is used, since its physical properties are such that the dimensions may be kept constant by temperature control and the element can withstand,

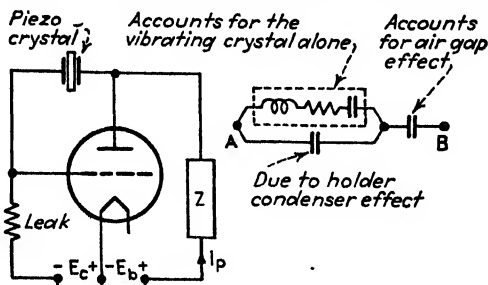


FIG. 62.—Original G. W. Pierce circuit (A to B is equivalent network of oscillating crystal with holder mounting).

for normal operation, the strains which exist when in a state of oscillation. The Pierce circuit, shown in Fig. 62, uses a quartz element across the grid and the plate of the tube and an external load Z which consists of a large inductance coil or a high resistance. Since the piezo-electric element with its holder, also taking into consideration the air-gap effect, is equivalent to an electric network as indicated, it acts like a resonating system of a natural period which is due to one of the possible modes of crystal vibration. For a circular crystal element in the Curie cut and of thickness t^{mm} and diameter d^{mm} , the principal possible vibrations have the frequencies

$$f_1 = \frac{2715}{d} \text{ kc/sec; } f_2 = \frac{3830}{d} \text{ kc/sec; } f_3 = \frac{2870}{t} \text{ kc/sec} \quad (141)$$

and, for a proper magnitude of Z , sustained oscillations of one of the foregoing frequencies will be noted in the plate branch. The magnitude of Z has no appreciable effect on the frequency except that for certain

¹ PIERCE, G. W., *Proc. Am. Acad. Arts Sci.*, **63**, 1, 1928, or *Proc. I.R.E.*, **17**, 42, 1929; L. W. MCKEEHAN and P. P. CIOFFI, *Phys. Rev.*, July, 1926; W. L. WEBSTER, *Proc. Roy. Soc. (London)*, December, 1925; A. SCHULZE, *Z. Physik*, p. 448, 1928; K. C. BLACK, *Proc. Am. Acad. Arts Sci.*, **63**, 49, 1928; E. H. LANGE and J. A. MYERS, *Proc. I.R.E.*, **17**, 1687, 1929.

² HORTON, J. W., and W. A. MARRISON, *Proc. I.R.E.*, **16**, 137, 1928.

values sustained oscillations are not possible. The oscillations are piezo-electrically controlled and are practically dependent only on the dimensions of the piezo-electric element. Experiments confirm theory in showing that, with such a connection, sustained piezo-electric oscillations are possible only when Z is capacitive. Hence when Z is a coil, the resonance frequency of Z must be lower than that of the piezo-electric oscillation which is set up. For this reason, Pierce found experimentally that a large inductance L must be used in place of Z or a high resistance R . In the first case, the distributed capacitance of R , together with the plate-filament capacitance, must produce a capacity effect. Therefore

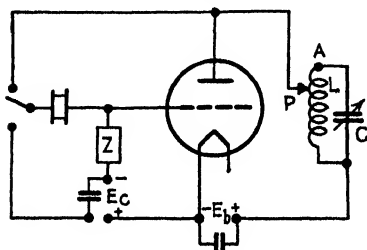


FIG. 63.—The J. M. Miller circuit.

the Pierce circuit with a large inductance in the plate circuit is nothing but the original tube oscillator since the crystal connected between the grid and the plate acts like a tuned circuit in producing piezo-electric oscillations. The feedback necessary for sustaining the Pierce oscillations is by means of the grid-filament capacitance.

Figure 63 gives the J. M. Miller circuit. The same circuit was also independently developed at the Bureau of Standards. Z denotes either a grid leak or a choke coil. The latter is especially useful for the production of piezo-electric oscillations of very high frequency. It is noted that the crystal can be connected between grid and plate, and in this case the external plate reactance must be capacitive in order to sustain piezo oscillations. When the crystal is connected between the grid and the filament, the feedback occurs by means of the plate-grid interelectrode capacitance and the external plate reactance must be *inductive* in order to satisfy the condition of oscillation. When the sliding contact P is at A , and the crystal across the filament and the grid, the natural frequency of the CL circuit must be above that of the crystal in order to set up the oscillation. With increasing capacity setting, the amplitude of the piezo-electric oscillation increases until, for a certain value of C , the natural frequency of the CL circuit reaches that of the piezo-electric oscillation when the oscillation breaks off. When the crystal is across the grid and plate, a much larger C setting must be chosen (corresponding to a lower natural frequency of CL branch) in order to produce capacity reactance and set up the piezo-electric oscillation; and as C is decreased toward current resonance of the CL branch (P at A), the amplitude of the oscillation is increased until for resonance the oscillations stop entirely. Near the resonance point the frequency of the oscillations is greatly affected by the reactance in the external plate circuit, while for adjustments farther away from the resonance point more or less true piezo-electric

frequencies exist. The tap P has the same function as in ordinary tube circuits. By means of it, a tuned-plate circuit can be used, thus excluding undesired oscillations. The variable tap P gives a means for matching the internal tube impedance to the circuit impedance so that maximum power transfer can be obtained.

This adjustment also is important when the piezo-electric oscillation is to have a large harmonic content. This is required when the piezo oscillator is to be used for calibrating frequency meters. The tuned-plate circuit with a low L/C ratio gives an external impedance of about the order of the internal plate impedance or greater, but only over a very narrow band of frequency. For large L/C ratios, the external impedance curve is broad and the harmonic content must be rich. Hence, for cases where a large harmonic content is required, a large inductance should be used in the plate circuit instead of the tuned CL branch and

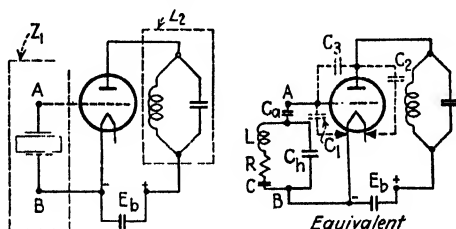


FIG. 64.—Equivalent electrical input for crystal between grid and hot cathode.

the plate tap at some point P as in Fig. 63, the crystal being connected across the grid and filament. Care must be taken that the inductance has a comparatively small distributed capacitance so that its natural frequency is higher than the fundamental frequency due to the piezo-electric element.

In order to obtain an idea of how the frequency of the piezo-electric crystal can be affected by circuit elements, reference is made to Fig. 64 where a quartz element is connected between the grid and the filament. For piezo-electric oscillations, the crystal can be imagined as a series combination of a coil (L, R) and a condenser (C) which is shunted by the capacitance C_h of the holder of the crystal. If any air gap between the upper electrode and the crystal is also taken into account, it is taken care of by the capacitance C_a . The interelectrode capacitances C_1, C_2 , and C_3 are also effective as far as the grid input is concerned. According to Sec. 34, we have the equivalent circuit of Fig. 65 since the grid gap acts as an effective impedance

$$Z_g = r_g \pm jX_g$$

even though the grid is properly biased. The circuit of Fig. 64 is nothing but the one shown in Fig. 44 where $Z_1 = R_1 \pm jX_1$ denotes the effect of

the quartz element with its holder, and $Z_2 = R_2 \pm jX_2$ the effect of the capacity-inductance branch in the external plate branch. From the theory given in Sec. 34 we note that, for certain adjustments of Z_2 , the effective grid-gap resistance r_g can be made negative—indeed so negative

that the losses in the piezo-electric element are outbalanced. If this is the case, the piezo circuit of Fig. 64 will sustain oscillations of a frequency which is practically determined by $Z_1 = 0$, that is, by the circuit constants L, R, C, C_a , and C_h . It is therefore essential that the crystal holder be well constructed; otherwise C_h as well as C_a will vary. From Fig. 65 it can be seen that, strictly speaking, r_g and X_g also affect the frequency somewhat, which means that for precision work the setting of the condenser in the plate circuit should be fixed and not too close to resonance, unless an anode tap P (as in Fig. 63) is employed.

FIG. 65.—Entire equivalent circuit for piezo oscillator of Fig. 64.

When a grid leak or a choke coil is used across the input side, a proper bias should be provided and, just as for ordinary tube circuits intended for high-precision work, the filament and plate supplies should be fixed. In order to minimize the effect of the load, a shield-grid tube amplifier can be used between the tube connected to the piezo element and the load circuit. The crystal should be temperature controlled and the holder so arranged that the spacing between the two electrodes is kept constant. To accomplish this constant spacing, several small quartz pegs are cut, in the same way from the same crystal as the piezo-electric element but somewhat thicker, so as to leave a small air gap between the upper electrode and the piezo-electric element. The magnitude of the air gap must be such that no standing supersonic waves (make smaller than half the wave length of the supersonic wave length) can be set up.¹

A piezo-electric oscillator with an acoustic backfeed, for which the anode reaction on the piezo-electric element is made very small, has been developed by L. P. Wheeler² and W. E. Bower. Figure 66 gives a con-

¹ For details on precision piezo oscillators see "High Frequency Measurements," McGraw-Hill Book Company, Inc., New York, 1933; *Proc. I.R.E.*, **16**, 1072, 1928.

² *Proc. I.R.E.*, **16**, 1035, 1928.

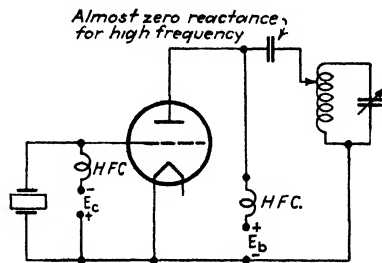
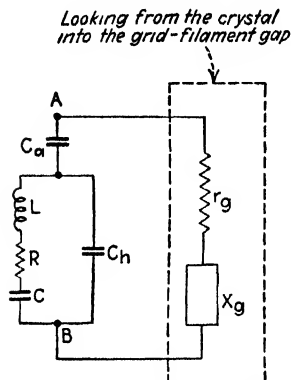


FIG. 66.—Piezo oscillator for very high frequencies. (Sometimes frequency doubling is used in the final amplifier stages of the oscillator.)

venient circuit for setting up piezo oscillations of very high frequencies (above 1500 kc/sec). The coils marked *H.F.C.* are high-frequency chokes which prevent any appreciable high-frequency currents from passing through these branches. Figure 67 gives circuits in which regenerative branches are used to produce piezo oscillations and a

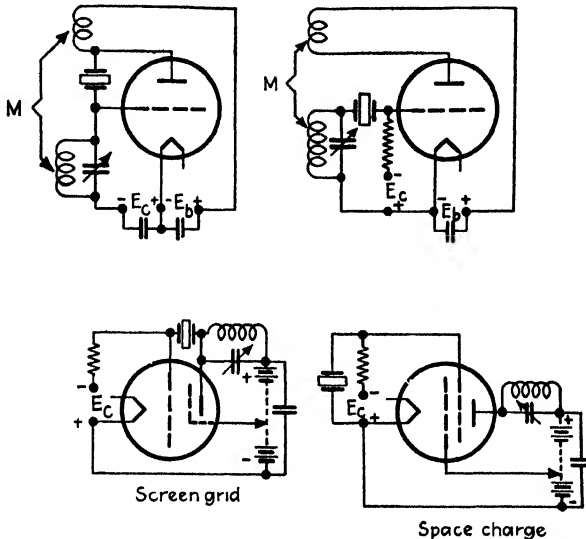


FIG. 67.—Regenerative and double-grid piezo oscillators.

double-grid tube is employed. Care must be taken in the case of these regenerative circuits to avoid the production of circuit oscillations. They can be avoided by choosing M small. The meaning of a screen grid is lost since in this particular connection the crystal acts as feedback

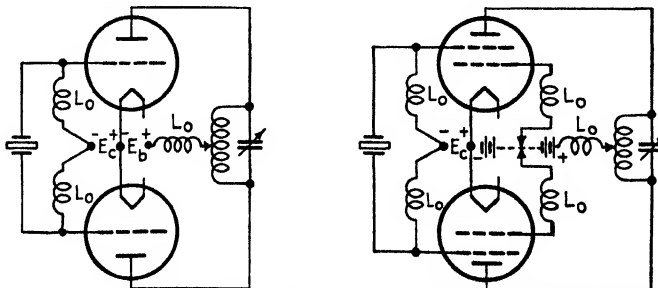


FIG. 68.—Push-pull piezo oscillators for the higher frequency range.

condenser. The grid leaks in these connections can be replaced by properly designed high-frequency chokes. Figure 68 gives a piezo oscillator in the ordinary and space-charge, push-pull connection. L_0 are high-frequency chokes. The L_0 chokes in the control-grid branches can also be replaced by high resistors.

44. Magnetostriction Oscillator.—The circuit shown in Fig. 69 is the work of G. W. Pierce.¹ The rod shown is magnetostrictive. When a coil surrounds it and an alternating current flows through it, at the peak of each half cycle the rod becomes magnetized and expands along its length irrespective of the polarity of magnetization. The rod will therefore expand and contract rhythmically, that is, vibrate longitudinally with a frequency double that of the magnetizing current. When, however, the coil carries both a direct and an alternating current and if the steady magnetization is greater than that due to the superimposed alternating current, the resultant magnetization will always be unipolar—it will only fluctuate or pulsate. Hence the rod will vibrate longitudinally

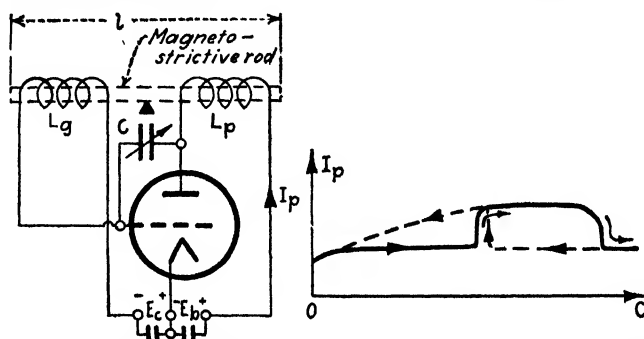


FIG. 69.—Stability curves of the G. W. Pierce magnetostriction oscillator

with the same frequency as the superimposed alternating current. As in the case of piezo-electric and any mechanically forced mechanical vibration, the effect is pronounced only when a natural mode of vibration is excited. The magnetostriction oscillator resembles the Hartley oscillator inasmuch as the plate and grid coils L_p and L_g form the resonance circuit. However, a close inspection shows that with the magnetostrictive rod the circuit has a tendency to be degenerative since L_p and L_g windings are such that the respective emission currents through them magnetize the rod in the same sense. A high- μ tube is used and the coils L_p and L_g surround the pivoted rod of length l freely. As the condenser setting C is gradually increased toward the natural frequency

$$f_0 = \frac{v}{2l}$$

of the rod, where v is the velocity of propagation along the rod, the plate current I_p suddenly rises to a maximum value as the rod goes into strong vibrations. When this condition is reached, the circuit is controlled by the rod since the setting of C can be either increased or decreased over a wide range without any appreciable change in frequency. The per-

¹ *Loc. cit.*

manent magnetization of the rod is due to the steady component of the plate current. Figure 69 shows the plate current when the magnetostriction oscillation is set up either with increasing C settings [corresponding to a natural frequency of the $C(L_g + L_p)$ branch which is higher than that of the fundamental longitudinal rod vibration] or for the case of decreasing C settings (which starts out with a natural circuit frequency which is lower). It is assumed that the spacing between L_g and L_p , and the capacitance, are of such magnitude as to make the electrical circuit nonoscillatory with the rod removed or held tight. Such an arrangement works well for frequencies below 3 kc/sec. But for shorter rods and frequencies from 3 to 50 kc/sec, the mutual inductance between L_g and L_p , and C , should be such as to make the electrical network oscillatory with the rod removed. For a proper C adjustment, the circuit will be controlled just the same by the dimensions of the rod. The building up of oscillations is as follows: Any current change in the plate coil L_p will change the degree of magnetization and the rod will be either shortened or elongated. This action is propagated along the rod and induces an e.m.f. in the grid coil L_g , which by means of the tube again gives an amplified action in the current passing through L_p .

Magnetostriction oscillators are of great value, no doubt, for frequency stabilization below 50 kc/sec, since piezo-electric quartz elements for such frequencies must be rather large. They form very effective supersonic sound sources and, like the piezo crystal, open up a large field for application.

45. Dynatron Oscillator.—The circuit shown in Fig. 70 is the work of A. W. Hull.¹ Oscillations are produced by means of the negative-resistance action ($-r_p$) of the tube. In dynatron tubes the perforated grid is more positive than the plate P . The electrons arriving at P are thus partly reflected back and with them secondary electrons. They finally reach the more positive grid. It is then possible that the plate current reverses its direction and a negative resistance action is produced. We have

$$\left. \begin{array}{l} \text{Damped} \\ \text{Undamped} \\ \text{Growing} \end{array} \right\} \text{oscillations for } \frac{R}{L} + \frac{1}{C(-r_p)} \begin{array}{l} < \\ = \\ > \end{array} 0$$

The current I_p which flows to the two branches of the actual oscillator circuit, for the straight portion of the tube characteristic, is given by the relation

$$I_p = \frac{E_p}{(-r_p)} + I_0$$

¹ *Proc. I.R.E.*, 6, 5, 1918; for details and applications, "High Frequency Measurements," McGraw-Hill Book Company, Inc., New York, 1933, pp. 27-28, 174-176, 328-329.

The quantity I_0 becomes zero if the anode return A is properly chosen. The quantity E_p denotes the resulting plate potential and $(-r_p)$ the drop of the straight portion of the characteristic of the tube. The oscillations are produced as follows: When the circuit is closed, the plate P receives electrons according to the values of $(-r_p)$ and C . The energy stored up

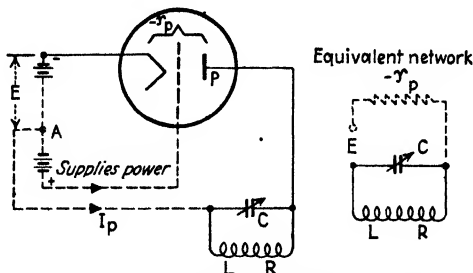


FIG. 70.—The A. W. Hull dynatron oscillator.

by condenser C discharges through coil L , R and the negative resistance. If

$$\frac{4}{CL} > \left[\frac{R}{L} + \frac{1}{C(-r_p)} \right]^2$$

we have for the frequency

$$f^{(-\text{sec})} = \frac{1}{2\pi} \sqrt{\frac{1}{CL} - \left[\frac{R}{2L} - \frac{1}{C(-r_p)} \right]^2} \cong \frac{1}{2\pi\sqrt{CL}}$$

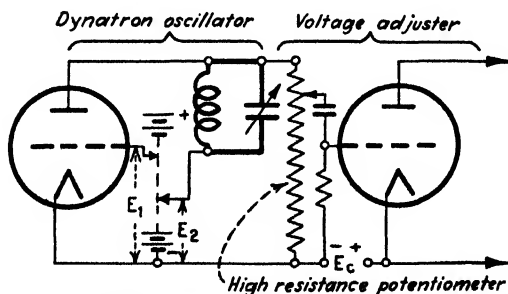


FIG. 71.—Dynatron source of good frequency constancy.

When a properly constructed tube is employed, the dynatron oscillator is a desirable generator for laboratory work since only the heavily drawn branch in the external plate circuit forms the oscillator and a back feed is not required. This is of advantage especially when working in the audio-frequency range. Figure 71 shows the principle of such an arrangement.

By means of a separate tube, the output voltage can be varied over a wide range without appreciably affecting the frequency calibration of the oscillator. The output voltage of the produced oscillations can also be varied by means of the ratio E_1/E_2 where E_1 and E_2 are the steady voltages taken from the supply battery.

46. Special Tube Generators (the Tungar, Negatron, Double-grid Oscillator, Square-wave Generator.)—Both the tungar and the nega-

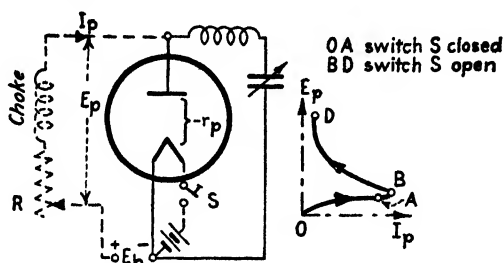


FIG. 72.—Tungar oscillator for negative resistance region *BD*.

tron generators are likewise founded upon negative-resistance action. The circuit indicated in Fig. 72 uses a tungar rectifier and is excited with a direct-current source. When the anode potential E_p is gradually increased, the anode current grows. For a sufficient ionic bombardment of the cathode, if the filament switch S is opened, the tube will continue to function. The plate current I_p will then at first increase with increased positive plate voltage until a certain plate potential is reached for which an unstable operation condition sets in and a falling voltage-current characteristic is produced. As indicated in Fig. 72, a negative tube characteristic of this kind can be obtained only by carefully adjusting the resistance R . Otherwise the tube either is injured or refuses to produce oscillations in the tank circuit parallel to it. In a similar way, oscillations can be produced in shunt with a mercury arc. In each case, however, much skill is required to set up oscillations.

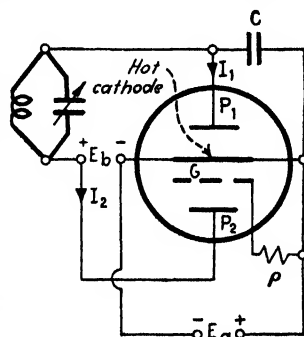


FIG. 73.—The negatron.

Figure 73 indicates the negatron oscillator of J. Scott-Taggart.¹ Two plates P_1 and P_2 are used as anodes and are at such potentials that I denotes the saturation current of the tube (see also Fig. 10). The oscillation circuit is connected across the main plate P_1 and the hot cathode, since any potential increase on P_1 produces a corresponding

¹ *London Electrician*, p. 386, 1921.

increase in E_g , that is, a current increase in I_2 and a decrease in I_1 . In the actual oscillator circuit, C denotes the back-feed condenser and ρ a high resistance. The grid is made positive with respect to the filament. Hence with increasing positive grid potential more electrons will pass toward P_2 than toward P_1 and the current I_1 decreases with increasing potential of P_1 .

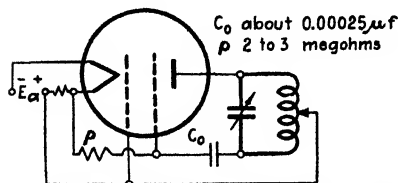


FIG. 74.—Double-grid uni-battery oscillator.

Figure 74 shows the double-grid tube in the oscillator connection. The only source is the low-potential A battery.

Figure 75 shows a square-wave generator. The grids of the first two tubes are connected together in such a way that the alternating grid voltage impressed on the second tube has a large amplitude. The biasing negative grid voltage E_c of the second tube is made so negative that the corresponding plate current I_2 becomes zero during the negative half cycle resulting from the oscillation of the first tube. During the same half period, the grid potential on the third tube is zero and a certain constant plate current I_3 flows through the load resistance R_3 . Since during the succeeding half period a large negative grid potential is impressed on the third tube, the current I_3 drops rather suddenly to zero. The rectangular high-frequency current I_3 is then as indicated in the figure since the second and third tube work during certain intervals below their characteristic curves. The load resistance R_3 , across which the rectangular high-frequency voltage is produced, is conveniently chosen equal to the internal plate resistance r_p of the third tube. The voltage of the rectangular wave is then equal to $E_3/2$. A generator of this kind was used by J. L. Bowman¹ in studying the mobility of ions. A generator of this kind also furnishes a high-frequency source which has a rich harmonic content. Therefore, if the fundamental frequency is chosen in the audio-frequency range, the higher harmonics can be used to calibrate frequency meters and the sudden voltage "jumps" to produce the linear time axis for a cathode-ray oscillograph.

Rectangular voltage waves can also be directly produced with generators for which the back feed is very pronounced. The resistance R_3 is connected in the plate circuit and in series with the plate coil. A tuned-grid oscillator is used.

47. Tube Oscillators for Very High Voltages and Oscillators for Very Large Currents.—Figure 76 gives circuits of tube generators used at abnormal voltages and currents. When large currents are needed, they can be obtained by a step-down (current) transformer. The coup-

¹ *Phys. Rev.*, **24**, 31, 1924.

ling coil is a copper tube which forms a single turn surrounded by the anode turns of the oscillator. For the production of high voltages, either the variometer or a slider arrangement as shown in the figure is useful. The values indicated in the figure hold for frequencies in the neighborhood

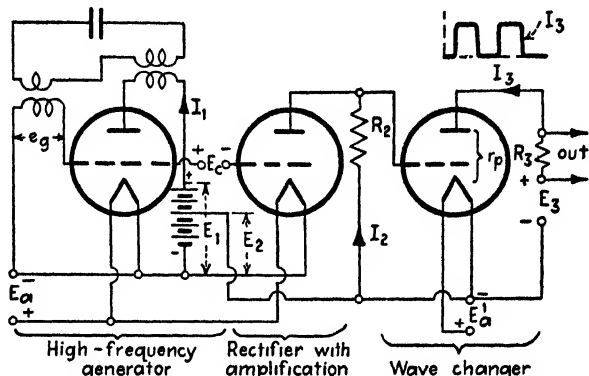


FIG. 75.—High-frequency generator with rectangular wave shape.

of 100 to 1000 kc/sec. The voltage can be computed by means of the condenser setting, the current through the condenser and the frequency.

48. Oscillators for Very High Frequency.—Inasmuch as condensers pass more displacement current as the frequency becomes higher, and inductances become effective chokes in the range of very high frequencies, capacitive back feeds are more advantageous for the generation of

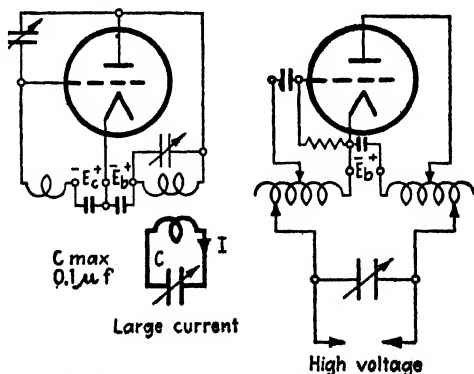


FIG. 76.—Oscillators for heavy currents and high voltages.

currents of ultrahigh frequencies. The Hartley circuit (Fig. 25) for frequencies above about 10 Mc/sec, that is, wave lengths below 30 m, is conveniently replaced by the Colpitts (Fig. 26) or some other circuit, and effective high-frequency chokes (*single layer*), must be used. Figure 77 shows a power oscillator which works at frequencies as high as

35 Mc/sec. The condensers C are from 0.0005 to 0.001 μf and the high-frequency chokes L_0 are conveniently long single-layer coils wound on $\frac{1}{2}$ -in glass tubing. It is easy to test the choking effect with a neon glow rod. If the glow tubing is moved along L_0 from 1 to 2, the glow must disappear toward 2. As far as oscillations are concerned, only half of one tube capacitance is effective across L since the circuit is dynamically in

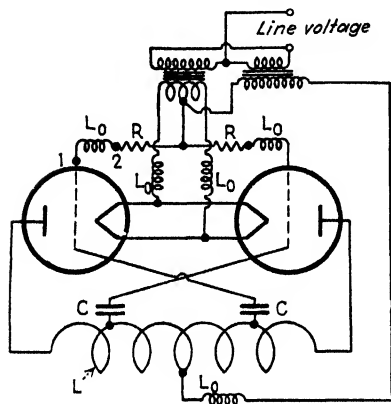


FIG. 77.—Oscillator for very high frequencies (up to 35 megacycles/sec) with self-rectification).

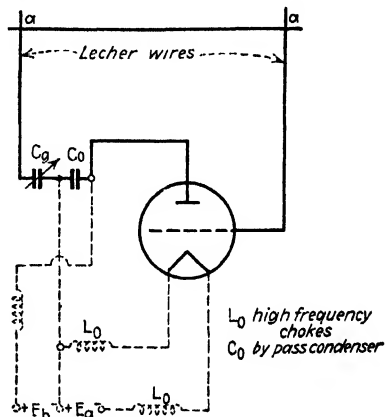


FIG. 78.—Oscillator up to 300 megacycles/sec (down to 1 m wave length).

push-pull. The plate power supply, however, is a parallel feed; that is, the high-voltage transformer is delivering power only every other half cycle. Hence it is necessary to rate for about twice as much watt dissipation in the secondary of the transformer as is required for the

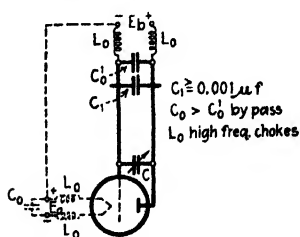


FIG. 79.—Lecher wire tube oscillator for frequencies up to 300 megacycles/sec.

primary which has to supply the plate power. It is also necessary to use enough iron since the self-rectified currents of both tubes are additive and not differential as for push-pull feed. The circuit of Fig. 78 gives still higher frequencies by varying C_0 and the size of the rectangular circuit. With a circuit of this kind, G. C. Southworth¹ succeeded in obtaining frequencies as high as 300 Mc/sec. In action this is a Colpitt oscillator since the missing external condenser between the filament

and the plate is now substituted by the tube capacitance. Another Lecher wire oscillator made by J. S. Townsend and J. H. Morrell² is shown in Fig. 79. C_1 , which should not be smaller than 1000 μf , forms a sliding bridge

¹ Loc. cit.

² *Phil Mag.* **42**, 265, 1921; see also A. MARCUS, *Phys. Rev.*, **27**, 250, 1926; W. C. HUXFORD, *Phys. Rev.*, **25**, 686, 1925.

(equal to a short circuit) along the parallel-wire system connected to the grid and the plate of the tube. The condenser C gives a fine and the movement of C_1 a coarse control of the frequency. The by-pass condenser C_0' prevents reflections of the waves at the terminals to which the B battery is connected. Figure 80 shows the high-frequency tube of A. Esau and the Lorenz Company which gives a few kilowatts power even at frequencies as high as 100 Mc/sec. According to E. Schliephake,¹ a Lorenz tube of this type for a plate potential of about 3500 volts, and 17-amp filament current at 30 volts, gives about 1.5 kw high-frequency power. As may be seen from circuit b of Fig. 80, the internal

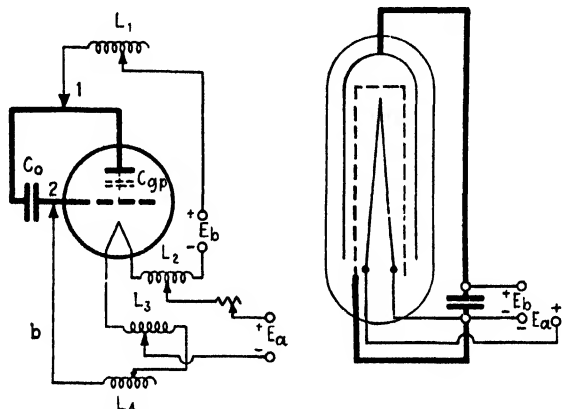


FIG. 80—Esau-Lorenz short-wave oscillator

grid-plate condenser C_{gp} and the connection between the grid and plate form the oscillatory circuit. C_0 denotes a small condenser which prevents the plate current from charging the grid. High-frequency choke coils L_1, L_2, L_3 , and L_4 must be inserted in all supply leads. By means of a suitable number of turns, the plate choke coil L_1 makes the back coupling most favorable. In the filament circuit, care must be taken that the lead-in wires do not subtract a substantial amount of energy from the actual oscillating branch. The high-frequency choke L_4 serves as a leak of the grid current. It is essential that all chokes be properly adjusted. The supply leads must therefore connect to places of voltage nodes. Such positions are found by sliding the contacts along the chokes until maximum high-frequency energy is indicated. In the same way, contacts 1 and 2 must be found. An ordinary small neon tube will glow up in the neighborhood of voltage loops. The inductance is formed by the heavily drawn connection, and the capacitance by the condenser formed by grid and plate.

¹ *Z. ges. expul. Med.*, 66, 212, 1929.

The upper frequency limit of the foregoing oscillations is given by the tube capacitance. Therefore push-pull¹ oscillators give a means of obtaining still higher frequencies. Figure 81 shows circuits of this type. For a symmetrical arrangement of the incoming leads, the same cannot conduct any high-frequency currents and therefore cannot affect the frequency. The reason is that the nodal point of the voltage coincides with the center tap. The plate and grid voltages are therefore applied at such nodal points. Because two tubes are used, the power output is doubled. A positive grid potential E_c (10 to 15 volts, according to the

anode potential) and properly designed high-frequency chokes L_0 must be provided.

Still higher frequencies can be obtained by Barkhausen-Kurz² oscillations with a circuit as shown in Fig. 82. Oscillations of this type give rise to frequencies as high as 750 Mc/sec (corresponding to wave lengths as short as 40 cm). The discovery of these oscillations resulted from the following observation made by H. Barkhausen

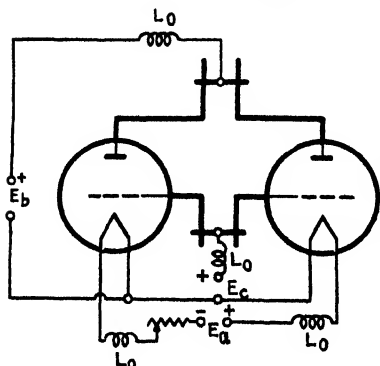


FIG. 81.—Push-pull Lecher wire oscillator.

and K. Kurz. When an ordinary

three-element tube with a cylindrical anode and grid and with the filament along the common axis is used, and when the grid is made a few hundred volts positive with respect to the filament and the plate (cylinder in this case) equal to the negative filament potential or even less negative, a plate current sometimes exists although one would, under such conditions, expect no plate current whatever. The plate current is due to oscillations which take place in the circuit and produce oscillating components of potential at the respective electrodes.

As has been brought out in the theory on page 18, the existence of these high-frequency oscillations can be explained by means of the "electron dance" between the cylindrical external electrode of diameter

¹ Originated by W. H. Eccles and F. W. Jordan, *London Electrician*, **83**, 299, 1919; F. Holborn, *Z. Physik*, **6**, 329, 1921; R. Mesny and P. David, *Compt. rend.*, **177**, 1106, 1923; R. Mesny, *L'onde élec.*, **3**, 25-37, 99-110, 1924; F. Kiebitz, *Jahrb. drahtl.*, **25**, 4, 1925; J. Taylor, *Exptl. Wireless*, **2**, 342, 1925.

² For the theory and references see p. 18. A good list of references on this subject is given by H. E. Hollmann, *Ann. Physik*, **86**, 129, 1928; *E.N.T.*, **6**, 253, 1929; *Proc. I.R.E.*, **17**, 229, 1929; and by K. Kohl, *Ann. Physik*, **85**, 1, 1928. References in connection with such oscillations are: L. Tonks, *Phys. Rev.*, **30**, 501, 1927; E. Pierret, *Compt. rend.*, **187**, 1132, 1928; G. Beauvais, *Rev. gen. élec.*, **25**, 393, 1929; H. G. Möller, *Jahrb. drahtl.*, **34**, 201, 1929; W. J. Kalinin, *J. Russ. Phys.-Chem. Soc.*, p. 131, 1929; also *Ann. Physik*, **2**, 498, 1929; G. Potapenko, *Z. tech. Physik*, **10**, 542, 1929.

D (Fig. 82) and the surface of the coaxial filament. As shown in the figure, either the negative filament potential or a negative potential E_b is applied to the outside cylinder of diameter D . A positive potential E_c , with respect to the negative end of the filament, is applied to the cylindrical grid. In some of the original experiments, the grid potential was $E_c = +80$ volts and the potential on the outside cylinder $E_b = -40$ volts. By means of the indicated parallel-wire system connected to the grid and the plate, the Lecher system can be tuned to the frequency of the oscillations. The frequency depends very little upon the circuit constants (inductance and capacitance) but is partly a dimensional quantity (diameter of cylinder and filament) and partly dependent upon

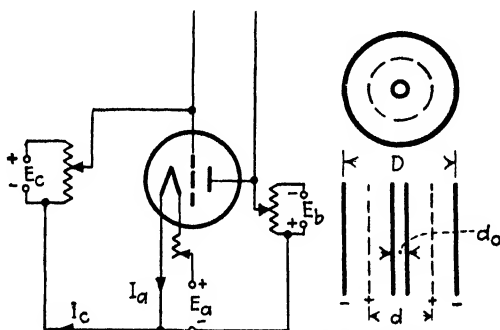


FIG. 82 Barkhausen-Kurz oscillator.

the filament current and supply voltages. Formula (31) on page 19 shows that for a positive grid potential of E_c volts with respect to the negative filament potential and with the outside cylinder at the negative potential of the filament (that is, $E_b = 0$) the frequency is

$$f = \frac{3 \times 10^4 \sqrt{E_c} \text{ (volts)}}{D \text{ (cm)}} \text{ kc/sec}$$

When the plate and cathode potential are unequal, that is, when a certain negative outside cylinder potential E_b exists, according to Eq. (32) on page 20, the frequency is

$$f = 3 \times 10^4 \sqrt{E_c} \frac{E_c - E_b}{D \cdot E_c - d \cdot E_b} \text{ kc/sec}$$

where the diameter D of the outside cylinder and the diameter d of the inside grid cylinder are again expressed in centimeters and the voltages E_b and E_c in volts. When this formula is expressed in wave length as measured along the parallel-wire system connected to the grid and the outside cylinder, we have the formula

$$\lambda = \frac{1000}{\sqrt{E_c}} \frac{D \cdot E_c - d \cdot E_b}{E_c - E_b}$$

for the wave length in centimeters. According to A. Scheibe,¹ this formula gives wave lengths which are somewhat longer than are found experimentally and an expression of the following form gives more accurate results:

$$\lambda^{(\text{cm})} = \frac{1000}{\sqrt{E_c}} \{ \varphi(x) + \Psi(y) \}$$

where in the functions of x and y

$$x = \sqrt{\log_e \frac{d}{d_0}} \quad y = \sqrt{\frac{E_c}{E_c - E_b} \log_e \frac{D}{d}}$$

and d_0 denotes the diameter of the filament. Figure 83 gives a push-pull arrangement for Barkhausen oscillations. M. T. Grechowa² used this type of circuit with a parallel-wire system and a sliding bridge across it. The plate potential was varied from -5 to $+15$ volts and the grid potentials from $+50$ to $+150$ volts. The frequency range is about the same as with the ordinary Barkhausen oscillations.

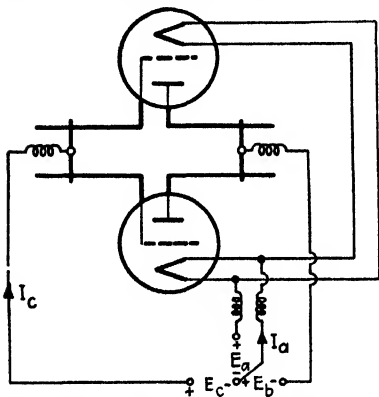


FIG. 83.—Electron oscillations in the push-pull connection.

As shown on page 21, the Barkhausen-Kurz oscillations can also be explained by the ordinary Thomson formula $f = 1/(2\pi\sqrt{CL})$ where C denotes the condenser formed between the electrodes between which the electrons vibrate. Because of the space charge in the tube, the dielectric constant no longer is equal to the conventional unity but is smaller and equal to $1 - (4\pi Nq^2)/(m\omega^2)$ if q and m denote the charge and mass, respectively, of each of the N electrons per unit volume. For resonance, the equivalent dielectric constant is zero; that is,

$$\omega^2 = \frac{4\pi Nq^2}{m}$$

We then have the equivalent case of a unit condenser $C = 1/4\pi$ shunted by an inductance $L = m/(Nq^2)$ since $\omega = 1/\sqrt{CL}$.

The Barkhausen theory explains only the action of the individual electrons that vibrate between the filament and the plate. But when

¹ *Ann. Physik*, **73**, 54, 1924. W. H. Moore, *Proc. I.R.E.*, **22**, 1021, 1934, shows that Barkhausen-Kurz oscillations can be produced in positive grid tubes without employing Lecher wires.

² *Z. Physik*, **35**, 50, 1925.

high-frequency oscillations are developed on the parallel-wire system as in Figs. 82 and 83, the space charge as a whole must oscillate from the filament through the grid to the plate and back again. This must happen in such a way that during one half cycle the space charge is mostly in the filament-grid space and during the following half cycle in the plate-grid space. According to the foregoing theory, we consider the filament-plate combination, with the space charge included, as a condenser and an inductance in parallel. The parallel system in the external tube circuit then acts as a direct-coupled resonator system. H. G. Möller¹ has followed up this case in detail.

The most favorable plate potential is that one where the electrons just reach the plate because of their deflection by the grid wires from their radial paths. A negative space charge then develops near the plate and instability within the tube takes place, giving rise to a negative-resistance action. Oscillations are then set up in the fictitious *CL* branch mentioned above.

For plane parallel electrodes² for a distance d cm between the grid and the plate we have for the wave length λ in centimeters

$$\lambda = \frac{4000d\sqrt{E_c - E}}{E_c - (4E/\pi^2)} \text{ (for Hollmann oscillations)}$$

if E_c is the steady grid voltage with an alternating voltage E superimposed on it. This relation comes to the form of the Barkhausen-Kurz formula for $E = 0$. If ρ stands for the ratio of the number of electrons within the volume enclosed by grid and plate to this volume (electron concentration), the wave length in centimeters for Barkhausen-Kurz oscillations is $3.35 \times 10^6/\sqrt{\rho}$. With the foregoing assumption that the grid plane is equidistant from plate and filament planes and from the assumption that the potential distribution V between the filament plane and the parallel plate follows closely a parabolic law, we have, for any distance x from the grid plane along a perpendicular to this plane, the relation $V = E_c[1 - (x/d)^2]$. The electric field \mathcal{E} for any distance x then becomes $\mathcal{E} = dV/dx = -2 \times E_c/d^2$. Since, for the electron charge q , the force on it is $\mathcal{E}q$, we find $-\mathcal{E}q = 2qE_c x/d^2$. Hence this force is proportional to the displacement of the electron and we have simple harmonic motion with a period of oscillation $T = 2\pi\sqrt{\frac{m}{q\mathcal{E}/x}}$ where m

¹ See footnote 2 (p. 132).

² GILL, E. W., and J. H. MORRELL, *Phil. Mag.*, **44**, 161, 1922; H. G. MÖLLER, *E.N.T.*, 298, 1930; H. E. HOLLMANN, *loc. cit.*; H. N. KOZANOWSKI, *Proc. I.R.E.*, **20**, 957, 1932; T. V. JONESCU, *Compt. rend.*, **193**, 575, 1931; A. ROSTAGNI, *Compt. rend.*, **193**, 1073, 1931.

denotes the electronic mass. Hence for the frequency $f = 1/T$ in cycles per second we find

$$f = \frac{1}{2\pi} \sqrt{\frac{2q}{m} \frac{\sqrt{E_0}}{d}} = K \frac{\sqrt{E_0}}{d}$$

This relation seems to hold for plate potentials that are either slightly negative or zero.

When working with Barkhausen-Kurz oscillations, the frequency depends essentially upon the electric field intermediate between the electrodes. A resonating system connected to the tube should therefore

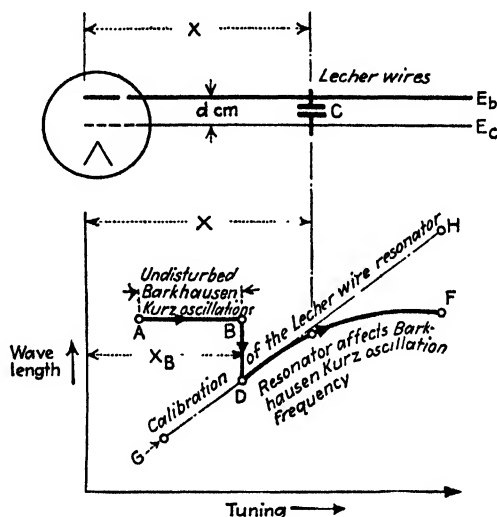


FIG. 84.—Hollmann oscillations for region DF.

not affect the frequency very much, except to increase the oscillating power of the tube. According to H. E. Hollmann, for certain coupling conditions to a resonator, the Barkhausen-Kurz frequency may jump suddenly to a value determined by the natural frequency of the resonator and then keep on varying as the natural frequency of the resonator is changed. This is illustrated in Fig. 84 where C denotes a condenser bridge across Lecher wires for changing the natural wave length of the external system of the tube. GH denotes the wave-length calibration of the Lecher wires for the corresponding positions X of the condenser bridge. As long as the distance X is less than X_B , the frequency is due to a true Barkhausen-Kurz oscillation and is not affected by the length X . But for the length $X = X_B$ the oscillation suddenly breaks off and jumps to an oscillation of the resonator frequency corresponding to point D . Since the wave length at this sudden change is decreased, the

frequency is correspondingly increased. A further shift of the condenser bridge toward larger values of X will produce frequencies corresponding to curve DF . The Barkhausen-Kurz formula is based on the steady grid potential E_c . In case of Hollmann oscillations the alternating potential E reacts all the more on the oscillating electron within the tube the more the natural frequency of the external resonating system approaches the value of the true electronic Barkhausen oscillation since E and E_c are superimposed on each other. Hence there must be a critical frequency ($X = X_n$) for which the Barkhausen-Kurz oscillation will suddenly jump to an oscillation due to the external-wire system. Applying the formula for Hollmann oscillations to the case for which the steady grid potential is $E_c = +500$ volts and the distance d between the grid and the plate is 0.5 cm, we have, for no reactive alternating potential E , a wave length of 89.5 cm, while for $E = 100$ volts $\lambda = 86.9$ cm and for $E = 400$ volts the wave length reduces to the small value of 58.8 cm.

Figure 85 shows a short-wave generator where oscillations are taken off by means of Lecher wires connected to the plate and filament instead of to plate and grid as for Barkhausen-Kurz oscillations. With such a system, H. N. Kozanowski¹ obtained with two 852-type tubes oscillations corresponding to wave lengths of about 70 cm. The length of the plate Lecher wire seems to determine the frequency of the oscillation, while the length of the filament Lecher wire has an effect on the amplitude of the oscillation.

Currents of very high frequencies can also be produced by piezo oscillators when frequency multiplication is used. It is then customary to use a piezo-electric quartz plate which is so thin that it has a fundamental frequency of about 7.5 Mc/sec (corresponding to 40-m wave length) and to tune the output of an amplifier to a harmonic. When, for instance, the plate circuit of the first amplifier is tuned to the second harmonic and this frequency is fed into the grid branch of another amplifier whose plate circuit is again tuned to twice the input, oscillations at a frequency of 30 Mc/sec are obtained. When the mounting of a piezo oscillator is properly chosen, the second harmonic can be excited directly.

¹ *Loc. cit.*

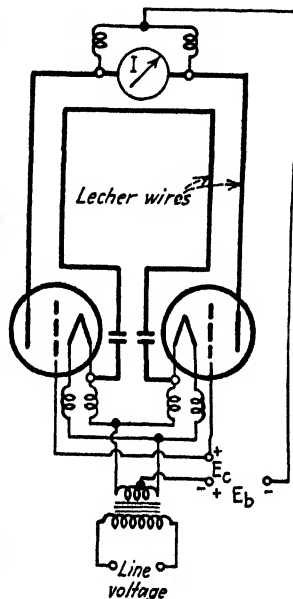


FIG. 85.—Oscillations for Lecher wires connected to filament and plate.

The magnetron¹ oscillator shown in Fig. 86 uses a push-pull connection and a split anode in a thermionic tube whose hot cathode is along the axis of symmetry of the two anodes. A negative-resistance action² is produced by means of a strong magnetic field whose lines of force are essentially parallel with the filament. In the external plate circuit, oscillations are produced in the CL branch in a similar manner to that in the dynatron and the Poulsen-arc circuit since the frequency is, to some extent, dependent on the oscillation constant CL . As brought out in detail in Sec. 13 beginning on page 32, the magnetic field due to the direct current I_0 causes the electrons to pass not along the radii toward

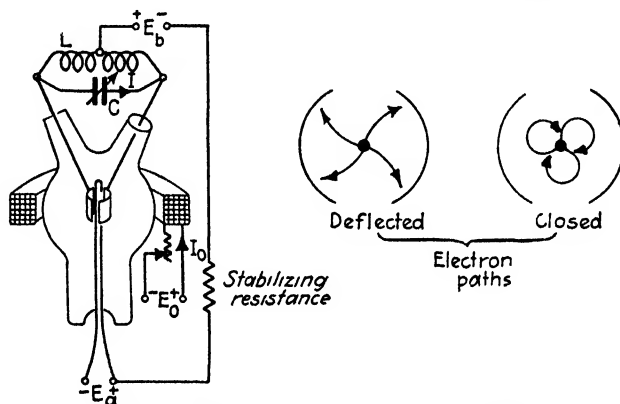


FIG. 86.- The split-anode magnetron oscillator

the anode but along a helical path as indicated in Fig. 86. When the magnetic intensity equals a certain critical value, the electrons just miss the anode and may set up a negative space charge near the split anodes. For very strong magnetic fields, the electrons turn completely around and return to the filament. The negative space charge near the anode may give rise to instability, that is, a negative-resistance action within the tube, and thus set the external CL branch into oscillations. Magnetron generators with considerable high-frequency output have been developed for frequencies up to 400 Mc/sec.³ For example, with certain designs 10 watts was obtained at 400 Mc/sec with a plate voltage of 1500 volts, and about 40 watts was obtained at 100 Mc/sec. With a water-cooled magnetron 1 kw at 85 Mc/sec was possible, while at 20 Mc as much as 5 kw was obtained, for each case the plate potential being 10 kv. With such power tubes the magnetizing current I_0 which produces the magnetic

¹ HULL, A. W., *J.A.I.E.E.*, **40**, 715, 1921; E. HABANN, A New Generator Tube, *Jahrb. drahtl.*, **24**, 115, 1924; H. YAGI, *Proc. I.R.E.*, **16**, 715, 1928; K. OKABE, *Proc. I.R.E.*, **17**, 652, 1929; W. C. WHITE, *Electronics*, **1**, 34, 1930.

² See p. 33.

³ WHITE, W. C., *loc. cit.*

field need only be of an order to produce instability (negative resistance within the tube) and is not critical with regard to the frequency of the oscillations since f is primarily dependent on the CL product of the external circuit. But for very high frequencies a circuit as indicated in Fig. 87 must be employed and the condenser C of the external plate circuit is omitted. It is noted that the external plate circuit again forms a parallel-wire (Lecher wire) system which can be adjusted to a suitable frequency. H. Yagi and K. Okabe¹ have obtained waves as short as 5.6 cm corresponding to 5350 Mc/sec with low-output oscillators of the split-anode type (Habann type). For such high frequencies, the strength of the applied magnetic field, according to formula (57) on page 39, gives a means of calculating the frequency.

The foregoing frequency is about the highest ever obtained directly with tube oscillators. For still higher frequencies, damped oscillators of the Hertzian type were used by several investigators.² E. F. Nichols and I. D. Tear produced wave lengths as short as 1.8 mm corresponding to a frequency as high as 166,500 Mc/sec, while M. Lewitsky as well as A. Glagolewa-Arkadiewa succeeded in producing fundamental wave lengths of 0.13 mm in length by means of sparks occurring between very small spheres or between metal filings. Such waves belong to the spectrum of heat radiation and correspond to 2.3 megamegacycles/sec.

The next step is the production of infrared³ and ultraviolet rays. The former can be generated by means of thermic radiators such as electric lamps and carbon arcs. About 36 per cent of the total emission of the carbon arc at 4,200°K lies between 0.7 and 1.1 μ . About 22 per cent of the radiation from a gas-filled lamp at 2400°K is infrared. Generally, it may be said that a carbon arc is rich in long and deficient in short wave-length radiations, while a tungsten arc is rich in all wave lengths. A tungsten arc is so rich in ultraviolet radiation that after 2 min an 8-amp tungsten arc will produce sunburn even at a distance of 18 in. Quartz-mercury lamps are good ultraviolet radiators. A condenser spark is rich in short ultraviolet radiation but deficient in long

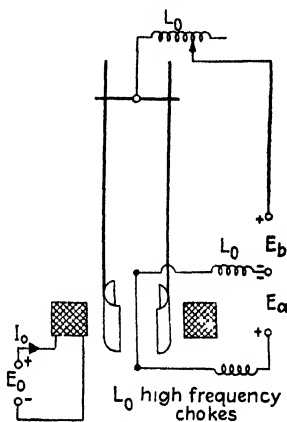


Fig. 87.—Magnetron oscillator for very high frequencies

¹ Loc. cit.

² MOEBIUS, W., *Ann. Physik*, **62**, 293, 1920; P. LEBEDEV, *Wied. Ann.*, **56**, 1, 1895; A. LAMPA, *Wiener Ber.*, **105**, 587, 1896; M. LEWITSKY, *Physik. Z.* **25**, 153, 1924; **27**, 177, 1926; E. F. NICHOLS and I. D. TEAR, *Phys. Rev.*, **21**, 587, 1923; A. GLAGOLEWA-ARKADIEWA, *Z. Physik*, **24**, 153, 1924.

³ SCHROETER, F., *E.N.T.*, **7**, 1, 1930.

ultraviolet radiation. The helium glow lamp is a very effective source for infrared radiation. This brings us to the class of gaseous infrared radiators with band emission. According to Paschen, the "metastable" orthohelium, which is produced from the normal parhelium by inelastic impact of 20.5-volt electrons, shows a characteristic absorption and reradiation at 1.08μ without loss or change in frequency. This infrared line which corresponds to $f = 2s - 2p$ is known as a "resonance line." A considerable emission of this resonance radiation should exist in the glow discharge of helium, since the energy difference between the "long-life" state $2s$ and the level $2p$ is compensated by the electron impacts in the case of high gas pressures and large current densities.

CHAPTER III

VOLTAGE AND CURRENT CHANGERS

Apparatus of this type plays an important part in high-frequency work since ordinary air coils can be used to bring about such changes. When relays of the ordinary, magnetic, or electron-tube type, respectively, are used, changes can be obtained where the power output is many times that at the input side. It is also possible to control one kind of current (for instance, direct current) by another kind of current (for instance, alternating current) or change alternating current of a certain frequency to alternating current of other frequencies.

49. Tesla's Transformer for Obtaining High Voltages of Discrete Wave Trains.—This scheme of voltage step-up combines the ordinary transformer step-up action with that due to resonance and thus produces very high voltages. An alternating-current source of about 10 to 30 kv is connected to the terminals of a condenser which is shunted by a series combination of an air-core coil of a few turns in series with a spark gap. The air-core coil is surrounded by a single-layer coil of many turns across whose terminals are produced the very high output voltages. Because of the resonance of the damped discharges which take place through the primary coil, a high voltage is generated across its terminals and in the secondary this voltage is still further increased according to the transformer ratio.

50. Resonance Transformer for Obtaining High Voltages of Sustained High-frequency Currents.—Figure 88 is an arrangement used by E. F. W. Alexanderson to obtain very high voltages. The operation is again due to the two actions brought out in the last section, except that the ordinary transformer action is utilized first and the resonance effect is used to obtain the final output voltage. Also, a separate high-frequency source is used and sustained voltages exist. The resonance system consists, for instance, of 24 pancake coils. The primary coil of the air-core transformer leads to the high-frequency source. The 24 coils are connected in such a way that two internal and then two external terminals always join consecutive coils. This reduces breakdown voltages. The tuning condenser is arranged on each side and is formed by copper tubing wound up conically. The capacitance is changed by the relative position of the two condenser poles. The coils, as well as these condensers, must be suspended so that no other metal parts are within the strong magnetic and electric fields. Dry hardwood can be used to hold them in place. In considering the effect of the air-core

transformer, an equivalent transformer ratio must be used since the voltage ratio also depends on the effective resistance, the capacity effects, and the external circuit reaction. For instance, at 100 kc, a turn ratio of 6:1 can give a voltage ratio of only 3.6:1.

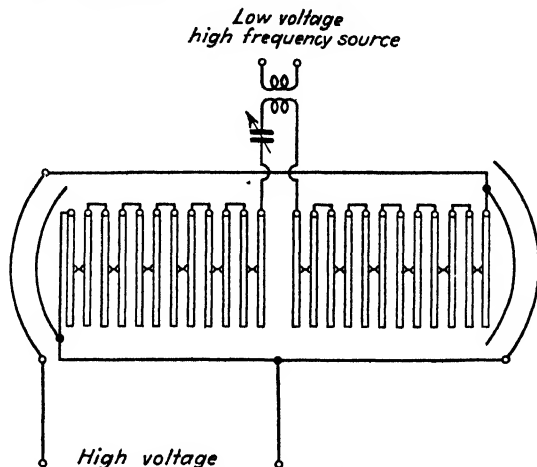


FIG. 88.—Production of high voltages.

51. Current Changes Using Shunts.—When shunts are used, the ratio of the currents I_1 and I_2 in the two branches with coils L_1 , R_1 and L_2 , R_2 , respectively, is

$$\frac{I_1}{I_2} = \frac{R_2 + j\omega L_2}{R_1 + j\omega L_1}$$

If the inductance is sufficiently large in comparison with the resistance, the current ratio is independent of the frequency and

$$I_2 = kI_1$$

If capacity effects exist in addition, we have

$$\frac{I_1}{I_2} = \frac{R_2 + j\omega L_2 + 1/(j\omega C_2)}{R_1 + j\omega L_1 + 1/(j\omega C_1)}$$

and for predominating capacity effects

$$I_2 = k'I_1$$

If the discrepancy is not to exceed η per cent, the values of L_2 and C_2 , respectively, must be chosen according to formulas

$$L_2 \leq \frac{R_2}{2\pi f \sqrt{1/[1 - \eta]^2 - 1}} \quad C_2 \leq \frac{\sqrt{1/[1 - \eta]^2 - 1}}{2\pi f R_2} \quad (1)$$

With respect to transformers, the subject matter is taken up at several places in the text.¹

¹ See also "High Frequency Measurements," McGraw-Hill Book Company, Inc., New York, pp. 10-16; 56-61, 100.

CHAPTER IV

PHASE CHANGERS

Ordinary inductances and condensers are phase changers and when properly combined in recurrent networks give rise to successive phase shifts. Rapid phase change takes place near the resonance setting and is known as "phase jump." It becomes more pronounced as the losses of the resonance system become smaller.

52. Phase Changers by Means of React-

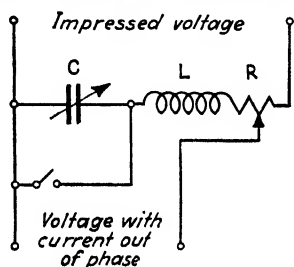


FIG. 89.—Production of phase displacements.

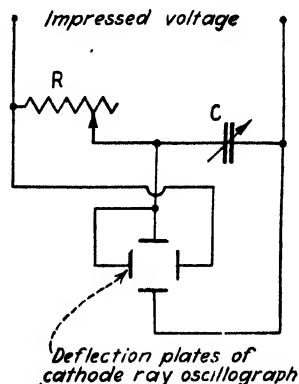


FIG. 90.—Phase changes up to 90 time degrees displacement.

ance and Resistance.—Figure 89 shows an arrangement where the phase is changed by C and L and R , respectively. For the latter case C is short-circuited. The case in which a variable condenser and variable resistance are connected, as in Fig. 90, is very convenient for obtaining a revolving electric field as used with cathode-ray tubes (Figs. 97 and 108). In order to secure a circular field, it is only necessary to make $R = 1/\omega C$. The schemes employing R and L , R and C , have the disadvantage of giving phase variations between 0 and 90 deg only, while the arrangement with C and L gives a 180-deg phase regulation. When mutual induction M as in Fig. 91 is used, the entire phase range can be covered. Figure 92 gives other schemes to produce different phases for the entire phase range (360 deg.).

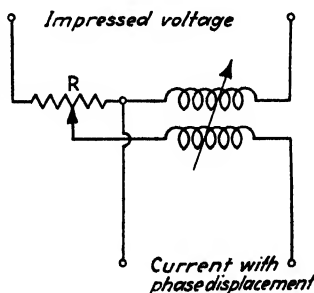


FIG. 91.—For phase displacement of entire phase range.

53. The Revolving-field Phase Changer and Phase Multiplier.—The arrangement indicated in Fig. 93 is based on a magnetic field which

revolves with an angular velocity $\omega = 2\pi f$ equal to that of the alternating e.m.f. impressed on the coil system L_1 and L_2 . The coils L_1 and L_2 are perpendicular to each other and produce a circular revolving field when L_1 , L_2 , C_1 , C_2 , and the ratio of the air-core transformer are chosen such that the magnetizing currents I_1 and I_2 are 90 time degrees (a quarter

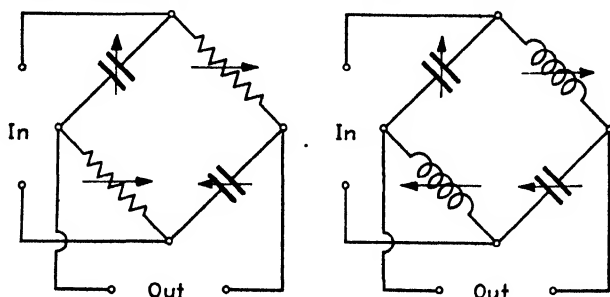


FIG. 92.—Phase changers.

of a period) out of phase and of the same amplitude. The induced voltages E_3 and E_4 have a phase difference equal to ψ . Any multiphase output system can then be obtained when secondary coils are properly located in the rotating field.

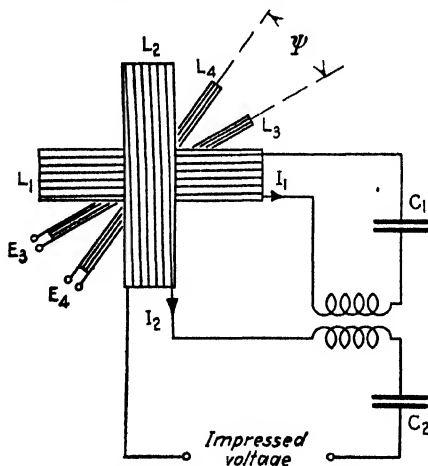


FIG. 93.—Phase changer.

54. Phase Changers and Phase Multipliers by Means of Out-of-phase Currents.—Figure 94 shows two transformers T_1 and T_2 which work through adjustable resistances R_1 , R_2 , and R_3 into a three-phase load. The e.m.f. across the output of transformer T_1 is different from that across the secondary of transformer T_2 since a choke coil is connected in the primary circuit of T_1 . By means of the resistances R_1 , R_2 , and R_3 three-phase balance is obtained.

Figure 95 shows a single-phase-three-phase converter for which equal phase amplitudes exist by virtue of the circuit. In this case, the phase conversion is applied to a piezo oscillator which produces a single-phase voltage between terminals a and b . The heavily drawn network is the phase multiplier for which 0-1, 0-2, and 0-3 are the three phases and 0 is the neutral point. In order not to load the piezo oscillator too much, the resistances R can be given high values and a stage of power amplification can be used for feeding a three-phase current into the primary of an

output transformer. That three-phase currents are obtained is evident from the adjustment relations $1/(\omega C) = R\sqrt{3}$ and $\omega L = R\sqrt{3}$ for equal resistances R in all three branches. Figure 96 gives another type of

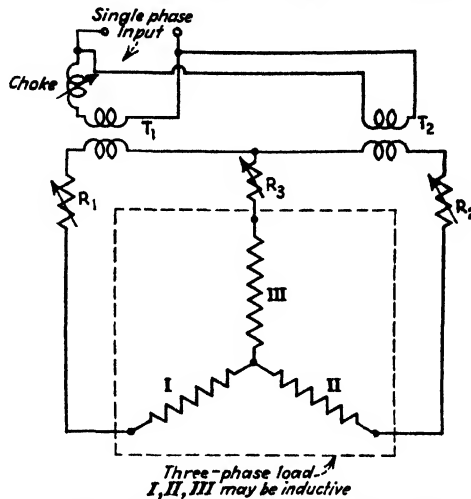


FIG. 94.—Single-phase-three-phase converter.

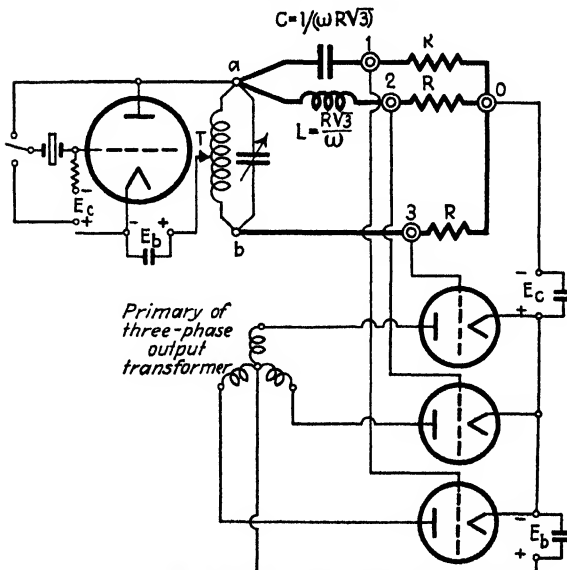


FIG. 95.—Piezo oscillator with three-phase output.

single-phase-three-phase converter utilizing the resistance-capacitance bridge circuit of Fig. 92. M denotes the center tap of the single-phase input. We have again a balanced Y output since $R_1 = 1/(\omega C_1\sqrt{3})$ and

$R_2 = 1/(\omega C_2 \sqrt{3})$ and these relations give $\tan 30^\circ = \omega CR = 1/\sqrt{3}$, as required in three-phase systems.

Figure 97 shows a cathode-ray-tube phase multiplier. For the sake of simplicity, the case of three-phase output is shown. By means of C and R for $R = 1/(\omega C)$ similar to the description given in connection with

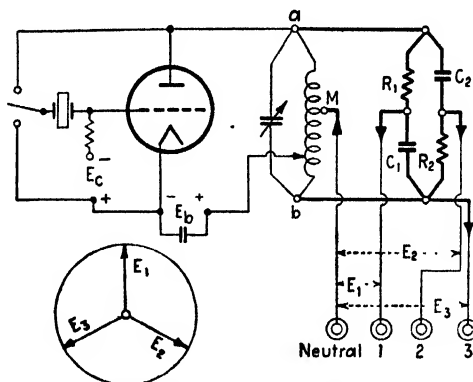


FIG. 96.—Single-phase-three-phase converter with input voltage of stabilized frequency across ab .

Fig. 90, the cathode-ray beam becomes circularly polarized on the screen of the tube; that is, the fluorescent spot describes one circular path for each complete cycle of the exciting single-phase voltage. Hence when either external¹ or internal metal electrodes are fastened to the end face

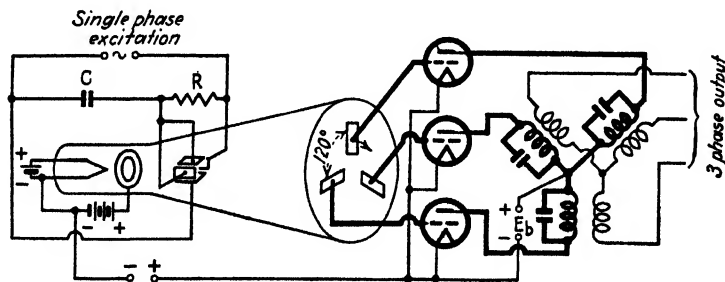


FIG. 97.—Cathode-ray tube as phase multiplier.

of the cathode-ray tube and are connected as indicated, three-phase excitation will occur on the grids when the metal sectors are spaced by 120° . The tank circuits will then charge up in three-phase relation and produce in the three output coils three-phase currents.

¹ External electrodes seem more practical, since any phase corrections can be readily made or any other phases can be quickly produced.

55. Phase Changers by Means of a Recurrent Network.—The principle is partially indicated in Fig. 98. The voltage e which is displaced in phase is produced across coil L which is free to slide inside a long single-layer coil (for high-frequency work) or many small coils (for low-frequency work). The individual sections of the recurrent network are made up of inductances L_1 along the line and capacitances C across it. The recurrent network is composed of many sections so that the current I at its end is attenuated practically to zero. As shown in connection

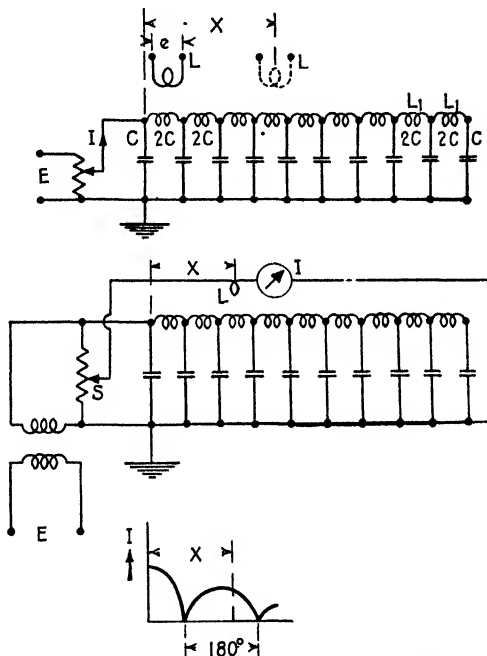


FIG. 98 — Distributed inductance and capacitance as phase shifter

with the theory of recurrent networks (pages 546 and 551, Fig. 322), a recurrent network of this kind (so-called "coil line"), when properly terminated, tends to pass only currents below a certain critical frequency f_0 ; for currents above this frequency, pronounced attenuation takes place. Figure 322 shows that such a network works as a phase changer up to this critical frequency. It is then possible to obtain phase variations *without amplitude changes* since attenuation takes place only for frequencies above f_0 . Hence if a small coil is moved inside the long coil (Fig. 98), the phase can be readily varied through 360 deg and more. This can be easily tested, as in the lower arrangement of Fig. 98, where two currents of different phases are produced and passed through a thermoelectric galvanometer. The galvanometer then gives deflections as indicated. For more accurate measurements, a tube voltmeter should

be used, so that coil L does not produce back reaction. The amplitude is adjusted by the sliding contact S .

56. Phase Changers by Means of Tube Circuits.—Figure 99 shows a system in which a sinusoidal current I_1 flows in at the input terminals and a current I_2 , which is out of phase with I_1 , is produced in the output circuit. The phase change is dependent on the magnitude of the oscillation constant CL , that is, by the setting of C . The phase of the current I_2 actually depends on the ratio CL/f , where f is the frequency of the current I_1 which was impressed on the system. The amplitude of I_2 depends on the coupling from I_1 to the grid branch and I_2 to the plate

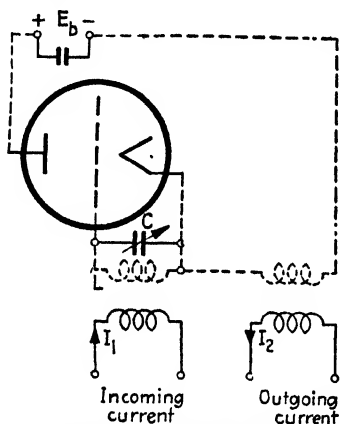


FIG. 99.—Tube phase shifter.

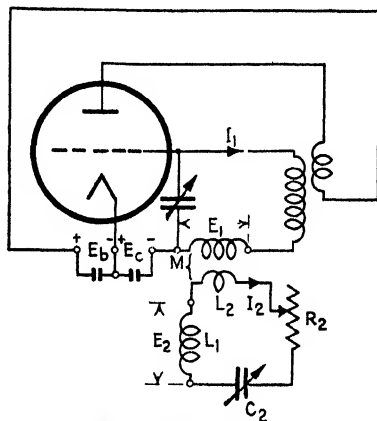


FIG. 100.—Tube oscillator for producing voltages E_1 and E_2 which are out of phase.

branch and the amplification factor of the tube. Figure 100 shows another tube arrangement for producing two voltages E_1 and E_2 of different phase. The current I_2 lags behind the current I_1 by an angle $(\pi/2) - \varphi$ where

$$\varphi = \tan^{-1} \frac{\omega[L_1 + L_2] - 1/(\omega C_2)}{R_2}$$

From this relation it is seen that, when the secondary circuit is almost tuned, small changes in C_2 produce pronounced changes in φ . Therefore the phase can be changed by C_2 , R_2 , and M . However, the disadvantage of this circuit is that a frequency jump (see page 103) may take place.

57. Phase and Corresponding Frequency Change.—Suppose a constant-frequency source affects a pick-up circuit in which the phase can be made to lag during a short interval and according to any law whatever. A deceleration (retardation of the phase) of the induced oscillation must then take place in the circuit. In a similar way when a transient circuit change causes a leading effect, a corresponding acceleration (advancement

of the phase) of the induced oscillation results irrespective of how constant the frequency of the supply.

Therefore when a sinusoidal variation of angular velocity $\omega = 2\pi f$ and a variable phase φ_t exists in such a pick-up or some transfer circuit, the voltage as well as the current in the circuit is at any instant

$$A_t = A_m \sin [\theta + \varphi_t]t$$

where $\theta/(2\pi t)$ now stands for the average frequency about which changes due to variable phase effects take place. If the phase φ_t varies according to an arbitrary time function, the corresponding frequency change δf is

$$\delta f = \frac{d\varphi_t}{dt}$$

If the phase varies according to a sine law $\varphi_t = \varphi_m \sin(2\pi f_1)t$, we have for the instantaneous value of voltage or current, neglecting their constant-phase displacement,

$$A_t = A_m \sin 2\pi[f + f_1]t = A_m \sin \Gamma$$

and the effective frequency at any instant becomes

$$f_t = \frac{1}{2\pi} \frac{d\Gamma}{dt} = f + \varphi_m f_1 \cos (2\pi f_1)t$$

with a maximum frequency shift $f_1\varphi_m$ if φ_m denotes the maximum phase shift.

CHAPTER V

FREQUENCY CHANGERS

The frequency impressed on certain circuits can be multiplied by means of magnetic, thermic, thermionic, and other devices. In some systems the desirable frequency mf is obtained by tuning to a harmonic mf of a distorted current of fundamental frequency f (current of an alternating-current arc, distorted currents of magnetic frequency multipliers). In other devices, current impulses are produced which either

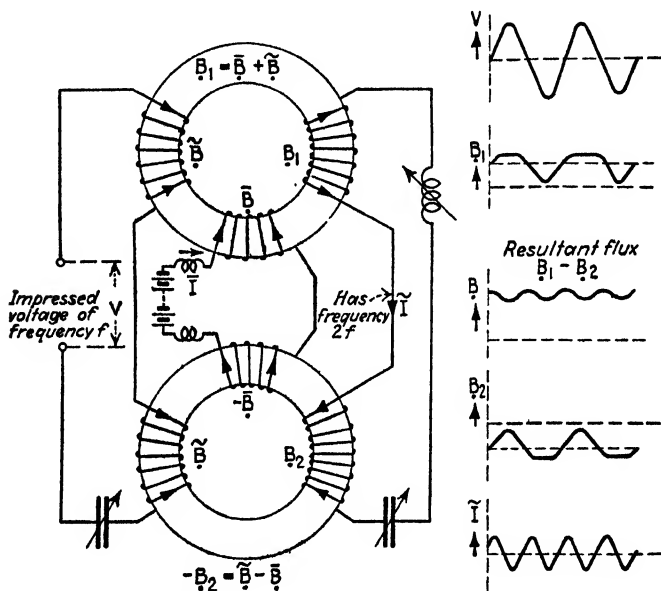


FIG. 101.—Doubling of frequency.

are distorted (certain magnetic multipliers) or form portions of sinusoids (tube multipliers). In methods which use two transformers, either the primary or the secondary coils are connected in opposition to the other coils so that their voltages are additive. If a double frequency is required, the dissymmetry in the transformers is produced by the superposition of a constant magnetic flux Φ (by means of a constant current I) and harmonic flux $\tilde{\Phi}$. Different degrees of magnetic saturation in the respective transformers are used to triple the frequency.

58. Triple Frequency by Means of the Alternating-current Arc (Zenneck).—When an electric arc is fed by an alternating current, the wave form becomes distorted with a pronounced third harmonic.

If a choke coil is inserted in the supply system and a capacity-inductance shunt parallel to the arc, a triple-frequency current can be got by resonance.

59. Double Frequency by Means of Unsymmetrical Magnetization (Arco).—Figure 101 shows the circuit. The primary coils of two similar transformers are connected in series, while the secondaries are connected in opposition through a variometer and a variable condenser. A direct

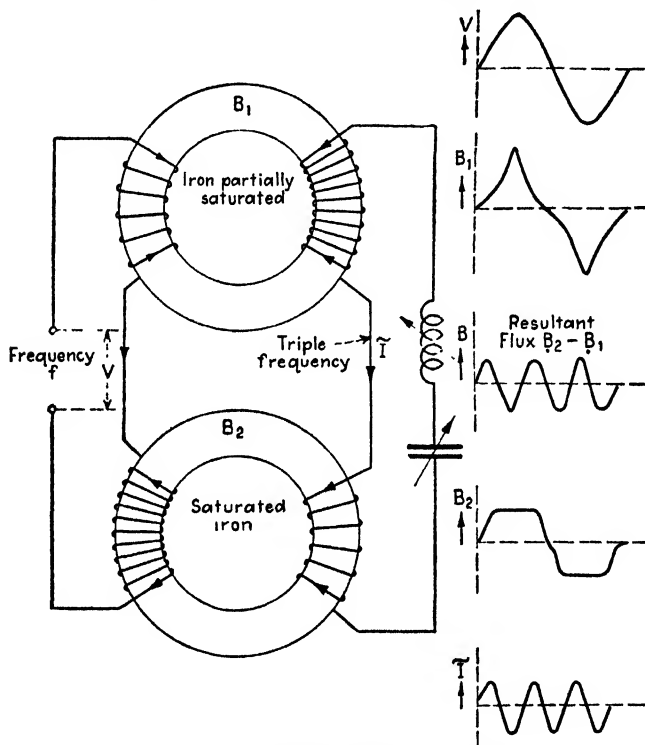


FIG. 102.—Threefold frequency output.

current I produces unsymmetrical magnetization. At the same instant, the alternating flux density \tilde{B} increases in one transformer to $+B_1 = \tilde{B} + \tilde{B}$ and decreases in the other transformer to $-B_2 = \tilde{B} - \tilde{B}$. Because of the opposing series connection of the secondaries, the flux densities act as $B_1 - B_2$ and are such that a strong double periodic-resonance current \tilde{I} flows in the output branch. By applying the reflection principle of R. Goldschmidt (page 59),¹ the frequency can be multiplied several times in steps.

60. Triple Frequency by Means of Transformers Which Are Magnetized to a Different Degree (Epstein, Joly).—The primary coils of the

¹ For details; "Hochfrequenzmesstechnik," 2d ed., Springer, Berlin, 1928, pp. 8-10.

arrangement of Fig. 102 are connected in indirect series and the secondaries in direct series. The condenser and the variometer in the output branch are used to tune to the triple frequency. The flux-density wave B_1 is peaked, since the corresponding transformer does not employ enough ampere-turns ($\bar{I}_{\max} < \text{saturation current}$), while the other transformer has sufficient turns to produce complete saturation of the core. Therefore the corresponding B_2 wave has a flattened shape. The

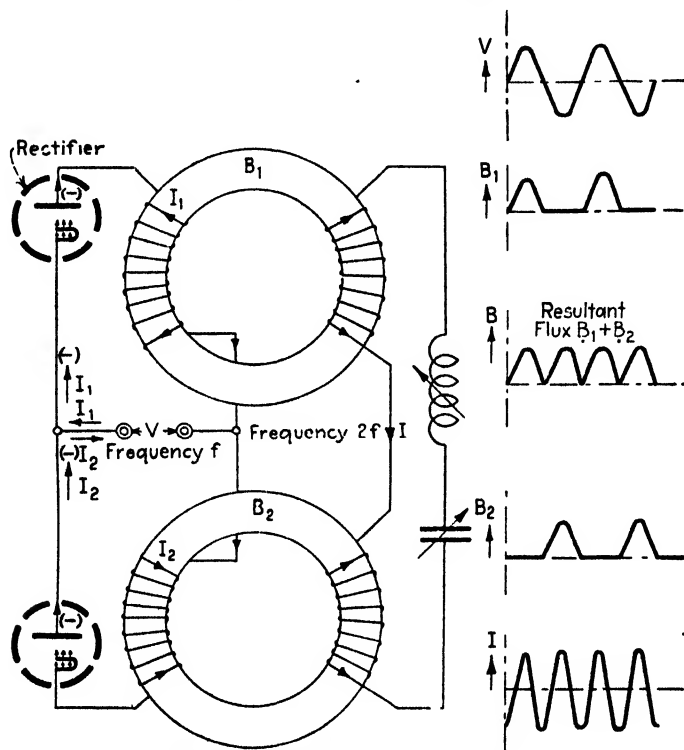


FIG. 103.—Double frequency output.

resulting density $B = B_2 - B_1$ is responsible for the output current I of triple frequency.

61. Double Frequency by Means of Rectified Half Waves.—The method indicated in Fig. 103 makes use of a hot-cathode rectifier (of ordinary or tungar kind) or any other rectifier (cuprox, etc). The primary coils are again in indirect series. Since the current I_1 produces B_1 pulses of opposite polarity (at times when I_1 does not act), a double periodic-resonance current can be taken off because $B = B_1 + B_2$ is effective.

62. Frequency Multiplier by K. Schmidt.—This method does not require static (direct-current) magnetization and needs only a single

autotransformer. The exciting ampere-turns are chosen so that the core is highly saturated. This causes sharply peaked induced voltages and a great number of powerful harmonics. The output frequency is produced by tuning to one of the higher harmonics.¹

63. Sixfold Frequency Multiplication by Means of a Full-wave Kenotron Rectifier Which Employs Temperature and Space-charge Effects.—With thermionic rectifiers, too low a cathode temperature flattens the rectified half waves, while insufficient plate potentials produce peaked half waves. Therefore, when the rectified current of a full-wave rectifier with a maximum plate potential $E_p < E_s$ (smaller than the saturation potential) is superimposed on a rectified current of another full-wave rectifier with an insufficient cathode temperature, a current of sixfold frequency can be selected by tuning. A sixfold frequency, however, requires the peaked caps to be added to the flattened caps. The space charge can also be controlled by changing the space-charge characteristic by means of one or two grids for each anode.

64. Frequency Multiplication by Means of Current Impulses.—Arrangements of this type make use of the principle that, when a condenser C (Fig. 104) receives unipolar current pulses (I_0 charging current) during t sec, and when during the intervals when $I_0 = 0$, which last for $(2m - 1)t$ sec, the condenser freely discharges through the inductance L , a sustained oscillation current I of frequency $F = mf$ can be selected by tuning the CL branch. The quantity f denotes either an imagined or an actual reference frequency which produces the variation of I_0 . For the former case, the current impulses I_0 (shaded caps of dotted sine waves in Fig. 104) are imagined as portions of sine waves. We then have $f = 1/T_0$. For the actual case, the sinusoidal curve denotes the reference time curve, of which the shaded portion only is utilized.

1. Hence, when regularly occurring voltage impulses E_0 produce the current impulses I_0 indicated in the upper representation of Fig. 104 (case $f = F$) and when the CL branch is adjusted so that

$$f = \frac{1}{2\pi\sqrt{CL}} = F$$

a sustained oscillation current I circulates in this branch. The negative-current halves have a somewhat smaller amplitude since the circuit losses must be supplied. This is not the case for the positive half waves, since during that interval the energy due to loss is being supplied.

2. When the regularly occurring current impulses I_0 occur somewhat slower than above and are such that the charging time lasts only t sec (t is only a fraction of a second), then the interval during which there is no energy supplied and the condenser C discharges itself becomes

¹ A similar system is described by W. Dornig, *E.T.Z.*, **39**, 223, 1925.

$$[2m - 1]t = 3t \text{ sec}$$

Then we have the case $F = 2f$, that is, a doubling of the supply frequency.

3. In the same way the illustrated cases for $F = 3f$, $= 4f$, etc., can be explained.

The shaded areas represent the quantity of electricity which is either supplied or sustained by the supply of voltage E_0 .

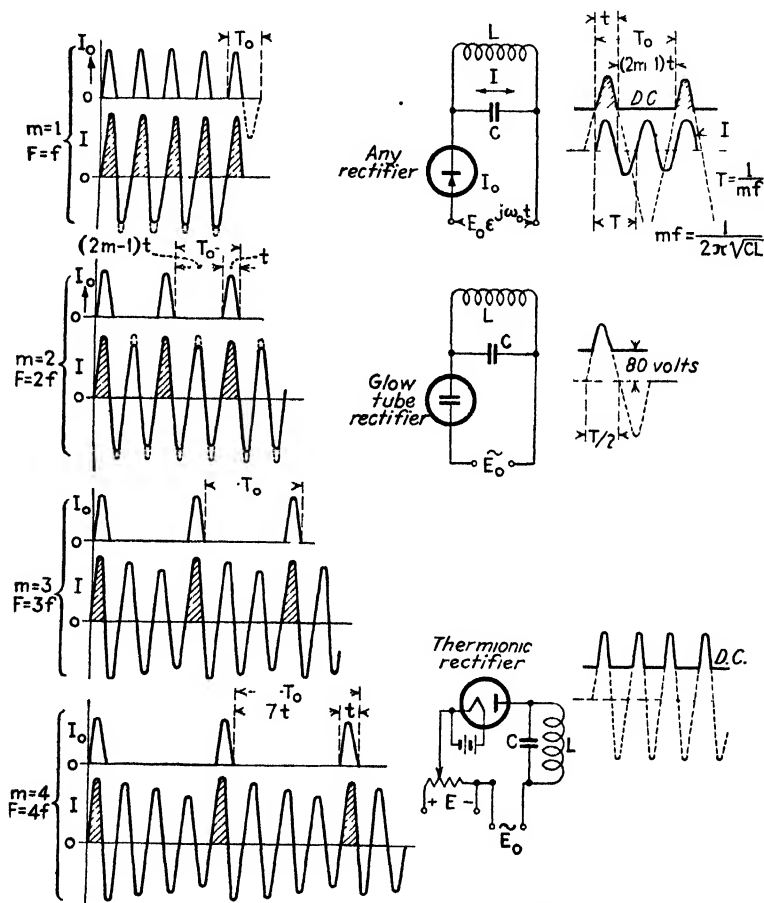


FIG. 104.—Frequency multiplication by impulse excitation.

The current impulses I_0 can be produced by commutator arrangements or by impulse transformers (which produce peaked positive half waves). They can also be produced by quenched spark gaps, arc oscillations of the pronounced second type, and the like. But, usually, it is far more expedient to use ordinary sinusoidal voltages for the supply E_0 . It is then only necessary to utilize "wave caps" of sufficient size.

This can be done by means of either certain types of rectifiers or ordinary electron tubes in which sufficient negative grid bias is provided. These schemes are described in more detail in the next sections.

Figure 105 shows the case in which the plate current of an ordinary three-element electron tube is of rectangular shape and can be expressed as

$$i_p = i_s[0.25 + 0.45 \cos \omega t + 0.32 \cos 2\omega t + \dots]$$

For the amplitude of the oscillation of double frequency, we have

$$i' = 0.32i_s$$

For the case of a triple frequency, 21 per cent of i_s would be available in the output current.

65. Two-element Tubes as Frequency Multiplier.—In Fig. 104, I_0 denotes the rectified current. An alternating voltage $E_0 e^{j\omega_0 t}$ of frequency $f = \omega_0/(2\pi)$ is impressed on the system. The rectifier is so adjusted that the condenser C receives a charge from E_0 during the time t , and the oscillation constant CL is chosen of such a magnitude that

$$T = 2\pi\sqrt{CL} = \frac{1}{mf}$$

where T is in seconds; C in farads, L in henries, and f in cycles per second. An oscillation current I of the m -fold frequency (equal to mf) is then obtained. For example, for a frequency multiplication of 5, we have $m = 5$, and the charging time to be maintained is $t = T_0/10 = 1/(10f)$ since we must satisfy the relation

$$t + [2m - 1]t = T_0/10 + [2 \times 5 - 1]T_0/10 = T_0.$$

The correct adjustment of t can be made with the help of a glow-discharge rectifier. This type of rectifier has an infinite resistance up to the lower critical voltage (in some cases 80 volts). But when this voltage is reached, the resistance suddenly decreases and a current flow sets in. Therefore it is possible to adjust for the proper charging time t by means of a suitable voltage. This can also be done by the superposition of a suitable steady voltage. An ordinary thermionic two-element tube can also be used. The time t is then obtained by means of a suitable negative bias in series with the alternating voltage.

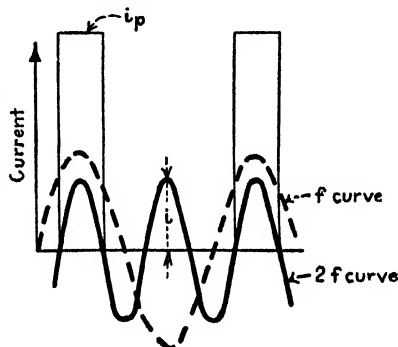


FIG. 105.—Frequency multiplication by means of rectangular plate current (i_p) impulses.

66. Three-element Tube as a Frequency Multiplier.—In the method indicated in Fig. 106, E_c' denotes a negative grid bias for which no plate current I_p is possible. Therefore, when such a negative bias E_c is chosen that the impressed voltage wave \tilde{E} of frequency f produces only current impulses I for the portions 1–2–3, 4–5–6, 7–8–9, etc., and the oscillation constant CL is properly chosen, a resonance current \tilde{I} of the m -fold frequency of f is obtained.

67. Magnetron as Frequency Doubler.—In the magnetron tube shown in Fig. 107 the magnetic field of the axial filament current is used

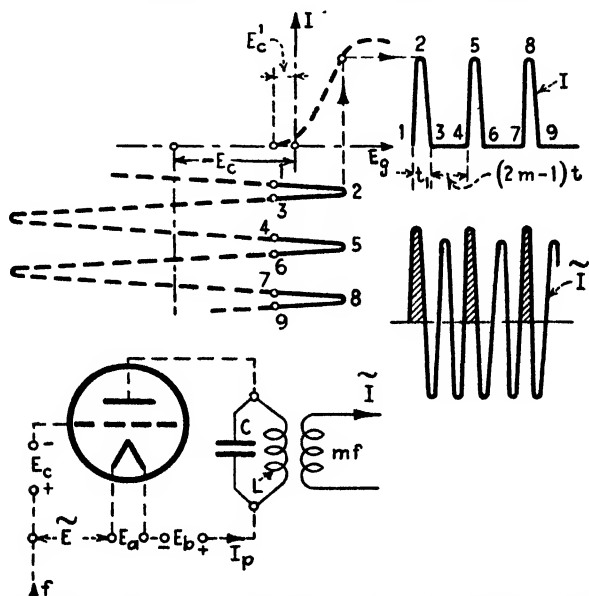


FIG. 106.—Frequency multiplication with a three-element tube.

to control the electron emission to the cylindrical anode. When a sufficiently heavy filament current is flowing, the electrons e , for a certain current, flow along the path as indicated. Hence, when an alternating current of frequency f heats the filament, electrons are deflected alternately upward and downward; while at the instants when zero instantaneous filament current exists, maximum electron current passes toward the cylindrical anode. When the heating current is sufficiently large, the anode current i_p will vanish completely at the instants for which the heating current has its maximum positive and negative value. In the CL circuit a pronounced double-frequency current can then be selected by tuning.

68. Cathode-ray Tube for Frequency Multiplication.—In Fig. 108 a cathode-ray tube is used which has external electrodes at the end surface of the tube. The eight metal electrodes are all connected to the grid of

an amplifier. The cathode ray is circularly polarized by means of the deflection condensers which are connected across the resistance R and condenser C , respectively. Hence for eight electrodes the grid will receive eight impulses per period and, if the CL circuit is tuned to $8f$, a current of this frequency will exist in the outgoing branch.

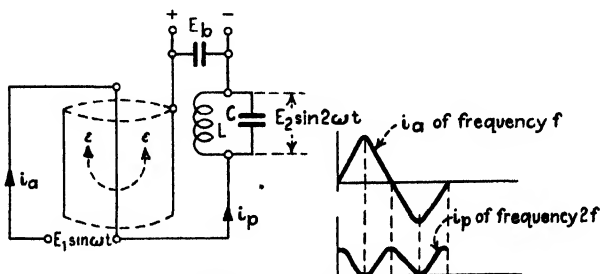


FIG. 107.—Magnetron frequency doubler.

69. Temperature Effect of a Hot Cathode as Frequency Doubler.—

The emission current which flows from the hot filament of a thermionic tube toward the anode can also be dynamically controlled (to some extent) by the temperature of the filament. For the static case, a small variation in the filament current (unless there is insufficient positive plate potential) produces an appreciable change in the current flowing to the anode. This is also true in the dynamic case when the frequency of the temperature variation is not too high. Because of the heat inertia

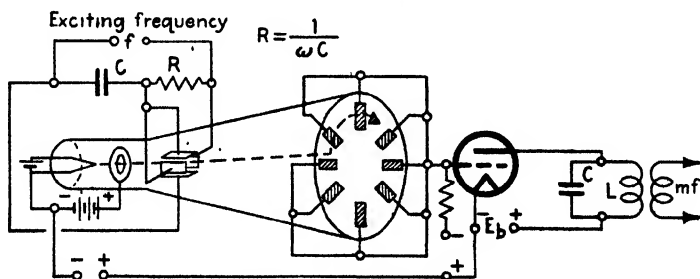


FIG. 108.—Cathode-ray tube as frequency multiplier.

of the filament, only current alternations up to about 500 cycles sec can produce sufficient double-frequency effects in the plate current. A doubling of the frequency is obtained since the temperature of the filament is proportional to the square of the filament current. The actual curve for the absolute temperature curve T can therefore be thought of as being due to a fictitious steady filament current I_A superimposed upon which is an alternating current I_B . The steady and variable components of the temperature can be computed from the expressions

$$T_A = \sqrt[4]{\frac{RI_A^2}{p \cdot S \cdot H}} \quad T_B = dI_B$$

for

$$d = D\epsilon^{-j\Psi} \quad D = \frac{B}{\sqrt{A^2 + \omega^2\eta^2}}$$

$$\Psi = \tan^{-1} \frac{\omega\eta}{4\rho S T_A^3} \quad \omega = 2\pi(2f)$$

if T is in Kelvin degrees, S the surface of the filament in square centimeters, the radiation constant $\rho = 1.37 \times 10^{-12}$ cal/cm² · sec · deg⁴, R effective average filament resistance, η the heat capacity of filament (equal to volume \times specific weight \times specific heat) and H the mechanical equivalent of heat (equal to 4.18 wattsec/cal). Therefore it can be seen that, for $I_p = I_m \epsilon^{j\omega t}$, the variation T_B has an amplitude DI_m and leads that current ripple by angle Ψ .

Undesirable hum in tubes whose cathodes are heated directly with alternating current can therefore be partly due to this effect, especially when the plate voltage is high enough so that small variations in the filament temperature can be thermally amplified into the plate branch. The same principle can be utilized to produce low-frequency oscillations with ordinary two-electrode thermionic tubes.

CHAPTER VI

RECTIFICATION AND INVERSION OF CURRENTS

A *rectifier* is a device for the conversion of some form of alternating-current wave into a unidirectional wave. An *inverter* changes some form of unidirectional current into some form of alternating current. The inversion of currents may open up in the near future more economic power transmission. Since a rectifier is an electrical conductor which offers less resistance to current in one direction than to current in the opposite direction, Ohm's law does not generally hold and, if it does, only for a certain range of current values and for a certain direction of

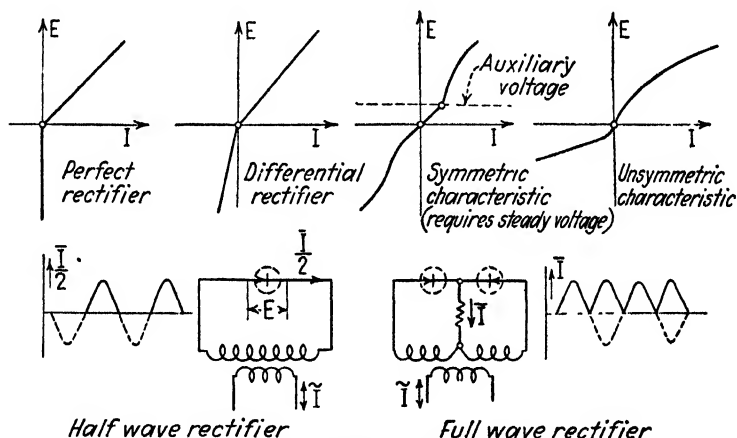


FIG. 109.—Rectifier characteristics.

current flow. Inasmuch as a rectified current is generally a pulsating direct current, it is of importance to distinguish between the effective current value I as indicated by a square-law instrument (thermoelectric, hot-wire meter, dynamometer, eddy-current meter) and the average current reading I_{av} as indicated on a direct-current meter (moving coil rotates between the poles of a permanent magnet). Hence, if a steady current component I_1 exists and a component $I_2 \sin \omega t$, the square-law meter will read the value $\sqrt{I_1^2 + 0.5I_2^2}$, while the direct-current meter registers only the value I_1 .

70. Basic Characteristics of Rectifiers.—Figure 109 includes the characteristics of nearly any type of rectifier.

1. A *perfect* rectifier is then one for which a current flow is possible in one direction only and for which Ohm's law holds for current flow in this direction. An infinite resistance is offered when the polarity is reversed. Most of the thermionic rectifiers belong practically to this class except that the internal-resistance line is straight for only a limited range of current flow. When saturation sets in, the current flow is independent of the voltage applied. This phenomenon is utilized in the linear time-axis apparatus used with cathode-ray tubes. Near points of zero voltage, the characteristic also bends toward the origin of the voltage-current coordinates.

2. An ideal *differential* rectifier offers less resistance to current in one direction than to current in the opposite direction. Ohm's law holds for the respective directions of flow only.

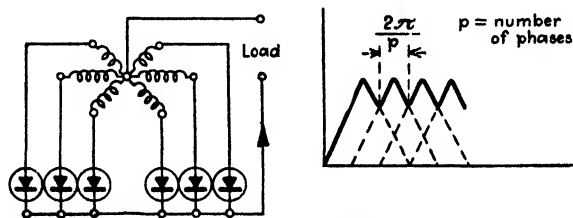


FIG. 110.—Six-phase rectifier ($p = 6$).

3. The third type of rectifier follows Ohm's law for a small range of current flow only, and the voltage-current curve is symmetrical with respect to the origin. Since such a device offers the same resistance to current flow in either direction, rectification is possible only when an appropriate steady voltage from a direct-current source is superimposed. This voltage disturbs the symmetry.

4. The fourth type of rectifier has an unsymmetrical internal characteristic, but here also the degree of rectification can be increased by superimposing an appropriate steady voltage. Many electrolytic and crystal rectifiers belong to this class. The lower representations of Fig. 109 show the case of a half-wave (single-phase) and a full-wave (biphase) rectifier. Figure 110 illustrates polyphase rectification.

71. Form Factor, Peak (Amplitude) Factor, and Useful Portion of a Rectified Current.—Since the energy of the rectified current is important, it is necessary to know not only the degree of the valve action of a certain rectifier but also the form of the rectified current. Many rectifiers distort the half waves, more or less, because the internal resistance R_v of the valve depends on the impressed voltage. Some types of practical rectifiers show small inverse currents so that only the differential effect is useful in the load branch. Figure 111 illustrates these cases. I_e denotes the effective current value measured, for instance, with a dyna-

mmometer type of instrument, and I_m the average value of the current as indicated by a direct-current meter. The dotted curves indicate the alternating current which would flow if no rectifier were in the circuit. The maximum amplitude I_1 of the rectified current is always smaller than I_{max} of the corresponding alternating current, since a certain rectifier resistance R_v is effective. In many cases the valve resistance R_v is vari-

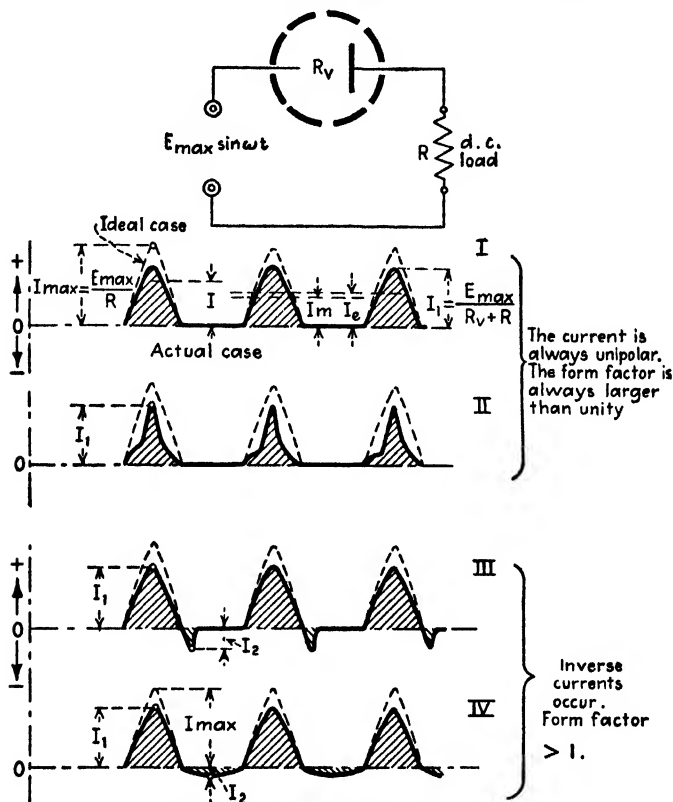


FIG. 111.—Possible rectifier actions.

able; for instance, a thermionic rectifier exhibits the smallest resistance when the impressed alternating voltage is either equal to or greater than the saturation anode potential¹ of the tube. In many cases, the effect of the variable rectifier resistance can be minimized by the load inductance or resistance. The magnitude of the load resistance R depends on the saturation current I_s as well as upon the alternating voltage, since R should be chosen so that $I_s[R + R_v] = E_{max}$. This is the condition for

¹ The saturation potential corresponds to the voltage between the hot cathode and the anode which, for a certain cathode temperature, just passes the full electron emission to the anode.

maximum energy conversion. Since the degree of rectification is equal to the ratio of useful current $I_m = I_{av}$ in the rectifier branch to the possible alternating current I , it is evident that the power delivered to the load is limited by the magnitude of the valve resistance R_v and that of the load. Since this ratio is given by

$$\xi = \frac{1}{2F \left[\frac{R_v}{R} + 1 \right]}$$

for a perfect rectifier, the maximum value for the useful load current occurs when $R_v = 0$. For a half-wave rectifier, the degree of rectification is practically equal to the reciprocal of twice the form factor F , or equal to $50/F$ per cent. When this result is combined with the relation of the internal rectifier resistance for maximum power conversion, optimum rectification effect is obtained

if F is not much greater than unity

and

$$R_v = \frac{E_{\max}}{I_s} - R \text{ is vanishingly small compared with } R$$

that is, R about E_{\max}/I_s , where I_s denotes the saturation current of the rectifier (for instance, of a tube). In this case, the current I_s must be equal to the maximum value I_1 since for a perfect rectifier $I_2 = 0$. For all other kinds of rectifiers, I_1 must be chosen so that the ratio of the maximum rectifier voltage to the effective internal resistance of the valve is equal to the value of I_1 .

The *peak factor* σ is defined by the relation

$$\sigma = \frac{\text{maximum instantaneous value}}{\text{effective value}} = \frac{I_{\max}}{I_e}$$

and the *form factor* by

$$F = \frac{\text{effective value}}{\text{average value}} = \frac{I_e}{I_{av}}$$

Hence, when rectification as in IV of Fig. 111 is under consideration, the peak factor becomes

$$\sigma = \frac{(I_1 + I_2)/2}{I_e}$$

when I_e denotes the current measured with an alternating-current meter in the direct-current branch. Since, for the average current I_{av} , measured in the direct-current branch with a direct-current meter,

$$I_{av} = \frac{I_{\max}}{\sigma F}$$

we find for the form factor in this particular case

$$F = \frac{(I_1 - I_2)/2}{\sigma I_{av}}$$

For a pure sine wave $F = 1.11$ and $\sigma = 1.414$. When the rectified cur-

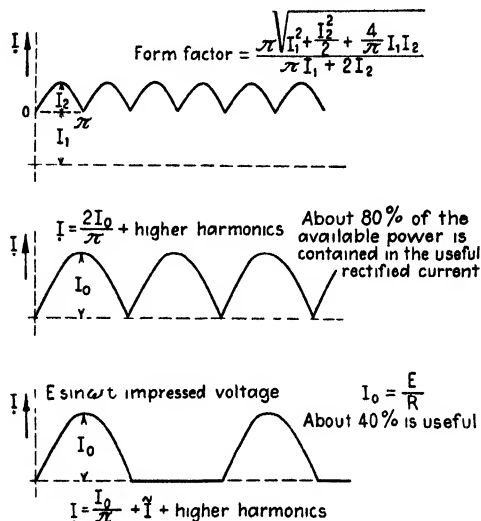


FIG. 112.—Form factor and useful power in different rectified currents.

rent is of the shape indicated in the upper curve of Fig. 112, the form factor becomes

$$F = \frac{\sqrt{\frac{2}{\pi} \int_0^{\frac{\pi}{2}} [I_1 + I_2 \sin \theta]^2 d\theta}}{2 \int_0^{\frac{\pi}{2}} [I_1 + I_2 \sin \theta] d\theta} = \frac{\pi \sqrt{I_1^2 + \frac{I_2^2}{2} + \frac{4}{\pi} I_1 I_2}}{\pi I_1 + 2 I_2}$$

and the peak (amplitude) factor is

$$\sigma = \frac{I_1 + I_2}{\sqrt{I_1^2 + (I_2^2/2) + 4I_1 I_2/\pi}}$$

Therefore by means of the peak and form factors the quality of rectifiers can be investigated.

For half-wave rectification (single phase rectified, sine wave, Fig. 112)

$$i = I = I_0 \left[\frac{1}{\pi} + \frac{1}{2} \sin 2\pi ft - \frac{1}{1 \times 3\pi} \cos 2\pi 2ft - \frac{2}{3 \times 5\pi} \cos 2\pi 4ft \dots \right]$$

$$I_0 = \frac{I_0}{2} \quad I_{av} = \frac{I_0}{\pi} \quad F = \frac{\pi}{2}$$

For double-phase rectification (Fig. 112),

$$i = I = I_0 \left[\frac{2}{\pi} - \frac{4}{\pi} \sum \frac{\cos 2m\theta}{[2m-1][2m+1]} \right]$$

$$= \frac{2I_0}{\pi} \left[1 - \frac{2}{3} \cos 2\pi 2ft - \frac{2}{3 \times 5} \cos 2\pi 4ft - \frac{2}{5 \times 7} \cos 2\pi 6ft \dots \right]$$

$$I_e = \frac{I_0}{\sqrt{2}}; \quad I_{av} = \frac{2I_0}{\pi}; \quad \sigma = \sqrt{2}; \quad F = \frac{\pi}{2\sqrt{2}}; \quad \theta = \omega t; \quad m = 1, 2, 3, \text{etc.}$$

For the polyphase case indicated in Fig. 110,

$$I = \frac{pI_0}{\pi} \sin \frac{\pi}{p} \left[1 + 2 \sum_{m=1}^{\infty} \frac{\cos m\pi \omega t}{1 - [mp]^2} \right]$$

where

p = number of phases

m = order of harmonic

$m = 1$ for the fundamental frequency

$$I_e = \sqrt{\frac{1}{2} + \frac{p}{4\pi} \sin \frac{2\pi}{p}} \quad \sigma = \frac{I_0}{\sqrt{\frac{1}{2} + \frac{p}{4\pi} \sin \frac{2\pi}{p}}}$$

$$I_{av} = \frac{p}{\pi} \sin \frac{\pi}{p} \quad F = \frac{\sqrt{\frac{1}{2} + \frac{p}{4\pi} \sin \frac{2\pi}{p}}}{\frac{p}{\pi} \sin \frac{\pi}{p}}$$

In order to get a more detailed picture of the energy of the rectified current, it is convenient to resolve the resultant current flowing in the direct branch into the various components.¹ By "useful current" is meant that component which determines the direct-current supply of energy to the load. Several components can be more or less wattless. The useful power determines the rectification effect and the efficiency of the rectifier. It is essential to distinguish between the degree of rectification and efficiency of an electric valve since a rectifier also has internal losses and acts as a power-limiting device.

In case of full-wave rectification, for which a symmetrically built thermionic or other rectifier of resistance R is used, if the plate and cathode excitations are chosen so that for an impressed voltage E both half waves are practically undistorted (middle curve of Fig. 112), the rectified current I at any instant is

¹ Proofs of various formulas given in this chapter are given in an article in *Elektrotech. u. Maschinenbau*, 40, 37, 1922; B. LIEBOWITZ, *Proc. I.R.E.*, 5, 33, 1917.

$$I = \frac{E}{R} \left[\frac{2}{\pi} - \frac{4}{\pi} \sum \frac{\cos m\omega t \cos^2(m\pi/2)}{m^2 - 1} \right] \text{ for } m = 2, 4, 6, 8.$$

$$= \frac{E}{R} \left[\frac{2}{\pi} \left[1 - \frac{2 \cos 2\omega t}{3} - \frac{2 \cos 4\omega t}{3 \times 5} - \frac{2 \cos 6\omega t}{5 \times 7} - \dots \right] \right]$$

Hence a continuous current $2E/(\pi R) = (2/\pi)I_0$ is superimposed on a double-frequency alternating current and a series of even higher harmonics. But since the useful current in the direct-current branch is $I = (2/\pi)I_0$ and the amplitude of the current of double frequency $I'' = (4/3\pi)I_0$, we note that

$$I = \frac{3}{2} I'' = \frac{3}{\sqrt{2}} I_e$$

which means that the useful current I in the direct-current branch is about 212 per cent as large as the superimposed double-frequency alternating current. The available power is $E^2/(2R)$ and the useful current carries the portion

$$I^2 R = \frac{4}{\pi^2} I_0^2 R = \frac{8}{\pi^2} \left[\frac{E^2}{2R} \right] = 81.1\%$$

of it, while there is associated with the alternating-current component of frequency $2f$, 18 per cent of power in unavailable form and with the remaining components of higher harmonic frequencies 0.9 per cent of the power in unavailable form, thus producing an unfavorable power factor of the alternating-current power supply. That this is true can be seen from the following calculation involving the effective double-frequency current I_e which gives

$$I_e^2 R = \left[\frac{4}{3\pi} \frac{I_0}{\sqrt{2}} \right]^2 R = \frac{16}{9\pi^2} \left[\frac{E^2}{2R} \right] = 18\% \text{ of } \left[\frac{E^2}{2R} \right]$$

For a half-wave rectifier (single phase, lower curve of Fig. 112) the instantaneous current I of the rectified current is

$$I = I_0 \left[\frac{1}{\pi} - \frac{1}{2} \cos \omega t + \frac{2}{3\pi} \cos 2\omega t - \frac{2}{3 \times 5\pi} \cos 4\omega t + \dots \right]$$

which means that a continuous current $I = I_0/\pi = E/(\pi R)$ has superimposed on it an alternating current I_e of the supply frequency, whose amplitude is $I' = I_0/2 = E/(2R)$. There is also a series of even higher harmonics. If the useful current I is again compared with the effective value of the fundamental current I_e which flows in the direct-current branch, for the effective value, we have

$$I_e = \frac{\pi}{2\sqrt{2}} I$$

since

$$I = \frac{2}{\pi} I' = \frac{2\sqrt{2}}{\pi} I_e$$

Hence the strength of the useful current I is only 90 per cent of the effective value I_e . For half-wave rectification, the available power is then only $E^2/(4R)$ and the useful current I takes only 40.55 per cent of the available current since

$$I^2 R = \frac{I_0^2}{\pi^2} R = \frac{4}{\pi^2} \left[\frac{E^2}{2R} \right]$$

Associated with the superposed fundamental current I_e there is unavailable power of an amount given by

$$I_e^2 R = \left[\frac{I_0}{2\sqrt{2}} \right]^2 R = \frac{1}{2} \left[\frac{E^2}{4R} \right] = 50\%$$

and associated with the even higher harmonics there is the remaining unavailable 9.45 per cent.

In a similar way the case of any multiphase rectified current, as in Fig. 110, may be analyzed by means of the relation

$$I = \frac{pI_0}{\pi} \sin \frac{\pi}{p} \left[1 + 2 \sum_{m=1}^{\infty} \cos \frac{mp\omega t}{[mp]^2} \right]$$

where p stands for the number of phases and m for the consecutive harmonics.

72. Direct-current Reading in Comparison with the Effective Value of the Second Harmonic.—It is always a comparatively easy matter to measure small direct currents (with microammeters, galvanometers, etc.). However, such measurements are rather difficult with small high-frequency currents since the best instruments (with thermocouples) are based on a square-law indication. The deductions in the last paragraph indicate a method by means of which a superimposed double-frequency current can be determined by a direct-current meter. It is then only necessary to have the reactance in the external circuit of the rectifier small compared with the resistance.

When ordinary two-element or three-element thermionic rectifiers (grid and anode connected together) are employed for rectification, we must deal with three cases, namely,

1. When very small currents are being rectified, in which case the current is practically proportional to the square of the impressed voltage.
2. When somewhat larger currents are rectified, in which case the current varies practically linearly with the voltage, and
3. When the rectifier is overloaded and an empirical law must be used.

The second case has been treated in the last paragraph and, for an impressed voltage $E \cos \omega t$, the current in the rectifier branch is proportional to the series

$$1 + \frac{\pi}{2} \sin \omega t - \frac{2}{3} \cos 2\omega t - \frac{2}{15} \cos 4\omega t - \dots$$

That is, a direct-current meter indicates half the amplitude value of the double-frequency component. For very small currents, the following series is obtained:

$$\frac{1}{4} + \frac{4}{3\pi} \sin \omega t - \frac{1}{4} \cos 2\omega t - \frac{4}{15\pi} \sin 3\omega t - \frac{4}{105\pi} \sin 5\omega t \dots$$

and the direct-current meter indicates directly the amplitude of the double periodic current. For measurements of very small currents, the rectifier must use such a negative auxiliary voltage that the current in the anode branch is just zero when no alternating voltage is applied (that is, the electron pressure must be balanced out).

73. Voltage, Current, and Power in a Rectifier Circuit.—As has already been stated, a rectified current may generally be thought of as being composed of a continuous current \bar{I} and a series of harmonic currents. If I_1, I_2, I_3 , etc., are the amplitudes of the various harmonic currents and E_1, E_2, E_3 , etc., the amplitudes of the corresponding voltages, and \bar{E} the steady voltage producing the continuous current \bar{I} , the effective values of the resultant voltage and current, according to ordinary alternating-current theory, are

$$\left. \begin{aligned} E &= \sqrt{\bar{E}^2 + 0.5[E_1^2 + E_2^2 + E_3^2 + \dots]} \\ I &= \sqrt{\bar{I}^2 + 0.5[I_1^2 + I_2^2 + I_3^2 + \dots]} \end{aligned} \right\}$$

The power in the rectifier branch is

$$W = \left\{ \begin{aligned} &\bar{E}\bar{I} + 0.5[E_1 I_1 \cos \varphi_1 + E_2 I_2 \cos \varphi_2 + E_3 I_3 \cos \varphi_3 + \dots] \\ &\quad \text{average power} \\ &EI = \sqrt{[\bar{E}^2 + 0.5(E_1^2 + E_2^2 + E_3^2 + \dots)][\bar{I}^2 + 0.5(I_1^2 + I_2^2 + I_3^2 + \dots)]} \\ &\quad \text{equivalent power} \end{aligned} \right.$$

If \bar{A}, A_1, A_2, A_3 , etc., are the corresponding amplitudes which stand for either voltage or current, it should be remembered that an *ordinary direct-current meter* (current flows through a moving coil which rotates between the magnet poles) inserted in the rectifier branch *indicates the value \bar{A}* , while a *dynamometric instrument* (a stationary and rotating coil in series carries the current which either measures current or expresses voltage, respectively) *indicates the value*

$$\sqrt{\bar{A}^2 + 0.5[A_1^2 + A_2^2 + A_3^2 + \dots]}$$

Hence, when a continuous current \bar{I} has superimposed on it an alternating ripple $I_1 \sin \omega t$; we have for $\rho = I_1/\bar{I}$

$$\frac{\text{Direct-current meter reading}}{\text{Square-law meter reading}} = \sqrt{1 + 0.5\rho^2} \cong 1 + \frac{1}{4}\rho^2 - \frac{1}{16}\rho^4 + \dots$$

making the ratio dependent on ρ . For very small ripples, both instruments then read alike.

For full-wave rectification as shown in Fig. 112 where all the harmonics are in phase with their voltages, the average power is

$$W = \frac{1}{2\pi} \int_0^{2\pi} e i d(\omega t) = \frac{1}{2\pi} \int_0^{2\pi} \left\{ E_0 \left[\frac{2}{\pi} - \frac{4}{3\pi} \cos 2\omega t - \frac{4}{15\pi} \cos 4\omega t \right] \right\} \\ \left\{ I_0 \left[\frac{2}{\pi} - \frac{4}{3\pi} \cos 2\omega t - \frac{4}{15\pi} \cos 4\omega t \right] \right\} d(\omega t) = \frac{E_0 I_0}{2} = EI$$

74. Derivation of the Rectification Law.—When dealing with a device which does not follow Ohm's law over the entire operating range, we are

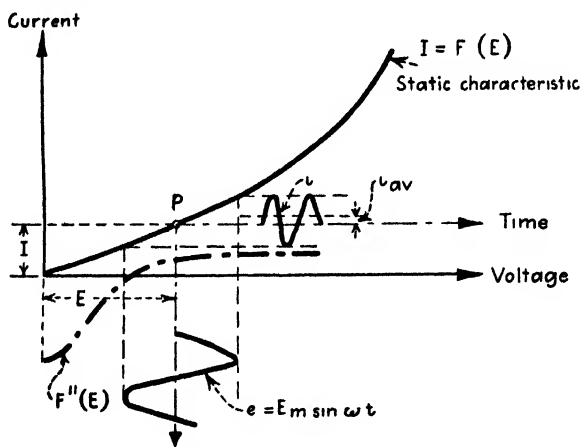


FIG. 113.—Rectification action.

concerned with voltage-current characteristics as shown in Fig. 109. We have a nonlinear static characteristic $I = F(E)$ as indicated in Fig. 113. A variable voltage e then gives, according to Taylor's theorem, if

$$\frac{d}{dE} F(E) = F'(E); \quad \frac{d^2}{dE^2} F(E) = F''(E), \text{ etc.,}$$

$$I + i = F[E + e] = F(E) + eF'(E) + \frac{e^2}{1 \times 2} F''(E) + \frac{e^3}{1 \times 2 \times 3} F'''(E) + \dots$$

and upon subtraction of $I = F(E)$ we have

$$i = eF'(E) + \frac{e^2}{2} F''(E) + \frac{e^3}{6} F'''(E) + \dots$$

For the operating point P , the average value I_{av} of the rectification is then

$$I_{av} = \frac{1}{T} \int_0^T i dt = \frac{1}{T} \left\{ F'(E) \int_0^T e dt + \frac{F''(E)}{2} \int_0^T e^2 dt + \frac{F'''(E)}{6} \int_0^T e^3 dt + \dots \right\}$$

But the average values of e , e^3 , etc., vanish for $e = E_m \sin \omega t$. With still higher powers neglected, the remaining term becomes

$$\frac{1}{T} \int e^2 dt = \frac{E_m^2}{2}$$

and

$$i_{av} = \frac{E_m^2}{4} F''(E) = \frac{E_m^2}{4} \frac{d^2 I}{dE^2} \dots \quad (1)$$

Hence the rectification effect increases with the square of the impressed voltage and the curvature $d^2 I/dE^2$ of the voltage-current characteristic at the operating point. Therefore no rectification is possible when the curvature vanishes. The rectification effect i_{av} , that is, the value of the net current, becomes a maximum when at the operating point P the maximum rate of change of slope occurs. This can also be seen from Fig. 120 where rectification with three-element tubes is considered and where the upper or, preferably, the lower bend of grid-voltage plate-current characteristic can be used for rectification. When the radius

$$r = \frac{\{1 + (dI/dE)^2\}^{1.5}}{d^2 I/dE^2}$$

of the curvature changes slowly, the slope dI/dE is mostly responsible for the rectification action which is then all the more pronounced the greater dI/dE .

If the impressed variable voltage is of the form

$$e = E_1 \sin \omega t + E_2 \sin 2\omega t + E_3 \sin 3\omega t + \dots$$

the change i_{av} of the mean rectifier current, or the rectification effect, is

$$i_{av} = \frac{E_1^2 + E_2^2 + E_3^2}{4} \frac{d^2 I}{dE^2} \quad (2)$$

When two high-frequency voltages of somewhat different frequencies f and $f + f_b$ are applied to a rectifier circuit (using, for instance, a crystal rectifier, a two-element thermionic tube, etc.) a beat-tone frequency f_b is heard in a telephone receiver inserted in the rectifier output circuit. The resultant impressed rectifier voltage is then of the form

$$e = E_1 \sin 2\pi f t + E_2 \sin 2\pi (f + f_b) t$$

and the rectification action, according to (1) becomes

$$\begin{aligned}
 i_{av} &= av \left[\frac{E_1 \sin 2\pi ft + E_2 \sin 2\pi(f + f_b)t}{2} \right]^2 \frac{d^2 I}{dE^2} \\
 &= \underbrace{\left\{ \frac{E_1^2}{4} + \frac{E_2^2}{4} + av[E_1 E_2 \sin 2\pi ft \sin 2\pi(f + f_b)t] \right\}}_{\text{cannot be heard}} \frac{d^2 I}{dE^2} \\
 &= \left\{ K + av \left[\frac{E_1 E_2}{2} (\cos 2\pi f_b t - \cos 2\pi(2f + f_b)t) \right] \right\} \frac{d^2 I}{dE^2}
 \end{aligned}$$

The average value of each cosine term vanishes but the cosine term of the beat frequency f_b varies so slowly¹ that a beat tone is produced in the telephone receiver, of intensity

$$J = \frac{E_1 E_2}{2} \cos 2\pi f_b t \frac{d^2 I}{dE^2} \quad (3)$$

Therefore, if the amplitude E_1 of the local oscillations is kept constant, the sound intensity is directly proportional to the amplitude of the unknown voltage E_2 and to the curvature of the rectifier characteristic. Hence great sensitivity for weak voltages is obtained with the beat method of detection since straight proportionality instead of a square law prevails.

75. Notes on the Application of Rectifier and Inverter Circuits.—

In the preceding paragraphs it has been shown that for full-wave rectification only about 80 per cent of the available energy can be used under the most favorable conditions. The remaining 20 per cent of energy oscillates uselessly to and fro in the system, like the 60 per cent for half-wave rectification. Therefore full-wave rectification is the better, even though there is still an unfavorable power factor produced at the input side. Therefore when a B eliminator of this type is used (Fig. 114), the voltage E and I cannot be in phase and the power company, as we might say, must deliver wattless current which is not registered by the watt-hour meter.

It is an easy matter to show that a loaded transformer is equivalent to a reactance and a resistance in series. The actual values of reactance and resistance are, however, not the same as the primary reactance and resistance when the secondary is open. When this scheme is applied to the case shown in Fig. 114, the B eliminator with the load can be represented by an effective inductance L_e and ohmic resistance R_e . The power-factor corrector 1 then consists of a resistance R with a series

¹ If the difference frequency f_b is greater than the smallest high frequency f , then the character of the resultant beat curve (interference curve) is lost, because then a variation of relatively high frequency is superimposed on a sinusoidal variation of comparatively much lower frequency.

capacity C in shunt with the input terminals and in many eliminators a capacitance of about 2 to 4 μf and a resistance R of about 50 to a few hundred ohms will correct the phase of the input current. Theory shows¹ that the entire eliminator with the RC shunt acts aperiodically; that is, E and I are in phase when

$$R = R_e = \sqrt{\frac{L_e}{C}}$$

and that the phase angle to be corrected is

$$\varphi = \tan^{-1} \frac{\omega L_e}{R_e}$$

If, as in some cases, the capacitance C comes out impractically high (up to 20 μf), the phase corrector 2 of Fig. 114 is more suitable. With

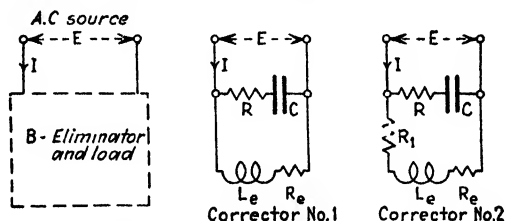


FIG. 114.—Power-factor correctors for battery eliminators.

resistances R_1 of a few ohms, the capacitance C can be brought down to reasonable values (about 2 μf). Resistance R_1 is then in series with R_e and $R_e + R_1$ must satisfy the square-root ratio.

Grid-controlled rectifiers are convenient means for changing direct current into alternating current.² The gas-filled tube acts as a switch to change the unidirectional flow of current from a direct-current source to alternate sections of transformer windings. An inversion with high efficiency is then possible as compared with the low-efficiency inversion in case of high-vacuum tubes. Grid-controlled rectifiers are used in this way in alternating-current radio receivers working on a direct-current supply.

76. Practical Rectifiers.—As to methods of operation, we can distinguish between mechanical rectifiers³ (commutator type, vibrating

¹ "High Frequency Measurements," McGraw-Hill Book Company, Inc., New York, 1933, pp. 9–10, and Fig. 5 on p. 9.

² For details, see K. Henney, "Electron Tubes in Industry," The McGraw-Hill Book Company, Inc., New York, 1934, pp. 199–215.

³ A good description of the action and application of rectifiers can be found in the following books: L. B. Jolley, "Alternating Current Rectification and Allied Problems," John Wiley & Sons, Inc., New York, 1928; A. Güntherschulze, "Electric Rectifiers and Valves," John Wiley & Sons, Inc., New York (translated and revised by N. A. DeBruyne); D. C. PRINCE and F. B. VOGDES, "Principles of Mercury Arc Rectifiers and Their Circuits," McGraw-Hill Book Company, Inc., New York, 1927

reeds, etc.), electrolytic small contact (includes all types of crystal detectors), thermoelectric converters, and also large surface-contact rectifiers such as the cuprox rectifier and tube rectifiers. For rectification of high-frequency currents, the mechanical types of rectifiers are not important. Thermoelectric converters (thermocouples) are very useful for indicating high-frequency currents by means of the direct-current output. Crystal rectifiers are likewise used for such purposes when great accuracy in calibration is not required. Tube rectifiers of the kenotron type are used to rectify currents in high-voltage circuits, while gaseous rectifiers (mercury arc, tungar, etc.) can be used for heavy-current work.

77. Electrolytic and Contact Rectifiers.—Electrolytic rectifiers can be used for the rectification of very small and moderately large currents. But it is understood that weak-current electrolytic rectifiers (for instance, the Schloemilch cell) cannot be used for heavy-current work and that electrolytic rectifiers used for heavier current work (such as the aluminum-lead rectifier using an electrolyte) are not efficient for the rectification of minute currents. Electrolytic rectifiers for the detection of weak high-frequency currents are due to Fessenden, Nernst, Pupin, Pierce, Schloemilch, Hausrath, Zenneck, and other investigators. Some electrolytic rectifiers of this type require a polarization voltage (Schloemilch cell) and therefore cannot be regarded as true rectifiers. They are more or less of historical interest. When the electrolytic cell shows a self-voltage, then polarization takes place without auxiliary voltage. This is always the case when two dissimilar electrodes act in an electrolyte. According to J. Zenneck, a rectifier consisting of lead and aluminum electrodes, respectively, and operating in a 5 per cent solution of ammonium phosphate can be used for currents up to several amperes without producing appreciable heating at the electrodes. A solution of zinc sulphate also may be used. But with the introduction of tungar, cuprox, and other rectifiers, this type of electrolytic rectifier is also practically out of date.

Contact rectifiers¹ of importance in the early days of radio are known as "crystal detectors." They consist of a small contact surface. One pole is formed by a small metal point, the other by some mineral, such as galena or carborundum. Much of the action is probably due to thermoelectric effects because with overloaded crystals a phenomenon similar to thermoelectric inversion can be observed. More recent investigations attribute some of the rectifying action to the same cause as that in electron tubes. It is then assumed that, at the small surface contact, field intensities are produced which liberate electrons and then accelerate them across the minute gap. If a carborundum crystal is used, an unsym-

¹ PIERCE, G. W., "Principles of Wireless Telegraphy," McGraw-Hill Book Company, Inc., New York, 1910, has an entire chapter devoted to such rectifiers.

metrical EI characteristic as in Fig. 109 exists and rectification is possible without an auxiliary steady voltage. The minerals used must show a certain conductivity, although the degree of conductivity is by no means a measure of the degree of rectification. Instead, the latter depends upon the asymmetry and the portion of the voltampere characteristic along which variations take place. It may be said that the rectifying sensitivity depends mostly upon the physical shape of the crystals and the chemical composition of the mineral. The contact surfaces must have a crystalline character and must be clean. A critical pressure of contact exists for which maximum sensitivity occurs and also a critical temperature for optimum rectification.

By means of a certain auxiliary potential, a further increase of rectification can be obtained. The resistance of crystal detectors depends a great deal upon the pressure of contact. Decreasing the pressure increases the resistance and in many cases produces better rectification action. Resistances up to 5000 ohms can be obtained. Since for most work stable operation is preferred to a great but unreliable sensitivity, fixed crystals are used which usually have a resistance between 500 and 2000 ohms. Crystals can be used only for the rectification of small currents up to several milliamperes. For the ordinary laboratory,

galena against a thin coiled brass wire gives a good rectifier for high-frequency currents. Carborundum is also good, but not so sensitive.

For the theory of the crystal rectifier, the rectifier law derived in Sec. 74 can be used.

For contact rectifiers with a large contact surface, reference is made to the two sections following.

78. Electrostatic Relay as a Rectifier.—The electrostatic relay shown in Fig. 115 utilizes the "Johnson-Rabbeek" effect.¹ The characteristic shows that the current passes more easily from the silver plate across the surface of contact toward the semiconductor (achat) than vice versa. The resistance resides mostly in the thin surface film between the metal and the semiconductor, so that a great electric-field strength is set up across the small thickness of separation. Hence great forces of attraction exist between the two plates. The metal plate, under the influence of the high field strength, readily conducts electrons, while

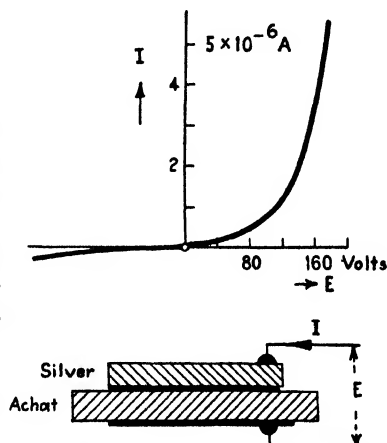


FIG. 115.—Rectification by means of distribution at surface of contact.

¹ KRAMER, W., *Z. Physik*, **28**, 74, 1924.

the semiconductor acts as a divider of ions. In place of achat, marble, slate, and the like, can also be used.

79. Cuprox Rectifier.—This rectifier, which is the work of L. O. Grondahl¹ and P. H. Geiger, is based on a similar action. A copper disk covered with a layer of cuprous oxide shows a greater resistance in one

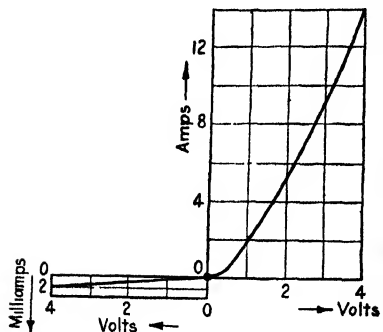


Fig. 116.—Copper-copper oxide rectifier.

than in the other direction. Figure 116 gives the characteristic of such a device. This rectifier will handle up to about 2 amp/sq in. without special cooling. For high-voltage work, the rectifier is built with many disks in series. It may then be assumed that, even at room temperature and with no voltage applied, a great number of electrons escape from the copper and pass into the cuprous oxide. The copper then acts like a thermionic emitter. Because of the short distance between the electrodes, the resistance to the flow of electron emission toward the copper oxide is then small. Hence, when a voltage is applied in the opposite direction, there is a tendency to drive the electrons back again into the copper. But this is opposed by the electron evaporation of the copper so that there will be an intense negative space charge near the surface of the copper. The resultant gradient in the electron density in the oxide then produces a potential gradient which opposes the electron flow in the oxide-to-copper direction.

80. The Two-electrode (Anode and Hot-cathode) Thermionic Rectifier.—Figure 117 illustrates the use of two-electrode thermionic tubes for half-wave and full-wave rectification. For the latter, either two tubes or a single tube with symmetrical anodes (as indicated in the figure) are employed. If high-vacuum thermionic tubes are used, very high voltages can be applied. They are then known as kenotron rectifiers. For voltages as high as 100,000 volts, the rectified current is of the order of several milliamperes. Since the thermionic tube can be saturated

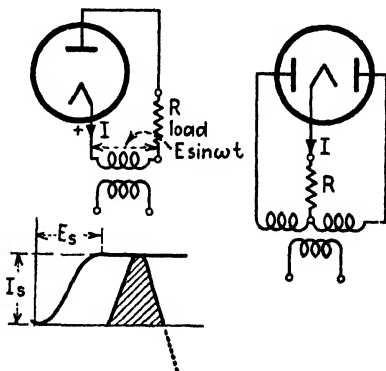


Fig. 117.—Thermionic half-wave and full-wave rectifier.

¹ GRONDAHL, L. O., *Phys. Rev.*, **27**, 813, 1926; L. O. GRONDAHL and P. H. GEIGER, *J. A.I.E.E.*, **46**, 215, 1927.

owing either to space charge or to filament temperature (Fig. 2) and the voltampere characteristic of the tube has the well-known S shape, the maximum value E of the impressed alternating voltage must be chosen so that the saturation current I_s is obtained. If E is just sufficient to produce saturation current, the case indicated in Fig. 117 exists, while with still higher supply voltages more rectangular current pulses I would be produced. The example illustrated on page 9 shows, for instance, that the voltage drop of a certain kenotron carrying just its saturation current I_s is only about 145 volts, in comparison with the supply voltage of 15,000 volts. Kenotrons have been built to give from 5 to 250 ma thermionic current for about 100 volts internal drop and with special designs up to 1 amp could be rectified. But, for such current values, gas-filled rectifiers seem more practical. Since the characteristic of such tubes follows the equation

$$I = kE^n$$

for the current and applied voltage, the static resistance is

$$R_p = \frac{E}{I}$$

while the effective dynamic resistance is

$$r_p = \frac{dE}{dI} = \frac{R_p}{n}$$

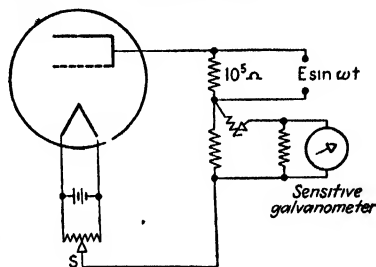


FIG. 118—Rectification of feeble high-frequency currents.

Hence, for the nonlinear portion of the characteristic, the dynamic resistance is smaller than R_p if $n > 1$. For the lower bend of the characteristic, it is about $r_p = R_p/2$. Along the saturation region, I remains constant for any further increase of the applied voltage E . This latter feature is used in obtaining a linear time axis for cathode-ray tubes.

When thermionic rectification is to be used to indicate a feeble high-frequency current by means of a direct-current meter, an ordinary three-element tube as in Fig. 118, with the grid connected to the plate, can be employed. The slider S provides a means for reducing to zero the electron current (owing to electron pressure) which would exist even at zero plate potential. A sensitive galvanometer can then be used and almost linear detection is possible.

81. Mercury-arc Rectifier.—Figure 119 shows a full-wave rectifier of this type. When a half-wave rectifier is used, an auxiliary steady current must be superimposed in order to sustain the arc during the semi-periods of no conduction. In the circuit indicated, the dotted branch serves to start the arc. The chokes to produce biphaserectification must also sustain the ionization of the mercury vapor when the alternating voltages reverse polarity. Heavy currents can be rectified with such a device.

82. Hot-cathode Mercury-vapor Rectifier.—This device combines the advantages of the high-vacuum tube (kenotron) with the low and nearly constant arc drop of the mercury-arc rectifier. These tubes operate in the presence of gas at a *low* pressure (1 to 30μ of mercury) and therefore can operate at relatively high voltages. A. W. Hull¹ found experimentally that cathode disintegration may be avoided if the arc drop is kept below a definite critical value and that for most common inert

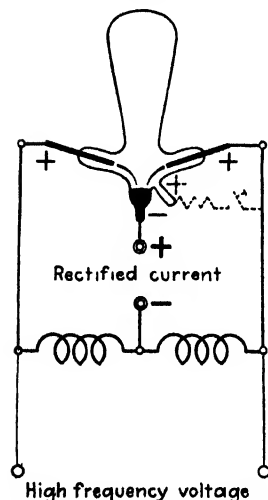


FIG. 119.—Full-wave mercury-arc rectifier.

gases this critical value, at which the positive ions acquire sufficient kinetic energy to disintegrate the cathode, lies between 20 and 25 volts. This caused K. H. Kingdon to introduce mercury vapor to neutralize the space charge present without this gas. The ionization potential of mercury vapor is 10.4 volts and the arc drop about 15 volts, well below the disintegration value, which for mercury vapor is about 22 volts.

The operation of the mercury-vapor hot-cathode tube is about the same as for the mercury-arc rectifier, since for either case the rectified current is determined by the electron emission of the cathode. For the arc rectifier, the emission depends on the size of the spot "dancing" on the mercury pool; that is, it is dependent on the current through the tube. The arc rectifier and the hot-cathode mercury-vapor tube emit a blue glow since the electrons, in passing from the cathode toward the anode, collide with mercury molecules and produce light.

Since the mercury-arc tube must use auxiliary anodes to sustain the cathode spot, ionization also exists during the blocking period but no electrons are received by the anode which happens to be passing through the negative cycle. For a mercury-vapor hot-cathode tube, no ionization can take place during the blocking period. Commercial tubes of this type have been built to give rectified power at potentials up to 10,000 volts, and even higher, and currents up to 2.5 amp. Other tubes of this type give a rectified output up to 400 kw at about 20 kv. In these tubes the space charge is limited by the arc drop of the vapor. It is practically constant in the range from 12 to 17 volts irrespective of the rectified current. The higher power tubes use tungsten cathodes.

¹ HULL, A. W., and W. F. WINTER, *Phys. Rev.*, **21**, 211, 1923 (abstract); A. W. HULL, *Trans. A.I.E.E.*, **47**, July, 1928; K. H. KINGDON, *Phys. Rev.*, **21**, 408, 1923; I. LANGMUIR, *Science*, **58**, 290, 1923; H. C. STEINER and H. T. MASER, *Proc. I.R.E.*, **18**, 67, 1930. The thyatron, an electrostatically controlled vapor rectifier, is described on p. 264.

83. The Tungar Rectifier.—This apparatus is likewise a product of the General Electric Research Laboratory, but unlike the hot-cathode mercury-vapor rectifier the space charge is neutralized by means of a gas at a relatively high pressure (3 to 8 cm of mercury) and the tube operates at low voltages only. The tungar uses pure argon gas at 3 to 8 cm pressure. The positive ionization of the argon gas decreases the negative space charge due to the thermionic cathode. The internal voltage drop of the tube then falls to about 15 volts or less, while without

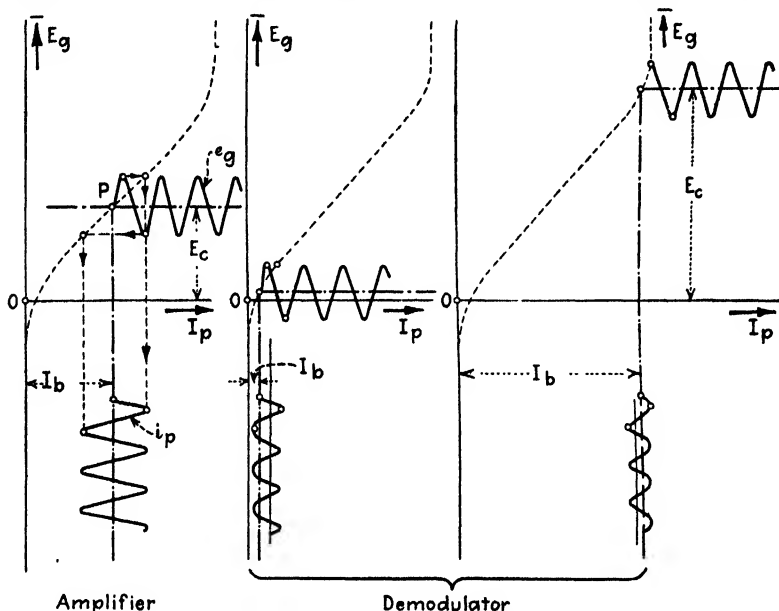


FIG. 120.—Plate rectification.

the presence of ionization some tubes would require from 100 to 500 volts to produce only about 300 ma. Rectifiers of this kind have been built to handle up to 60 amp of rectified current.

84. Rectification Action in an Ordinary Three-element Thermionic Tube When Used as a Demodulator.—Demodulation effects with three-element tubes occur again along the curved portion of the tube characteristic, as can be seen in Fig. 120. The curved portion near the origin is preferable since then the steady plate current supplied by the B battery is smallest. The rectification law [formula (1) on page 169] holds again if the effective tube characteristic is taken into consideration. For the rectifier action, that is, the change in average plate current, we have

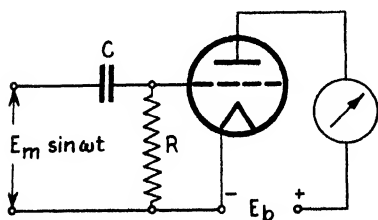
$$i_{av} = \frac{E_m^2}{4} \frac{\partial^2 i_p}{\partial e_g^2} \quad (4)$$

This is the relation known as *anode rectification* and the maximum value E_m' of the variable grid voltage must vary about a favorable operating point for which no power is absorbed by the grid from the exciting voltage source $E_m \sin \omega t$. Rectification action of this type is more pronounced than that for a two-element tube or a crystal rectifier since

$$\frac{\partial^2 i_p}{\partial e_g^2} > \frac{\partial^2 i}{\partial e^2},$$

where e and i are the voltage and current ordinates of the operating point of the diode and the crystal characteristic.

For the case of *grid rectification* (Fig. 121), the detection action is given by the relation



$$i_{av} = \frac{E_m^2}{4} \frac{\partial^2 i_g}{\partial e_g^2} \quad (5)$$

since the grid-voltage grid-current curvature plays a part and $E_m \sin \omega t$ acts practically across R for a low value of $1/(\omega C)$. The grid condenser is therefore of such a magnitude that its reactance is small compared with the grid-leak resistance R . A capacitance C of $0.0001 \mu f$ and a leak of 0.5 megohm give a negligible cutoff, although in many cases a capacitance of $0.00025 \mu f$ and R up to 2 megohms are used. The latter values seem of

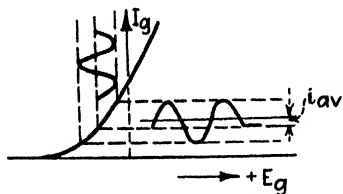


FIG. 121.—Grid rectification.

less advantage. The size of the grid leak changes the position of the operating point.

When two sinusoidal high-frequency voltages act either on the anode or on the grid rectifier and their fundamental frequencies f and $f + f_b$ lie within the same octave, according to formula (3) on page 170, the rectification actions for a constant amplitude of one of the impressed voltages (E_1) are proportional to

$$E_2 \frac{\partial^2 i_p}{\partial e_g^2} \text{ (for anode rectification)}$$

or to

$$E_2 \frac{\partial^2 i_g}{\partial e_g^2} \text{ (for grid rectification)}$$

Moreover, with reference to Fig. 122, it is noted that the approximate amplitude of the resultant voltage across a tube rectifier varies between $(E_1 + E_2)$ and $(E_1 - E_2)$, and its value lies along the straight portion of

the tube characteristic (grid voltage plate current and grid voltage grid current, respectively). Here, E_1 denotes the maximum value of the much larger constant local voltage impressed on the rectifier. Under such conditions, the sum of the two sinusoidal voltages $E_1 \sin 2\pi ft$ and $E_2 \sin 2\pi(f + f_b)t$, where f is about equal to $f + f_b$, can be imagined to be a single sine wave, the amplitude and phase of which are slow functions of time. The phase angle may be neglected as far as the beat current is concerned since E_2 is much smaller than E_1 and the resultant voltage acting on the rectifier is about $E_1 - E_2 \cos 2\pi f_b t$. The beat-frequency current is then proportional to

$$[E_2 \cos 2\pi f_b t] \frac{\partial i}{\partial e}$$

Thus the beat-frequency current, in case of anode rectification, is proportional to $E_2 g_m$, where g_m is the mutual conductance of the tube, and for the case of grid rectification it is proportional to $E_2 g_o$, where g_o is the grid conductance $\partial i_o / \partial e_o$. In the latter case, the plate current is decreased instead of increased.

Anode and grid rectification are important in connection with direct-reading tube voltmeters (of the Moulton type) and in broadcast receivers where the audio-frequency modulation of a radio-frequency carrier is, so to speak, separated by means of such devices. Square-law grid rectification is usually only possible when the impressed grid voltages are smaller than about $\frac{1}{10}$ volt. Under such conditions, the grid rectifier is more sensitive than the square-law plate rectifier, at the same time blocking off any positive plate potentials required for the preceding tube. The increased sensitivity is due to the fact that rectification takes place in the grid branch and the audible components separated in that circuit are then amplified into the plate branch. For anode rectification, the only possible amplification must be at radio frequency, before rectification takes place. Also, the plate circuit must have a low high-frequency resistance, and consequently the possible amplification is somewhat less than that obtained for grid rectification. In addition, the wave form for grid rectification is better than for anode rectification, when proper C and R values are chosen ($0.0001\mu f$, 0.5 megohm).

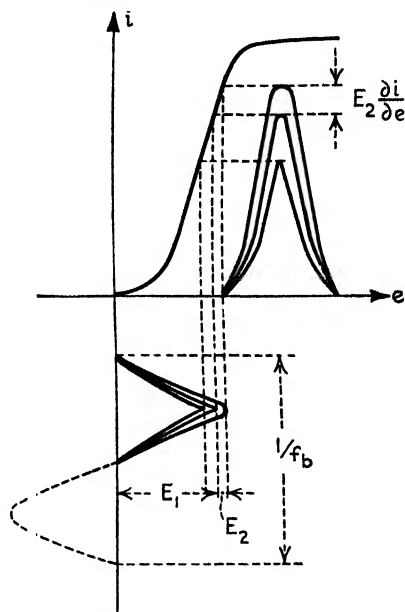


FIG. 122.—Beat-frequency effect.

The use of power rectification (power detection) has become good practice in modern receiver design. For such detectors, the tube rectifier gives sufficient audio-frequency voltage outputs to operate directly into the final output tube. Much higher modulated high-frequency voltages are applied to this type of tube rectifier (several volts against less than $\frac{1}{10}$ volt). Approximately linear, instead of square-law, rectification then takes place. Hence but little detection distortion should occur. Grid-leak power rectification is again more efficient than the anode or *C*-bias rectification when the same input voltages prevail. However, the audio-frequency output-voltage-carrier input-voltage characteristic is more linear for the anode power rectifier.

85. Rectification by Means of Cold-electrode Tubes.—Some of the representatives of this type are based on the principle of the glow-dis-

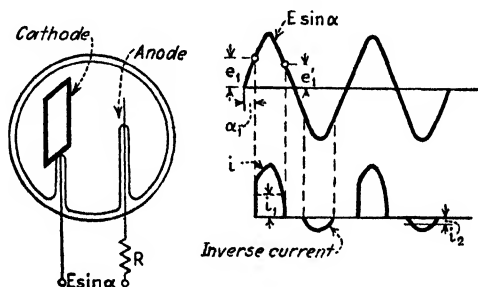


FIG. 123.—Glow-tube rectifier.

charge tubes described on pages 42 to 45. Rectification can be produced in several ways and results from a comparatively large current flow in one direction and a smaller flow (inverse current) in the opposite direction. It can be obtained by using either two electrodes with an active surface of different size or electrodes of different materials which produce different cathode drops. For instance, an aluminum electrode requires much less energy for liberating electrons than does a nickel electrode. Hence rectification can be obtained by means of an aluminum cathode and nickel anode.

Figure 123 indicates the performance of such a rectifier when a small rod electrode and a large plate electrode or a rod electrode inside a cylindrical electrode is used in an atmosphere of neon. For a suitable gas pressure, a negative glow discharge about 3 mm in thickness will cover the electrode which is acting as cathode. When an alternating voltage $E \sin \alpha$ is applied to the two electrodes, more current will flow if the large plate or the surrounding cylinder, respectively, is negative than if the polarity is reversed and the rod acts as cathode. Therefore we have the case of a differential rectifier (page 159). The ratio of the average current in one direction to the average current in the other

direction is approximately equal to the ratio of the respective effective electrode surfaces. The empirical relation between the instantaneous current and the voltages of such a rectifier is

$$i = \frac{e - e_1}{(1/kS) + R} = \frac{e - e_1}{A}$$

if e denotes the instantaneous supply voltage and e_1 the ignition voltage of the tube. As has been mentioned on page 42, there are two critical voltages e_1 and e_1' for starting and interrupting a glow discharge. S denotes the effective area of the cathode (covered with glow discharge) during the active portion of the respective half cycle, k the slope of the tube characteristic per unit area of the cathode, and R the protective series resistance. Such a stabilizing resistance is essential in glow-discharge devices since, after igniting a glow discharge a small increase in voltage greatly increases the current flow.

From Fig. 123, it can be seen that only current caps produce the larger current in one direction and the small inverse current in the other direction. This disadvantage can, however, be utilized in obtaining impulse excitation for frequency multiplication (page 154).

If i_1 is the average current when the large electrode of surface $S = S_1$ is negative and i_2 the average inverse current when the small electrode of surface $S = S_2$ is negative, the rectified current is

$$i_s = i_1 - i_2$$

where

$$i_1 = \frac{\int_{\alpha_1}^{\pi - \alpha_1} [E \sin \alpha - e_1] d\alpha}{2\pi A_1} = \frac{\frac{E \cos \alpha_1}{\pi} - e_1 \left[0.5 - \frac{\alpha_1}{\pi} \right]}{A_1} = \frac{\beta}{A_1}$$

$$i_2 = \frac{\beta}{A_2}$$

$$A_1 = \frac{1}{kS_1 + R} \quad A_2 = \frac{1}{kS_2 + R}$$

if it is assumed that the two critical voltages e_1 and e_1' are nearly equal.

Another construction of a rectifier tube is that in which a large cylindrical electrode of aluminum, which readily emits electrons, surrounds a small tip electrode of nickel which even when heated has no electron emission. The anode tip just reaches out of the upper end of a glow-preventing glass tube which carries the lead-in wire. A construction of this type is most suitable for unidirectional electron movement.

The S tube rectifier of V. Bush and C. G. Smith¹ uses either magnetic or space-charge control to produce rectification action. When the electrodes in a neon tube which uses neon gas of about 2 mm mercury

¹ *Proc. I.R.E.*, 10, 41, 1922.

pressure are only 1 mm apart, several thousand volts are not sufficient to produce a discharge current, while a few hundred volts will produce a discharge if the electrodes are separated by about 25 mm. The reason for this is that ionization by collision can take place only when electrons are able to collide with sufficient speed. Hence, when a large tube is used and the electrons are deflected along a longer curved path, the chances of ionizing collisions with gas molecules are increased and ionization takes place. Such deflections can be obtained by means of a magnetic field (page 33). Further, the positively charged nucleuses resulting from such collisions will be attracted by the cathode and will consequently bombard it. This will free other electrons and still further increase the electron flow toward the anode. In the magnetically controlled tube of Bush and Smith the magnetic field is built up until, for a critical field strength H_c , a space current starts to flow within the tube. Tubes based upon this principle have been built to pass space currents up to $\frac{1}{4}$ amp for voltage drops as low as about 200 volts. Rectification action is then obtained by superimposing an alternating magnetic field on the steady field and adjusting their intensities until the tube passes current only every other half cycle.

The other type of S tube uses space-charge control and depends upon the fact that the heavier positive ions move more slowly than the electrons which move in the other direction. The outcome is that the less mobile positive ions must form a positively charged cloud between the electrodes of the tube. When a hollow electrode with an opening is used together with a solid electrode, the positive space charge is not neutralized for each half cycle and the tube acts as a rectifier. Tubes of this kind have been built to give up to 150 ma rectified with a drop of about 200 volts. The rectification action is then somewhat as follows: When an alternating voltage is applied, current will—practically—flow only when the hollow electrode is negative since then the electrons pass toward the other electrode (anode) and the positive ions bombard the inside walls of the cathode after passing through the opening and liberate new electrons which move toward the anode. On their way to the anode they produce increased ionization through collision with gas molecules. At times when the hollow electrode is positive, some of the positive ions pass only slowly through the opening toward the cathode. If an electron should be liberated at the solid cathode, it will be attracted to the positive space charge and only a few will reach the anode, thus producing a very small inverse current flow.

86. Rectifiers for Obtaining B and Other Voltages for Tube Circuits.—Figure 124 shows the full-wave rectification obtained by the use of two thermionic diodes. A single tube with two symmetrical anodes will accomplish the same result. When no smoothing device is used, rectified

impulses I , as indicated, will be obtained. As in the case of all rectifiers of this type, the cathode forms the *positive* terminal for the direct-current load. The figure also brings out the effect on the wave shape of tem-

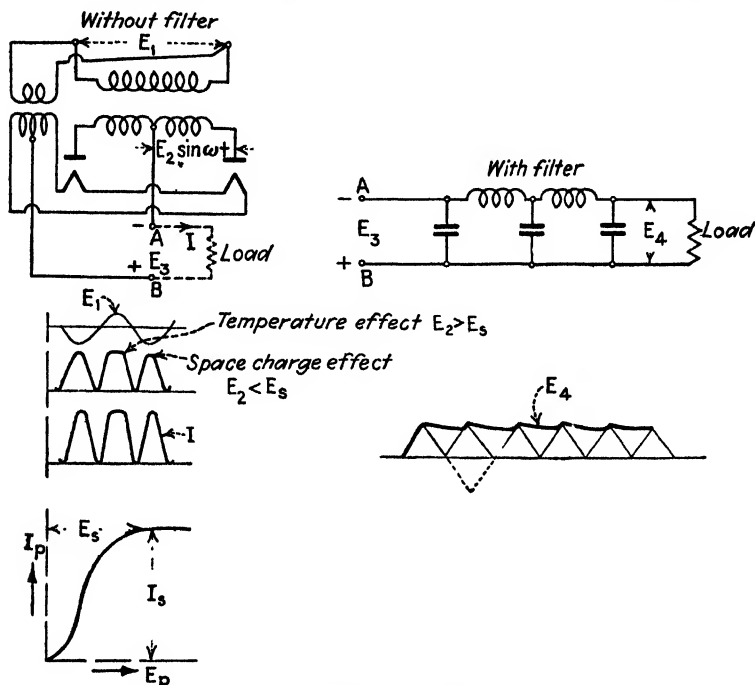


FIG. 124.—Full-wave thermionic rectifier action with and without "brute-force" filter.

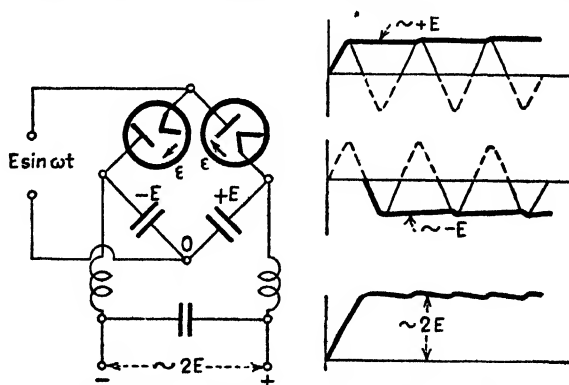


FIG. 125.—Double voltage in output branch.

perature and space-charge effects, respectively, which tend to limit the current flow. In the case of a full-wave rectifier with a "brute-force" filter, as used in commercial receiving sets, the voltage E_4 across the

output is about as indicated. A smoothing device of this kind, though satisfactory for receiver work, is by no means a filter in the true sense and merely smooths out the impulse charges by means of choke coils (about 30 henries each). The condensers of 4 and more microfarads serve as storage tanks in order to keep the output voltage fairly constant. This is, however, true only for small load currents. We must distinguish between *condenser-input* filter (large condenser connected directly across the output of the rectifier) and *choke-input* filter (rectifier output goes to a choke coil and then is bridged by a large condenser). The condenser-input filter gives higher output voltages but poor voltage regulation and higher rectifier peak current. The choke-input gives good voltage regulation and smaller rectifier peak current.

Figure 125 shows a circuit which obtains a direct-current supply with a voltage of about twice the amplitude value of the alternating voltage. The rectifier to the left conducts the electrons (e) to the left condenser, the upper plate of which is charged to potential $-E$, while the other rectifier attracts about the same number of electrons from the hot cathode. Therefore the upper plate of the condenser to the right becomes charged to potential $+E$. The voltage difference between the two upper plates of the left and right condensers is then $2E$ volts.

CHAPTER VII

VOLTAGE, CURRENT, AND POWER AMPLIFIERS

An amplifier is a device for increasing the amplitude of electric current or voltage through the control by the input power of a larger amount of power supplied to the output circuit by a local source. We can distinguish between voltage, current, and power amplification. The first is given by the ratio of variable voltage produced at the output terminals to the variable voltage impressed on the input terminals, while current amplification is the ratio of the variable current which flows in the output branch to the variable current supplied to the input circuit. By "power amplification" is understood the ratio of the variable power produced in the output branch to variable power supplied to the input circuit. When the output power reacts back on the input branch, the amplification may be either increased or decreased, depending upon whether or not the phase of the regenerative or the feedback voltage produces a higher or a lower input voltage than without the back action. The different kinds of direct-current amplification are defined in a similar way except that it is understood that the output refers only to that portion which is the change due to the input. Relays also belong to this class but by their use more or less power can be released which is normally of a different character from that acting at the input. A relay is, for example, a device by means of which contacts in one circuit are operated by a change in conditions in either the same or associated circuits.

87. Magnetic Amplifiers.¹—The system indicated in Fig. 126 used in the Alexanderson modulation arrangement affects the high-frequency energy by a comparatively small current with a periodicity which may have any value or follow any transient law. As in all magnetic-modulation schemes, the action is based on the degree of magnetic saturation. When an iron core is partially magnetized by a direct current, the inductance of a high-frequency coil wound on the same core will be different from that for no direct-current flow. For a sufficient number of direct-current ampere-turns, the inductance of the high-frequency coil can be reduced so that it acts like an air coil. This system has the advantage

¹ KUEHN, L., *Jahrb. dr. Tel.*, **7**, 221, 1913; *ETZ*, **35**, 916, 1018, 1914; E. F. W. ALEXANDERSON and S. P. NIXDORFF, *Proc. I.R.E.* **4**, 101, 1916; R. V. Hartley, U. S. Patent No. 1287982, suggests two separate ferromagnetica in order to diminish the distortion of the high-frequency current; A. Feige, *E.N.T.*, **2**, 96, 1925, describes the magnetic modulator with special reference to the system of L. Pungs.

that no direct power transfer occurs between the control coils and the high-frequency coils. In order to accomplish this, the high-frequency turns are so wound that their magnetic flux affects the control turns just as much in one direction as in the other. Therefore the resultant e.m.f. vanishes. In spite of such a neutralization, the effect upon the permeability still exists.

Impedance curves of one high-frequency coil dependent upon the direct-current magnetization are also shown in Fig. 126. It can be

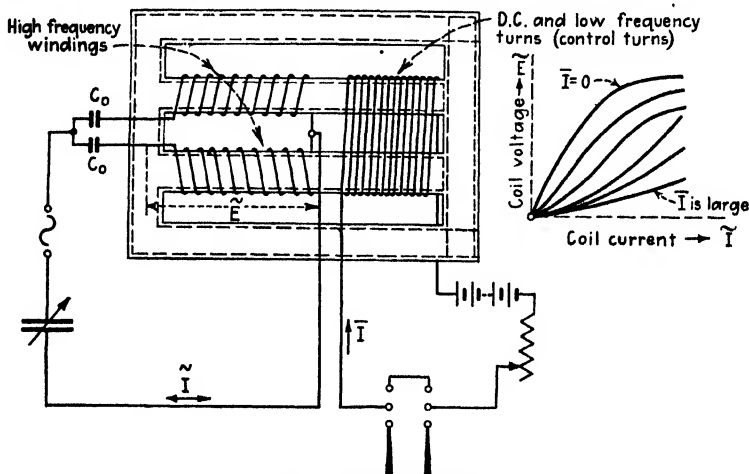


FIG. 126.—Magnetic amplifier.

seen that, for zero direct current in the control turns, the highest high-frequency impedance is obtained, while for a certain direct-current magnetization, so to speak, only a portion of the high-frequency turns are affected by the presence of iron if it is assumed that some of the turns act as coils with an iron core and the remaining turns as air coils. The following derivations explain these statements: If

A = cross-sectional area of iron in square centimeters

E = voltage across high-frequency coil in volts

i = instantaneous current in amperes

L = inductance in henries

l = length of magnetic path in centimeters

μ = permeability

N = number of turns

Φ = flux interlinked with coil

then

$$\Phi = \frac{\text{m.m.f.}}{\text{magnetic resistance}} = \frac{(4\pi/10)Ni}{l/(\mu A)}$$

$$d\Phi = \mu \frac{4\pi AN}{10l} di$$

$$E = -\frac{N}{10^8} \frac{d\Phi}{dt} = -[L] \frac{di}{dt} = -\left[\frac{4\pi AN^2}{10^9 l}\right] \frac{di}{dt}$$

that is,

$$L = \mu \frac{4\pi AN^2}{10^9 l}$$

or

L is a function of μ

As already mentioned, the parallel connection of the two high-frequency coils avoids a power transfer to the control coil. This is also the case when the iron is unsymmetrically magnetized. Moreover, the parallel connection forms a short circuit for the second harmonic which is another advantage. The two stoppage condensers C_0 prevent the existence of any low-frequency changes in the high-frequency coils; otherwise short-circuit currents would flow and the average value of the inductance L would be unchanged.

88. The Ordinary Triode as an Amplifier.—When a tube of this type is used for the amplification of variations impressed between the grid and the hot cathode, the deductions in Sec. 25 (page 66) show that the tube acts as a generator (Fig. 31) of voltage μe_g through the internal dynamic plate resistance r_p . When the variations are confined to an almost linear portion of the dynamic tube characteristic (Fig. 33), the instantaneous values of the variable plate current and grid voltage acting through an external plate resistance R are then interconnected by the relation

$$i_p = \frac{\mu e_g}{r_p + R} \quad (1)$$

It should be remembered that this relation¹ holds strictly only for

¹ Strictly, $i_p = ae_g + be_g^2 + \dots$ and

$$i_p = \frac{\mu e_g}{r_p + R} + 0.5 \left[\frac{-\mu^2 r_p \frac{\partial r_p}{\partial E_p} + \mu \frac{\partial \mu}{\partial E_p} [r_p^2 - R^2] + \frac{\partial \mu}{\partial E_g} [r_p + R]^2}{[r_p + R]^3} \right] e_g^2$$

which for a constant amplification factor $\mu = \frac{\partial I_p / \partial E_g}{\partial I_p / \partial E_p}$ holding for a constant-emission current gives the Carson equation

$$i_p = \frac{\mu e_g}{r_p + R} - \frac{1}{2} \frac{\mu^2 r_p (\partial r_p / \partial E_p)}{[r_p + R]^3} e_g^2 + \dots$$

(Carson, J. R., *Proc. I.R.E.*, 7, 187, 1919; F. B. Llewellyn, *Bell System Tech. J.*, 5, 433, 1926.) Unless the load resistance R is small compared with the internal plate resistance r_p , the modulation due to variations in μ may be appreciable. For a negative grid bias, the general i_p —expression can be simplified by making use of the approximation $\mu \partial \mu / \partial E_p = \partial \mu / \partial E_g$. For no convection current flowing across the

relatively small variations and special precautions must be taken when it is applied to output tubes where the variation e_g is large and considerable power output is required. Since the amplification factor μ , internal plate resistance r_p , and mutual conductance g_m are interlinked by the relation

$$r_p g_m = \mu \quad (2)$$

because

$$\left. \begin{aligned} r_p &= \frac{\partial e_p}{\partial i_p} \\ g_m &= \frac{\partial i_p}{\partial e_g} \\ \mu &= \frac{\partial e_p}{\partial e_g} \end{aligned} \right\} \begin{array}{l} \text{(for constant grid voltage, plate voltage,} \\ \text{and plate current, respectively)} \end{array}$$

we need consider only two of these three characteristic¹ quantities. Therefore, by knowing g_m and μ of a tube, the internal plate resistance r_p is given by (2). Since small voltages across the grid and the hot cathode should produce large variations in the plate current, it is essential that the operating point be chosen on a steep portion of the I_p , E_g characteristic. The steepness is expressed by the mutual tube conductance g_m . Its magnitude is limited in practical tubes, since the negative space-charge effect tends to reduce it. The closer the grid is placed to the filament, the greater is g_m . It also increases with the active surface of the filament and is, to some extent, also dependent on the area of the plate. For the ordinary three-element type of receiving tube, much

grid-filament electron path of an amplifier (class A amplifier), the output current i_p can then be computed from e_g by means of

$$i_p = \frac{\mu}{r_p + R} e_g - \frac{1}{2} \left[\frac{\mu^2 r_p \partial r_p / \partial E_p}{[r_p + R]^2} - \underbrace{\frac{2 r_p (\partial \mu / \partial E_g)}{[r_p + R]^2}}_{\mu \text{ modulation term}} \right] e_g^2 + \dots$$

¹ Since the instantaneous plate and grid potentials $E_p = E_b + e_p$ and

$$E_g = E_s + e_g$$

are composed of the steady terms E_b and E_s , respectively (owing to plate supply and grid bias), and the corresponding instantaneous plate current $I_p = I_b + i_p$, we have the more specific definition

$$r_p = \left(\frac{\partial E_p}{\partial I_p} \right)_{E_p=\text{constant}} \quad g_m = \left(\frac{\partial I_p}{\partial E_g} \right)_{E_p=\text{constant}} \quad \mu = \left(\frac{\partial E_p}{\partial E_g} \right)_{I_p=\text{constant}}$$

The variations take place about the steady values E_b , E_s , and I_b , fixed by the operating point whose position along the tube characteristic is of special importance for r_p and g_m . To express r_p , g_m , and μ in terms of the variable components e_p , e_g , i_p is justified from a mathematical point of view, if it is understood that the position of the operating point about which the variations take place has an effect.

better values than about $g_m = 2$ ma/volt are not customary and the g_m varies with different types of receiving tubes from 0.2 to 2 ma/V. The maximum value of g_m for a particular tube is obtained along the middle portion of the I_p , E_g characteristic for which g_m may be considered constant. Such a favorable operating point P is maintained by the negative grid bias E_c (amplifier representation of Fig. 120). Tubes with a high value of g_m are in general more efficient amplifiers if they are compared with tubes of similar characteristics. The amplification factor μ is affected but little by the location of the operating point except for extreme portions of the characteristic but μ is more or less dependent upon the grid mesh, being larger for a mesh that is finer. The applied voltages do not much affect the value of μ except that at low plate potentials there is a slight decrease. There seems to be no limit to the magnitude of μ as for g_m , and for proper grid designs it can be made up to 30 and even higher. From Eq. (1), it can be seen that a variable grid potential e_g acts in the plate branch μ -fold. Hence a certain variation in the plate potential is only $1/\mu$ th as effective on the plate current as would be the same variation applied to the grid. This is of use in measuring very high voltages by smaller compensating voltages applied to the grid. Some writers use the reciprocal value of μ to express the same tube property. It is then known as the "through grip" $D = 1/\mu$ of the tube. For example, $D = 4$ per cent corresponds to an amplification factor of $\mu = 25$.

Since, for an external load resistance R ohms, $e_p = -i_p R$, we have

$$e_p = -\frac{\mu e_g}{R_p + R} R \quad (3)$$

Inasmuch as the dynamic tube resistance $r_p = \mu/g_m$ has a meaning only when current changes i_p are concerned, it is a tube constant depending, because of the denominator g_m , upon the operating point P along the I_p , E_g characteristic (Fig. 120). It becomes smallest when g_m is largest (at the middle, almost straight, portion). It can be seen that an ordinary three-element tube always has a low internal plate resistance r_p when the amplification factor μ is low. Thus an output tube of about $r_p = 2000\Omega$ has a μ of only about 3 to 4 for $g_m = 1.8$ ma/V, while a high- μ tube of $\mu = 30$, for instance, has $r_p = 150,000\Omega$ and $g_m = 0.2$ ma/V. Figure 127 gives the variations of the tube constants of a commercial receiving tube (Cunningham CX-301A or its equivalent) for normal plate voltage.

An amplifier should draw no appreciable grid current so that the input voltage does not undergo a change and true voltage amplification is possible. A proper negative grid bias will accomplish this unless the frequency of the impressed grid voltage is so high that the tube capacitance becomes so pronounced that the passage of an appreciable dis-

placement¹ current is made possible. When selecting a tube for amplification work, we must distinguish between voltage, current, and power amplification. The amplification factor μ can also be termed "voltage amplification factor" since it determines the degree of voltage gain. The quantity μ denotes the quotient of

$$\frac{\text{Change of anode potential}}{\text{Change of grid potential}}$$

for one and the same change in the anode current. Since it is almost constant for most of the voltage range used on a tube, it is an easy matter to determine this quantity.

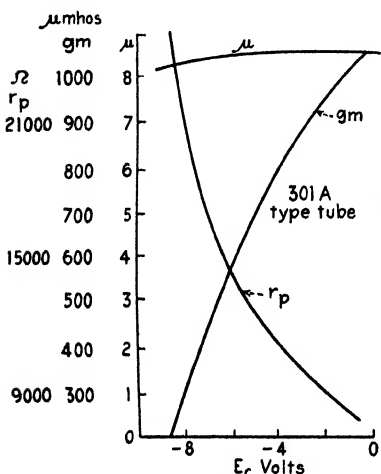


FIG. 127.—Tube factors.

1. *The voltage amplification* of a tube is almost identical with the amplification factor only when the plate load is a very high impedance. Such amplification is normally used not to produce large power outputs but merely to obtain amplified voltages in the plate circuit and to affect, with the magnified variations, another stage of amplification or an output tube. The formula for the voltage amplification, obtained from (3), is

$$A_v = \frac{e_p}{e_g} = \mu \frac{R}{r_p + R} \quad (4)$$

which becomes a maximum and equal to μ when the external plate resistance R is very large compared with r_p . It is customary to make R or $X = \omega L$ (for a choke load) not more than about $10r_p$ (page 207) since the voltage amplification proceeds asymptotically toward the limiting value μ , and for $R = 10r_p$ the voltage amplification is already 0.9μ .

2. *The current amplification* is defined as current output per volt input and is given by the expression

$$A_i = \frac{\mu}{r_p + R} \quad (5)$$

It can be seen that current amplification is always smaller than μ .

3. *The power amplification* is given by

$$A_p = \frac{\mu^2 R}{[r_p + R]^2} \quad (6)$$

when expressed by power output per volt squared input. This formula is obtained from the power output which is $W = i_p^2 R = \mu^2 e_g^2 R / [r_p + R]^2$.

¹ For effective input resistance and tube capacitances, see p. 203.

Maximum power amplification occurs when $R = r_p$, which can also be seen from Fig. 137.

89. Special Remarks on Voltage and Power Amplification.—From formulas (4) and (6) it can be seen that, for a load resistance $R = \infty$, no plate current at all can exist, and $\mu e_g = -e_p$. The plate reaction completely neutralizes the action of the grid. Hence by using a very high resistance R in the external plate branch and by measuring e_p with a tube voltmeter across R , the ratio e_p/e_g practically gives the amplification factor. Choosing a load resistance R which is low compared with r_p , the voltage amplification becomes

$$A_e \cong \frac{\mu R}{r_p} \quad (4a)$$

since $\frac{R}{r_p + R} = \frac{1}{1 + \frac{r_p}{R}} \cong \frac{1}{\frac{r_p}{R}}$. Therefore it is evident that the voltage

amplification must be correspondingly small. For example, for $\mu = 8$, $r_p = 5000 \Omega$, and a load resistance of $R = 500 \Omega$ A_e is

$$\frac{8 \times 500}{5000} = 0.8,$$

which means that the output voltage is only 80 per cent of the voltage impressed across the grid and the filament and deamplification occurs. Choosing $R = r_p$ provides maximum power transfer from the tube to the load resistance R although not without some distortion.

A distinction must be made between the case of a resistance R' reflected back into the external plate branch by means of an output transformer and that of the load resistance R connected directly in the plate circuit. With respect to the notation of Fig. 128, the anode voltage at any instant is

$$E_p = E_b - RI_p$$

while for the transformer output it is

$$E_p = E_b - R'i_p = E_b - \rho^2 R_2 i_p$$

if the resistance of the primary turns is neglected. The quantity ρ denotes the ratio of transformation of the transformer and R_2 the load resistance. This method is employed in order to match tube resistance r_p with a fixed load resistance R_2 .

When a certain number of tubes of similar design (same filament, same electrode areas, etc.) but of different μ and g_m are available, the particular tube to be used will depend on the purpose for which the amplifier is intended, especially when the load resistance is not fixed and can be adjusted. Hence, when a maximum power output is desired, R is

or by using the plate-voltage plate-current characteristic¹ where the plate current and plate voltage at any instant are given by the function

$$I_p = F(E_p, \mu E_g)$$

and therefore

$$E_p = E_b - I_p R$$

The first equation is not linear since the plate-current plate-voltage curves for different values of grid bias are as indicated in Fig. 128. For the supply voltage E_b of the plate battery, the relation $E_p = E_b - I_p R$ is a slanting line of slope $1/R$ and passes through the operating point P for which the constant supply voltage is E_b . The resistance line $1/R$ with R in Ω , the plate voltage in volts, and, as customary, the plate current in milliamperes gives the scale $10^3/R^\Omega$. For a load resistance of 5000Ω , the slope of the resistance line would be 1:5. Between the dot-and-dash horizontal lines for the minimum and maximum values of the plate current I_p , the various static characteristics are essentially linear. This linearity is even more pronounced when the external plate branch is loaded by a resistance R . The characteristics are then as indicated by the heavily drawn set of curves (Fig. 129 for $R = r_p$), while the dotted set of curves represents the corresponding charac-

¹ WARNER, J. C., and A. V. LONGHREN, *Proc. I.R.E.*, **14**, 735, 1926; the case of output power of vacuum tubes has also been treated by G. W. Kellog, Design of Non-distorting Power Amplifiers, *J. A.I.E.E.*, **44**, 490, 1925; discussion 645, 1925; W. P. Radt, Über Maximalleistungen von Verstärkerröhren (On the Maximum Power of Amplifier Tubes), *E.N.T.*, **3**, 21, 1926; F. B. Llewellyn, Operation of Thermionic Vacuum Tube Circuits, *Bell System Tech. J.*, **5**, 433, 1926; F. C. Willis and L. E. Melhuish, Load Carrying Capacity of Amplifiers, *Bell System. Tech. J.*, **5**, 573, October, 1926; A. Clavier and I. Podliasky, Sur les amplificateurs de puissance sans distorsion (On Power Amplifiers without Distortion), *L'onde élec.*, **6**, 71, 1927; A. Forstmann and E. Schramm, Über Arbeitskennlinien und die Bestimmung des günstigsten Durchgriffes von Verstärkerröhren, (On Working Characteristics and the Determination of the Most Favorable Amplification Factor of Tubes), *Jahrb. drahtl.*, **30**, 89, 1927; Über Maximalleistungen von Verstärkerröhren (On Maximum Output of Amplifier Tubes), *Jahrb. drahtl.*, **32**, 195, 1928; A. Forstmann reviews the entire subject matter, *Jahrb. drahtl.*, **35**, 1109, 1930; C. R. Hanna, L. Sutherland, and C. B. Upp, Development of a New Power Amplifier Tube, *Proc. I.R.E.*, **16**, 462, 1928; B. D. D. H. Tellegan Endverstärkerprobleme (Problems of Amplification in Output Tubes), *Jahrb. drahtl.*, **31**, 183, 1928; M. von Ardenne, On the Theory of Power Amplification, *Proc. I.R.E.*, **16**, 193, 1928; H. Bartels, Über Höchstleistungen und Verzerrungen bei Endverstärkern (Optimum Output and Distortion in Output Amplifiers), *E.N.T.*, **6**, 9, 1929; B. C. Brain, Output Characteristic of Thermionic Amplifiers, derives his formulas by means of the actual tube characteristics since the assumption of the linearity of the $E_p - E_g$ curves is not quite true and gives a formula from which the proper load resistance can be calculated from the alternating-current resistance r_p at the specified grid bias, *Exptl. Wireless*, **6**, 119, 1929; H. A. Pidgeon and J. O. McNally, A Study of the Output Power Obtained from Vacuum Tubes of Different Types, *Proc. I.R.E.*, **18**, 266, 1930.

teristics for $R = 0$. With a load resistance R which is still higher in comparison with the internal tube resistance r_p , the characteristic is rotated still more about the operating point P toward the horizontal for $R = \infty$. Therefore, the *higher* R is chosen the more horizontal the characteristic and the *less distortion* in the variable plate current i_p since the load characteristic cuts all the static characteristics (for $R = 0$ and different values of E_c) at almost the same angle. Thus distortion due to plate-voltage plate-current curvature is more or less avoided. The power output is, however, small. Therefore a high-quality output amplifier cannot be very efficient since, besides avoiding distortion effects due to E_p , I_p curvature, care must also be taken that the grid is at no time positive. Otherwise the input impedance might vary as the result

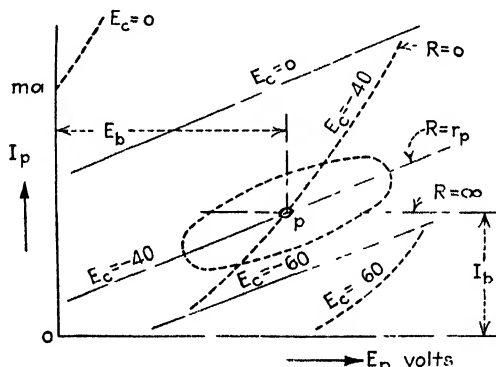


FIG. 129.—Shows that for full-line ($R = r_p$) characteristics almost no distortion compared to the case of dotted characteristics ($R = 0$).

of changing grid currents. For this reason, some engineers design their output amplifiers according to one of three classes.

1. *Class A amplifiers* are high-grade repeaters for which the variable plate current i_p is of practically the same shape as the impressed variable grid voltage e_g and the distortion due to the tube does not exceed 5 per cent. By "distortion" is meant the amount of second harmonic in i_p which is not present in e_g . The load resistance R is then usually about $2r_p$, where r_p is the alternating-current resistance of the tube for the specified operating voltages. In some cases values of R in the neighborhood of 1.6 to $1.8r_p$ give sufficiently good results. The power amplification $\mu^2 R / [R + r_p]^2$ is then high but the efficiency is rather low. The reason for this is that the negative grid bias is chosen so that plate current flows at all times during the cycle of e_g , and the grid voltage e_g is of such a small magnitude that the dynamic operating characteristics are essentially linear. Even at the respective maximum values of e_g no grid current flows and the minimum of I_p ($I_p = I_{\min}$, Fig. 128) is large

enough so that it does not reach into the curvature region of the plate-voltage plate-current characteristic.

2. *Class B amplifiers* are not true repeaters since a negative grid bias E_c is chosen so that the power output is proportional to e_o . To do this efficiently, the lower bend of the tube characteristic is employed and E_c chosen so negative that there is practically no plate current when e_o is not applied. The grid voltage is made of such a magnitude that the variable plate current i_p consists essentially of half sine waves corresponding to the positive half cycles of the applied variable grid voltage e_o . For such amplifiers some grid current may flow when e_o swings through the very positive peak of the cycle and harmonics with a specially pronounced double-frequency content are produced in i_p . They must be eliminated by tuning out or by using two equal tubes amplifying in push-pull. An amplifier of this type has a relatively low ratio of power amplification, but an efficiency which is higher than that for the class A amplifier.

3. *Class C amplifiers* are for work in which the wave shape of i_p is of no concern, but a high efficiency is of importance, even if the power amplification ratio is small. The negative grid bias E_c is then chosen so great that it is more than sufficient to produce zero plate current if no variable grid voltage e_o is impressed. The applied grid voltage e_o is made large enough so that large amplitudes of i_p are produced during the most positive portion of the positive e_o half cycle. Almost rectangular i_p impulses are produced since the saturation tube current will flow during each very positive swing of e_o . Within limits, the output varies as the square of the plate voltage, which accounts for the high efficiency.

4. Devices for which the working characteristic of special tubes¹ lies practically in the positive region of grid potentials may be added as *class D amplifiers*. A grid current is then essential since the grid bias is quite positive and the entire operation about this potential is essentially positive except that the instantaneous grid potential $E_g = E_c + e_o$ must always be less than the instantaneous plate potential $E_p = E_b + e_p$. Such special tubes give a comparatively large emission current at moderate plate voltages (I_p about 150 ma, $I_o = 30$ ma at $E_p = 200$ volts and $E_g = +100$ volts; the fixed grid bias is then about $E_c = +45$ volts). High- μ tubes (μ about 30) with a comparatively high mutual conductance g_m (about 1.5 ma/volt) are then used. For maximum power transfer, the relation $R = r_p$, which holds for tubes in the negative potential region, no longer holds but a load resistance

$$R = \frac{2r_p}{1 + \mu}$$

¹ RADT, W. P., *E.N.T.*, 3, 21, 1926.

gives a pronounced power output

$$W = \frac{1 + \mu}{16r_p} E_b^2$$

for a grid bias

$$E_c = \frac{\mu - 3}{4\mu} E_b$$

if E_b denotes the voltage of the steady B supply in the plate branch and $r_p = \mu/g_m$. The theoretical optimum output for an ordinary output tube with a working characteristic which is substantially in the region of negative grid voltages would be

$$W = \frac{E_b^2}{16r_p}$$

Therefore the optimum power output of the class D amplifier is more than for ordinary output tubes. It must be remembered, however, that because of working practically all of the time in the positive—and even in the highly positive—grid-potential region, considerable power is required on the grid side and care must be taken that the previous stage can supply the power which operates the grid. This grid dissipation is

$$W_o = \frac{E_b^2}{16r_o'} \left[1 + \frac{3}{\mu} \right]^2$$

if r_o' denotes the effective internal resistance between grid and filament. This input power is, for instance, of the order of $\frac{1}{2}$ watt if about 10 watts of power is delivered to the load resistance R .

When the load in the external plate branch is an impedance Z , we have for the voltage amplification

$$A_v = \frac{e_p}{e_g} = \mu \frac{Z}{r_p + Z}$$

and, as is shown in Figs. 129 and 34 as well as on page 69, the dynamic characteristic forms a closed area which, when working over almost linear sections of the static characteristics, generally forms an inclined ellipse. This is because the plate current and grid voltage are no longer in phase. Generally, for a load impedance $Z = R \pm jX$, the effective value of alternating plate current I for an effective alternating grid voltage E is

$$I = \frac{\mu E}{\sqrt{[r_p + R]^2 + X^2}}$$

and the phase difference between E and I is

$$\varphi = \tan^{-1} \frac{\pm X}{r_p + R}$$

The instantaneous values of the alternating grid voltage and corresponding plate current for the impedance $Z = R \pm jX$ are given by

$$\begin{aligned} e_g &= E\epsilon^{j\omega t} \\ i_p &= I\epsilon^{j\omega t} \end{aligned}$$

where the complex amplitudes are of the form $A = A_m\epsilon^{j\varphi}$, that is, contain the amplitudes A_m and the phase φ . Hence for an impedance

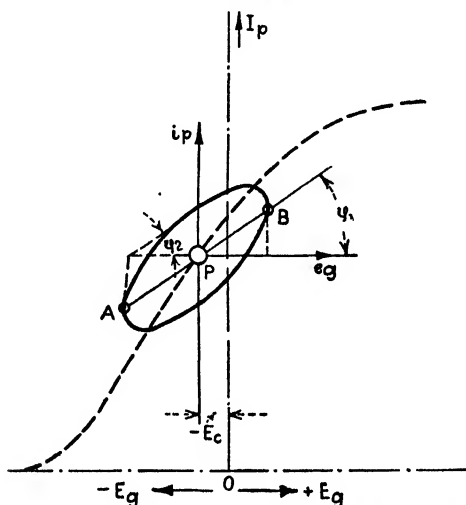


FIG. 130.—Dynamic characteristic is an ellipse.

$Z = R \pm jX$, the phase of the ratio I/E must give the same phase as exists between e_g and i_p , and we find for the vector ratio

$$\frac{I}{E} = \tan \varphi_1 + j \tan \varphi_2$$

determining the dynamic characteristic, which is an ellipse, as indicated in Fig. 130. For a pure resistance load $Z = R$, the vector ratio is $I/E = \tan \varphi_1$ and gives the well-known dynamic characteristic indicated by the line AB .

Moreover, according to Eq. (2), Eq. (1) can also be written in the form

$$i_p = \frac{g_m \cdot r_p}{r_p + R} e_g = \frac{g_m}{1 + (R/r_p)} e_g \quad (10)$$

and

$$g_w = \frac{g_m}{1 + (R/r_p)} \quad (11)$$

gives the steepness of the work curve of the amplifier in comparison with the steepness g_m of the I_p , E_g characteristic. It becomes larger as g_m

increases, and Eq. (11) shows that it becomes flatter (more horizontal) the higher the ratio R/r_p . Also, introducing the steepness g_w of the work curve in the expressions for voltage, current, and power amplification gives the simple expressions

$$A_v = g_w R; \quad A_i = g_w; \quad A_p = g_w^2 R \quad (12)$$

The power amplification as given by A_p in (12) and A_p in (6) expresses only the ratio of the power output delivered to the load in the plate branch to the square of the impressed grid voltage. Normally, under true power amplification, the ratio of the power output in the plate circuit to power input in the grid branch is taken and we have

$$A_w = \frac{W_p}{W_g} = \frac{E_2 I_2}{E_1^2 / r_g} \quad (13)$$

where E_1 and E_2 denote the effective values of the alternating input and output voltages acting on the grid and plate, respectively, I_2 the effective inphase value of the plate alternating current, and r_g the grid resistance. But for a resistance load R ,

$$E_2 = -\frac{\mu E_1}{r_p + R} R \quad I_2 = \frac{\mu E_1}{r_p + R}$$

the minus sign indicates that the plate potential decreases with an increase of plate current. Hence

$$A_w = \frac{\mu^2 R r_g}{[r_p + R]^2} \quad (13a)$$

For optimum true power amplification ($R = r_p$) but not without distortion, we then find

$$A_{\max} = \frac{\mu^2 r_g}{4 r_p} \quad (14)$$

Assuming for a particular case $r_g = 10^6 \Omega$ and using a tube of $\mu = 2$ and $r_p = 2000 \Omega$, the optimum power amplification becomes five-hundred fold. When the grid goes appreciably positive, the value of r_g becomes lower, the amplification decreases, and the distortion increases. In the foregoing example, the tube amplifies only for grid resistances larger than 2000Ω . The effect of the tube capacitance, as is brought out on page 203, is to make amplification difficult at very high frequencies. If the case for which maximum power amplification with practically no distortion (R about equal to $2r_p$) is chosen, then

$$A' = 0.222 \mu^2 \frac{r_g}{r_p} \quad (15)$$

which shows that true power amplification is not so much smaller than for optimum condition $\left(0.25\mu^2\frac{r_p}{r_p}\right)$ with distortion. The square-root value of true power amplification [Eqs. (13), (13a), (14), and (15)] is then a linear amplification. It corresponds in proper amplifiers to voltage amplification and is identical with it when $r_p = R$.

90. Estimation of Power Output and Amount of Second-harmonic Distortion.—Reference to Fig. 128, the power output is

$$W = 0.125(E_{\max} - E_{\min})(I_{\max} - I_{\min}) \quad (16)$$

and second-harmonic distortion is given by

$$D_2 = \frac{0.5[I_{\max} + I_{\min}] - I_b}{I_{\max} - I_{\min}} \quad (17)$$

If this distortion becomes more than 5 per cent, the load resistance R should be chosen higher. As previously mentioned, $R = (1.6 \text{ to } 2.0)r_p$, as a rule, provides good repeater action. If the dynamic plate resistance r_p is unknown for a particular operating point P , it can be found graphically as indicated in Fig. 131 where the static I_p/E_p characteristic for the desired constant grid bias E_c is drawn. A tangent along the operating point P for any two points A and B gives the slope at this point and

$$r_p = \frac{E_2 - E_1}{I_2 - I_1} \quad (18)$$

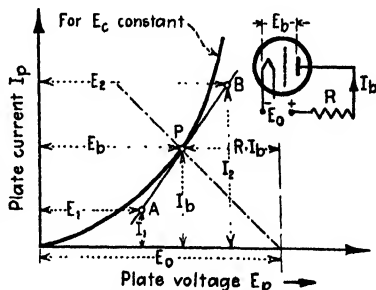


FIG. 131.—Graphical method for finding dynamic plate resistance.

From the relation [Eq. (8) on page 192] for the effective values E and I of alternating grid voltage and plate current, respectively, and for optimum power output ($R = r_p$), we obtain

$$W = I^2 R = \frac{\mu^2 E^2}{4r_p} = \frac{\mu g_m}{4} E^2 = Q E^2 \quad (19)$$

where Q denotes the quality of an amplifier tube.

91. Plate-current Grid-voltage Characteristic and Grid Bias for Loaded Plate Circuits.—The heavily drawn characteristic of Fig. 132 denotes the static $I_p - E_c$ characteristic when the plate is directly connected through the B source to the filament, and the dot-dash curve the corresponding dynamic characteristic for a resistance load R in the external plate branch. The working characteristic for optimum power transfer ($R = r_p$) has the steepness $g_m/2$ only. For maximum undistorted power output ($R = 2r_p$) the fraction $g_m/3$ only is effective. The

negative grid bias E_c can be found by the construction indicated in Fig. 133. For optimum power output extend the straight portion of the static characteristic until it intersects the $I_p = 0$ line at A and draw the line AB of steepness $g_m/2$. The line OC , with C as mid-point of AB , intersects the static characteristic at the operating point P , giving the desired grid bias E_c .

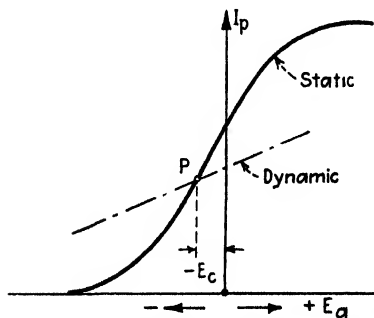


FIG. 132.—Static and dynamic steepness characteristics.

For undistorted maximum power transfer, the lower curvature of the I_p , E_g characteristic cannot be used. Hence draw reference line XY which eliminates this curvature and a line UV a distance of about -1.5 volts. Practically no grid current exists for such negative voltages. The intersection of these two lines is O' , and the construction is as before.

92. Uses of Lumped Characteristics.—Suppose the plate of a triode is connected through a B battery of negligible resistance to the negative end of the filament and a steady grid bias connected between the grid and the negative end of the filament. The lumped tube voltage is then given by

$$E_l = E_b + \mu E_c \quad (20)$$

and by plotting E_l against the plate current we have the lumped tube characteristic. When a positive grid bias E_c is added, more plate

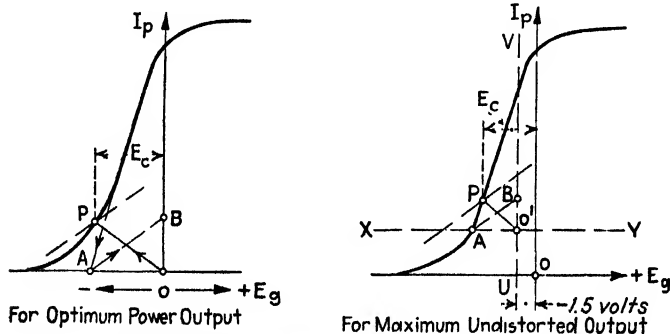


FIG. 133.—Graphical solution for correct grid bias E_c .

current flows. The same can also be accomplished by increasing E_b by a voltage equal to μE_c . The opposite effect results when the grid bias is made more negative. Since for zero grid potential the lumped tube voltage is identical with the effective plate potential, the static plate-current plate-voltage characteristic for $E_c = 0$ (Fig. 134) can be used to

compute the plate current for any condition of plate voltage and grid-bias. Suppose that the characteristic indicated in the figure refers to a tube with $\mu = 3.3$ and that $E_p = 70$ volts corresponds to $I_p = 8$ ma. In order to find I_p at -5 volts grid bias we have

$$E_i = E_p + \mu E_c = 70 - 3.3 \times 5 = 53.5 \text{ (volts)}$$

and 53.5 volts on the lumped characteristic for $E_c = 0$ gives about 4.7 ma, which is the desired current value. By choosing several different values of plate voltage and finding the plate current when $E_c = -5$ volts, the characteristic for such a grid bias is obtained.

In dealing with lumped triode voltages, a distinction must be made between the effects of the steady voltage of the grid and plate battery and those due to the variable voltages.

When a sinusoidal voltage $e_a = e_o' \sin \omega t$ is impressed on the grid of an amplifier, with a fixed grid bias E_c and plate supply voltage E_b , we have for the resultant lumped voltage

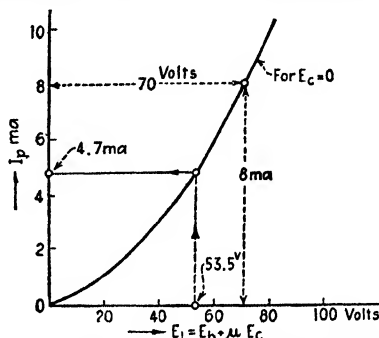


FIG. 134.—Lumped characteristic for finding I_p for any E_c bias.

$$E_r = E_i + e_i' \sin \omega t = \mu E_c + E_b + [\mu e_o' - e_p'] \sin \omega t \quad (21)$$

A minus sign occurs since the plate voltage $e_p = e_p' \sin \omega t$ decreases with the load current $i_p = i_p' \sin \omega t$ which flows through the external anode resistance. This was used on page 66 when the formula for the variable-current tube resistance of a triode was derived. The amplitude of the variable lumped triode voltage $e_i = e_i' \sin \omega t$ becomes

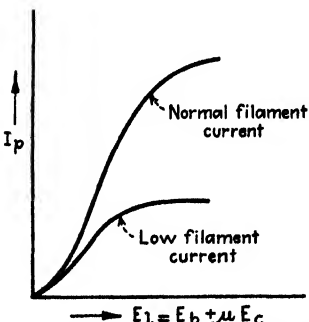


FIG. 135.—Lumped static characteristics.

$$e_i' = [\mu e_o' - e_p'] = e_o' \left[\mu - \frac{e_p'}{e_o'} \right] \quad (22)$$

Hence, when μ reaches the value of e_p'/e_o' , the dynamic lumped voltage e_i' vanishes. From Eq. (22) it can be seen that the amplification factor μ must be made larger the higher the operating voltages of a tube.

As far as static lumped characteristics are concerned, reference is made to Fig. 135 where each characteristic corresponds to a certain constant-filament current. Each curve is given by the function

$$I_p = F[E_p + \mu E_c] = F(E_i) \quad (23)$$

where E_p is for unloaded external plate circuit ($R = 0$) equal to the voltage of the plate supply. The steepness of this curve represents a conductance and is not constant but is

$$g = \frac{\partial I_p}{\partial E_l} = \frac{\partial F(E_l)}{\partial E_l} \quad (24)$$

A small change δE_p in E_p produces a change δI_p in I_p and $\partial F(E_l)/\partial E_l$ is practically the same as $\partial I_p/\partial E_p$. With this in mind

$$\frac{\partial E_l}{\partial F(E_l)} = r_p \quad (25)$$

For the almost straight-line region of the lumped characteristic, $\partial r_p/\partial F(E_l)$ is very small while for the curved portion this is not true. When the external plate branch is loaded by an ohmic resistance R , the plate current $I_p = I_b$ sinks to some value $I_p = I_1$ and the effective lumped tube voltage to a correspondingly smaller value E_1 and we have for the voltage E_b of the B battery

$$I_1 = F[(E_b - I_1 R) + \mu E_g] = F(E_1) \quad (26)$$

When the tube is used as an amplifier, some small variable grid voltage e_g is superimposed on the constant grid bias and produces a variable i_p in the plate current so that, besides the voltage contribution μe_g in the plate circuit, the external drop $e_p = -i_p R$ must also be taken into account. Then

$$I_1 + i_p = F(E_1) + F(\mu e_g - i_p R) = F(E_1 + \rho)$$

if $\rho = \mu e_g - i_p R$. Expanding the right side according to Taylor's theorem, we find

$$I_1 + i_p = F(E_1) + \rho \frac{\partial F(E_1)}{\partial E_1} + \frac{\rho^2}{2} \frac{\partial^2 F(E_1)}{\partial E_1^2} + \frac{\rho^3}{6} \frac{\partial^3 F(E_1)}{\partial E_1^3} \quad (27)$$

Substituting the value of (26) and (27), we find for the variable-current component

$$i_p = \rho \frac{\partial F(E_1)}{\partial E_1} + \frac{\rho^2}{2} \frac{\partial^2 F(E_1)}{\partial E_1^2} + \frac{\rho^3}{6} \frac{\partial^3 F(E_1)}{\partial E_1^3} \quad (28)$$

which indicates, for small values of ρ , a linear voltage amplification since only the first term remains and the well-known tube relation

$$i_p = \frac{\mu e_g - i_p R}{r_p} \quad \text{or} \quad i_p = \frac{\mu e_g}{r_p + R}$$

is obtained because $\partial F(E_1)/\partial E_1 = 1/r_p$ and $\rho = \mu e_g - i_p R$. Unless this relation is obtained, distortion occurs in the amplifier since terms in e_g^2 and higher powers become important.

93. Effect of Interelectrode Capacitance and Grid Resistance on the Amplification.—As brought out in Sec. 34, the effective grid capacitance and dynamic grid resistance are by no means the geometrical capacitance C_{gf} and the resistance $R_g = E_g/I_g$, respectively, but are values which depend on the load in the external plate branch since any actions which take place in the plate circuit react back through the plate-grid capacitance C_{gp} into the input circuit. The static grid resistance R_g due to any convection current through the electron path from filament to grid is not the value to be taken, since the dynamic input resistance depends upon the rate of change of the grid current with the grid voltage. For instance, when the saturation value of steady grid current is flowing, $\partial I_g/\partial E_g$ gives zero grid conductance and an infinite value for the dynamic resistance r_g , although the static resistance is fairly low. When the input impedance is represented by an apparent resistance r_g' in parallel with an apparent capacitance C_g' , as in Fig. 136, and the effect of the plate capacitance together with the load resistance R is assumed to be that given by the dynamic tube resistance r_p , we have, for a properly biased tube,

$$\left. \begin{aligned} r_g' &= \frac{\beta}{\alpha r_p [2 + \mu]} & \alpha &= \omega^2 C_{gp}^2 \\ C_g' &= \underbrace{C_{gf}}_{\text{geometrical grid-filament capacitance with tube alone (without plate return)}} + 2C_{gp} \frac{2 + \mu}{\beta} & \beta &= 4 + \alpha r_p^2 \end{aligned} \right\} \quad (29)$$

The geometrical interelectrode capacitance at the input side, when the tube is connected as in the indicated circuit, is $C_{gf} + C_{gp}$. Therefore, it is evident that the apparent capacitance in each case is larger than the geometrical value. For instance, taking a commercial receiving semi-power output tube (112A or its equivalent), we have

$$\mu = 8; \quad \underbrace{C_{gp} = 10.5; \quad C_{gf} = 6; \quad C_{pf} = 5.5}_{\mu\mu\text{f}}$$

$r_p = 5000\Omega$ for 135 volts supply voltage on plate and 9 volts negative grid bias

We then find the values in Table IV.

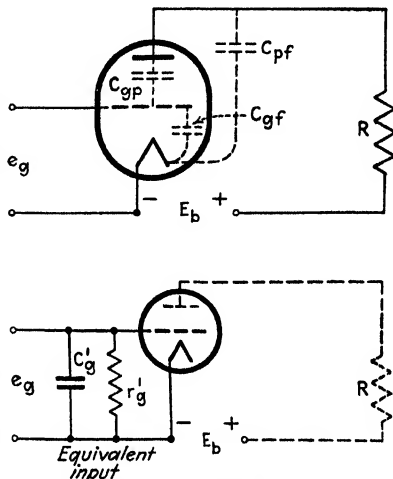


FIG. 136.—Tube taking interelectrode tube capacitances into account.

TABLE IV

f , kc/sec	$C_g' = \left[6 + \frac{210}{\beta} \right] 10^{-12}$ $\cong 58.5 \times 10^{-12}$, farads	$\frac{1}{\omega C_g'}$ ohms	$r_g' = \frac{\beta}{5 \times 10^4 \alpha}$, ohms	Remarks
1	58.5×10^{-12}	2.72×10^6	1.84×10^{10}	$\beta = 4 + \delta$, where δ is usually small compared with 4. For this example $\delta = 0.109$ at 1000 kc/sec, and 1.09×10^{-7} at 1 kc which is the other limit
10	58.5×10^{-12}	2.72×10^5	1.84×10^8	
100	58.5×10^{-12}	2.72×10^4	1.84×10^6	
1000	57×10^{-12}	2.79×10^3	1.89×10^4	

It can be seen that the effective dynamic resistance offered by the grid-filament gap as well as the reactance of the effective parallel capacity are high enough in the audio-frequency range to require the use of grid leaks of several megohms resistance in resistance-coupled amplifiers. Also, even at frequencies as low as 100 kc/sec, the capacity reactance is so low that it practically determines the voltage drop across the input side. In the broadcast range, the effective input impedance offered by this tube is already very low and at 100 kc/sec we deal with impedances of only a few thousand ohms, and grid leaks in the megohm range would be useless. It should be understood that the example refers to a semi-power output tube with a fairly low plate resistance r_p and loaded for maximum power transfer. As seen from formulas (29), the apparent resistance r_g' becomes higher with a higher external load resistance R and the apparent capacitance C_g' becomes correspondingly smaller.

The apparent tube capacitance can be understood by considering the charging current which flows toward the input side of a tube. It divides into a current which charges the geometrical grid-filament condenser to the voltage e_g and a current which charges the geometrical grid-plate condenser to the voltage $e_g + e_p$. The voltage amplification is $A_s = e_p/e_g$ and therefore

$$e_g + e_p = e_g[1 + A_s]$$

If e_g and e_p' are the respective maximum values of alternating grid and plate voltages and i' the maximum value of the corresponding total charging current which flows toward the input side of the tube, we have

$$\begin{aligned}
 i' &= \underbrace{\omega e_g' C_{gf}}_{\text{charges } C_{gf}} + \underbrace{\omega [e_g' - e_p'] C_{gp}}_{\text{charges } C_{gp}} \\
 &= \omega e_g' [C_{gf} + (1 + A_s) C_{gp}] = \omega e_g' C_g'
 \end{aligned}$$

or

$$\begin{aligned}
 C_g' &= C_{gf} + [1 + A_s]C_{gp} \\
 &= C_{gf} + \underbrace{C_{gp}}_{\substack{\text{geometrical input capacitance} \\ \text{with tube connected in circuit}}} + A_s C_{gp}
 \end{aligned} \tag{30}$$

This formula shows that the apparent capacitance varies with any factors that affect the voltage amplification and is especially useful if audio-frequency amplifiers with resistance-capacitance or resistance coupling are under consideration. According to Eq. (4), the voltage amplification for a load resistance R is equal to $\mu R / (r_p + R)$ and, ignoring the effect of the plate-filament capacitance, we have for the apparent input capacitance

$$C_g' = C_{gf} + C_{gp} \left[1 + \frac{\mu R}{R + r_p} \right] \tag{31}$$

which is exactly the same result as obtained in formula (69) on page 86. Taking the case of maximum power amplification which occurs for $R \cong r_p$, we have

$$C_g' = C_{gf} + C_{gp} \left[1 + \frac{\mu}{2} \right] \tag{32}$$

and, applying this to the tube used in computing Table IV, we find that

$$C_g' = [6 + 10.5 \times 5] \times 10^{-12} = 58.5 \times 10^{-12} \text{ farad}$$

checking, of course, with the results in the table if only the lower frequencies, and especially the audio-frequency range, are to be considered.

The capacity reactance $1/(\omega C_g')$ for the highest operating frequency is quite important. Suppose the tube forms the final stage of an audio-frequency amplifier which is to amplify audio currents up to 10 kc/sec without appreciable distortion. No frequency dependency should exist for the entire range and the critical test is that for the most severe limit, which is 10 kc/sec, and the reactance $1/(\omega C_g') = 2.72 \times 10^5$ ohms should be much larger than the load resistance R in the plate branch of the preceding tube.

When the dynamic grid resistance is derived from the static grid-voltage grid-current curve, the lower portion of this curve plays a part only when a proper grid bias is chosen and any e_g variations—so to speak—sweep into the “starting grid-current” range for which a small current flow for small negative grid potentials (small retarding potentials) is possible. Then the ordinary tube law no longer holds but rather Eq. (10) on page 7 for which

$$\left. \begin{aligned} I_g &= I_{g0} e^{-\frac{qE_g}{kT}} \\ \frac{q}{k} &= \frac{10^5}{8.6} \text{ }^\circ\text{K/volt} \end{aligned} \right\} \tag{33}$$

It is assumed that the entire available electron current given by this relation passes to the grid. The quantity T denotes the absolute temperature of the filament and I_0 the current for zero electrode potential. The theoretical dynamic input resistance of the tube is then

$$r_g = \frac{dE_g}{dI_g} = \left[\frac{I_s e^{-\frac{E_g}{8.6 \times 10^{-5} T}}}{8.6 \times 10^{-5} T} \right]^{-1} \quad (34)$$

Assuming a tungsten filament operating at 2300°K , we have

$$\frac{10^5}{8.6 T} = \frac{10^5}{8.6 \times 2300} = 5.06 \text{ per volt}$$

and

$$r_g^{(\text{ohms})} = \frac{198 e^{5.06 E_g}}{I_s} \quad (34a)$$

if I_s is, as usual, in milliamperes and the effective grid voltage E_g in volts. Suppose the saturation current I_s is 20 ma. For the different effective grid potentials we then find the values of r_g given in Table V, showing

TABLE V	
Negative Grid Potential E_g , Volts	$r_g = 99 e^{5.06 E_g}$, Ohms
-0.5	1230
-1	15,600
-2	2.46×10^5
-2.5	31×10^5

that near zero grid potential very unfavorable low grid resistances can prevail.

94. Resistance- and Resistance-capacitance-coupled Amplifiers.—From Eqs. (4), (5), and (6) we obtain, for an effective value E of the variable grid voltage, output curves for voltage, current, and power as indicated in Fig. 137 when a load resistance R is used in the external plate branch. Putting

$$R = \alpha \cdot r_p \quad (35)$$

for the degree of plate loading R in terms of the internal dynamic tube resistance r_p , the variable power output becomes

$$\begin{aligned} W &= \frac{\alpha}{r_p [1 + \alpha]^2} \mu^2 E^2 \\ &= \frac{4\alpha}{[1 + \alpha]^2} W_{\max} \end{aligned} \quad (36)$$

Hence, when choosing R half as small ($R = r_p/2$) and twice as large ($R = 2r_p$) as for optimum power output ($R = r_p$), we find for each case ($\alpha = 1/2$ and $\alpha = 2$, respectively)

$$W' = \frac{8}{9} W_{\max}$$

that is, 11.1 per cent less output than for optimum condition. The range from $\alpha = \frac{1}{2}$ to $\alpha = 2$ still gives considerable power output and $R = (1.6 \text{ to } 2)r_p$ for undistorted output does not mean so much power reduction after all. For the voltage output, we have

$$E_1 = \frac{\alpha}{1 + \alpha} \mu E \quad (37)$$

Hence, for $R = 4r_p$ only, that is, $\alpha = 4$, already 80 per cent of the maxi-

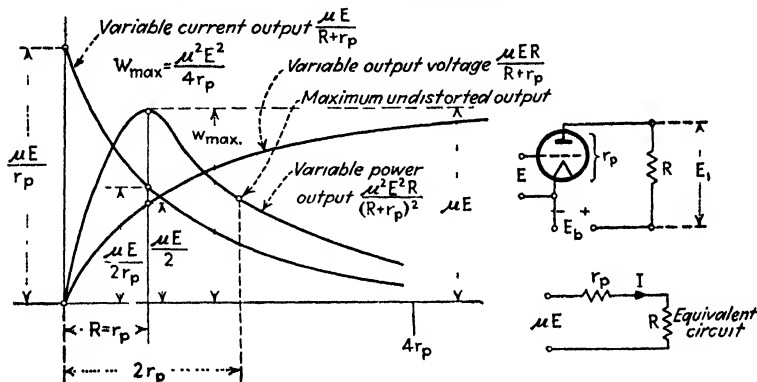


FIG. 137.—Performance in a resistance-loaded amplifier.

mum obtainable voltage amplification and, for $\alpha = 10$, practically maximum voltage amplification is obtained. For maximum undistorted output, α about equal to 2, the voltage amplification is 66.7 per cent of the maximum obtainable value. Since the effective value of the variable output current is

$$I = \frac{\mu E}{[1 + \alpha]r_p} \quad (38)$$

the current amplification of a resistance-coupled amplifier becomes greater the smaller α , that is, the smaller the external load resistance, and reaches its maximum value $\mu E/r_p$ for $R = 0$.

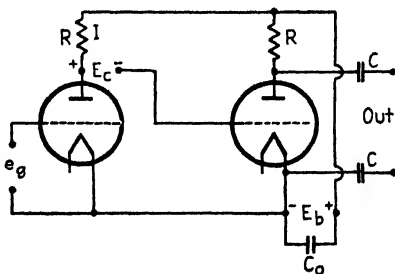


FIG. 138.—Resistance-coupled (aperiodic) amplifier.

For several stages of voltage amplification either resistance coupling (Fig. 138), with comparatively large grid bias, must be used in order to compensate the positive plate potential or resistance-capacitance coupling (Fig. 139) employed. The straight resistance amplifier (Fig. 138) is also known as a direct-current amplifier (when no output condensers C are used) since it amplifies down to the lowest frequencies as well as amplifying direct-current changes. The amplification per stage

can be readily measured by noting the change i in the plate current I when a certain small direct potential e_g is impressed. The voltage amplification is then $e_p/e_g = R \cdot i/e_g$. Usually the output tube of a cascade amplifier as in Fig. 139 has a much lower plate resistance and requires a different grid bias from that of the two first tubes which are conveniently high- μ tubes of the same rating.

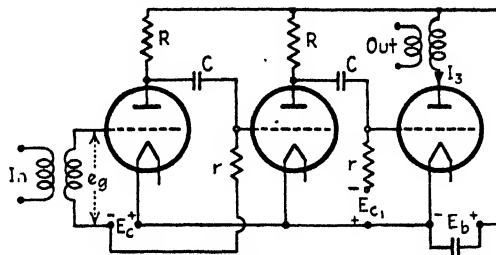


FIG. 139.—Resistance-capacitance-coupled amplifier.

95. Supply Voltages for Resistance-coupled Amplifiers.—The normal voltage specified by the manufacturer should be used for the filament supply. However, the grid bias depends upon whether a class A amplifier (working practically with no distortion) or an amplifier with more or less grid current (working characteristic reaches into the positive region) is to be used. In each case, the steady positive plate potential $E_b = E_B - RI_b$ due to the voltage E_B of the B battery and the amplification factor μ determines the suitable value of the bias, although the graphical construction shown in Fig. 133 can be used to find the value of E_c . If $k = (R + r_p)/r_p$, the supply voltage of the B battery is

$$E_B = kE_b \quad (39)$$

Hence, for optimum power output, the supply voltage must be $2E_b$, or double the specified value, while for maximum undistorted output ($R = 2r_p$) it must be three times the normal value specified by the tube manufacturer. For values of the load resistance R that are small in comparison with the internal plate resistance r_p , the plate and supply voltages do not differ greatly and the grid bias may be calculated from

$$E_c = -\frac{E_b}{1.5\mu} \quad (40)$$

Hence, for a tube of $\mu = 3$, we find for $E_B = 180$ volts the bias $E_c = -40$ volts, and for $E_B = 135$ the value -30 volts. Such small load resistances would be of little use for amplification work. For the average resistance loading, the bias may be found approximately from

$$E_c = -\frac{E_B}{2\mu} \quad (41)$$

which, for a supply voltage $E_B = 180$ volts in the foregoing example, would require only -30 volts bias. The $I_p - E_g$ characteristic is less steep and the working value of g_m correspondingly smaller.

96. Effect of Capacitance-resistance Coupling and Grid-plate Inter-electrode Capacitance on the Frequency Characteristic of an Amplifier.—The coupling condenser C in the amplifier section indicated in Fig. 140 absorbs a certain part of the available plate potential. When e_p denotes the vector of the alternating voltage across the load resistance R , it produces a current i in the equivalent variable-current network and leaves the vector value e_g to be passed on to the grid of the succeeding tubes. Since $e_g = ir$ and $e_p = i[r + 1/(j\omega C)] = i[(\omega Cr - j)/(\omega C)]$, we obtain for the effective voltage ratio of e_g/e_p

$$\rho = \frac{p}{\sqrt{1 + p^2}} \quad (42)$$

if $p = \omega Cr$ because the absolute value

of $\frac{\omega Cr - j}{\omega C} = \frac{\sqrt{\omega^2 C^2 r^2 + 1}}{\omega C}$. This

factor is always smaller than unity and increases, for a fixed coupling capacitance C , toward unity as the frequency becomes higher. For a fixed frequency, it approaches unity as the capacitance is increased. Since in amplifiers C is fixed, ρ is a function of the frequency only and should be such that it changes but little for the range of frequency for which the amplifier is used. Hence, when an amplifier is to be designed to cover the range from 15 to 100 kc/sec, the voltage loss due to C coupling should at any frequency not exceed a certain percentage. Suppose the limit required is 5 per cent, then $\rho = 0.95$ and $p = 3$. Assuming the grid leak to be $r = 10^6$ ohms,

$$C = \frac{p10^6}{r\omega} = \frac{3 \times 10^6}{2\pi \times 15 \times 10^3 \times 10^6 \times 10^6} = 0.000032 \mu\text{f}$$

If a coupling capacitance $C = 0.002 \mu\text{f}$ were used instead of the computed value, we should have

$$p = \omega Cr10^{-6} = 6.28 \times 15 \times 10^3 \times 2 \times 10^{-3} \times 10^6 \times 10^{-6} = 188.5$$

which corresponds to hardly any voltage drop in C for the most severe limit (15 kc/sec) of the frequencies to be transmitted through the amplifier.

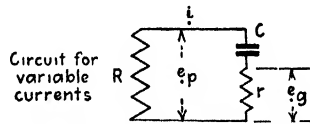
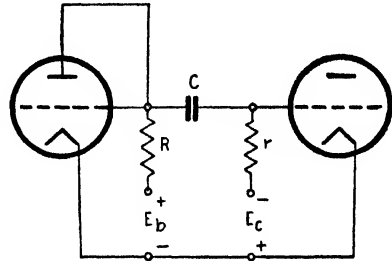
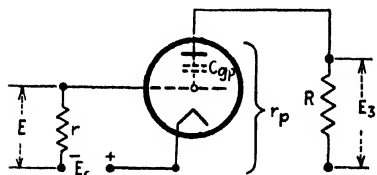


FIG. 140.—Interstage coupling.

Figure 141 shows the case in which the grid-plate interelectrode capacitance is effective and feeds some of the plate voltage back into the input branch of the tube. The grid-filament and plate-filament interelectrode capacitances are not taken into consideration here since they are in parallel with r and R , respectively, and r and R are to be chosen according to the frequency range. (These capacitances are discussed in the analysis of Sec. 98.) If $E = E_1 + E_2$ denotes the effective value of the variable voltage which exists between the grid and the filament, it is made up of two components, one due to the actual impressed grid voltage and the other due to the back action of the plate on the grid by means of the interelectrode capacitance C_{gp} . The latter component is



$$E_1 = \frac{rE_3}{\sqrt{r^2 + 1/(\omega^2 C_{gp}^2)}} = \beta E_3$$

FIG. 141.—Grid-plate capacitance feeds voltage back.

if E_3 denotes the effective value of the variable output voltage across the load resistance R . This voltage is produced by the effective value of the voltage between the grid and the cathode.

For

$$E = -\frac{E_3}{\gamma} \quad (43)$$

we find

$$\begin{aligned} E_3 &= -\gamma E = -\gamma[E_1 + E_2] = -\gamma[\beta E_3 + E_2] \\ E_3[1 + \beta\gamma] &= -\gamma E_2 \end{aligned}$$

The effective voltage gain is the ratio of the plate voltage to the impressed grid voltage. The ratio of the plate voltage to the effective grid voltage is always γ . Hence for the gain per stage

$$\frac{E_3}{E_2} = -\frac{\gamma}{1 + \beta\gamma} \quad (44)$$

This relation is of importance in the higher frequency range of resistance-capacitance-coupled amplifiers, while in the normal audio-frequency range the reactance $1/(\omega C_{gp})$ is comparatively high. The ratio of high-frequency to low-frequency amplification

$$\rho' = \frac{\gamma}{1 + \beta\gamma} \cdot \frac{1}{\gamma} = \frac{1}{1 + \beta\gamma} \quad (45)$$

is then a measure of the faithfulness of the resistance-loaded amplifier due to back feed.

97. Special Remarks on the Design of Resistance-capacitance-coupled Amplifiers.—A closer inspection of formula (45) shows that the factor ρ' decreases when either the frequency or γ is increased. The former effect expresses the well-known fact that a resistance-coupled amplifier becomes most inefficient in the higher frequency range. With ordinary receiving tubes, the voltage amplification falls off considerably for frequencies higher than about 300 kc/sec, and for frequencies as high as those used in the middle broadcast range (1000 kc/sec) practically no useful voltage amplification occurs.

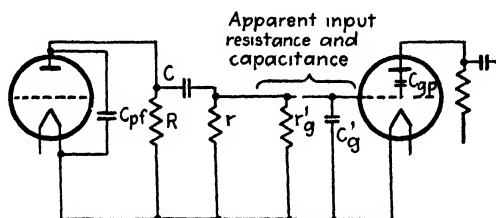


FIG. 142.—Interstage network for variable currents.

The decrease of ρ' with an increase in $\gamma = \mu R / (R + r_p) = \mu K$, for a fixed loading, shows that in the higher frequency range μ should not be chosen unreasonably high (not more than about 20). For the lower frequency range for which γ denotes practically the voltage amplification, high- μ tubes are of advantage. The internal plate resistance r_p is also higher and consequently R can be higher, since it can be the value of r_p . It is to be noted, however, that, for high- μ tubes, the grid-voltage plate-current characteristic is less displaced into the region of negative grid voltage. In many cases, higher plate-supply voltages bring the working portion more into the negative region. If there is no objection to distortion, the operating point can be chosen more toward the lower bend of the E_p, I_p characteristic, which simultaneously increases the value of r_p .

To judge the usefulness of a cascade amplifier of this type over the entire frequency range, we must compare the effects of all resistances and capacity reactances (Fig. 142). It should be noted again that C_g' and r_g' denote the effective dynamic grid-filament capacitance and resistance offered by the grid-filament gap for a particular loading and that C_g' is larger than the geometrical capacitance C_{gf} (pages 86 and 203). In the design of such an amplifier, the following points are then of interest.

1. Decrease in amplification due to reactance of coupling condenser [formula (42)].
2. Change in amplification due to back feed from plate [formula (45)].
3. Decrease in amplification due to reactance of input interelectrode capacitance C_g' [formula (31), page 205, for C_g'].

4. Decrease in amplification due to effective resistance r_o' experienced between grid and filament.

5. Change in amplification due to C_{pf} capacitance.

6. Time constant $C \cdot r_o$ if effect of e_o' is neglected and $r_o = \frac{r \cdot r_o'}{r + r_o'}$.

Cases 1, 2, and 5 have been discussed in Sec. 96. As far as the effect of the reactance of the interelectrode input reactance is concerned, we note from Table IV on page 204 that in the low-frequency range this reactance can be assumed to be several megohms. This reactance is in multiple with the grid-leak resistance r and there is, therefore, no gain in using leak resistances much higher than 5 megohms in amplifiers used for the audio-frequency band. We note from Table IV that the input capacity reactance for frequencies only as high as the broadcast range can be as low as several thousand ohms, indicating again the unsuitability of such amplifiers for the higher frequency range. From the same table, it can be seen that in the lower and audio-frequency range the effective resistance r_o' which is also in parallel with the grid leak r , is high enough to allow high grid leaks up to 10 megohms. If, however, the reactance $1/(\omega C_o')$ is comparatively low, grid leaks of lower resistance can be of use only (about 0.5 to 5 megohms). For the high-frequency range, Table IV indicates that r_o' can assume quite low values, although the shunting effect of $1/(\omega C_o')$ calls for even smaller values of r .

The C_{pf} capacitance shunts the load resistance R and limits its magnitude, that is, the value of α in formula (35) on page 206. For many receiving tubes, the reactance due to this capacitance is very high in the low-frequency range (about 100 megohms at 60 cycles/sec) and about 1 megohm in the middle audio-frequency range. But for frequencies only as high as 50 kc/sec, it drops to values of about 0.1 megohm. In the lower broadcast range (500 kc/sec), this reactance has values in the neighborhood of 10,000 ohms. The voltage amplification of resistance-coupled amplifiers is also limited by this capacitance and the value of α in formula (35) can only be chosen high (up to 10) when working up to medium frequencies. It can also be seen that, owing to this capacity effect, such amplifiers are useless for the broadcast range and give no voltage amplification at all for frequencies in the short-wave band. This statement can be readily checked by means of the generalized formula for the voltage amplification. It is obtained from Eq. (4a) on page 191 as

$$A_v \cong \frac{\mu Z}{r_p}$$

for the case of an effective load impedance Z low in comparison with r_p . Such a low value will result from the parallel combination of the load resistance R and the reactance $1/(\omega C_{pf})$. This happens when $1/(\omega C_{pf})$

practically determines the value of Z in the higher frequency band. Consider a high- μ tube with the constants $\mu = 25$, $C_{pf} = 6 \times 10^{-12}$, $r_p = 250,000 \Omega$ at the operating voltage and a load resistance R of about 0.5 megohm when the supply voltage is about 200 volts. At 3000 kc/sec, we have $1/(\omega C_{pf}) = 8850 \Omega$. This reactance practically determines the plate load impedance Z and $A_r = 25 \times 8850/250,000$, which is smaller than unity. Therefore a decrease in voltage instead of voltage amplification is obtained. This speculation, of course, has reference only to what happens as a result of the effect of the plate-filament interelectrode capacitance. As a rule, such receiving tubes with a high- μ value have a comparatively large effective input capacitance so that for this reason alone it would have value as an audio-frequency amplifier only. Therefore, it can again be seen that a tube with a high- μ value does not necessarily guarantee high-voltage amplification when applying it to the high-frequency range. From the effects due to r_a' , C_a' , and C_{pf} as well as μ , it is evident that a fixed grid leak r and a fixed coupling condenser C for a certain tube by no means give a good transmission characteristic in a resistance-coupled amplifier when working over a wide range of frequency. The quality of transmission is evidently dependent on the width of the frequency band and the lowest pass frequency. Such an amplifier when used in the audio-frequency range may work satisfactorily, for instance, when using a leak resistance $r = 2$ megohms and a coupling condenser $C = 0.003 \mu f$ but requires a much smaller leak resistance for the higher frequency range and therefore also a smaller coupling capacitance, since the reactance of the effective input capacitance may have values as low as a few thousand ohms. A coupling condenser of about 0.0005 may be more satisfactory. When high- μ tubes (such as the UX240 or its equivalent) are used, they give fairly good transmission characteristics in the audio-frequency band when their load resistance R is made about $2r_p$ and a coupling condenser $C = 0.006 \mu f$ is used. A leak resistance $r = 2 \times 10^6$ ohms is suitable. With many amplifiers of this type, it does not seem to be an advantage to give r_a a high value, especially when cascade amplification is under consideration, since multistage amplifiers are much more stable if r_a is not much higher than about $1/2$ megohm.

Another important point is the proper choice of the time constant τ . If the value $C(\mu f) \times r_0(\text{megohms}) = \tau(\text{sec})$ is not properly chosen for

$$r_0 = \frac{r \cdot r_a'}{r + r_a'}$$

the amplifier may block (no plate current) during certain intervals. The $C \cdot r_0$ product denotes the time in seconds for C to discharge to 37 per cent of its original value (falls off to $1/2.718$ th). When a dis-

turbing impulse enters the input side of the amplifier and C is chosen too large, it may take altogether too much time to charge C of the first coupling condenser and the plate current of the succeeding tube may fall to zero so that this tube ceases to function for quite an interval of time. This action passes through all stages and the various capacity couplings may produce different time constants, so that the disturbing pulse may set up a circulating disturbance which is fed back again to the input, propagated again, and so on. This is more apt to happen when a common B battery with quite an appreciable internal resistance is used. Therefore it is essential that the effective resistance across the grid and filament be properly proportioned in comparison with the coupling condenser C . With respect to Fig. 140 and formula (42), we have, for the effective voltage ratio $\rho = e_g/e_p$ and $C \cdot r_0 = \tau$, the expression

$$\rho = \frac{\omega\tau}{\sqrt{1 + \omega^2\tau^2}} \quad (46)$$

The quantity ρ is always smaller than unity and expresses the loss of voltage due to the coupling condenser for a certain time constant τ and frequency $\omega/(2\pi)$. The magnitude of the coupling condenser C is found by means of (46) by at first assuming a suitable grid-leak resistance r (somewhere between 0.5 and 5 megohms). For the low-frequency range where the alternating-current resistance of the grid-filament gap is one to several megohms, the upper limit for r is chosen; but for the range of high frequencies where the apparent dynamic resistance r_g' is of the order of a few thousand ohms, the value of $r_0 = r_g' \cdot r/(r_g' + r)$ becomes correspondingly low. Hence the coupling condenser C is not the same for each case. When, for instance, a single-stage amplifier is under consideration and the audio-frequency band is to be covered, a time constant of about $\tau = 0.005$ sec is suitable. Putting this value in Eq. (46) for the lowest frequency gives the percentage voltage loss $(1 - \rho) 100$ due to the C coupling at this frequency and the ratio τ/r_0 for r_0 in megohms gives the coupling in microfarads. Since with two and three stages of amplification the values are to be taken as about p^2 and p^3 , the time constant τ must be increased.

98. Design Formulas for Resistance-coupled Amplifiers and Width of Pass Band.—As noted above, a resistance-coupled amplifier is especially suitable for voltage amplification over a considerable frequency band, provided the band does not reach into the very high-frequency range. It is possible to obtain almost undistorted amplification. It was shown that the voltage amplification increases with the μ of the tube as well as with the load resistance R but that in many cases R can be increased only when the B voltage in the plate branch is correspondingly higher in order to bring the operating point to the middle of the

straight portion of the I_p, E_o characteristic again. When only ordinary B voltages (120 to 200 volts) are used, the plate load cannot be made too high (about 50,000 for ordinary tubes) in an attempt to increase the voltage output $\mu e_o \frac{R}{R + r_p}$. For high- μ tubes, such as UX240 or its equivalent, R is then chosen about equal to $2r_p = 250,000\Omega$ with a supply voltage of about 180 volts. Resistance-coupled amplifiers of such proportions are most frequently used and the derivation¹ of the performance for a certain frequency band is then an easy matter. On the other hand, experiment and theory show² that very high plate resistances (R up to 3 megohms) can be used at ordinary supply voltages ($E_b = 90$ to 150 volts) so that only about 10 to 30 volts can be operative on the plate. The operating point would then seem to be far down on the curved portion of the characteristic. Nevertheless, the working characteristic is again almost linear and high-voltage amplification is possible, even with normal supply voltages. This can be readily understood from Eq. (28) on page 202 which refers to a straight-line dynamic lumped characteristic when the quantity $\rho = \mu e_o - i_p R$ is small, since the higher powers of ρ such as ρ^2, ρ^3 , etc., must make the terms to which they belong negligible in comparison with $\rho \partial F(E_1)/\partial E_1$. We have again the well-known relation

$$i_p R = \frac{\mu e_o R}{R + r_p}$$

for the voltage output which, because of the high value of R , must be pronounced. Therefore, with a high- μ tube, the quantity μe_o in

$$\rho = \mu e_o - i_p R$$

can be large as long as R is high enough to make ρ sufficiently small.

As far as the frequency characteristic of the resistance-capacitance-coupled amplifier is concerned, a lower and an upper frequency limit exists since, according to Fig. 143 (where all effective resistances and reactances are considered), the coupling condenser C partially determines the lower frequency limit, and the apparent interelectrode capacitance C_o and the plate-filament capacitance C_s partially determine the upper limit. These cutoff frequencies may be called f_l and f_u , respectively, and they can be approximately computed from

$$f_l = \frac{1}{2\pi C r_o} \quad (47)$$

$$f_u = \frac{1}{2\pi C_o R_o} \quad (48)$$

¹ WIGGE, H., *Z. Hochfreq.*, **36**, 24, 1930.

² VON ARDENNE, M., "Der Bau von Widerstandsverstärkern" (Design of Resistance Amplifiers), 2d ed., R. C. Schmidt, Berlin, 1927; F. M. COLEBROOK, *Exptl. Wireless*, **4**, 195, 1927.

and the frequency at which maximum amplification occurs is

$$f_0 = \frac{1}{2\pi\sqrt{r_0 k_1 [C_1 C_4 + C C_5]}} \quad (49)$$

if

$$\frac{1}{R_0} = \frac{1}{R} + \frac{1}{r_p} + \frac{1}{r_0}; \quad \frac{1}{R_1} = \frac{1}{R} + \frac{1}{r_p}; \quad C_4 = C_2 + C_3; \\ C_5 = C_1 + C_4; \quad (50)$$

C_0 about $50 \mu\text{f}$ and is mostly due to $C_1 + C_3$ and the socket capacitances. The width of the pass band is then

$$w = f_u - f_l \quad (51)$$

for

$$A_e = A_{\max} \left[1 - \frac{\eta}{100} \right] \quad (52)$$

where it is understood that f_l and f_u are such cut-off frequencies that beyond them (outside the pass band) the voltage amplification A_e is

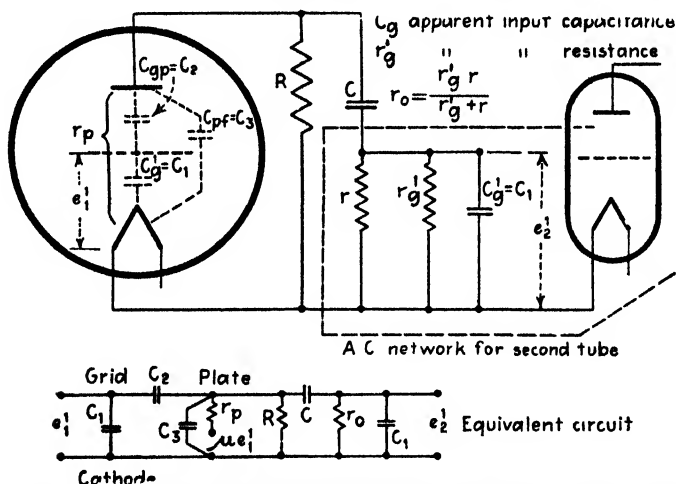


FIG. 143.—Equivalent network of resistance-capacitance-coupled amplifier.

never more than $\eta = 30$ per cent of the maximum amplification A_{\max} which occurs for frequency f_0 somewhere in the pass band. The justification for these formulas can be readily obtained from the network of Fig. 143 if e_1' denotes the maximum value of a sinusoidal e.m.f. impressed across the grid and filament of the first tube and e_2' the maximum value available across the filament and grid of the succeeding tube. The solution becomes simpler when it is assumed that the variations take place only about the operating point of least distortion, that is, only along the almost straight portion of the plate-current grid-voltage charac-

teristic. Then g_m is the maximum value of the mutual conductance (steepness) and the internal plate resistance r_p is at its minimum value. The voltage amplification is

$$A_e = \frac{e_2'}{e_1'} = \frac{\mu \left[1 - \frac{j\omega C_2}{g_m} \right]}{\left\{ \left[1 + \frac{C_1}{C} + \frac{1}{j\omega C r_0} \right] [1 + a + j\omega C_4 r_p] + b + j\omega C_1 r_p \right\}} \quad (53)$$

for

$$R_s = \frac{r_p}{a} \quad \text{and} \quad r_0 = \frac{r_p}{b} \quad (53a)$$

For frequencies which are not too high, ωC_2 is much smaller than g_m and the numerator of (53) becomes practically equal to the amplification factor μ and we find

$$\begin{aligned} A_e &= \frac{g_m}{\frac{1}{R_0} + j\omega C_5 - \frac{j}{\omega C r_0 R_1} + \frac{C_1}{C R_1} + \frac{C_4 r_0}{C} + j\omega \frac{C_1 C_4}{C}} \\ &= \frac{g_m}{A + jB} = \frac{g_m}{\sqrt{A^2 + B^2}} \end{aligned} \quad (54)$$

for

$$\left. \begin{aligned} A &= \frac{1 + \frac{C_1}{C}}{R_1} + \frac{1 + \frac{C_4}{C}}{r_0} \\ B &= \omega \left[C_5 + \frac{C_1 C_4}{C} \right] - \frac{1}{\omega C R_1 r_0} = \omega C_5 - \frac{D}{\omega} \end{aligned} \right\} \quad (54a)$$

Maximum voltage amplification takes place when the term B , which contains the frequency $\omega/2\pi$, vanishes, that is, for

$$A_{\max} = \frac{g_m}{A} = \frac{\mu}{r_p A} = \frac{\mu}{r_p} \frac{1}{\left[1 + \frac{C_1}{C} \right] \left[\frac{1}{r_p} + \frac{1}{R} \right] + \left[1 + \frac{C_2 + C_3}{C} \right] \frac{1}{r_0}} \quad (55)$$

This happens at the frequency $f_0 = \omega/2\pi$ found from $B = 0$, or

$$\omega \left[C_5 + \frac{C_1 C_4}{C} \right] = \frac{1}{\omega C R_1 r_0} \quad (55a)$$

which confirms formula (49). According to (55), A_{\max} reaches an optimum value when the loading resistance R and the effective input resistance r_0 across the grid and filament are both high compared with r_p and the interelectrode capacitances are small compared with the coupling capacitance C . For such a condition,

$$A_{\text{opt}} = \frac{\mu}{r_p} \frac{1}{1/r_p} = \mu \quad (55b)$$

On the other hand, when the interelectrode capacitances are small compared with the coupling capacitance C , the terms C_1/C and $(C_2 + C_3)/C$ in (55) will be small compared with unity and

$$A_{\max} = \frac{\mu}{r_p} R_0 = g_m R_0 \quad (55c)$$

If the amplification drop is η per cent [Eq. (52)] and is chosen small for the pass band w of the amplifier, the voltage amplification for the entire band is given by the approximation

$$A_e = \frac{g_m}{\frac{1}{R} + \frac{1}{r_p} + \frac{1}{r_0}} \quad (56)$$

Hence for a tube with $g_m = 200 \times 10^{-6}$ mho, $r_p = 150,000\Omega$, $R = 250,000\Omega$, and an effective input resistance $r_0 = r_o' \cdot r / (r_o' + r) = 10^6\Omega$, in the audio-frequency range, the voltage amplification for the entire pass band would be seventeenfold instead of about $\mu = g_m r_p =$ thirtyfold as for the optimum condition. From the foregoing formula, it will be evident that it is convenient to use tubes with a large mutual conductance g_m and an amplification factor somewhere between 10 and 30.

The width w of the frequency band for which the amplifier must work depends upon the maximum percentage decrease η [Eq. (52)] of the voltage amplification from the maximum value at frequency f_0 [Eq. (49)]. Combining (52) with $A_{\max} = g_m/A$ from (55) and A , from (54), we find

$$\frac{g_m}{\sqrt{A^2 + B^2}} = \frac{g_m}{A} \left[1 - \frac{\eta}{100} \right]$$

or

$$B = \pm A \sqrt{\frac{1}{[1 - (\eta/100)]^2} - 1} = \pm A\Gamma \quad (57)$$

Substituting this result in the expression for B of Eq. (54a) leads to the quadratic equation

$$\omega^2 C_6 \mp \omega A\Gamma - D = 0$$

or

$$\omega = \pm \frac{A\Gamma}{2C_6} + \sqrt{\left(\frac{A\Gamma}{2C_6}\right)^2 + \frac{D}{C_6}} \quad (58)$$

since only the plus sign before the square root gives positive frequencies $\omega/2\pi$. The frequency limits f_l and f_u , between which the voltage amplification A_e never drops more than η per cent, are then

$$\begin{aligned} f_l &= \frac{1}{2\pi} \left[\sqrt{\left(\frac{A\Gamma}{2C_6}\right)^2 + \frac{D}{C_6}} - \frac{A\Gamma}{2C_6} \right] \\ f_u &= \frac{1}{2\pi} \left[\sqrt{\left(\frac{A\Gamma}{2C_6}\right)^2 + \frac{D}{C_6}} + \frac{A\Gamma}{2C_6} \right] \end{aligned} \quad (59)$$

giving a pass-band width

$$w = f_u - f_l = \frac{A\Gamma}{2\pi C_6} \quad (60)$$

where, according to (50) and (54a),

$$\left. \begin{aligned} A &= \left[1 + \frac{C_1}{C} \right] \left[\frac{1}{R} + \frac{1}{r_p} \right] + \left[1 + \frac{C_2 + C_3}{C} \right] \left[\frac{1}{r_o'} + \frac{1}{r} \right] \\ C_6 &= C_1 + C_2 + C_3 + \frac{C_1[C_2 + C_3]}{C} \\ D &= \frac{1}{CR_1r_0} \quad \text{and} \quad \Gamma = \sqrt{\frac{1}{[1 - (\eta/100)^2] - 1}} \end{aligned} \right\} \quad (61)$$

Hence, when the interelectrode capacitances are small compared with the coupling capacitance C , we have the approximation

$$A \cong \frac{1}{R} + \frac{1}{r_p} + \frac{1}{r_o'} + \frac{1}{r}$$

and Eq. (60) leads to a pass-band width

$$f_u - f_l = \frac{\left[\frac{1}{R} + \frac{1}{r_p} + \frac{1}{r_o'} + \frac{1}{r} \right] \Gamma}{2\pi C_6} = \frac{\Gamma}{2\pi C_6 R_0} \quad (60a)$$

Making the load resistance R about ten times the internal plate resistance r_p as is conveniently done in the audio-frequency range, and realizing that the apparent grid resistance r_o' as well as that of the grid leak r is also usually large compared with r_p when the frequency is not too high, leads to

$$f_u - f_l = \frac{\sqrt{\frac{1}{[1 - (\eta/100)^2] - 1}}}{2\pi C_6 r_p} \quad (60b)$$

Therefore, the pass band is widest for the straight portion of the tube characteristic because r_p is then smallest, and an increase in the interelectrode capacitances C_1 , C_2 , and C_3 decreases the pass band, while an increase of the coupling capacitance C makes the pass band wider.

Since, according to (59),

$$f_l \cdot f_u = \frac{D}{4\pi^2 C_6}$$

and, according to (55a), the frequency f_0 for which maximum voltage amplification occurs is given for $B = 0$, from (54a) $\omega C_6 - (D/\omega) = 0$ we obtain

$$f_0 = \frac{1}{2\pi} \sqrt{\frac{D}{C_6}}$$

Hence

$$f_0 = \sqrt{f_l \cdot f_u} \quad (62)$$

and the frequency for maximum voltage amplification is the geometrical mean of the two limit frequencies. For this reason, when the amplifier is to work between 16 cycles and 10 kc, maximum amplification occurs at $f_0 = \sqrt{16 \times 10,000} = 400$ cycles, while for the lower limit at 30 cycles this frequency would be shifted to 550 cycles. Since, for R several times the internal plate resistance r_p in $1/R_1 = 1/R + 1/r_p \cong 1/r_p$ and in (49), $C_1 C_4$ is small compared with CC_5 , the maximum frequency can also be approximately computed from

$$f_0 = \frac{1}{2\pi\sqrt{r_0 r_p C C_5}} \quad (63)$$

where $C_5 = C_1 + C_2 + C_3$ with the tubes in their sockets and in operating conditions may be as high as $50 \mu\mu\text{f}$. If a resistance-capacitance-coupled amplifier is to be designed for the band whose lower limit $f_l = 16$ cycles/sec, and whose upper limit $f_u = 10$ kc/sec, we find from Eq. (62) that the maximum voltage amplification occurs at $f_0 = 400$ cycles/sec. Using tubes with $r_p = 30,000 \Omega$ and assuming that the parasite capacitances C_5 do not exceed $50 \mu\mu\text{f}$ and that r_0 is 2 megohms, we find, from (63), that the coupling capacitance

$$C = \frac{1}{4\pi^2 f_0^2 r_0 r_p C_5} = \frac{1}{4\pi^2 400^2 \times 2 \times 10^6 \times 30,000 \times 50 \times 10^{-12}}$$

that is, about $0.021 \mu\text{f}$. If the capacitance approximation is also made as in Eq. (60b), we have $C_s = C_5$ and

$$\Gamma = \sqrt{\frac{1}{[1 - (\eta/100)]^2} - 1} = 6.28 r_p \cdot w \cdot C_s$$

which gives $\Gamma = 0.094$ for $w = (10,000 - 16)$. In Fig. 144, the voltage amplification in the pass band never deviates more than $\eta = 0.44$ per cent from the value at 400 cycles/sec, which corresponds to maximum amplification. Hence almost distortionless amplification should prevail. From this example it can be seen that formulas (59) need not be applied at all and that the entire calculation may be based upon the application of the formulas used in the example.

The approximate formulas (47) and (48) are used when the voltage amplification does not deviate anywhere in the pass band more than about 30 per cent from the maximum voltage amplification. When several frequencies occur at the same time, such a deviation can hardly be noticed. Hence, for the foregoing example when $r_p = 30,000 \Omega$ and

$r_0 = 2 \times 10^6$ ohms, we find, for $\eta = 30$ per cent, that $\Gamma = 1.04$ and from (60b) the width of the band becomes

$$w = \frac{1.04}{6.28 \times 50 \times 10^{-12} \times 30,000} = 110,000 \text{ cycles/sec}$$

For the sake of simplicity, by taking this width to be about 100,000, we find, for the limits $f_l = 16$ cycles/sec and $f_u = 100,016$ cycles/sec, that at $f_0 = \sqrt{16 \times 100,016} = 1267$ cycles/sec maximum voltage amplification takes place. From (63), the coupling capacitance becomes

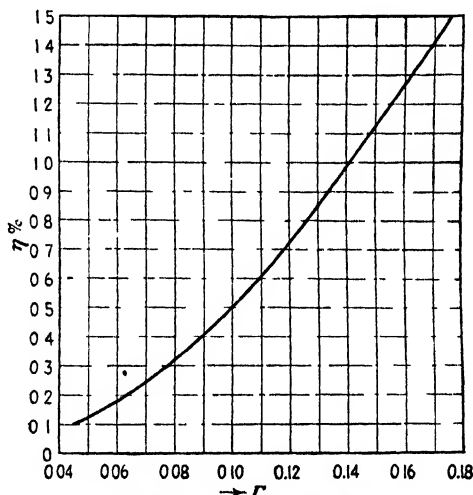


FIG. 144.—Curve for Γ against η %.

$C = 0.0053 \mu\text{f}$. The approximate formulas (47) and (48) for $R = 10r_p$ would give

$$f_l = \frac{1}{6.28 \times 0.0053 \times 10^{-6} \times 2 \times 10^6} = 16.9 \text{ cycles/sec}$$

$$f_u = \frac{0.367 \times 10^{-4}}{6.28 \times 50 \times 10^{-12}} = 116,000 \text{ cycles/sec}$$

since $1/R_0 = 1/R + 1/r_p + 1/r_0 = 0.367 \times 10^{-4}$. The formula for f_u also shows that the upper cutoff frequencies are limited since r_0 must be chosen much smaller for the high-frequency range and because the plate-filament capacity reactance cannot be taken very high.

When a straight resistance-coupled amplifier as in Fig. 138 is used, the alternating-current network is as in Fig. 145. The voltage amplification becomes

$$A_v = \frac{e_2'}{e_1'} = \frac{g_m}{\sqrt{A^2 + B^2}} \quad (64)$$

for

$$\left. \begin{aligned} A &= \frac{1}{r_p} + \frac{1}{r_0} \\ B &= \omega(C_1 + C_2 + C_3) \end{aligned} \right\} \quad (64a)$$

Maximum amplification then occurs for direct currents since, for $B = 0$, the frequency $f_0 = 0$. The width of the pass band is the same as for the resistance-capacitance amplifier and is

$$w = f_u = \frac{\Gamma}{6.28 r_p [C_1 + C_2 + C_3]} \quad (65)$$

when R as well as r_o' is large compared with r_p . This width gives directly the upper cutoff for a maximum amplification variation of η per cent within the pass band since the lower limit is at zero frequency.

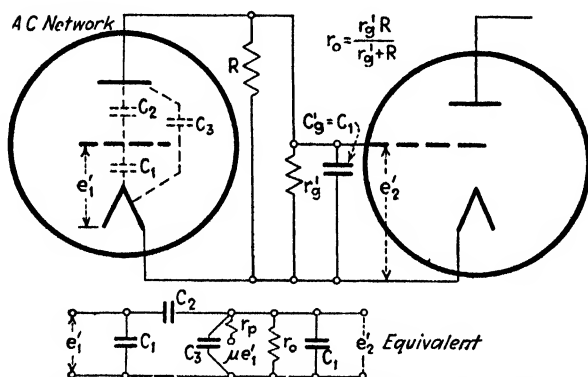


FIG. 145.—Equivalent network of resistance-coupled amplifier.

99. The Transformer-coupled Amplifier.—In the arrangement of Fig. 146, the effective value E_1 of the variable plate voltage of the first tube is passed on to the next tube by means of a transformer. Therefore the effective voltage E_2 applied to the second grid can also be increased by means of the step-up ratio of the transformer. The equivalent circuit also contains the components C_g' and r_o' of the dynamic input impedance Z_g of the grid-filament gap where, according to Eq. (30), C_g' can be computed from

$$C_g' = C_{gf} + [1 + A_e]C_{vp}$$

if A_e stands for the voltage amplification E_3/E_2 due to the second stage. When the transformer L_1, L_2 is matched to the respective terminating impedances, the number of primary and secondary turns N_1 and N_2 , respectively, are given by

$$\frac{N_1}{N_2} = \sqrt{\frac{Z_p}{Z_g}} \quad (66)$$

if Z_p stands for the impedance formed by the parallel branches of r_p and C_{pf} . This expression gives the turn ratio only. The absolute values are limited by the coil capacitances, especially that of the secondary which has more turns, and the ohmic resistance.

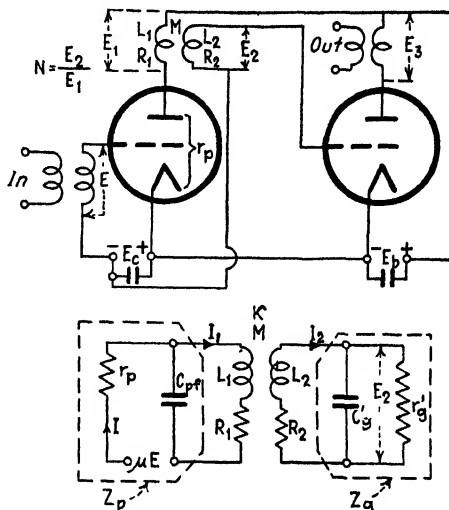


FIG. 146.—Equivalent transformer-coupled amplifier.

If the input capacitance C_o' as well as the distributed capacitance of the transformer windings are at first neglected, the secondary of the transformer is essentially loaded by r_o' and, as in the case of matching a filter in the external plate circuit (page 590), the resistance value r_o'/N^2 is reflected back into the primary. This means that, for no leakage and negligible coil resistances R_1 and R_2 , the equivalent circuit of Fig. 146

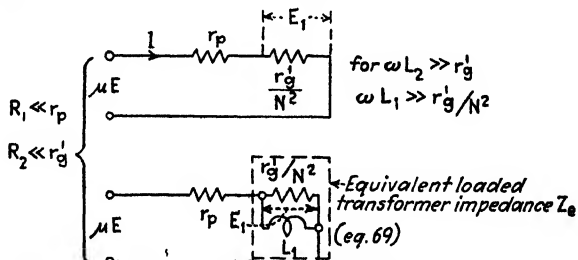


FIG. 147.—Equivalent network for transformer-coupled amplifier.

simplifies to the network shown in Fig. 147, if the plate-filament capacitance is also neglected. The effective value I of the current is then

$$I = \frac{\mu E}{r_p + (r_o'/N^2)}$$

The effective value E_1 of the plate voltage is the drop across the equivalent load, that is, $E_1 = I r_o' / N^2$, and the voltage amplification with respect to the primary terminals of the transformer becomes

$$A_e = \frac{E_1}{E} = \frac{\mu r_o' N}{r_o' + N^2 r_p}$$

This value must be multiplied by the transformer ratio $N = E_2/E_1$ in order to give the expression for the entire voltage amplification per stage which is

$$A_e' = \frac{E_2}{E_1} = \frac{\mu N r_o'}{r_o' + N^2 r_p} \quad (67)$$

Now, since r_p is fixed and the loading r_o' is held constant, the only variable that can affect the degree of voltage amplification is the ratio N of transformation. It becomes a maximum for

$$N = \sqrt{\frac{r_o'}{r_p}}$$

Inserting this in (66) gives

$$A_{\max} = 0.5\mu \sqrt{\frac{r_o'}{r_p}} = 0.5\mu N \quad (68)$$

This maximum condition requires that

$$\frac{X_1}{X_2} = \frac{\omega L_1}{\omega L_2} = \frac{L_1}{L_2} = \frac{r_p}{r_o'} = \frac{1}{N^2} \quad (68a)$$

and large primary and secondary reactances compared with r_p and r_o' , respectively, should be used. But, by taking the tube capacitance C_{pf} and the effective input capacitance C_o' as well as the distributed coil capacitances of the transformer windings into consideration, it can be seen that a good frequency characteristic can be obtained only within the audio range. A good frequency characteristic requires that the transformer be effective at frequencies considerably below its lowest natural frequency. Therefore it is customary to use ordinary transformers only in the low- and medium-frequency range and to employ tuned transformers and tuned reactances in the high-frequency band.

When the transformer exhibits leakage flux, we find from Fig. 146, for negligible tube capacitances and coil resistances R_1 and R_2 and the coupling coefficient $\kappa = M/\sqrt{L_1 L_2}$,

$$\begin{aligned} \mu E &= I_1[r_p + j\omega L_1] + j\omega I_2 \kappa \sqrt{L_1 L_2} \} \\ 0 &= I_2[r_o' + j\omega L_2] + j\omega I_1 \kappa \sqrt{L_1 L_2} \} \end{aligned}$$

or

$$\mu E = I_1 \left[r_p + j\omega L_1 + \underbrace{\frac{\omega^2 \kappa^2 L_1 L_2}{r_o' + j\omega L_2}}_{Z_e} \right] \quad (69)$$

The interstage transformer with the r_o' load acts like an equivalent impedance

$$Z_e = \frac{\omega^2 L_1 L_2 [\kappa^2 - 1] + j\omega L_1 r_o'}{r_o' + j\omega L_2} \quad (70)$$

Hence the closer the coupling, the smaller the factor $(\kappa^2 - 1)$, and for no leakage ($\kappa = 1$) the reflected impedance becomes

$$Z_e = \frac{j\omega L_1 r_o'}{r_o' + j\omega L_2} = \frac{(j\omega L_1)(r_o'/N^2)}{j\omega L_1 + \frac{r_o'}{N^2}} \quad (71)$$

showing that the portion r_o'/N^2 of the grid resistance is reflected back as though it were connected across the primary inductance L_1 with the secondary circuit of the transformer entirely removed (Fig. 147). Hence the primary reactance $X_1 = \omega L_1$ (no load on the transformer) must be large compared with r_o'/N^2 . But, according to (68a), $1/N^2 = L_1/L_2$ and for efficient voltage amplification the condition $\omega L_2 \gg r_o'$ is to be satisfied to prove the requirement brought out in connection with (68a). When iron-core transformers are used, the core losses must also be taken into account, since the no-load primary current is changed accordingly. Additional resistance r_c which takes care of these losses acts in series with L_1 . Moreover, from (69), we find

$$\begin{aligned} \mu E &= I_1 \left[\left(r_p + \frac{\omega^2 \kappa^2 L_1 L_2 r_o'}{r_o'^2 + \omega^2 L_2^2} \right) + j\omega \left(L_1 - \frac{\omega^2 \kappa^2 L_1 L_2^2}{r_o'^2 + \omega^2 L_2^2} \right) \right] \\ &\cong I_1 \left[\left(r_p + \kappa^2 \frac{L_1}{L_2} r_o' \right) + j\omega (L_1 - \kappa^2 L_1) \right] \quad (72) \end{aligned}$$

if $r_o'^2 \ll \omega^2 L_2^2$, showing again that for no leakage ($\kappa = 1$) and large secondary reactance only a pure resistance

$$(L_1/L_2)r_o' = (N_1/N_2)^2 r_o' = r_o'/N^2$$

is reflected back into the plate branch.

When the secondary of the tube transformer works into an impedance (telephone receiver, loud-speaker, etc.), we have the equivalent circuits of Fig. 148. For the ideal audio-frequency transformer ($\kappa = 1$; $R_1 \ll r_p$; $R_2 \ll R$; open-circuit impedance of secondary winding $\gg Z$), the simplified equivalent diagram holds. If R_1' and L_0 are neglected, and if the ratio N_1 of primary to N_2 of secondary turns is equal to the reciprocal

$1/N$ of the transformation ratio, we have the approximation that the load impedance Z across the secondary is $1/N^2$ fold reflected back into the plate branch of the tube. Hence, if the step-up ratio of an audio-frequency transformer is $N = 4$, a condenser load $C = 100\mu\text{mf}$ across the secondary will act as though $1600\mu\text{mf}$ were connected across the no-load primary inductance L_1 . A telephone receiver, as the load Z of effective resistance r and inductance L , acts as a series combination of r/N^2 and L/N^2 across L_1 .

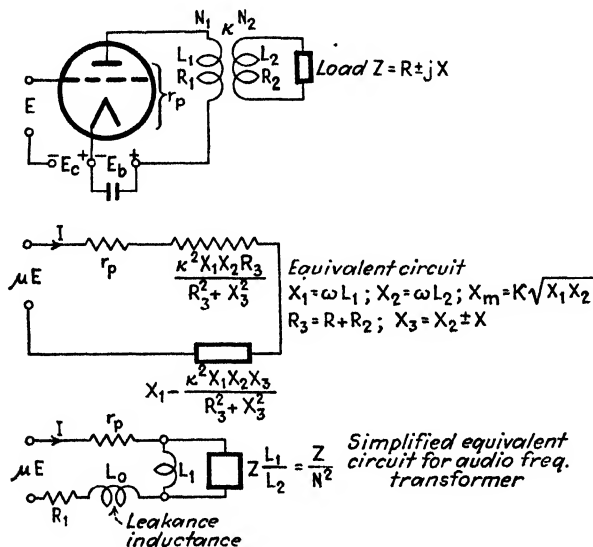


FIG. 148.-- Equivalent networks for high and audio frequencies.

100. Remarks on the Design of Transformer-coupled Amplifiers.—

Iron-core transformers are customary because for efficient voltage amplification over a wide frequency range practically only the audio-frequency range can be covered.

For interstage transformers, according to the previous section, the ratio of secondary to primary turns is given by

$$\frac{N_2}{N_1} = \sqrt{\frac{r_p'}{r_p}} \quad (73)$$

For $r_p = 10,000\Omega$ and an effective grid resistance $r_p' = 10^6$ ohms, this formula would lead to a tenfold transformation. But, according to Fig. 147, the primary reactance L_1 must be large compared with $r_p'(N_1/N_2)^2$ and a tenfold ratio would require that ωL_1 be large compared with $10,000\Omega$. Using $\omega/2\pi = 25$ cycles/sec, to calculate the lower limit would lead to a very high secondary inductance L_2 which, unless designed very elaborately, would include considerable self-capacitance and ohmic

resistance drop. For this reason, it is customary not to go much higher than $N_2/N_1 = 3$ to 4 for interstage transformers. Of course, L_1 can also be made large without too many turns by using a larger cross section of the core. The dynamic inductance L_1 can be computed, given the cross-sectional area A , the length l_i of the iron path, and the dynamic permeability μ' , from

$$L_1 = \frac{\mu' k A N_1^2}{l_i} \text{ henries} \quad (74)$$

where

$$k = \begin{cases} 0.4\pi \times 10^{-8} = 1.256 \times 10^{-8} & \text{(for the core dimensions in centi-} \\ & \text{meters)} \\ 3.2 \times 10^{-8} & \text{(for core dimensions in inches)} \end{cases} \quad (74a)$$

If an air gap of length l is used, the formula is

$$L_1 = \frac{k A N_1^2}{(l_i/\mu') + l} \quad (75)$$

The dynamic, that is, the incremental, permeability μ' is to be taken since the diagonal slope of the superimposed hysteresis loop must be considered and not the tangent to the static B - H curve at the operating point. The value of μ' changes with the location of the operating point for a given current in the winding, and the dynamic inductance L_1 may be much smaller when the steady plate current I_b through the primary of the transformer is present. Often L_1 can be increased by using an air gap. This is true only when both direct and alternating currents pass through L_1 . This can be understood when it is realized that, in order to force the flux across the air gap l and the iron path l_i , the ampere-turns required for each path are simply to be added along the direction of the H coordinate. Therefore the hysteresis loop is sheared over. A given steady plate current I_b will produce a smaller value of flux density B . It is possible that the operating point about which the small dynamic hysteresis loop is described may be moved from the almost saturated portion downward along the large static B - H curve to a point of more effective dynamic steepness. For a certain path l_i , a definite air gap l must exist for which μ' , that is, L_1 , becomes a maximum. In many cases it is sufficient to assume that, for 14- to 20-mil high-grade audio-transformer iron, μ' is about 500 when considerable plate current flows as in single-output tubes, while for push-pull transformers $\mu' = 1000$ to 1200. The reactance ωL_1 is made about double the value of r_p since actual tests show that not so much is gained (although theoretically desirable) by making this reactance much larger.

Hence when using a 201-A tube or its equivalent with $r_p = 10,000\Omega$ at 135 volts on the plate, we have $\omega L_1 = 20,000\Omega$ for the lowest frequency of interest, since r_g'/N^2 , which is in shunt with L_1 , is affected mostly by

the magnitude of ωL_1 at the lower end of the pass band. Choosing this frequency at 30 cycles/sec, we find $L_1 = 106$ henries which is quite a large value. If a shell-type transformer core with 14-mil laminations is assumed, with $A = 1$ sq in and $l_1 = 6$ in, according to (74) with the dimension constant $k = 3.2 \times 10^{-8}$, we find

$$N_1 = \sqrt{\frac{106 \times 6}{500 \times 3.2 \times 10^{-8}}} = 6300 \text{ turns}$$

and with a step-up ratio of 3 this would require $N_2 = 18,900$ secondary turns. When standard cores of fixed A and l_1 are available, it is convenient to use, as in ordinary transformer engineering, a specific number N_0 of turns which gives 1 henry inductance exactly under normal operating conditions. If f_i denotes the lower frequency of interest, we find from $2\pi f_i L_1 = 2\pi f_i (N_1/N_0)^2$ with a matching impedance equal to $2r_p$

$$N_1 = N_0 \sqrt{\frac{r_p}{\pi f_i}} \quad (76)$$

For the core in the foregoing example, N_0 is about 610 turns/henry. This is a comparatively small specific number of turns compared with the cores used in the earlier days of radio when very compact transformers had values of N_0 up to 3000 and more turns per henry. With step-up ratios not more than about 4 and properly designed windings on conservatively large cores, the resistance of the coils will be comparatively small and the self-capacitance such that the lowest natural frequency is much higher than in transformers of an earlier date. When C_0 denotes the self-capacitance of the secondary winding (with more turns), the resonance frequency can be computed from

$$f_0 = \frac{N_0}{6.28 N_2 \sqrt{C_0}} \quad (77)$$

For the design of the output transformer of any amplifier, it is also necessary to know the frequency characteristic of the load. Suppose we have the case of an old-time loud-speaker which, for instance, has $L = 0.25$ henry average inductance and $R = 1500\Omega$ average resistance. According to the simplified equivalent circuit (Fig. 148), R and L act as though R/N^2 and L/N^2 were connected in series across the no-load inductance L_1 of the transformer, if N is equal to the turn ratio N_2/N_1 . At first, neglecting the primary resistance R_1 and the leakage inductance L_0 , and assuming a frequency $\omega/2\pi$ high enough so that, because of the increased value of ωL_1 , most of the current passes through the parallel branch with L/N^2 and R/N^2 in series,

$$\frac{\omega L}{N^2} = r_p + \frac{R}{N^2}$$

the voltage μE will give such geometrical components across $(r_p + R/N^2)$ and L/N^2 , respectively, that their values are equal but smaller than $\mu E/2$ since a phase angle of 45 deg produces a power factor of 0.707. Hence, about 30 per cent of the voltage is lost. For a twofold matching, that is,

$$\frac{\omega L}{N^2} = 2 \left[r_p + \frac{R}{N^2} \right]$$

only about 10 per cent would be lost. In each case the ear would hardly notice the difference for compound output tones, since 30 per cent is about the upper limit permissible for mixed frequencies. If f_u is the upper frequency limit for which the voltage loss is 30 per cent, we find the turn ratio

$$\frac{N_2}{N_1} = \sqrt{\frac{6.28 f_u L}{r_p} - \frac{R}{N^2}} \quad (78)$$

if L is in henries, R and r_p in ohms, and f_u in cycles per second. If the upper frequency range only were concerned and if the upper limit of $f_u = 5000$ cycles/sec were satisfactory, the turn ratio, according to (78), becomes about $N = 1.6$ for an output tube whose plate resistance $r_p = 2500\Omega$. From Table VI it can be seen that, for the upper frequency range, $\omega L/N^2$ is almost equal to Z/N^2 while, for the medium- and lower

TABLE VI

f , cycles per second	$L = 1.57f$, ohms	Actual impedance load $Z = \sqrt{R^2 + \omega^2 L^2}$, ohms	ωL_1 , ohms for L_1		Equivalent load Z/N^2 , ohms for $N = 1.6$	Remarks
			5 hen-ries	10 hen-ries		
10	15.7	1500	314	628	585	$R = 1500\Omega$
20	31.4	1500	628	1,256	585	
40	62.8	1500	1,256	2,512	585	$L = 0.25$ henries
100	157	1510	3,140	6,280	590	
200	314	1532	6,280	12,560	597	$r_p = 2500\Omega$
500	785	1692	15,700	31,400	660	
1000	1570	2170	31,400	62,800	846	
2000	3140	3480	62,800	125,600	1360	
4000	6280	6450	125,600	251,200	2520	
5000	7850	8000	157,000	314,000	3130	

frequency range, the term R/N^2 determines more or less the reflected impedance Z/N^2 . Hence for the lower frequency range, R/N^2 and L_1 act practically in parallel. When f_1 denotes the lower limit of important

pass frequencies and with a 30 per cent voltage loss because of the presence of ωL_1 , we have

$$6.28f_i L_1 = \frac{R}{N^2}$$

and

$$L_1 = \frac{0.159R}{f_i N^2} \quad (79)$$

where all quantities are in practical units as in (78). If a 10 per cent loss (twofold matching), that is, $6.28f_i L_1 = 2R/N^2$ is used, the inductance must be twice as large as found from (79). If the lower cutoff frequency f_i is chosen as the value below which sound can no longer be perceived, a no-load primary inductance of about $L_1 = 5$ henries for 30 per cent

voltage loss and 10 henries for 10 per cent voltage loss at this frequency is obtained. The performance over the frequency range from 10 to 5000 cycles can be understood from Table VI.

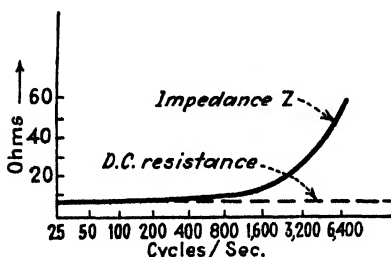


FIG. 149.—Frequency characteristic of a dynamic speaker.

In modern radio engineering the last tube usually works into dynamic speakers with a characteristic of about the shape indicated in Fig. 149. It is then customary to consider a speaker as an impedance Z equal to

either the direct-current resistance or the direct-current value increased by 10 per cent. Using this assumption, and calling the load resistance of a certain speaker $R = 6\Omega$, with a tube of about 2500Ω plate resistance, we can put the reflected speaker load R/N^2 equal to either r_p or $2r_p$. Taking the latter value, we have the formula for the turn ratio

$$\frac{N_1}{N_2} = \sqrt{\frac{2r_p}{R}} \quad (80)$$

which for the foregoing example requires about ninety-onfold step-down ratio. For a straight energy matching ($R/N^2 = r_p$) only a fourth of this value is needed. Since we deal here with step-down transformers fed by tubes of comparatively low plate resistance, the condition of a no-load transformer primary reactance ωL_1 that is large in comparison with the plate resistance r_p of the tube can be more readily fulfilled without too much increase in coil capacitance. Therefore it is customary to make

$$\omega L_1 = (6 \text{ to } 8)r_p \quad (81)$$

at the lowest frequency f_i to be passed. Matching against $6.28 r_p$ leads to the simple formula

$$L_1 = \frac{r_p}{f_l} \text{ henries} \quad (81a)$$

if r_p is in ohms and f_l in cycles per second. For $r_p = 2500\Omega$ and the audio-frequency band extending down to $f_l = 50$ cycles/sec, $L_1 = 50$ henries is needed. Again introducing, for a core of fixed dimensions and material, the number N_0 of primary turns per henry, we have

$$N_1 = N_0 \sqrt{L_1} = N_0 \sqrt{\frac{r_p}{f_l}} \quad (82)$$

When the core¹ with $l_c = 6$ in. and $A = 1$ sq in. and $\mu' = 50$ is used, we have the specific number $N_0 = 610$, and 4300 primary turns are needed. According to (80), in this particular case we need $4300/91 = 47$ secondary turns.

In all the cases brought out in these examples, care must be taken that the magnetic flux variation does not reach into the saturation region and in the foregoing example a suitable air gap [formula (75)] will avoid this. Also the leakage inductance L_0 (Fig. 150) must be a small percentage of the useful inductance L_1 . This is especially important for output transformers. If this inductance is too large, the frequency-transmission curve of the output tube will fall off at the higher frequency end of the pass band since ωL_0 will consume more voltage as f increases. If L_0 were only as much as 1 per cent of the useful inductance L_1 , its value for the foregoing example would be 0.5 henry and would lead to the reactance drop indicated in Table VII. Of course, this drop acts in quadrature with r_p and R/N^2 but its magnitude shows that the leakage inductance should be even smaller than one-tenth of 1 per cent if a good

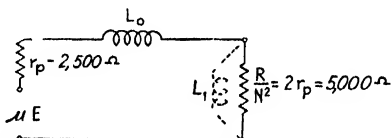


FIG. 150 Equivalent circuit for ωL_1 high compared with R/N^2

TABLE VII

f , cycles per second	Leakance reactance L_0 in Ω for	
	$L_0 = 0.01L_1$	$L_0 = 0.001L_1$
10	31.4	3.14
20	62.8	6.28
40	125.6	12.6
100	314	31.4
500	1,570	157
1000	3,140	314
2000	6,280	628
4000	12,560	1256
5000	15,700	1570

¹ See Fig. 192, p. 239, "High-frequency Measurements."

frequency characteristic is to exist in the upper audio-frequency band. The frequency characteristic can also be improved by connecting a suitable resistance load or other equalizing shunt across the speaker. For interstage transformers, the leakage inductance is determined by measuring the inductance of the secondary with the primary short-circuited and open. The value measured with short-circuited primary should always be smaller than $\frac{1}{20}$ of the value with the primary open.

For the design of the input transformer, the same procedure is followed.

When push-pull transformers are working properly, the direct-current magnetization of the core (even for the practical unbalance which always exists) can be considered to be only about 10 per cent of that due to the normal plate current. An air gap can then be dispensed with and a permeability value of about 1000 to 1200 assumed for high-grade transformer laminations (14- to 20-mil laminations work well). For ordinary single-tube output stages, the dynamic permeability μ' is about 500 and an air gap is required [formula (75)]. For input transformers and interstage transformers of ample dimensions, $\mu' = 1000$ to 1200 can be used since the steady magnetization is small.

101. Tuned Amplifier.—As brought out in the preceding section, ordinary transformer-coupled amplifiers are as a rule efficient only over a large frequency band when in the audio-frequency range.¹ High-voltage amplification is obtained when the external plate impedance is large compared with r_p . Therefore if a coil L , R in parallel with a condenser C forms the external plate load, a high external plate impedance

$$Z = \frac{L}{RC}$$

is obtained if the parallel branch is tuned to the frequency of the grid exciting voltage.² However, an amplifier of this type requires a coupling condenser or considerable negative grid bias in order to prevent grid currents due to the positive plate potential of the preceding tube. To avoid this, a resonance transformer with coupling inductance M is used. For the condition $\omega^2 M^2 = r_p R_2$ which gives maximum voltage output of a resonance transformer, we have the expression

$$A_{\max} = 0.5 \frac{\mu \omega L_2}{\sqrt{R_2 \cdot r_p}} \quad (83)$$

¹ LOWELL, P. D., *Bur. Standards, Sci. Paper* 449, describes special constructions of air- and iron-core transformers which also work in the higher frequency range. The air-core transformers, although working more efficiently, have only a small pass band, while open-cored iron transformers, although less efficient, can be made to work over a somewhat wider band.

² For details, see "High-frequency Measurements," McGraw-Hill Book Company, Inc., New York, 1933, pp. 58-61.

for maximum voltage amplification. Hence for a given tube (r_p and μ fixed), the optimum voltage amplification is proportional to the reactance of the secondary coil L_2 and inversely proportional to the square root of its resistance R_2 . The tube chosen should have a large ratio $\mu/\sqrt{r_p}$. Only the mutual inductance M is important in this case, and the ratio of secondary to primary turns does not matter. Where only a few primary turns are used, the coupling must be made closer in order to make M the same value as for more primary turns and a looser coupling. If the mutual inductance M is smaller than for optimum amplification

$$M_{\text{opt}} = \frac{\sqrt{R_2 \cdot r_p}}{\omega},$$

both R_2 and r_p play a greater part in the voltage amplification and their effect lies somewhere between the square-root value and the first power of the resistance. From these results, it can be seen that the ratio $\mu/\sqrt{r_p}$ for tuned radio-frequency amplifiers plays the same part as the mutual conductance in resistance-coupled amplifiers, while the ratio $\omega L_2/\sqrt{R_2}$, which refers only to the secondary coil, characterizes the usefulness of this coil.

The foregoing formulas do not take into account the capacity coupling between the primary and secondary coil of the resonance transformer.

The presence of such capacitive coupling changes the amount of mutual inductance¹ necessary to obtain optimum amplification at a given frequency; that is, it reduces the optimum voltage gain. The equivalent circuit is as in Fig. 151, where C_m denotes the equivalent lumped capac-

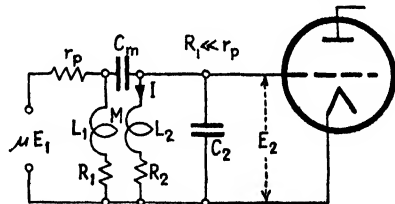


FIG. 151.—Equivalent-variable current network with capacitance effects between primary and secondary transformer windings.

ity coupling between the primary and secondary coil of the resonance transformer. The amplified voltage E_2 passed on to the next stage is then at a maximum when the resonance current I reaches an optimum value. This happens for

$$I_{\text{opt}} = \frac{j\mu E_1 [MC_2 - (L_1 - M)C_m]}{(L_1/\omega) - \omega R_2 r_p L_1 C_2 C_m - [\omega(L_1 L_2 - M^2) - (R_2 r_p/\omega)][C_2 + C_m]} \quad (84)$$

Now since $E_2 \cong \omega L_2 I$, the voltage amplification becomes

$$A_v = \frac{E_2}{E_1} = \frac{\omega L_2 I}{E_1} \quad (85)$$

¹ DIAMOND, H., and E. Z. STOWELL, *Proc. I.R.E.*, **16**, 1194, 1928.

Therefore the optimum amplification is obtained by inserting the value of I_{opt} in (85) and occurs at resonance, obtained by making the capacity

$$C_2 = \frac{(1/\omega^2) - C_m[L_1 + L_2 - 2M]}{L_2 - \omega^2 C_m[L_1 L_2 - M^2]} \quad (86)$$

If the coupling capacitance were neglected ($C_m = 0$), this setting would satisfy the ordinary resonance law

$$C_2 = \frac{1}{\omega^2 L_2}$$

and the optimum current would become $j\omega\mu M E_1/(\omega^2 M^2 + R_2 r_p)$.

When a tuned circuit with an anode tap is under consideration, the equivalent circuit is as shown in Fig. 152. The impedance of the external

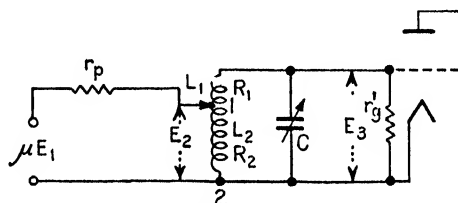


FIG. 152.—Tuned circuit with anode tap.

plate circuit acting between points 1 and 2 for the resonance frequency $\omega/(2\pi)$ and $m = M + L_2$ is

$$Z = \frac{m^2 \omega^2}{R_e}$$

for

$$R_e = R_1 + R_2 + \frac{\omega^2 L^2}{r_g}; \quad L = L_1 + L_2 + 2M$$

The dynamic grid capacitance may be thought of as a part of C . We then have

$$\frac{E_2}{E_1} = \frac{\mu E_1 Z}{Z + r_p}$$

and

$$\frac{E_3}{E_2} \cong \frac{L}{m}$$

since $r_p \gg m\omega$. The total voltage gain at the grid of the next tube is

$$\frac{E_3}{E_1} = \frac{\mu \omega^2 m L}{m^2 \omega^2 + r_p R_e}$$

The anode tap determines the coupling and with it the step-up ratio of the tuned autotransformer. The maximum value of the over-all ampli-

fication is obtained by means of $\frac{d[E_3/E_1]}{dm} = 0$, which leads to the simple result that the plate resistance r_p and the external plate impedance Z must be equal. Hence maximum voltage amplification gives the value

$$A_{\max} = 0.5 \frac{\mu \omega L}{\sqrt{r_p \cdot R_s}} \quad (87)$$

an expression resembling formula (83) which holds for the tuned resonance transformer used as coupling between tubes. Also in this case we can split up the result of (87) into two factors. The factor $\mu/\sqrt{r_p}$ determines the quality of the tube for this kind of coupling and should be as large as possible, and the factor $\omega L/\sqrt{R_s} \cong \omega L/\sqrt{R_1 + R_2}$ determines the quality of the entire winding of the autotransformer and indicates that maximum amplification is directly proportional to the reactance of the entire winding and inversely proportional to the square root of the entire resistance.

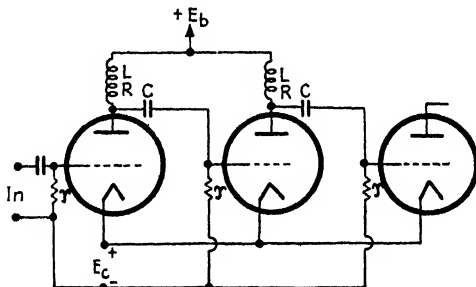


FIG. 153.—Choke-condenser coupling.

102. The Amplifier with Choke-capacitance Coupling.—The amplifier shown in Fig. 153 has an advantage over the resistance-capacitance-coupled amplifier because a choke coil L is used in place of a resistance for the external plate load. Practically the full voltage of the B battery is effective on the plate if the resistance R of the plate choke is made low. When the amplifier is to cover quite a frequency range in the lower high-frequency band, it is customary to wind the choke coil of resistance wire so that its lowest natural frequency is about 100 kc/sec. In the range of lower frequencies the resistance R is mostly responsible for the amplification, while in the upper range of the pass band the reactance ωL determines the output voltage mostly. An amplifier of this type will cover a range between 15 and about 150 kc/sec. Maximum amplification in this particular case will take place at 100 kc/sec and for frequencies higher than 100 kc, that is, above the natural frequency of the external plate load, the amplification rapidly decreases. Open-core laminated-

iron chokes are also used to obtain a more even frequency characteristic in the pass region. Iron-core chokes when properly designed can be used up to about 1000 kc/sec. When air-core chokes are used, single-layer coils of fine resistance wire are used for pass bands above 200 kc/sec, and a value of several millihenries is chosen for L . The core then consists conveniently of bakelite tubing of about $\frac{1}{2}$ in. diameter and about 4 in. in length. If fine resistance wire is used, the resistance of the choke may be

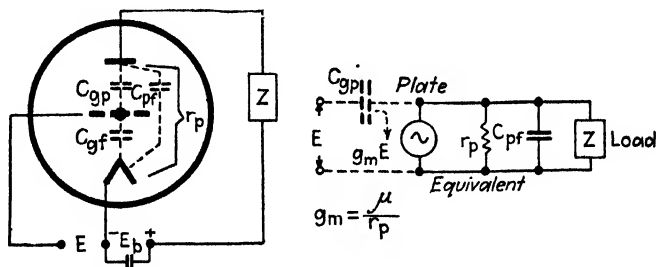


FIG. 154.—Equivalent circuit with constant-current output $g_m E$.

made a few thousand ohms and the self-capacitance kept about of the order of the plate-filament interelectrode capacitance. The choke-coil amplifier can be used up to very high frequencies (up to 6000 kc/sec) when current resonance is provided. The value of L is then small and ordinary copper wire is used. The magnitude of L is chosen such that,

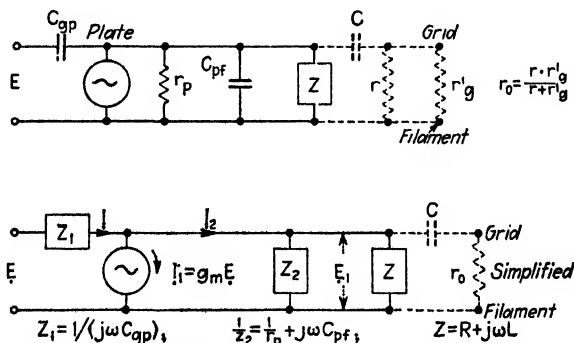


FIG. 155.—Equivalent and simplified equivalent circuit.

for multistage amplifiers, resonance occurs by means of the effective interelectrode capacitance $C_1 = C_p' + C_{pf}$ and the self-capacitance C_2 of the choke. The choke coil acts like a resistance $L/[(C_1 + C_2)R]$. If the amplifier is to work over a band of frequencies, the value of L is chosen different for each stage and such that the resonance frequencies of the successive chokes are evenly distributed over the band. The coupling condenser C and the grid leak r are chosen as in resistance-

capacitance-coupled amplifiers so that $1/(\omega C)$ for the lowest pass frequency is small compared with the effective grid resistance $r_g' \cdot r/(r_g' + r)$. Not much is gained by making r too high, especially in the higher frequency range. For the range from 10 to about 200 kc, values from 3 to 0.5 megohms are satisfactory. Moreover, since the equivalent tube circuit can also be treated as a constant-current generator of current $\mu E/r_p = g_m E$ with the dynamic plate resistance r_p in parallel¹ (Fig. 154), we find, for one stage of the amplifier shown in Fig. 153, the equivalent network indicated in Fig. 155. If all the voltages and currents indicated are vector values, according to Kirchhoff's law, we have

$$E = Z_1 I + \frac{Z Z_2}{Z + Z_2} I_2 \quad \text{and} \quad I = g_m E + I_2$$

The added input impedance becomes

$$\frac{E}{I} = \frac{Z[Z_1 + Z_2] + Z_1 Z_2}{Z[1 + g_m Z_2] + Z_2} \quad (88)$$

For the equivalent constant-current generator, the effective plate load is equal to

$$Z_3 = \frac{Z Z_2}{Z + Z_2} \quad (89)$$

to which parallel combination the current

$$I_2 = \frac{[1 - g_m Z_1][Z + Z_2]}{Z[Z_1 + Z_2] + Z_1 Z_2} E$$

flows. Hence the output voltage

$$E_1 = I_2 Z_3$$

and the voltage amplification

$$\frac{E_1}{E} = \frac{[1 - g_m Z_1] Z Z_2}{Z[Z_1 + Z_2] + Z_1 Z_2} \quad (90)$$

Since, for the pass band of a properly designed amplifier, the voltage drop across the coupling condenser C is small compared with that applied to grid and filament of the succeeding tube, the resultant grid resistance r_0 (including the grid leak r and apparent grid resistance r_g') is also in multiple with Z_2 and Z , and I_2 flows into the load Z_4 determined by

$$\frac{1}{Z_4} = \frac{1}{Z_2} + \frac{1}{Z} + \frac{1}{r_0} = \frac{1}{r_p} + j\omega C_{pf} + \frac{1}{R + j\omega L} + \frac{1}{r_0}$$

¹ MAYER, H. F., *Telegr. Fernsprech. Tech.*, November, 1926; N. R. BLIGH, *Exptl. Wireless*, 7, 480, 1930 (also editor's reference in this paper to a manuscript of W. S. Percival).

The output voltage is then

$$E_1' = I_2 Z_4 \quad (91)$$

and E_1'/E gives the entire amplification per stage from which the frequency characteristic for negligible $1/(\omega C)$ drop can be computed. For the higher frequency range, the effective grid capacitance C_g' must also be taken into consideration since it is practically in multiple with C_{pf} of the preceding tube and can be added to this capacitance. The value of C_g' can be computed from the reactive term of (88). For a more accurate analysis, the method in Sec. 98 for the resistance-capacitance amplifier can be used.

When the tuning capacitance $C_1 = C_g' + C_{pf}$ plus the self-capacitance C_2 of L is set for current resonance, the effect of the choke load acts, as brought out above, like a resistance $L/[(C_1 + C_2)R]$ and the shunt resistance r_p should be large in order to give a sharp resonance setting. The equivalent circuit of Fig. 155 also confirms Eq. (56). This equation holds approximately for the resistance-coupled amplifier for which, in the pass region, the tube resistance r_p , load resistance R , and the total input resistance $r_0 = r_g'r/(r_g' + r)$

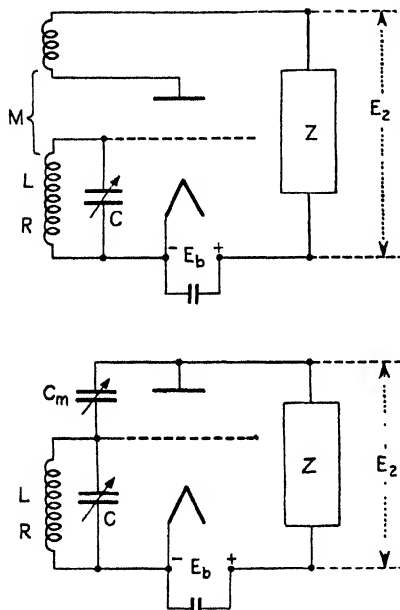


FIG. 156.—Regenerative amplifiers.

may be considered to be in multiple. Hence r_p as well as g_m should be large; that is, high- μ tubes are better.

103. Regenerative Amplifiers.—Regeneration in tubes can cause increased amplitude without any appreciable effect on the frequency. It can also give rise to an increase in frequency¹ when working in the ultrahigh-frequency band. Figure 156 indicates two tube circuits where the amplified voltage E_2 across the load Z is again fed back to the input side by a mutual inductance M or by a capacitance C_m or by both. When the voltage fed back into the grid has a component in phase with the original grid voltage, the ultimate resulting grid voltage will be greater and the ratio of final output voltage to original grid voltage can be considerably higher than without regeneration. When the feedback

¹ With respect to frequency regeneration, see pp. 18 and 136. It can also give rise to the generation of new electrons and ions (see p. 272).

voltage is in antiphase, the resultant amplification will be less. The amplification usually takes place for a case in which the back-feed voltage is more or less out of phase but is such that regeneration, that is, increased voltage gain results. As brought out in the consideration of tube generators, the back-feed voltage affects the *CLR* branch connected across the input by either increasing or decreasing its effective resistance. When the negative resistance action due to a regenerative back feed just neutralizes the value of R , the amplifier becomes a generator. This condition sets the upper limit for normal regeneration. A more effective back feed without self-oscillation may be secured by the use of super-regeneration, in which the grid and plate are made alternately positive and negative (by means of an auxiliary source).

For no back feed, the voltage amplification is

$$A_e = \frac{E_2}{E_1} = \frac{\mu Z}{r_p + \bar{Z}} \quad (92)$$

if for simplicity's sake E_1 and E_2 denote the maximum values of the alternating input voltage across the grid and filament and the output voltage across the external plate load Z , respectively. If E denotes the resultant output voltage, amplification with back feed is defined as

$$A_r = \frac{E}{E_1} \quad (93)$$

Hence, when $A_r > A_e$, regeneration takes place, and

$$\rho = \frac{A_r}{A_e} = \frac{EE_1}{E_1E_2} \quad (94)$$

is the resultant back-feed factor which must be larger than unity for regeneration.

The derivation for the ultimate grid voltage, which exists after a series of back reflections, is as follows: The original grid voltage E_1 (which would exist without back feed) is amplified into the plate circuit and a certain portion of it acts backward, adding to the original voltage E_1 , the portion $pE_1\epsilon^{j\varphi}$. After amplification of this portion, the voltage $E_1(p\epsilon^{j\varphi})^2$ must be added at the input side, etc. The final input voltage is

$$\begin{aligned} E' &= E_1[1 + p\epsilon^{j\varphi} + (p\epsilon^{j\varphi})^2 + (p\epsilon^{j\varphi})^3 + \cdots] \\ &= E_1 \frac{1 - [p\epsilon^{j\varphi}]^m}{1 - p\epsilon^{j\varphi}} \bigg|_{m=1}^{m=\infty} \end{aligned} \quad (95)$$

The result shows that, for back feeds for which $p > 1$, the resultant voltage E' grows to an unlimited high value which is, of course, limited by the saturation condition and energy balance of the tube. The

amplifier turns into an oscillator and any impressed signals will beat with the self-oscillations. The result produces the well-known whistling and howls. If, however, $p < 1$, the series in Eq. (95) reduces to

$$E'' = \frac{E_1}{1 - p\epsilon^{j\varphi}} \quad (96)$$

and the resultant input voltage E'' is larger than the original voltage E_1 when the denominator $(1 - p\epsilon^{j\varphi})$ is smaller than unity. Figure 157 indicates this case where for the sake of simplicity only a few terms are used instead of the entire series.

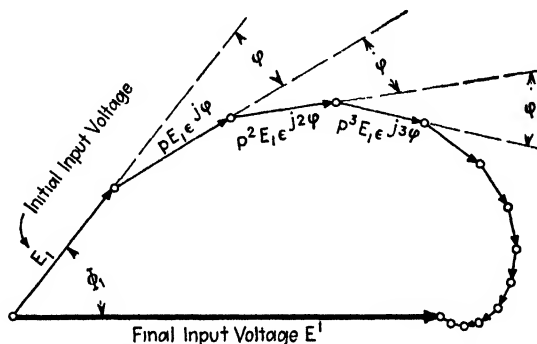


FIG. 157.—Building-up of the final input voltage E' due to regeneration.

The same process of derivation can be used for the resultant final output voltage. If $e_o = E_1\epsilon^{j\omega t}$ is the original input voltage which would be maintained for no back feed, the output voltage across any load impedance Z in the external plate circuit is

$$e_p = A_e E_1 \epsilon^{j(\omega t - \varphi_1)} \quad (97)$$

if φ_1 denotes the difference in phase produced by the amplifier and A_e again denotes the normal voltage amplification without back feed. If, as above, p stands for the back-feed factor, we obtain the additional grid voltage

$$e_1 = p e_p \epsilon^{-j\varphi_1} \quad (98)$$

since the portion of the reflected original plate voltage e_p is generally out of phase by an angle φ_2 . The new input voltage is $e_o + e_1$ and the new output voltage becomes

$$e_1 = A_e [e_o + e_1] \epsilon^{-j\varphi_1} \quad (99)$$

This feeds back the next additional grid voltage

$$e_2 = p [A_e e_1 \epsilon^{-j\varphi_1}] \epsilon^{-j\varphi_1} \quad (100)$$

since only the portion p of $A_e e_1 \epsilon^{-j\varphi_1}$ is reflected back with a phase angle φ_2 with respect to the original grid voltage e_g . The additional component amplified into the plate load is then $A_e e_2 \epsilon^{-j\varphi_1}$ and the new output voltage becomes

$$e_{II} = A_e [e_g + e_1 + e_2] \epsilon^{-j\varphi_1} \quad (101)$$

leading for the final output voltage to the series

$$E''' = A_e [e_g + e_1 + e_2 + e_3 + e_4 + \dots] \epsilon^{-j\varphi_1} \quad (102)$$

where

$$\frac{e_m}{e_{m-1}} = \frac{e_4}{e_3} = \frac{e_3}{e_2} = \frac{e_2}{e_1} = \frac{e_1}{e_g} = p A_e \epsilon^{-j\beta}$$

for $\beta = \varphi_1 + \varphi_2$. The graphical vector solution for the final output

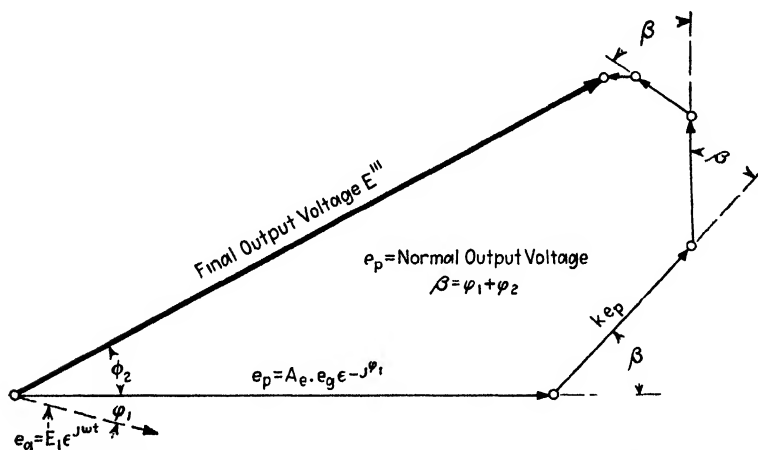


FIG 158.—Graphical construction of the final output voltage E''' in a regenerative receiver

voltage E''' is as indicated in Fig. 158 since, for $k = p A_e \epsilon^{-j\beta}$, the geometrical series

$$\begin{aligned} E''' &= A_e \epsilon^{-j\varphi_1} [1 + k + k^2 + k^3 + k^4 + \dots] e_g \\ &= [1 + \underbrace{k + k^2 + k^3 + k^4 + \dots}_{\text{due to regeneration}}] e_p \\ &= e_p \frac{1 - k^m}{1 - k} \quad \text{or} \quad = e_p \frac{k^m - 1}{k - 1} \bigg|_{m=1}^{m=\infty} \end{aligned} \quad (102a)$$

is obtained.

For the analytical evaluation, Eq. (102a) can be used or Eq. (102) by means of $e_g = E_1 \epsilon^{j\omega t}$ written in the form

$$E''' = \underbrace{A_e E_1 \epsilon^{j(\omega t - \varphi_1)}}_{\text{normal output voltage}} + \underbrace{p A_e^2 E_1 \epsilon^{j(\omega t - 2\varphi_1 - \varphi_2)} + p^2 A_e^3 E_1 \epsilon^{j(\omega t - 3\varphi_1 - 2\varphi_2)} + \dots + p^n A_e^{n+1} \epsilon^{j(\omega t - n\beta - \varphi_1)}}_{\text{due to back feed}} + \dots \quad (102b)$$

if the significant general terms hold from $n = 0$ to $n = \infty$ since, for $n = 0$, the normal voltage output is obtained. From (102a), we obtain, for an infinite number of terms and k smaller than unity, the final output voltage

$$E''' = \frac{e_p}{1 - k} = \frac{A_e E_1 \epsilon^{j\alpha}}{1 - p A_e \epsilon^{-j\beta}} \quad (103)$$

if $\alpha = \omega t - \varphi_1$ and $\beta = \varphi_1 + \varphi_2$. Maximum output voltage in a regenerative amplifier is obtained when $\beta = \varphi_1 + \varphi_2 = 0$, since the phase angle φ_1 produced by the external and internal plate impedance must be equal and opposite to that due to the phase angle φ_1 of the back feed. We then have

$$E'''_{\max} = \frac{A_e E_1 \epsilon^{j\alpha}}{1 - p A_e} \quad (104)$$

For regenerative and maximum regenerative voltage amplification, we find according to (93), (103), and (104) that

$$\left. \begin{aligned} A_r &= \frac{e_p}{[1 - k]e_o} = \frac{A_e}{1 - k} = \frac{A_e}{1 - p A_e \epsilon^{-j\beta}} \\ A_{\max} &= \frac{A_e}{1 - p A_e} \end{aligned} \right\} \quad (105)$$

From these formulas it can be seen that the maximum amplification can be increased to an optimum value by properly choosing the back-feed factor p with respect to the normal voltage amplification A_e . The more the product $p A_e$ approaches unity, the larger the maximum amplification, and for $p = 1/A_e$ the amplification would become infinite and would set up its own oscillations.

In order to express (105) in absolute values, we put

$$\begin{aligned} A_r &= \frac{A_e}{1 - p A_e \epsilon^{-j\beta}} = \frac{A_e}{1 - p A_e [\cos \beta - j \sin \beta]} = \frac{A_e}{[1 - p A_e \cos \beta] + j p A_e \sin \beta} \\ &= \frac{A_e [1 - p A_e \cos \beta]}{1 - 2p A_e \cos \beta + p^2 A_e^2} - j \frac{p A_e^2 \sin \beta}{1 - 2p A_e \cos \beta + p^2 A_e^2} \\ &= \frac{a}{-jb} \end{aligned} \quad (105a)$$

The absolute value of A_r is then

$$|A_r| = \sqrt{a^2 + b^2} = \frac{A_e}{\sqrt{1 - 2p A_e \cos \beta + p^2 A_e^2}} \quad (105b)$$

which for $\beta = 0$ confirms the value $A_e/(1 - pA_e)$ already found in (105) and holds for maximum regenerative amplification when phase compensation is provided. Since self-oscillations just begin for $pA_e = 1$, according to (105b), the upper limit of amplification without whistles must always be smaller than

$$\frac{A_e}{\sqrt{1 - 2 \cos \beta + 1}} = \frac{A_e}{2 \sin \beta/2} \quad (106)$$

The phase angle Φ_2 (Fig. 158) between the final and the normal output voltage is

$$\Phi_2 = \sin^{-1} \frac{b}{\sqrt{a^2 + b^2}} = |A_r| \cdot p \sin \beta \quad (107)$$

The angle φ_1 (Fig. 157) can be found by the same procedure. In the total phase shift $\beta = \varphi_1 + \varphi_2$, for any external plate impedance

$$Z = R \pm jX$$

and internal plate resistance r_p , the angle φ_1 is

$$\varphi_1 = \tan^{-1} \frac{\pm X}{R + r_p}$$

The angle φ_2 is likewise determined by the reactive and resistance components of the input side. Hence, when, for instance, the variable plate current is fed back to the grid coil by coupling output and input coils to one another, for a constant frequency the angle φ_2 can be assumed constant even though the amplification is varied by means of the degree of back coupling. The degree of coupling affects the back-feed factor p only and the optimum value of p is obtained from

$$\left. \frac{d|A_r|}{dp} \right|_0 = A_e \frac{d[1 - 2pA_e \cos \beta + p^2A_e^2]^{-1/2}}{dp} = 0$$

giving the optimum back-feed factor

$$p_{\text{opt}} = \frac{\cos \beta}{A_e} \quad (108)$$

Inserting this value in (105b) leads to the optimum amplification

$$A_{\text{opt}} = \frac{A_e}{\sin \beta} \quad (109)$$

104. Notes on Practical Regenerative Amplifiers.—Any one of the tube generators with insufficient back coupling to the input side to produce oscillations acts as a regenerative amplifier. Unless a resistance-capacitance-coupled amplifier with a resistance back feed is employed,

regenerative amplifiers do not give a good frequency characteristic over a wide frequency band. If a variable voltage is impressed on the grid coil LR of the tuned-grid circuit shown in Fig. 24, the arrangement may act as a regenerative amplifier. In that case, the back coupling M is connected with the other circuit constants as in

$$R + \frac{g_m M}{C} > 0 \quad (110)$$

where $g_m = \mu/r_p$. The regenerative amplifier begins to set up self-oscillations when the expression of (110) vanishes. This condition fixes the possible upper limit of maximum regeneration, unless superregeneration is employed. The correctness of (110) can be readily understood by a closer inspection of Eq. (13) on page 71 where, in the expression for $n = \alpha \pm j\omega$, the effective damping factor of the input resonator

$$\alpha = \underbrace{\frac{R}{2L}}_{\text{true damping factor of } CL \text{ circuit}} + \underbrace{\frac{g_m M}{2CL}}_{\text{increase or decrease due to back feed } M} = \frac{1}{2L} \overbrace{\left[\underbrace{R}_{\text{true resistance of } CL \text{ circuit}} + \underbrace{\frac{g_m M}{C}}_{\text{increase or decrease due to back feed}} \right]}^{\text{effective resonator resistance}}$$

This relation shows that the back feed for regenerative output must be such that M is negative in order to reduce the effective resistance R of the grid coil L and increase, as a consequence of the greater selectivity, the resultant grid voltage. Therefore plate and grid coils must be wound in opposition (as in tube generators) unless a small back-feed coil (tickler) wound in the proper direction causes a negative value of mutual inductance. Taking the proper direction of the back-feed coil, we must choose M such that it is never larger than RC/g_m . Otherwise the effective resonator resistance is either zero or negative and the amplifier produces self-oscillations. For the tuned-plate circuit shown in Fig. 37 (not so important for amplifier work), effective regenerative amplification occurs when the magnetic back feed is chosen such that

$$M < \frac{CRr_p + L}{\mu} \quad (111)$$

and close to $(CRr_p + L)/\mu$.

Figure 46 illustrates a case in which regeneration takes place by means of the back-feed condenser C_3 when

$$C_3 > \frac{L_2[\mu L_1 - L_2]}{[L_1 + L_2][R_1 + R_2]r_p} \quad (112)$$

Regeneration becomes more effective the closer C_3 is to the expression on the right side. Equation (112) is the outcome of Eq. (85) on page 91 when applied to the case of no oscillations.

For the three-tube resistance-coupled and resistance-capacitance-coupled amplifier shown in Figs. 138 and 139, any change δI_3 in the plate current of the third tube will, for a common plate-battery supply of internal resistance r_B , produce a potential drop $r_B \cdot \delta I_3$ at the plate of the first tube. A potential drop is also produced at the grid of the second tube which finally increases the original change δI_3 in I_3 . Therefore regeneration takes place and in some cases is responsible for self-oscillations in resistance-coupled amplifiers. In such cases, the oscillations can be suppressed by biasing the B-battery supply with a large condenser (about $2 \mu\text{f}$). Figure 159 shows a circuit in which this method of feedback is utilized. Since the back feed for a proper resistance r_b is

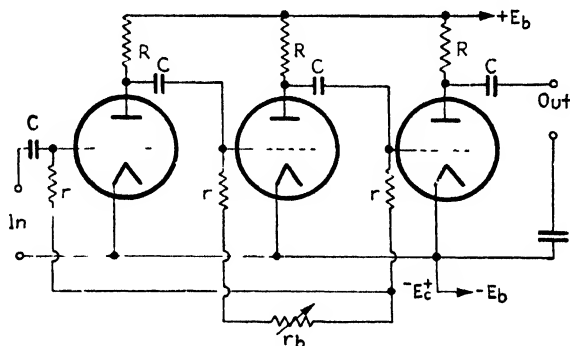


FIG. 159.—Resistance-capacitance-coupled amplifier with resistance (r_b) back feed.

independent of the frequency, this regenerative amplifier works faithfully over a wide band of frequency and with an amplification which is several times the value of the normal amplification (without regeneration). The back-feed resistance r_b is usually in the neighborhood of a few thousand ohms and should be made adjustable in order to control the degree of amplification. If A_n again denotes the normal amplification and A_r the effective amplification when regeneration is present, we have

$$A_r = \frac{A_n}{\sqrt{1 - \frac{r_b}{r_0 + r_0} A_n^2}} \quad (113)$$

where r_0 denotes the effective grid resistance $r_0' \cdot r / (r_0' + r)$ which, for the lower frequency range, is about equal to the grid-leak resistance r . According to Eq. (56), the normal amplification A_n for the pass band can be computed from

$$A_n = \frac{g_m}{(1/R) + (1/r_p) + (1/r_0)}$$

It should be noted that, because grid and plate potentials of the same tube are in antiphase, the back feed must bridge over an even number of tubes.

104a. Superregenerative Circuits.—As indicated in Sec. 103, maximum regeneration occurs near the point where self-oscillations set in. In dealing with the tuned-grid amplifier (which is the most important), the input circuit becomes very selective for optimum regeneration and a modulated voltage wave may be distorted by amplifying the side bands much less than the portions near the carrier.

To increase the regeneration either the "superregenerative" circuit of E. H. Armstrong¹ or the Flewelling circuit may be used. In the latter system, rhythmic grid charges are provided in order to suppress transient

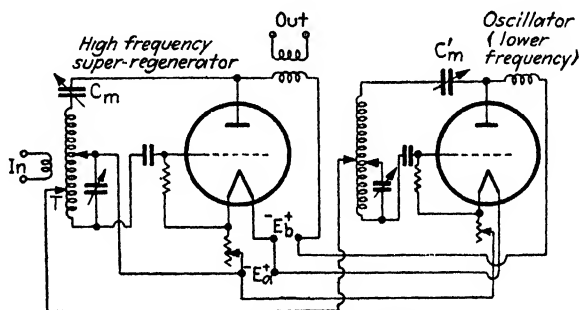


FIG. 160.—Superregenerator.

self-oscillations of the amplifier. In the Armstrong circuits, oscillations are interrupted for certain intervals by changing the effective resistance of the grid circuit or the plate circuit abruptly. In both schemes, increased regeneration is possible since during certain times the amplifier input has a negative resistance (is superregenerative). Figure 160 shows such a superregenerative amplifier in which the left tube acts as an amplifier and the back feed is obtained by means of $C_m = 0.0003\mu\text{f}$. The resistance of the grid circuit is varied by means of oscillations of much lower frequency produced by the tube circuit to the right. In this particular case, the lower frequency oscillation affects the grid circuit although it could be made to affect the plate circuit. By means of C_m , the regenerative back feed of the amplifier circuit is increased just until self-oscillations set in. The back feed C_m' of the oscillator, as well as the tap T coupling the oscillations into the amplifier circuit, is varied until the whistling just disappears and a very pronounced regenerative amplification sets in. When the circuit is used for amplification in the broadcast band, the frequency of the oscillator to the right is about 30 to 50 kc/sec. This system has never gained much prominence in broadcast

¹ *Proc. I.R.E.*, 10, 244, 1922; see also *Electronics*, p. 42, February, 1934.

receivers since the critical adjustment and the "spilling over" of the amplifier make it useful only in the hands of a skillful operator. But for the amplification of very high frequencies, the superregenerative amplifier works in a rather stable manner and shows much promise. Figure 161 shows a superregenerator with a single tube which acts simultaneously as a radio-frequency superregenerative amplifier and as a low-frequency oscillator. L_2C_2 has a natural frequency of about 20 kc/sec. By means of the feedback M , an oscillation of this low frequency is maintained.

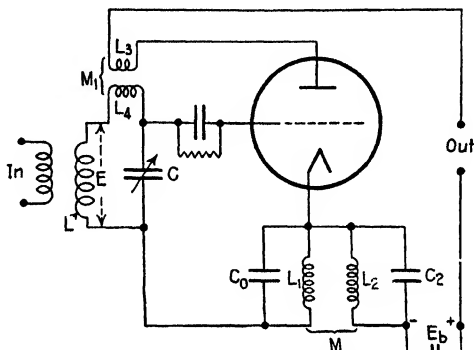


FIG. 161.—Single tube superregenerator.

The grid coil L_1 of the low-frequency generator circuit is shunted by a high-frequency by-pass condenser C_0 of about $0.002\mu\text{f}$. The auxiliary voltage of the lower frequency in this circuit is in series with the voltage of the B battery and impressed on the plate. This again affects the effective resistance of the circuit LL_4C and a tight back coupling M_1 between the amplifier coils L_3 and L_4 is thus made possible. When a voltage variation E of the same frequency as that given by

$$[2\pi\sqrt{C(L + L_4)}]^{-1}$$

acts in the grid circuit, a number of cycles can occur before the low-frequency cycle of the local oscillations is completed. The circuit acts so that no free oscillations are generated when no impulse is impressed on the grid circuit. But, when E acts, free oscillations of 20 kc/sec exist and the corresponding current in the input branch of the tube attains an amplitude which is proportional to that of the value of E at the instant the free oscillation begins to build up. Therefore the rectified plate current consists of a series of 20-kc impacts, the envelope of which is the greatly amplified modulation of the incoming voltage E .

The Flewelling circuit shown in Fig. 162 acts so that the variable plate current makes the grid more negative and the tube can produce oscillations only during certain intervals. In order to accomplish this,

plate and grid circuits must be interlinked in addition to the back coupling L_b, L . For this reason, the upper end of the back-feed coil L_b is connected directly to the grid branch (connected a, b) but a $0.00025\text{-}\mu\text{f}$ condenser is interposed in order to separate the direct connection from the hot cathode. The variable current i , which is a component of the

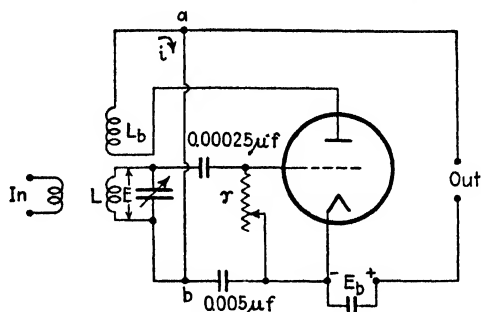


FIG. 162.—Flewelling circuit.

plate current, will then flow through the $0.005\text{-}\mu\text{f}$ condenser; and when a high enough grid leak r (from 3 to 6 megohms) is employed, self-oscillations occur only intermittently.

105. Self-oscillations in Cascade Amplifiers and Their Prevention.—The general network of a cascade amplifier is as shown in the lower repre-

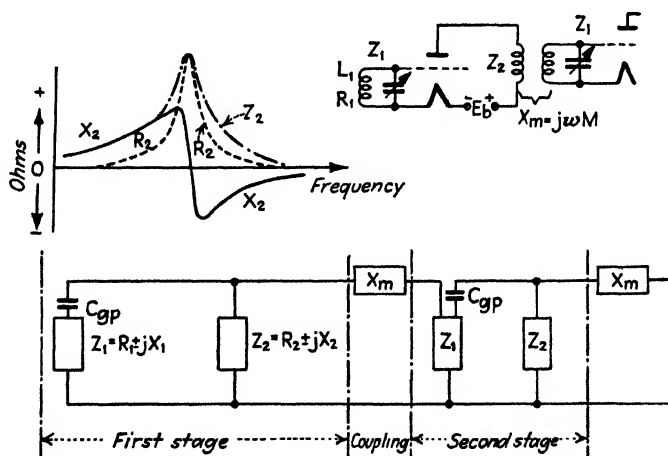


FIG. 163.—General network of cascade amplifier.

sensation of Fig. 163. The external input impedance across the grid and filament is $Z_1 = R_1 \pm jX_1$ and the load impedance in the external plate branch is $Z_2 = R_2 \pm jX_2$. The coupling between two successive stages is X_m and may be a coupling condenser, as in resistance-capacitance-coupled and choke-coupled amplifiers, or a mutual inductance as for a

tuned-grid amplifier as shown above. The grid-plate interelectrode capacitance C_{gp} forms a path for the alternating current so that an energy exchange is possible from grid to plate as well as from the plate to grid branch. It is the latter which, for certain conditions, gives rise to undesirable self-oscillations in amplifiers. This subject has been described in detail in Sec. 34 and it was shown that the input impedance of a tube depends upon the plate load even though a proper grid bias is provided. The reaction of the plate load is such that the grid gap acts in effect as an impedance

$$Z_g = r_g - jX_g \quad (114)$$

When the plate load is a pure resistance ($Z_2 = R_2$), as in resistance-coupled amplifiers, the effective grid-gap impedance is

$$Z_g = r_g + \frac{1}{\omega C_g} \quad (115)$$

that is, it acts as an ohmic resistance r_g in series with a capacitance $C_g = C_I + C_{II}$. The first part $C_I = C_{gf} + C_{gp}$ is the true or geometrical grid capacitance, while $C_{II} = \mu R_2 C_{gp} / (R_2 + r_p)$ denotes an apparent increase. For an inductive reactance load ($Z_2 = \omega L_2$), we have

$$Z_g = -\mu \frac{L_2 C_{gp}}{C_I^2} + \frac{1}{\omega C_I} = -r_g - jX_I \quad (116)$$

showing that a negative resistance r_g is reflected into the input gap as well as a negative reactance. Unless the coil resistance R_2 is large, r_g will always be negative and Z_g , together with the input impedance Z_I , may cause a resultant zero or even negative resistance and produce self-oscillations. For a capacitive load $Z_2 = 1/(j\omega C_2)$, the resistance component r_g of Z_g is always positive. For the tuned-grid amplifier shown in the upper diagram, all three cases may occur and experience shows that negative-resistance action takes place with tuned-grid amplifiers employing several stages unless special precautions are provided. A very effective means for avoiding self-oscillations would be to choose R_1 of L_1 high or work with reduced filament current or low plate voltages. But all of these expedients result in rather low-efficiency amplifiers. When Z_1 and Z_2 are both inductances L_1 and L_2 , respectively, of resistance R_1 and R_2 , the grid-plate capacitance C_{gp} will give rise to self-oscillation whose frequency is determined by the oscillation constant $C_{gp}[L_1 + L_2]$ if

$$C_{gp} < \frac{L_2[\mu L_1 - L_2]}{[L_1 + L_2][R_1 + R_2]r_p} \quad (117)$$

as can be proved by Eq. (85) on pages 84-89. The oscillations can be stopped by connecting a variable condenser C across the grid and

the plate and increasing its value until $(C + C_{op})$ reaches a value which is just larger than the right side of (117). An alternative method of preventing oscillations is to increase either R_1 or R_2 . While any of these expedients may be used, no one of them strikes at the cause of oscillations and each will result in reduced amplification. Although, according to Eq. (114), a resistance-coupled as well as a resistance-capacitance-coupled amplifier cannot give rise to self-oscillations due to interelectrode back feed, self-oscillations are possible due to external back feed as in all other amplifiers. This case is described in Sec. 104 in connection with Fig. 159.

All these examples have reference to one stage only, for which in ordinary amplifiers no self-oscillations due to interelectrode back feed as a rule, occur. When several stages are added, the external plate impedance Z_2 is usually lowered to some value $Z_2 - \Delta Z$ and consequently the voltage amplification to some value

$$A_e' = A_e - \Delta A_e = \frac{\mu[Z_2 - \Delta Z]}{[Z_2 - \Delta Z] + r_p} = FA_e,$$

because some voltage acts through the interstage coupling to excite the grid impedance of the succeeding tube. If this happens, there is less tendency to self-oscillations although the effect is usually small. As in the case for external back feed we can assume that by means of the C_{op} capacitance a certain amount of the output voltage acting across Z_2 is fed back. When the amplification of the N stages produces an output voltage $F^{(N-1)}A_e^N E$ for an effective input voltage E , F is a factor for multistages (N more than 1) which is smaller than unity. For N stages, the portion $pF^{(N-1)}A_e^N E$ is reflected back to the input side, while for one stage ($F^{(N-1)} = 1$ and $N = 1$) only $pA_e E$ is reflected back. Hence the first requirement is that pA_e be smaller than unity so that a single stage will not give rise to self-oscillations. p is usually a small fraction for customary values of C_{op} and plate loads. But from

$$pF^{(N-1)}A_e^N E,$$

it is evident that, even with the foregoing requirement, a critical number of stages exist above which $pF^{(N-1)}A_e^N$ exceeds unity and the amplifier sets up oscillations.

The effect of the interelectrode back feed can be balanced out in several ways, as suggested by C. W. Rice, L. A. Hazeltine,¹ and others. It can also be avoided by using double-grid tubes² in the screen-grid connection. Figure 164 shows a tuned radio-frequency amplifier where, by means of the setting of the neutralizing condenser C_n and the tap T ,

¹ RICE, C. W., U.S. Patent No. 1334118; L. A. HAZELTINE, *Proc. Radio Club Am.*, 2, No. 8, March, 1923; U.S. Patent Nos. 1489228 and 1533858; J. F. DREYER *Proc. I.R.E.*, 14, 217, 1926; R. S. GLASGOW, *J. A.I.E.E.*, 47, 327, 1928.

² See pp. 27-32, 251-254.

the displacement current through the grid-plate capacitance is balanced out. Although the neutralization has a frequency term, for instance, for the broadcast range, it is possible to find a setting which holds practically over the entire range although at the higher end of the frequency band there is a tendency toward oscillations. When new tubes are inserted, the setting of C_n must be changed accordingly. For a proper

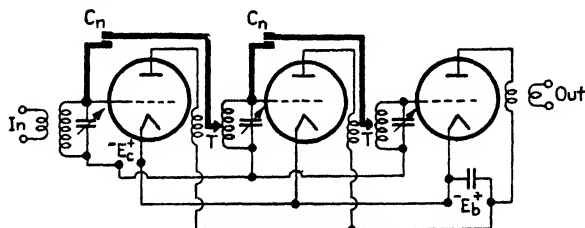


FIG. 164 — Neutralization by means of external condenser C_n and tap T .

tap T , C_n is about of the order of the C_{gp} capacitance. Figure 165 illustrates how the effect of the C_{gp} interelectrode capacitance can be neutralized. An inductive load is used as an external plate load. If $L_1 = L_2 = L$, the steady B-battery voltage is supplied to the center tap T of coil $L + L$. For this case, T forms a voltage node and the potentials $+e_p$ and $-e_p$ exist at the ends of the coils. Because of the grid-plate capacitance, the current $I_{gp} = j\omega C_{gp} e_p$ flows toward the input circuit. Therefore, if $C_n = C_{gp}$, the current $I_n = -j\omega C_n e_p$ neutralizes the effect of the back feed. This compensation assumes that the effect of the interelectrode capacitance between plate and filament is small. This capacitance (C_{pf}) acts across coil L_1 . The input capacitance C_g' of the following tube also has a small effect. Figure 166 shows several schemes of neutralization used in tuned high-frequency amplifiers.

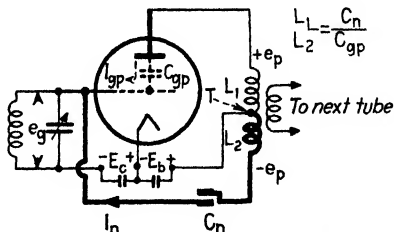


FIG. 165 — Current I_n neutralizes displacement current I_{gp} .

Another method of utilizing the full amplification of a multistage amplifier is by the use of shield-grid tubes for which the grid-plate capacitance can be reduced to about 1 per cent of the value that could be attained with ordinary single-grid tubes. Tubes having back-feed capacitances with respect to the control grid as low as $C_{gp} = 28 \times 10^{-15}$ farad are then possible. Consequently, according to A. W. Hull,¹

¹ *Phys. Rev.*, **27**, 439, 1926. With three-grid tubes (control grid, space-charge grid, and shield grid due to W. Schottky, *Arch. Elektrotech.*, **8**, 821, 1919) voltage amplifications up to 100 per stage are possible without self-oscillations if the frequency is not higher than about 1000 kc/sec. For still higher frequencies A_v decreases.

tuned high-frequency amplifiers can be built with a voltage amplification per stage as high as 45 at 1000 kc/sec, while at 10,000 kc stable amplification of about $A_e = 18$ is possible. The theory of A. W. Hull is briefly as follows: In the alternating-current network of Fig. 167, the back feed

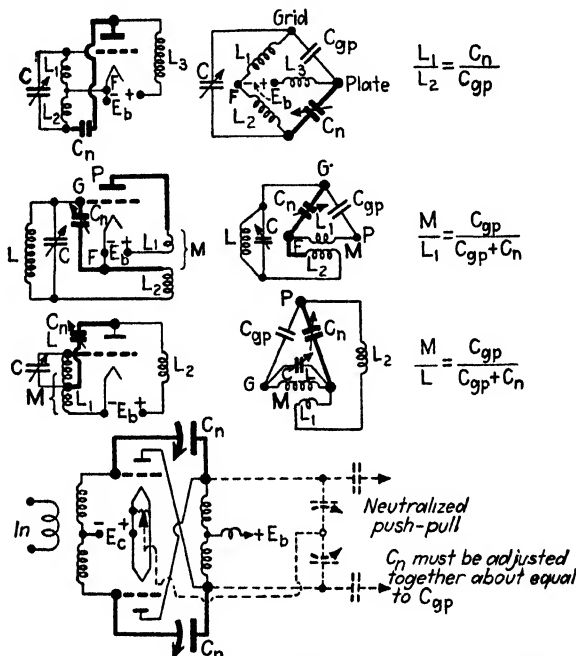


FIG. 166.—Conditions for different neutralized circuits.

occurs through the grid-plate interelectrode capacitances and, for tuned-plate circuits (coil L , R in parallel with a tuning condenser C), the effective external plate resistance is practically $R_e = L/(CR)$. The effect of the coupling condenser C_m (not shown) between the external plate load and

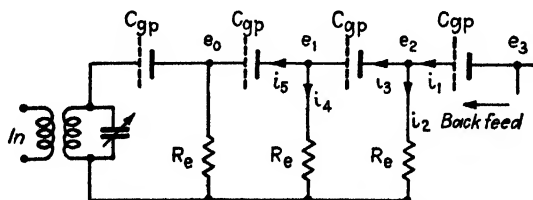


FIG. 167.—A.c. network for the back feed of a cascade tuned-plate amplifier.

the grid of the next tube is neglected, as is that of the grid leak, which acts in parallel with R_e . If the grid-leak resistance r and the effective grid resistance r_0' are also taken into account, $r_0 = r \cdot r_0' / (r + r_0')$ acts practically in multiple with R_e and the equivalent resistance becomes

$R_e \cdot r_0 / (R_e + r_0)$. Since e_0, e_1, e_2 , etc., denote the plate potentials producing the back-feed currents i_1, i_2, i_3 , etc., we have

$$\left. \begin{aligned} i_1 &= (e_3 - e_2)\omega C_{gp}; & i_2 &= \frac{e_2}{R_e}; & i_3 &= (e_2 - e_1)\omega C_{gp}; & i_4 &= \frac{e_1}{R_e}; \\ i_5 &= \frac{e_1}{\sqrt{R_e^2 + (1/\omega C_{gp})^2}}; & i_1 - i_2 - i_3 &= 0; & i_3 - i_4 - i_5 &= 0 \end{aligned} \right\}$$

The value of $(1/\omega C_{gp})^2$ for high-frequency currents is very great and much larger than R_e^2 so that R_e^2 may be neglected and, upon elimination of e_2, i_1, i_2, i_3, i_4 , and i_5 , we have the attenuation

$$\frac{e_3}{e_1} = \left[\frac{1}{\omega C_{gp} R_e} + 2 \right]^2 - 1$$

But this decay ratio extending over two stages of amplification must, for stable high-frequency amplification, outweigh the voltage amplification A_e^2 holding for two stages. That is,

$$\left[\frac{1}{\omega C_{gp} R_e} + 2 \right]^2 - 1 > A_e^2$$

which leads to the approximation

$$A_e < \frac{1}{\omega C_{gp} R_e} + 2 \quad (118)$$

But, according to Eq. (56), for a comparatively large effective grid resistance r_0 , we find $A_e = \frac{g_m}{\frac{1}{R_e} + \frac{1}{r_p}}$ and

$$A_e < \sqrt{\frac{g_m}{\omega C_{gp}} + \left[\frac{1}{2\omega C_{gp} r_p} - 1 \right]^2} - \frac{1}{2\omega C_{gp} r_p} + 1 \quad (119)$$

which gives the condition for stable amplification. Hence the voltage amplification A_e per stage must always be smaller than the expression to the right and Eq. (119) can be used to find the optimum amplification that can be employed without self-oscillations. Thus, with an ordinary single tube having $g_m = 400 \mu\text{mhos}$, $r_p = 30,000\Omega$, and $C_{gp} = 2.5 \mu\text{mf}$, the maximum stable voltage amplification is $A_e = 5$ at 1000 kc/sec. For a double-grid tube in the *space-charge* connection with a steepness which is considerably greater (g_m about 1600 mhos) and r_p and C_{gp} as above, A_e can be as high as 10. Now, when the same tube is used in the *shield-grid* connection, the effective back-feed capacitance C_{gp} with respect to the control grid can be made very small indeed—only about 1 per cent of the geometrical capacitance. For screen-grid tubes, r_p

is very high and the term $1/r_p$ in Eq. (119) can therefore be neglected, and the optimum condition for stable voltage amplification is

$$A_e < \sqrt{\frac{g_m}{\omega C_{gp}}} + 1 + 1 \quad (120)$$

Hence for a tube with $g_m = 400 \times 10^{-6}$, C_{gp} as low as 28×10^{-15} farad, at 10 Mc/sec the voltage amplification A_e per stage must be less than 19. When a tube with a space charge and shield grid is employed, very stable amplification is possible since g_m is then much higher. From the relation

$$A_e = \frac{g_m}{(1/R_e) + (1/r_p)} = g_m R' \cong g_m R_e \quad (121)$$

it can be seen that for a given g_m the amplification A_e per stage can be increased by making R_e higher. This condition can be only partially fulfilled and, when tuned-plate amplifiers in the shield-grid connection are used, the condition of (120) is usually satisfied since for a grid leak r

$$g_m = \frac{A_e[r + R']}{R' \cdot r}$$

that is, the value of $rR'/(r + R')$ must be very high in order to approach quality in Eq. (120). With shield-grid amplifiers, the circuit conditions of the load and the coupling are normally such that the effective-stage amplification is well within the region of great stability. A. W. Hull¹ reports a case where the maximum-stage amplification was about $A_e = 7$ at 10 Mc/sec, while formula (120) would call for stable amplification up to $A_e = 19$. A load impedance as high as $R_e = 45,000\Omega$ (which seems impractically high) would have to be provided to make A_e about 19.

From the foregoing analysis of stability conditions, it is seen that the back-feed current depends upon the reactance $1/(\omega C_{gp})$, that is, on the frequency. Hence an amplifier becomes more stable the lower the frequency. For this reason, a modulated high-frequency current of carrier frequency f_1 is sometimes made to beat with an auxiliary high-frequency current of frequency f_2 within the same octave, and, upon rectification, the beat frequency $f_1 - f_2 = f_b$ of lower frequency value than f_1 is amplified in the usual way, then rectified again in order to separate the low-frequency components from the high-frequency carrier of frequency f_b . A very sensitive and selective detector system is secured in this way and is known as the "superheterodyne." Figure 168 indicates the principle of such a circuit where, for instance, $f_1 = 1000$ kc, $f_2 = 900$ kc/sec. $f_b = 100$ kc, a frequency for which stable amplification

¹ *Loc. cit.*

is readily obtainable. The auxiliary frequency f_1 is obtained by means of an autodyne detector although a separate heterodyne oscillator can be used. Amplification systems of this type can be used to great advantage in the determination of field intensities.

106. Notes on Frequency Limitation and Tube¹ and Other Noises in Amplifiers.—As far as the frequency limitation is concerned, amplifications are possible from the lowest frequency ($f = 0$ cycle/sec, direct current) up to the condition for which the "schrott effect" (or "shot effect," 1918) becomes important. The duration of an impulse to be amplified cannot be shorter than the time taken for an electron to pass from the filament to the plate.

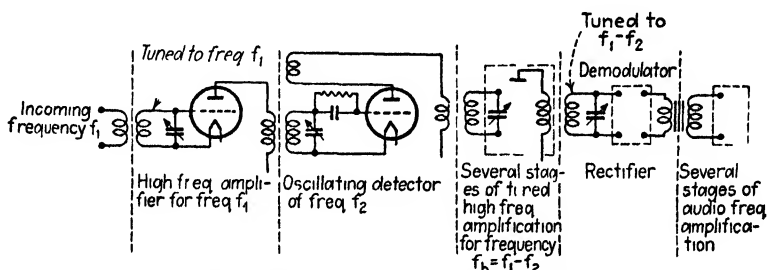


FIG. 168 —Principle of superheterodyne reception.

If no space charge is present, the true shot effect takes place and amplification noise can be observed due to irregularities in the stream of the individual electrons which pass toward the plate. When temperature saturation of the hot cathode prevails, the shot effect disappears and the noises still existing are due to the ions within the tube, to production of secondary electrons or ions, or to thermal agitation, the last playing a large part in high-vacuum tubes. Noises produced by ions are more pronounced when the grid is very negative. In any conductor, electric charges are in a state of thermal agitation. They are in a thermodynamic equilibrium with the heat motion of the atoms in the conductor. Hence at the terminals of the conductor a corresponding variation of the potential difference must take place. Therefore when a high-impedance input circuit is used the potential fluctuations due to thermal agitation are amplified, while for a low-input impedance only those thermal noises resulting from the heat motion of atoms within the conductors in the plate circuit occur. Therefore noises due to thermal agitation can be greatly reduced when low-impedance input circuits are employed. This condition, however, cannot always be fulfilled.

¹ HULL, A. W., and N. H. WILLIAMS, *Phys. Rev.*, **25**, 147, 1925, and **27**, 432, 1926; T. C. FRY, *J. Franklin Inst.*, **199**, No. 2, February, 1925; H. NYQUIST, *Phys. Rev.*, **32**, 110, 1928; J. B. JOHNSON, *Phys. Rev.*, **32**, 97, 1928; F. B. LLEWELLYN, *Proc. I.R.E.*, **18**, 243, 1930, gives a very clear discussion of this subject.

There are also noises due to the microphonicness of the tubes and for this reason it is customary to mount tubes in elastic sockets and keep the tubes mechanically shielded so that sound waves from a powerful loud-speaker cannot form an acoustic back feed. It has already been indicated that the time constant of the grid leak r and the coupling condenser C_m must be properly chosen. Threshold howls can also occur. They are due not to the interstage coupling but to back feeds partly controlled by the inductive reactance in the external plate load. To find out whether a threshold howl or an interstage-coupling noise exists, vary somewhat the value of the grid leak r or of the coupling condenser. When the pitch of the howl is not changed, we have a threshold howl. The coupling howl depends upon the $C_m \cdot r$ product, while the threshold howl is partly determined by the time constant L/ρ if ρ denotes the entire series resistance (including r_p) through which the current producing the noise flows and L the apparent inductance in the plate branch. Therefore a decrease in L or an increase in ρ gives a rise in pitch of the observed disturbance.

In the upper limit of voltage amplification, for amplifiers working in the lower frequency range (audio frequency), noises other than those due to shot effect and thermal agitation are more prominent and it may be said that total voltage amplification much higher than about 50,000 to 100,000 can with ordinary means hardly be called practical. But, as far as tuned high-frequency amplifiers with proper tubes (multiple-grid tubes) are concerned, total voltage amplifications up to a few millionfold seem possible, especially when the shot effect is practically avoided by means of temperature saturation of the filament. It is then only necessary to keep the noises due to thermal agitation and due to ions and formation of secondary electrons as low as possible. With the modern power detector which uses several volts on the grid, the ratio of noise voltage to useful voltage can be smaller than with old detector tubes in which about 0.5 volt variable grid voltage was the allowable maximum voltage. When no precautions were taken with respect to the shot effect, the shot voltage of an ordinary receiving tube would also produce about 1 volt if the total voltage amplification were one millionfold.

107. Notes on Push-pull Amplifiers.—The arrangements of Fig. 169 have the advantage that the two tubes working in push-pull produce only currents of the fundamental frequency and its odd harmonics in the output branch since, for equal work characteristics for both tubes, the effects of even harmonics are balanced out. By “fundamental frequency” is understood the frequency of the impressed input voltage. However, when the input voltage is distorted and contains even harmonics, the output of the push-pull amplifier will also contain even components.

The symmetrical push-pull amplifier avoids only even harmonics in the output branch that are due to the characteristic of the amplifier. It should be noted that, for the ideal case, the steady plate current vanishes. In practical amplifiers on account of lack of symmetry, about 10 per cent of the direct-current component remains, but it is still possible to design output transformers without an air gap since the remaining direct-current component does not shift the operating point of the magnetization into the neighborhood of saturation. Since second-harmonic distortion is a very important kind of distortion, the push-pull output amplifier should avoid much of the distortion, as can be seen from the I_3 wave shape

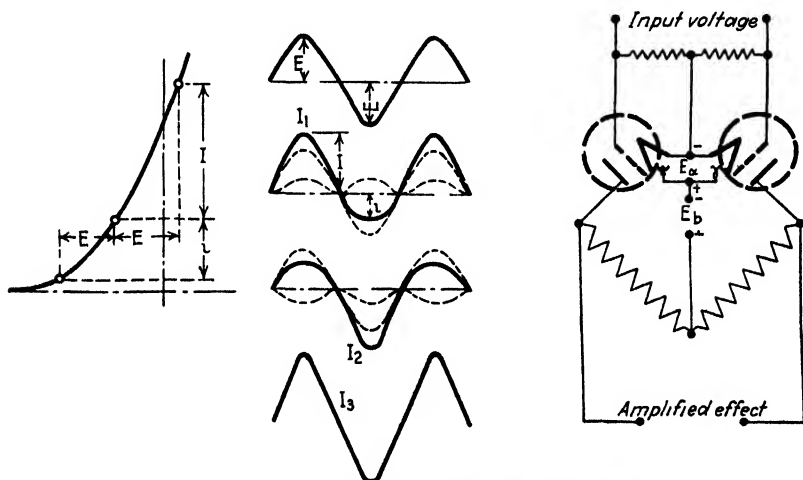


FIG. 169.—Action in push-pull amplifiers.

indicated in Fig. 169. This figure shows also a push-pull amplifier with resistance coupling. It can be used for the lower frequency range down to the amplification of voltages due to direct currents.

Balanced tube circuits can also be used to separate frequencies according to their respective phase relations in two or more similar modulating circuits since the phases of the output components depend upon the relative phases of the input currents. Such applications are the work of J. R. Carson (U. S. Patent No. 1343306) and have been described by E. Peterson and C. R. Keith.¹ With filters it would be hardly possible to suppress a carrier frequency and second-order side-band frequencies which are very close to it. Figure 170 indicates what happens in such circuits. Ordinary push-pull amplifiers are also convenient when amplified output currents are to be indicated by an ordinary oscillograph since the direct-current component is practically zero. It is unnecessary to

¹ *Bell System Tech. J.*, 7, 106, 1928.

offset the zero position of the image of the vibrator mirror. This is of interest especially when amplified impulses, for instance, those due to

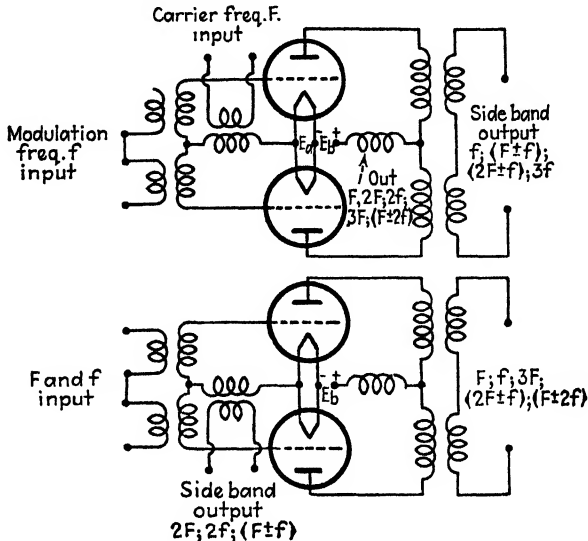


FIG. 170.—Push-pull circuits for the separation of frequencies.

reflection echoes from the ionized layer, are to be pictured. When no push-pull amplifier is available, this zero adjustment can be made by the arrangement indicated in Fig. 171, where the neutral position of the image of the vibrator mirror is set by means of the slider S of the potentiometer.

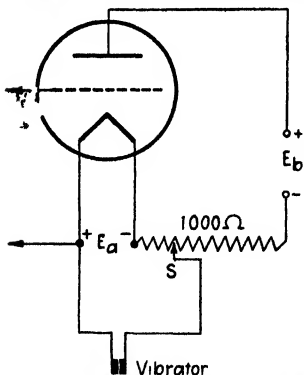


FIG. 171.—Single tube for registering current impulses.

When a 210-type tube or its equivalent, with about 350 volts on the plate is used as the last stage of an amplifier, a vibrator of ordinary sensitivity can be readily operated.

108. Notes on Amplifiers Using Tubes with Several Grids.—The action of tubes using two and three grids, respectively, is described in Secs. 11 and 12. An amplifier using double-grid tubes in the space-charge connection has a very steep work characteristic with a moderate supply voltage E_b in the plate branch. An appropriate positive potential on the grid next to the filament minimizes the negative space charge. The mutual conductance of the tube becomes very high and, if the filament were an equipotential surface and all electrons were emitted with zero initial velocity along radii, an infinite mutual conductance would be obtained. With such grid connections, for a low control voltage (slightly negative), some

negative space charge. The mutual conductance of the tube becomes very high and, if the filament were an equipotential surface and all electrons were emitted with zero initial velocity along radii, an infinite mutual conductance would be obtained. With such grid connections, for a low control voltage (slightly negative), some

of the electrons emitted from the filament fall through the space-charge grid and, on coming close to the control grid, turn around and pass either to the positive space-charge grid or through its openings to the region near the hot cathode. After this they are returned again, and so on, until finally the space-charge grid has captured all of the electrons. But, as soon as the control grid becomes positive, the electrons fall through its openings to the plate.

In order that the tubes in an amplifier should have a high amplification factor, together with a comparatively low plate voltage and negligible grid current, the grid next to the plate (shield grid) is given a positive potential. Since, for a proper constant shield-grid potential, the plate is electrostatically screened off from the control grid, any potential variations on the plate can react only slightly on the control grid. Therefore a high- μ value is obtained as can be understood from the formulas of Sec. 11. The tube characteristic is then sufficiently displaced into the region of negative control-grid voltages so that the control grid is rendered a true electrostatic electrode.

Generally it may be said that the double-grid tube in the shield-grid connection is of great value for high-frequency amplification, while the double-grid tube in the space-charge connection is a ready means for obtaining a very efficient amplifier in the audio-frequency range. It is also possible with such connections to build a very effective direct-current amplifier with which can be amplified, for instance, very weak thermoelectric currents even though these come from a source of a low internal resistance (a few ohms).

When the two grids of a double-grid tube are connected together, the internal resistance r_p becomes high and the tube acts like a high- μ tube.

For three-grid tubes, it is of utmost importance to distinguish between tubes which are for amplifier output stages and tubes which are for voltage amplification only, that is, for use in the preceding stages. When a three-element tube is used for output work, it should be operated so that it has a comparatively low output resistance. It is then of little value as an efficient voltage amplifier. But when a three-grid tube is so designed and operated that it acts as a high-resistance low-power output tube, that is, of the screen-grid type, it is most suitable for voltage amplification. Tubes with three grids are known as "pentodes." The pentode that acts as an efficient voltage amplifier is to be credited to W. Schottky and its arrangement is shown in Fig. 13. It combines the features of the shield-grid tube with those of the space-charge-grid tube. The control grid is placed between the space-charge grid, which is next to the filament, and the shield grid which must be next to the plate in order to reduce the plate-control-grid interelectrode capacitance. The control grid again has a negative bias of about 1.5 volts so that practically no grid current

flows. An electrode arrangement of this type practically removes the negative space charge and increases the resultant amplification factor of the tube without decreasing its mutual conductance at the operating points. When, for the sake of simplicity, it is assumed that all electrons leave the filament with zero velocity, some of them pass through the openings of the space-charge grid with a velocity of 25 volts; that is, $v = 600\sqrt{25} = 3000$ km/sec, and then lose velocity until, when they are

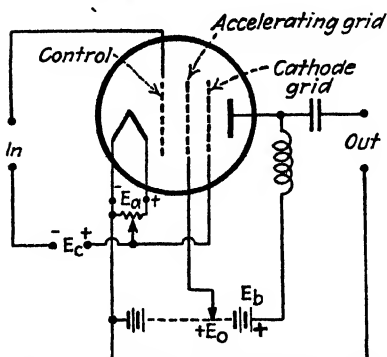


FIG. 172.—Output of triple grid tube.

close to the control grid, which is at $E_c = -1.5$ volts, zero speed is obtained again. Hence, for a symmetrical electrode arrangement (cylindrical electrodes), the apparent emitter of the electrons is a cylinder somewhat smaller than the cylinder of the control grid and, when D denotes the diameter of the control grid and d that of the filament forming the axis of the grid cylinder, the space-charge density is reduced to d/D th of the original value. The shield

grid, which in Fig. 13 is at a positive potential of about +50 volts, acts like a screen and practically all electric lines of force coming from the plate terminate on its mesh. Hence the space between space-charge and shield grid is practically free from variable lines of force due to variations in the plate potential, even though the control grid has a wide mesh and therefore a high value of effective mutual conductance g_m exists.

Reference is made to Fig. 172 for the arrangement of an output pentode. It will be noted that the control grid is again next to the filament, as for the ordinary single-grid tube and the two-grid tube in the shield-grid connection. The grid next to the control grid may be called the *accelerating grid* because its primary function is to speed up the electrons. The mesh is wide open so that only a small portion of the arriving electrons are attracted to the grid wire but the majority pass on to the plate. This grid should not be confused with a screen grid because its function is not necessarily to prevent the output from reacting back on the input side by means of the plate control-grid capacitance. It is also not a space-charge grid in the true sense although it does tend to reduce the space-charge effect near the cathode. The accelerating grid is the cause of the high resultant μ value as well as for the resultant g_m value of this tube. For ordinary double-grid tubes, the normal rated plate voltage and auxiliary accelerating grid voltage are such that secondary emission of electrons (plate produces secondary electrons) does not occur to an appreciable extent. But with output pentodes the electrons

flying through the wide meshes of the accelerating grid meet the plate with sufficient velocity to produce secondary electrons through impact and at times the accelerating voltage is higher than the effective plate potential. Consequently secondary electrons are pulled to the more positive accelerating grid. The secondary electrons speeding back to the accelerating grid then produce a negative resistance action as in the dynatron and, under certain conditions, an increase in the plate potential can produce a decrease in the plate current. In order to reduce the formation of secondary electrons and check their flow toward the accelerating grid, the cathode grid (at the average potential of the cathode) is interposed between the plate and the high-voltage accelerating grid. Since the center or neutral point of the filament usually leads to ground, the cathode grid acts like a grounded shield and increases the

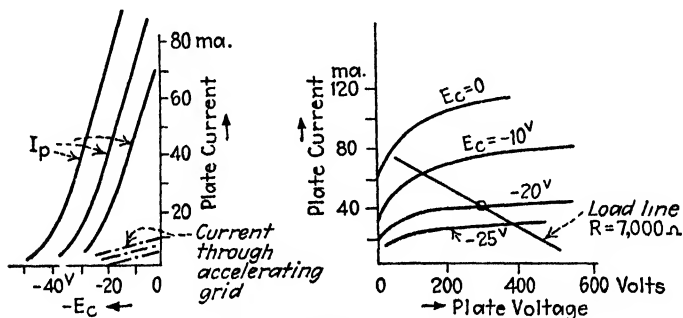


FIG. 173 — Characteristics for a triple grid tube.

voltage gradient toward the positive field of the plate. Thus the emission of secondary electrons is greatly reduced and the output is freer from distortion. The power output may then be very great, for instance, equivalent to that of a 171-type tube or its equivalent, but with increased sensitivity since the accelerating voltage decreases the internal plate resistance.

Tubes of this type have, for instance, the following constants: filament voltage 5 volts, plate voltage +300 volts, accelerating voltage +150 volts, control-grid bias -20 volts, normal plate current 40 ma, current due to the electrons captured by the accelerating grid about 2.5 ma, alternating-current plate resistance 38,000 Ω , effective mutual conductance $g_m = 2500 \mu\text{mhos}$, effective amplification factor $\mu = 95$, and optimum external load resistance $R = 7000\Omega$. The tube characteristics are as in Fig. 173. For the mesh of the cathode grid, a compromise must be made with respect to the electron flow toward the plate and the flow of secondary electrons from plate toward the acceleration grid. The cathode grid keeps the voltage gradient near the plate more or less posi-

tive so that secondary electrons are absorbed near the plate and kept from the accelerating grid. This action becomes more pronounced the finer the mesh of the cathode grid. But for a fine mesh fewer electrons pass toward the plate and thus the internal plate resistance is increased, while for too coarse a grid too many secondary electrons reach the accelerating grid. A suitable mesh and relative spacing of the electrodes is therefore essential. It must also be remembered that r_p as well as μ is variable through wide limits but can be considered fixed for a certain operating point.

109. Amplifiers Utilizing Devices with Negative Resistance.—High amplifications are possible especially when a positive and a negative

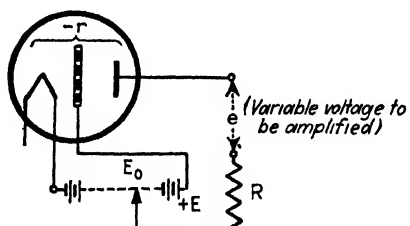


FIG. 174.—Voltage amplification by negative resistance action.

resistance are either in series or in multiple. For the series connection voltage amplification and for the parallel connection current amplification take place. The dynatron, credited to A. W. Hull,¹ is a device which exhibits a negative resistance over quite a range of its plate-voltage plate-current characteristic.

Figure 174 shows a dynatron amplifier in which e is the variable voltage to be amplified and R the positive load resistance. The amplified voltage is taken off across R or across $(-r)$. The voltage amplification increases as R approaches the value of the negative plate resistance $-r$. The dynatron is especially effective when a grid is added. The resulting device is known as the "pliodynatron." The grid potential changes the space-charge condition as in the ordinary double-grid tube. Hence the electron emission toward the plate and the number of secondary electrons reflected back from the plate can be varied by the grid potential. Since the tube resistance is negative and the plate potential has but little effect on the emission of primary electrons, it is evident that any voltage variation between grid and filament must produce corresponding amplified variations in the plate circuit.

Very effective amplification can also be obtained in the parallel connection of a negative and positive resistance. Applying this to the case of a dynatron in multiple with an ordinary three-element electron tube, we have the amplifier shown in Fig. 175. When the dynatron voltage is properly chosen, the respective plate currents I_p and I_p' are equal and in antiphase. A very sensitive current indicator can then be inserted in the supply lead and the amplification actions noted thereby.

¹ *Proc. I.R.E.*, 6, 5, 1918; see also "Hochfrequenzmesstechnik," 2d ed., Julius Springer, Berlin, 1928, pp. 326-335.

According to A. W. Hull,¹ if the tube in parallel with the dynatron has a positive plate resistance $r_p = 10,000\Omega$ and if the positive load resistance $R = 250,000\Omega$, the twelvefold amplification of the ordinary tube could

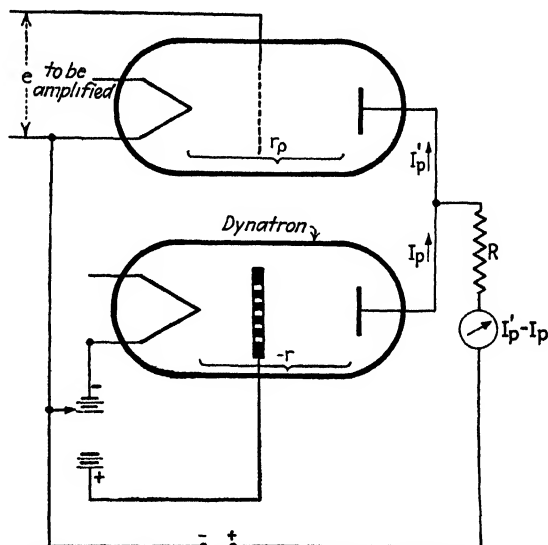


FIG. 175.—Negative resistance ($-r$) in parallel with positive tube resistance r_p .

be increased to a 650-fold amplification. Figure 176 shows the kallirotion amplifier of L. B. Turner² where E denotes the voltage to be amplified and in which two ordinary three-element tubes are aperiodically coupled back by means of the resistances R_1 and R_2 . If g_1 and g_2 denote the steepness of the respective work characteristics $I_1 - E_1$ and $I_2 - E_2$, we have

$$\left. \begin{aligned} I_1 &= g_1 E_1 = g_1 [E + R_2 I_2] \\ I_2 &= g_2 E_2 = g_2 R_1 I_1 \end{aligned} \right\}$$

Hence

$$I_1 = \frac{g_1 E}{1 - g_2 R_1 R_2} \quad (122)$$

and, by increasing the back-feed resistances R_1 and R_2 , the value of I_1 can be greatly increased. The amplification action can also be understood by direct inspection of the circuit. A rise in the impressed voltage E causes an increase in I_1 and a fall of potential across R_1 , that is, a fall of potential in E_2 . This reduces the current I_2 and tends to increase E_1 , and so on. When a load resistance R is used instead of the indicator,

¹ *Loc. cit.*

² *Radio Rev.*, **1**, 317, 1920; see also *Jahrb. drahtl.*, **17**, 52, 1921.

the voltage E_s across it denotes the output voltage and E_s/E the voltage amplification, which can be several thousandfold.

110. Notes on Special Grid Tubes.—

Grids can also be used outside the glass bulb. When an ordinary thermionic two-element tube with a coaxial external grid is used, we have the Weagant tube. Such a device has a dynamic tube characteristic only, since any steady potentials taken from a direct-current source cannot affect the plate current. This can be understood when it is realized that, for N electrons of charge q and velocity v , the electron emission Nqv toward the inner glass wall is equal to

$$\frac{E}{r} + k \frac{dE}{dt}$$

and for any steady grid potentials

$$Nqv = \frac{E}{r} = 0 \text{ (practically)}$$

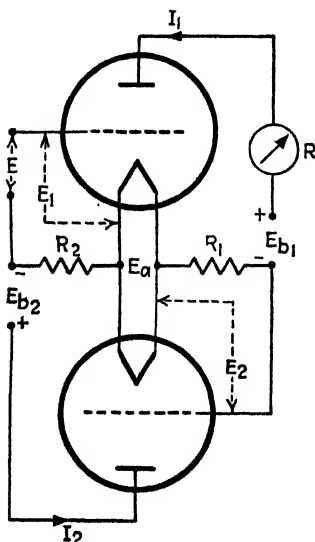


FIG. 176.—The kallitron amplifier.

the grid is useful practically only when the discharge sets in since, under operating conditions, both negative and positive ions are present in such tubes and there is not a pure electron discharge as in ordinary

since the resistance r of the glass wall is high.

There are also single-grid tubes such as the thyatron¹ and grid-glow tube,² in which

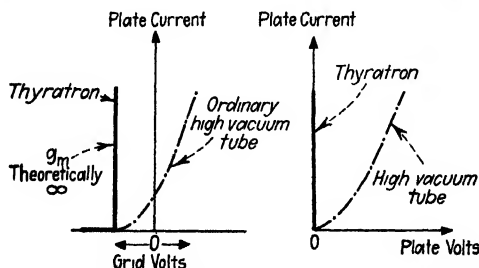


FIG. 177.—Thyatron and high vacuum tube compared.

vacuum tubes. The characteristics of such tubes therefore change abruptly at the time when the plate current is suddenly allowed to flow

¹ LANGMUIR, I., U.S. Patent No. 1289823; P. TOULON, U.S. Patent No. 1654949; I. LANGMUIR, *Science*, **58**, 290, 1923; *Gen. Elec. Rev.*, **26**, 731, 1923; I. LANGMUIR and H. M. MOTT-SMITH, *Gen. Elec. Rev.*, **27**, 449, 538, 616, 762, 810, 1924; L. DUNOYER and P. TOULON, *J. Phys.*, **5**, 257, 289, 1924; A. W. HULL, *J.A.I.E.E.*, **47**, 798, 1928; *Radio Industries*, p. 233, 1930; D. C. PRINCE, *Gen. Elec. Rev.*, **31**, 347, 1928.

² For references and more details, see pp. 42-45.

and are roughly as indicated in Fig. 177. The starting amplification or grid-control ratio corresponding to the true amplification factor at the instant when the discharge sets in is

$$\mu = \frac{e_p}{e_g}$$

since no current exists just before the discharge sets in. It can be as high as 100; that is, a much smaller voltage acting on the grid can suddenly start the operation. Hence, as far as preventing a plate-current flow from the hot cathode to the plate is concerned, the grid functions as in an ordinary high-vacuum tube and as long as the grid bias can produce a negative field around the hot cathode no plate current is possible. After the discharge is formed, the grid no longer controls the discharge current passing to the plate. It can neither modulate nor stop it unless the plate voltage goes off. However, when an alternating plate voltage is used, the discharge goes off intermittently and the grid voltage controls the average current. Theoretically (Fig. 177) the plate current rises to infinity since $g_m = \infty$ and $r_p = 0$. However, this is not strictly true since the external load resistance sets a limit to the current flow and the number of original electrons depends upon the size, material, and temperature of the hot cathode.

In order to understand why the grid-controlled arc rectifier can control only the *average* but not the *instantaneous* value as in an ordinary high-vacuum tube, reference is made to Langmuir's¹ positive-ion sheaths (Fig. 178). Suppose we have an ionized gas as in any glow-discharge tube. The current is then generally carried jointly by electrons and negative and positive ions. These charged particles are distributed through the space between the cathode (cold cathode in a grid-glow tube, hot cathode in a thyatron) and the plate. While the discharge currents flow, there will be places where the negative-charge density is in excess and places like those near the cathode where the positive-ion density is larger. Hence there must be places where there are an equal number of positive and negative ions. On the other hand, in high-vacuum tubes, for normal operating conditions, there are practically only electrons and, while a positive grid may attract some of them, a negatively charged grid cannot since it repels electrons. But in the presence of positive and negative ions an interposed grid, for a definite critical potential, will cause positive and negative ions to arrive at equal rates. When a more negative grid potential than the critical potential is chosen, some of the arriving electrons will be rejected and an excess of positive ions will exist near the grid. For a more positive grid potential, the negative-charge

¹ *Phys. Rev.*, **2**, 450, 1913; also I. LANGMUIR and K. B. BLODGETT, *Phys. Rev.*, **22**, 347, 1923, and A. W. HULL, *Radio Industries*, p. 233, 1930.

density next to the grid will outweigh the positive charges. We have then either a positive- or a negative-charge layer near the grid. Since the discharge current passing toward the plate may be appreciable, the positive and negative sheaths are rather thin and affect the value of the plate current but little. For small discharge currents, the sheaths grow in thickness. For the minute currents existing before the discharge is allowed to start, the sheaths must be very thick and positive and act like a screen to prevent the formation of a discharge current. For this con-

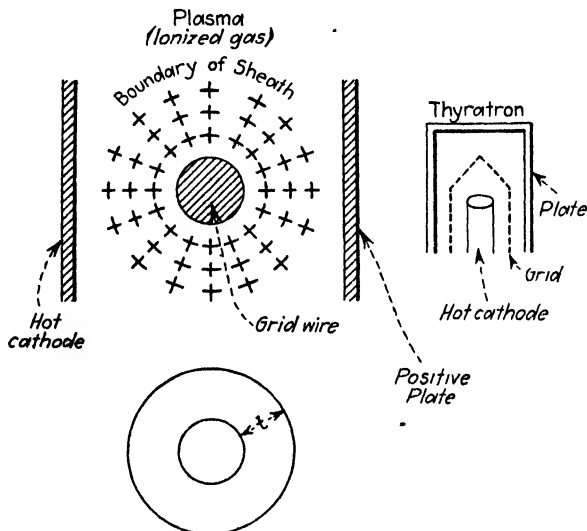


FIG. 178.—Langmuir's positive-ion sheath explaining trigger action of thyatron and grid-glow tubes.

dition, the normal plate current existing after ignition is prevented. Therefore it can be seen that the charge sheath acts as an insulating layer and, whatever the potential of the grid forming the inner surface of the sheath, the potential of the outer surface is that of the effective discharge. When, during the normal operation of the tube, the grid is made more negative, the only effect is as though the grid wire were made somewhat thicker. Since, for normal discharges, the sheath is not thick compared with the diameter of the grid wire, it is evident that a grid with a sheath (when the grid is negative) acts (as far as physical dimensions are concerned) like a grid without an insulating layer but without any controlling voltage on the grid. Therefore the grid has hardly any effect upon the plate current. But when the plate current is kept very low, the sheath around each grid is very thick and can become so thick that the outside surfaces (boundary of sheath) of the adjacent sheaths touch each other and prevent plate-current flow altogether. For a small gap between

sheaths, a small current is possible. This case refers to a continuously¹ controlled arc discharge, and the grid can modulate and act as in any high-vacuum tube. From the foregoing it can be seen, however, that the available plate current must be small and a suitable vapor pressure must be chosen. It is a question whether the ordinary high-vacuum tube is not better.

Now, for tubes in which the plate current passes through an ionized gas, the total number of positive ions is about equal to the number of electrons and in the case of a thyratron there are about 10^{10} to 10^{12} ions/cc. Since the retarding potential of the grid must be negative, the *positive* ions attracted toward the grid region form the positive sleeves around the grid wires (Fig. 178), while the electrons are repelled by the negative grid. The positive grid sleeves appear as dark spaces or dark sheaths around the grid. According to Langmuir,² the thickness $t^{(em)}$ of the sleeve depends upon the *negative* grid bias $E_c^{(volta)}$ and the positive-ion current. Hence, for plane electrodes, Langmuir's well-known space-charge equation for the current density

$$\frac{I}{S} = 2.33 \times 10^{-6} \frac{E_c^{1.5}}{nt^2} \quad (123)$$

holds, where the number $n = 608$ depends on the mass of the ion and accounts for the mercury vapor in the thyratron tube. It is obtained by extracting the square root of the ratio of the mass of the mercury ion to the mass of the electron. When positive ionization is due to traces of helium gas as in certain glow-discharge tubes, the number 86 is obtained. For neon ions $n = 193$, and for argon ions $n = 271$. The symbol S denotes the surface of the electrode in square centimeters, and I the positive-ion current to the electrode in amperes. It should be noted that E_c denotes the negative potential in volts of the electrode with respect to the surrounding gas. For cylindrical electrodes (l = length, and d = diameter in centimeters) we have, for the positive current per centimeter length,

$$\frac{I}{l} = \frac{29.38 \times 10^{-6} E_c^{1.5}}{\beta^2 \cdot n \cdot d}$$

where the factor β depends on the ratio D/d and D denotes the outside diameter of the insulating sleeve. Putting $\gamma = \log (D/d)$, β can be computed from

$$\beta = \gamma - (2\frac{1}{3})\gamma^2 + (11\frac{1}{20})\gamma^3 - (47\frac{1}{300})\gamma^4 + \quad (124)$$

which holds only when γ is small. The value obtained will be somewhat

¹ LUEBCKE, *Z. tech. Physik*, **8**, 445, 1927.

² *Loc. cit.*

smaller than the correct value. For more accurate values, the formula by H. M. Mott-Smith¹ can be used. The values are tabulated in the paper by I. Langmuir and K. B. Blodgett.

It is evident from formula (123) that the thickness t of the positive grid sleeve increases with the three-fourth power of the negative grid potential but decreases as the square root of the current density of the positive ions increases. But the number of positive ions is proportional to the discharge current coming from the hot cathode, and the thickness of the insulating sleeve is consequently inversely proportional to the square root of the emission current. The same relation holds approximately for cylindrical electrodes when t is small compared with d . This shows that, for normal space current coming from the cathode, the thickness t must be very small and D almost equal to d , whereas for a blocking grid bias and a condition close to the grid potential which will just allow the discharge to occur, the sheath must be thick. From this it is evident that the control ratio $\mu = e_p/e_g$ is determined by the largest opening in the grid mesh, while for the ordinary high-vacuum amplifier tube the grid-control ratio depends on the average plate current and the average grid mesh.

From the action of such tubes it can be seen that they behave as a trigger relay and as an intermittent relay if the plate voltage is made to vary in cycles. When either a pulsating or an alternating plate voltage is applied, the plate current can be made to vanish on each zero point of the voltage wave and the control grid can be used either to prevent or to allow the current to start again during the next half cycle.

The positive ionization in thyratron tubes results from the presence of mercury vapor at a pressure between 1 to 50 μ , while in the tungar bulbs pressures of about 5 cm are used. For other gases and especially for helium, somewhat higher pressures than for thyratrons are used for the best operation. In order to obtain mercury vapor at the required low pressure, a small drop of mercury (about a cubic millimeter is sufficient for moderate-size tubes) is inserted at the bottom of the tube and at about 40°C the pressure is 5 μ , so that the tube can operate anywhere from room temperature to 60°C. Since the drop of mercury is at the bottom where no direct heating exists, the temperature of the filament and of the remainder of the tube has little effect.

For the grid-glow tube, reference is made to Fig. 179 where the small tip reaching out of a thin glass stem denotes a nickel anode which has great electronic affinity and therefore shows little tendency to liberate electrons under the conditions encountered in the normal operation of such tubes. A well-insulated nickel grid bends toward the anode, while an aluminum cylinder (emits electrons readily) surrounds these two

¹ See paper by I. Langmuir and K. B. Blodgett, *op. cit.*, footnote 1, p. 265.

electrodes and acts as the cold cathode. All electrodes are under a pressure of about 10 mm of neon gas expressed in terms of the mercury column. Suppose that, when the grid is connected to the anode, the discharge begins at $E_p = 350$ volts where E_p denotes the positive anode potential. When the grid floats freely, that is, without any impressed potential, it acquires electrons emitted from the cathode cylinder and, as

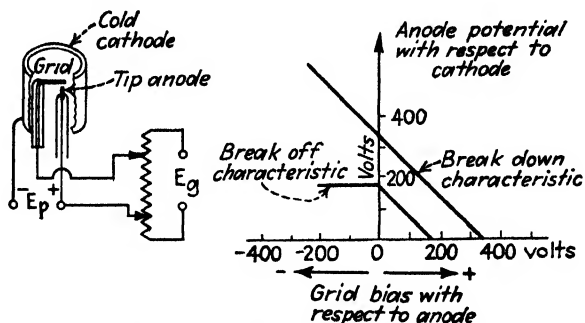


FIG. 179.—Action in grid-glow tube.

the plate voltage $+E_p$ is gradually raised, the grid captures and holds electrons, thus producing a negative space charge next to the anode. Such conditions are maintained until the critical potential is reached at which the discharge occurs, and they have a tendency to repel the approaching electrons and thus to cut down their average velocity. Hence a much higher voltage than the critical breakdown value of

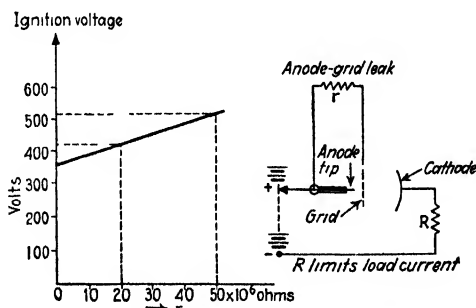


FIG. 180.—Breakdown voltage increases with r .

350 volts will now be required. The breakdown will occur instead at a voltage which may be as high as 1000 volts, depending upon the degree of grid insulation. Figure 180 indicates approximately how the insulation resistance r affects the ignition voltage.

When in Fig. 179 the grid is made positive, the electrons are accelerated and produce ionization at a correspondingly lower plate voltage than 350 volts. The plate voltage required can be readily calculated

since the active ionization voltage now acts between the grid and the cathode as $(E_p + E_g)$ and for the start of a discharge current must be equal to the upper critical voltage E_u , that is,

$$E_u = E_p + E_g \quad (125)$$

When 100 volts positive grid bias exists, $350 = E_p + 100$ and only 250 volts are needed between the cathode and plate, while, for a negative grid bias of 100 volts, $350 = E_p - 100$ or $E_p = 450$ volts required to bring about a glow discharge. As in the case of the thyratron tube, after the discharge current is established, the grid bias can have practically no effect because of the positive insulating layer about the grid.

If the plate voltage is reduced below the lower critical glow-discharge voltage E_l , the discharge current will disappear again, as is indicated by the breakoff characteristic of Fig. 179. It can be seen that, for any negative grid bias, a plate voltage of about 180 volts will maintain the discharge. Hence the original plate voltage, when higher than 180 volts, could be reduced almost to $E_p = 180$ volts without stopping the discharge. This is not true when a positive grid bias assists the starting of the discharge or when the grid bias is changed to some positive value after the discharge current exists. For zero grid bias, the lower critical or breakoff voltage must be the same as for a negative bias and is the same as would exist with a two-element glow tube (no grid present). With a positive bias of $E_g = +180$ volts, the grid voltage alone is sufficient to support the discharge. For any positive grid voltage between 0 and 180, that is, between 0 and the normal lower critical voltage, we have the law

$$E_l = E_p + E_g \quad (126)$$

while for negative grid biases $E_l = E_p$ holds. For a positive grid-biasing potential of 100 volts, $180 = E_p + 100$, the plate voltage could be lowered to 80 volts before the discharge current breaks off. Formulas (125) and (126) show that the grid-control ratio or amplification factor (since no current flows before discharge exists) to start the glow discharge is only unity and not a large value as it is for the thyratron. For positive grid biases, the grid-control ratio is again unity, while for negative biases it is zero since the grid voltage has no effect whatsoever. That the grid-control ratio of the glow-discharge tubes does not show any gain does not matter since the sensitivity of the device is utilized to trigger off a larger amount of energy. The sensitivity of the tube increases as the negative grid bias approaches zero grid potential and becomes very high near the point at which the discharge current builds up. In some tubes, only about $10\mu\mu$ watts is dissipated in the grid circuit when the negative grid bias is about to allow a discharge current. Usually an alternating grid voltage is used to control the grid-glow relay. It is to be noted that the

maximum value of the voltage wave is to be taken into account and not the effective value. When both E_p and E_a denote alternating voltages of the same frequency, Eqs. (125) and (126) hold if the quantities are added vectorially.

111. Glow-tube Amplifiers.¹—Grid-glow tubes and thyratrons cannot be used as amplifiers for modulations, etc., since amplification exists only in the threshold state, that is, at the time when the discharge just sets in. Recent experiments have shown that it is possible to make a glow tube amplify and therefore also oscillate like an ordinary thermionic tube

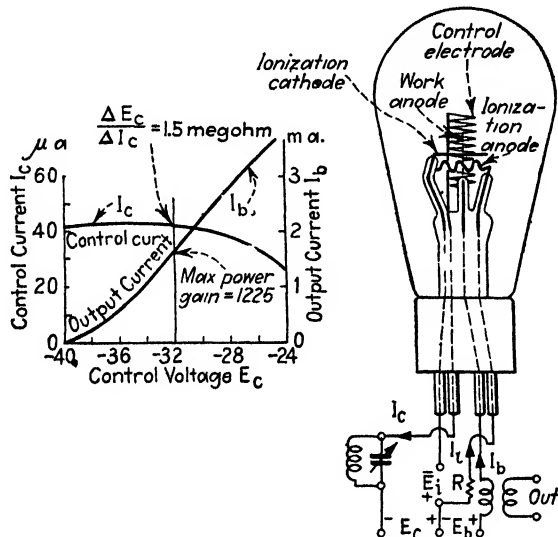


FIG. 181.—Action in a glow-tube amplifier.

One way of accomplishing this is to produce in the space next to the control electrode either an excess of positive ions or an excess of negative ions. The latter is more useful since it is then possible to utilize the more mobile electrons. Figure 181 shows a glow tube of this type in a typical circuit. In order to segregate negative ions from positive ions, an arrangement of four electrodes is used. With canal rays (positive rays) it would be an easy matter to segregate positive ions, especially when carbon dioxide gas is used. Such a tube would need only three electrodes but its frequency characteristic would not be very good since the current flow would depend on the motions of the relatively heavy ions.

Tubes of the four-electrode glow type may be readily compared with ordinary three-element thermionic tubes. Instead of the incandescent filament, a primary ionization (glow discharge) is produced, for example,

¹ Developed in the Research Laboratory of Wired Radio, Inc., North American Company.

between a ring-shaped ionization cathode and a wavy circular ionization anode. For a proper gas pressure, only the tips of the wavy anode will show a glow although the ionization cathode will be fully covered with its characteristic glow. The excitation of these glows is brought about by a direct-current source of voltage E_i . R denotes a protective resistance. Instead of the plate of a thermionic tube we have, for the tube shown in Fig. 181, a work anode along the axis of the control electrode which corresponds to the grid of a thermionic tube. The work anode is at a potential E_a volts above the potential of the ionization anode. The potential is chosen so high that a *secondary* glow appears in the space between the work anode and the helical control electrode although no streamer discharge passes through the control turns. The secondary glow is an essential feature of this tube since without it practically no power would be available in the output branch. Instead of the high vacuum in thermionic tubes, a gas—nitrogen at a pressure of about 25 mm or some other suitable gas—is used.

These are glow tubes and therefore the glow should be used, so to speak, for all that it is worth. Tubes without secondary glow and requiring very pure neon gas at about 6 mm of mercury have been experimented with by G. Seibt and H. Bley. They require special electrode design since they are based on the "edge effect" for which only those electrons can be useful which sweep around the edges of the positive exciter electrode. The work-anode potential is then only a few volts because it is necessary to avoid secondary glow and any glow in the space between the grid and the anode. The power output with neon gas at such a low pressure can be only very small. Tubes utilizing secondary ionization and higher gas pressures can operate at high work-anode potentials and large space currents are possible. Their operating range of current and voltage is of the same order of magnitude as that of ordinary thermionic tubes. This is due to the fact that the original electrons which pass through the control openings produce electronic regeneration in the space between the control electrode and the work anode. Many new electrons are generated in this space by electrons which were controlled by the grid; the presence of these new electrons accordingly increases the current collected by the work anode. When glow-tube amplifiers of this type are considered, it must be remembered that it is more convenient to refer the control voltage E_c to the potential of the ionization anode since the control electrode in these tubes must accelerate the electrons. Otherwise they could never reach the work anode in time. With such a reference, the negative control-electrode potentials are of the same order as those for thermionic tubes. In glow tubes of this type, a steady control current I_c flows, its magnitude usually being about $50\mu\text{a}$. However, this does not matter since the operating point must be chosen such that it corresponds

to a portion of the I_c curve which is more or less horizontal; then the dynamic input resistance is high. It is about 1.5 megohms for the case indicated in Fig. 181. The tube indicated in this figure may be termed a glow tube with *external* primary ionization since the primary glow is produced outside and the useful electrons are driven inside toward the axial work anode. It is just as easy to design a tube for which the primary glow discharge is produced centrally and to have the work anode and the secondary glow discharge around it, as is shown in Fig. 18. The four electrodes are again concentric. The ionization cathode is centrally disposed and made in the shape of a coil, while the ionization anode forms only 1 turn and is likewise centrally disposed. Surrounding

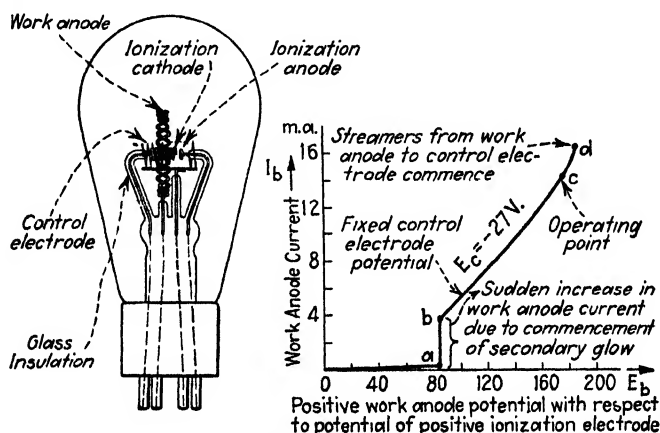


FIG. 182.—Useful discharge region $b-d$ for a glow-tube amplifier.

the ionization electrodes, which together produce the primary glow discharge, is a helical control electrode and around the latter a wavy work anode.

The characteristic shown gives the work-anode potential E_b with respect to the useful work-anode current I_b when a bias of $E_c = -27$ volts is impressed on the control electrode. As mentioned above, both the work-anode potential E_b and the control bias E_c are measured with respect to the potential of the ionization anode. Owing to the scale on which the current values are plotted, the characteristic appears to start at 0 and to ascend very slightly toward the point a . Careful measurements, however, show that, with no external voltage E_b applied between the work anode and the ionization anode, a minute flow of current exists which apparently is due to the primary ionization (or spills through the control openings) toward the work anode. This minute current is comparable in magnitude with that customarily found in thermionic tubes when the plate is directly connected to the negative

end of the filament. In that case it results from the "electron pressure." It is of no significance in ordinary uses of these tubes. At about 80 volts of work-anode potential, the current jumps suddenly from point *a* to point *b*, that is, approximately from 0.25 to 3.8 ma. This is due to the

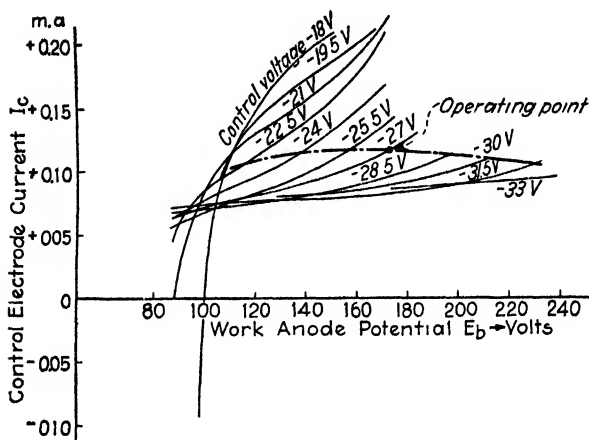
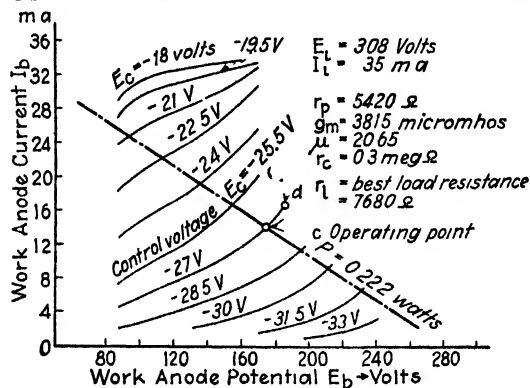


FIG. 183.—Characteristics of glow-tube amplifier with load line.

beginning of the secondary glow discharge in the region between control electrode and work anode. With further increase of the work-anode potential, the work-anode current increases rapidly up to point *d*, where a streamer discharge sets in between the work anode and the control electrode.

The unstable condition of the tube between *a* and *b* and the streamer discharge beyond point *d* determine the useful ranges for operating the tube as a customary demodulator, amplifier, and oscillator. The useful ranges are therefore between *b* and *d*, also between 0 and *a*. The former

is much to be preferred, however, since in that range it is possible to control considerably more output power with a given fluctuation in the input potential applied to the control electrode. Where the tube is intended to function only as a threshold amplifier or trip relay, the operating voltage may be swung over the range which straddles the critical points *a* and *b*. An alternative is to operate about the point *d* so that a large streamer discharge current may be initiated with only a very slight variation in control potential.

In Fig. 183, a number of characteristics corresponding to the useful operating range *b-d*, as indicated in Fig. 182, are given. The different curves were obtained experimentally under the conditions of control-electrode bias shown. The dot-and-dash line passing through the operating point *c* indicates the region for which best undistorted operation prevails. It is near the region of saturation and far from the region of streamer discharge *d*. The dot-and-dash line is chosen, in contrast to usual thermionic work, not only with respect to the I_b , E_b characteristics¹ but also with respect to the I_c , E_c curves since with gas-filled tubes steady grid currents I_c exist and care must be taken that the dynamic input resistance is high for the operating region. From the values given in Fig. 183, it will be noted that the ionization voltage E_i for this particular tube is 308 volts and that the work-anode current I_b can swing well toward the ionization-current value $I_i = 35$ ma without serious distortion. This means that the tube will deliver to the work-anode branch practically all the available power controlled by the glow discharge. It is also of interest to note that the mutual conductance g_m of the tube is better than that of commercial three-element thermionic tubes. Values of g_m as high as 10,000 have been obtained. The following table gives

TABLE VIII

E_i (volt)	I_i (ma)	E_b (volt)	I_b (ma)	E_c (volt)	r_p Ω	g_m (μ mhos)	μ
372	35	123	17.0	-4.5	4,820	3,665	17.65
303	35	123	16.0	-3.0	4,100	5,800	24.0
300	40	166	28.0	-3.0	3,760	7,600	26.0
310	45	115	26.5	-1.5	2,625	10,830	28.43
305	50	250	24.0	-3.0	4,280	6,700	28.65
388	40	140	21.0	-1.5	5,900	10,720	63.5
265	60	345	21.6	-22.8	16,000	6,000	90.0
312	30	230	13.5	-3.0	7,050	5,270	37.3
271	40	163	19.2	-1.5	1,750	5,520	9.7
301	35	133	17.2	-7.5	1,750	4,190	7.3
296	35	133	23.0	-3.0	4,700	3,540	16.7
300	35	90	25.0	-18.0	1,640	1,721	34.7

¹ See also Fig. 128 for thermionic amplifier, on p. 192.

data of several experimental glow tubes, most of them using nitrogen gas from 15 to 40 mm of mercury pressure.

In the tube of Fig. 182, the primary ionization due to the voltage E_i takes place between the helical central cathode and a small central anode turn. The negative ions which are segregated move radially outward

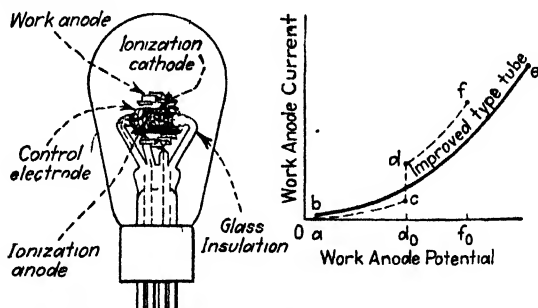


FIG. 184.—Ionization anode inside of perforated ionization cathode cylinder.

from the ionization cathode. In the tube shown in Fig. 184, the ionization cathode is a perforated cylinder which is centrally located and surrounded by a helically shaped control electrode and a work anode in the form of a crimped cylindrical band. Inside the hollow ionization cathode and along its axis is the ionization anode. Hence the primary

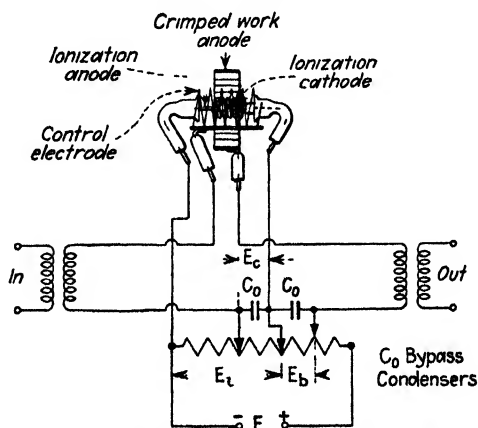


FIG. 185.—Tube can be excited from a single source.

ionization will cause electrons to pass toward the inside of the perforated cathode cylinder as well as toward the work anode. This means that electrons will be traveling in opposite directions. Consequently most of the electrons passing toward the work anode can start out with almost zero velocity and their motion is essentially due to the field produced by the work anode and the control electrode. A much more effective

segregation of electrons and positive ions must therefore take place. This can also be seen from the heavily drawn characteristic of Fig. 184. The very long portion *b* to *e* of this characteristic is useful in amplifier work. For other types of tubes, the characteristic is as indicated by the broken line *Oacdf*, with *df* as the useful portion. The portions from 0 to *a* and 0 to *c*, respectively, again represent conditions for which the output power is insufficient to set up a secondary glow discharge in the region between the work anode and a place close to the control electrode. A comparison of the full-line and broken-line characteristics shows clearly the greatly increased operating range through which the work-anode current may be controlled, that is, between *b* and *e*. The minimum point *b* is very close to the zero value. Figure 185 shows how such glow-tube amplifiers can be excited from a single source. Another form of tube with improved electronic segregation is also shown. The ionization cathode is again centrally located and formed by a helical wire within which and along the axis is located the ionization anode.

112. Trigger Circuits.—Circuits in which a large amount of energy is to be released (triggered off) may employ either grid-glow tubes or

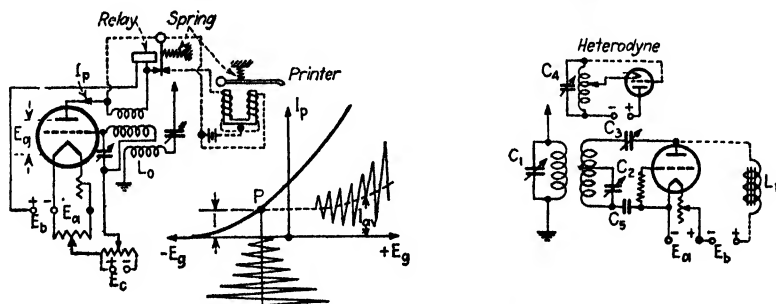


FIG. 186.—Trigger circuits.

thyratrons. It is then only necessary to set the grid bias near the critical breakdown voltage, so that a small superimposed voltage will set the tube into operation. Figure 186 gives trigger circuits which are highly regenerative, that is, on the verge of oscillation. Hence a very small voltage on the grid starts up self-oscillations. The circuit with the printer is the Bureau of Standard's adaptation of a scheme originally described by L. B. Turner¹ to the reception of time signals from long-distance stations. The method utilizes a potentiometer across the A battery and a potentiometer across a grid battery in order to set the circuit for a very regenerative condition. The negative bias E_c is just sufficient to prevent self-oscillations when no outside voltage acts on the

¹ *London Electrician*, p. 4, July 4, 1919; E. A. ECKHARDT and J. C. KARCHER, *Wash. Acad. Sci.*, 11, 303, 1921.

grid. This condition corresponds to operating point P and plate current I as measured with a direct-current meter. It exists when g_m is somewhat smaller than RC/M , in which R denotes the effective resistance of the grid coil and M the magnetic back feed from the plate coil. Hence when a small alternating voltage is induced in the pick-up coil L_0 , the positive half waves of the induced voltage produce, because of the curvature of the E_g, I_p characteristic, larger positive than negative fluctuations in the anode current and therefore also a larger average value I_{av} . Self-oscillations can then build up and the plate current can assume values which are many times the original value I , even though the frequency of the incoming voltage is quite different from the natural frequency of the tube oscillation. An equality of impressed and circuit frequency increases the trigger action. The disadvantage of this system is that the condition of self-oscillation prevails after the trigger voltage due to the incoming signal stops. But the original condition of high regeneration and no oscillations can be restored automatically if the contact point to the left of the coil relay causes a short circuit on the plate coil. When a dash signal arrives, the starting self-oscillation pulls the contact arm to the left, stops the oscillation, springs back to the natural position, is attracted again to the left, and so on. The contact arm thus rattles to and fro during the duration of the dash and can be made to operate a recorder whose differential winding becomes unbalanced during such periods. An ordinary receiver tube can be used with a coil relay operating at about 2 ma. The critical current for which no oscillations exist is then set to about 0.25 ma.

The other arrangement indicated in Fig. 186 was used by E. Alberti and G. Leithäuser to measure the frequencies of remote stations. A capacitive back-feed adjustment C_3 was utilized so that the condition of self-oscillation could be very closely approached. A parallel-plate supply through the choke coil L_1 was then necessary. This coil also served to feed into an audio-frequency amplifier the audible beat currents produced in conjunction with the heterodyne. To obtain a highly regenerative system, the condenser C_3 was varied until oscillations just appeared. The coil of the antenna was gradually coupled to the self-oscillating detector until the self-oscillations suddenly stopped. Voltages induced in the antenna would then trigger off the detector circuit.

113. Thermal Amplifiers.—Oscillators and amplifiers of this type have been investigated by Yoji Ito.¹ They depend on the fact that the electron emission can be varied by variations in the temperature of the hot cathode. Any changes in the filament temperature can be made to control the plate current and an ordinary two-element tube (filament and plate only) can be made to amplify by thermal action. Because of the

¹ *Z. Hochfreq.*, **35**, 12, 1930.

sluggishness of the thermal action, such amplification can be useful only in the low-frequency range. In a similar manner, undesirable low-frequency modulations may be set up when the hot cathode is directly heated by commercial alternating current. A useful amplifier of the thermic type is indicated in Fig. 187, in which the effect of a small low-frequency voltage $E \sin \omega t$ is to produce a magnified action in the plate current. Assuming that the average value of the hot cathode during

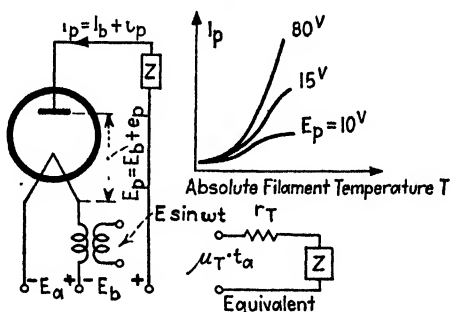


FIG. 187.—Actual and equivalent thermal amplifier.

the cyclic change is r ohms, we have for the loss W of the incandescent body which follows the black-body-radiation law

$$W = kST^4 \quad (127)$$

if T stands for the absolute temperature and S the surface in square centimeters of the filament. The quantity

$$k = 1.37 \times 10^{-12} \frac{\text{cal}}{\text{cm}^2 \text{ sec} \cdot \text{deg}^4}$$

denotes the radiation constant. Since the filament has a certain heat capacity $Q = \text{volume} \times \text{density} \times \text{specific heat}$, and the heat equivalent H is 4.18 wattsec/cal, we have, for the instantaneous value i of heating current,

$$\frac{r \cdot i^2}{H} - W = Q \frac{dT}{dt} \quad (128)$$

The filament current is made up of a steady direct-current value I_a and a small alternating component i_a resulting in a constant temperature T_a about which small temperature fluctuations t_a take place. We have for T^4 and i^2 in (127) and (128)

$$\begin{aligned} T^4 &= [T_a + t_a]^4 \cong T_a^4 + 4T_a^3 t_a \\ i^2 &= [I_a + i_a]^2 \cong I_a^2 + 2I_a \cdot i_a \end{aligned}$$

Since $i_a = I_m e^{j\omega t}$, for the energy balance we obtain

$$Q \frac{dt_a}{dt} + A \cdot t_a - BI_m e^{j\omega t} = 0 \quad (129)$$

for

$$A = 4kST_a^3; \quad B = \frac{2I_a \cdot r}{H} \quad (129a)$$

The steady and the variable component of the absolute temperature of the hot cathode can therefore be computed from

$$T_a = \sqrt{I_a} \sqrt[4]{\frac{r}{kHS}} \quad (130)$$

$$t_a = D e^{-j\psi} I_m e^{j\omega t} = G \cdot i_a$$

$$D = \frac{B}{\sqrt{A^2 + \omega^2 Q^2}}; \quad G = D e^{-j\psi}; \quad \psi = \tan^{-1} \frac{\omega Q}{4kST_a^3} \quad (130a)$$

Therefore the alternating temperature fluctuation t_a has the amplitude DI_m and lags behind the amplitude I_m of the alternating current which produces it by the phase angle ψ . Since the plate current is a function of the plate voltage and the filament temperature, we have, for the instantaneous values,

$$I_p = I_b + i_p = F(T, E_p) = F(T_a, E_b) + \frac{\partial F(T, E_p)}{\partial T} t_a + \frac{\partial F(T, E_p)}{\partial E_p} e_p$$

Subtracting from this expression the relation for the constant components which is

$$I_b = F(T_a, E_b)$$

we obtain for the remaining components

$$\begin{aligned} i_p &= \frac{\partial F(T, E_p)}{\partial T} t_a + \frac{\partial F(T, E_p)}{\partial E_p} e_p \\ &= \frac{\partial I_p}{\partial T} t_a + \frac{\partial I_p}{\partial E_p} e_p \end{aligned} \quad (131)$$

This result resembles the one obtained for the three-element tube using a grid as the third electrode. Hence by putting

$$\left. \begin{aligned} \left(\frac{\partial I_p}{\partial T} \right)_{E_p = \text{constant}} &= g_r = \text{(thermal mutual conductance or thermal dynamic steepness of the control characteristic)} \\ \left(\frac{\partial I_p}{\partial E_p} \right)_{T = \text{constant}} &= r_p = \text{(thermal internal dynamic plate resistance)} \end{aligned} \right\}$$

we obtain from (131)

$$i_p = g_r t_a + \frac{e_p}{r_p} = \frac{g_r \cdot r_p \cdot t_a + e_p}{r_p} \quad (131a)$$

But for the three-element tube $\mu = g_m \cdot r_p$; hence the corresponding thermal amplification factor $\mu_T = g_T \cdot r_T$ and (131a) leads to

$$i_p \cdot r_T = \mu_T t_a + e_p \quad (132)$$

But since, for an external plate load Z , the change in plate potential $e_p = -i_p Z$, Eq. (132) yields, for the variable plate current, the relation

$$i_p = \frac{\mu_T t_a}{r_T + Z} \quad (133)$$

where the temperature fluctuation t_a takes the place of the variable grid voltage e_g in the case of an ordinary three-element tube. This result confirms the equivalent circuit (Fig. 187) for thermal amplification since the two-element tube acts toward variable currents as though an increased temperature fluctuation $\mu_T t_a$ acted directly in the plate circuit comprising the internal thermal plate resistance and the external impedance Z . The product $\mu_T t_a$ has the dimension of a voltage.

Since the temperature variation t_a is due to a small variable e.m.f. impressed on the filament, voltage amplification is possible, $i_p \cdot Z$ being the amplified output voltage. The thermal amplification factor is given by the relation

$$\mu_T = \left(\frac{\partial E_p}{\partial T} \right)_{I_p = \text{constant}} \quad (134)$$

expressed in volts per Kelvin degrees, while the work characteristic has a thermal steepness g_T which may be expressed in milliamperes per Kelvin degree. The thermal resistance r_T is in ohms. Since, for saturation current, Richardson's law

$$I_p = a \cdot S \cdot T^2 \epsilon^{-\frac{b}{T}}$$

holds for the material constants a and b , we have, for the region ($E_p \geq E_{\text{saturation}}$), the thermal steepness

$$g_T = \left(\frac{\partial I_p}{\partial T} \right)_{E_p = \text{constant}} = a \cdot S [2T + b] \epsilon^{-\frac{b}{T}} \quad (135)$$

When negative space charge is present ($E_p < E_{\text{saturation}}$), the three-halves-power law holds; that is,

$$I_p = K E_p^{\frac{3}{2}}$$

and I_p is independent of the absolute temperature T of the filament. The dynamic thermal steepness g_T is therefore zero and, since $\mu_T = g_T \cdot r_T$, theoretically no thermal amplification is possible in the space-charge operating region, which is a basic criterion for thermal amplification.

Since in theory for complete saturation $\mu_r = \infty$, it can be assumed that in the saturation region the thermal amplification factor is generally very high, while it must generally be almost zero in the space-charge operating region. Hence, unlike the case of three-element tubes, the thermal amplification factor μ_r of a two-element tube varies greatly along the characteristic; it depends to a great extent upon the operating point. From these deductions it is also evident that, for complete saturation, the thermal internal plate resistance r_r becomes infinite although, according to (135), the steepness $g_m = \mu_r/r_r$ has a finite value because μ_r is also exceedingly high. On the other hand, in the operating space-charge region $g_r = 0$ and $\mu_r = 0$, the resistance $r_r = \mu_r/g_r$ has a finite value.

114. Notes on Telephone Receivers and Their Amplification Action.—

We must distinguish between two classes of indicating instruments which may be connected in the output branch of the last tube. Those in the first class give indications which are directly proportional to the output current, while those in the second give indications proportional to the square of the output current. Thermoelectric arrangements of the ordinary type, hot-wire instruments, etc., give deflections varying with the square of the indicator current. Those telephone receivers which utilize a strong permanent magnet have a response directly proportional to the current, while a receiver whose magnetic effect depends upon the magnetic effect of the pulsating armature current follows only a square law, which makes the indication of very small currents difficult.

First, examining the telephone receiver with a strong permanent magnet, we find that an amplification effect occurs. When $\Phi = \Phi$ denotes the vector of the permanent magnetic flux and Φ' that of the variable flux due to the variable telephone current I , the instantaneous value F of the force which moves the diaphragm of the receiver is

$$\begin{aligned} F &= k_1[\Phi + \Phi']^2 = k_1[\Phi + k_2 I]^2 \\ &= k_1 \Phi^2 \quad (\text{constant pull on diaphragm which acts at all times}) \\ &\quad + k_1 k_2^2 I^2 \quad (\text{variable pull, depending on the current to be indicated}) \\ &\quad + 2k_1 k_2 \Phi I \quad (\text{pull which depends on constant and variable magnetic flux}) \end{aligned}$$

When the constant flux due to the permanent magnetic system is chosen sufficiently large, the variable pull due to the exciter current can be neglected. The telephone receiver then responds directly proportionally to I , that is, is just as sensitive to small currents and works almost without distortion since

$$F \cong k_1 \Phi^2 + 2k_1 k_2 \Phi I = k_1[\Phi + 2k_2 I] = k_1[\Phi + k_2 I] \quad (136)$$

From the final result of (136) it is evident that a large force acts as though Φ were zero or very small. An indicator of this type is useful when audible currents are to be observed.

For heterodyne circuits, one component must be audible. Therefore it can be seen that, for receivers which respond proportionally to the resulting current due to two currents of different frequency, either the frequency f_1 or the frequency f_2 must be in the audible range, while, for receivers which do not follow a straight-line law, audible effects can be produced even though two high-frequency currents of different periodicity are superimposed, provided their difference frequency

$$f = \frac{\omega}{2\pi} = \frac{\omega_2 - \omega_1}{2\pi}$$

is in the audible range. This can readily be seen from the following solution for a telephone receiver which responds to the square of the resulting current I . If I_1 and I_2 are the constituent currents, we have

$$I^2 = [I_1^2 + I_2^2] = \left[\sum_{+j}^{-j} I_1 e^{j\omega_1 t} \right]^2 + 2 \sum_{+j}^{-j} I_1 e^{j\omega_1 t} \sum_{+j}^{-j} I_2 e^{j(\omega_1 + \omega)t} + \left[\sum_{+j}^{-j} I_2 e^{j(\omega_1 + \omega)t} \right]^2$$

and the detailed derivation given hereafter shows that the effect on the diaphragm of the receiver is proportional to the square of the audio current of frequency f , while all other currents of frequencies $2f_1$, $2f_2$, $f_1 + f_2$, zero frequency, are not audible.

Detailed solution:

$$\begin{aligned} & I_1^2 \{ e^{j\omega_1 t} - e^{-j\omega_1 t} \}^2 \\ & + 2I_1 I_2 \{ e^{j\omega_1 t} - e^{-j\omega_1 t} \} \{ e^{j(\omega_1 + \omega)t} - e^{-j(\omega_1 + \omega)t} \} \\ & + I_2^2 \{ e^{j(\omega_1 + \omega)t} - e^{-j(\omega_1 + \omega)t} \}^2 \\ & = -2I_1^2 \left. \begin{aligned} & -2I_2^2 \end{aligned} \right\} \text{(of zero frequency and therefore not audible)} \\ & -2I_1 I_2 \{ e^{j\omega t} + e^{-j\omega t} \} \quad \left(\text{of frequency } \frac{\omega}{2\pi} = f \text{ and audible in the} \right. \\ & \qquad \qquad \qquad \left. \text{receiver} \right) \\ & \left. \begin{aligned} & + I_1^2 \{ e^{j(2\omega_1)t} + e^{-j(2\omega_1)t} \} \quad \left(\text{of frequency } \frac{2\omega_1}{2\pi} = 2f_1, \text{ that is, double} \right. \\ & \qquad \qquad \qquad \left. \text{periodicity of the } f_1 \text{ oscillation} \right) \\ & + 2I_1 I_2 \{ e^{j(2\omega_1 + \omega)t} + e^{-j(2\omega_1 + \omega)t} \} \quad \left(\text{of frequency } 2f_1 + f = f_1 + \right. \\ & \qquad \qquad \qquad \left. f_2, \text{ that is, equal to the sum} \right. \\ & \qquad \qquad \qquad \left. \text{of the component frequen-} \right. \\ & \qquad \qquad \qquad \left. \text{cies} \right) \\ & + I_2^2 \{ e^{j2(\omega_1 + \omega)t} + e^{-j2(\omega_1 + \omega)t} \} \quad \left(\text{of frequency } 2(f_1 + f) = 2f_2, \right. \\ & \qquad \qquad \qquad \left. \text{that is, double periodicity of} \right. \\ & \qquad \qquad \qquad \left. \text{the } f_2 \text{ oscillation} \right) \end{aligned} \right\} \quad (137) \end{aligned}$$

(High-frequency currents which are not audible)

CHAPTER VIII

THEORY OF ELECTROSTRICTION WITH SPECIAL REFERENCE TO PIEZO ELECTRICITY IN QUARTZ

The following is an outline of the classical experiments and theory¹ of piezo electricity and its application to crystal quartz.

The stabilization of frequency in quartz oscillators and resonators is due to electrostriction, which is caused by the piezo-electric effect (pressure effect). Electrostriction includes both the direct and reverse effect. The former deals with the separation of electric charges as the result of mechanical stress, thus producing an electric field, and the latter deals with the production of mechanical strain when an electric field is applied.

115. Experimental Evidence.—When a crystal of quartz (Fig. 188) is compressed in the direction of one of the three electric axes, the six

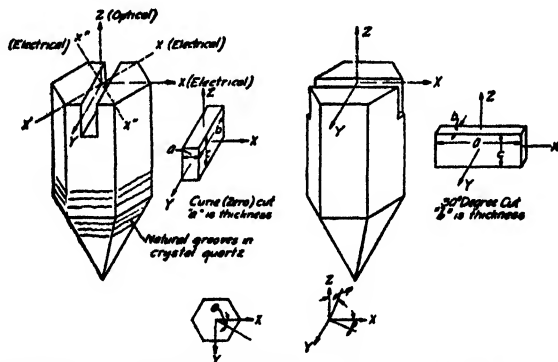


FIG. 188.—Zero (Curie) and 30-deg-cut piezo-electric elements.

edges of the prism become electrically charged. In the parallelepiped as indicated in the figure, X denotes one of the three twofold electrical axes of the crystal, and Z its optical axis about which threefold symmetry exists. The dimension a denotes the thickness and, for the Curie cut, is along the electrical axis for which maximum piezo-electric effect exists.

¹ VOIGT, W., "Lehrbuch der Kristalloptik," pp. 801-964; J. CURIE, and P. CURIE, *Comp. rend.*, **95**, 914-917, 1882; *C.R.T.*, **91**, 294, 1880; *J. phys.*, **8**, 149, 1889; M. G. LEFFMAN, *Ann. chim. phys.*, **24**, 164-167, 1881; E. RIECKE and W. VOIGT, *Ann. Physik* (Wiedemann), **45**, 523-552, 1892; F. POCKELS, *Abt. Kön. Ges. Wiss., Göttingen*, **30**, 268, 1893; W. G. Cady, *Proc. I.R.E.*, **10**, 83-114, 1922; A. F. JORRE, "The Physics of Crystals," McGraw-Hill Book Company, Inc., New York, 1928, Lecture VII, pp. 87-69; M. F. BERNEAU, *Mémoires des Sc. Physiques, Fascicule VI*, 1928.

For a parallelepiped cut, Curie found that charges could be produced on metal layers bounding the plate of quartz of thickness a . The charge q per unit area on one of the coatings is proportional to the pressure X along the electric axis; that is,

$$q = -\delta \cdot X$$

The total charge Q developed on one of the two coatings is

$$\begin{aligned} Q &= b \cdot c \cdot q \\ &= -\delta \cdot F \end{aligned} \quad (1)$$

if F denotes the total force along the electrical axis acting on the face bc . The quantity δ is known as the "piezo-electric modulus" and measurements show that it is

$$\delta = 6.32 \times 10^{-2} \text{ e.s. charge units/kg}$$

The sign of this quantity depends on the direction of the electric axis. Suppose the face of the quartz touching the metal electrode is $bc = 5 \text{ cm}^2$, and the thickness a of the quartz plate such that the electrodes with the quartz between them form a condenser of capacity $C_1 = 7 \text{ cm}$ in e.s. The electrodes are connected to an electrometer of capacity $C_2 = 3 \text{ cm}$. If the quartz is loaded with a weight W which produces a pressure $p = 10 \text{ kg/cm}^2$ across the face bc , the electrometer will indicate a voltage

$$V = \frac{p \cdot b \cdot c \cdot \delta}{C_1 + C_2} = \frac{10 \times 5 \times 6.32 \times 10^{-2}}{10} 300 = 94.8 \text{ volts}$$

When the same force acts, for a Curie cut, along the Y -axis and across faces $a \cdot c$, the total charge

$$Q = +\delta \cdot F \frac{b}{a} = \delta \cdot F \frac{\text{coated area}}{\text{pressed area}} \quad (2)$$

is obtained. Forces along the Z -axis (optical) produce no charges.

Lippman predicted the converse effect. When a certain potential difference V is applied to the coating, the thickness of the interposed quartz slab must change accordingly. The linear compression or dilation is

$$x = \delta \cdot V \quad (3)$$

Since, according to these experimental facts, the charge per unit area is directly proportional to the force and independent of the thickness, it may be shown, by applying Hooke's law and Eq. (3), that the electric-field intensity is proportional to the strain. This relation forms the basis of the classical theory of piezo electricity.

Now, if the two metal coatings in the foregoing example are connected to a thermomilliammeter, and a sinusoidal pressure of amplitude $p = 5 \text{ kg/cm}^2$ and frequency 10^6 cycles/sec is applied between the coatings, the milliammeter indicates a current of

$$I = \frac{2\pi 10^6 p \cdot b \cdot c \cdot \delta}{3 \times 10^9} = \frac{2\pi 10^6 \times 5 \times 5 \times 6.32 \times 10^{-8}}{3 \times 10^9} = 3.3 \text{ ma}$$

Since the voltage in the crystal is not uniformly distributed for oscillating crystals, we have to deal with a space charge of density

$$\rho = \delta \frac{dp}{dx} \quad (4)$$

which forms a basic equation for the *dynamic* theory of piezo electricity and explains oscillations (for instance, torsional oscillations)¹ with crystals cut along the optical axis. From Eq. (4), it is seen if p varies with respect to x , according to a sine law, the space-charge density will vary according to a cosine law.

116. Relation of Curie and Lippman Effects to the Ny Tsi Ze Saturation Phenomenon.—Ny Tsi Ze² has shown that the deformations in a quartz crystal are proportional to the voltage up to about 3000 volts but above this voltage tend toward a limit. The piezo-electric modulus δ acts as though it were a factor rather than a constant. With respect to Fig. 188 it was shown that, for the *direct* Curie effect, a force X acting across each unit area of face $b \cdot c$ produces a charge $q = \delta \cdot X = \delta \cdot p$ where $\delta = 6.32 \times 10^{-8}$, if expressed in absolute c.g.s. units. Relation (3) holds for the Lippman *converse* effect showing that the dilation along the piezo-electric axis is independent of the dimensions of the quartz element. As far as the Curie effect is concerned, no electric charges are produced when mechanical forces act along the optical axis; but when electric fields act along this axis, *dielectric* distortion results. It was also shown by (2) that the same force acting along the axis which is perpendicular to the piezo-electric and optic axis develops, for the same pressure p , a charge per unit area on the faces $b \cdot c$ which is equal to $q = \delta' \cdot Y = \delta' \cdot p$ if $\delta' = (b/a)\delta$. Hence a potential difference V between the coatings of the $b \cdot c$ faces gives the linear dilation $x = -\delta' \cdot V$ in the thickness dimension. The dimensions of the piezo-electric element then play a part and the dimensional change in thickness can be increased by choosing the ratio b/a in δ' large. Applying the principle of conservation of electricity, the change in charge received for each square centimeter of faces $b \cdot c$, according to M. G. Lippman,³ is

$$dq = CdV + kdp$$

¹ *Bur. Standards, Research Paper 156*, vol. IV, March, 1930.

² *J. phys. radium*, 9, 13, 1928; *Compt. rend.*, 184, 1645, 1927.

³ *Loc. cit.*

if C denotes the capacitance of the piezo-electric condenser and k is a negative constant. Hence the energy change dW due to the variable external force leads to

$$dW = p db + V dq \quad \text{and} \quad da = A dV + B dp$$

But dq , dW , as well as da , are exact differentials and

$$\frac{\partial C}{\partial p} = \frac{\partial k}{\partial V}; \quad \frac{\partial A}{\partial p} = \frac{\partial B}{\partial V}; \quad \frac{\partial(pA + CV)}{\partial p} = \frac{\partial(pB + kV)}{\partial V}$$

The development of the last expression shows that $A = k$; that is, $\partial a / \partial V = \partial q / \partial p$. Hence the charge q of the piezo-electric condenser of 1 sq cm area is

$$q = CV - \delta \cdot p$$

where δ may have values equal to δ , $\delta' = (b/a)\delta$, or zero. We have also

$$\frac{\partial q}{\partial p} = V \frac{\partial C}{\partial p} - \delta = \frac{\partial a}{\partial V}$$

Since the variation of the capacitance C due to the pressure p , that is, $\partial C / \partial p$, is very small and C is hardly affected by V , the value of $\partial C / \partial p$ may be thought of as independent of V and we obtain

$$\Delta b = - \underbrace{\int_0^V \delta \cdot dV}_{\text{piezo-electric effect}} + \underbrace{\left(\frac{1}{C} \frac{\partial C}{\partial p} \right) \frac{CV^2}{2}}_{\text{common with all dielectrics}}$$

The dimensional changes along a , b , and c become

$$\left. \begin{aligned} \Delta a &= \delta V + \left[\frac{1}{C} \frac{\partial C}{\partial p} \right]_a \frac{CV^2}{2} && \text{(along the piezo-electric X-axis)} \\ \Delta b &= -\delta' V + \left[\frac{1}{C} \frac{\partial C}{\partial p} \right]_b \frac{CV^2}{2} && \text{(along the Y-axis)} \\ \Delta c &= \left[\frac{1}{C} \frac{\partial C}{\partial p} \right]_c \frac{CV^2}{2} && \text{(along the optic Z-axis)} \\ \delta' &= \frac{b}{a} \delta \end{aligned} \right\}$$

If the mechanical pressure p increases more and more, according to Curie, the charge q for each unit area of the $b \cdot c$ face increases accordingly and with it the voltage V across the coatings. But, according to the Lippman converse effect, we obtain a contraction which acts against the pressure p and as such opposes the original action. The resultant

effect is as though δ decreased. If $d\delta$ denotes the decrease which is assumed proportional to the contraction $\delta \cdot dV$, we have for an increase dV of potential difference

$$d\delta = -\beta \cdot \delta \cdot dV \quad \text{or} \quad \delta = \delta_0 \epsilon^{-\beta V}$$

where ϵ (for this particular formula) stands for the base of the system of natural logarithms, δ_0 is the limit of the piezo-electric modulus (for $V = 0$, practically equal to the Curie value), and δ is the modulus for any voltage V acting across the coating. Since an increase in V works against a decrease in δ , the sign of β is such that βV is positive. The dimensional changes along the b dimension are

$$\begin{aligned} \Delta b &= - \int_0^V \delta \cdot dV + \left(\frac{1}{C} \frac{\partial C}{\partial p} \right) \frac{CV^2}{2} \\ &= - \frac{\delta_0}{\beta} [1 - \epsilon^{-\beta V}] + \left(\frac{1}{C} \frac{\partial C}{\partial p} \right) \frac{CV^2}{2} \end{aligned}$$

and the saturation value of the piezo-electric deformation is δ_0/β . The dielectric term $\left(\frac{1}{C} \frac{\partial C}{\partial p} \right) \frac{CV^2}{2}$ of the deformation can be solved as follows: For the total capacitance C_t of the condenser of the area $b \cdot c$ sq cm, we have, for a dielectric constant κ ,

$$C_t = \frac{\kappa b \cdot c}{4\pi a}$$

and

$$\frac{1}{C_t} \frac{\partial C_t}{\partial p} = \frac{1}{\kappa} \frac{\partial \kappa}{\partial p} + \frac{1}{b} \frac{\partial b}{\partial p} + \frac{1}{c} \frac{\partial c}{\partial p} - \frac{1}{a} \frac{\partial a}{\partial p}$$

The dielectric deformation along the piezo-electric axis, that is, along the thickness a , then becomes

$$\left[\frac{1}{C_t} \frac{\partial C_t}{\partial p} \right]_a = \left[K - \frac{\sigma_y}{E} - \frac{\sigma_z}{E} - \frac{1}{E} \right] \frac{1}{b \cdot c}$$

where E is Young's modulus along the electric axis, σ_y Poisson's coefficient in the direction perpendicular to optic and electric axis, σ_z along the optic axis, and K the coefficient of variation κ by the force acting along the lines of force. Ny Tsi Ze has measured the deformations along the a , b , and c dimensions and for δ has found the value of 6.4×10^{-8} which checks well the Curie constant of 6.32×10^{-8} and substantiates the Lippman theory. By also observing the saturation phenomenon he found, for feeble piezo-electric quartz vibrations, the variations in centimeters along the a , b , and c dimension to be, respectively,

$$\left. \begin{aligned} \Delta a &= 6.4 \times 10^{-8} \times 114 \left[1 - \epsilon^{-\frac{V}{114}} \right] + 1.1 \times 10^{-11} \left[\frac{V}{a} \right]^2 \\ \Delta b &= -6.4 \times 10^{-8} \frac{b}{a} 114 \left[1 - \epsilon^{-\frac{V}{114}} \right] + 1.3 \times 10^{-11} \left[\frac{V}{a} \right]^2 \\ \Delta c &= 6.5 \times 10^{-12} c \left[\frac{V}{a} \right]^2 \end{aligned} \right\}$$

of which Δc is purely dielectric since no piezo-electric effect occurs along the optical axis.

117. Static Theory of Piezo Electricity.—Generally speaking, any stress will produce a strain, which is resolvable into six components. The electric field has three components; hence $3 \times 6 = 18$ equations with 18 constants are necessary for the complete definition of an electric effect in a crystal.

The electric state at any place in the interior of a crystal is given by the components P_1 , P_2 , and P_3 of the electric moment per unit volume. At the same place we have three dilations x_x , y_y , and z_z (elongations or contractions per unit length) and three angle changes x_y , y_z , and z_x .

The components of the electric moment per unit volume along the three coordinate axes are P_{x_0} , P_{y_0} and P_{z_0} . Their effects are always compensated by charges of opposite sign on the exterior surface so that the moments are not noticeable at once. But when forces are applied and deformations take place, new values P_x , P_y , and P_z appear. The differences

$$\left. \begin{aligned} P_1 &= P_x - P_{x_0} \\ P_2 &= P_y - P_{y_0} \\ P_3 &= P_z - P_{z_0} \end{aligned} \right\} \quad (5)$$

occur immediately after the deformation takes place and with their full intensity. For many crystals, including *quartz*, the symmetry is so good that the permanent moment

$$P_{x_0} = P_{y_0} = P_{z_0} = 0$$

and the observed moments, also known as "polarizations," are equal to those due to the deformation.

Using the theory of elasticity, we can assume that for small deformations a linear relation exists between the polarization and deformation. Hence along the three coordinates

$$\left. \begin{aligned} P_x &= \overbrace{\epsilon_{11}x_x + \epsilon_{12}y_y + \epsilon_{13}z_z}^{\text{dilation components}} + \overbrace{\epsilon_{14}y_z + \epsilon_{15}z_x + \epsilon_{16}x_y}^{\text{shear (angle) component}} \\ P_y &= \epsilon_{21}x_x + \epsilon_{22}y_y + \epsilon_{23}z_z + \epsilon_{24}y_z + \epsilon_{25}z_x + \epsilon_{26}x_y \\ P_z &= \epsilon_{31}x_x + \epsilon_{32}y_y + \epsilon_{33}z_z + \epsilon_{34}y_z + \epsilon_{35}z_x + \epsilon_{36}x_y \end{aligned} \right\} \quad (6)$$

According to Voigt, ϵ denote the piezo-electric constants. Their values depend on the kind of crystal and the position of its coordinate system with respect to the main axis. When the crystal possesses symmetry and the coordinate system is properly chosen, the number of components become less and the equations reduce to simple expressions. Voigt originally derived the foregoing equations by taking the thermodynamic potential ξ along the components of the electric-field strength \mathcal{E} , that is, from

$$-\frac{\partial \xi}{\partial \mathcal{E}_i} = P_i = \sum_h \epsilon_{ih} \cdot x_h$$

Since, in the classical experiments of the Curie brothers as well as for the vibrating crystals of today of W. Cady¹ (resonator) and G. W. Pierce² (first single-tube oscillator), the effective pressures X_x , Y_y , and Z_z along the three coordinate axes are of more practical importance, they are introduced in the following equations³ instead of the deformations x_x , y_y , and z_z . We obtain

$$\left. \begin{aligned} -P_x &= \overbrace{\delta_{11}X_x + \delta_{12}Y_y + \delta_{13}Z_z}^{\text{translation components}} + \overbrace{\delta_{14}Y_z + \delta_{15}Z_x + \delta_{16}X_y}^{\text{shear components}} \\ -P_y &= \delta_{21}X_x + \delta_{22}Y_y + \delta_{23}Z_z + \delta_{24}Y_z + \delta_{25}Z_x + \delta_{26}X_y \\ -P_z &= \delta_{31}X_x + \delta_{32}Y_y + \delta_{33}Z_z + \delta_{34}Y_z + \delta_{35}Z_x + \delta_{36}X_y \end{aligned} \right\} \quad (7)$$

where δ_{ik} denotes again a piezo-electric modulus and is found experimentally as is the piezo-electric constant ϵ_{ih} . They are connected through the relation

$$\delta_{ik} = \sum_h \epsilon_{ih} s_{hk} \quad \epsilon_{ih} = \sum_k \delta_{ik} c_{hk} \quad (8)$$

The factors s_{hk} and c_{hk} are the principal elastic factors, since from them can be computed the piezo-electric constants and moduli as well as Young's moduli, etc. For quartz at room temperature (unit stress 10^9 dynes cm^2), they have the values

$$\left. \begin{array}{lll} s_{11} & 1298 \times 10^{-6} & c_{11} \quad 851 \\ s_{33} & 990 \times 10^{-6} & c_{33} \quad 1053 \\ s_{44} & 2005 \times 10^{-6} & c_{44} \quad 571 \\ s_{12} & -166 \times 10^{-6} & c_{12} \quad 69.5 \\ s_{13} & -152 \times 10^{-6} & c_{13} \quad 141 \\ s_{14} & -431 \times 10^{-6} & c_{14} \quad 168 \end{array} \right\} \quad (9)$$

¹ CADY, W., *loc. cit.*

² PIERCE, G. W., *Proc. Am. Acad. Arts Sci.*, 59, No. 4, 81, 1923.

³ The deformations are linear functions of the pressure components and such that $x_x = c_{11}X_x + c_{12}Y_y + c_{13}Z_z + c_{14}Y_z + c_{15}Z_x + c_{16}X_y$, etc., from which it follows that $x_y = s_{11}X_x + s_{12}Y_y + s_{13}Z_z + s_{14}Y_z + s_{15}Z_x + s_{16}X_y$.

The various factors can be computed from

$$\left. \begin{aligned} \epsilon_{11} &= \delta_{11}[c_{11} - c_{12}] + \delta_{14}c_{14} \\ \epsilon_{14} &= 2\delta_{11}c_{14} + \delta_{14}c_{44} \\ \delta_{11} &= \epsilon_{11}[s_{11} - s_{12}] + \epsilon_{14}s_{14} \\ \delta_{14} &= 2\epsilon_{11}s_{14} + \epsilon_{14}s_{44} \end{aligned} \right\} \quad (10)$$

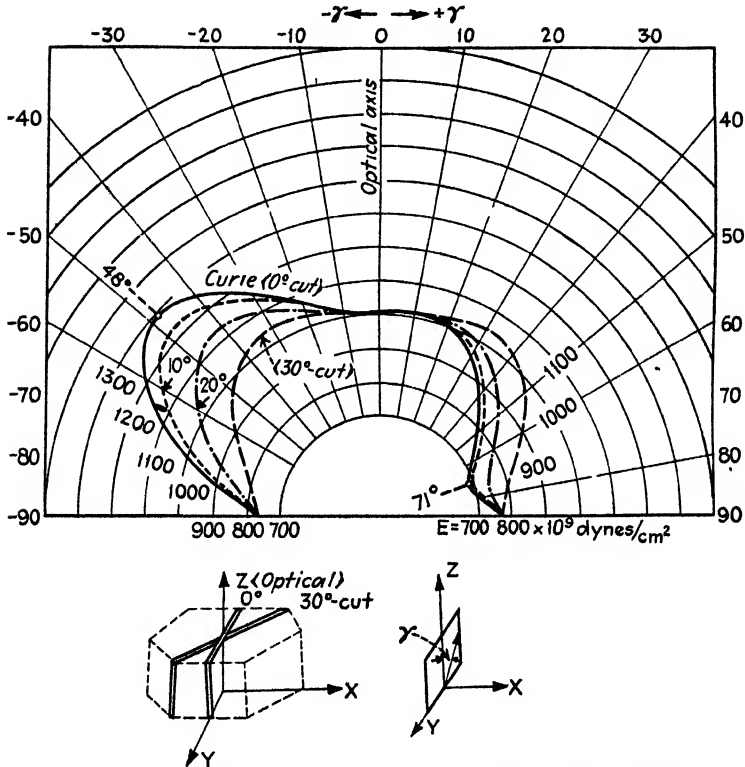


FIG. 189.—Modulus of elasticity E in any direction in space for zero degree (Curie), 10-, 20-, and 30-deg quartz cuts.

Since *Young's modulus* E changes with the direction except in the equatorial plane perpendicular to the optical axis, we have

$$\left. \begin{aligned} E_1 &= \frac{1}{s_{33}} = \frac{10^{-6}}{990} = 1010 \times 10^9 \text{ dynes/cm}^2 \text{ along the optical axis} \\ E_2 &= \frac{1}{s_{11}} = \frac{10^{-6}}{1298} = 770 \times 10^9 \text{ dynes/cm}^2 \text{ in the equatorial plane} \end{aligned} \right\} \quad (11)$$

Young's modulus in any direction given by the direction cosines α , β , and γ with respect to the coordinate axes X , Y , and Z can be calculated from

$$\frac{1}{E} = s_{11}[1 - \gamma^2]^2 + [s_{44} + 2s_{13}]\gamma^2[1 - \gamma^2] + s_{33}\gamma^4 + 2s_{14}\beta\gamma[3\alpha^2 - \beta^2] \quad (12)$$

The angles are as shown in Fig. 192 on page 302 while in the foregoing equation α , β , γ are written, for the sake of simplicity, instead of $\cos \alpha$, $\cos \beta$, and $\cos \gamma$. This is an important formula since it gives a means for finding maximum and minimum values of elasticities for different cuts as is shown in Fig. 189. By its use, the velocities of propagation in quartz can be computed since the density is constant and the empirical disk formulas (page 119)¹ can be theoretically explained.

Table IX contains the moduli of elasticity E underlying the curves shown in Fig. 189. It can be seen that—for the Curie cut—maximum and minimum values of E exist at (-48) and at $(+71)$ deg with respect to the optical axis.

TABLE IX

(cos ⁻¹ γ = φ) angle φ against optical axis	Modulus of elasticity E, 10 ⁹ dynes/cm ²				φ	E			
	Angle against the Curie cut, deg					Angle against the Curie cut, deg			
	0	10	20	30		0	10	20	30
-90	770	770	770	770	0	1010	1010	1010	1010
-85	810	810	795	775	5	1011	1011	1011	1011
-80	885	870	830	785	10	1015	1015 +	1015 +	1017
-75	965	942	877	805	15	1010	1010	1016	1023
-70	1045	1010	930	831	20	1000	1005	1015	1032
-60	1208	1150	1027	900	25	980	990	1010	1036
-55	1260	1202	1072	935	30	953	965	996	1045
-48	1285	1234	1116	985	35	915	930	975	1040
-45	1280	1231	1127	1000	40	870	890	945	1025
-40	1250	1215	1127	1025	50	785	805	867	970
-35	1210	1180	1118	1041	60	720	738	798	900
-30	1162	1145	1100	1046	65	700	717	775	862
-25	1117	1106	1078	1043	71	648	707	753	825
-20	1075	1070	1055	1035	75	695	705	745	805
-15	1045	1041	1035	1025	80	707	718	745	786
-10	1023	1022	1020	1020	90	770	770	770	770
- 5	1012	1012	1012	1012					

Equations (6) and (7) become much simpler for quartz when the coordinate system is properly chosen. First, by putting Z along the optical axis, we have threefold symmetry about this axis. We can turn the system by 120 deg without changing the relation between the electric

¹ *Proc. I.R.E.*, 16, 447, 1926.

moments and the deformations. This leads to the following simplification in the piezo-electric constants:

$$\left. \begin{aligned} \epsilon_{11} &= -\epsilon_{12} = -\epsilon_{26} \\ \epsilon_{22} &= -\epsilon_{21} = -\epsilon_{16} \\ \epsilon_{15} &= \epsilon_{24} \\ \epsilon_{14} &= -\epsilon_{25} \\ \epsilon_{31} &= \epsilon_{32} \\ \epsilon_{13} &= \epsilon_{23} = \epsilon_{34} = \epsilon_{35} = \epsilon_{36} = 0 \end{aligned} \right\} \quad (13)$$

In addition to this, the quartz also has three twofold symmetry axes (in Fig. 188 along the X -axis). Therefore, we can turn the system by 180 deg about such an axis without disturbing the foregoing relations between the electric moments and the deformations. This gives the following simplifications:

$$\epsilon_{15} = \epsilon_{22} = \epsilon_{31} = \epsilon_{33} = 0 \quad (14)$$

and Eqs. (6) and (7) simplify to

$$\left. \begin{aligned} P_x &= \epsilon_{11}[x_x - y_y] + \epsilon_{14}y_z \\ P_y &= -\epsilon_{14}x_x - \epsilon_{11}y_y \\ P_z &= 0 \end{aligned} \right\} \quad (15)$$

and

$$\left. \begin{aligned} -P_x &= \delta_{11}[X_x - Y_y] + \delta_{14}Y_z \\ + P_y &= \delta_{14}X_x + 2\delta_{11}Y_y \\ P_z &= 0 \end{aligned} \right\} \quad (16)$$

since

$$\delta_{11} = -\delta_{12} = (\frac{1}{2})\delta_{26} \quad \text{and} \quad \delta_{25} = -\delta_{14}$$

Both sets of equations show that there can be no piezo-electric effect along the optical axis. It is evident that the Y -component is produced only by shear strains, while the polarization P_x is produced by linear and angular changes. According to Voigt, the values for the piezo-electric moduli¹ in c.g.s.e.s. units are

$$\left. \begin{aligned} \delta_{11} &= -6.45 \times 10^{-8} \\ \delta_{14} &= -1.45 \times 10^{-8} \end{aligned} \right\} \text{ (in c.g.s.e.s. units)} \quad (17)$$

and the piezo-electric constants, according to the elasticity constants given on page 290 and formulas (10), become

¹ According to Sosman, the most probable values of the moduli at room temperature are $\delta_{11} = -69 \times 10^{-9}$ and $\delta_{14} = 17 \times 10^{-9}$ where the pressures are in dynes per square centimeter and the electric charge in e.s.c.g.s. units per square centimeter. (R. B. Sosman, "The Properties of Silica," *Am. Chem. Soc. monograph ser.*, Chap. XXVIII, beginning with p. 555. This chapter is a very clear exposition of piezo electricity in quartz).

$$\left. \begin{aligned} \epsilon_{11} &= -4.77 \times 10^4 \\ \epsilon_{14} &= 1.73 \times 10^4 \end{aligned} \right\} \text{ (in c.g.s.e.s. units)} \quad (18)$$

Now using the shears, we obtain

$$P_x = \epsilon_{11}x_x - \epsilon_{11}y_y \quad (19)$$

and

$$-P_x = \underbrace{\delta_{11}X_x}_{\substack{\text{effect} \\ \text{along} \\ \text{piezo-} \\ \text{electric} \\ \text{axis}}} - \underbrace{\delta_{11}Y_y}_{\substack{\text{effect} \\ \text{along} \\ Y\text{-axis}}} \quad (20)$$

Hence only terms dealing with the thickness and transverse effects remain.

For oscillator and resonator work a quartz element is often excited by an electric field \mathcal{E}_x acting along the piezo-electric X -axis (Curie cut). The pressure components along the X - and Y -axes are then given by

$$\left. \begin{aligned} -X_x &= \epsilon_{11}\mathcal{E}_x \\ Y_y &= \epsilon_{11}\mathcal{E}_x \end{aligned} \right\} \quad (21)$$

and the corresponding deformation equations are

$$\left. \begin{aligned} x_x &= \delta_{11}\mathcal{E}_x \text{ (thickness effect)} \\ y_y &= -\delta_{11}\mathcal{E}_x \text{ (transverse effect)} \end{aligned} \right\} \quad (22)$$

Thus the absolute values of the tensions X_x and Y_y due to the electric field are equal, as are the numerical values of the dilations x_x , and y_y .

When a voltage V is applied to the metal coatings whose planes are perpendicular to the X - (electric-) axis, the field strength, according to Figs. 188 and 195,

$$\mathcal{E}_x = \frac{V}{a}$$

and the total force produced on one coating of area $b \cdot c$, when the coating on the opposite face of the piezo-electric quartz element is kept fixed, becomes

$$\begin{aligned} F &= X \cdot b \cdot c = -\epsilon_{11}\mathcal{E}_x \cdot b \cdot c \\ &= 4.77 \times 10^4 \frac{\text{coated area}}{\text{thickness}} V \end{aligned} \quad (23)$$

where F is in dynes and the space dimensions¹ of the crystal in centimeters, and the voltage in e.s.c.g.s. units.

From the deformation Eq. (22), we find

$$x_x = \delta_{11} \frac{V}{a}$$

¹ The piezo-electric constants ϵ have the dimension of an electrostatic polarization, and the moduli δ the dimension of the reciprocal of an electric intensity.

and the total elongation or contraction for the thickness a , along one of the electric axes of quartz is

$$x = a \cdot x_z = 6.45 \times 10^{-8} V \quad (24)$$

At this point it may be of interest to know how the static piezo-electric effect compares with the dielectric effect. Suppose a plate of quartz the Curie cut has a thickness of 0.1 cm and an electrode face perpendicular to the X -axis of 2×2 cm². From Eq. (23) we can calculate what force results from the application of a certain voltage, say 300 volts, if the crystal is tightly clamped between the electrodes and the polarization is such as to tend to cause an expansion. Bearing in mind that 300 volts are 300/300 e.s.u., for the *piezo-electric force* we obtain

$$F = 4.77 \times 10^4 \frac{4}{0.1} \text{ dynes}$$

or 1.905 kg, since 1 g = 981 dynes. However, there is also an electrostatic or dielectric force as for any plate condenser whose dielectric is no piezo electric. This force can be computed from

$$F = 442 \times 10^{-9} \frac{\text{coated area}}{(\text{thickness})^2} \kappa V^2 \text{ dynes} \quad (25)$$

which, for the foregoing case and for a dielectric constant $\kappa = 4.6$ along the electric axis, gives a *dielectric force*

$$F = 73.2 \text{ dynes}$$

The piezo-electric force is, therefore, about 25,000 times as great as the force due to the electrostatic effect.

The total change in thickness can also be found by use of Eq. (24). It is only 6.45×10^{-8} cm for 300 volts.

By means of Eq. (20) it is possible to prove the empirical formulas [Eqs. (1) and (2)] of the Curie brothers. When $S_x = b \cdot c$ stands for the area of the crystal face perpendicular to the X -axis, and $S_y = a \cdot c$ for the faces perpendicular to the Y -axis, we obtain, for a total force F acting along X and across S_x

$$-P_x = \delta_{11} X_x = \delta_{11} \frac{F}{S_x}$$

since there is no force applied along the Y -axis. Hence the total charge

$$Q = P_x S_x = -\delta_{11} F$$

which confirms Eq. (1).

When the total force F acts along the Y -axis and across face S_y , the term $\delta_{11} X_x$ disappears in Eq. (20) and

$$P_z = \delta_{11}Y_y = \delta_{11}\frac{F}{S_y}$$

or

$$Q = P_z S_z = \delta_{11}\frac{S_z}{S_y}F = \delta_{11}\frac{b}{a}F$$

proving Eq. (2), since S_y now denotes the pressed area. It shows that the charge¹ is larger, the longer the length b compared with thickness a .

When a disk is cut out of a crystal in any arbitrary direction, and a pressure p is applied perpendicular to the circular face, and α , β , and γ denote the direction cosines of the cylinder axis of the disk, the components of piezo-electric polarization (electric moment per unit volume) of Eq. (16) become

$$\left. \begin{aligned} P_x &= [\delta_{11}(\alpha^2 - \beta^2) + \delta_{14}\beta\gamma]p \\ P_y &= \alpha[\delta_{14}\gamma + 2\delta_{11}\beta]p \\ P_z &= 0 \end{aligned} \right\} \quad (26)$$

because the elastic pressures along the coordinate axes are

$$X_x = p\alpha^2; \quad X_y = p\beta^2; \quad X_z = p\gamma^2$$

and the shear components become

$$Y_x = p\beta\gamma; \quad Z_x = p\alpha\gamma; \quad X_y = p\alpha\beta$$

The piezo-electric moment P in any direction, with direction cosines α_1 , β_1 , and γ_1 , is then

$$P = \alpha_1 P_x + \beta_1 P_y \quad (27)$$

since $\gamma_1 P_z$ is zero for quartz. When P is perpendicular to a surface, it represents the surface density of charge and gives a means for calculating the total charge.

Equation (26) gives another way of checking Curie's empirical law since, for a pressure $p = X_z$ acting along the electrical axis, we have $\alpha = 1$ and $\beta = \gamma = 0$, giving again $P_x = -\delta_{11}p = -\delta_{11}X_z$.

118. Notes on Dynamic Piezo Electricity.—The static theory as originally given by W. Voigt can also be applied to vibrating quartz crystals as long as the temperature is not higher than 300°C, because the piezo activity is practically constant within the range of temperature²

¹ For the total charge produced, the capacity effect must be taken into account [formulas (40) and (41)].

² PERRIER, A., and B. DE MANDROT, *Compt. rend.*, **175**, 622-624, corrections on p. 1006, 1922; *Mem. soc. Vandoise, sci. nat.*, **1**, 333-364, 1923; S. NAMBA, and S. MATSUMURA, *Researches of the Electrotechnical Laboratory, Japan*, No. 248, April, 1929; F. R. LACK, *Proc. I.R.E.*, **17**, 1123-1141, 1929.

from 20 to 300°C. Above 300°C the piezo-electric moduli decrease considerably. At about 200°C a slight maximum in δ is also noted.

In dealing with quartz oscillators and resonators, the piezo-electric element constitutes an extremely complex vibration system with a great number of degrees of freedom which for the most part are combinations of certain fundamental types of vibrations. According to the static theory, crystal quartz requires six constants to express the relation between stress and strain, while fused quartz, which is fairly isotropic, involves only two constants. The particular constants for crystal quartz which apply to certain modes of vibration depend upon the orientation of the quartz plate with respect to the threefold optical and twofold electrical axes.

We must distinguish among longitudinal, flexural (lateral, transverse, or bending), and torsional vibrations. Each of these has many higher modes. This subdivision is especially useful for the case of vibrating rods and long bars.

Applying Voigt's theory to vibrating systems, Laue¹ found that there is a free potential energy per unit volume for the alternate effect between electric field and elastic tensions according to

$$U = [\delta_{11}X_x - \delta_{11}Y_y + \delta_{14}Y_z]\mathcal{E}_x - [\delta_{14}Z_x + 2\delta_{11}X_y]\mathcal{E}_y \quad (28)$$

since for the corresponding deformations

$$U = -[\epsilon_{11}x_x - \epsilon_{11}y_y + \epsilon_{14}y_z]\mathcal{E}_x + [\epsilon_{14}z_x + \epsilon_{11}x_y]\mathcal{E}_y \quad (29)$$

where \mathcal{E}_x and \mathcal{E}_y are the components of the electric field, since \mathcal{E}_z has zero effect, because it acts along the optical axis. For the displacement² components u , v , and w , we have

$$x_x = \frac{\partial u}{\partial x}; \quad y_y = \frac{\partial v}{\partial y}; \quad y_z = \frac{\partial v}{\partial z} + \frac{\partial w}{\partial y}; \quad z_x = \frac{\partial w}{\partial x} + \frac{\partial u}{\partial z}; \quad x_y = \frac{\partial u}{\partial y} + \frac{\partial v}{\partial x}$$

119. Design Formulas for Curie-cut Quartz Elements Producing Longitudinal Vibrations.—When a crystal is cut as in Fig. 188 and the exciting electrodes arranged parallel to faces $b \cdot c$, two alternate effects are possible, according to the Curie-Lippman laws—one along the thickness a , and one along the dimension b . No electrical effects can be set up along the optical dimension c . Therefore vibrations can be produced at least along the X or along the Y dimension when an electric alternating field acts along the piezo-electric axis X . If the frequency of the applied alternating field is the same as that of a possible mode of vibration along either of these two dimensions, an oscillation of pronounced amplitude must occur.

¹ VON LAUE, M., *Z. Physik*, **34**, 347, 1925.

² Generally a portion of a body has displacements δx , δy , and δz . But when actual displacements exist, the displacement components, u , v , and w replace δx , δy , and δz .

With the customary mounting (one electrode on each side along the entire $b \cdot c$ face) it may be assumed that a longitudinal thickness vibration occurs along a , and that for the fundamental mode $a = \lambda/2$, where λ denotes the wave length of the stationary wave system set up in the quartz element because of resonance (natural vibration). Since the density of crystal quartz is known ($= 2.654$ g/cc) and Young's modulus of elasticity E , according to Eq. (11), is equal¹ to 770×10^9 g cm⁻¹ sec⁻², we have for the velocity of propagation in crystal quartz anywhere in the XY -plane or parallel to it

$$v = \sqrt{\frac{E}{D}} = 540 \times 10^3 \text{ cm/sec}$$

Hence the supersonic sound waves are in the equatorial plane propagated with a velocity which is 16.3 times as great as in the air. Now, since $\lambda f = v$ and $2a = \lambda$, we find that the frequency

$$f = \frac{v}{2a} = \frac{2700}{a} \text{ kc/sec} \quad (30)$$

when the thickness a is expressed in millimeters. This corresponds to 111.1 m electromagnetic wave length for each millimeter thickness, since $f^{(\text{kc/sec})} = 3 \times 10^5$ m/sec. However, experiments² show that for Curie plates of nearly any shape the thickness constant is somewhat smaller and close to a value 104.6 m/mm. This leads to the *design formula*

$$f_1 = \frac{2870}{a_{(\text{mm})}} \text{ kc/sec (Curie-cut thickness formula)} \quad (31)$$

which holds for pressure variations X_x with the electric field along the X -axis. The small discrepancy between the theoretical and the design formula is probably due to the fact that, as the quartz plate contracts and expands along the thickness a , it also bulges in and out along the cross dimension b along the Y -axis. Therefore it produces small shearing effects which ought to be taken into account in the theoretical formula (30).

Another natural fundamental longitudinal vibration is due to Y_y stress variations which likewise occur along the equatorial plane. We have again the velocity $v = 540 \times 10^3$ cm/sec, in quartz, and find the design formula for the dimension b along the Y -axis

$$f_2 = \frac{2700}{b_{(\text{mm})}} \text{ kc/sec (Curie-cut width formula)} \quad (32)$$

In this case, the constant 2700 corresponding to 111.1 m wave length per millimeter width can be better satisfied with the theoretical formula,

¹ Since in the physical-unit system the unit of a force 1 g cm/sec² = 1 dyne.

² *Proc. I.R.E.*, 16, 447, 1926, Tables I and II.

since any resonance vibration along the b dimension is less affected by any corresponding thickness effects that may occur since the thickness, as a rule, is much smaller than the width. This formula is, therefore, especially useful when low-frequency crystals are to be designed. Today such crystals are employed for stepping the frequency down to still lower values by means of relaxation oscillators, and up for frequency meter-calibration work. The rectangular bar shown in Fig. 190 according to measurement gives 30 kc/sec. Design formula (32) gives 30.7 kc/sec.

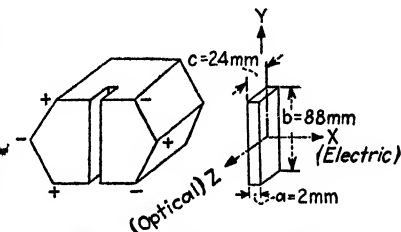


FIG. 190.—Piezo-electric quartz element.

Experiment shows, however, still another pronounced fundamental oscillator¹ frequency. It may be called the "coupling frequency." For a square plate it is ($b = c$, Fig. 188)

$$f_3 = \frac{3330}{b(\text{mm})} \text{ kc/sec (Curie-cut coupling frequency of square plate of side } b) \quad (33)$$

This coupling frequency exists even for a nonsquare form, as long as one of the two dimensions b and c along the Y - and optical axes is not unreasonably small compared with the other. But when b and c are not equal, the constant 3330 in (33) is also different. For instance, for a Curie plate $a = 7.1$ mm, $b = 42.08$ mm, and $c = 39.62$ mm, the frequencies $f_1 = 404$, $f_2 = 66.05$, and $f_3 = 85.43$ kc/sec were measured and values $f_1 a = 2870$, $f_2 b = 2780$, and $f_3 b = 3590$ were obtained instead of 3330.

There are more reliable design formulas for circular crystals. For a thickness a in millimeters along the electrical X -axis, and a diameter d in millimeters, anywhere in the XY -plane or parallel to it, they are

$$\left. \begin{aligned} f_1 &= \frac{2870}{a(\text{mm})} \\ f_2 &= \frac{2715}{d(\text{mm})} \\ f_3 &= \frac{3830}{d(\text{mm})} \end{aligned} \right\} \text{kc/sec (Curie-cut disk formulas)} \quad (34)$$

¹ Oscillator frequencies must be distinguished from resonator frequencies, since very many response frequencies can be observed when the crystal is connected up in a resonator circuit. For a Curie crystal in an oscillator circuit, we obtain normally three different frequencies (thickness frequency, width or Y frequency, and coupling frequency) for rectangular plates of the Curie cut. There are also three frequencies for circular Curie cuts.

These formulas have been applied to the design of disk crystals since 1923 for nearly every useful size and seem to hold within about 1 per cent. These disk formulas can be theoretically explained. The thickness formula is the same as proved above. However, for the diameter expressions, it does not seem correct to assume that we have a vibration along the Y -axis together with a coupling frequency, wherever and whatever it may be, since the physical boundary is now a circle and, for the isotropic case, any wavelike disturbance traveling along a certain diameter would experience the same reflection at the boundary as along any other diameter. But, for the Curie cuts, the modulus of elasticity E and consequently the velocity of propagation depend on the direction of the diameter (Fig. 189). Therefore the equivalent boundary curve is no longer a circle but a curve which can be derived from the polar curve of Fig. 189 by extracting the square root of each radius vector E and multiplying it by a constant. The constant is the reciprocal of the square-root value of the density of the crystal quartz (2.654 g/cc). The velocity of propagation can be calculated from the diameter formulas since, according to (34), the frequency constants are

$$\left. \begin{aligned} K_2 &= f_2 d = 2715 \\ K_3 &= f_3 d = 3830 \end{aligned} \right\}$$

and the respective velocities and moduli of elasticity are

$$\left. \begin{aligned} v_2 &= 2K_2 = 543 \\ v_3 &= 2K_3 = 766 \end{aligned} \right\} \times 10^3 \text{ cm/sec} \quad \text{and} \quad \left. \begin{aligned} E_2 &= 2.654v_2^2 = 780 \\ E_3 &= 2.654v_3^2 = 1560 \end{aligned} \right\} \times 10^9 \text{ g cm}^{-1} \text{ sec}^{-2} \quad (34a)$$

The velocity ratio is $v_3/v_2 = \sqrt{2}$, and the corresponding elasticity ratio $E_3/E_2 = 2$, a simple result which needs further investigation.

A. Meissner,¹ who has also experimented with circular crystals, gives Kundt's dust figure as shown in Fig. 191. When the lines along the optical Z -axis and places of maximum powder displacement are drawn, it will be noticed that at an angle (-48°) with the optical axis the longitudinal vibration of frequency f_3 occurs, and at an angle of $+71^\circ$ the longitudinal vibration of frequency f_2 takes place. Strictly speaking, maximum excitation occurs along these directions when either the f_3 or the f_2 vibrations set in, and the supersonic air waves blow away the dust along these directions. From the elasticity curves of Fig. 189, we note

¹ MEISSNER, A., *Physik. Z.*, **28**, 621-625, 1927; A. KUNDT, *Ber. Akad.*, **16**, 421, 1883. (Lycopodium powder is distributed uniformly over crystal plate and around it.)

that, for a Curie cut, these directions coincide with the values $E_{\max} = E_{-48} = 1285 \times 10^9$ dynes/cm² and $E_{\min} = E_{+71} = 648 \times 10^9$ dynes/cm², which gives an elasticity ratio $E_{-48}/E_{+71} = 1.985$, that is, almost 2. The slight difference is due, no doubt, to slide-rule errors in evaluating Eq. (12)¹ (Table IX, page 292).

When the principal elastic factors as given by W. Voigt² are used instead of the more recent values used above, the constants of the elasticity equation become $A = 1273$, $B = 1669$, $C = 970$, and $D = 846$, and

$$E_{-48}/E_{+71} = 1310/660 = 1310/660 = 1.985.$$

Again, a ratio value which is practically 2 as found from the empirical disk formulas given in Eq. (34).

120. Design Formulas for the 30-deg-cut Crystal.—A 30-deg crystal

cut as indicated in Fig. 188 has its electrode faces $a \cdot c$ parallel to the XZ -plane, and the electric field is applied along the Y -axis. As a rule, it seems to oscillate much more readily than a Curie-cut crystal. We can assume that vibrations are possible along the X -axis, that is, along the width a , and along the thickness b which is along the lines of electric force of the applied field. For thin plates of large area $a \cdot c$, the approximate design formula for the thickness vibration is

$$f_1 = \frac{1960}{b} \text{ kc/sec (30-deg.-cut thickness formula)} \quad (35)$$

¹ For computations, Eq. (12) is conveniently put in the form

$$E = \frac{10^9}{A[1 - \cos^2 \gamma]^2 + B \cos^2 \gamma[1 - \cos^2 \gamma] + C \cos^4 \gamma - D \cos \gamma \sin^2 \gamma \sin 3\psi}$$

where $\sin 3\psi = -1$ for the Curie cut, since, according to Fig. 192, ψ denotes the angle of the cut (perpendicular to the equatorial XY -plane) with the electric axis and is 90 deg. The constants are according to the principal elastic factors given in Eq. (9): $A = 1298$; $B = 1701$; $C = 990$; and $D = 862$. For $\gamma = -48^\circ$; $\cos \gamma = 0.6691$; $\cos^2 \gamma = 0.446$; $\cos^4 \gamma = 0.2$; $1 - \cos^2 \gamma = 0.554$; $[1 - \cos^2 \gamma]^2 = 0.306$; $\sin \gamma = -0.7431$; $\sin^2 \gamma = -0.41$ and $E_{-48} = \frac{10^9}{397 + 420 + 198 - 236} = 1285$ dynes/cm². For $+71$ deg, we find $\cos \gamma = 0.3256$; $\cos^2 \gamma = 0.106$; $\cos^4 \gamma = 0.1062$; $1 - \cos^2 \gamma = 0.894$; $[1 - \cos^2 \gamma]^2 = 0.8$; $\sin \gamma = 0.9455$; $\sin^2 \gamma = 0.845$; hence

$$E_{+71} = \frac{10^9}{1038 + 161 + 105 + 237} = 648 \text{ dynes/cm.}^2$$

² Voigt, W., *Pogg. Ann.*, 33, 464, 1887; F. SAVART, *Pogg. Ann.*, 16, 206, 1829.

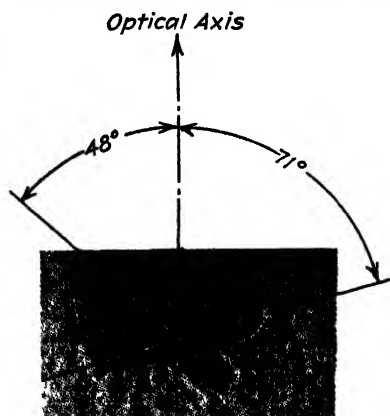


Fig. 191.—Dust pattern of a circular quartz disk in the Curie cut.

where b is in millimeters, since an electromagnetic wave length of about 153 m corresponds to each millimeter of thickness.¹ It can be seen that 30-deg-cut crystals give a lower frequency than Curie-cut crystals of the same thickness. Since the constant 1960 in Eq. (35) stands because of the relation

$$f = \frac{v}{2b}$$

for the velocity of propagation along the thickness dimension b , we have

$$v = 392 \times 10^3 \text{ cm/sec} = \sqrt{\frac{E}{D}}$$

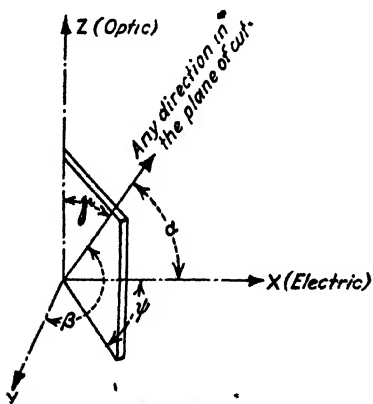


FIG. 192.— $\cos \alpha = \sin \gamma \cos \psi$ and $\cos \beta = \sin \gamma \sin \psi$.

giving a modulus of elasticity $E = 392^2 \times 10^6 \times 2.654 = 408 \times 10^9$ dynes/cm². According to Fig. 189 and Table IX (page 292) this cannot be a longitudinal modulus, since it is altogether too small. The wave disturbance in the crystal must therefore follow a law

which is more complex. Such a magnitude of the modulus is shown to be possible if we assume, as Cady² did, that a shear vibration occurs according to a shearing stress X_y in the XY -plane; then we should obtain $v = 360 \times 10^3$ cm/sec instead of 392×10^3 cm/sec. However, this assumption requires that the shear modulus give rise to a positive temperature coefficient.³ The thickness dimension of a 30-deg cut quite often gives two response frequencies which are almost alike (about 1 kc/sec apart).

The other possible oscillation is a longitudinal vibration along the X -axis and can be calculated from the ordinary formula

$$f_2 = \frac{2860}{a_{(\text{mm})}} \text{ kc/sec (30-deg-cut width formula)} \quad (36)$$

121. Temperature⁴ Coefficients of Curie-cut and 30-deg-cut Quartz Elements.—For the thickness and Y vibrations in a Curie-cut crystal and the width vibrations along the X -axis of a 30-deg crystal, the temperature coefficient of the frequency is *negative* since it depends mainly

¹ When the plates are not very thin and of large area, the electromagnetic wavelength constant varies considerably with the dimension a . In some cases, this constant lies anywhere between 140 to 165 m/(mm dimension).

² Cady, W. G., *Phys. Rev.*, **29**, 617, 1927.

³ Lack, F. R., *Proc. I.R.E.*, **17**, 1128, footnote 9, 1929.

⁴ Ferrier, A., and B. de Mandrot, *loc. cit.*; S. Namba and S. Matsumura, *loc. cit.*; F. R. Lack, *loc. cit.*

upon the temperature coefficient of Young's modulus in the equatorial XY -plane. The temperature effects on the density and the dimension play a minor part only. Figure 193 gives the variations¹ for the X and the Y direction. The average temperature coefficients are

$$\left. \begin{aligned} K_{t_x} &= -0.002 \text{ to } -0.0035\% \text{ (Along electric axis for Curie and 30-deg cut)} \\ K_{t_y} &= -0.005 \text{ to } -0.007\% \text{ (Along } Y\text{-axis for Curie cut)} \\ K_t &= -0.004 \text{ to } -0.007\% \text{ (For coupling frequency of Curie cut)} \end{aligned} \right\} \quad (37)$$

That is, from 20 to 35 cycles in one million is the change in frequency for each degree centigrade for thickness vibrations of Curie-cut crystals and for vibrations along the X -axis for 30-deg-cut plates.

The temperature coefficient of the thickness frequency of a 30-deg-cut crystal is usually *positive* and varies with the dimension along the X -axis of the plate, and in addition it is also dependent upon the temperature. It is

$$K_{t_x} = (+0.01) \text{ to } (-0.002)\% \text{ (Along thickness of 30-deg-cut crystal)} \quad (37a)$$

which means that the thickness frequency varies from +100 cycles in a million per degree centigrade to -20 cycles. Hence there must be a case for which zero temperature coefficient exists. Moreover, for 30-deg-cut crystals, abrupt changes in oscillation frequency are observed at several points of temperature. Further, experiment shows that the temperature coefficient for plates cut in the same plane varies also with the size and shape of the plate.

Since the thermal expansion coefficients² of quartz are known with great accuracy and their mean values between 0 and 20°C. are, for a direction parallel with the optic axis, $k_x = 7.3 \times 10^{-6}$ and, perpendicular to it, $k_{xy} = 13.5 \times 10^{-6}$, we can find the temperature coefficient e of the modulus of elasticity E since the temperature coefficient K of the fre-

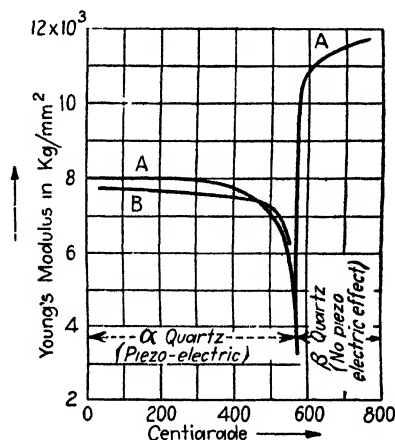


FIG. 193.—Curve A gives Young's modulus along the electric X -axis. (A. Perrier and B. de Mandrot.) Curve B along the Y -axis. (S. Namba and S. Matsumura.)

¹ Below 570°C, crystal quartz has a trigonal-trapezohedral symmetry and is known as α quartz, but above this temperature it turns into β quartz which is of a hexagonal trapezohedral type and loses piezo-electric activity since the atomic arrangement is somewhat changed.

² KOHLRAUSCH, F., "Lehrbuch der praktischen Physik," 16th ed., 1930, p. 158; E. GIEBE and A. SCHEIBE (Z. Hochfreq., 35, 165, 1930) have discussed this subject for luminous-rod resonators.

quency can be found experimentally. If a quartz rod is excited as in Fig. 198, it produces transverse (or flexural) vibrations. According to Eq. (58) on page 315, the fundamental frequency f is proportional to $(c/b^2)\sqrt{E/D}$ if b denotes the long dimension along the Y -axis and c is the dimension along the optic axis. The effect of the temperature t on the temperature coefficient K_1 is measured for the flexural-rod oscillation

$$f[1 + K_1 t] = \frac{[1 + k_s t]c}{[1 + 2k_{xy} t]b^2} \sqrt{\frac{[1 + et]E}{[1 - (2k_{xy} + k_s)t]D}}$$

from which

$$K_1 = 1.5k_s - k_{xy} + 0.5e$$

or

$$e = 2K_1 + 2k_{xy} - 3k_s$$

For the fundamental mode of the longitudinal vibration along the b dimension and excited in the usual Curie fashion along the electrical X -axis, that is, along the a dimension, we have the frequency formula $f = (1/2b)\sqrt{E/D}$. Calling K_2 the temperature coefficient of the frequency for this kind of oscillation, we find, by the same procedure as above, $K_2 = 0.5(k_s + e)$; that is,

$$e = 2K_2 - k_s$$

We can therefore compute the temperature coefficient e of the modulus of elasticity E either from the experimental value K_1 obtained from the fundamental transverse vibration or from the experimental value K_2 when the rod is excited in the fundamental longitudinal mode. The value of e is then very small and about -10^{-5} . By eliminating e from the two expressions obtained for it, we find

$$K_2 - K_1 = k_{xy} - k_s$$

which can be checked experimentally since K_2 and K_1 may be found by measuring the respective fundamental frequencies at two different temperatures.

122. Air-gap and Pressure Effect on Frequency.¹—As will be shown in Sec. 124 giving the equivalent electric circuit of quartz, the frequency is also affected by a change in the air gaps between the main crystal faces and the electrodes. Figure 194 shows the effect of both the pressure and the air-gap effect. If a mechanical load such as a heavy metal electrode is put on the piezo-electric element, its frequency is increased. If the electrode is very gradually removed, the true crystal frequency is produced for a moment (when the effect of the tube and the rest of the circuit

¹ PIERCE, G. W., *Proc. Am. Acad. Arts. Sci.*, **10**, 271, 1925; see also *Proc. I. R. E.*, **16**, 1072, 1928.

is neglected), while a very small air gap again gives a somewhat higher frequency. For the case shown in Fig. 194, two large disk crystals (Curie cut) were excited in the thickness vibration (frequency about 130 kc/sec) and the output branches coupled to a common coil with a rectifier in the circuit. The air gap of one crystal was varied. The ordinates give the beat frequency and the abscissas the air-gap distance in inches. It can be seen that, with the upper electrode just resting in the piezo-electric element, the beat frequency is about 118 cycles/sec. It then drops to a value of about 116 cycles/sec and ascends again as indicated until the oscillation suddenly stops, since the condition for one-half wave length of

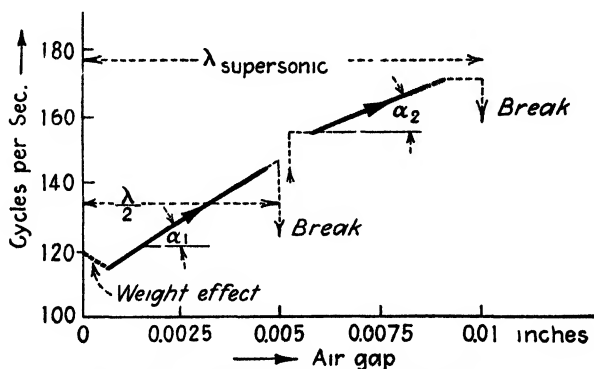


FIG. 194.—Frequency change with air gap.

the supersonic sound wave exists, and from the $\lambda/2$ as well as the λ condition, etc., the sound velocity in the gap is found to be

$$v = 0.258064 \times 131,240 = 338.68 \text{ m/sec,}$$

at 24.5°C, that is, about of the order of audible sound waves in air. If l denotes the length of the gap, v the velocity of supersonic sound waves in centimeters per second, f the frequency in cycles per second, and $p = 1, 2, 3 \dots$, the air column between the upper face of the quartz and the upper electrode will be set into resonance and oscillations will stop when

$$l = \frac{pv}{2f} \quad (38)$$

When stable oscillations are desired, air gaps of about this length should be avoided.

123. Total Values of Polarization, Displacement Current, and Charge for Mounted Quartz Elements.—Suppose a Curie cut of thickness a , with one electrode face of the plate fixed and the other free to move when an alternating field due to a voltage V is applied along the a direction (X direction). The *total polarization* is then

$$\begin{aligned}
 P &= P_1 + P_2 \\
 &= \underbrace{\frac{\kappa V}{4\pi a}}_{\text{due to condenser action}} + \underbrace{\frac{2\epsilon x}{a}}_{\text{due to piezo-electric action}}
 \end{aligned} \tag{39}$$

where $\kappa = 4.55$ denotes the dielectric constant of crystal quartz along the X direction, x the amplitude of the movable surface, and $\epsilon = -4.77 \times 10^4$ the piezo-electric constant along a . The first term is well known, and the second term is due to Eq. (15), since $P_2 = P_x$ and only the term $\epsilon_{11}x_x$ is of interest here. We have $2x = ax_x$ in $P_2 = \epsilon x_x$ because the actual maximum elongation or contraction of the thickness of the plate is $2x$.

The total displacement current of a condenser with a piezo-electric dielectric, is

$$i = S \frac{dP}{dt} = \underbrace{\frac{\kappa S}{4\pi a} \frac{dV}{dt}}_{\text{proportional to change in voltage}} + \underbrace{\frac{2\epsilon S}{a} \frac{dx}{dt}}_{\text{proportional to velocity}} \tag{39a}$$

where S denotes the area $b \cdot c$ of the main crystal (Fig. 188) faces which are assumed to be the same size as the electrodes.

If V and the charge Q are expressed in the c.s.e.g.s. system, the force F in dynes (Eq. 23), and the dimensions of the quartz plate in centimeters, we have, for the extension Δa of the a dimension and the charge Q liberated at either electrode, when a variable force F acts across faces $S = b \cdot c$,

$$\begin{aligned}
 \Delta a &= \frac{a}{S \cdot E} F - \delta \cdot V \\
 Q &= \underbrace{\frac{\kappa S}{4\pi a} V}_{\text{dielectric effect}} + \underbrace{\delta \cdot F}_{\text{piezo-electric contribution}}
 \end{aligned} \left\{ \begin{array}{l} \text{for force } F = X_x S \\ \text{across face } S = b \cdot c \\ \text{(thickness effect)} \end{array} \right. \tag{40}$$

where $E = 770 \times 10^9$ dynes/cm² the modulus of elasticity, and $\delta = -6.45 \times 10^{-8}$ e.s.c.g.s. the piezo-electric modulus along the thickness a . When the force F is applied along the Y dimension, the signs are reversed [Eq. (22)], and we obtain for the extension or contraction Δb of the b dimension and the charge

$$\begin{aligned}
 \Delta b &= \frac{b}{S_1 E} + \frac{b}{a} \delta \cdot V \\
 Q &= \frac{\kappa S}{4\pi a} V - \frac{b}{a} \delta \cdot F
 \end{aligned} \left\{ \begin{array}{l} \text{force } F = Y_y \cdot S_1 \text{ acts} \\ \text{across face } S_1 = a \cdot c, \\ \text{condenser area } S = b \cdot c \\ \text{(transverse effect)} \end{array} \right. \tag{41}$$

When no mechanical forces F are directly applied either along the X - or along the Y -axis but a voltage V acts along the X direction, alter-

nate elongations and contractions will be produced along the a dimension and corresponding alternate contractions and elongations along the b dimension. These can be observed when the frequency of the exciting field is equal to the frequency of a pronounced natural vibration of the crystal plate.

124. Theory of the Vibrating Quartz Rod and Its Equivalent Electric Circuit.—The theoretical investigation is easiest when long quartz rods are under consideration. For instance, this is the case when a rod is

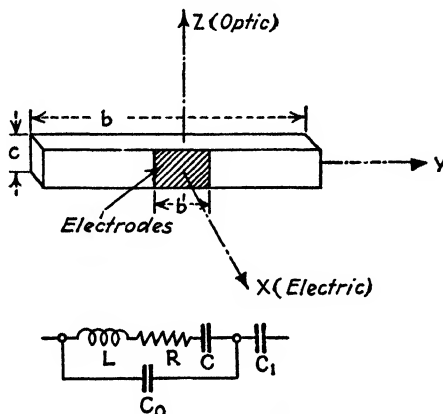


FIG. 195.—Vibrating piezo-electric rod.

electrically excited along a comparatively short X dimension (lines of applied force along X dimension), but the fundamental vibration¹ exists along a comparatively long Y dimension (Fig. 195).

According to Lamb,² the general equation of motion is

$$\frac{\partial^2 \xi}{\partial t^2} = A \frac{\partial^2 \xi}{\partial u^2} + B \frac{\partial^3 \xi}{\partial^2 u \partial t}$$

when ξ denotes the displacement at instant t of a point on the rod whose undisturbed coordinate is u . Then, for negligible damping (small viscosity B),

$$A = v^2 = \frac{E_y}{D} = [540 \times 10^3 \text{ cm/sec}]^2$$

¹ CADY, W. G., *Phys. Rev.*, **19**, 1, 1922 (also equivalent electrical constants presented at the U.R.S.I., 1926, unpublished); M. VON LAUE, *Z. Physik*, **34**, 347, 1925; Y. WATANABA, *I.E.E. (Japan)*, No. 466, 506, 1927; *E.N.T.*, **5**, 45, 1928; D. W. DYE, *Proc. Phys. Soc. London*, **38**, 399, 1926 (a detailed description of the quartz resonator and its equivalent circuit, using the method of S. Butterworth, *Proc. Phys. Soc. London*, **27**, 410, 1915, to obtain the equivalent constants); K. S. VAN DYKE, *Proc. I.R.E.*, **16**, 742, 1928 (follows up Cady's work, also derivation for equivalent network, and gives formulas for both thickness and Y vibrations of a Curie cut).

² Lamb's "Dynamic Theory of Sound," 1910.

Since the condition of resonance, or at least close to resonance (when taking resonance curves), is of interest for practical work, according to Cady the rod can be imagined as a body of equivalent mass

$$\alpha = \frac{a \cdot b \cdot c}{2} D$$

that is, half the magnitude of the actual mass, possessing 1 deg of freedom. The quantity D is again the density ($= 2.654 \text{ g/cc}$). The equation of motion of a displacement¹ y at any time t for a sinusoidal voltage V applied to the electrodes of the quartz rod is

$$\underbrace{\alpha \frac{d^2 y}{dt^2}}_{\text{involves moment of inertia}} + \underbrace{\beta \frac{dy}{dt}}_{\text{involves damping}} + \underbrace{\gamma y}_{\text{involves elastic forces due to deformation } y} = F = \underbrace{F_0 \cos \omega t}_{\text{driving force due to voltage } V} = kV \quad (42)$$

where

$$\beta = \frac{\pi^2 a c D b}{2b} \quad \text{and} \quad \gamma = \alpha \omega_0^2$$

are the mechanical resistance and stiffness of the quartz rod. Hence, α , β , and γ correspond to inductance, resistance, and the reciprocal of capacitance in an electric circuit. Since, for the fundamental longitudinal mode of vibration along dimension b ,

$$f_0 = \frac{1}{2b} \sqrt{\frac{E}{D}} \quad \left\{ \right. \\ \omega_0 = \frac{\pi}{b} \sqrt{\frac{E}{D}} \quad \left. \right\}$$

we have

$$\gamma = \frac{a c \pi^2 E}{2b}$$

where E denotes Young's modulus of elasticity along the Y -axis ($E_y = 770 \times 10^9 \text{ dynes/cm}^2$).

The displacing force F is proportional to the applied voltage V ; that is,

$$F = kV$$

The power supplied by V to maintain the rod in a state of vibration is $W = F(dy/dt)$. Introducing now the symbolic notation $dy/dt = ny = j\omega y$; $d^2y/dt^2 = n^2y$ since sustained sinusoidal vibrations are of interest only, we obtain from (42)

$$\left. \begin{aligned} [\alpha n^2 + \beta n + \gamma]y &= F \\ W &= VI = Fny \end{aligned} \right\} \quad (43)$$

¹ Actual contraction or elongation of entire rod is at any instant equal to $2y$.

The equivalent impedance¹ $Z_e = V/I$ is obtained from (43) through elimination of y and writing kV for F . We have then the equivalent impedance

$$Z_e = \frac{n\alpha + \beta + \frac{\gamma}{n}}{k^2} = \frac{\beta}{k^2} + j \left[\frac{\omega \alpha}{k^2} - \frac{\gamma}{\omega k^2} \right] \quad (44)$$

Comparing this result with

$$Z_e = R + j \left[\omega L - \frac{1}{\omega C} \right]$$

for a series combination of resistance, inductance, and capacitance (Fig. 195), we obtain

$$\left. \begin{aligned} L &= \frac{\alpha}{k^2} = 1.3 \times 10^2 \frac{a \cdot b}{c} \text{ henries} \\ R &= \frac{\beta}{k^2} = 1.3 \times 10^5 \frac{a}{b \cdot c} \text{ ohms} \\ C &= \frac{k^2}{\gamma} = 22 \times 10^{-4} \frac{b \cdot c}{a} \mu\text{mf} \end{aligned} \right\} \begin{array}{l} \text{for a rod vibrating longitudinally along the } Y \text{ dimension} \\ \text{but excited by an electric field along the } X\text{-axis} \end{array} \quad (45)$$

since $k = 2\epsilon c = 9.54 \times 10^4 c$ and, according to Eq. (21), the actual stress $Y_y = \epsilon_{11} \mathcal{E}_x = \epsilon V/a$, which acts throughout the entire length of the rod. According to the law of superposition, this stress is equal to two forces $F/2 = acY_y$ acting on both sides in opposite directions; that is,

$$F = 2acY_y = 2\epsilon V = kV$$

where V and Y_y denote instantaneous values of the applied e.m.f. and stress. The dimensions a , b , c of the rod in Eq. (45) are measured in centimeters. The derivation for the final equivalent-inductance expression is, for instance, based upon the evaluation of

$$L = \frac{a \cdot b \cdot c \cdot 2.654}{2} \frac{9 \times 10^{11}}{9.54^2 \times 10^8 c^2}$$

¹ The mechanical impedance Z_m can be derived from the first equation of (43) by realizing that the velocity of vibration $dy/dt = ny$ corresponds to the current, and the force F to the applied e.m.f. in an electric circuit since, for $n = j\omega$ and with the transient terms neglected,

$$[an^2 + \beta n + \gamma]y = F = F_0 e^{nt}$$

and

$$y = \frac{F_0}{j\omega Z_m} e^{j\omega t} \quad \text{for} \quad Z_m = \beta + j \left[\alpha\omega - \frac{\gamma}{\omega} \right]$$

where e stands for the base of the system of natural logarithms in this case.

henries where 9×10^{11} is the conversion factor for changing from the e.s.c.g.s. system to the henry units. The final resistance value of Eq. (45) is obtained by assuming, in the expression for $\beta = \pi^2 \times 2.654(ac/2b)B$, the apparent viscosity B about equal to 100, since the effects of air friction and the friction of the quartz rod against the mounting must be taken into account. In the International Critical Tables,¹ W. G. Cady gives for ϵ_{11} the value -5.1×10^4 e.s.c.g.s. and k would be $10.2 \times 10^4 c$, making $L = 1.147 \times 10^2(ab/c)$ henries. From Eqs. (39) and (39a), it can be seen that the current has one component which is due to the dielectric effect of the electrode condenser with the quartz as a dielectric. This means that the crystal holder capacity C_0 is in parallel (Fig. 195) with the equivalent series combination of L , R , and C and its value for the dielectric constant $\kappa = 4.55$ can be calculated from the ordinary formula

$$C_0 = \kappa \frac{b'c10^{-5}}{a36\pi} \mu f = 0.4 \frac{b'c}{a} \mu \mu f \quad (46)$$

since the actual coating in the case of a rod resonator generally extends only along the length b' . Strictly speaking, this condenser has an apparent dielectric constant which is slightly greater than the dielectric constant if the quartz rod were not piezo electric. The capacity is increased by about 1 per cent thereby.

For a quartz rod of dimensions $a = 0.2$ cm, $b = 5.4$ cm, and $c = 0.8$ cm, according to Eq. (32) for the fundament Y vibration, we find a frequency $f_2 = 2700/54 = 50$ kc/sec and, according to (45), the equivalent electrical constants

$$L = 1.3 \times 10^2 \frac{0.2 \times 5.4}{0.8} = 175.5 \text{ henries}$$

$$R = 1.3 \times 10^5 \frac{0.2}{5.4 \times 0.8} = 6000 \text{ ohms}$$

$$C = 22 \times 10^{-4} \frac{5.4 \times 0.8}{0.2} = 0.0475 \mu f$$

Assuming the electrodes along the entire $b \cdot c$ faces, we have the capacity $C_0 = \frac{0.4 \times 5.4 \times 0.8}{0.2} = 8.65 \mu \mu f$. Therefore, the vibrations have a very small decrement. Moreover we found

$$\frac{dy}{dt} = \frac{F_0 \cos \omega t}{\beta + j \left[\alpha \omega - \frac{\gamma}{\omega} \right]}$$

¹ Vol. VI, 1929, p. 207,

which, upon integration, gives for the displacement

$$y = \frac{F_0 \sin \omega t}{\omega \left[\beta^2 + j \left(\alpha \omega - \frac{\gamma}{\omega} \right) \right]}$$

and is 90 deg out of phase with the velocity.

The maximum amplitude at any frequency $f = \omega/2\pi$ is

$$y_0 = \frac{F_0}{\omega \sqrt{\beta^2 + \left[\alpha \omega - \frac{\gamma}{\omega} \right]^2}} \quad (47)$$

and at resonance $\alpha \omega_0 = \gamma/\omega_0$; that is,

$$f_0 = \frac{1}{2\pi} \sqrt{\frac{\gamma}{\alpha}} = \frac{1}{2b} \sqrt{\frac{E}{D}} = \frac{2700}{b_{(\text{mm})}} \text{ kc/sec} \quad (48)$$

and the resonance amplitude

$$y_r = \frac{F_0}{\omega_0 \beta} \quad (49)$$

But

$$F_0 = 2c\epsilon V_0 = 9.54 \times 10^4 c V_0$$

and for any maximum mechanical displacement of the rod in terms of its resonance amplitude y_r , according to Fig. 196, we obtain for any frequency the expression

$$y_0 = y_r \cos \varphi = \frac{F_0}{\omega_0 \beta} \cos \varphi = \frac{9.54 \times 10^4 c V_0}{\omega_0 \beta} \cos \varphi \quad (50)$$

where, according to Eq. (48),

$$\omega_0 = \frac{54 \times 10^4 \pi}{b} \quad (51)$$

when b is expressed in centimeters, and the resonance frequency f_0 in cycles per second. Therefore, the amplitude of vibration at any frequency f , by making the substitutions $\beta = \pi^2 acDB/2b$; $B = 100$, is

$$y_0 = 43 \times 10^{-8} \frac{b^2}{a} V_0 \cos \varphi$$

Bearing in mind that 1 e.s.c.g.s. unit of V_0 is equal to 300 volts, the amplitude of vibration at any forced frequency f becomes

$$y_0 = 14.33 \times 10^{-8} \frac{b^2}{a} V_0 \cos \varphi \quad (52)$$

where all dimensions are in centimeters, and the maximum voltage V_0 in volts. With respect to the expression for $\cos \varphi$ (see Fig. 196) all dimensions are in c.g.s.u. Hence, when a quartz rod of dimensions $a = 0.2$ cm, $b = 5.4$ cm, and $c = 0.8$ cm vibrates in its fundamental longitudinal mode along the b dimension, we have for a maximum voltage $V_0 = 300$ volts across the electrodes for the resonance amplitude $y_0 = y_r$ of vibration: $y_r = 14.33 \times 10^{-8}(5.4^2/0.2)300 = 0.00626$ cm since at resonance $\cos \varphi = 1$. When comparing this with the static elongation or contrac-

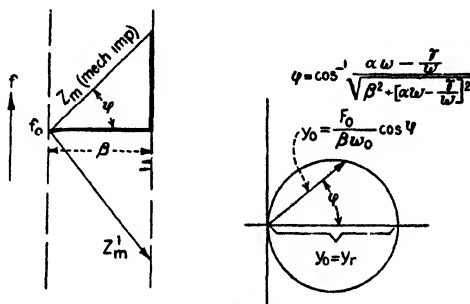


FIG. 196.—Vector diagram of vibrating rod

tion y along the b dimension (for $f = 0$ cycles/sec), we find, according to Eq. (22), for the static elongation or contraction per unit length

$$y_v = -6.45 \times 10^{-8} \frac{V_0}{a}$$

and for the *total static change* of dimension b

$$y = y_v \cdot b = -6.45 \times 10^{-8} \frac{b}{a} V_0 \quad (53)$$

where V_0 is expressed in e.s.c.g.s. units. The minus sign indicates that a total compression x along the thickness dimension corresponds to an elongation y along the Y dimension. Hence, for a steady voltage $V_0 = 300$ volts = 1 e.s.u., $y = -6.45(5.4/0.2)10^{-8}$ is only 174×10^{-9} cm. The dynamic amplitude y_r is therefore $y_r/y = 3600$ times greater than the static dilation (depending upon the polarity of V_0). Of course, this large ratio is due to the resonance effect and shows that, for oscillating crystals, the amplitude of mechanical vibration is appreciable and that the static-dimension change is negligible.

Comparing the results of (52) and (53), we note that the amplitude y_0 of vibration is proportional to the square of the length of the rod and inversely proportional to the thickness, while for the static effect the latter relation holds also, but the dilation increases only linearly with the dimension b , which shows again that, for long rods along the y

dimensions, the resonance amplitude becomes very pronounced. The ratio of *dynamic amplitude to static dimension change* at any frequency is

$$\frac{y_0}{y} = 666b \cos \varphi \quad (54)$$

which, for resonance, that is, for the fundamental longitudinal Y vibration, is

$$\frac{y_r}{y} = 666b \quad (55)$$

where b is in centimeters and it is assumed that the static voltage V_0 is adjusted to the value of maximum alternating voltage across the electrodes of the oscillating crystal.

The damping factor d of the mechanical vibration, according to Eq. (45), is

$$d = \frac{R}{2L} = \frac{\beta}{2\alpha} = \frac{500}{b^2} \quad (56)$$

Hence the logarithmic decrement Δ per cycle for the fundamental vibration along the b dimension is

$$\Delta = \frac{d}{f_0} = \frac{0.00202}{b^{(\text{cm})}} \quad (57)$$

that is, very small, and becomes smaller the longer the rod.

125. Longitudinal, Transverse, and Torsional Quartz Oscillations.—

These three divisions of characteristic types of oscillations¹ are suitable when dealing with quartz rods although for disks and plates the oscillations are more complex. The vibrations described so far are longitudinal; that is, the direction of vibration is along the direction of propagation. Figure 197 shows the stress, velocity, and charge distributions when the indicated quartz rod is excited by means of electrodes which apply the alternating field across the electric X -axis. It can be seen that the fundamental mode can be excited by electrodes along the $b\ c$ faces or smaller faces $b'c$ as indicated in Fig. 195. The second harmonic cannot be excited by electrodes covering the entire $b\ c$ face but by electrodes as

¹ GIEBE, E., and A. SCHEIBE, *Z. Physik*, **33**, 335, 1925; *E.N.T.*, **5**, 65, 1928; *Z. Physik*, Jan. 25, 1928 (describes longitudinal, transverse, and torsional vibrations, when the quartz acts as a resonator); J. R. HARRISON, *Proc. I.R.E.*, **15**, 1040, 1927 (describes method of flexural—transverse—oscillations in the length-breadth plane, thickness along electric axis, quartz acts as oscillator); S. NAMBA and S. MATSUMURA, *loc. cit.* (describes the Giebe-Scheibe experiments and applies their luminous method as well as Kundt's dust method to quartz plates and disks, quartz oscillator, and resonator for longitudinal and transverse oscillations); *Bur. Standards Research Paper* 156, 1930 (torsional, transverse, and longitudinal vibrations in cylinders cut along the optical axis, quartz acts as oscillator).

indicated in Fig. 197. When second-mode vibrations are excited in rectangular plates and circular disks, the frequency of the second mode for the former is about twice that of the fundamental mode, while for the latter it is smaller than $2f$.

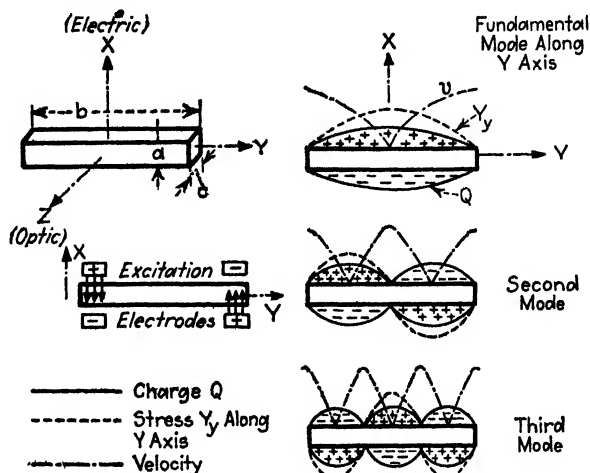


FIG. 197.—Distributions for longitudinal-rod vibrations.

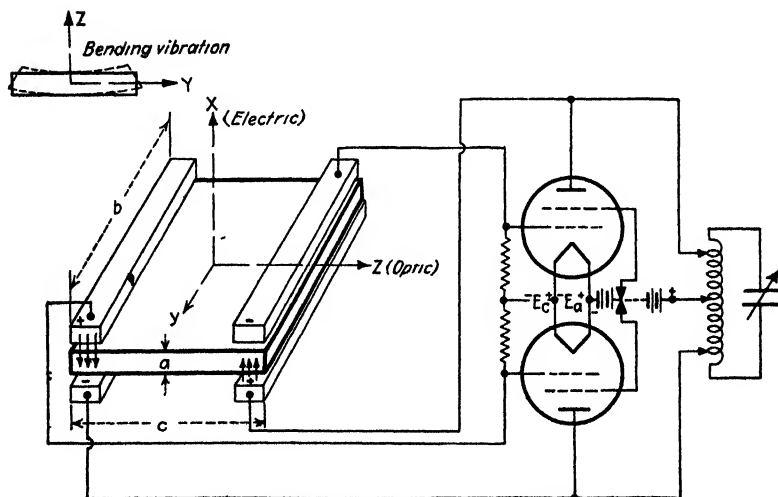


FIG. 198.—Excitation of a transverse oscillation.

Transverse vibrations can be excited with the circuit indicated in Fig. 198. The transverse Y_y stress is employed and the fundamental frequency is much lower than for longitudinal or for torsional modes. Theoretically the frequency for $a b c$ dimensions along the X -, Y -, and Z -axes is in c.g.s. units

$$f = \frac{\Psi^2}{4\pi\sqrt{3}} \frac{c}{b^2} \sqrt{\frac{E}{D}} \quad (58)$$

where $\Psi = [p + \frac{1}{2}]\pi$ and p denotes the order of the harmonic. This leads, for the fundamental transverse mode, to the theoretical frequency formula

$$f = 551 \frac{c}{b^2} \text{ kc/sec (theoretical formula for flexural vibrations)} \quad (59)$$

when the dimensions b and c are in centimeters. Measurements show that the theoretical low-frequency value is only approximated when the ratio of length b to width c is large.

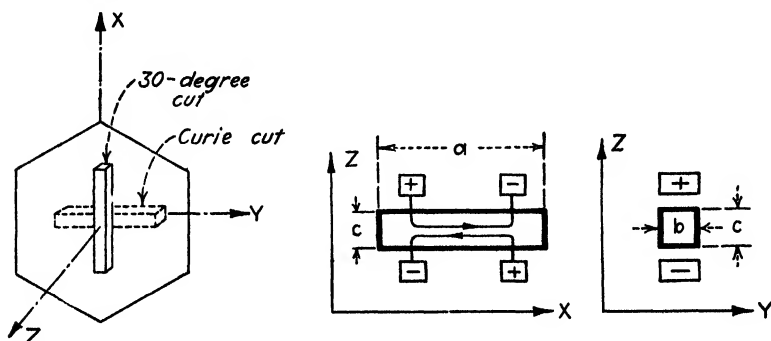


Fig. 199.—Transverse oscillation for 30-deg-cut rod.

When 30-deg-cut crystals are used, the rod can be excited in a transverse (flexural) mode along the Z -axis by a stray field which is along the electric X -axis as indicated in Fig. 199. With mountings of this and similar types, Giebe and Scheibe¹ have produced their glow-discharge patterns. In Fig. 200, torsional oscillations are produced by means of Curie- and 30-deg-cut bars of rectangular cross section.

It has been found that longitudinal, transverse (flexural), and torsional oscillations can also be produced when quartz cylinders are cut along the optical (Z -) axis. The electrodes may then be mounted as in Fig. 201a where a surrounding metal ring acts as one electrode, and the two metal end faces may be used either singly or in parallel as the other electrode. The mounting indicated in *b* uses electrodes around the cylinder, and mounting *c* uses six such electrodes. The latter mounting suggests itself from the piezo-electric structure of the cylinder. When the axis of the cylinder is long compared with the diameter of the cross section, we can again distinguish between longitudinal, torsional, and transverse oscillations involving the velocities of propagation v_1 , v_2 , and v_3 , respectively. The first two of these are due to the linear modulus of

¹ *Loc. cit.*

elasticity E_1 and a torsional modulus E_2 , which must be dealt with in case of longitudinal and torsional cylinder vibrations, respectively. The

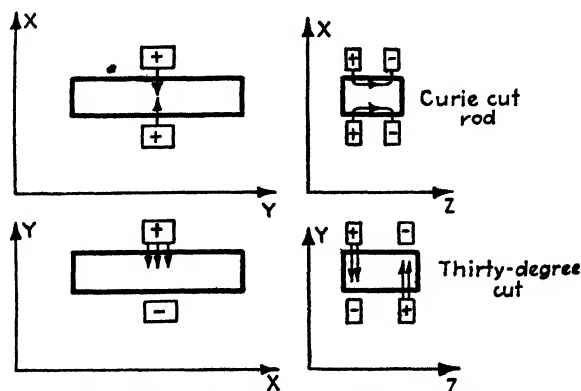


FIG. 200.—Excitation of torsional oscillations.

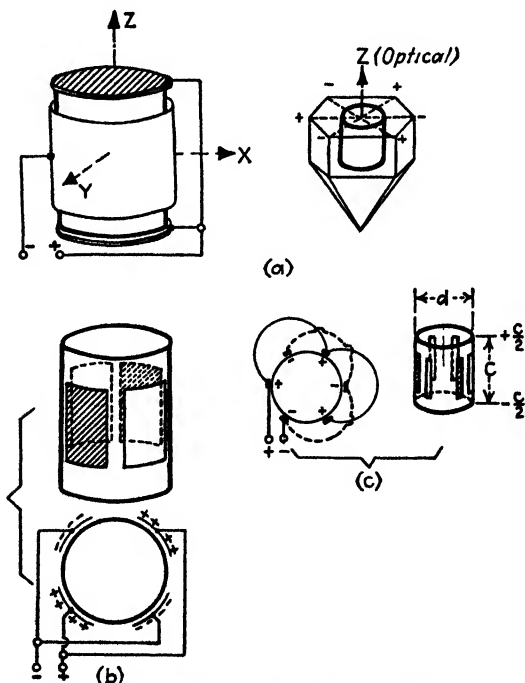


FIG. 201.—Electrodes for exciting oscillations in quartz cylinders cut along the optical axis.

third velocity is due to what we may consider as a corresponding E_2 , effective in the case of transverse vibrations. If D again denotes the density ($= 2.654 \text{ g/cc}$) of the cylinder, we have

$$\left. \begin{aligned} v_1^2 &= E_1 D^{-1} \\ v_2^2 &= E_2 D^{-1} \\ v_3^2 &= E_3 D^{-1} \end{aligned} \right\} \quad (60)$$

A simple relation is found to exist between E_1 and E_3 so that we may conveniently write for the corresponding frequencies of vibration

$$\left. \begin{aligned} f_{\text{long}} &= \frac{p}{2c} \sqrt{\frac{E_1}{D}} \\ f_{\text{tors}} &= \frac{p}{2c} \sqrt{\frac{E_2}{D}} \\ f_{\text{trans}} &= \frac{\psi_p^2 d}{8\pi c^2} \sqrt{\frac{E_1}{D}} \end{aligned} \right\} \quad (61)$$

where p stands for the order of the mode ($p = 1$ for the fundamental), d and c denote the diameter and height of the cylinder, respectively.

The values of ψ_p for the fundamental and some of its higher modes are $\psi_1 = 4.71$; $\psi_2 = 7.85$; $\psi_3 = 11.0$; $\psi_4 = 14.1$; $\psi_5 = 17.3$. From this it can be seen that, even for long cylinders, the transverse modes of oscillations are still affected by the size of the cross section, that is, by the diameter. The formulas for torsional and transverse vibrations are conveniently expressed in terms of longitudinal vibrations. Thus we find

$$f_{\text{tors}} = \frac{f_{\text{long}}}{\sqrt{2[1 + \mu]}} \quad (62)$$

where μ may have values between 0.2 and 0.5 depending upon the values of E_1 and E_2 . For the transverse frequency, we obtain

$$f_{\text{trans}} = \frac{\pi[2p + 1]^2 d}{16p} \frac{d}{c} f_{\text{long}} \quad (63)$$

from which, for the *fundamental mode* ($p = 1$),

$$f_{\text{trans}} = 1.767 \frac{d}{c} f_{\text{long}} \quad (64)$$

Of course, these formulas will give reasonable values only when the proper modulus of elasticity is used. Fortunately, earlier experimenters¹ in the field have determined the longitudinal modulus E_1 as well as the torsional modulus E_2 along the optic axis. They are

$$\left. \begin{aligned} E_1 &= 1030.4 \times 10^9 \text{ dynes/cm}^2 \\ E_2 &= 508.5 \times 10^9 \text{ dynes/cm}^2 \end{aligned} \right\} \quad (65)$$

¹ Voigt, Riecke, Pockels, and others.

and give the corresponding velocities of propagation

$$\left. \begin{array}{l} v_1 = 6.24 \\ v_2 = 4.38 \end{array} \right\} \times 10^5 \text{ cm/sec} \quad (66)$$

For the longitudinal and torsional modes of vibration of a cylinder of crystal quartz cut along the optical axis, therefore, we have

$$\left. \begin{array}{l} f_{\text{long}} = \frac{312p}{c} \\ f_{\text{tors}} = \frac{219p}{c} \end{array} \right\} \text{ kc/sec} \quad (67)$$

where the height c of the cylinder is expressed in centimeters, and p stands for 1, 2, 3, 4, etc., according to the order of the mode. For the transverse modes, the expression in (61) together with the value of v_1 in (66) gives

$$f_{\text{trans}} = 24.8 \frac{\psi_p^2 d}{c^2} \text{ kc/sec} \quad (68)$$

where both the length c and the diameter d of the cylinder are expressed in centimeters. For the *fundamental mode* ($\psi_p = 4.71$)

$$f_{\text{trans}} = 550 \frac{d}{c^2} \text{ kc/sec} \quad (69)$$

Formula (68) must be considered as an approximation because of the lateral effect.¹

126. Surface and Space Charges.—Glow-discharge pictures of Giebe and Scheibe² and others on resonating and oscillating crystals show that we have resultant charge effects which give definite charge functions along rods and cylinders. Giebe and Scheibe² have interpreted their patterns by means of Voigt's ("Lehrbuch der Kristalloptik") theory of surface and equivalent space charges. The space charges are only equivalent since in each quartz element there are as many positive as negative charges.

With reference to surface charges, the surface distribution can be calculated when the function of the surface density of charge along a rod or cylinder is known. This can be done by means of the piezo-electric polarization P since, according to its definition, it gives the surface charge per unit area directly when standing normal to the unit area.

¹ E. P., Tawil, *Comptes Rendus des séances de l'Académie des Sciences*, April, 1935, p. 1306, confirmed these formulas experimentally.

² *Loc. cit.*

Hence, if τ denotes the angle which the direction of polarization P_i makes with the normal to any unit surface,

$$\sigma_i = P_i \cos \tau \quad (70)$$

is the surface density of charge.

The volume or space-charge density inside the quartz can be computed likewise from the polarization and is given by the relation

$$\rho = - \left[\frac{\partial P_x}{\partial x} + \frac{\partial P_y}{\partial y} + \frac{\partial P_z}{\partial z} \right] \quad (71)$$

The formation of equivalent space charges for the 30-deg-cut rod indicated in Fig. 202 can be explained as follows: The dotted line denotes the

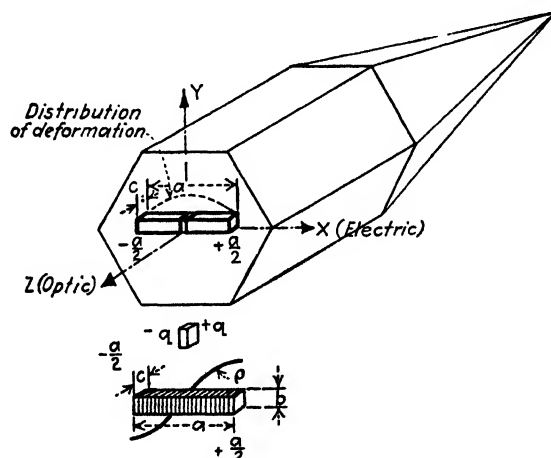


FIG. 202.—Formation of equivalent space charge ρ for a 30-deg-cut rod.

distribution of deformation along the a dimension, the driving electrodes being along faces $a \cdot c$. Suppose the rod is cut into infinitely thin slices as indicated, and at first each slice is imagined to be separate but acted upon by the deformation which exists for it when part of the rod. Each side face ($b \cdot c$) of the slice taken out of the rod will have unequal charges because the deformation changes along its thickness except for the slice cut out at the center of the rod.

The excess of charges between that on the left side of the slice and that on the right side becomes greater as the rapidity of the change of deformation along the thickness of the slice is increased. Hence the excess increases from a zero value for slices at the center of the rod to a maximum value for the slices at each end of it, since one face of each end slice is subject to no deformation at all. When the infinitely thin slices are, as in reality, all touching each other, the excess of the surface charges

of the touching faces form space charges within the quartz rod which must vary according to a sine law, if the deformation is as indicated. Therefore, when the strain X_x along the X -axis is nonuniform, for instance, as in Fig. 203, the space charge varies according to Eq. (4). The case of sinusoidal-pressure distribution is of importance only for oscillating

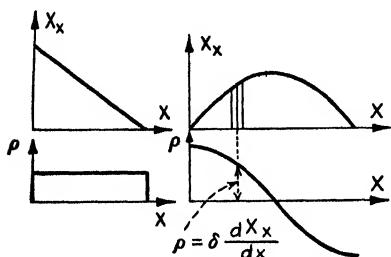


FIG. 203.—Strain and corresponding space-charge distributions.

crystals since, for the various natural modes of vibrations, the voltage across the driving electrodes is sinusoidal.

Suppose we have the case of a Curie-cut rod as indicated in Fig. 188. The electrodes are perpendicular to the electric X -axis. The resultant polarization P then takes place along the X -axis, which means that the components P_y and P_z in Eq. (16) are

both zero and the shears do not play a part in this method of excitation. When the rod is set in longitudinal vibrations along the Y dimension, Eq. (16) for a static polarization gives

$$P_x = \delta_{11} Y_y = -6.45 \times 10^{-8} Y_y \quad (72)$$

Since for this case $\tau = 0$ in Eq. (70), we obtain on the respective electrodes the static surface densities

$$\sigma_x = \mp 6.45 \times 10^{-8} Y_y \quad (73)$$

The stress Y_y is constant over the cross section $a \cdot c$ but varies according to a cosine law for all odd modes of possible longitudinal Y vibrations; that is,

$$Y_y = Y_0 \cos \frac{p\pi y}{b} \quad (74)$$

Here, $p = 1$ for the fundamental mode, $p = 3, 5$, etc., for the third, fifth, etc., mode. For even modes

$$Y_y = Y_0 \sin \frac{p\pi y}{b} \quad (75)$$

for $p = 2, 4, 6$, etc. For both surfaces $\pm a/2$, a distance a apart, we have, according to Eqs. (73) and (74) at any instant opposite and equal surface charges which are

$$\sigma_x = \mp 6.45 \times 10^{-8} Y_0 \cos \frac{p\pi y}{b} \quad (76)$$

and, according to (71), the space-charge density

$$\rho = -\frac{\partial P_x}{\partial x} = 0 \quad (77)$$

since the stress Y_y in Eq. (72) is constant¹ over the entire cross section ac . The glow discharge in this case is due to the true surface charges only. For the fundamental mode $p = 1$, and for the end faces $y = \pm b/2$ which are a distance b apart, the surface density becomes zero, while at the middle of the rod ($y = 0$) the surface density becomes a maximum ($= \mp 6.45 \times 10^{-8} Y_0$) and the rod shows a glow discharge at the center of it.

For the 30-deg-cut rod indicated in Fig. 202,

$$P_x = -\delta_{11}X_x = 6.45 \times 10^{-8}X_x = \pm\sigma_x \quad (78)$$

for longitudinal effects along the X -axis, where the stress is

$$X_x = X_0 \cos \frac{p\pi x}{a} \quad (79)$$

Combining these two equations, we note that because of the relation

$$\sigma_x = 6.45 \times 10^{-8}X_0 \cos \frac{p\pi x}{a} \quad (80)$$

no surface charges can exist on the end faces ($x = \pm a/2$) of the rod, although such charges would be produced by a static polarization $X_x = X_0$. However, it must be realized that, with the 30-deg cut, the equivalent space-charge effect does not vanish but is

$$\rho = -\frac{\partial P_x}{\partial x} = 6.45 \times 10^{-8}X_0 \frac{p\pi}{a} \sin \frac{p\pi x}{a} \quad (81)$$

For the fundamental mode $p = 1$, and at the ends $x = \pm a/2$, we have the maximum effects $\rho = \pm 6.45 \times 10^{-8}(\pi/a)X_0$ which produce glow discharges.

When torsional oscillations² about the optical axis (Fig. 201) are to be theoretically confirmed, we use the expression

$$U = [\delta_{11}(X_x - Y_y) + \delta_{14}Y_x]\varepsilon_x - [\delta_{14}Z_x + 2\delta_{11}X_y]\varepsilon_y \quad (82)$$

for the free potential energy per unit volume. This expression can be obtained by utilizing the relation of the thermodynamic potential (page 293) in Eq. (16). It is the energy relation given by Laue [Eq. (28)].

When torsional vibrations take place, they must be due to tangential forces which, according to Eq. (82), are given by the tension³ components Y_x and Z_x for cylinders along the optical axis. Only the smaller⁴ modulus

¹ Slices must be parallel to ac faces.

² Footnote 1, p. 313.

³ Capital letters give direction of tensions and suffixes the planes.

⁴ $\delta_{14} = -1.45 \times 10^{-8}$ while the usual modulus $\delta_{11} = -6.45 \times 10^{-8}$.

δ_{14} is now effective and this may be the reason why this kind of oscillations was only recently discovered. It takes special circuits (regenerative amplifiers on the verge of self-oscillations) to produce torsional oscillations about the optical axis. According to Eq. (16), only polarizations P_x and P_y can exist and are, for this particular case,

$$\left. \begin{aligned} P_x &= -\delta_{14} Y_z = 1.45 \times 10^{-8} Y_z \\ P_y &= \delta_{14} Z_x = -1.45 \times 10^{-8} Z_x \end{aligned} \right\} \quad (83)$$

where the proportionality

$$\left. \begin{aligned} Y_z &= -kx \\ Z_x &= ky \end{aligned} \right\} \quad (83a)$$

for static torsion exists. According to Voigt,

$$Y_z = \frac{\partial \Omega}{\partial x} \quad \text{and} \quad Z_x = -\frac{\partial \Omega}{\partial y} \quad (84)$$

where Ω is a function of x and y , and $\Omega = 0$ is the equation of the boundary curve of the cross section of the cylinder—a circle in this case.

Because of the harmonic variation along the Z -axis, Eqs. (83a) for oscillations become

$$\left. \begin{aligned} Y_z &= -kx \cos \frac{p\pi z}{c} \\ Z_x &= ky \cos \frac{p\pi z}{c} \end{aligned} \right\} \quad (85)$$

where p denotes the order of the mode, and for cosine distributions $p = 1, 3, 5, 7 \dots$, while for sine distributions $\sin p\pi z/c$ has the values $p = 2, 4, 6, 8 \dots$, etc. The end surfaces of the cylinder (Fig. 201) have the position $z = \pm(c/2)$. According to Eqs. (83) and (85), we have the polarizations

$$\left. \begin{aligned} P_x &= \delta_{14} mx \\ P_y &= \delta_{14} my \end{aligned} \right\} \quad (86)$$

for $m = k \cos p\pi z/c$.

By means of these relations we can find the surface charges around the cylinder (end effects neglected) and the space charge inside the quartz cylinder and can learn whether an exterior field is possible. Only for such a condition can external electrodes produce oscillations. When σ_α stands for the surface density, we have

$$\sigma_\alpha = P_x \cos \alpha + P_y \sin \alpha \quad (87)$$

Since the cylinder cross section is a circle of radius $d/2$,

$$x = \frac{d}{2} \cos \alpha \quad \text{and} \quad y = \frac{d}{2} \sin \alpha$$

and, according to (86) and (87), the surface density is

$$\sigma_{\alpha} = \frac{md}{2}\delta_{14} = -725 \times 10^{-11}md \quad (88)$$

The space-charge density ρ , according to Eq. (71), is

$$\begin{aligned} \rho &= -\left[\frac{\partial P_x}{\partial x} + \frac{\partial P_y}{\partial y}\right] \\ &= -2m\delta_{14} = 2900 \times 10^{-11}m \end{aligned} \quad (89)$$

Therefore, for each cross section z , around the *circumference* we have the *surface charge*

$$\Sigma = \pi d \left[\frac{md}{2} \delta_{14} \right] = -725 \times 10^{-11} \pi m d^2 \quad (90)$$

and the space charge Q for the same cylinder section is

$$Q = \frac{\pi d^2}{4} [-2m\delta_{14}] = 725 \times 10^{-11} m d^2 \quad (91)$$

Hence, in dealing with static torsions, the distribution function is unity and $m = 1$ for which case

$$Q = -\Sigma \quad (92)$$

proving Voigt's results that there can be no charges present for static twists. However, this is not true for dynamic torsions (oscillations) since the distribution function along the cylinder gives rise to places where the surface charge does not neutralize the space charge and lines of force can either enter the cylindrical envelope or leave it. An external field can therefore produce oscillations and vice versa, and the experimental results of torsional oscillations with quartz cylinders cut along the optical axis are justified.

CHAPTER IX

ELECTROMAGNETIC THEORY

The following derivations are based on laws by Gauss, Ampère, and Faraday, including Maxwell's conception of displacement current, and lead to the electromagnetic-field equations which play an important part in field-intensity measurements and propagation of waves in space. They have also a bearing on the dynamic theory of piezo electricity.

127. Gauss' Theorem.—According to Gauss, the total normal electric induction over a closed surface is equal to 4π times the total charge within

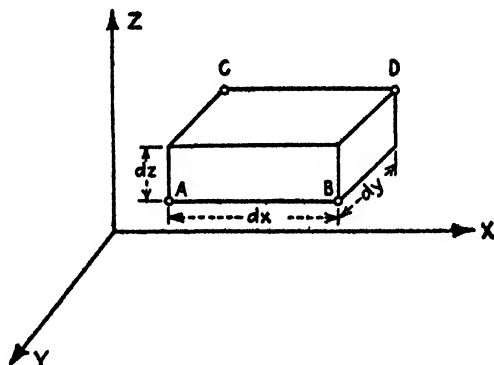


FIG. 204.—Parallelepiped filled with matter of volume density ρ .

it. Generalized, it states: If a mass of attracting matter is placed at any point and if we describe around it any closed surface S , and at each point of that surface resolve the force normally to the surface and take the product of this normal force F and the surface element dS , we find the surface integral FdS equal to 4π times the total quantity of attracting matter within the surface *irrespective* of its distribution.

$ACBD$ of Fig. 204 denotes a small parallelepiped filled with matter of volume density ρ . The total matter of the parallelepiped is therefore $\rho dx \cdot dy \cdot dz$. In our case we deal with either electric or magnetic forces.

If at A an electric force \mathcal{E} acts with the components \mathcal{E}_x , \mathcal{E}_y , and \mathcal{E}_z , the normal component over face AC is \mathcal{E}_z , and that over face BD is $\mathcal{E}_z + (\partial \mathcal{E}_z / \partial z) dz$. The normal electric induction over face AC is therefore $\kappa \mathcal{E}_z dy \cdot dz$ and that over face BD is $\kappa [\mathcal{E}_z + (\partial \mathcal{E}_z / \partial z) dz] dy \cdot dz$, if κ stands for the dielectric constant. The difference between these two is the *contribution* of the two faces AC and BD to the total normal induction over the whole surface. It is

$$\kappa \left\{ \left[\varepsilon_x + \frac{\partial \varepsilon_z}{\partial x} dx \right] dy \cdot dz - \varepsilon_x \cdot dy \cdot dz \right\} = \kappa \frac{\partial \varepsilon_x}{\partial x} dx \cdot dy \cdot dz$$

Treating the other two pairs of faces in the same way, we obtain the contributions $\kappa(\partial \varepsilon_y / \partial y) dx dy dz$ and $\kappa(\partial \varepsilon_z / \partial z) dx dy dz$. Since ρ denotes the electric volume density and $\rho dx dy dz$ the enclosed charge within the parallelepiped, we have from the Gauss theorem,

$$\kappa \left[\frac{\partial \varepsilon_x}{\partial x} + \frac{\partial \varepsilon_y}{\partial y} + \frac{\partial \varepsilon_z}{\partial z} \right] dx dy dz = 4\pi(\rho dx dy dz)$$

or

$$\frac{\partial \varepsilon_x}{\partial x} + \frac{\partial \varepsilon_y}{\partial y} + \frac{\partial \varepsilon_z}{\partial z} = \frac{4\pi\rho}{\kappa} \quad (1)$$

In a similar manner, the expression

$$\frac{\partial H_x}{\partial x} + \frac{\partial H_y}{\partial y} + \frac{\partial H_z}{\partial z} = \frac{4\pi\rho}{\mu} \quad (2)$$

for the resultant magnetic intensity H and permeability μ is found. The quantity ρ has reference to the magnetic density. The operator $\partial/\partial x + \partial/\partial y + \partial/\partial z$ is called the "divergence" (div) of the vector and (1) can be written

$$\text{div } \varepsilon = \frac{4\pi\rho}{\kappa} \quad (1a)$$

and stands for the quantity of ε which originates or diverges from a unit volume of space. If the potential function V is used,¹ the corresponding equation, known as Poisson's equation

$$\nabla^2 V = -\frac{4\pi\rho}{\kappa} \quad (3)$$

where

$$\nabla^2 = \frac{\partial^2}{\partial x^2} + \frac{\partial^2}{\partial y^2} + \frac{\partial^2}{\partial z^2}$$

is obtained.² By means of it the volume density can be calculated at any point in the field if the potential V is known at that point. For $\nabla^2 V = 0$ there can be no attracting matter or electricity and we have Laplace's equation.

$$^1 \varepsilon_x = -\frac{\partial V}{\partial x}; \varepsilon_y = -\frac{\partial V}{\partial y}; \varepsilon_z = -\frac{\partial V}{\partial z}$$

² For *cylindrical coordinates* in the x, y plane, together with the unmodified z coordinate ($x = r \cos \alpha; y = r \sin \alpha$), the Poisson equation reads

$$\nabla^2 V = \frac{1}{r} \frac{\partial}{\partial r} \left(r \frac{\partial V}{\partial r} \right) + \frac{1}{r^2} \frac{\partial^2 V}{\partial \alpha^2} + \frac{\partial^2 V}{\partial z^2} = -\frac{4\pi\rho}{\kappa}$$

while for *spherical polar coordinates* where r is the radius vector from the origin, β the azimuth (longitude), that is, the angle between the meridian plane and the x, z plane, α the zenith angle, that is, the angle between r and the Z -axis, we have $x = r \sin \alpha \cos \beta; y = r \sin \alpha \sin \beta; z = r \cos \alpha$; and

$$\nabla^2 V = \frac{1}{r^2} \frac{\partial}{\partial r} \left(r^2 \frac{\partial V}{\partial r} \right) + \frac{1}{r^2 \sin \alpha} \frac{\partial}{\partial \alpha} \left(\sin \alpha \frac{\partial V}{\partial \alpha} \right) + \frac{1}{r^2 \sin^2 \alpha} \frac{\partial^2 V}{\partial \beta^2} = -\frac{4\pi\rho}{\kappa}$$

128. Application of Poisson's Equation.—By means of Eq. (3), Langmuir derived the well-known space-charge law for electron tubes with pure electron emission under the assumption that the initial velocity of the electrons given off at the hot cathode is negligible. The solution is simpler when both the cathode and the anode are two infinite parallel plates as shown in Fig. 205. For a cold cathode, no electrons are emitted

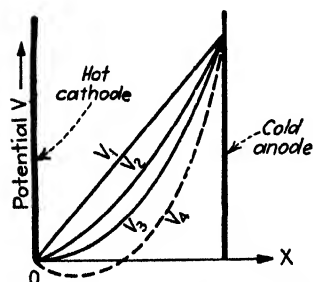


FIG. 205. — Application of Poisson's equation

and the potential V_1 between the two electrodes varies linearly.¹ But when the cathode is slightly hot, an emission current passes toward the anode and produces the parabolic potential distribution V_2 . The electrons then move with a velocity depending upon the potential drop through which they have passed. If the current density is I_x and if it is assumed at first that the electrons move with a constant velocity v across the space, we have a space charge $\rho = I_x/v$ per unit volume. If the velocities of the electrons are uniform, the space charge will fall off according to Poisson's equation which for negative charges (electrons) is

$$\frac{\partial^2 V}{\partial x^2} + \frac{\partial^2 V}{\partial y^2} + \frac{\partial^2 V}{\partial z^2} = 4\pi\rho$$

Since the electrodes are parallel to the YZ plane, the foregoing equation simplifies to

$$\frac{d^2 V}{dx^2} = 4\pi\rho$$

and indicates the shape of V_2 . As the temperature of the cathode is increased, the emission density I_x increases until finally saturation takes place. This happens for distribution V_3 for which OX is the tangent at O . A distribution such as that indicated by V_4 is impossible for zero initial velocity since the electrons could not start out against gradients below

¹ This is true only for a very high degree of vacuum. Generally, if we deal with two infinite metal planes perpendicular to the x -axis, we have

$$-\frac{\partial^2 V}{\partial x^2} = 4\pi[Q_1 - Q_2] \text{ (for positive ions and electrons)}$$

for instance, for glow tubes. There can be places where the net charge is negative, where the positives are in excess, and where the positive and negative charges have the same amount per unit volume. The plot of potential V against distance x likewise gives curved and straight lines as in Fig. 205. The straight-line condition shows that the positive and negative charges Q_2 and Q_1 are equal for unit space. When the plot is a curve which is concave upward, the negative charges Q_1 are in excess, while for a curve which is concave downward the positive charges Q_2 are predominating.

the OX -axis. The effect of the space charge ρ therefore automatically limits the emission current. If m denotes the mass and q the charge of an electron with no losses between the plates, we have

$$\frac{1}{2}mv^2 = V \cdot q$$

where V is the potential at a distance x from the hot cathode. From this equation we find the velocity

$$v = \sqrt{\frac{2V \cdot q}{m}}$$

which together with $I_x = \rho \cdot v$ gives the space-charge density

$$\rho = \frac{\sqrt{m/q} I_x}{\sqrt{2} \sqrt{V}}$$

and

$$\frac{d^2V}{dx^2} = 2\pi\sqrt{2} \sqrt{\frac{m}{q}} V^{-1/2} \cdot I_x$$

in e.s. units. The solution gives

$$I_x = 2.33 \times 10^{-6} \frac{V^{3/2}}{x^2}$$

where I_x is the maximum current density in amperes per square centimeter, V in volts, and x in centimeters.

A more practical case is that of a cylindrical anode with the cathode along its axis. R_a is the radius of the anode cylinder and r that of the incandescent wire forming the cathode. The thermionic current per unit length is

$$I = 2\pi R \rho v$$

for any cylinder of radius R since $2\pi R$ is the area per unit length of the cylinder surface. If V denotes the corresponding potential, we obtain from the foregoing expression and

$$\frac{1}{2}mv^2 = V \cdot q$$

the space-charge density

$$\rho = \frac{\sqrt{m/q} I}{2\pi R \sqrt{2} \sqrt{V}}$$

This, introduced in Poisson's equation with cylindrical coordinates for negative charges, is

$$\nabla^2 V = \frac{1}{R} \frac{d}{dR} \left[R \frac{dV}{dR} \right] = -4\pi\rho$$

or

$$R \frac{d^2 V}{dR^2} + \frac{dV}{dR} = 4\pi\rho R$$

giving

$$R \frac{d^2 V}{dR^2} + \frac{dV}{dR} = \sqrt{2} \sqrt{\frac{m}{q}} V^{-1/2}$$

The solution gives

$$I = \frac{1.465 \times 10^{-5} V^{3/2}}{R_a}$$

where the radius R_a of the anode cylinder is in centimeters, the anode potential V in volts, and the current per centimeter length I in amperes. Another application of Poisson's equation is given on page 319 in connection with space and surface charges in oscillatory quartz cylinders.

129. Ampère's Law.— This law states that the work done in carrying a unit magnetic pole around a closed path across which a current is flowing is equal to 4π times the current.

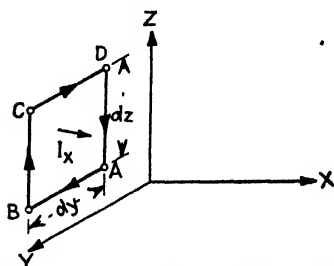


FIG. 206.—Diagram for Ampère's law.

Suppose a current flows across the small rectangular cross section $ABCD$ of sides dy and dz as shown in Fig. 206. The current density at A is I with the components I_x , I_y , and I_z . The components of the magnetic vector H are H_x , H_y , and H_z . The magnetic component along AB is then H_y and that along CD is $-[H_y + (\partial H_y / \partial z) dz]$. The work done by the field when a unit pole is taken from A to B is force times distance, that is, $H_y dy$, and when taken from C to D it is $-[H_y + (\partial H_y / \partial z) dz] dy$. The total work done when taken around the rectangular figure $ABCD$ then becomes

$$H_y dy + \left[H_z + \frac{\partial H_z}{\partial y} dy \right] dz - \left[H_y + \frac{\partial H_y}{\partial z} dz \right] dy - H_x dz = \left[\frac{\partial H_z}{\partial y} - \frac{\partial H_y}{\partial z} \right] dy dz$$

But this, according to Ampère's law, is equal to 4π times the current flowing normally through area $ABCD$, that is, equal to $4\pi I_x dy dz$. Hence

$$4\pi I_x = \frac{\partial H_z}{\partial y} - \frac{\partial H_y}{\partial z} \quad (4a)$$

In a similar way, we obtain for the other two component current densities

$$\left. \begin{aligned} 4\pi I_y &= \frac{\partial H_x}{\partial z} - \frac{\partial H_z}{\partial x} \\ 4\pi I_z &= \frac{\partial H_y}{\partial x} - \frac{\partial H_x}{\partial y} \end{aligned} \right\} \quad (4b)$$

which reads in the general form

$$4\pi I = \text{curl } H \quad (5)$$

and gives

$$\text{div } I = 0 \quad (5a)$$

since, according to (4a) and (4b),

$$\operatorname{div} I = \frac{\partial I_x}{\partial x} + \frac{\partial I_y}{\partial y} + \frac{\partial I_z}{\partial z} = \frac{1}{4\pi} [0]$$

electricity cannot be destroyed or created at any point.

130. Maxwell's Displacement Current.—In high-frequency systems we have to do with variable currents which flow partially along conductors and partially as displacement currents in dielectrics, usually of constant κ . Equations (5) and (5a) must therefore be generalized by using the total current density I' instead of I , which holds only for the conduction current. We have then¹

$$\begin{aligned} I' &= \underbrace{I}_{\substack{\text{current density of} \\ \text{the conduction current}}} + \underbrace{\frac{\partial D}{\partial t}}_{\substack{\text{current density of the} \\ \text{displacement current}}} \\ &= \sigma \mathcal{E} + \frac{1}{4\pi c^2} \frac{\partial \kappa \mathcal{E}}{\partial t} \end{aligned} \quad (6)$$

since, for a dielectric, the time variation $\partial D/\partial t$ of the displacement D gives the current per unit area and

$$\begin{aligned} D &= \frac{\kappa \mathcal{E}}{4\pi c^2} \\ c &= 3 \times 10^{10} \text{ cm/sec} \\ \mathcal{E} &\cdots (1 \text{ e.m.u.} = 10^{-8} \text{ volts cm}^{-1}) \end{aligned}$$

It should be noted that for the conduction current, whether in the conductor or in the dielectric, we always have $I = \sigma \mathcal{E}$ if σ denotes the specific conductivity ($1 \text{ e.m.u.} = 10^9 \Omega^{-1} \text{ cm}^{-1}$). The generalized equations for (5) and (5a) are therefore

$$\begin{aligned} \operatorname{curl} H &= 4\pi I' \\ &= 4\pi \sigma \mathcal{E} + \frac{\kappa}{c^2} \frac{\partial \mathcal{E}}{\partial t} \end{aligned} \quad (7)$$

and

$$\operatorname{div} \left[\sigma \mathcal{E} + \frac{\kappa}{4\pi c^2} \frac{\partial \mathcal{E}}{\partial t} \right] = 0 \quad (7a)$$

In (7) and (7a) attention is called to the three different kinds of conductors, namely, (1) conductors (metals), (2) semiconductors (different kinds of the earth crust), (3) nonconductors (insulating materials).

In Eq. (7) the electric-field strength \mathcal{E} enters in both the conduction and the displacement component. Its maximum possible value depends upon the nature of the substance. For ordinary conductors, the heat

¹ All quantities are expressed in the e.m. c.g.s. system unless especially noted since at times the Gaussian system facilitates the solution.

formation per unit volume ($= \mathcal{E} \cdot I = \sigma \mathcal{E}^2$ watts/cc) determines the upper limit which gives, for example, for copper a value of \mathcal{E}_{\max} of only about 3.5×10^{-3} volts/cm. For nonconductors, however, \mathcal{E}_{\max} can be several thousand volts per centimeter, since σ is theoretically zero. Although the magnitude of the dielectric constant κ of conductors is not known, it is a fact that the displacement current can be neglected. For semiconductors, the conduction and the displacement currents are of about the same order, while for nonconductors only the displacement component remains. Now whether we deal with a semi- or nonconductor depends upon the frequency. Thus, for instance, ordinary ground can be considered, for very low frequencies (commercial frequencies), as a conductor of high resistance depending upon the condition and composition of the ground. However, as the frequency becomes higher, for the wave band (200 m to 20 km) the ground is considered as a substance conducting well enough to act as an electric mirror. But, for still shorter waves, the displacement component begins to play a part, and at about $\lambda = 15$ m the displacement current in the ground is of about the same order as the conduction current, whereas for still shorter waves the ground acts like a dielectric.

For moist ground, the specific conductivity σ is about 8×10^{-14} c.g.s. units in comparison with 5.9×10^{-4} c.g.s. for copper. For expressions in practical units, we have the values of Table X.

TABLE X

Substance	Specific conductivity σ $\frac{1}{\text{ohm} \cdot \text{cm}}$	Dielectric constant κ
Wet ground.....	10^{-4} to 10^{-5}	5 to 15
Dry ground.....	10^{-6} to 10^{-14}	2 to 6
Average river water.....	10^{-5}	80
Salt water (ocean).....	10^{-2} to 5×10^{-2}	80
Heaviside layer.....	About 10^{-15} [see also formula (15) on p. 378]	See formulas (11) and (12) on p. 375, formula (13) on p. 377 and formula (15) on p. 378

For electromagnetic waves in free space, Eq. (7) simplifies to

$$\text{curl } H = \frac{\kappa}{c^2} \frac{\partial \mathcal{E}}{\partial t} \quad (7b)$$

since σ is practically zero.

131. First Field Equation for the Ionized Medium.—When electromagnetic waves pass into the ionized region (Heaviside-Kennelly layer), they set the ions into oscillations and the ions contribute to the electric

current. The Maxwellian equation (7) must then be changed¹ to

$$\text{curl } H = \underbrace{\frac{\kappa}{c^2} \frac{\partial \mathcal{E}}{\partial t}}_{\text{due to displacement component}} + \underbrace{4\pi Nq \frac{\partial s}{\partial t}}_{\text{due to ions of charge } q} \quad (8)$$

where N denotes the number of ions per cubic centimeter and s the displacement of each ion from its original position. The second term is therefore $4\pi q \Sigma v$ if Σv stands for the geometric sum of all field velocities per unit volume. The average effect of the motions of the ions due to thermal agitation practically cancels out and therefore needs no consideration. The correctness of the second term can be readily understood by realizing that, for N ions per cubic centimeter moving with a velocity $v = \partial s / \partial t$, a current density $I = Nqv$ is produced which when multiplied by 4π , according to Ampère's law, gives the second term. Generally, the equation of motion of the free ion, when acted upon by an electric field \mathcal{E} of a wave and in addition by the magnetic field H_e of the earth, is

$$m \frac{d^2 s}{dt^2} = q \left[\mathcal{E} + \frac{1}{c} \frac{ds}{dt} \times H_e \right]$$

¹ We note from (8) that the ions have no restoring force of the dielectric type. The motion of the ion produces a convection current which reacts back on the electromagnetic wave and changes the velocity of propagation. Owing to collisions and recombinations, energy will pass continuously from the electromagnetic field and increase the energy of agitation of neutral molecules. Since the process is irreversible, energy is subtracted from the electromagnetic field. When collisions take place in the ionized medium, the last term of (8) becomes complex as brought out on pages 376-377 and (8) can be written either in the form (Gaussian units)

$$\text{curl } H = \frac{1}{c} \kappa'_e \frac{\partial \mathcal{E}}{\partial t}$$

where κ'_e is the complex dielectric constant, or in the form

$$\text{curl } H = \frac{1}{c} \kappa_e \frac{\partial \mathcal{E}}{\partial t} + \frac{4\pi\sigma}{c} \mathcal{E}$$

where κ_e is the true dielectric constant and σ the true conductivity.

Since the ion forms a portion of the gaseous medium, it will participate in the thermal agitation of the gas molecules and the kinetic theory requires that the kinetic energy of the ions for such a motion is equal to that of the molecules of the medium (gas). Hence their velocity varies as the square root of the mass of the ion. It is to be remembered that even at ordinary temperatures, the thermal velocities are very large. For instance, for air the average molecular velocity at atmospheric pressure and 0°C is as high as 48.5×10^3 cm/sec. Since these velocities are distributed equally in all directions, the number of ions carried by thermal agitations across any plane in the gaseous medium in one direction is equal to the number of ions crossing the plane in the opposite direction. Hence no electric charges can be transferred in this way. The only effect which thermal agitations produce is to control the number of collisions.

when expressed in Gaussian units and m denotes the mass of the ion. The total current density I is then found from

$$4\pi I = \frac{d\varepsilon}{dt} + \Sigma 4\pi Nq \frac{ds}{dt} = \kappa_e \frac{d\varepsilon}{dt} \quad (8a)$$

when the summation refers again to different kinds of ions and κ_e is the effective dielectric constant instead of κ which would be unity for ether.

132. Faraday's Induction Law.—This law gives the e.m.f. around a circuit through which the magnetic flux Φ varies. For an elementary area dS , it is $e = -\frac{\partial\Phi}{\partial t} = -\frac{\partial B}{\partial t}dS = -\frac{\partial(\mu H)}{\partial t}dS$. The flux Φ through the rectangle $ABCD$ of Fig. 206 is $\mu H_x dy \cdot dz$ and the rate of variation of magnetic flux is $dydz(\partial\mu H_x/\partial t)$. If the component of the electric-field strength ε along AB is ε_y , then along CD it is $\varepsilon_y + (\partial\varepsilon_y/\partial z)dz$, and similarly for the other two sides. We have therefore for the induced e.m.f. around the rectangle $ABCD$

$$\varepsilon_y dy + \left[\varepsilon_z + \frac{\partial\varepsilon_z}{\partial y}dy \right] dz - \left[\varepsilon_y + \frac{\partial\varepsilon_y}{\partial z}dz \right] - \varepsilon_x dz = \left[\frac{\partial\varepsilon_z}{\partial y} - \frac{\partial\varepsilon_y}{\partial z} \right] dydz$$

Hence

$$\left[\frac{\partial\varepsilon_z}{\partial y} - \frac{\partial\varepsilon_y}{\partial z} \right] dydz = -dydz \frac{\partial\mu H_x}{\partial t}$$

or, for μ constant,

$$-\mu \frac{\partial H_x}{\partial t} = \frac{\partial\varepsilon_z}{\partial y} - \frac{\partial\varepsilon_y}{\partial z} \quad (9)$$

In the same way we find the other two components

$$\left. \begin{aligned} -\mu \frac{\partial H_y}{\partial t} &= \frac{\partial\varepsilon_x}{\partial z} - \frac{\partial\varepsilon_z}{\partial x} \\ -\mu \frac{\partial H_z}{\partial t} &= \frac{\partial\varepsilon_y}{\partial x} - \frac{\partial\varepsilon_x}{\partial y} \end{aligned} \right\} \quad (10)$$

Equations (9) and (10) lead to the second Maxwellian field equation

$$\frac{\partial B}{\partial t} = \frac{\partial(\mu H)}{\partial t} = -\text{curl } \varepsilon \quad (11)$$

133. Field Equations for the Dielectric and for Conductors (Stationary Bodies).—According to (7b) and (11), we have for a dielectric with negligible conduction currents

$$\left. \begin{aligned} \text{curl } H &= \frac{\kappa}{c^2} \frac{d\varepsilon}{dt} \\ \text{curl } \varepsilon &= -\mu \frac{dH}{dt} \end{aligned} \right\} \quad (12)$$

and for conductors with negligible displacement currents, according to (5) and (11),

$$\left. \begin{aligned} \text{curl } H &= 4\pi I \\ \text{curl } \mathcal{E} &= -\frac{dB}{dt} \end{aligned} \right\} \quad (13)$$

in the differential form. These results read, in the integral form,

$$\left. \begin{aligned} \text{M.m.f.} &= \oint H dl = 4\pi I_t \\ \text{Induced e.m.f.} &= \oint \mathcal{E} dl = -\frac{d\Phi}{dt} \end{aligned} \right\} \quad (13a)$$

where $I_t = \int I dS$.

134. Application of the Field Equations to the Case of Penetration into a Conductor. Case A. For a Plane Slab.—When electromagnetic

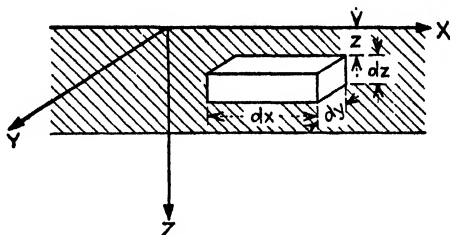


FIG. 207.—Penetration of electromagnetic waves.

waves pass over conductors (metal, sea water, ground, etc.), they induce currents in them. The penetration becomes smaller as the frequency becomes higher. Figure 207 represents a slab of a conductor with a flat surface. Imagine again a small parallelepiped $dx dy dz$ with its top face a depth z below the top face of the slab. When a high-frequency e.m.f. acts parallel to the flat surface, the corresponding current flow diminishes as we go below the surface. If I_z denotes the current density perpendicular to face $dy dz$, we have, according to (13),

$$\begin{aligned} \frac{\partial H_y}{\partial z} &= -4\pi I_z \\ \frac{\partial \mathcal{E}_x}{\partial z} &= -\mu \frac{\partial H_y}{\partial t} \end{aligned}$$

since in the corresponding component equations (4a) and (10) the components H_z and \mathcal{E}_z are zero. Differentiating the first equation with respect to t and the second with respect to z gives upon elimination of $\partial^2 H_y / \partial z \partial t$

$$\frac{\partial^2 I_z}{\partial z^2} = 4\pi\mu\sigma \frac{\partial I_z}{\partial t}$$

since for the specific conductivity σ of the conductor $I_z = \sigma \mathcal{E}_z$. Assuming a sinusoidal variation $I_z = I_0 e^{j\omega t}$ gives for $\omega = 2\pi f$

$$\begin{aligned} \frac{d^2 I_z}{dz^2} &= j\omega 4\pi\mu\sigma I_z \\ &= \alpha^2 [j + 1]^2 I_z \end{aligned} \quad (14)$$

for

$$\alpha = 2\pi\sqrt{\mu\sigma f} \quad (15)$$

since $2j = (j + 1)^2$.

Equation (14) is of the form $d^2 y/dx^2 = a^2 y$ with the well-known solution

$$y = A e^{-\alpha z} + B e^{+\alpha z}$$

We have therefore an expression for the current density I_z at any depth z with the solution

$$I_z = A e^{-(j+1)\alpha z} + B e^{(j+1)\alpha z}$$

The constant B must be zero; otherwise I_z could not become zero at an infinite depth z . If I_0 denotes the maximum value of the current density at the surface of the conductor, we have the solution

$$I_z = I_0 e^{j\omega t} e^{-(j+1)\alpha z} = I_0 e^{-\alpha z} e^{j(\omega t - \alpha z)} = I_0 e^{-\alpha z} \{ \cos(\omega t - \alpha z) + j \sin(\omega t - \alpha z) \} \quad (16)$$

Hence α is the damping constant with respect to the depth. It is therefore possible to calculate the thickness of the skin for which noticeable currents can flow. For ϵ^{-4} we have about $0.02I_0$, that is, only about 2 per cent of the surface current density. Taking this as the limit, we have $z = 4/\alpha$ and, according to (15),

$$z = \frac{0.636}{\sqrt{\mu\sigma f}} \text{ cm} \quad (17)$$

The field equation used in the derivation was expressed in the e.m.c.g.s. system; hence the specific conductivity σ and the permeability as well as the distance z are also in these units. The frequency f is in cycles per second. This gives, for $f = 10^5$ cycles/sec, assuming iron with about $\sigma = 10^{-4}$ c.g.s.u. and $\mu = 10^3$, a penetration of 0.00636 cm, while for 1,000,000 cycles/sec the penetration would be only about 0.002 cm deep. Moreover, according to (16), it is evident that

$$I_z = I_0 e^{-z} \sqrt{\frac{2\pi\omega\mu}{\rho}} \sin\left(\omega t - z\sqrt{\frac{2\pi\omega\mu}{\rho}}\right) \quad (16a)$$

if ρ denotes the specific resistance in abohms per cubic centimeter. It is therefore possible to calculate how deep an electromagnetic wave penetrates into ground. We have, for the equation of penetration,

$$H_z = H_0 e^{-\alpha z}$$

where

$$\alpha = \sqrt{\frac{2\pi\omega\mu}{\rho}}$$

and H_0 and H_z are the field intensities at the surface and z cm below it. For ocean water, $\mu = 1$; $\rho \cong 10^{11}$ abohms/cc. Assuming that a signal H_z of 1 per cent of H_0 is still detectable, we have

$$e^{-2\pi z} \sqrt{\frac{1}{\rho}} = 0.01$$

and, for a wave length $\lambda = 10,000$ m, we find that reception below $z = 15$ m is questionable. It is seen that with longer waves greater depths can be reached.

If the earth were a perfect conductor, the electric-field vector \mathcal{E} would be everywhere perpendicular to ground and electric waves could not penetrate into the ground. But because of the dielectric constant κ and the specific conductivity σ , the electric field \mathcal{E} tilts somewhat forward and energy is subtracted by the ground from the electromagnetic wave passing over it.¹ According to G. W. O. Howe,² the penetration t of the waves into ground (for a decrease to 10 per cent of the current density

TABLE XI.—PENETRATION OF WAVES INTO GROUND

Frequency, kc/sec	Dry ground		Wet ground		River water	Ocean
	$\sigma = 10^{-8}$ $\kappa = 2$	$\sigma = 10^{-8}$ $\kappa = 6$	$\sigma = 10^{-5}$ $\kappa = 5$	$\sigma = 10^{-5}$ $\kappa = 15$	$\sigma = 10^{-5}$ $\kappa = 80$	$\sigma = 10^{-2}$ $\kappa = 80$
9.55	$t = 1190$ m	$t = 1200$ m	$t = 375$ m	$t = 375$ m	$t = 384$ m	$t = 11.86$ m
47.76	545	580	169	171	186	5.3
477.6	216	311	51	63.5	112	1.68
4776	172	298	29	47.4	109	0.54
47760	172	298	23.6	47.2	108.5	0.19

at the surface) is as in Table XI. Hence for transmission over the ocean, even the long waves hardly penetrate below the surface.

Case B. For a Straight Wire.—Figure 208 shows the cross section of a circular conductor of radius r_1 . For the solution, the integral form of (13a) is convenient. It is therefore necessary to calculate the total current density for each ring of radii r and $r + dr$ in order to evaluate the line integral $\oint H dl = 4\pi I$. We then have for the current density I along the wire

$$H_{r+dr} 2\pi(r + dr) - H 2\pi r = 4\pi I (2\pi r dr)$$

¹ The case of attenuation along the X, Y, and Z dimension in ground is treated in "High Frequency Measurements," pp. 292-294, McGraw-Hill Book Company Inc., 1933.

² *London Electrician*, 1925.

But

$$H_{r+dr} = H_r + \frac{\partial H_r}{\partial r} dr$$

hence

$$\frac{\partial H_r}{\partial r} + \frac{1}{r} H_r = 4\pi I$$

which is the first Maxwellian equation in cylinder coordinates. According to (13a), we have for the Faraday-Maxwell induction law the line

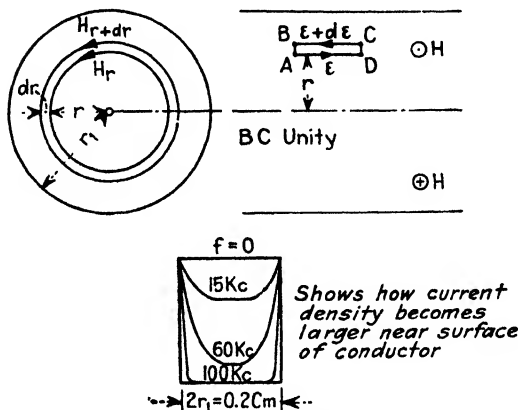


FIG. 208.—Current distribution in cross section of a conductor.

integral $\oint \mathcal{E} dl = -d\Phi/dt = -\mu(dH/dt)$. Through the rectangle ABCD of unit length and width dr the induction flux $\mu H dr$ passes and leads to

$$\mathcal{E} - \left(\mathcal{E} + \frac{\partial \mathcal{E}}{\partial r} dr \right) = -\frac{\partial}{\partial t} \mu H dr$$

or

$$\frac{\partial \mathcal{E}}{\partial r} = \mu \frac{\partial H}{\partial t}$$

For the specific conductivity σ , we have $I = \sigma \mathcal{E}$ and

$$\frac{1}{\sigma} \frac{\partial I}{\partial r} = \mu \frac{\partial H}{\partial t}$$

which is the other Maxwellian equation in cylindrical coordinates. For high-frequency work, we are interested in harmonic currents and the two main equations treated symbolically by means of $H, \mathcal{E} e^{j\omega t}$ give

$$\left. \begin{aligned} 4\pi I &= \frac{\partial H_r}{\partial r} + \frac{1}{r} H_r \\ \frac{\partial I}{\partial r} &= j\omega \sigma \mu H_r \end{aligned} \right\}$$

where I and H now denote complex functions of r whose scalar value at each place is equal to the amplitude. For the sake of simplicity, no special notation for the two quantities is introduced. Eliminating H , gives the differential equation

$$\frac{\partial^2 I}{\partial r^2} + \frac{1}{r} \frac{\partial I}{\partial r} - 4\pi j\omega\mu\sigma I = 0$$

Putting $4\pi\sigma\mu\omega = m^2$ and $mr = x$ gives

$$\frac{\partial^2 I}{\partial x^2} + \frac{1}{x} \frac{\partial I}{\partial x} = jI \quad \{$$

or

$$\frac{\partial}{\partial x} \left(x \frac{\partial I}{\partial x} \right) = j \cdot I \cdot x$$

The integral of this expression is a Bessel function of the first kind. According to Lord Kelvin, it can be expressed by a real and an imaginary term as

$$I = k(\text{ber } x + j \text{bei } x)$$

and inserting this in the foregoing equation leads to

$$\begin{aligned} \frac{\partial}{\partial x}(x \text{bei}' x) &= x \text{ber } x \\ \frac{\partial}{\partial x}(x \text{ber}' x) &= -x \text{bei } x \end{aligned}$$

where

$$\begin{aligned} \text{ber } x &= 1 - \frac{x^4}{(2 \times 4)^2} + \frac{x^8}{(2 \times 4 \times 6 \times 8)^2} - \dots \\ \text{bei } x &= \frac{x^2}{2^2} - \frac{x^6}{(2 \times 4 \times 6)^2} + \dots \end{aligned}$$

For the center of the conductor, $r = 0$ and $k = I_0$ and, for the surface, $r = r_1$ and

$$I_1 = k(\text{ber } mr_1 + j \text{bei } mr_1).$$

Hence the ratio of the current density at the center to that at the surface becomes

$$\frac{I_0}{I_1} = [\text{ber}^2 mr_1 + \text{bei}^2 mr_1]^{-1/2}$$

and the phase displacement ψ between these two current densities is

$$\tan \psi = \frac{\text{bei } mr_1}{\text{ber } mr_1}$$

the phase angle indicates that an internal self-induction exists. Putting

$$x_1 = \frac{mr_1}{2\sqrt{2}} = \pi r_1 \sqrt{\mu \sigma f}$$

since $m = \sqrt{4\pi\mu\sigma\omega}$

we have for small and large arguments the following approximate formulas:

$$\left. \begin{array}{l} \text{For } x_1 = 0 \text{ to } 0.8, \\ \frac{R}{R_0} = 1 + \frac{x_1^4}{3} - \frac{4}{45}x_1^8 \\ \text{For } x_1 = 1.5 \text{ to } 10, \\ \frac{R}{R_0} = 0.997x_1 + 0.277 \\ \text{For } x_1 > 2, \\ \frac{R}{R_0} = x_1 + \frac{1}{4} + \frac{3}{64x_1} \end{array} \right\} \begin{array}{l} \\ \\ (R \text{ high-frequency resistance.} \\ R_0 \text{ direct-current resistance}) \\ \end{array}$$

For the range $x_1 = 0.8$ to 1.5 , we have

TABLE XII

x_1	R/R_0	x_1	R/R_0	x_1	R/R_0	x_1	R/R_0
0.7	1.07	0.9	1.18	1.1	1.35	1.3	1.56
0.75	1.09	0.95	1.22	1.15	1.4	1.35	1.61
0.8	1.11	1.0	1.26	1.2	1.45	1.4	1.66
0.85	1.14	1.05	1.31	1.25	1.5	1.45	1.72

Figure 208 shows also the distribution of the current amplitudes for a circular copper wire with a diameter of 0.2 cm. The skin effect is already pronounced even at a frequency of only 100 kc/sec.

135. Propagation of Electromagnetic Waves.—The two main field equations are

$$\left. \begin{array}{l} \text{curl } H = 4\pi\sigma\mathcal{E} + \frac{\kappa}{c^2} \frac{d\mathcal{E}}{dt} \\ \text{curl } \mathcal{E} = -\frac{d(\mu H)}{dt} \end{array} \right\} \quad (18)$$

and the components of the first of these equations are

$$\left. \begin{array}{l} \frac{\partial H_z}{\partial y} - \frac{\partial H_y}{\partial z} = 4\pi\sigma\mathcal{E}_x + \frac{\kappa}{c^2} \frac{\partial \mathcal{E}_x}{\partial t} \\ \frac{\partial H_x}{\partial z} - \frac{\partial H_z}{\partial x} = 4\pi\sigma\mathcal{E}_y + \frac{\kappa}{c^2} \frac{\partial \mathcal{E}_y}{\partial t} \\ \frac{\partial H_y}{\partial x} - \frac{\partial H_x}{\partial y} = 4\pi\sigma\mathcal{E}_z + \frac{\kappa}{c^2} \frac{\partial \mathcal{E}_z}{\partial t} \end{array} \right\} \quad (18a)$$

The components of the second equation of (18) are given by (9) and (10). These expressions can be combined to give the equations of motion of the electromagnetic field. Differentiating the first equation with respect to t gives for the x component

$$\frac{\partial}{\partial y} \left(\frac{\partial H_z}{\partial t} \right) - \frac{\partial}{\partial z} \left(\frac{\partial H_y}{\partial t} \right) = 4\pi\sigma \frac{\partial \mathcal{E}_x}{\partial t} + \frac{\kappa}{c^2} \frac{\partial^2 \mathcal{E}_x}{\partial t^2}$$

Inserting from (10) the values for $\partial H_y/\partial t$ and $\partial H_z/\partial t$ leads to

$$\frac{1}{\mu} \left[\frac{\partial}{\partial y} \left(\frac{\partial \mathcal{E}_x}{\partial y} - \frac{\partial \mathcal{E}_y}{\partial x} \right) - \frac{\partial}{\partial z} \left(\frac{\partial \mathcal{E}_x}{\partial x} - \frac{\partial \mathcal{E}_x}{\partial z} \right) \right] = 4\pi\sigma \frac{\partial \mathcal{E}_x}{\partial t} + \frac{\kappa}{c^2} \frac{\partial^2 \mathcal{E}_x}{\partial t^2}$$

or

$$4\pi\sigma \frac{\partial \mathcal{E}_x}{\partial t} + \frac{\kappa}{c^2} \frac{\partial^2 \mathcal{E}_x}{\partial t^2} = \frac{1}{\mu} \left[\nabla^2 \mathcal{E}_x - \frac{\partial}{\partial x} (\text{div } \mathcal{E}) \right] \quad (19)$$

since

$$\nabla^2 \mathcal{E}_x = \frac{\partial^2 \mathcal{E}_x}{\partial x^2} + \frac{\partial^2 \mathcal{E}_x}{\partial y^2} + \frac{\partial^2 \mathcal{E}_x}{\partial z^2}$$

and

$$\text{div } \mathcal{E} = \frac{\partial \mathcal{E}_x}{\partial x} + \frac{\partial \mathcal{E}_y}{\partial y} + \frac{\partial \mathcal{E}_z}{\partial z}$$

In a similar manner, the other two components become

$$\left. \begin{aligned} 4\pi\sigma \frac{\partial \mathcal{E}_y}{\partial t} + \frac{\kappa}{c^2} \frac{\partial^2 \mathcal{E}_y}{\partial t^2} &= \frac{1}{\mu} \left[\nabla^2 \mathcal{E}_y - \frac{\partial}{\partial y} (\text{div } \mathcal{E}) \right] \\ 4\pi\sigma \frac{\partial \mathcal{E}_z}{\partial t} + \frac{\kappa}{c^2} \frac{\partial^2 \mathcal{E}_z}{\partial t^2} &= \frac{1}{\mu} \left[\nabla^2 \mathcal{E}_z - \frac{\partial}{\partial z} (\text{div } \mathcal{E}) \right] \end{aligned} \right\} \quad (20)$$

Differentiating the first equation of (18) with respect to x , the second with respect to y , and the third with respect to z , and adding, results in

$$4\pi\sigma \left[\frac{\partial \mathcal{E}_x}{\partial x} + \frac{\partial \mathcal{E}_y}{\partial y} + \frac{\partial \mathcal{E}_z}{\partial z} \right] + \frac{\kappa}{c^2} \left[\frac{\partial^2 \mathcal{E}_x}{\partial x \partial t} + \frac{\partial^2 \mathcal{E}_y}{\partial y \partial t} + \frac{\partial^2 \mathcal{E}_z}{\partial z \partial t} \right] = 0$$

or

$$4\pi\sigma (\text{div } \mathcal{E}) + \frac{\kappa}{c^2} \frac{\partial}{\partial t} (\text{div } \mathcal{E}) = 0 \quad (21)$$

Hence

$$\text{div } \mathcal{E} = \text{constant } e^{-\frac{4\pi\sigma\kappa}{c^2}t} \quad (22)$$

since Eq. (21) has the form

$$\frac{dy}{dt} + \frac{a}{b}y = 0$$

where $a = 4\pi\sigma$, $b = \kappa/c^2$, and the solution $y = Ae^{-at/b}$. For nonconductors ($\sigma = 0$), the result is $\text{div } \mathcal{E} = \text{constant}$. For periodic changes,

$\text{div } (\epsilon)$ as well as $\text{div } (H)$ can be put equal to zero. When a medium shows a certain conductivity (as, for instance, the ground), the $\text{div } \epsilon$ will decrease. The decrease is more pronounced as the relaxation time T_0 becomes smaller. It is

$$T_0 = \frac{\kappa}{4\pi c^2 \sigma}$$

Putting $\text{div } \epsilon = 0$ in Eq. (19) gives

$$\frac{\partial^2 \epsilon_x}{\partial t^2} + \frac{4\pi c^2 \sigma}{\kappa} \frac{\partial \epsilon_x}{\partial t} = v^2 \nabla^2 \epsilon_x \quad (23)$$

where

$$\left. \begin{aligned} v &= \frac{c}{\sqrt{\mu\kappa}} \\ c &= 3 \times 10^{10} \text{ cm/sec} \end{aligned} \right\} \quad (23a)$$

denote the velocity of propagation of the electromagnetic disturbance and the velocity of light, respectively. For ether, $\mu = \kappa = 1$. Similar equations can be obtained for (20). When Eq. (9) is differentiated with respect to t and the values for $\partial \epsilon_v / \partial t$ and $\partial \epsilon_r / \partial t$ from (18) are inserted, we have, for the x component,

$$4\pi\sigma \frac{\partial H_x}{\partial t} + \frac{\kappa}{c^2} \frac{\partial^2 H_x}{\partial t^2} = \frac{1}{\mu} \left[\nabla^2 H_x - \frac{\partial}{\partial r} (\text{div } H) \right] \quad (24)$$

and similar expressions for the other two components of H . We have therefore the corresponding equation of motion for $\text{div } H = 0$

$$\frac{\partial^2 H_x}{\partial t^2} + \frac{4\pi c^2 \sigma}{\kappa} \frac{\partial H_x}{\partial t} = v^2 \nabla^2 H_x \quad (25)$$

Both (23) and (25) have the form

$$\frac{\partial^2 P}{\partial t^2} + \frac{1}{T_0} \frac{\partial P}{\partial t} = v^2 \nabla^2 P \quad (26)$$

of the wave equation. For plane waves in the direction of the x -axis, an equation of this type leads, for instance, to the telegraph equation

$$\frac{\partial^2 P}{\partial t^2} + \frac{1}{T_0} \frac{\partial P}{\partial t} = v^2 \frac{\partial^2 P}{\partial x^2} \quad (27)$$

and for free waves in insulators for which the relaxation time T_0 is infinite, we have

$$\frac{\partial^2 P}{\partial t^2} = v^2 \frac{\partial^2 P}{\partial x^2} \quad (28)$$

with the well-known solution

$$P = F_1(x - vt) + F_2(x + vt) \quad (28a)$$

For an isotropic dielectric, the foregoing equations become

$$\left. \begin{aligned} \frac{\partial^2 \mathcal{E}}{\partial t^2} &= \frac{c^2}{\mu\kappa} \nabla^2 \mathcal{E} \\ \frac{\partial^2 H}{\partial t^2} &= \frac{c^2}{\mu\kappa} \nabla^2 H \end{aligned} \right\} \quad (29)$$

where $\nabla^2 \mathcal{E} = (\partial^2 \mathcal{E} / \partial x^2) + (\partial^2 \mathcal{E} / \partial y^2) + (\partial^2 \mathcal{E} / \partial z^2)$ and similarly for $\nabla^2 H$. These results can also be directly derived from the curl equations (18) by neglecting the conduction term $4\pi\sigma\mathcal{E}$. Hence

$$\left. \begin{aligned} \text{curl } H &= \frac{\kappa}{c^2} \frac{\partial \mathcal{E}}{\partial t} \\ \text{curl } \mathcal{E} &= -\mu \frac{\partial H}{\partial t} \end{aligned} \right\}$$

Differentiating the second equation with respect to t gives

$$\frac{\partial}{\partial t} \text{curl } \mathcal{E} = -\mu \frac{\partial^2 H}{\partial t^2}$$

and substituting the value of $\partial \mathcal{E} / \partial t$ of the first equation gives

$$\frac{c^2}{\kappa} \text{curl}^2 H = -\mu \frac{\partial^2 H}{\partial t^2}$$

or

$$\frac{\partial^2 H}{\partial t^2} = -\frac{c^2}{\mu\kappa} \text{curl}^2 H = \frac{c}{\mu\kappa} \left[\frac{\partial^2 H}{\partial x^2} + \frac{\partial^2 H}{\partial y^2} + \frac{\partial^2 H}{\partial z^2} \right] = \frac{c^2}{\mu\kappa} \nabla^2 H$$

For very long Hertzian waves (in semiconductors), the displacement current may be neglected in comparison with the conduction current and (23) and (25) lead to

$$\left. \begin{aligned} \frac{\partial \mathcal{E}}{\partial t} &= \frac{1}{4\pi\sigma\mu} \nabla^2 \mathcal{E} \\ \frac{\partial H}{\partial t} &= \frac{1}{4\pi\sigma\mu} \nabla^2 H \end{aligned} \right\} \quad (30)$$

From the complete solutions of (23) and (25), it can be seen why Hertzian waves cannot penetrate very far into sea water and ground. The term with the first time derivative ($\partial \mathcal{E} / \partial t$ and $\partial H / \partial t$, respectively) affects the speed of propagation and the attenuation. Since for propagation in free space [if not in the ionized medium, see Eq. (8)] Eq. (29) is sufficient, we have, for the field strength \mathcal{E} a distance d from the excitation,

$$\mathcal{E} = \frac{1}{d} \left[F_1 \left(d - \frac{c}{\sqrt{\mu\kappa}} t \right) + F_2 \left(d + \frac{c}{\sqrt{\mu\kappa}} t \right) \right] \quad (31)$$

A similar expression may be obtained for H . In this solution F_1 and F_2 are arbitrary functions. In our case, F_1 represents a spherical wave which spreads away from the center of excitation, and F_2 a wave which converges toward the center, both traveling with a velocity $v = c/\sqrt{\mu\kappa}$. But $\lambda = vT$ for the wave length λ and period T and, expressing F_1 as a trigonometric function, leads to

$$\varepsilon = \frac{\varepsilon_0}{d} \cos 2\pi \left(\frac{d}{\lambda} - \frac{t}{T} \right) \quad (32)$$

where ε_0 denotes the amplitude at the center of excitation. A similar expression can be obtained for H . The H and ε vibrations are perpendicular to each other and to the direction of propagation. For large distances d , the waves may be considered to be plane rather than spherical and we have

$$H_0 = \sqrt{\frac{\kappa}{\mu}} \frac{\varepsilon_0}{c} \quad (33)$$

since $H_0 = (\kappa/c^2)(\lambda/T)\varepsilon_0$. For ether, $\kappa = \mu = 1$ and

$$\begin{aligned} \varepsilon &= cH \\ \varepsilon \text{ (volts/cm)} &= 300H \text{ (gilberts/cm)} \end{aligned} \quad (34)$$

an important relation for field-intensity measurements.

When Hertzian waves pass from a medium κ_1, μ_1 to one of constants κ_2, μ_2 , the index n of refraction of the wave is equal to the ratio of the velocities of propagation; that is,

$$n = \sqrt{\frac{\mu_1 \kappa_1}{\mu_2 \kappa_2}} \quad (35)$$

This expression determines the bending of the path along which radio waves are propagated when the constants of the medium change gradually. For instance, for the ionized layer of the atmosphere where $\mu_1 = \mu_2 = 1$, the bending depends only upon the change of the apparent dielectric constant.

136. Scalar and Vector Potentials.—Maxwell's field equations are a means whereby the current may be calculated when the magnetic field is known. But in order to calculate the magnetic field from an electric current, the vector potential Λ is conveniently used. If the field at a distance (as in the case of the space field due to current in a distant antenna) is to be computed, *retarded* vector potentials are employed. A knowledge of these is necessary since the Hertzian equations are based upon such potentials.

The integral $\int \frac{q d\tau}{r}$ is called a scalar potential¹ if q denotes any scalar quantity which is arbitrarily distributed in a region with volume elements $d\tau$, and r is the distance from $d\tau$ to some fixed point. If q denotes a vector function of position instead of a scalar function, the integral gives the vector potential.² This has in addition to magnitude also a direction. Hence if $q = \rho$ denotes the electric volume density, then $\int \frac{\rho d\tau}{r}$ is the electric scalar potential at the fixed point. But if we deal with the distribution of an electric current density I in the element $d\tau$, we have the vector potential

$$\mathbf{A} = \int \frac{I d\tau}{r} \quad (36)$$

Now if the field is without sources

$$(\text{div } \mathbf{A} = 0),$$

we have

$$\left. \begin{aligned} 4\pi I &= -\nabla^2 \mathbf{A} \\ H &= \text{curl } \mathbf{A} \end{aligned} \right\} \quad (37)$$

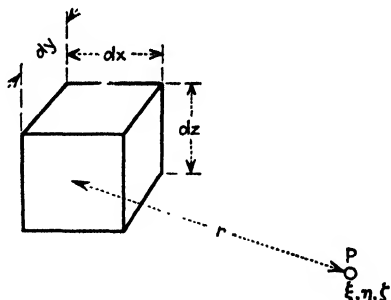


FIG. 209.—Volume element $d\tau$ of coordinates x, y , and z and point P of coordinates ξ, η, ζ .

Hence the vector potential of moving charges (that is, of a current) is such that its curl gives the magnetic-field strength due to the current at any given point. The last equation serves to calculate H from the current density. If the volume element $d\tau$ has the coordinates x, y, z and the components I_x, I_y , and I_z for the current density, we have for point P (Fig. 209), whose coordinates are ξ, η, ζ , the three components of the vector potential

$$\left. \begin{aligned} A_\xi &= \int \frac{I_x d\tau}{r} \\ A_\eta &= \int \frac{I_y d\tau}{r} \\ A_\zeta &= \int \frac{I_z d\tau}{r} \end{aligned} \right\} \quad (38)$$

After these components are known, the components of the magnetic-field strength are calculated from

¹ The electric field due to stationary charges is a vector \mathbf{E} which can be derived from a scalar potential V according to $\mathbf{E} = -\text{grad } V$.

² The vector potential \mathbf{A} can also be considered as a vector such that the line integral of \mathbf{A} around any closed path equals the magnetic flux through that path, or $\oint \mathbf{A} \cos \alpha d\ell = \iint \mu H \cos \beta dS$.

$$\left. \begin{aligned} H_{\xi} &= \frac{\partial \Lambda_{\zeta}}{\partial \eta} - \frac{\partial \Lambda_{\eta}}{\partial \zeta} \\ H_{\eta} &= \frac{\partial \Lambda_{\xi}}{\partial \zeta} - \frac{\partial \Lambda_{\zeta}}{\partial \xi} \\ H_{\zeta} &= \frac{\partial \Lambda_{\eta}}{\partial \xi} - \frac{\partial \Lambda_{\xi}}{\partial \eta} \end{aligned} \right\} \quad (39)$$

By inserting (39) in (4a) and (4b) and putting

$$\frac{\partial \Lambda_{\xi}}{\partial \xi} + \frac{\partial \Lambda_{\eta}}{\partial \eta} + \frac{\partial \Lambda_{\zeta}}{\partial \zeta} = 0$$

the correctness of (39) is proved since the first relation of (37) is obtained. According to the definitions given above, the scalar potential V at a fixed point, for an electric volume density ρ in the element $d\tau = dx dy dz$, is

$$V = \frac{1}{\kappa_0} \iiint \frac{\rho}{r} dx dy dz$$

and the vector potential for the current density I in the same volume element is

$$\Lambda = \mu_0 \iiint \frac{I}{r} dx dy dz$$

The corresponding retarded potentials are

$$\left. \begin{aligned} V_r &= \frac{1}{\kappa_0} \iiint \frac{[\rho]}{r} \frac{t-r}{c} dx dy dz \\ \Lambda_r &= \mu_0 \iiint \frac{[I]}{r} \frac{t-r}{c} dx dy dz \end{aligned} \right\} \quad (40)$$

since the potentials due to a periodically varying space charge ρ and a current density I , respectively, act at a point at a distance r somewhat later (are retarded), and the instantaneous value, for example, of I is not I_t but $I_{t-(r/c)}$, if c is the velocity of propagation. We have $\mu_0 = 1$ and $\kappa_0 = 1/c^2$ in the e.m.c.g.s. system, and in the e.s.c.g.s. system $\kappa_0 = 1$ and $\mu_0 = 1/c^2$. For any further considerations, the subscript r for the retarded potentials will be omitted for the sake of simplicity. Now if Gaussian units are employed for which ϵ , I are in e.s.c.g.s. and H in e.m.c.g.s. units, the electric and magnetic forces at any point due to the current-density I are found by first calculating the scalar and vector potentials by integration and then evaluating ϵ and H from

$$\begin{aligned}\mathcal{E} &= -\text{grad } V - \frac{1}{c} \frac{\partial \Lambda}{\partial t} \Big\} \\ H &= \text{curl } \Lambda\end{aligned}\quad (40a)$$

for

$$\Lambda = \iiint \frac{[I]_t - \frac{r}{c}}{r} d\tau \quad \text{and} \quad V = \iiint \frac{[\rho]_t - \frac{r}{c}}{r} d\tau$$

Examples.—If the current element is at the origin and x , y , and z the point at which H_x , H_y , and H_z are the components of the magnetic-field strength and Λ_x , Λ_y , and Λ_z the components of the vector potential, we have to put in (39) $\xi = x$, $\eta = y$, and $\zeta = z$. For an antenna AB as indicated in Fig. 210, we have, if the current element dh is at the origin, for point x , y , z

$$\Lambda_x = \Lambda_y = 0 \quad \text{and} \quad \Lambda_z = \frac{idh}{r}$$

Equation (39) therefore reduces to

$$\left. \begin{aligned} H_x &= \frac{\partial \Lambda_z}{\partial y} \\ H_y &= -\frac{\partial \Lambda_z}{\partial x} \\ H_z &= 0 \end{aligned} \right\} \quad (39a)$$

or

$$H = \sqrt{H_x^2 + H_y^2}$$

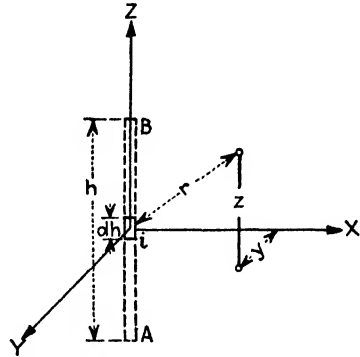


FIG. 210.—Current element i of height dh for finding radiation effect of an open circuit (vertical aerial AB).

In the equatorial plane for a point x , 0, 0, Eq. (39a) reduces to

$$H_y = -\frac{\partial \Lambda_z}{\partial x} \quad (39b)$$

since also $\partial \Lambda_z / \partial y = 0$. For a sinusoidal current, we have the vector potential

$$\Lambda_z = \frac{I_m dh}{x} \sin \omega \left(t - \frac{x}{c} \right)$$

and for any distance x the instantaneous value of the magnetic-field strength

$$\begin{aligned} H_t &= -0.1 \frac{\partial \Lambda_z}{\partial x} = -0.1 \left\{ \frac{\omega \cdot dh \cdot I_m}{cx} \cos \omega \left(t - \frac{x}{c} \right) + \frac{dh \cdot I_m}{x^2} \sin \omega \left(t - \frac{x}{c} \right) \right\} \quad (39c) \\ &= \underbrace{\quad a \quad}_{\text{power or watt component due to radiated field}} + \underbrace{\quad jb \quad}_{\text{wattless component due to field which is interlinked with the current element } dh} \end{aligned}$$

According to (34),

$$\mathcal{E} \text{ (volt/cm)} = 300 H \text{ (gilbert/cm)}$$

the electric-field strength may also be found. According to the figure, it is evident that the field strength H_t as well as \mathcal{E} , varies as the cosine of the altitude of the point

The first term L is the self-induction of the circuit which is the only term important for slowly varying currents (low frequency). The last terms become more important as the frequency increases. For sinusoidal currents, the current density is

$$I = I_m \cos \omega t$$

and

$$E = (L - \omega^2 L_2) \frac{dI}{dt} - \underbrace{(\omega^2 L_1 - \omega^4 L_3)}_{\text{in phase with } I} I$$

The parenthesis value of the inphase term must be a resistance in order to produce an e.m.f. and denotes the radiation resistance

$$R = -\omega^2 L_1 + \omega^4 L_3$$

137. Spherical, Cylindrical, and Beam Wave Propagation.—The solutions for uni-, two-, and three-dimensional radiation of a single outgoing sinusoidal wave train are

$$\left. \begin{aligned} \varepsilon_z &= \varepsilon_0 \sin \omega \left(t - \frac{r}{c} \right) \cdots \text{linear } (r = x) \\ \varepsilon_z &= \frac{\varepsilon_0}{\sqrt{r}} \sin \omega \left(t - \frac{r}{c} \right) \cdots \text{cylindrical } (r = \sqrt{x^2 + y^2}) \\ \Lambda &= \frac{\Lambda_0}{r} \sin \omega \left(t - \frac{r}{c} \right) \cdots \text{spherical } (r = \sqrt{x^2 + y^2 + z^2}) \end{aligned} \right\} \quad (41)$$

for large distances r . ε_0 and Λ_0 denote the values at the source. Uni-dimensional or beam transmission is therefore the most efficient since *no attenuation due to wave spread* occurs (amplitude the same at all distances if there is no absorption in space). When electromagnetic waves are propagated in two dimensions, ε is a function of x , y , and t and the amplitude decreases as $1/\sqrt{r}$. For three-dimensional radiation, the retarded vector potential Λ is a function of x , y , z , and t and the wave-spread attenuation factor varies inversely with the distance. For the foregoing solution, the linear propagation occurs along the x -axis and the electric-field vector ε is parallel to the z -axis. The z component corresponding to (23) gives, for free space, the wave equation (28) with the solution (28a); that is,

$$\varepsilon_z = F_1(x - ct) + F_2(x + ct)$$

since $P = \varepsilon_z$ which for the outgoing term $(x - ct)$ gives the first equation of (41). The corresponding magnetic-field component is

$$H_y = H_0 \sin \omega \left(t - \frac{r}{c} \right)$$

indicating that the electric and magnetic fields are always in phase during the wave propagation. Hence, if at a certain place in space ε has

a maximum value, the magnetic vector H has also maximum strength. This is, of course, not true for standing waves since there are times when the energy is wholly electric and times when it is wholly magnetic.

For spherical wave motion, Euler has given the solution

$$\Delta = \frac{1}{r}[F_1(r - vt) + F_2(r + vt)] \quad (42)$$

if v denotes the velocity of propagation. The third equation of (41) is obtained from (42) for the case of a single sinusoidal wave train moving away from the exciter with a velocity $v = c$. The wave equation then reads

$$\frac{\partial^2(r\Delta)}{\partial r^2} = \frac{\mu\kappa}{c^2} \frac{\partial^2\Delta}{\partial t^2} \quad (43)$$

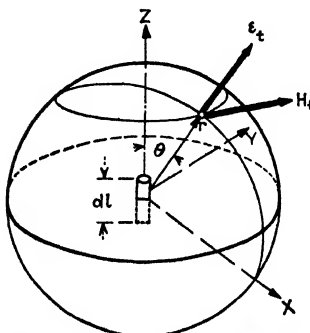


FIG. 212.—Radiation resistance of a current element dl .

where $v = c/\sqrt{\mu\kappa}$.

138. Magnitude and Direction of the Electric and Magnetic Field of a Current Element and Radiation Resistance.—Poynting's theorem is expressed by

$$dW = \frac{1}{4\pi} \epsilon_t H_t dS dt \quad (44)$$

where dW/dt denotes the rate at which energy is supplied to the field by a current-carrying conductor dl through the surface element dS of radius r as shown in Fig. 212. ϵ_t and H_t are the instantaneous values of the electric and magnetic forces, ϵ_t being along r and H_t horizontal.

According to Maxwell's equations,¹ for a current $i = I_0 \sin \omega t$ with a uniform distribution along dl

$$\left. \begin{aligned} \epsilon_t &= \frac{c\lambda I_0}{2\pi} \frac{dl}{r^3} \sin \theta \left[\sin \varphi + \frac{2\pi r}{\lambda} \cos \varphi - \left(\frac{2\pi r}{\lambda} \right)^2 \sin \varphi \right] \\ H_t &= \frac{\lambda I_0}{2\pi} \frac{dl}{r^3} \sin \theta \left[\cos \varphi - \frac{2\pi r}{\lambda} \sin \varphi \right] \end{aligned} \right\} \quad (45)$$

for

$$\varphi = \omega \left(t - \frac{r}{c} \right)$$

These equations have terms which become negligibly small for long distances r and we have, for any distance r large in comparison with the wave length λ ,

¹ The derivation for a vertical antenna is given on p. 351.

$$\left. \begin{aligned} \mathcal{E}_t &= \frac{2\pi c I_0 dl}{\lambda \cdot r} \sin \theta \sin \omega \left(t - \frac{r}{c} \right) \\ H_t &= -\frac{2\pi I_0 dl}{\lambda \cdot r} \sin \theta \sin \omega \left(t - \frac{r}{c} \right) \end{aligned} \right\} \text{(for distant radiation region)} \quad (46)$$

Therefore \mathcal{E}_t and H_t always have the same phase in the true radiation field as has already been found from the first equation of (41) and its corresponding H_y equation. We see, furthermore, that the energy flow is always away from the source.

If, however, r is small compared with λ and yet large compared with the height dl of the original current element, of the sender, we have

$$\left. \begin{aligned} \mathcal{E}_t &= -\frac{c\lambda I_0 dl}{2\pi r^3} \sin \theta \sin \omega \left(t - \frac{r}{c} \right) \\ H_t &= \frac{I_0 dl}{r^3} \sin \theta \cos \omega \left(t - \frac{r}{c} \right) \end{aligned} \right\} \text{(near exciter antenna)} \quad (47)$$

Hence in the region near the source H_t lags \mathcal{E}_t by 90 deg; that is, in the neighborhood of the sender dl the product $\mathcal{E}_t H_t$ must change its sign. Consequently during one half cycle the radiated energy passes into the field and during the following half cycle it passes partially back to dl . This to-and-fro motion of the energy flow, according to (46), does not exist in the distant region. Since $dS = 2\pi r^2 \sin \theta d\theta$, we have, according to (44) for the radiation region,

$$\frac{1}{4\pi} \mathcal{E}_t H_t dS dt = 2\pi^2 c \left(\frac{dl}{\lambda} \right)^2 I_0^2 \sin^3 \theta d\theta \sin^2 \left[\omega \left(t - \frac{r}{c} \right) \right] dt$$

But

$$\frac{1}{T} \int_0^T \sin^2 \left[\omega \left(t - \frac{r}{c} \right) \right] dt = \frac{1}{2}$$

and

$$\int_0^\pi \sin^3 \theta d\theta = \frac{4}{3}$$

Hence for the entire surface of the sphere, the average value of the radiation energy is

$$W = \frac{4}{3} \pi^2 c \left(\frac{dl}{\lambda} \right)^2 I_0^2 \text{ ergs/sec} = 1579 \left(\frac{dl}{\lambda} \right)^2 I^2 \text{ watts} \quad (48)$$

where I denotes the effective value of the current flowing along dl . Since $W = R_r I^2$, the radiation resistance becomes

$$R_r = 1579 \left(\frac{dl}{\lambda} \right)^2 \text{ ohms} \quad (49)$$

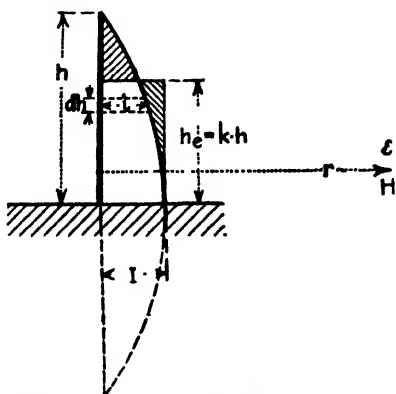
By omitting the time function, we find in the equatorial plane ($\theta = 90^\circ$) for the radiation region

$$\left. \begin{aligned} \mathcal{E}_0 &= \frac{2\pi c I_0 dl}{\lambda \cdot r} \text{ c.g.s.} \\ H_0 &= \frac{2\pi I_0 dl}{\lambda \cdot r} \text{ c.g.s.} \end{aligned} \right\} \quad (50)$$

For a vertical antenna standing on ground and having a geometrical height h , we have, according to Fig. 213, in the equatorial plane¹

$$\left. \begin{aligned} \mathcal{E} &= \frac{4\pi c I h_e}{\lambda \cdot r} \text{ c.g.s.} = \frac{377 I^4 h_e^{(om)}}{\lambda^{(om)} r^{(om)}} \text{ volts/cm} \\ H &= \frac{4\pi I h_e}{\lambda \cdot r} \text{ c.g.s.} \end{aligned} \right\} \quad (50a)$$

since on account of the image effect the radiation is the same as that of



the real antenna and an imaginary one extending an equal distance below the surface of the ground. The conductor element dl is therefore to be replaced by $2h_e$, if h_e denotes the effective height for which a uniform current distribution I has the same effect as that of the actual distribution along h . If I denotes the effective current measured at the ground side, the effective height is

$$h_e = \frac{1}{I} \int i dh \quad (51)$$

FIG. 213.—Field intensities at a distance r from a vertical aerial.

if i is the effective current in any element dh of h . Making the same substitution in (48), we find again for the radiation resistance of a vertical grounded antenna

$$R_r = 1579 \left(\frac{h_e}{\lambda} \right)^2 \text{ ohms} \quad (52)$$

since radiation takes place only over the hemisphere which is above ground. When a vertical antenna oscillates in its fundamental mode, a quarter-wave-length distribution (Fig. 213) exists; that is, $h = \lambda/4$ and $k = 2/\pi$ since

$$h_e = \frac{1}{I} \int_0^{\lambda} I \cos \frac{2\pi h}{\lambda} dh = \frac{1}{I} \left[\frac{I \lambda}{2\pi} \sin \frac{2\pi h}{\lambda} \right]_0^{\lambda} = \frac{\lambda}{2\pi} = \frac{4h}{2\pi}$$

The radiation resistance then becomes $R = 1579(0.636/4)^2 \cong 40\Omega$.

¹ For more details see Sec. 139.

For a vertical antenna on good conducting ground, the length dl of Fig. 212 corresponds to length $2a$ in Fig. 214. The radius r of the sphere is again large compared with the operating wave length λ . We have $r' = r - z \cos \theta$. For any wave length λ , the current at any place of the vertical wire is

$$I \sin \left\{ \frac{2\pi}{\lambda} (a - z) \right\} \sin \omega t = I_0 \frac{\sin \left\{ (2\pi/\lambda)(a - z) \right\}}{\sin (2\pi a/\lambda)} \sin \omega t$$

For the fundamental wave length $\lambda_0 = 4a$, we find

$$p = \frac{2\pi a}{\lambda} = \frac{\pi \lambda_0}{2\lambda}$$

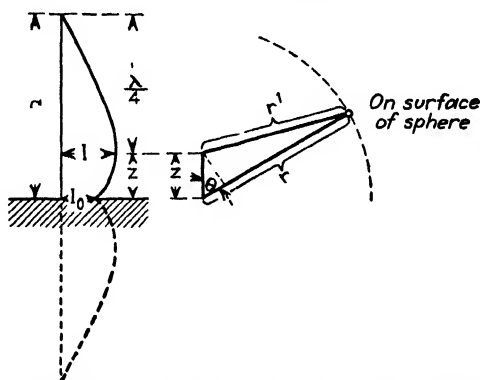


FIG. 214.—Vertical length longer than one-quarter of the exciting wave length.

According to (40a), we have in Gaussian units for the retarded vector potential

$$\Lambda = \frac{I}{c} \int_0^a \sin \left\{ \frac{2\pi}{\lambda} (a - z) \right\} \sin \omega \left(t - \frac{r'}{c} \right) \frac{dz}{r'} + \int_0^{-a} \text{image}$$

at the surface of the sphere of radius r and at a distance r' from the integration element. For the image integral, we have only to reverse the sign of $\cos \theta$. We then find at point r, θ

$$\Lambda = -\frac{I\lambda}{\pi rc} \sin \omega \left(t - \frac{r}{c} \right) \frac{[\cos p - \cos (p \cos \theta)]}{\sin^2 \theta}$$

Since \mathcal{E} and H are equal and perpendicular to each other, we have, for the electric-field strength,

$$\mathcal{E}_\theta = H_\gamma = \text{curl}_\gamma \Lambda = \sin \theta \frac{\partial \Lambda}{\partial r} + \frac{\cos \theta}{r} \frac{\partial \Lambda}{\partial \theta}$$

and

$$\mathcal{E}_\theta = \frac{2I}{c \cdot r} \cos \omega \left(t - \frac{r}{c} \right) \frac{\cos p - \cos (p \cos \theta)}{\sin \theta} \quad (53)$$

where \mathcal{E}_θ is longitudinal and H_γ latitudinal.

It should be noted that, for these formulas, the ground is assumed to be a good conductor so that \mathcal{E} is always perpendicular to the surface of the earth. This assumption, however, is often far from being true and besides depends very much upon the frequency. The electric vector is usually somewhat inclined, a forward tilt existing in the direction of propagation. If τ denotes the angle¹ with the vertical and if the time phase between the two components of the field is considered to be zero, the tilt can be computed from

$$\tan \tau = \sqrt{\frac{1}{\frac{4\pi \cdot 9 \times 10^{11} \sigma}{\omega^2}}} = \sqrt{\frac{f}{\frac{18 \times 10^8 \sigma}{\kappa^2}}} = \sqrt{\frac{1}{1 + \left[\frac{\kappa f}{18 \times 10^8 \sigma}\right]^2}} \quad (54)$$

If f denotes the frequency in kilocycles per second, the dielectric constant κ of the ground has its customary numeric value with respect to that of air and the specific conductivity σ is in $1/(\text{ohm cm})$. According to Table X (page 330), we have for ocean water $\kappa = 80$ and $\sigma = 10^{-2}$, and for dry ground $\kappa = 2$ and $\sigma = 10^{-6}$. We have for the forward tilt over ocean and over dry ground the values given in Table XIII and Fig. 215.

TABLE XIII

Frequency, kc	Over ocean	Over dry ground
20	$\tau = 0^\circ 2.5'$	$\tau = 4^\circ 18'$
200	$0^\circ 8'$	$13^\circ 30'$
2,000	$0^\circ 25'$	$32^\circ 12'$
20,000	$1^\circ 23'$	35°

From this table and the figure it can be seen that for ocean communication, even with very *short waves*, the electric vector \mathcal{E} remains practically perpendicular to the surface of the earth, while for dry ground consider-

¹ This is based upon Sommerfeld's theory (*Ann. Physik*, **28**, 665, 1909, and *Jahrb. dr. Tel.*, **4**, 157, 1911) for surface waves for which the electric field consists of two components which have a phase difference as to time. The refraction law [Eq. (35)] then appears in a complex form and the angle which the maximum amplitude of the elliptic rotation field makes with the normal to the ground plays a part and can be used for determining the electrical constants of the ground. Putting the permeability for ground and air equal to unity as well as the dielectric constant in air $\kappa_{\text{air}} = 1$, we have $\tan \tau = \mathcal{E}_x / \mathcal{E}_z = \sqrt{\kappa_{\text{air}} / \kappa'}$. But $\kappa' = \kappa + (\sigma / j\omega)$ and

$$\tan \tau = \sqrt{\frac{1}{\sqrt{\kappa^2 + (\sigma/\omega)^2}}} = \sqrt{\frac{\omega/\sigma}{\sqrt{(\omega\kappa/\sigma)^2 + 1}}}$$

For other details see "High Frequency Measurements," McGraw-Hill Book Company, Inc., New York, 1933, pp. 292-293.

able tilts can occur for shorter waves and that, even for long waves, a noticeable inclination exists.

According to J. Zenneck,¹ we have the relation

$$-\frac{\varepsilon_x}{\varepsilon_z} = \epsilon^{j\theta} \tan \tau = \epsilon^{j\theta} \sqrt{\frac{9 \times 10^{11} \sigma_1 + \frac{j\omega\kappa_1}{4\pi}}{9 \times 10^{11} \sigma_2 + \frac{j\omega\kappa_2}{4\pi}}} \quad (54a)$$

for the horizontal (ε_x) and the vertical (ε_z) components of a plane electromagnetic wave propagated along a plane surface between two media 1 and 2. Here σ_1 and σ_2 are again the specific conductivities of the respec-

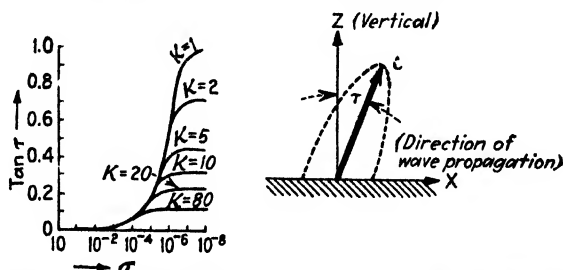


FIG. 215.—Forward tilt of electric-field vector for different values of specific conductivity σ and dielectric constant κ .

tive media in mhos per centimeter cube, κ_1 , κ_2 the dielectric constants, and θ the phase angle. If we consider again the case where medium 1 is air and medium 2 the ground, put $\sigma_1 = 0$, $\kappa_1 = 1$, $\sigma_2 = \sigma$, $\kappa_2 = \kappa$, and express the frequency f in kilocycles per second, we have

$$-\frac{\varepsilon_x}{\varepsilon_z} = \epsilon^{j\theta} \tan \tau = \frac{1}{\sqrt{\kappa}} \left[\frac{\left(\frac{\kappa f}{18 \times 10^8 \sigma} \right)^2}{1 + \left(\frac{\kappa f}{18 \times 10^8 \sigma} \right)^2} \right]^{\frac{1}{4}} \epsilon^{j \left[\frac{1}{2} \tan^{-1} \left(\frac{18 \times 10^8 \sigma}{\kappa f} \right) \right]} \quad (54b)$$

Now when the time phase between the horizontal and the vertical component of ε is zero ($\theta = 0$), the angle τ represents the angle of forward inclination of the propagated wave front. But, in general, θ is not equal to zero and the angle of tilt of the major axis of the ellipse traced by the electric vector is less than τ . In such a case it is better to

¹ ZENNECK, J., On the Propagation of Plane Electromagnetic Waves along a Plane Conducting Surface and Its Relation to Wireless Telegraphy, *Ann. Physik*, **23**, 846, 1907. This theory was followed up by F. Breisig, "Theoretische Telegraphie," 2d ed., Braunschweig, 1924, pp. 482-487, and applied to the case of waves reaching a wave antenna by A. Bailey, S. W. Dean, and W. T. Wintringham, *Proc. I.R.E.*, **18**, 1645, 1928. In foregoing formulas, the positive direction of the horizontal component is in the direction of propagation and the positive direction of the vertical component is downward.

speak of a quasitilt angle. From the expression for θ and $\tan \tau$, we can find the value of the time phase and the specific conductivity as

$$\left. \begin{aligned} \theta &= \frac{1}{2} \cos^{-1} (\kappa \tan^2 \tau) \\ \sigma &= \frac{f}{18 \times 10^8} \frac{\sqrt{1 - \kappa^2 \tan^4 \tau}}{\tan^2 \tau} \end{aligned} \right\} \quad (54c)$$

139. Radiation Resistance of Commercial Antennas.—The radiation resistance of commercial antennas can be computed approximately from Eq. (52). But for more accurate formulas of complicated aerial systems, it is better to calculate the Poynting vector for each point¹ in space and integrate the normal energy flow through any surface enclosing

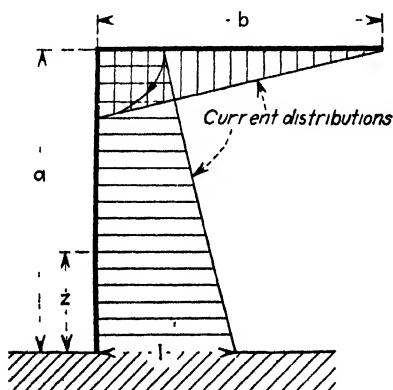


FIG. 216.—Distributions for heavy coil loading of aerial.

the antenna. The radiation resistance can also be derived by means of the induced e.m.f. method² utilizing the electromagnetic-field equations in the form employing the retarded potentials of Lorentz (for details, see page 344). For the first method, a doublet of infinitesimal length is assumed at each point of the aerial. The electric- and magnetic-field strengths at a distant point are summed up for all the doublets taking account of the difference in phase. If this is done for all points of a distant sphere surrounding the

antenna, we obtain the total electric and magnetic forces at all points of the sphere. Then integrating the Poynting vector over the sphere gives the total power radiated. The ratio of the radiated energy to the square of the current at the loop gives the radiation resistance.

For heavy coil loading of the antenna, the current distribution along it decreases almost linearly toward the end as is indicated in Fig. 216 and we can, according to F. Cutting,³ calculate the approximate radiation resistance by means of (49) in the form

¹ G. W. Pierce has in the *Proc. Am. Acad. Arts Sci.*, **52**, 192, 196, 1916 as well as in his textbook "Electric Oscillations and Electric Waves," McGraw-Hill Book Company, Inc., New York, followed up the Poynting vector method in detail. See also B. van der Pol, Jr., *Proc. Phys. Soc. London*, **13**, 217, 1917; S. Ballantine, *Proc. I.R.E.*, **12**, 823, 1924; **15**, 245, 1927; M. A. Bontsch-Bruewitsch, *Ann. Physik*, **81**, 425, 1926; S. A. Levin and C. J. Young, *Proc. I.R.E.*, **14**, 675, 1926.

² BAILLOUIN, M. L., *Radioélectricité*, **3**, 147, April, 1922; A. A. PISTOLKORS, *Proc. I.R.E.*, **17**, 561, March, 1929.

³ CUTTING, F., *Proc. I.R.E.*, **10**, 129, 1922.

$$R_r = 1579 \left(\frac{h}{\lambda} \right)^2 \frac{I_e^2}{I^2} \quad (55)$$

that is, the radiation resistance is the value given by the doublet formula multiplied by the ratio of the mean squared vertical current to the square of the current at the base. This assumes that no appreciable radiation takes place from the flat top. With the distribution indicated in Fig. 216,

$$i = I \left[1 - \frac{z}{a+b} \right]$$

and

$$\begin{aligned} I_e^2 &= \frac{1}{a} \int_0^a i^2 dz \\ &= \frac{I^2}{a} \int_0^a \left(1 - \frac{2z}{a+b} + \frac{z^2}{(a+b)^2} \right) dz \\ &= I^2 \left[1 - \frac{a}{a+b} + \frac{1}{3} \frac{a^2}{(a+b)^2} \right] \end{aligned}$$

The radiation resistance then becomes

$$R_r^\Omega = 1579 \left[\frac{a}{\lambda} \right]^2 \left[1 - \frac{a}{a+b} + \frac{1}{3} \frac{a^2}{(a+b)^2} \right] \quad (56)$$

Hence when the flat top b is longer than the vertical portion a , the last term can be neglected and

$$R_r^\Omega = 1579 \left[\frac{a}{\lambda} \right]^2 \left(\frac{b}{a+b} \right) \quad (56a)$$

The more accurate formula for the radiation resistance due to the vertical portion is, according to G. W. Pierce,

$$R_r^\Omega = \frac{1}{\sin^2 \frac{q}{2}} \{ R_1 - R_2 \cos q - R_3 \sin q \} \quad (56b)$$

for

$$\begin{aligned} R_1 &= 15 \left\{ \frac{2+2}{3!2} k^2 - \frac{4+2}{5!4} k^4 + \frac{6+2}{7!6} k^6 - \dots \right\} \\ R_2 &= 15 \left\{ \frac{2^2+2^2-4}{3!2} k^2 - \frac{4^2+2^4-6}{5!4} k^4 + \frac{6^2+2^6-8}{7!6} k^6 - \dots \right\} \\ R_3 &= 15 \left\{ \frac{3^2+2^3-5}{4!3} k^3 - \frac{5^2+2^5-7}{6!5} k^5 + \frac{7^2+2^7-9}{8!7} k^7 - \dots \right\} \\ q &= \frac{\pi \lambda_0}{\lambda} \quad \text{and} \quad k = \frac{4\pi a}{\lambda} \end{aligned}$$

where

λ_0 = wave length without loading coil

λ = wave length with loading coil

Formulas (56) and (56a) agree fairly well with Pierce's formulas¹ as long as λ is not close to the natural wave length λ_0 , for which, of course, sinusoidal current distribution is approached.

Since the radiation effect of the flat top is neglected, a T antenna can be taken as an inverted L antenna of the same length and height and the

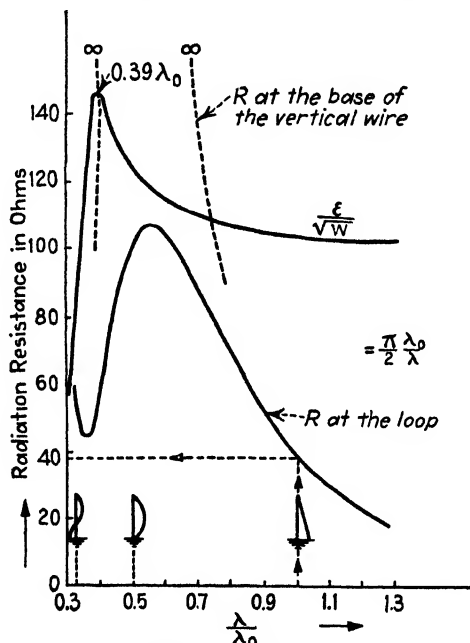


FIG. 217.--Radiation resistance of vertical aerials.

radiation resistance can be calculated by means of (56). For a vertical wire of height a and heavy coil loading at the base, we have

$$R_r^a = 526 \left(\frac{a}{\lambda} \right)^2 \quad (57)$$

since $b = 0$ and the value of the expression in the last bracket of (56) is then $\frac{1}{3}$.

Figure 217 gives the values of the radiation resistance R_r at the current loop and at the base of a vertical antenna over good conducting ground.²

¹ G. W. Pierce (*loc. cit.*) has in addition derived a formula which also takes the radiation of the flat top into account and gives tables at the end of his book for the ready use of the formulas.

² BALLANTINE, S., *loc. cit.*

Since, for the received energy, only the field intensity on the horizon is of importance, we have

$$\varepsilon = \frac{2I}{c \cdot r} [1 - \cos p] \quad (58)$$

for $p = \frac{\pi \lambda_0}{2 \lambda} = \frac{\pi f}{2 f_0}$, if I denotes the effective current at the loop. The foregoing expression is obtained by putting $\theta = 90^\circ$ in (53). For a radiation resistance R_r at the current loop, the radiated energy becomes $W = I^2 R_r$ and $I = \sqrt{W/R_r}$. The maximum efficiency of the sender antenna occurs when ε/\sqrt{W} becomes a maximum. Eliminating I in the preceding expressions, we have

$$\frac{\varepsilon}{\sqrt{W}} = \frac{2[1 - \cos p]}{c \cdot r \sqrt{R_r}} \quad (59)$$

and find $0.39\lambda_0$ the most efficient wave length.

When the flat top of an aerial is not horizontal but is as indicated in Fig. 218, the height in the doublet formula (55) for a heavy coil loading is

$$h = a + b \cdot \sin \alpha$$

and

$$I_e^2 = \frac{I^2}{a + b \sin \alpha} \left\{ \int_0^a \left[1 - \frac{z}{a+b} \right]^2 dz + \left[1 - \frac{a}{a+b} \right]^2 \int_0^{b \sin \alpha} \left[1 - \frac{z}{b \sin \alpha} \right]^2 dz \right\}$$

Hence

$$R_r^{\Omega} = 1579 \left[\frac{a + b \sin \alpha}{\lambda} \right]^2 \left\{ a \left[1 - \frac{a}{a+b} + \frac{1}{3} \left(\frac{a}{a+b} \right)^2 \right] + \frac{b \sin \alpha}{3} \left(\frac{b}{a+b} \right)^2 \right\} \quad (60)$$

140. Derivation of the Formulas for the Electric- and Magnetic-field Intensity Due to a Sender Antenna (Induction and Radiation Fields, and Received Current).—The case for a very short current element is treated in Secs. 136 and 137 in connection with Figs. 210 and 212. For a sender antenna (Fig. 213) of geometrical height h , twice the effective height (that is, $2h_e$) must be used in the formulas instead of the current element dh in order to account for the image effect and the current distribution along the antenna. The factor 2 is correct only

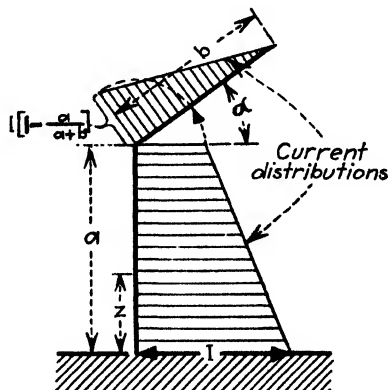


FIG. 218.—Inclined top aerial.

for good conducting ground, being smaller than 2 in the case of a poorly grounded antenna. According to Eq. (51), the effective height is

$$\int_0^h i dh = I \cdot h_e$$

if i denotes the effective current in the antenna element dh and I the effective value of the current at the base of the aerial. Since the horizontal components of the vector potential Λ are zero for the vertical antenna, we have, according to Eq. (39a), in the equatorial plane ($x, y, 0$) for spherical wave motion the resultant magnetic-field intensity

$$H_t = \sqrt{\left(\frac{\partial \Lambda_z}{\partial x}\right)^2 + \left(\frac{\partial \Lambda_z}{\partial y}\right)^2} \quad (61)$$

in which for a sinusoidal transmitter current

$$\Lambda_z = \frac{2h_e I_m \sin \omega \left(t - \frac{r}{c}\right)}{r}$$

$r = \sqrt{x^2 + y^2}$ denoting the distance from the foot of the aerial to the point ($x, y, 0$) at which H and \mathcal{E} are to be determined (Fig. 213).

But

$$\frac{\partial \Lambda_z}{\partial x} = \frac{\partial \Lambda_z}{\partial r} \frac{\partial r}{\partial x} = \frac{x}{r} \frac{\partial \Lambda_z}{\partial r} \quad \text{and} \quad \frac{\partial \Lambda_z}{\partial y} = \frac{y}{r} \frac{\partial \Lambda_z}{\partial r}$$

hence the instantaneous value of the magnetic-field intensity

$$H_t = 0.1 \frac{d\Lambda_z}{dr} = -0.2 \left[\underbrace{\frac{\omega h_e I_m}{c \cdot r} \cos \omega \left(t - \frac{r}{c}\right)}_{\text{power or watt component due to radiated field}} + \underbrace{\frac{h_e \cdot I_m}{r^2} \sin \omega \left(t - \frac{r}{c}\right)}_{\text{wattless component due to field interlinked with sender antenna}} \right]$$

For $c = \lambda f$; $\omega = 2\pi f$, and if the effective sender current $I_s = \frac{I_m}{\sqrt{2}}$ at the

foot of the aerial, the effective magnetic-field intensity becomes

$$\begin{aligned} H_{(\text{gilbert/cm})} &= 12.56 \times 10^{-3} \frac{h_{es}^{(m)} I_s^{(\text{amp})}}{\lambda^{(m)} r^{(m)}} + j 2 \times 10^{-3} \frac{h_{es} I_s}{r^2} \quad (62) \\ &= \underbrace{P}_{\text{radiation field}} + \underbrace{j Q}_{\text{induction field interlinked with aerial}} \end{aligned}$$

The imaginary term decreases with the square of the distance r and can be neglected for large distances. For a distance $r = \lambda/(2\pi)$, both fields have the same strength. Therefore, for distances smaller than 0.1592λ , the induction field plays the most important part for the received current.

For a distance of about 16λ , the induction field is only 1 per cent of the radiation field and can be neglected as in the case of large distances. For large values of r , the wave front becomes substantially plane and the term P which is everywhere parallel to the equatorial plane must, according to Maxwell, be accompanied by a changing electric field perpendicular to it and to the direction of its movement. The two fields must be equivalent as expressed by Eq. (34), which is

$$\mathcal{E} \text{ (volt/cm)} = 300H \text{ (gilbert/cm)}$$

and we find that, for large distances d from the sender,¹ the effective values

$$\begin{aligned} H \text{ (gilbert/cm)} &= 12.56 \times 10^{-3} \frac{h_e I_s}{\lambda d} \\ \mathcal{E} \text{ (volt/m)} &= 377 \frac{h_e I_s}{\lambda d} \end{aligned} \quad (63)$$

where h_e , d , and λ are in meters and the current I_s in amperes.

Since $\lambda^{(m)} f^{(ko)} = 3 \times 10^8 \text{ m/sec}$, the electric-field intensity for large distances expressed in kilometers becomes

$$\mathcal{E} \text{ (}\mu\text{volt/m)} = 1.256 \frac{h_e I_s f}{d} \quad (64)$$

if h_e is in meters, d in kilometers, f in kilocycles per second, and I_s in amperes. The expressions in (63) and (64) are very useful for field-intensity measurements. If a receiving aerial of effective height h_e stands at distance d , an effective e.m.f.

$$E_r = \mathcal{E} \cdot h_e = I_r R$$

will be induced in the tuned aerial if I_r denotes the resonance current measured at the foot of the antenna² and R its effective resistance. Hence

$$\mathcal{E} = \frac{I_r R}{h_e}$$

and the received current becomes

$$I_r \text{ (}\mu\text{amp)} = 1.256 \frac{h_e h_e I_s f}{R d} \quad (65)$$

if h_e is in meters, d in kilometers, f in kilocycles per second, R in ohms, and I_s in amperes. This expression, however, is correct only when the

¹ The letter r instead of d for the distance was used only in the derivation in order to avoid any confusion with the differential sign.

² For an untuned aerial, it is $I \cdot Z$ where Z is the aerial impedance.

distance d is not too large.¹ Otherwise an absorption factor must be used. In the transmission formulas, the space-absorption factor has the form $\epsilon^{-\alpha}$ where $\alpha = kd^2/\lambda^2$. For instance, according to Austin-Cohen, $\alpha = 0.0015d/\sqrt{\lambda}$ for long waves. In some cases, the author found $\alpha = 0.00129d/\lambda^{0.61}$ a good value for long waves. For distances less than 10λ , the absorption factor can be neglected and (65) can be used to determine the effective height of an aerial if either the h_e or the h_{ϵ} is

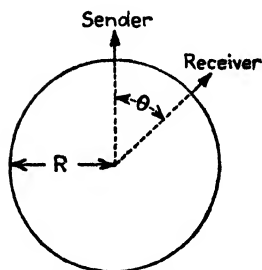


FIG. 219.—Curvature of earth surface taken into account.

known. When the curvature of the earth² is taken into consideration, instead of Eq. (64) we have the expression

$$\epsilon = 1.256 \frac{h_e I_s f}{d} \sqrt{\frac{\theta}{\sin \theta}} \epsilon^{-\alpha} \quad (66)$$

where α has the same form as above and θ is the angle subtended by the stations at the center of the earth as indicated in Fig. 219. The correction has, however, no meaning for $\theta = 180$ deg since ϵ would have an infinite value. But for such distances the ordinary transmission formula

does not hold, as is brought out in more detail on page 367. Moreover, the correction term for the curvature is used for angles greater than 60 deg since, even for $\theta = 60^\circ$, the factor $\sqrt{\theta/\sin \theta}$ is only about 1.1. For $\theta = 90^\circ$, it is 1.25 and for 120 deg it becomes 1.56, etc. Hence for distances of about 2000, 7000, and 10,000 km, the field strength is greater by 1, 10, and 25 per cent if the correction term is not used.

G. N. Watson³ has derived a transmission formula which takes into consideration the propagation between two concentric spheres, that is, a formula which includes the effect of the ionized layer. The formula is

$$\epsilon = k \frac{h_e I_s f}{\sqrt{R \sin \theta}} \epsilon^{-\alpha} \quad (66a)$$

for $\alpha = \beta d/\sqrt{\lambda}$ and k and β constant.

$$\beta = \frac{1}{2H} \left\{ \left(\frac{\mu_1}{2c\sigma_1} \right)^{1/2} + \left(\frac{\mu_2}{2c\sigma_2} \right)^{1/2} \right\}$$

¹ Since then the ionized layer makes spherical wave motion doubtful (for distances of 300 miles and more) and in addition appreciable energy is absorbed. If this is the case, the resultant field intensity at the receiver for large distances can be even higher owing to the wave return from the layer.

² This can be neglected up to 60 miles since, for the same distance d (but along the surface of the earth), the energy passes through an area which is smaller in the ratio $(\sin \theta)/\theta$.

³ For more information, see p. 368.

where

H = height of ionized layer (40 to 100 km) .

μ_1 and μ_2 = permeability of layer and ground, respectively

σ_1 and σ_2 = specific conductivity of layer and ground, respectively (σ_1 about 10^{-15} e.m.c.g.s. and σ_2 of the order of 10^{-11} to 5×10^{-11} for ocean)

$c = 3 \times 10^{10}$ cm/sec

β varies from 0.001 to 0.0015

The theoretical damping term in Watson's formula is based on two-dimensional propagation and is about the same as the Austin-Cohen empirical term $\epsilon^{-\alpha}$, although the theoretical term in the Austin-Cohen formula assumes three-dimensional propagation (Hertzian radiation).

If we have true beam transmission (one-dimensional propagation), the field strength becomes

$$\mathcal{E} = 1.256 \frac{h_e I_s f}{d} \epsilon^{-kd} \quad (67)$$

141. Notes on Wave Propagation with Respect to Wave Length and Distance.—Whether we have to deal with two- or three-dimensional propagation is in many cases difficult to decide unless the wave length, the distance, and other factors are known. According to formulas (41), it is evident that three-dimensional radiation can play a part only for comparatively short distances (up to about 300 miles), while two-dimensional propagation seems to be the case for long-distance work and one-dimensional propagation occurs when beam transmission is provided (which from a practical point of view is possible only for very short waves).

Normally an antenna stands on ground and a certain portion of the energy glides along the surface of the earth. We can, therefore, distinguish between

1. Surface waves (along the ground).
2. Space waves (proceeding between ground and the ionized layer).
3. Space waves (which detach themselves from ground and are either reflected or refracted from the ionized layer toward the receiving aerial).

For waves which are several kilometers¹ long (up to 20 km), the propagation is probably largely due to the surface waves together with space waves of kind 2 since, for such long waves with comparatively low frequency (down to 15 kc), the absorption in the ground is not so great, this being especially so when transmission occurs across the ocean.

For the broadcast band (200 to 550 m corresponding to a frequency range from 1500 to 545 kc), no considerable distances can be reached (up to about 100 to 200 miles only). For this reason, these stations can

¹ Since, according to Sommerfeld's theory, one kind of wave always supplies energy to the other if the latter should lose too much energy.

hardly be heard over long distances during the daytime, while good transmissions are possible during the night only because of the return wave from the ionized layer.

For waves from 10 to 100 m corresponding to 30,000 to 3000 kc, the surface waves are so attenuated that the reflected (refracted in the true sense) waves are responsible for the long distances obtained. We have then the well-known dead zones of no reception (skip distances, Fig. 220). For still shorter waves (50 cm to about 10 m),¹ there are practically no surface waves and no effect from the ionized layer. We have then true space waves which behave very much like light rays. The higher the

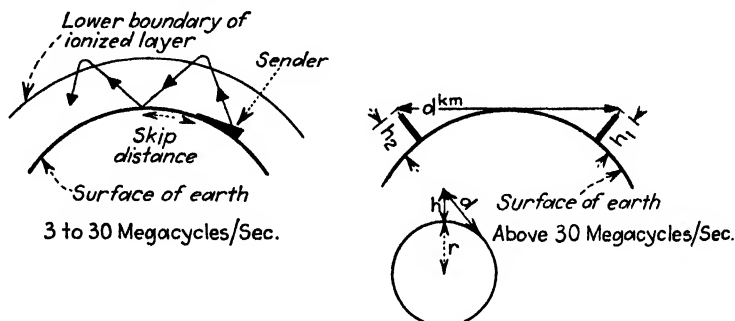


FIG. 220.—Wave propagation.

small dipoles are placed above the ground (Fig. 220), the longer is the reach d and the distance d in kilometers can be found from

$$d = 3.55[\sqrt{h_1} + \sqrt{h_2}] \quad (68)$$

This formula depends upon the following derivation: If h denotes the height of the sender dipole over ground, d denotes the greatest distance over which direct radiation is possible. But the length of the tangent d is

$$d = \sqrt{2rh - h^2} \cong \sqrt{2rh}$$

Hence

$$d^{(\text{km})} = 3.55\sqrt{h^{(\text{m})}}$$

since $r = 6.4 \times 10^3$ km. These waves cannot pass through obstacles (buildings, etc.) which are large compared with the wave length. Shadows are produced as for light but fog may be penetrated. The amplitude of the energy flow decreases in the region of direct radiation as the square of the distance. Beam transmission is readily obtained by the use of parabolic mirrors. Inasmuch as such waves near the surface of the ground will on account of the density of the air follow a somewhat

¹ Experiments by A. Esau, Jena; W. Hahnemann (see also F. Gerth and W. Scheppmann), *Jahrb. drahtl.*, **33**, 3, 1929.

curved path (successive refraction, radius of curvature about four times that of the earth) somewhat longer radiation distances will be experienced than expressed by the above formulas. This is all the more true during night hours when the density of the atmosphere becomes greatest. When the distance found from above formulas is multiplied by 1.2 the experimental distance will be approximately obtained.

142. Sommerfeld's Surface and Space Waves and Numerical Distance.¹—We must distinguish between space and surface waves. Both waves depend upon each other and an energy loss in one causes the other wave to supply power to the weaker, since both are the result of the integration of the Maxwellian field equations with the true conditions of the ground taken into account.

The *space waves* are radiated from an antenna into space without detaching themselves completely from the ground. The energy flow passes through hemispherical surfaces (assuming a grounded antenna) and decreases with the square of the distance d since the surfaces of the sphere increase as d^2 . The field strength is therefore proportional to $1/d$, as can also be seen from Eqs. (50a) and from the third equation of (41).

Inasmuch as the ground is not a perfect conductor but instead has a finite conductivity σ and a dielectric constant κ , we also have to deal with *surface waves* which pass along a layer in the ground of approximately the same thickness. Therefore the energy flows through cylindrical surfaces of equal height. But since such surfaces increase in direct proportion with d , the energy of the surface waves is proportional to $1/d$ and the field strength changes as $1/\sqrt{d}$, which can also be seen from the second equation of (41).

The amplitudes of the waves experience a *geometrical* decrease as the waves pass on (attenuation due to wave spread). In addition, the attenuation due to absorption in the ground itself and due to other causes must be considered. If the absorption in the ground is small, the progressive waves at a large distance must turn into pure surface waves.

According to Sommerfeld, the propagation of the waves for no ideal ground depends upon the expression

$$\beta = 2\pi f \sqrt{\frac{d_n}{2c\sigma}} \quad (69)$$

where d_n denotes the numerical distance, σ the specific conductivity in $1/(\text{ohm} \cdot \text{cm})$, f the frequency in cycles per second, and $c = 3 \times 10^{10}$ cm/sec. If \mathcal{E} is the field strength of the wave at a distance d from the source when the waves pass over perfect conducting ground, and \mathcal{E}_s

¹ SOMMERFELD, A., *Ann. Physik*, **28**, 665, 1909; R. L. SMITH ROSE and R. H. BARFIELD, *J.I.E.E.*, **64**, 766, 1926; R. H. BARFIELD, *J.I.E.E.*, **66**, 204, 1928.

denotes the actual field strength when the waves pass over imperfect conducting ground, then

$$\begin{aligned}\varepsilon_a &= \varepsilon F(\alpha \cdot d) \\ &= \varepsilon F(d_n)\end{aligned}\quad (70)$$

where F is a function sign. Therefore the numerical distance depends upon the frequency f , the conductivity σ , and the horizontal distance d , and the character and intensity of the waves depend upon d_n instead

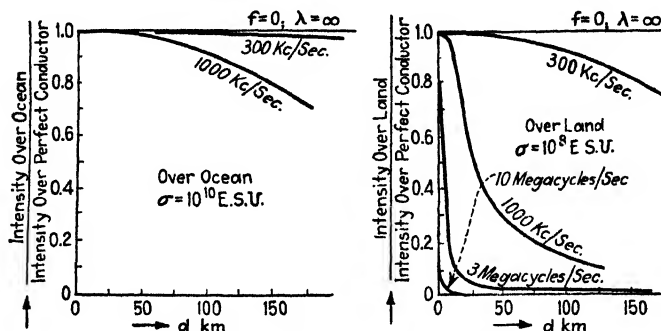


FIG. 221.—Absorption due to ground.

of d . The foregoing expression assumes $\sigma/f \gg 2\pi$. If $\beta \ll 1$ and $d_n \ll \lambda$, from the Hertzian equations we obtain for the potential P

$$P = 2q \left[\underbrace{\frac{\sin \omega \left(t - \frac{d}{c} \right)}{d}}_{\text{due to space wave}} + \beta \sqrt{\pi - \underbrace{\frac{\cos \omega \left(t - \frac{d}{c} \right)}{d}}_{\text{due to surface wave}}} \right] \quad (71)$$

where q is the maximum value of the moment of the dipole. Thus for $\lambda = 2$ km and $d = 240$ km, the potential due to the surface wave is only about 10 per cent of the potential due to the space wave if the transmission takes place over the ocean, while over moist ground the same values are attained after a distance of only 1 km. When waves pass over land, the effect of absorption due to higher ground resistance is rather pronounced for wave lengths shorter than 1 km and a 1-km wave over land is attenuated as much as a 30-m wave over the ocean. However, for a 300-m wave, the intensity at a distance of 150 km over land is only 8 per cent of the value over sea and, for a 30-m wave for $d = 10$ km distance, it is reduced to 1 per cent of its value for perfect ground. For more details, Fig. 221 is added. If the curvature of the earth¹ is neglected,

¹ The specific conductivity σ of the earth differs with the locality. Average values in the e.m.c.g.s. system are given in Table X, page 330. According to Smith Rose, and Barfield (*loc. cit.*), in England over land $\sigma = 10^8$ e.s.c.g.s. That is, $10^8/c^2 \approx 10^{-12}$ e.m.c.g.s. or about 10,000 ohms/cm².

assuming $2\sigma/f \gg 1$, the quantity $2\sigma/f$ will exceed 10 for all wave lengths above 15 m.

If κ denotes the dielectric constant of the ground and σ its conductivity, and f the frequency, then we have the effective value $\kappa' = \kappa + 2\sigma/jf$ and the refractive index of ground $n = \sqrt{\kappa'}$, since κ for air is equal to 1. Sommerfeld now finds a series for the vector¹ potential P and the numerical distance

$$d_n = \frac{\pi}{n^2} \frac{d}{\lambda} \quad (72)$$

which for $2\sigma/f \gg \kappa$; that is, the conduction current in the ground exceeds the displacement current considerably. Hence

$$d_n \cong \frac{\pi f}{2\sigma} \frac{d}{\lambda} = \frac{\pi c d}{2\sigma \lambda^2} \quad (73)$$

Here d has the same unit as the wave length λ , the conductivity σ is expressed in the e.s.c.g.s. system, and f is in cycles per second. For the same absolute distance d , the numerical distance d_n becomes smaller as the wave length λ becomes larger. The same value for the field strength requires the same value of d_n . For oversea transmission and $d_n = 1$, we have $d = 77 \times 10^3$ km and $\lambda = 2$ km or $d = 2.1 \times 10^3$ km and $\lambda = 333$ m. For river water, the same field strength is obtained for $d = 90$ and $\lambda = 2$ km since $d_n = 1$. For surfaces of high specific conductivity as, for instance, the ocean, the space wave plays the most important part and for this reason the Austin-Cohen semiempirical formula is justified because \mathcal{E} is then proportional to $1/d$.

For the numerical distance d_n not less than 10, we have the approximate expression

$$P = - \left[\frac{1}{2d_n} + \frac{1 \times 3}{2 \times 2d_n^2} + \frac{1 \times 3 \times 5}{2 \times 2 \times 2d_n^3} + \dots \right] \frac{e^{j2\pi(d/\lambda)}}{d} \quad (74)$$

for a very large d_n

$$P = \frac{k\lambda^2}{d^2} \quad (75)$$

Moreover, the energy subtracted from the surface wave per unit area is

$$W_o = \frac{c\mathcal{E}^2}{4\pi} \sqrt{\frac{f}{2\sigma}} \quad (76)$$

since² the wave passing over ground must be regarded as inclined to

¹ Equal to the distance rate of the radiated magnetic field, that is, equal to $\partial H / \partial d$.

² BOUTHAILLON, *L'onde élec.*, 2, 275, 345, 1923. Generally, if an electromagnetic wave passes over ground and the electric component is not perpendicular to the

the surface at a constant angle of incidence for which, according to electro-optics, the reflected waves vanish (Fig. 222). We then have

$$\cos \gamma = \sqrt{\frac{f}{2\sigma}} \quad (77)$$

With no reflection, the incident waves at the angle γ must pass completely into the ground. The energy subtracted from the surface wave is for each square centimeter surface equal to $(c\varepsilon^2/4\pi) \cos \gamma$ which confirms Eq. (76).

From (76), we find that

$$\frac{f}{2\sigma} = \frac{16\pi^2 W_o^2}{c^2 \varepsilon^4}$$

and the numerical distance [Eq. (73)] can also be expressed as

$$d_n = \frac{16\pi^3}{9 \times 10^{20}} \frac{d}{\lambda} \frac{W_o^2}{\varepsilon^4} \quad (73a)$$

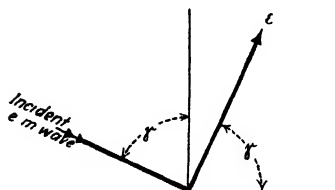


FIG. 222.—Nature of surface waves and Brewster angle γ .

This expression is conveniently written in the form

$$\frac{W_o}{\varepsilon^2} = \frac{3 \times 10^{10}}{4\pi} \sqrt{\frac{d_n \lambda}{\pi d}}$$

and gives the ratio of the energy absorbed per unit surface of the earth to the square of the electric-field intensity.¹ It should be noted that in the foregoing expression both the effect of the ionized layer and the curvature of the earth have been neglected.

surface, current will be induced in the ground, if its conductivity is not zero, and this will reduce the transmitted energy. Only perpendicular components will not be reduced. Hence if the earth were a perfect conductor, the electromagnetic fields passing over it would be polarized so that their electric component would be perpendicular and their magnetic component parallel to it. Since the earth is not a perfect conductor, the wave front is not quite perpendicular. For descending waves coming from dipole antennas on high towers or from aeroplanes or the ionized layer, the penetration of the polarized magnetic fields is usually pronounced when the surface is a poor conductor.

¹ With such formulas R. H. Barfield and G. H. Munro have made calculations for the energy absorption over towns where many vertical metal poles subtract energy from the wave.

CHAPTER X

THEORY OF THE IONIZED LAYER

(Heaviside-Kennelly Layer)

Field intensities that actually exist in space are often different from the value predicted by the theoretical formulas derived in the previous chapter. There are even instances where the observed field intensity is much greater than the theoretical value. In other cases (for instance

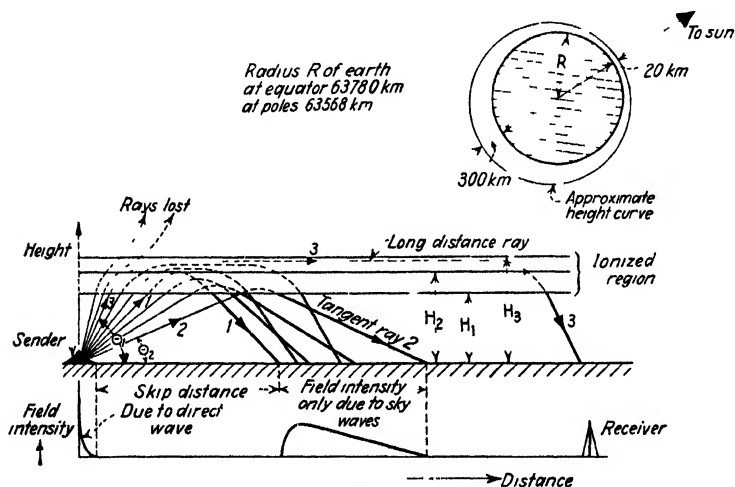


FIG. 223.—Wave propagation.

with waves between 20 and 100 m corresponding to a range of 15,000 to 3000 kc/sec), no field is observed for certain distances, even comparatively close to the sender (Fig. 223) (dead zones, skip distances) although farther away from the sender zones of reception and zones of no field intensity occur alternately. This behavior occurs irregularly depending upon the weather, the location of the sun with respect to the sender and receiver, the season, etc. The intensity varies especially erratically during periods of sunrise and sunset.

143. Causes of Abnormal Field Intensities and the Ionization of the Upper Atmosphere.—In order to account for abnormal received field intensities, Heaviside¹ and Kennelly in 1902 suggested independently of

¹ This hypothesis was at first followed up by Poincaré, Blondel, and Guillaume.

each other the existence of an ionized layer about 100 km above the surface of the earth. According to some of their followers, the upper portion of the layer consists largely of free electrons, while the lower portion contains in addition many ions. From this layer, radio waves are again bent back to the earth. It is believed that free electrons and ions produce the bending and that the electrons accelerate the propagation of the waves. A retardation occurs when the electrons moved by the waves collide with the ions and give up their energy, that is, produce damping. Therefore in the upper portion of the layer an acceleration of the wave front occurs, while the wave front in the lower portion falls behind; that is, the wave front is tilted forward and again moves down toward the earth. The motion of the electrons is considerably more active for the longer waves than for the shorter ones. Hence, for long waves, more electrons collide with the heavy ions in the lower wave front and the bending effect is very pronounced, which explains the fact that, for very large distance and longer waves, a good deal of the observed field intensity is still due to the direct space wave.

The successful theoretical work began with the investigations of W. H. Eccles¹ and G. N. Watson,² each attacking the problem from a different angle. The attack of Eccles formed the beginning of the present theory and was still more successfully carried on by J. Larmor³ and others. According to Eccles, the atmosphere at about 80 km acts as a conductive layer and waves can be reflected. In the lower portion of the layer, ionization takes place during the day only but becomes less as the surface of the earth is approached. Therefore the index of refrac-

¹ ECCLES, W. H., *London Electrician*, **69**, 1015, 1912; **71**, 969, 1913.

² WATSON, G. N., *Proc. Roy. Soc. (London)*, (A), **95**, 546, 1919.

³ LARMOR, J., *Phil. Mag.*, **48**, 1025, 1924; H. W. NICHOLS and I. C. SCHELLENG, *Bell System Tech. J.*, **4**, 215, 1925; E. V. APPLETON, *Proc. Phys. Soc. London*, **37**, 160, 1925; G. ELIAS, *E.N.T.*, **2**, 351, 1925; C. T. R. WILSON, *Proc. Phys. Soc. London*, **37**, 320, 1925; E. O. HULBURT, *J. Franklin Inst.*, **201**, 597, 1926; G. BREIT and M. A. TUVE, *Phys. Rev.*, **28**, 554, 1926; E. O. HULBURT and A. H. TAYLOR, *Phys. Rev.*, **27**, 189, 1926; M. LARDRY, *L'onde élec.*, **449**, 502, 1924; **355**, 401, 1925; R. MESNY, *L'onde élec.*, **434**, 1926, with a long list of references; W. G. BAKER and C. W. RICE, *A.I.E.E.*, **45**, 1535, 1926; H. LASSEN, *E.N.T.*, **4**, 324, 1927; S. GOLDSTEIN, *Proc. Roy. Soc. (London)*, **121A**, 260-285, 1928; LT. GUGOT, *L'onde élec.*, **7**, 509, 1928; G. W. KENRICK and C. K. JEN, *Proc. I.R.E.*, **17**, 711, 1929; E. V. APPLETON, *J.I.E.E. (London)*, **71**, 642, 1932. T. R. GILLILAND, G. W. KENRICK, K. A. NORTON, *Proc. I.R.E.*, **20**, 286, 1932, discuss observations and height of two ionized layers, *E* and *F*, which correspond to the virtual heights of the *E* and *F* regions of E. V. Appleton; L. TONKS, *Nature*, **132**, 101, 1933; J. A. RATCLIFFE and E. L. C. WHITE, *Proc. Phys. Soc. London*, **45**, 399, 1933; *Nature*, **131**, 873, 1933; K. A. NORTON, *Nature*, **132**, 676, 1933; L. V. BERKNER and D. M. STUART, *Bur. Standards, J. Res.*, **12**, 15, 1934; *Proc. I.R.E.*, **22**, 481, 1934; L. V. BERKNER and H. W. WELLS, *Proc. I.R.E.*, **22**, 1102, 1934, identify three layers, *E*, *F*₁, and *F*₂; E. O. HULBURT, *Phys. Rev.*, **46**, 822, 1934, reports on recent measurements in the ionized media.

tion varies, increasing with decreasing ionization—hence the bending of the wave path. During the night the atmosphere between ground and the ionized layer acts as a perfect dielectric. The electric waves are therefore propagated between the conductive surfaces with very little absorption and successive reflections take place between the layer and ground. During the day the atmosphere between the layer and ground is no longer a perfect dielectric and the waves undergo refraction as they pass higher up. The absorption is then great. Watson assumes, however, that the atmosphere behaves like a dielectric. The ground forms one conducting shell and the layer another conducting shell of infinitely greater conductivity. There is an energy decrease with distance as in a transmission line. For his final formula, Watson assumes that the ground is not a perfect conductor and arrives at formula (66a) on page 360.

The existence of the layer can be attributed to several causes. The main causes are probably the corpuscular radiation from the sun and the ionization effect of the ultraviolet light of the sun.

1. The sun shoots off corpuscles, mainly electrons, which reach the upper portion of the atmosphere¹ and strongly ionize it (Swann). Owing to the earth's magnetic-field action, the electrons can also reach that portion of the earth which is not directly illuminated by the sun (Stoermer, Birkland, Villard).

2. The wave radiation of the sun, especially that in the ultraviolet portion of the spectrum, ionizes² the layer during the day. The ionization gradually, but not completely, dies off during the night (Eccles, Lassen). Other less probable origins of the ionization are

3. The radium emanation of the earth passes into the air and ionizes the atmosphere uniformly during day and night. But in this case the ionization can exist only in the lowest portions of the atmosphere and therefore can hardly explain the condition in the higher portions of it.

4. Ionization could also be brought about by the action of cosmic radiation, the so-called *Höhenstrahlung*, which comes from the empty space.

The following can be said about the absorption in the layer. For wave propagation without absorption, no collisions between ions (which are set in motion by electromagnetic waves) can occur. Hence the amplitude of the oscillations must be small compared with the mean free path of the ions and electrons, respectively. In other words, the period of the oscillations must be small in comparison with the time it takes the electrons and the ions, respectively, to travel through their mean free path. It can be shown that, for a height of 100 km above ground and a wave length $\lambda = 1000$ m (300 kc/sec), these conditions are fulfilled for

¹ For a pressure of about 0.01 mm mercury. Direct bombardment of the outer layers of the earth's atmosphere by electrons mostly thrown off from sun spots.

² The ultraviolet light breaks up the neutral gas molecules of the upper atmosphere into positive and negative constituents.

the hydrogen ions. For the electrons, however, several collisions are possible.

Recently the existence of three ionized layers, namely, the E , F_1 , and F_2 layers, have been experimentally verified. All three layers have, so to speak, an upper and lower boundary which cannot, of course, be well defined. The E layer is next to the surface of the earth and the F_2 region on the side next to the sun. According to L. V. Berkner and H. W. Wells, the maximum ionization of the F_1 region is about 2.5×10^5 electrons/cc, while the density of heavier ions is not greater than about 10^7 /cc. The maximum ionization of the F_2 region reaches 1.1×10^6 electrons/cc. The F_1 layer seems to be caused by a separation from a general F region during the morning rather than direct ionization of a separate layer. Two reflection components are found near the maximum ionization of the F_1 and F_2 regions. These components attain critical values at different transmission frequencies. A dip in the critical frequency of the F_2 region often occurs in the morning in summer. This may have something to do with the appearance of the F_1 region. The critical frequency for the F_2 region is somewhere between 2 and 3 Mc/sec. Diurnal and seasonal data for the E region seem to agree with the ultraviolet theory for ions, giving a value of order 10^{-12} for the ionic recombination loss. Data for the F_1 region agree with the ultraviolet theory for electrons, giving a value of 10^{-4} for the loss of electrons by attachment to oxygen molecules. Virtual heights between 100 and 150 km correspond to the E region. These heights have been verified at 1.6, 2, and 3 Mc/sec. The reflection from ionized layers during thunderstorms shows that the lower E layer was about 125 km above ground before a thunderstorm arrived. During the storm the electrical discharge pushed the layer down to about 105 km. Immediately after the storm the layer rose again to 125 km and mounted to about 150 km after 15 min. Hence during thunderstorms the layer seems to move up and down.

Inasmuch as the verification of multi-ionized regions is only of recent date, it does not seem advisable to present more details before all the facts are well understood. For this reason, the following sections are based on a general ionized layer.

144. Direct and Indirect Rays, Their Phase Difference and Dead Zones.—Figure 223 (direct and indirect rays) pictures waves below 100 m (above 3 Mc/sec). The direct rays produce field strengths which can be estimated by means of the theoretical formulas given in the last chapter. The diagram at the top indicates the indirect rays which are refracted back from the ionized layer. For the sake of clearness, the height of the layer is drawn out of proportion. We note that the thickness of the layer is $H_2 - H_1$ and may be 20 km if the lower surface H_1 is about 90 to 100 km above the earth. The height of the layer is by no

means fixed as can also be seen from the upper diagram of this figure. For a certain wave length, two limiting angles θ_1 and θ_2 exist. Between these angles we have refraction, that is, bending of the wave front, and the waves return to the earth as sky or indirect rays. If a ray ascends more steeply than is indicated by the angle θ_1 , the energy is probably lost unless it is assumed that the ray, after passing through the layer, is reflected back to the earth from the electron walls of the Stoermer electron pockets or some other ionized regions above the layer. Such rays would probably be of little use for commercial applications since they would produce echo effects (arrive, for instance, several seconds later on account of the immense dimensions of the pockets) which would blanket out signals of the direct rays and the normal indirect rays. The other limiting angle θ_2 is determined by the tangent to the surface of the earth. It will be noted that the rays enter farther into the layer when they leave the sender at a greater angle with the ground, until the angle is such that they reach a height H_2 . At this height the index of refraction, which so far has decreased almost linearly with the height, gradually decreases more slowly. For a somewhat greater angle, therefore, abnormal indirect rays are produced which travel for long distances within the layer and thus may account for reception at a very great distance.

Figure 224 gives approximate average transmission data for different wave lengths (10 to 1000 m) at different distances.¹ The received signal is assumed to have a field strength of 10μ volts/m. To the left of the line marked "limit of ground wave" it should be possible to receive at all times. This corresponds to the ordinary transmission formulas based on spherical wave motion. After that, one must use a pair of curves of the same kind, that is, for the same time; then if the distance is within the curves, one should hear a signal. Thus a 30-m wave should be reliable at all times up to 70 miles. From there up to 400 miles its daylight performance will probably be uncertain, while beyond 400 miles it will gradually die down until at 4600 miles it will again be below 10μ volts/m. From these figures, it is possible to estimate the skip distances.

If, as in Fig. 223, we consider the case of a single reflection (strictly, refraction) from the ionized layer, we have one direct path of length d_1 between sender and receiver and an indirect path of length d_2 which, so to speak, travels up toward the layer through a distance $d_2/2$ and is reflected down toward the receiver through a distance $d_2/2$. If H denotes the height of the layer, the phase difference between the received waves is given by the phase angle

$$\varphi_1 = \omega \left[t - \frac{d_1}{c} \right]$$

¹ The curves are printed with the permission of the American Radio Relay League (taken from "The Radio Amateurs' Handbook").

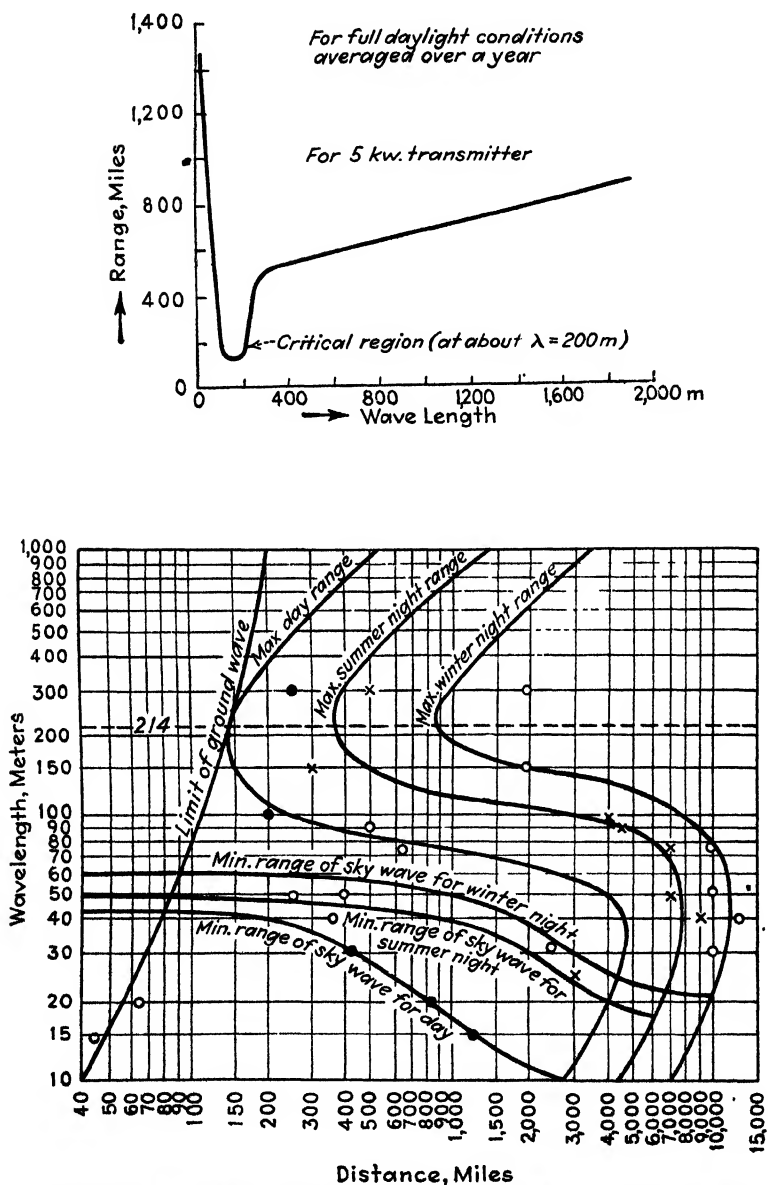


FIG. 224.—Transmission performance and selective absorption near $\lambda = 200$ m.

of the direct¹ wave and the phase angle

$$\varphi_2 = \omega \left(t - \frac{d_2}{c} \right) = \omega t - \frac{d_1 \omega}{c} \sqrt{1 + \left(\frac{2H}{d_1} \right)^2}$$

of the indirect wave. Therefore, we have at the receiver the phase difference

$$\begin{aligned} \varphi &= \varphi_2 - \varphi_1 = \frac{d_1 \omega}{c} \left[1 - \sqrt{1 + \left(\frac{2H}{d_1} \right)^2} \right] \\ &= \frac{2\pi}{\lambda} d_1 \left[1 - \sqrt{1 + \left(\frac{2H}{d_1} \right)^2} \right] \\ &= \frac{2\pi}{\lambda} d_1 p \end{aligned} \quad (1)$$

If $(d_1/\lambda)p$ denotes a whole number, maximum signal intensity will be received; but if $(d_1/\lambda)p$ is half of an odd integer, we have to deal with phase opposition. Such phase effects do exist but are often obscured by multiple reflection which partially blankets out the inphase and opposite-phase relations.

145. Effective Dielectric Constant of the Ionized Medium.—The field equation for the ionized medium has already been treated in Sec. 131 [Eqs. (8) and (8a)]. Assuming a plane wave moving in the x direction, we find from the curl equations²

$$\left. \begin{aligned} \text{curl } \mathcal{E} &= -\mu \frac{\partial H}{\partial t} \\ \text{curl } H &= \frac{\kappa}{c^2} \frac{\partial \mathcal{E}}{\partial t} + 4\pi q \sum v \end{aligned} \right\} \quad (2)$$

that only the components \mathcal{E}_z and H_y exist in the component relations (9), (10), and (18a) of page 338 if, instead of the term $4\pi\sigma\mathcal{E}$, the ionic contribution $4\pi q \sum v$ is used. We have then only

$$\begin{aligned} \frac{\partial \mathcal{E}_z}{\partial x} &= \mu \frac{\partial H_y}{\partial t} \\ \frac{\partial H_y}{\partial x} &= \frac{\kappa}{c^2} \frac{\partial \mathcal{E}_z}{\partial t} + 4\pi q \sum v \end{aligned}$$

Differentiating the first equation with respect to x , the second with respect to t , and eliminating $\partial^2 H_y / (\partial x \partial t)$ results in

¹ This phase equation is, of course, only approximately correct since, for a portion of the path d_1 (within the layer), the group velocity is smaller than c and the deduction is based on simple reflection.

² Where $\sum v$ stands for the geometric sum of all field velocities of the ions per unit volume (1 cc in this case) and q for the charge of particular ion.

$$\frac{\partial^2 \mathcal{E}_z}{\partial x^2} = \frac{\mu \kappa}{c^2} \frac{\partial^2 \mathcal{E}_z}{\partial t^2} + 4\pi\mu \frac{\partial}{\partial t} \left(q \sum v \right) \quad (\text{equation of motion for the ionized medium}) \quad (3)$$

From this expression, it can be seen that the effective (or phase) velocity c' is different from the velocity c since we have an effective dielectric constant κ_e instead of κ only. The latter has already been brought out in Eq. (8a) on page 332. If for the sake of brevity we call \mathcal{E} the z component of the electric-field intensity and assume sinusoidal excitation, we have

$$\mathcal{E}_z = \mathcal{E} = \mathcal{E}_0 \sin \omega t$$

According to Eq. (2), this field strength produces two currents in the ionized medium. One current results from the linear to-and-fro vibration of the ion and the other is the Maxwellian displacement current. Both are due to \mathcal{E} and agree with the direction of this electric force. If m denotes the mass of an ion of charge q , we have the equation of ionic motion

$$m \frac{d^2 z}{dt^2} + F \frac{dz}{dt} = q \mathcal{E} \quad (4)$$

Here z denotes the displacement of each ion from its original position and $F(dz/dt) = F \cdot v$ is the friction term. If it is assumed that for free ions no elastic restoring or dissipating force exists (effects due to collisions are neglected), then Fv can also be neglected in comparison with $m(dv/dt)$ and we find

$$m \frac{dv}{dt} = q \mathcal{E} \quad (5)$$

This expression omits the less important motions of the ion.¹ Integrating this equation and putting the constant of integration equal to zero, since we are not concerned with the random velocities, we obtain

$$v = \frac{q}{m} \int \mathcal{E} dt = -\frac{q}{m\omega} \mathcal{E}_0 \cos \omega t \quad (6)$$

which expressed symbolically is

$$v = \frac{j q}{m \omega} \mathcal{E} \quad (7)$$

¹ Strictly speaking, the equation of motion for each ion is

$$m \frac{dv}{dt} = q \mathcal{E} + \frac{\mathcal{E}}{c} [vH] + \frac{2}{3} \frac{\mathcal{E}^2}{c^2} \frac{dv}{dt} \quad \text{for} \quad \text{curl } \mathcal{E} = -\frac{\mu}{c} \frac{\partial H}{\partial t}$$

and

$$\text{curl } H = \frac{\kappa}{c} \frac{\partial \mathcal{E}}{\partial t} + \frac{4\pi q}{c} \sum v$$

For motions due to thermal agitations, see footnote 1, page 331.

Now the motion of N ions/cc contributes a current

$$i_1 = Nqv = -\frac{Nq^2}{m\omega} \varepsilon_0 \cos \omega t \quad (8)$$

In addition to this we have the ordinary displacement current flowing across a unit cube. The potential difference between two planes 1 cm apart is ε times 1 cm. The capacity of the fictitious condenser with plates 1 cm² in area and 1 cm apart is $\kappa/(4\pi) = 1/(4\pi)$ since $\kappa = 1$ and the charging current becomes

$$i_2 = \frac{1}{4\pi} \frac{d\varepsilon}{dt} = \frac{\omega}{4\pi} \varepsilon_0 \cos \omega t \quad (9)$$

This expression could have been directly obtained from the definition for the Maxwellian displacement.¹ Hence the total current is

$$\begin{aligned} i &= i_1 + i_2 = \frac{1}{4\pi} \left\{ 1 - \frac{4\pi Nq^2}{m\omega^2} \right\} \omega \varepsilon_0 \cos \omega t \\ &= \frac{1}{4\pi} \left\{ 1 - \frac{4\pi Nq^2}{m\omega^2} \right\} \frac{d\varepsilon}{dt} \\ &= \frac{\kappa_e}{4\pi} \frac{d\varepsilon}{dt} \end{aligned} \quad (10)$$

from which the effective dielectric constant κ_e of an ion medium² is

$$\kappa_e = 1 - \frac{4\pi Nq^2}{m\omega^2} \quad (11)$$

where all quantities are in the e.s. c.g.s. system. We see from this that the dielectric constant is smaller than for ether, and that the effect of gas ions on the effective dielectric constant can be neglected in comparison with the effect due to electrons. This can be understood if it is remembered that even the lightest ion, the hydrogen ion, has a mass of about 1800 times the mass of an electron. If the ions collide ν times per second, the dielectric constant becomes

$$\kappa_e' = 1 - \frac{4\pi Nq^2}{m\omega\sqrt{\omega^2 + \nu^2}} \quad (12)$$

when all collisions are assumed inelastic. The derivation of (12) is as follows: Take any ion which had its most recent collision at $t = t_0$ and can move freely under the influence of the electric field. Assume that after the collision it has lost its velocity in the direction of the electric

$$1. \frac{dD}{dt} = \frac{dQ}{dt} = i_1 = \frac{\kappa}{4\pi} \frac{d\varepsilon}{dt}.$$

² Another expression for κ_e is given in Eq. (37).

field \mathcal{E} . The velocity of an ion, according to (6), is, in the symbolical form,

$$v = -\frac{jq}{m\omega}P(\epsilon^{j\omega t} - \epsilon^{j\omega t_0})$$

since

$$m\frac{dv}{dt} = q\mathcal{E} = qP\epsilon^{j\omega t}$$

It is furthermore assumed that the number of collisions ν per second of an ion with other molecules is the same whether the electric field is present or not. Then the formula for the kinetic-gas theory can be applied. Now during the interval dt there occur $N\nu dt$ collisions for each cubic centimeter of volume. The number of ions which collide during the interval between t and $t + dt$ (but for the interval $t' = t - t_0$ pass freely) is

$$(N\nu dt)\nu\epsilon^{-\nu'(t-t')}$$

Each ion when colliding loses the velocity

$$v = -\frac{jq}{m\omega}P[\epsilon^{j\omega t} - \epsilon^{j\omega(t-t')}]$$

and the sum of the velocity changes of all ions colliding at t becomes

$$\sum_{dt} v = N\nu^2 dt \int_0^\infty \nu\epsilon^{-\nu' t'} dt' = \frac{Nq}{m} \frac{\nu}{\nu + j\omega} \mathcal{E} dt$$

Then the velocity change per cubic centimeter during the interval dt due to collisions is $-\sum_{dt} v$. But for no collisions we have the velocity change per cubic centimeter during dt

$$\frac{Nq}{m} \mathcal{E} dt$$

and the resulting velocity change becomes

$$d\left(\sum v\right) = \frac{Nq}{m} \left[1 - \frac{\nu}{\nu + j\omega}\right] \mathcal{E} dt = \frac{Nq}{m} \frac{j\omega}{\nu + j\omega} \mathcal{E} dt$$

which gives, upon integration,

$$\sum v = \frac{Nq}{m} \frac{\mathcal{E}}{\nu + j\omega}$$

We have therefore for the ionic current contribution

$$i_1 = q \sum v = \frac{Nq^2}{m} \frac{\mathcal{E}}{\nu + j\omega}$$

and the displacement current, according to (9),

$$i_2 = \frac{1}{4\pi} \frac{d\varepsilon}{dt} = \frac{j\omega}{4\pi} \varepsilon$$

Hence the total current

$$\begin{aligned} i &= i_1 + i_2 = \left[\frac{j\omega}{4\pi} + \frac{Nq^2}{m(\nu + j\omega)} \right] \varepsilon \\ &= \frac{1}{4\pi} \left[1 + \frac{4\pi Nq^2}{m(j\omega\nu - \omega^2)} \right] \frac{d\varepsilon}{dt} = \frac{1}{4\pi} \left[1 - \frac{4\pi Nq^2}{m\omega^2 \left[1 - j\frac{\nu}{\omega} \right]} \right] \frac{d\varepsilon}{dt} \\ &= \frac{\kappa_e'}{4\pi} \frac{d\varepsilon}{dt} \end{aligned}$$

that is, the apparent dielectric constant for a medium with collisions is

$$\kappa_e' = 1 - \frac{4\pi Nq^2}{m\omega^2 \left[1 - j\frac{\nu}{\omega} \right]} \quad (13)$$

The dielectric constant is therefore *complex* and must have a power (or watt) and a wattless component if expressed in this form. This can readily be seen from the following derivation where the ordinary instead of the symbolic method is employed. We have, for $\varepsilon = \varepsilon_0 \cos \omega t$,

$$v = \frac{q\varepsilon_0}{m\omega} [\sin \omega t - \sin \omega t_0]$$

and each ion when colliding loses the velocity

$$v = \frac{q\varepsilon_0}{m\omega} [\sin \omega t - \sin \omega(t - t')]$$

and the resulting velocity change becomes

$$\begin{aligned} d\left(\sum v\right) &= \left\{ \frac{Nq}{m} \frac{\omega/\nu^2}{1 + (\omega/\nu)^2} \varepsilon_0 \cos \omega t - \frac{Nq}{m} \frac{\omega/\nu}{1 + (\omega/\nu)^2} \varepsilon_0 \sin \omega t \right\} dt \\ &= \{ \alpha \varepsilon_0 \cos \omega t - \beta \varepsilon_0 \sin \omega t \} dt \end{aligned}$$

Integration yields

$$\Sigma v = \underbrace{\gamma \varepsilon_0 \sin \omega t}_{\substack{90 \text{ deg out of} \\ \text{phase with } \varepsilon; \\ \text{hence displac-} \\ \text{ement (wattless)} \\ \text{component}}} + \underbrace{\delta \varepsilon_0 \cos \omega t}_{\substack{\text{in phase with } \varepsilon; \\ \text{hence absorp-} \\ \text{tion (watt)} \\ \text{component}}}$$

for $\gamma = \alpha/\omega$ and $\delta = \beta/\omega$. Inserting these results in the main equation

$$\text{curl } H = \frac{1}{c} \frac{\partial \varepsilon}{\partial t} + \frac{4\pi q}{c} \Sigma v$$

for the ionized medium, yields

$$\text{curl } H = \frac{1}{c} \frac{\partial \mathcal{E}}{\partial t} + \frac{4\pi q}{c} [\gamma \mathcal{E}_0 \sin \omega t + \delta \mathcal{E}_0 \cos \omega t]$$

But $\mathcal{E} = \mathcal{E}_0 \cos \omega t$; hence $\mathcal{E}_0 \sin \omega t = -\partial \mathcal{E} / \partial t$ and

$$\text{curl } H = \frac{1}{c} \underbrace{[1 - 4\pi q \gamma]}_{\kappa_e} \frac{\partial \mathcal{E}}{\partial t} + \underbrace{\frac{4\pi q \delta}{c}}_{4\pi \sigma / c} \mathcal{E} \quad (14)$$

Therefore, for the ionized layer with ν collisions per second, the true dielectric constant κ_e and true conductivity σ are

$$\left. \begin{aligned} \kappa_e &= 1 - \frac{4\pi N q^2}{m(\omega^2 + \nu^2)} \\ \sigma &= \frac{N q^2 \nu}{m(\omega^2 + \nu^2)} \end{aligned} \right\} \quad (15)$$

146. Phase Velocity, Group Velocity of Propagation, Index of Refraction, and Critical Frequency.—Since the permeability of the ionized medium remains unchanged and the dielectric constant κ_e alone changes and the velocity of propagation of an electromagnetic wave in a medium is inversely proportional to the square root of the permeability times the dielectric constant of the medium, we have for the phase velocity

$$c' = \frac{c}{\sqrt{\kappa_e}} = \frac{c}{\sqrt{1 - \frac{4\pi N q^2}{m\omega^2}}} \quad (16)$$

since $\mu = 1$. We therefore see that the phase velocity is greater than the velocity c of light. Phase velocity must be distinguished from group velocity.

The phase velocity c' is the speed at which an infinitely long sinusoidal wave train travels through a medium.

The group velocity c'' is the speed at which the energy travels through a medium. For our case, we have the simple relation

$$c'c'' = c^2 = 9 \times 10^{20} \text{ cm}^2/\text{sec}^2 \quad (17)$$

that is, when the phase velocity c' is greater than the velocity c in free ether, the group velocity c'' is smaller than c . Hence high phase velocity means that the energy received arrives somewhat later. This is a very important point when dealing with electromagnetic echo effects which often occur seconds after the direct signal has been received.¹

From these definitions, it is evident that the phase velocity is of no practical value except when unmodulated time signals present themselves.

¹ For details, see p. 403.

But as soon as a wave is modulated or we receive impulses, we deal with the group velocity c'' . Stokes first called attention to a general formula for group velocity and he regards the group as due to two infinitely long trains of waves of equal amplitudes and nearly equal wave lengths advancing in the same direction. Rayleigh shows more generally that, if c' is the velocity of propagation of any wave length λ where $k = 2\pi/\lambda$,

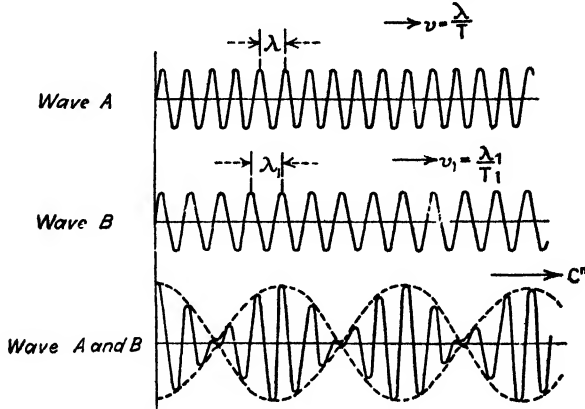


FIG. 225.—Illustrates group velocity c'' .

then the group velocity c'' of a group composed of a great number of waves and moving into an undisturbed part of the medium is

$$c'' = \frac{\partial(kc')}{\partial k} \quad (18)$$

The derivation is briefly as follows. Referring to Fig. 225, we have for two infinitely long waves represented by

$$y_1 = \cos k(vt - x) \quad \text{and} \quad y_2 = \cos k_1(v_1t - x)$$

a resulting wave (1 + 2)

$$y = 2 \cos \left\{ \frac{k_1 v_1 - kv}{2} t - \frac{k_1 - k}{2} x \right\} \cos \left\{ \frac{k_1 v_1 + kv}{2} t - \frac{k_1 + k}{2} x \right\}$$

where

$$k = \frac{2\pi}{\lambda}$$

$$k_1 = \frac{2\pi}{\lambda_1}$$

At time $t = 0$, the resultant wave has a maximum at the point of origin ($x = 0$). If the wave lengths are almost equal, that is, $k_1 - k$ and $v_1 - v$ small, we have a train of waves whose amplitude varies slowly from one part to another between 0 and 2, forming a series of groups separated

from one another by regions comparatively free of disturbances. The position at the time t of the middle of the group which was initially at the origin ($x = 0$) moves on with a group velocity c'' determined by

$$(k_1 v_1 - kv) - (k_1 - k) = 0$$

which shows that the group velocity is $(k_1 v_1 - k_2 v_2)/(k_1 - k)$ which, in the limit, yields

$$\begin{aligned} c'' &= \frac{d(kv)}{dk} \\ &= v - \lambda \frac{dv}{d\lambda} \end{aligned} \quad (19)$$

and checks formula (18). From this derivation, it is evident that, when wave trains λ and λ_1 travel with equal speeds, the speed of the interference beat would be equal to the speed common to both component waves.

The index of refraction n is defined as the ratio of the velocity of propagation in vacuum to that in the medium;¹ that is, for the ionized medium it becomes

$$n = \frac{c}{c'} = \sqrt{1 - \frac{4\pi N q^2}{m\omega^2}} \quad (20)$$

This equation determines the degree of bending in the ionized layer. If during 1 sec ν ionic collisions occur, then according to (12) and (13) we obtain a complex index of refraction since

$$\begin{aligned} n &= \sqrt{1 - \frac{4\pi N q^2}{m\omega\sqrt{\omega^2 + \nu^2}}} \\ &= \sqrt{1 - \frac{4\pi N q^2}{m\omega^2 \left[1 - j\frac{\nu}{\omega}\right]}} \end{aligned} \quad (21)$$

and hence absorption takes place. But, at heights greater than 80 km, the atmosphere is so dilute that ν is very small (Table XV, page 384) and for short waves ν/ω is small in comparison with unity. Consequently a real index of refraction as given by (20) exists. Combining (19) and (20), we find another expression for the group velocity

$$c'' = \frac{\partial(f)}{\partial(f/c')} = c \frac{\partial(f)}{\partial(nf)} \quad (22)$$

and

$$\frac{1}{c''} = \frac{1}{c} \frac{\partial(nf)}{\partial f} = \frac{1}{c} \left(n + f \frac{\partial n}{\partial f} \right)$$

¹ Another expression for n is given in Eq. (37).

and for any path

$$c \int \frac{ds}{c'} = \int n ds - f \int \frac{\partial n}{\partial f} ds \quad (23)$$

if ds denotes the element of the path and f the frequency.

In order to prove Eq. (17), we have to investigate Eq. (3), the equation of motion for the ionized medium. Since the time factor of the field strength \mathcal{E} of Eq. (4) is $e^{i\omega t}$, we find for the velocity v of one ion, when the frictional term $F(dz/dt)$ is included,

$$v = \frac{q\mathcal{E}}{F + jm\omega}$$

and (3) becomes for N ions/cc

$$\frac{\partial^2 \mathcal{E}}{\partial x^2} = \frac{\mu\kappa}{c^2} \frac{\partial^2 \mathcal{E}}{\partial t^2} + \frac{4\pi\mu Nq^2}{F + jm\omega} \frac{\partial \mathcal{E}}{\partial t} \quad (24)$$

if \mathcal{E} denotes the remaining z component and like ions are considered. The solution of this expression is of the form

$$\mathcal{E} = A e^{-\alpha x + j\omega \left(t - \frac{x}{c'}\right)}$$

Neglecting the frictional term ($F = 0$) we obtain for the phase velocity

$$c' = \frac{c}{\sqrt{1 - \frac{4\pi Nq^2}{m\omega^2}}} = c \sqrt{1 + \frac{\lambda^2}{\lambda_1^2}} = c \sqrt{1 + \frac{k_1^2}{k^2}}$$

for $\mu\kappa = 1$; $k = 2\pi/\lambda$; $k_1 = 2\pi/\lambda_1$; $\lambda_1^2 = \pi mc^2/(Nq^2)$

But, according to (18), the group velocity is

$$c'' = \frac{\partial(kc')}{\partial k} = \frac{c}{\sqrt{1 + \frac{k_1^2}{k^2}}}$$

Hence

$$c' \cdot c'' = c^2$$

and the group velocity becomes

$$c'' = c \sqrt{1 - \frac{4\pi Nq^2}{m\omega^2}} = c \sqrt{1 - \left(\frac{f}{f_0}\right)^2} \quad (25)$$

if f_0 denotes the resonance frequency for which selective absorption occurs. Since the group as well as the phase velocity for the ionized medium is often very different from the velocity c in a vacuum, we have to distinguish the three cases.

1. If $4\pi Nq^2/m\omega^2 < 1$, then the phase velocity in the ionized medium is greater and the group velocity correspondingly smaller than the velocity of propagation in empty space.

2. If the group velocity c'' vanishes, then, according to (25)

$$\frac{4\pi Nq^2}{m\omega^2} = 1 \quad (26)$$

for which case the phase velocity (16) is infinite. Hence, for a given number of ions a frequency f_0 exists for which electromagnetic waves can no longer pass and that portion of the layer is opaque to waves of this frequency. From (26) we find that the critical frequency

$$f_0 = q\sqrt{\frac{N}{m\pi}} \quad (27)$$

3. If $4\pi Nq^2/m\omega^2 > 1$, we have to deal with an imaginary group velocity. The value of the critical frequency is difficult to calculate since the number of ions and the kind of ions have to be assumed. Certain authors assume the action to be due to electrons and give values ranging from 10^5 to 3×10^6 electrons/cc. For $N = 10^6$ electrons/cc, we had $f_0 = 2840$ kc/sec, corresponding to a critical wave length of 106 m; this absorption was never observed. For electrons $q = 4.77 \times 10^{-10}$ e.s.c.g.s.; $m = 8.97 \times 10^{-28}$ g, and $4\pi q^2/m = 3.2 \times 10^9$ e.s.c.g.s. The index of refraction for 10^6 electrons/cc and short waves becomes

$$n = \sqrt{1 - \left(\frac{\lambda}{75}\right)^2} \quad (28)$$

when λ is measured in meters.

147. Dispersive Properties of the Ionized Layer.—From (16), (25), and (27), we find for the phase and group velocity

$$\left. \begin{aligned} c' &= \frac{c}{\sqrt{1 - (f_0/f)^2}} \\ c'' &= c\sqrt{1 - \left(\frac{f_0}{f}\right)^2} \end{aligned} \right\} \quad (29)$$

and from (20) for the refractive index,

$$n = \sqrt{1 - \left(\frac{f_0}{f}\right)^2} \quad (30)$$

where f_0 denotes the resonance frequency and f the frequency of the wave. These results show that the ionized layer has dispersing properties and rays of higher frequency pass at a greater speed than those of lower frequency. A modulated wave ($f + \Sigma\delta f$ and $f - \Sigma\delta f$, respectively) with side bands must therefore arrive somewhat distorted. The effect is more pronounced the larger $\delta f/f$. Hence the *distortion for shorter waves is less* since $(f + \delta f)/f$ is almost unity. Besides this velocity effect we see from (23) that different frequencies can follow different paths.

148. Notes on the Physics of the Atmosphere¹ and Selective Absorption.—The earth's atmosphere is composed of two concentric shells. The inner shell is called the "trophosphere" and the outer the "stratosphere."

The trophosphere has a temperature gradient which decreases from the ground upward, the mean gradient being about 6°C/km. The radial height of the trophosphere is 10 to 15 km and masses of air are continually moved about to places where the pressure is different.

In the stratosphere no temperature gradient exists. This is an isothermal shell and convection currents of air cease at a radial height of about 20 km since the temperature is there only about -54°C, consequently there are no large mass movements.

With respect to the main elements contained in the atmosphere we have the volume percentages of nitrogen, oxygen, hydrogen, and helium as in Table XIV². We see that at a height of 70 km there is a rather

TABLE XIV

Height, km	Pressure, mm mercury	Nitrogen	Oxygen	Hydrogen	Helium
0	760	78.1	20.9	0.033	0.005
20	41.7	85	15		
40	1.92	88	11	1	
60	0.106	77	6	16	1
80	0.019	21	1	74	4
100	0.013	1	.	95	4
120	0.011			97	3
200	0.006	99	1
500	0.0016	100	

marked dividing line. From this height on, the lightest gas, hydrogen, forms the main constituent of the air. The volume percentage for the content of hydrogen is somewhat doubtful since Jeans gives a value which is 3.3×10^{-5} against a value of 3.3×10^{-3} as in this table.

Ionization is brought about as explained on page 369, and Table XV, the work of S. Chapman and E. A. Milne,³ gives the approximate values

¹ HUMPHREY, W. J. "Physics of the Air," J. B. Lippincott Company, Philadelphia, 1920; WEGENER, "Thermodynamik der Atmosphäre," 1911, p. 46; S. CHAPMAN in Glazebrook, "Dictionary of Applied Physics," Vol. II, The Macmillan Company, New York, 1926, p. 543; LORD RAYLEIGH, *Proc. Roy. Soc. (London)*, **109**, 428, 1925; W. R. G. BAKER and C. W. RICE, *A.I.E.E.* **45**, 535, 1926; H. LASSEN, *E.N.T.*, **4**, 324, 1927; S. CHAPMAN and E. A. MILNE, *Quart. J. Roy. Met. Soc.*, **46**, 357, 1920; J. J. THOMSON, *Phil. Mag.*, **47**, 337, 1924.

² WEGENER, *loc. cit.* In this table the hypothetical gas geocornium is included with hydrogen.

³ *Loc. cit.*

TABLE XV

Height, km	Pressure, dynes/cm ²	Number of molecules/cc	Molecular mean free path, cm	Electron collision, frequency per sec ($\nu = 1/\tau$) between an electron and a gas molecule
0	1.01×10^5	2.7×10^{19}	9×10^{-6}	9.5×10^{11}
12	1.92×10^5	6.5×10^{18}	4×10^{-6}	2.1×10^{11}
20	5.53×10^4	1.9×10^{18}	1×10^{-4}	8.5×10^{10}
40	2.55×10^3	8.6×10^{16}	3×10^{-3}	2.8×10^9
60	1.24×10^2	4.2×10^{15}	6×10^{-2}	1.4×10^8
80	6.27	2.1×10^{14}	1	8.5×10^6
100	0.363	1.2×10^{13}	20	4.3×10^6
150	1.49×10^{-2}	5.0×10^{11}	500	1.7×10^4
200	5.62×10^{-3}	1.8×10^{11}	1000	8.5×10^3
300	6.99×10^{-4}	2.4×10^{10}	1×10^4	8.5×10^2
400	1.05×10^{-4}	3.6×10^9	7×10^4	1.2×10^2
600	2.59×10^{-6}	8.8×10^7	3×10^6	2.8
800	7.97×10^{-8}	2.7×10^6	9×10^7	0.95
1000	2.92×10^{-9}	9.9×10^4	3×10^9	2.8×10^{-3}

of pressure, molecular concentration, mean free path between molecules, and collision frequency. The molecular mean free path l is calculated from

$$l = \frac{1}{\pi\sqrt{2}MD^2} \text{ cm} \quad (31)$$

where M denotes the number of molecules per cubic centimeter and D the molecular diameter (assuming 3×10^{-8} cm, and that no account is taken of air as a mixture). For the electronic free path l_e , we have the approximate formula

$$l_e = \frac{1}{M\pi D_1^2 \sqrt{1 + \frac{m_e}{m}}} \text{ cm} \\ \cong \frac{4}{\pi MD^2} \text{ cm} \quad (32)$$

where M , the number of molecules per cubic centimeter, is assumed large compared with the number of electrons, $D_1 = (D + D_e)/2$ is the average value of the diameters of the molecules and electrons, m_e and m are the masses of an electron and a molecule, respectively. The second expression is obtained when the mass and diameter of the electron are neglected in comparison with those of a molecule. The radius of the electron at rest is only 1.85×10^{-13} cm, but that of the lightest atom, a hydrogen atom,

is 1.085×10^{-8} cm. We see that the electron mean free path is about $4\sqrt{2}$ times the molecular mean free path. Since the average electron velocity is

$$v = \sqrt{\frac{8kT}{\pi m_e}} \text{ m/sec}$$

where the universal gas constant $k = 1.37 \times 10^{-16}$, T is in Kelvin degrees ($273 + C^\circ$), and¹ $m_e = 8.995 \times 10^{-28}$ g, then the average collision frequency ν between the electrons and a gas molecule is

$$\nu = \frac{v}{l_e} = MD^2 \sqrt{\frac{k\pi T}{2m_e}} \quad (33)$$

We note from Table XV that selective absorption takes place at $h = 70$ km for a frequency of 5000 kc/sec, since the collision frequency ν equals $\omega = 3.14 \times 10^7$ at a height of about 70 km. Hence, if the lower boundary of the ionized layer is much above 70 km, the electromagnetic waves will not be subjected to large absorption.

By means of Eq. (4), the amplitude z of the motion of an ion can be found, and we have for

$$m \frac{d^2 z}{dt^2} + F \frac{dz}{dt} = q \mathcal{E}_0 \sin \omega t$$

a solution of the form^{*}

$$z = A \sin \omega t + B \cos \omega t$$

Hence

$$\begin{aligned} \frac{dz}{dt} &= \omega A \cos \omega t - \omega B \sin \omega t \\ \frac{d^2 z}{dt^2} &= -\omega^2 A \sin \omega t - \omega^2 B \cos \omega t \end{aligned}$$

and the equation of motion reads

$$-\omega^2 A \sin \omega t - \omega^2 B \cos \omega t + \frac{F}{m} A \sin \omega t + \frac{F}{m} B \cos \omega t$$

for $\omega t = \pi/2$; $\sin \omega t = 1$ and $\cos \omega t = 0$; hence

$$-\omega^2 A + \frac{F}{m} A = \frac{q}{m} \mathcal{E}_m$$

¹ This is the mass $m_e = m_0$ which is correct up to velocities $= c/5 = 60,000$ km/sec. It should be remembered that the entire energy W of an electron in motion is $W = W_e + 0.5m_0 v^2$ where the first term denotes the magnetic-field energy due to the electronic charge q in motion, and the second term the energy required to move the uncharged mass of the electron with a velocity v .

and for $\omega t = 0$; $\sin \omega t = 0$ and $\cos \omega t = 1$

$$-\omega^2 B + \frac{F}{m} B = 0$$

Hence

$$A = \frac{(q/m) \varepsilon_0}{(F/m) - \omega^2} \quad \text{and} \quad B = 0$$

and the amplitude z for any frequency $f = \omega/2\pi$, after steady-state conditions have been attained, is

$$z = \frac{(q/m) \varepsilon_0}{(F/m) - \omega^2} \quad (34)$$

which shows that, for a frequency

$$f_0 = \frac{1}{2\pi} \sqrt{\frac{F}{m}} \quad (35)$$

a theoretically infinite amplitude would be reached if the ion did not collide with its neighbors and thus consume energy from the wave which produces the vibration along the direction of ε . In (35), the quantity F denotes the restoring force per unit displacement and is, according to (27)

$$F = 4\pi Nq^2$$

Thus we find for the amplitude of the ionic oscillation due to $\varepsilon_0 \sin \omega t$ from (34),

$$z = \frac{(q/m) \varepsilon_0}{\omega_0^2 - \omega^2} = \frac{q \varepsilon_0}{4\pi^2 m (f_0^2 - f^2)} \quad (36)$$

From the relation (8) for the ionic contribution, we find

$$i_1 = Nqv = Nq \frac{dz}{dt}$$

or

$$D_1 = \int i_1 dt = Nqz$$

which is nothing more than the component of *electric* displacement due to N ions. From (9), we find for the unit cube

$$D_2 = \int i_2 dt = \frac{\varepsilon}{4\pi}$$

which is nothing more than the *dielectric* displacement in the fictitious condenser since the field strength per unit length is numerically equal to the potential difference. The resultant effect is, therefore, if we deal with maximum values,

$$D_0 = \frac{\varepsilon_0}{4\pi} + Nqz = \frac{\varepsilon_0}{4\pi} + \frac{Nq^2 \varepsilon_0}{4\pi^2 m (f_0^2 - f^2)}$$

and

$$\begin{aligned} 4\pi D_0 &= \epsilon_0 \left[1 + \frac{Nq^2}{\pi m(f_0^2 - f^2)} \right] \\ &= \epsilon_0 \kappa \end{aligned}$$

Hence the dielectric constant κ_e and index of refraction n can also be expressed in a dispersive medium as

$$\left. \begin{aligned} \kappa_e &= 1 + \frac{Nq^2}{\pi m(f_0^2 - f^2)} \\ n &= \sqrt{\kappa_e} \end{aligned} \right\} \quad (37)$$

These results, however, are of value only when the atoms are so far apart that the free periods of the ions are not affected by the presence of the neighboring atoms and there is only one critical frequency f_0 .

With reference to ionization due to ultraviolet rays ($\lambda < 400\mu\mu$) from the sun, the following is added: The action of such rays liberates an electron from a neutral molecule. It leaves behind a positively charged nucleus. The electron can either remain free or join another gas molecule and thus produce a negative ion. Generally nitrogen and oxygen are ionized in this way, while hydrogen is hardly affected by ultraviolet rays.

If A denotes the absorption ability of air at the surface of the earth and assuming that A is proportional to the number of molecules per cubic centimeter, and therefore also proportional to the pressure, the absorption ability at any height $h^{(om)}$ becomes

$$a = A\epsilon^{-kh}$$

for $k = 1.3 \times 10^{-6}$ (ratio of specific gravity and pressure at 0°C). But where there is strong absorption, there is also strong ionization. Hence the change in the intensity of the rays at any height becomes

$$dJ = aJdh = A\epsilon^{-kh}Jdh$$

or

$$\frac{dJ}{J} = A\epsilon^{-kh}dh$$

and

$$J = J_0\epsilon^{-\frac{A}{k}\epsilon^{-kh}}$$

where J_0 denotes the intensity of the ultraviolet rays at $h = \infty$, that is, before absorption begins. We find for the absorption

$$\frac{dJ}{dh} = A\epsilon^{-kh}J$$

The coefficient A for a monatomic gas is given in the formula for the intensity of ultraviolet light

$$J = J_0\epsilon^{-Ax}$$

if the rays pass along in the direction of x . According to Lenard and Ramsauer, the ionization effect of the ultraviolet light is, after passing through an air distance of x cm, 100 relative ionization numbers for $x = 0.5$; 6.8 relative numbers for $x = 1.5$; and only 0.3 relative numbers for a distance of 2.5 cm. Hence $A = 2.7$. Figure 226 gives the functions of J and dJ/dh . The latter is a relative measure of the number of ion pairs produced at any height h per unit volume and in unit time.

The strongest ionization takes place in a layer of about 30 km thickness and the maximum ionization is, according to

$$\frac{dJ}{dh} = A\epsilon^{-kh}J$$

for

$$h = \frac{1}{k} \log_{\epsilon} \frac{A}{k} = 112 \text{ km}$$

Above and below this height, the ionization decreases and more decrease takes place below 112 km. Accordingly, the ionized layer is at about 100 km.

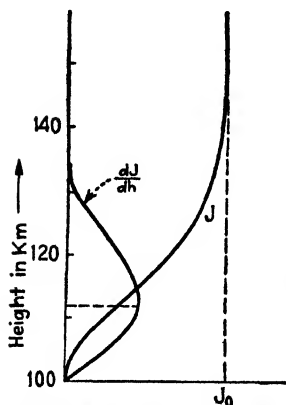


FIG. 226.—Degree of ionization above ground.

Now the question arises whether the electrons remain as free electrons or join a neutral gas molecule and produce a negative ion of molecular magnitude. Since at the foregoing height hardly any oxygen exists, the electrons can join with nitrogen or hydrogen molecules only. But the former has, like the noble gases, no great tendency to catch free electrons, and therefore hydrogen seems to be the only gas that can at this height act as a negative ion after absorbing an electron. Hence we have to deal with such negative ions and with free electrons.

149. Bending and Path of the Rays.—We have seen that the distribution of ionization in the ionized stratum will at first increase with height, reaching a maximum, and will then decrease again to a small value at very great heights.

The effective refraction index [Eq. (20)] of the medium is reduced on account of the free electrons which are in the ionized layer and some of the waves moving toward the layer will be bent and return to earth. For the treatment of the path, we can therefore consider the energy flow like light rays.

According to (16), we have for the phase velocity

$$c' = \frac{3 \times 10^{10}}{\sqrt{1 - \frac{4\pi Nq^2}{m\omega^2}}} \cong 3 \times 10^{10} \left[1 + \frac{2\pi Nq^2}{m\omega^2} \right] \quad (38)$$

the approximation to the right being permissible for short waves (below 100 m). In order to realize the effect of the variable phase velocity of propagation, we imagine (in Fig. 227) an infinitely narrow wave element dz which is cut out of the wave front. The wave front will be at time t at AB and at time $t + dt$ along ED . Hence it takes the wave the same time to go from A to E as from B to D . But the distance from A to E is $(c' + dc')dt$ and from B to D is $c'dt$ for the velocities indicated in the figure. The wave element has turned itself through angle $\Delta\theta$, which is

$$\Delta\theta = \frac{(c' + dc')dt - c'dt}{dz} = \frac{dc'dt}{dz}$$

and the path of the ray is therefore curved owing to the variable velocity c' of propagation. The radius ρ of the curvature can be found from the relation

$$\rho\Delta\theta = c'dt$$

Hence

$$\frac{1}{\rho} = \frac{dc'dt/dz}{c'dt} = \frac{dc'/dz}{c'} = \frac{d(\log_e c')}{dz} \quad (39)$$

In order that the rays shall have sufficient intensity at the receiving end, the maximum value of ρ cannot be greater than the radius $R = 6.37 \times 10^8$ cm of the earth. With $\rho = R$, we find from (39) the curvature

$$\frac{1}{R} = \frac{1}{c'} \frac{dc'}{dz}$$

Hence if the number N of ions increases along z , then c' increases and the rays will bend downward with a curvature $c'^{-1} \partial c' / \partial z$.

Introducing from (20) the refractive index n , we obtain from

$$c' = \frac{c}{n} = \frac{3 \times 10^{10}}{n}$$

for the equation of bending

$$\frac{1}{R} = -\frac{1}{n} \frac{dn}{dz} \quad (40)$$

where z is perpendicular to the direction of the ray. Eq. (40) is therefore the equation of the path if n is everywhere known. Since n is practically unity except at the critical frequency, this curvature is $0.5(dn^2/ds)$. If the ray is to follow the curvature of the earth, it is

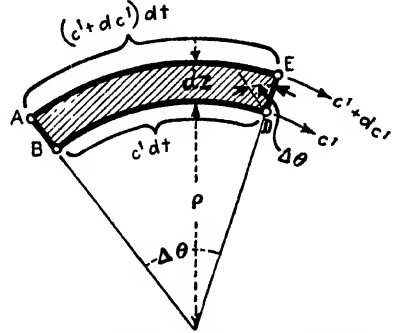


FIG. 227. -- Wave element dz of wave front

evident that n must decrease at higher altitudes; that is, dn^2/dz must be negative.

As the ray passes into the ionized layer (Fig. 228), the angle Φ_0 changes to some angle Φ since the index n of refraction decreases within the layer and gives the smallest value at some critical height in the ionized medium. From there on, n increases again toward the limiting value 1. Assuming a definite small electron concentration N below the layer, we find from (20) that for short waves the index of refraction is practically unity and a real quantity.

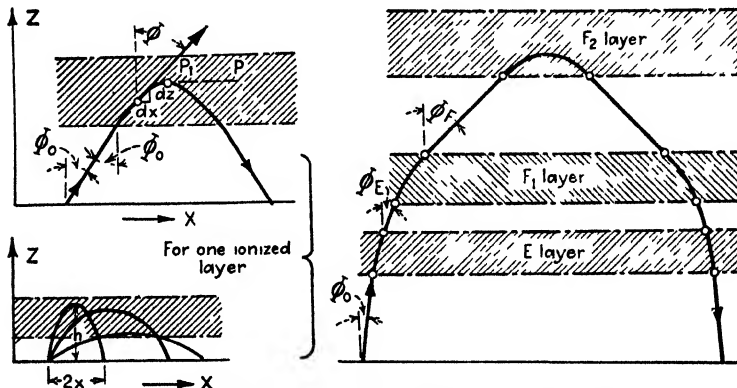


FIG. 228.—Path of sky ray for single- and multi-layers.

Within the layer, Snell's law

$$n \sin \Phi = \text{constant} \quad (41)$$

can be applied. But since n decreases at first with z , the angle Φ grows until the path is horizontal. But, according to Gans, just before $\Phi = 90^\circ$ at a critical plane $P_1 - P$ in the layer, the refraction law breaks down and total reflection takes place at point P_1 . After that, refraction occurs again and it is justifiable to apply the refraction law

$$n_0 \sin \Phi_0 = n \sin \Phi \quad (42)$$

with the condition that a critical plane must exist in order to bring the ray back toward the earth. This condition requires $\Phi = 90^\circ$ or $\sin \Phi = 1$. Hence $n = n_0 \sin \Phi_0 = \sin \Phi_0$ since, for short waves below the layer, $n_0 = 1$. The number of electrons per cubic centimeter can be calculated since the expression introduced in (20) yields

$$\begin{aligned} \sin \Phi_0 &= \sqrt{1 - \frac{4\pi Nq^2}{m\omega^2}} \\ &\cong 1 - \frac{2\pi Nq^2}{m\omega^2} \end{aligned}$$

the latter approximation holding only for short waves. Hence the electron density

$$N = \frac{m\omega^2(1 - \sin \Phi_0)}{2\pi q^2} \quad (43)$$

An angle $\Phi_0 = 80^\circ$ corresponds for $\lambda = 14$ m to a ray which is tangent to the surface of the earth and from this value we can calculate the number of electrons per cubic centimeter or hydrogen ions per cubic centimeter, respectively, which exist for this frequency. Most authors assume an electron concentration N since the hydrogen ion seems altogether too heavy to account for the transmission phenomena. Assuming a certain number of electrons per cubic centimeter, we see from (43) that, with increasing frequency ($\omega/2\pi$), the refraction becomes smaller and smaller until, above a certain frequency, the ray can no longer be refracted back. This frequency seems to be in the neighborhood of 20 Mc/sec. When the curvature of the earth is to be taken into account, we use the relation

$$\frac{d(\log_e n)}{dr} = \frac{1}{R}$$

assuming that a ray which was once parallel to the ground becomes again parallel to the ground. The quantity r denotes the distance from the center of the earth and R the radius of the earth. In this formula the height of the ionized layer is neglected in comparison with R . If we deal, for instance, with waves below 100 m in length, we have again $n \cong 1 - (2\pi Nq^2/m\omega^2)$ and, according to the curvature condition,

$$\begin{aligned} \Delta N &= \frac{m\omega^2}{2\pi q^2 R} \Delta r \\ &= \frac{2\pi m f^2}{q^2 R} \Delta r \end{aligned} \quad (44)$$

This equation gives a means for determining how much the electron density must change for a certain height Δr in order to keep the ray parallel to the surface of the earth. For instance, for a wave of

$$\lambda = 80 \text{ m } (= 3.748 \times 10^6 \text{ cycles/sec}),$$

we find for the increase of N per kilometer height ($\Delta r = 1$ km) if we assume the presence of electrons only

$$\Delta N = \frac{6.28 \times 9.02 \times 10^{-28} \times 3.748^2 \times 10^{12} \times 10^5}{4.774^2 \times 10^{-20} \times 6.378 \times 10^8} = 55 \text{ electrons/km}$$

Hence if the curvature of the surface of the earth is taken into account, the electron density is slightly larger. With respect to the path of the ray, we find from Fig. 228

$$\frac{dx}{dz} = \tan \Phi = \frac{\sin \Phi}{\sqrt{1 - \sin^2 \Phi}}$$

and combining this with (42) for $n_0 = 1$ gives

$$\frac{dx}{dz} = \frac{\sin \Phi_0}{\sqrt{n^2 - \sin^2 \Phi_0}}$$

which gives

$$x = \sin \Phi_0 \int_0^z \frac{dz}{\sqrt{n^2 - \sin^2 \Phi_0}} \quad (45)$$

This integral can be evaluated when n is known as a function of the height z .

From this point, assumptions have to be made. E. O. Hulburt¹ assumes, for instance, as one possibility that the electron density is proportional to the height and finds for $n^2 = 1 - \gamma z$ for the path of the ray an expression

$$x^2 = \frac{4 \sin^2 \Phi_0 (1 - \sin^2 \Phi_0 - \gamma z)}{\gamma^2}$$

which is a parabola. The maximum height h above ground then is

$$h = \frac{1 - \sin^2 \Phi_0}{\gamma} \quad (46)$$

and the ray comes down again at a distance $2x = 4h \tan \Phi_0$ (Fig. 228). On the other hand, H. Lassen¹ calculates the index of refraction n also with respect to z (Fig. 229) and assumes $z = 0$ at a height of 95 km above ground (lowest level of the layer). The index of refraction then becomes

$$n = \sqrt{1 - 2.3 \times 10^{-9} \lambda^2 \left(z - \frac{z^2}{34} \right)}$$

if z is expressed in kilometers and the wave length in centimeters. The rays which are incident in the layer at an angle Φ_i to the normal from ground will pass parallel to the ground when

$$\cos \Phi_i = 1.4 \times 10^{-4} \lambda^{(\text{cm})} \quad (47)$$

This corresponds to an angle of $\theta = 0^\circ$ at the sender. Table XVI is obtained from Eq. (47). The table shows that waves below 14 m in length can never return from the layer. The limiting angles assume, however, a plane earth.

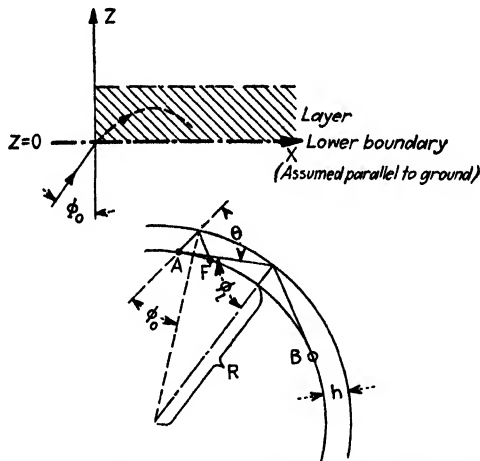
¹ *Loc. cit.*

TABLE XVI

$\lambda^{(m)}$	Φ_i , deg	θ , deg
14	79	0
20	73	13
30	65	22
40	56	32
60	33	56

Moreover, in Eq. (28) we found, for short waves and $N = 10^6$ electrons/cc, an index of refraction

$$n = \sqrt{1 + \left(\frac{\lambda}{75}\right)^2}$$

FIG. 229.—Limiting angle Φ_i for sky waves.

if λ is expressed in meters. Hence, for a certain angle Φ_i of incidence into the layer, there is no longer refraction but only total reflection given by

$$\sin \Phi_i = n$$

or

$$\cos \Phi_i = \frac{\lambda}{75} \quad (48)$$

This formula yields about the same results as those obtained from (47) and given in Table XVI. Now, in Fig. 229, the distance AB represents the normal limit reached by short waves if we do not take into consideration the rays which travel for long distances completely within

the layer (Fig. 223) and may account for abnormal distances and probably some long time-interval echo effects. This distance is approximately

$$\begin{aligned} d = AB &\cong 2\sqrt{(R+h)^2 - R^2} \\ &= 2\sqrt{2Rh + h^2} \\ &= 2\sqrt{12,760h + h^2} \end{aligned} \quad (49)$$

But

$$\sin \Phi_i = \frac{R}{R+h}$$

and

$$\left(\frac{R}{R+h}\right)^2 = 1 - \left(\frac{\lambda}{75}\right)^2$$

or

$$\lambda = \frac{75}{R+h} \sqrt{h^2 + 2Rh}$$

which together with (49) gives

$$\begin{aligned} \lambda &= \frac{75}{2(R+h)} d \cong \frac{75}{2R} d \\ &= \frac{75}{12,760} d \end{aligned}$$

or

$$d^{(\text{km})} = 170\lambda^{(\text{km})} \quad (50)$$

The distance $AF = d_1$ for angle Φ_0 of incidence (Fig. 229) becomes

$$d_1^{(\text{km})} = 2h^{(\text{km})} \tan \Phi_0 \quad (51)$$

150. Effect of the Earth's Magnetic Field on the Path of Transmission and Selective Absorption Due to Electron Motions.—The magnetic field of the earth is derived from a potential which is approximately

$$\Gamma = 0.32R^3r^{-2} \cos \alpha \quad (52)$$

if R denotes the radius of the earth and α the angular distance from a hypothetical magnetic north pole. The magnetic north pole lies in the neighborhood of the geographic south pole. The deviation from the geographic north-south direction is about 8 deg. The angle of the magnetic axis with the horizon is about 66 deg. At a height of 50 km, the horizontal and vertical components of the resultant magnetic-field intensity are

$$\begin{aligned} H_h &= 0.31 \sin \alpha \\ H_v &= 0.62 \cos \alpha \end{aligned}$$

When the wave passes into the ionized layer at an angle θ in the direction of the magnetic field, we have

$$\begin{aligned}H_z &= -H \cos \theta \\H_x &= H \sin \theta\end{aligned}$$

When long-distance transmission takes place and the ray is horizontal and at an angle θ with the magnetic meridian, then

$$\begin{aligned}H_z &= -H_h \cos \theta \\H_x &= \sqrt{H_h^2 \sin^2 \theta + H_v^2}\end{aligned}$$

and the total field varies from the horizontal and a value of 0.33 at the magnetic equator to the vertical and a value of 0.62 at the poles; the average value therefore¹ is

$$H_r = 0.5 \text{ gauss} \quad (53)$$

Omitting the less important motions of the ions and electrons, we have seen from the preceding sections that ions can be excited by the electric vector \mathcal{E} of a wave and that the ions execute linear to-and-fro motions along the direction of \mathcal{E} . It will be shown in the following that the ions for an appropriate orientation of the electromagnetic alternating field with respect to the magnetic field of the earth can be caused to oscillate along ellipses and circles, by means of which the polarization of the existing wave will be changed. The original linear polarized wave is then for the general case *elliptically* polarized. Special cases, circular and linear polarization, respectively, can occur. Besides this, selective absorption exists for a different critical frequency f_0 from that given by the theory originally suggested by Eccles and Larmor.

As is well known, a free ion moving in a magnetic field has a force (due to the magnetic field) acting upon it at right angles to its velocity and to the magnetic field. If the ion has a simple periodic electric force impressed upon it, it will execute a free oscillation together with a forced oscillation whose projection on a plane is in the general case an ellipse traversed in one period of the applied force. The component velocities are linear functions of the components of the electric field and the natural frequency f_0 depends only on the magnetic field and the ratio of the charge to the mass of the ion. The components would then become infinite if energy dissipation due to collision did not take place.

The simplest case is that in which the electric field \mathcal{E} which accelerates the ion is assumed to act perpendicularly to the earth's magnetic field H_e and it is assumed that the magnetic field H due to the wave is negligible. For a vanishing electric field, the force due to H_e causes the ion to move along a circular path. The direction of rotation depends upon the polarity of the charge of the ion. If ω_0 denotes the angular velocity of

¹ This corresponds to a flux density of 0.5 maxwell/cm² since $\mu = 1$ and is the value used in our calculations.

the ion, and R the radius of the circular path, we must satisfy the condition of balanced forces

$$\underbrace{\frac{1}{c}H_e R q \omega_0}_{\text{mechanical force due to } H_e} = \underbrace{m R \omega_0^2}_{\text{centrifugal force due to motion of ion}} \quad (54)$$

for which the ion remains moving along the circular path with the velocity $v = \omega_0 R$. The correctness of the left side is evident if it is realized that, for the ionized medium, the flux density $B = \mu H_e = H_e$ and that the force due to the earth's field H_e on the ion is

$$F = \frac{B}{c} q v$$

The natural frequency $\omega_0/2\pi$ of any ion becomes therefore

$$f_0 (\text{cycles/sec}) = 53 \times 10^{-13} H_e (\text{gauss}) \frac{q}{m} \quad (55)$$

if the charge of the ion is expressed in e.s.c.g.s. units and its mass in grams. For electrons, we have $q = 4.774 \times 10^{-10} \text{ cm}\sqrt{\text{dynes}}$ and $m = 9.02 \times 10^{-28} \text{ g}$. Combining this with the value $H_e = 0.5 \text{ gauss}$ of (53), we find that the resonance frequency of the electron is 1395 kc/sec, corresponding to a wave length of $\lambda = 215 \text{ m}$ which is in the vicinity of the selective absorption noted in the experiments of A. H. Taylor (Fig. 224). The other resonance frequency that might occur would be that due to the hydrogen ion which has a ratio q/m , equal to 1/1800 of that of the electron. Putting this value into (55), we find

$$f_0 = \frac{1.395 \times 10^6}{18 \times 10^2} = 775 \text{ cycles/sec}$$

corresponding to $\lambda_0 = 387 \text{ km}$, that is, a value in the audio-frequency range, which could not occur in this class of work. Hence for the selective absorption, which in this case has also been experimentally confirmed, the ions cannot play a part and the action of the free electrons together with the earth's magnetic field seems alone to be responsible for it.

Now if we include the action of the electric field

$$\mathcal{E} = \frac{\mathcal{E}_0}{2} [e^{i(\omega t - \varphi)} + e^{-i(\omega t + \varphi)}] = \mathcal{E}_1 + \mathcal{E}_2$$

of an electromagnetic wave where φ is the angle with respect to the direction of the alternating field \mathcal{E} , we note that we have a left- and a right-handed revolving field. One component must have the same direc-

tion of rotation as the ion and the other must revolve in the opposite direction. It should be noted, however, that, when \mathcal{E} also acts, the forced oscillating frequency of the ion is due to the frequency of \mathcal{E} . The action of the H_e field then affects the orbit velocity $v = R\omega$ only, since H_e determines the radius R of the ion path. According to the two revolving fields \mathcal{E}_1 and \mathcal{E}_2 , we have two components for the balanced forces [similar to Eq. (54)] for the stationary state

$$\underbrace{\frac{1}{c}H_e R q \omega}_{\text{mechanical force due to earth field } H_e} + \underbrace{\frac{\mathcal{E}_0}{2}q}_{\text{mechanical force due to electric field } \mathcal{E}_1} = \underbrace{mR\omega^2}_{\text{balancing centrifugal force}}$$

and for the other rotation

$$-\frac{1}{c}H_e R q \omega + \frac{\mathcal{E}_0}{2}q = mR\omega^2$$

Upon rearranging the terms and utilizing the resonance condition [Eq. (55)]

$$\omega_0 = \frac{H_e}{c} \frac{q}{m}$$

we obtain the relations

$$\left. \begin{aligned} \omega R &= \frac{0.5 \mathcal{E}_0 q}{m\omega - \frac{1}{c}H_e q} = \frac{0.5(q/m)\mathcal{E}_0}{\omega - \omega_0} = \frac{(q/m)\mathcal{E}_0}{4\pi(f - f_0)} \quad \left(\begin{array}{l} \text{for field in the same} \\ \text{direction as the cir-} \\ \text{culation of the ion} \end{array} \right) \\ \omega R &= \frac{(q/m)\mathcal{E}_0}{4\pi(f + f_0)} \quad \left(\begin{array}{l} \text{for field in the opposite direction} \end{array} \right) \end{aligned} \right\} \quad (56)$$

These results give the relations for the velocity $v = \omega R$ of the ions. The ionic current contribution due to the first expression of (56) for N ions is

$$i_1' = Nqv = \frac{0.5Nq^2\mathcal{E}_0}{m(\omega - \omega_0)} = \frac{Nq^2\mathcal{E}_1}{m(\omega - \omega_0)} \quad (57)$$

For the other component, we find

$$i_1'' = \frac{Nq^2\mathcal{E}_2}{m(\omega + \omega_0)} \quad (58)$$

The displacement current i_2 is

$$i_2 = \frac{0.5}{4\pi} \frac{d\mathcal{E}_0}{dt} \quad (59)$$

It is, however, to be noted that the ions are moving in the direction of the field when the revolving-field components are perpendicular to it since the velocity of the ions lags 90 deg behind the exciting field. Bearing

this in mind, we find for a wave propagation in the direction of the earth's field (about north-south transmission) for the total current as in solution (10)

$$\begin{aligned} i'_e &= i_1' + i_2 = \frac{1}{4\pi} \left[1 - \frac{4\pi Nq^2}{m\omega(\omega - \omega_0)} \right] \frac{d\varepsilon_1}{dt} \\ &= \frac{\kappa_e'}{4\pi} \frac{d\varepsilon_1}{dt} \end{aligned} \quad (60)$$

and for the other component

$$\begin{aligned} i_1'' &= i_1'' + i_2 = \frac{1}{4\pi} \left[1 - \frac{4\pi Nq^2}{m\omega(\omega + \omega_0)} \right] \frac{d\varepsilon_2}{dt} \\ &= \frac{\kappa_e''}{4\pi} \frac{d\varepsilon_2}{dt} \end{aligned} \quad (61)$$

The effective dielectric constant κ_e for the two cases is therefore

$$\kappa_e = 1 - \frac{4\pi Nq^2}{m\omega(\omega \mp \omega_0)} \quad (62)$$

We have also two different indices of refractions

$$n = \sqrt{1 - \frac{4\pi Nq^2}{m\omega(\omega \mp \omega_0)}} \quad (63)$$

as well as the phase velocities¹

$$c' = \frac{c}{\sqrt{1 - \frac{4\pi Nq^2}{m\omega(\omega \mp \omega_0)}}} \quad (64)$$

The wave therefore breaks up into two oppositely circularly polarized components traveling with different phase velocities $c_1' = c/\sqrt{\kappa_e'}$ and $c_2' = c/\sqrt{\kappa_e''}$. The plane of polarization of the resulting alternating field is rotated through an angle θ with respect to the field in the plane $d = 0$ which is

$$\theta = \frac{\omega d}{c_1'} - \frac{\omega d}{c_2'} = \frac{\omega d}{c} [\sqrt{\kappa_e'} - \sqrt{\kappa_e''}] \quad (65)$$

¹ If τ denotes the time between two impacts of an electron and gas molecules, the absorption coefficient for the wave is

$$\alpha = \frac{1}{2\tau c} \frac{4\pi Nq^2}{m(\omega \mp \omega_0)^2}$$

The minus sign stands for the counterclockwise-polarized wave and the plus sign for the clockwise-polarized wave. Hence one wave has more decrement than the other and in many cases only one will arrive with sufficient intensity.

since the wave after passing through a distance d has one component

$$\varepsilon_1 = 0.5\varepsilon_0 e^{j\left(\omega t - \varphi - \frac{\omega d}{c_1'}\right)}$$

and another component

$$\varepsilon_2 = 0.5\varepsilon_0 e^{-j\left(\omega t + \varphi - \frac{\omega d}{c_1'}\right)}$$

We must, however, realize that the two circularly polarized components remain coherent only if the index of refraction is not too great and the distance of propagation is small. If the two components are separated by greater refraction or distance, each will proceed as a circularly polarized wave. This can be understood from Eq. (40). We can calculate from it the curvature by means of the simplified formula $0.5(dn^2/dz)$ if z is taken perpendicular to the direction of the ray. When this is done, it will be seen that the curvatures of the two components are also different.

For short waves (below 100 m), that is, $\omega \gg \omega_0$, the two dielectric constants κ_e' and κ_e'' become almost equal and the rotation of the plane of polarization occurs only for long distances. For $\omega = \omega_0$, only the natural period of the electron oscillation plays a part. The dielectric constant κ_e' decreases as ω approaches ω_0 until it becomes negative; that is, the phase velocity c_1' becomes imaginary and the first-component wave becomes extremely damped. The reason for this is that the radius R of the electron orbit would become infinite if the energy absorption due to collisions did not interfere and produce the well-known selective absorption at about $\lambda = 215$ m (Fig. 224).

Fading in the broadcast range may be due to changes in the phase velocities and absorption by small changes in the electron density N or the strength of H_e .

For long waves ($\omega \ll \omega_0$), only one of the two circularly polarized rays will normally be returned from the ionized layer since the component of the dielectric constant κ_e' has a value greater than the dielectric constant κ of ether. The phase velocity is therefore smaller than that of c and the ray will curve upward and be lost.

In case the earth's magnetic field is perpendicular to the direction of wave propagation (about east-west direction), we can decompose the electric field ε into a component parallel to the H_e field and a component perpendicular to it. The phase velocity c_1' for the ε oscillations parallel to the magnetic field cannot be disturbed by this field and is

$$c_1' = \frac{c}{\sqrt{1 - \frac{4\pi Nq^2}{m\omega^2}}} \quad (66)$$

since the dielectric constant $\kappa_e' = \kappa_e$ has the same value as for absence of the magnetic field. The same is also true for the index refraction

since $n' = n$ [Eqs. (11), (16), and (20)]. For the other component, the total ionic current contribution is the sum of the ion motions due to both revolving fields. The other dielectric constant becomes

$$\begin{aligned}\kappa_e'' &= \left[1 - 0.5 \left(\frac{4\pi N q^2}{m\omega(\omega - \omega_0)} + \frac{4\pi N q^2}{m\omega(\omega + \omega_0)} \right) \right] \\ &= \left[1 - \frac{4\pi N q^2}{m(\omega^2 - \omega_0^2)} \right]\end{aligned}\quad (67)$$

and

$$n'' = \sqrt{1 - \frac{4\pi N q^2}{m(\omega^2 - \omega_0^2)}} \quad (68)$$

with a phase velocity

$$c_2' = \frac{c}{\sqrt{1 - \frac{4\pi N q^2}{m(\omega^2 - \omega_0^2)}}} \quad (69)$$

From these expressions we see that, for the earth's field perpendicular to the direction of propagation, double refraction takes place. The original ray is therefore split into *ordinary* and *extraordinary* rays which behave quite differently. The path is also entirely different. One ray can bend away from the earth, while the other returns to earth. Abnormal curvatures can occur in the path of a ray in the neighborhood of the critical frequency $\omega/2\pi = \omega_0/2\pi$.

151. Polarization of the Received Electromagnetic Waves and Fading.—Since, in the actual case, the direction of propagation does not always occur along the earth's field or perpendicular to it but is usually oblique to it, the received sky wave at the receiver antenna is generally an *elliptically* polarized wave, since the wave is split into two elliptically polarized waves traveling at different velocities. The magnetic vector lies in the wave front but the electrical vector is oblique to it. The axes of the magnetic ellipse are along and perpendicular to the component in the wave front of the imposed magnetic field. One of the axes of the electric ellipse (Fig. 230) is in the direction of this component also. The paths of the ions are ellipses in a plane oblique to the wave front. Usually the inclination of the electric vector to the wave front is small but the inclination to the wave front of the plane in which the paths of the ions lie will in general be appreciable. The electric vector of the downcoming ray *CO* is conveniently resolved into a component \mathcal{E}_y' along the *Y*-axis and a vector \mathcal{E}' in the vertical plane and perpendicular to *CO*. The vector \mathcal{E}' is then resolved into components \mathcal{E}_x' and \mathcal{E}_z' . The polarization of ray *EDO* is changed upon reflection and is resolved into \mathcal{E}'' and \mathcal{E}_y'' where \mathcal{E}'' has again the subcomponents \mathcal{E}_x'' and \mathcal{E}_z'' .

The components of the resultant electric vector \mathcal{E} at O are then

$$\left. \begin{aligned} \mathcal{E}_x &= \mathcal{E}_x' + \mathcal{E}_x'' \\ \mathcal{E}_y &= \mathcal{E}_y' + \mathcal{E}_y'' \\ \mathcal{E}_z &= \mathcal{E}_z' + \mathcal{E}_z'' + \mathcal{E}_z''' \end{aligned} \right\} \quad (70)$$

which is an ellipsoid with O at its mid-point. The eccentricity varies if the phase velocities and curvatures of the paths vary owing to variations in the effective ionic concentration N and changes in the effective value of H_e . Thus the variations of field intensity (fading) at the receiver and the bearing errors in direction finding are explained.

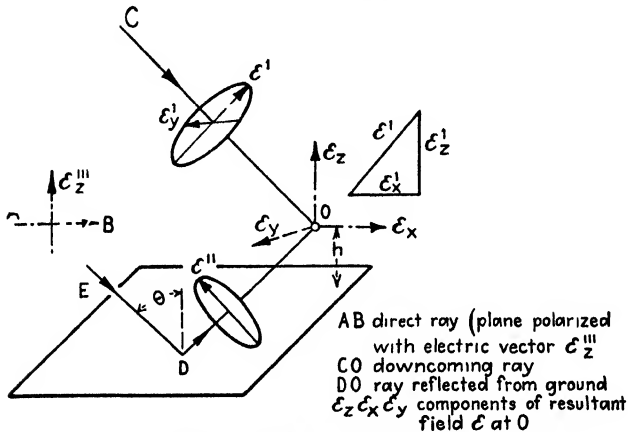


FIG. 230.—Elliptical polarization of electromagnetic waves.

By fading we mean a variation of the field strength at the receiver end with time. This can only be true for a constant transmitter intensity when the ion concentration N or the earth's field H_e or both are functions of time. If this is true, then the velocities of propagation, refraction, absorption, and rotation of the plane of polarization will also be variable and the amplitude of variation will depend on N , dN/ds , H_e , dH_e/ds , and f if s is the path. The effect of H_e and dH_e/ds on fading is probably only secondary. Probably owing to the irregularities of the ionic distribution in the layer, the wave front, soon after entering the layer, develops irregularities which become more and more pronounced as the wave goes on. The irregularities can be obtained by a Huygen construction at any point. In the neighborhood of a receiving antenna we can imagine regions in which the wave front is convex and regions where it is concave. Hence at certain portions of the wave front energy will be scattered, while at other parts it will be concentrated and the e.m.f. induced in the antenna will be very sensitive to changes in the ionic distribution along all the paths ds of the elementary rays contributing to the effect at the receiver.

According to experiments by Hollingworth, the downcoming waves longer than 10,000 m are usually plane polarized. The direction of the plane is approximately constant during the day but during sunset and sunrise it varies in a manner depending upon the distance between the transmitter and the receiver. At some distances the plane is turned in one direction and at other distances it is turned in the opposite direction.

For waves of 400 m wave-length at distances of 100 miles, the downcoming components are circularly polarized, which means that both the electric and magnetic vectors have a constant amplitude but rotate synchronously in the direction of rotation depending on the direction of the earth's magnetic field. A left-handed rotation is found in all parts of the Northern Hemisphere.

✓ For very short waves, 15 and 50 m, T. L. Eckersley finds the downcoming waves to be almost plane polarized, the plane rotating slowly with a period of a few seconds which should produce fading when a vertical or a horizontal aerial is used for receiving. Owing to the probable irregularities in the wave front at the receiver, it is evident that time variations in the ionic contribution should be very marked for short waves.¹ ✓ But single fading seems to be due to a change in the intensity of the downcoming waves rather than to a change of phase with respect to the ground wave.

✓ For waves of the broadcast range, similar rotations of the plane of polarization of the downcoming waves were found, according to experiments carried on by T. Parkinson² of the Bureau of Standards, and seem to be the cause of much fading. This is especially pronounced during the sunset period. At other times fading can occur at 1-min intervals. (The periodicity of fading is, of course, irregular.) ✓ Fading caused by interference between direct (surface and normal space waves of the Sommerfeld type) and indirect waves seems to occur only for receiving stations sufficiently near to produce appreciable direct waves. The night-time field intensity is then usually less than the daytime intensity because of the constant direct wave. The out-of-phase indirect wave often partially and sometimes completely neutralizes the effect of the direct wave, even for short distances. Fading due to a fluctuating height of the ionized layer has not been found, but evidence of refraction of the indirect wave from a rising layer is found in the fact that the received field intensity in a frame antenna at minimum position starts at zero in daylight and gradually increases during sunset.

¹ For long waves, the region of the medium comparable in dimension to a wave length has to undergo a very great change dN/ds before it can affect the field strength at the receiver.

² *Proc. I.R.E.*, 17, 1042, 1929.

For waves of 400 m wave length and a distance of 80 miles, the apparent height¹ of the ionized layer changes during the night from 90 km at sunset to about 130 km at 1 hr before sunrise. At times during the winter months, heights as high as 300 km and more have been measured. One method of determining the apparent height (method with interference fringes) often gives two sets of fringes, one corresponding to a height of about 100 km and the other about 250 km. Hence there must be two regions in the layer where the ionization density tends to become a maximum after several hours of darkness. The lower maximum can transmit an incident wave downward to the receiver. During the middle of the day, a third layer less than 10 km high can exist (probably the Lindemann-Dobson layer). It has, however, little refracting power and causes only attenuation.

Returning to the theoretical speculations, it may be said that, for waves longer than 1 km, reflection practically takes place during day and night. For waves between 100 and 1000 m, refractions in the layer are possible during the day and especially at night since during daytime a very pronounced absorption occurs. Waves between 15 and 100 m are refracted during the day and night but only during the day does absorption play a part for longer waves of this range. Very short waves below 20 m cannot return again to earth during the night but refract back to earth with appreciable absorption during daylight hours. Waves much below 15 m ($1\frac{1}{2}$ to 3 m) behave like light rays and travel, it might be said, in straight lines. The distances can be increased only by placing the small dipole sender on high towers.² Such waves, of course, can never extend to very long distances (at present about 50 to 100 km maximum) but, nevertheless, seem to have a promising future because of the beam and shadow effects which can be utilized to great advantage in certain kinds of work.

152. Long-time-interval Echo Effects.³—It has been observed that within the range of short waves a definite signal which has been given off at a transmitter repeats itself several times at a receiving station. Such echo effects have been reported by Taylor and Young, Hoag and Andrew, Quack and Moegel; they correspond to 0.005- to 0.08-sec

¹ Apparent height is somewhat higher than the actual height of the layer. For details, see "High Frequency Measurements," McGraw-Hill Book Company, Inc., New York, 1933, pp. 411-417.

² For details, see p. 362.

³ STOERMER, C., *L'onde élec.*, **7**, 531-533, 1928; *Compt. rend.*, **187**, November, 1928; *Nature* (London), Nov. 3, 1928; H. S. J. JELSTRUP, *L'onde élec.*, **7**, 538-540, 1928; B. VAN DER POL, *L'onde élec.*, **7**, 534-537, December, 1928; Echos von Hertzian Wellen (Echoes of Hertzian Waves), editorial, *E.N.T.*, **5**, 488, December, 1928; J. B. HOAG, and V. J. ANDREW, *Proc. I.R.E.*, **16**, 1368-1374, October, 1928; L. C. VERMAN, S. T. CHAR, ALJAB MOHAMMED, *Proc. I.R.E.*, **22**, 906-922, 1934.

intervals and seem to be due to a layer about 1500 km above the earth, from the polar night-light zone or from the sunset-shadow wall.

C. Stoermer and J. Hals and Van der Pol have reported long-time-interval echo effects in which the echo arrived as much as 3 to 15 sec. after the direct signal was received for a wave length of 31.4 m. Echoes have also been heard even after 30 sec. Direct layer reflection could occur only if it were at an immense distance from the earth—for instance, as far as to the moon.¹ This means that the echoes must have passed through a distance of from 1 to 5×10^6 km. For this reason, some writers have claimed that the wave experiences multiple reflections between the ionized layer and the earth—so-called round-the-world

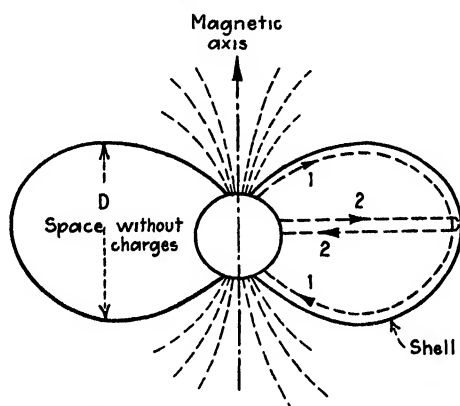


FIG. 231.—The C. Stoermer electron shells in the universe.

signals. Stoermer applies his theory of the Aurora Borealis² and assumes reflections or refractions on the electron envelope of empty pockets of very great dimensions. The pockets are of oval shape as indicated in Fig. 231 with the smallest width

$$D = (\sqrt{2} - 1) \sqrt{\frac{qM}{mv}} \text{ cm} \quad (71)$$

in which the magnetic moment of the earth $M = 8.4 \times 10^{25}$, m is the mass and q the charge of the particles, and certain initial velocities are represented by v in centimeters per second. The origin of these immense empty pockets surrounded by electron shells may be due to electrons which are shot off from the sun and travel through very great distances. Some of them reach the earth and are deflected by its magnetic field. The ovals are tangent to the magnetic axis passing through the center of the earth. Some rays either pass directly through the ionized layer

¹ Moon to earth 384×10^3 km; sun to earth 150×10^6 km.

² STOERMER, C., *Arch. sci. phys. nat.*, Genf, 1907.

or are so refracted that they curve away from the earth. After passing through the ionized layer, they pass into the empty pockets and either undergo reflection at the inside of the ionized oval or refract back again to earth. According to Table XVII, if it is assumed that an electromagnetic wave passes along path 1, that is, along the electron shell, then

TABLE XVII

Kind of particles	mv/q	D , km	T_1 , sec	T_2 , sec
Cathode rays.....	About 300	2.2×10^6	22	15
β rays.....	Up to 4000	6×10^5	6	4
α rays.....	300 000	7×10^4	0.7	0.5

T_1 is the interval between the main signal and echo. For path 2, we have the time interval T_2 . The echo interval is calculated by multiplying the distance by 2 and dividing by the velocity of light.

According to Eqs. (17) and (20) and Fig. 223, it is evident that, although the Stoermer explanation gives reasonable values, the long time intervals can also be explained by means of the immense phase velocities which can occur in the layer. The group velocity c'' with which the echo arrives is then very small and can easily correspond to such time intervals as were noted in the Stoermer-Hals experiments.

If a "moon echo" of radio signals could be established, it might be used by astronomers to gain better pictures of the moon's somewhat erratic travel path.

As far as wave propagations through ionized layers are concerned, there should be an ample field not only for the radio engineer but also for the physicist since it seems that from so many strange reception phenomena we could, by means of experimental data and theoretical speculation, also enrich other applied fields of physics!

CHAPTER XI

LINES OF LONG AND SHORT ELECTRICAL LENGTH WITH SPECIAL REFERENCE TO ANTENNA PROBLEMS¹

High-frequency currents are often conducted either along single or along double lines. Single-wire and Lecher-wire feeds for Hertzian aerials are representative. For aerials operating with short wave lengths a concentric line feed is often advantageous to Lecher-wire (parallel-wire) feed since for practical dimensions the characteristic impedance can be made as low as 10 to 150 Ω , while for the Lecher-wire feed, it would be in the range from about 400 to 750 ohms. Twisted cable feed is also used. In telephonic multichannel communication, systems with supersonic carrier frequencies are also often used. Carrier currents of supersonic frequency are likewise used when radio programs are transmitted directly over power lines. Treating certain aerial problems like problems in transmission lines gives a means for accounting, to a fair degree of approximation, for wave distributions and possible natural frequencies.

153. Formation of Progressive and Standing Waves along an Electrical Line and Impedance at the Generator End.—When a high-frequency e.m.f. which follows a sine law is impressed on a line, a considerable portion of the wave length is usually developed along the line. The effective values of voltage and current have different values along the line. Points for which the effective voltage is a minimum may be regarded as pseudonodes² since the prevailing voltage is just sufficient to supply the power for the conductor loss, that is, sufficient to keep the line in a state of oscillation.

The following constants hold for the high-frequency two-wire system (go and return) as well as for the long horizontal antenna. For the former, the following constants belong to the section mentioned including the go-and-return conductor (Fig. 232).

¹ For other details, see *Elektrotech. u. Maschinenbau*, Heft **26**, **34**, **37**, **45**, 1920; *Bur. Standards, Sci. Paper* 491, 1924; *Proc. I.R.E.*, **8**, 424, 1920. E. J. Sterba and C. B. Feldman, *Proc. I.R.E.* **20**, 1163, 1932; W. C. Tinus, *Electronics*, **8**, 239, 1935.

² If the voltage or current distribution is represented in a plane (two coordinates only), it is not possible to show the pseudonodes. But if the wave diagram is represented in space (three coordinates), then the wave winds around the line as it passes on and the pseudonodes correspond to points where it curves closest to the line of reference.

$r^{(\text{ohm})}$ resistance per unit length (centimeter), apparent (static) value for uniform current distribution

$L^{(\text{henry})}$ inductance per centimeter of length for uniform current distribution.

$C^{(\text{farad})}$ capacity per centimeter of length for uniform voltage distribution.

$g^{(\text{mho})}$ leakage (or conductance) per centimeter of length for uniform voltage distribution.

$E^{(\text{volt})}$ maximum value of the voltage at any distance x from the distribution end of the wires (is a complex function of x).

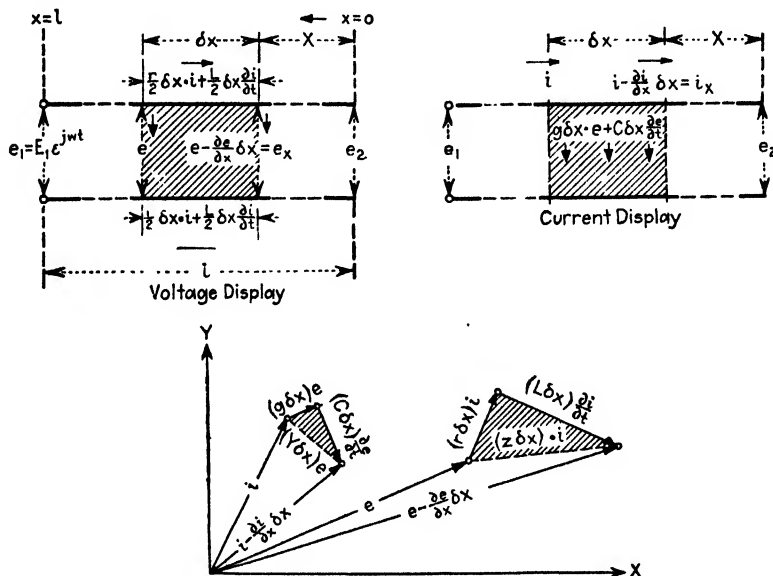


FIG. 232.—Vector representations of Eqs. 1 and 2.

E_1 maximum value at the input.

E_2 maximum value at the end of the wires.

e instantaneous value of voltage, the real part $E e^{j\omega t} = \mathcal{E}$ where \mathcal{E} is the vector $I^{(\text{amp})}$ maximum value of current at any place x .

I_1 current at input.

I_2 current at output.

i instantaneous value of current; the real part of $I e^{j\omega t} = \mathcal{I}$.

$z^{(\text{ohm})}$ impedance $r + j\omega L$ per centimeter length.

$y^{(\text{mho})}$ admittance $(g + j\omega C)$ per centimeter length across the line.

l geometric length of the line.

$\Omega = nl$ electric length of the line.

$Z_0 = \sqrt{z/y}$ surge impedance of the line.

$n = \alpha + j\beta = \sqrt{zy}$ generalized angular velocity, also known as "propagation constant" in the case of lines.

α space = attenuation constant.

β wave = length constant.

Let dx be a small section of the parallel-wire system shown in Fig. 232. The distance is first measured from the right toward the source of the e.m.f. $E_1 e^{j\omega t}$. The voltage drop per unit length $[ri + L(\partial i/\partial t)]$ is equal to the decrease $\partial e/\partial x$ of the voltage; that is,

$$\frac{\partial e}{\partial x} = ri + L \frac{\partial i}{\partial t} \quad (1)$$

and the loss of current per unit length $[ge + C(\partial e/\partial t)]$ must be equal to the decrease $\partial i/\partial x$; hence

$$\frac{\partial i}{\partial x} = ge + C \frac{\partial e}{\partial t} \quad (2)$$

The particular solution of Eqs. (1) and (2) of interest here is that for which both e and i are simple harmonic functions of the time. The instantaneous potential difference e is the real part of $Ee^{j\omega t}$, and the current i the real part of $Ie^{j\omega t}$, where E and I are complex functions of x . The corresponding vector equations of (1) and (2) which can also be directly read from the vector diagram of Fig. 232 are

$$\left. \begin{aligned} \frac{\partial E}{\partial x} &= zI \\ \frac{\partial I}{\partial x} &= yE \end{aligned} \right\} \quad (3)$$

for $z = r + j\omega L$ and $y = g + j\omega C$. A partial differentiation of (3) with respect to x leads to

$$\left. \begin{aligned} \frac{\partial^2 E}{\partial x^2} &= n^2 E \\ \frac{\partial^2 I}{\partial x^2} &= n^2 I \end{aligned} \right\} \quad \text{and} \quad n = \sqrt{yz} = \alpha \pm j\beta \quad (4)$$

The quantity n is known as the propagation constant and the value $\sqrt{z/y} = Z_0$ as the surge impedance of the line. It is also known as the characteristic impedance. The expression

$$E = ae^{nx} + be^{-nx} \quad (5)$$

is the solution of the first equation of (4) and, by means of the first equation of (3) and Eq. (5), the solution of the current is

$$I = \frac{ae^{nx} - be^{-nx}}{Z_0} \quad (6)$$

The quantity n is generally complex, and both relations show that the potential as well as the current at any point of the line is, in general, caused by wavelike disturbances moving in opposite directions. Suppose the parallel-wire system is bridged at the end with an indicating instrument of impedance Z_1 . Then there will be at that point, for which $x = 0$, a voltage $E = E_1$ and a current $I = I_1$ where $e_1 = E_1 e^{j\omega t}$ and $i_1 = I_1 e^{j\omega t}$. This, when used in (5) and (6), gives the constants

$$a = \frac{E_1 + Z_0 I_1}{2} \quad b = \frac{E_1 - Z_0 I_1}{2}$$

The maximum values of voltage and current at any point, therefore, are

$$\left. \begin{aligned} E &= \frac{1}{2} \{ E_1 [e^{nx} + e^{-nx}] + Z_0 I_1 [e^{nx} - e^{-nx}] \} = E_1 \cosh nx + Z_0 I_1 \sinh nx \\ I &= \frac{1}{2} \left\{ I_1 [e^{nx} + e^{-nx}] + \frac{E_1}{Z_0} [e^{nx} - e^{-nx}] \right\} = I_1 \cosh nx + \frac{E_1}{Z_0} \sinh nx \end{aligned} \right\} \quad (7)$$

Therefore, if a parallel-wire system is connected at the far end to a load impedance Z_2 , we have, for the voltage at the input end of the line of length $x = l$,

$$E_1 = E_2 \cosh nl + Z_0 I_2 \sinh nl$$

At the output end we have the current I_2 and $Z_2 = E_2/I_2$. Hence the driving impedance with respect to generator voltage and output current is

$$\frac{E_1}{I_2} = Z_2 \cosh nl + Z_0 \sinh nl$$

This is a very important relation when a line is used for feeding power into aerial systems, where it is imperative that the load shall not change the relationship of the driving impedance. If the line is such that the attenuation α can be neglected, we have for this impedance

$$\frac{E_1}{I_2} = Z_2 \cos \beta l + jZ_0 \sin \beta l$$

and when the length l is equal to a quarter wave length (etc.)

$$\frac{E_1}{I_2} = jZ_0$$

which means that the load current I_2 has a *constant* relation to the generator voltage E_1 . In such cases it is often desirable that generator and load impedance be properly related. This can readily be done with an impedance-matching device which in case of high-frequency currents may be a simple air-core transformer for which the Q value (also known as $\omega L/R$ ratio) of primary and secondary turns is large compared with the load impedance, and for which the coupling coefficient is high. The turns ratio of the transformer is then equal to the square root of the ratio of the impedances to be matched.

For the instrument disconnected (line open, that is, $I_2 = 0$),

$$\left. \begin{aligned} E &= E_2 \cosh nx \\ I &= \frac{E_2}{Z_0} \sinh nx \end{aligned} \right\} \quad \text{hence} \quad Z = \frac{E}{I} = Z_0 \coth nx \quad (8)$$

For the line short-circuited ($E_2 = 0$),

$$\left. \begin{aligned} E &= Z_0 I_2 \sinh nx \\ I &= I_2 \cosh nx \end{aligned} \right\} \quad \text{hence} \quad Z = Z_0 \tanh nx \quad (9)$$

where I_2 denotes the maximum value of the current, and E and I are the maximum values of voltage and current at any distance x from the end.

From (8) and (9), we note that the impedances Z are either *hyperbolic* cotangent or tangent functions according to whether the line is open or short-circuited at the end. Hence at the input side ($x = l^{(\text{ant})}$) we have $E = E_1$ and $I = I_1$ and $Z = Z_1$, and for the line open at the free end,

$$Z_1 = Z_0 \coth \Omega \quad (10)$$

for the electrical length $\Omega = nl$. This denotes the *impedance* with which either an open-ended parallel-wire system or a single-wire antenna acts *against the generator* and is a most important relation for studying the conditions along such lines.

Calling Z_{op} and Z_{sc} the open and the short-circuited line impedance experienced at the beginning of the line, we have

$$\left. \begin{aligned} Z_{op} &= Z_0 \coth \Omega \\ Z_{sc} &= Z_0 \tanh \Omega \end{aligned} \right\}$$

From which

$$\frac{Z_{op} + Z_{sc}}{Z_{op} - Z_{sc}} = \frac{\coth \Omega + \tanh \Omega}{\coth \Omega - \tanh \Omega} = \frac{\cosh^2 \Omega + \sinh^2 \Omega}{\cosh^2 \Omega - \sinh^2 \Omega} = \cosh 2\Omega$$

Hence the electrical length $\Omega = nl = (\alpha + j\beta)l$ is given by

$$\Omega = \frac{1}{2} \cosh^{-1} \frac{Z_{op} + Z_{sc}}{Z_{op} - Z_{sc}} = \frac{1}{2} \cosh^{-1} P$$

where $P \equiv p|\varphi$ and, since $P > 1$, we have the expression

$$\cosh^{-1} P = \log_e 2P - \frac{1}{2} \cdot \frac{1}{2} \left[\frac{1}{P} \right]^2 - \frac{1}{2} \cdot \frac{3}{4} \cdot \frac{1}{4} \left[\frac{1}{P} \right]^4 - \frac{1}{2} \cdot \frac{3}{4} \cdot \frac{5}{6} \cdot \frac{1}{6} \left[\frac{1}{P} \right]^6 - \dots$$

and

$$\left. \begin{aligned} \alpha l &= \frac{1}{2} \left[\log_e 2p - \frac{\cos 2\varphi}{4p^2} - \frac{3 \cos 4\varphi}{32p^4} - \dots \right] \\ \beta l &= \frac{1}{2} \left[2\pi q + \varphi + \frac{\sin 2\varphi}{4p^2} + \frac{3 \sin 4\varphi}{32p^4} + \dots \right] \end{aligned} \right\} \quad (11)$$

if q is an integer. The approximations of (11) for large values of Ω are

$$\left. \begin{aligned} \alpha l &= \frac{1}{2} \log_e 2p \\ \beta l &= q\pi + \frac{\varphi}{2} \end{aligned} \right\} \quad (12)$$

For this case, we also have the approximation

$$Z_0 = \frac{Z_{op} + Z_{sc}}{2} \quad (13)$$

since

$$\begin{aligned} Z_{op} + Z_{sc} &= Z_0[\cotanh \Omega + \tanh \Omega] \\ &= 2Z_0 \frac{\epsilon^{2\Omega} + \epsilon^{-2\Omega}}{\epsilon^{2\Omega} - \epsilon^{-2\Omega}} = 2Z_0[1 + \epsilon^{-4\Omega}]\{1 - \epsilon^{-4\Omega}\}^{-1} \\ &= 2Z_0[1 + 2\epsilon^{-4\Omega} + 4\epsilon^{-8\Omega} + \dots] \\ &\cong 2Z_0[1 + 2\epsilon^{-4\Omega}] \end{aligned}$$

Formulas (12) and (13) are convenient approximations when determinations have to be made on certain lines and filters.

If R_1 and R_2 are the resistances measured for the open and short-circuited condition and X_1 and X_2 the corresponding reactances, we have

$$\frac{p}{\varphi} = \frac{Z_{op} + Z_{sc}}{Z_{op} - Z_{sc}} = \frac{[R_1 + R_2] + j[X_1 + X_2]}{[R_1 - R_2] + j[X_1 - X_2]}$$

Putting $R_a = R_1 + R_2$; $X_1 + X_2 = X_a$; $R_1 - R_2 = R_b$; and

$$X_1 - X_2 = X_b,$$

we have

$$p^2 = \frac{R_a^2 + X_a^2}{R_b^2 + X_b^2} \quad (14)$$

and the attenuation α , the wave-length constant β for unit length and surge impedance Z_0 , according to Eq. (12), can be computed from

$$\left. \begin{aligned} \alpha &\cong 0.25 \log_e 4p^2 \cong 576 \times 10^{-3} \log_{10} 4p^2 \text{ nepers} \\ &\cong 5 \log_{10} 4p^2 \text{ decibels} \\ \beta &\cong \left[\pi q + \frac{\varphi_a - \varphi_b}{2} \right] \text{ radians} \\ Z_0 &\cong \frac{1}{2}[Z_{op} + Z_c] \cong (0.5\sqrt{R_a^2 + X_a^2})/\varphi_a \end{aligned} \right\} \quad (15)$$

where q is a suitable integer and

$$\left. \begin{aligned} \varphi_a &= \tan^{-1} \frac{X_1 + X_2}{R_1 + R_2} \\ \varphi_b &= \tan^{-1} \frac{X_1 - X_2}{R_1 - R_2} \end{aligned} \right\} \quad (16)$$

154. Time and Space Functions, Velocity of Propagation, and Preparation Constant.—If the end of the parallel-wire system is bridged with a wire which has practically only low resistance, the voltage and current are in phase and the complete solution (space and time functions) becomes

$$\left. \begin{aligned} E &= \frac{\epsilon^{j\omega t}}{2} \{ E_2[\epsilon^{nz} + \epsilon^{-nz}] + Z_0 I_2[\epsilon^{nz} - \epsilon^{-nz}] \} \\ I &= \frac{\epsilon^{j\omega t}}{2} \left\{ I_2[\epsilon^{nz} + \epsilon^{-nz}] + \frac{E_2}{Z_0}[\epsilon^{nz} - \epsilon^{-nz}] \right\} \end{aligned} \right\} \quad (17)$$

which for the short-circuited line ($E_2 = 0$) yields

$$\left. \begin{aligned} E &= \frac{Z_0 I_2}{2} \{ e^{[\alpha x + j(\omega t + \beta x)]} - e^{[-\alpha x + j(\omega t - \beta x)]} \} \\ I &= \frac{I_2}{2} \{ e^{[\alpha x + j(\omega t + \beta x)]} + e^{[-\alpha x + j(\omega t - \beta x)]} \} \end{aligned} \right\} \quad (18)$$

which shows that at each point the amplitude varies harmonically with the time, and that similar space distributions exist along the line. The phase of the current or voltage is either ahead of or behind the state at the end of the line by an amount βx . Hence at points for which x differs¹ by $2\pi/\beta = \lambda$, the same phases exist at the same time. The distance corresponds to the time interval of $1/f$ sec, if the current feeding into the line performs f cycles/sec. The velocity of propagation is then given by

$$v = \frac{\lambda}{1/f} = \frac{\omega}{\beta} = c[1 - \Delta]$$

This velocity differs by a small amount Δc from the exact recognized value $c = 2.9982 \times 10^{10}$ cm/sec. Grouping the real and imaginary terms of Eq. (4), we have for the propagation constant

$$\begin{aligned} n = \alpha + j\beta &= \sqrt{yz} = \sqrt{[g + j\omega C][r + j\omega L]} \\ &= \sqrt{\frac{1}{2}[yz + rg - \omega^2 CL]} + \\ &\quad j\sqrt{\frac{1}{2}[yz - rg + \omega^2 CL]} \end{aligned} \quad (19)$$

The rigorous formula for the phase velocity becomes

$$v = \frac{\omega}{\sqrt{\frac{1}{2}[yz - rg + \omega^2 CL]}} \quad (20)$$

If we bear in mind that the leakance g across the line or from a single antenna wire is negligible, we obtain for the propagation constant n the solution

$$n = \sqrt{yz} = \sqrt{j\omega C[r + j\omega L]} = j\omega\sqrt{CL}\sqrt{1 + \frac{r}{j\omega L}} \cong j\omega\sqrt{CL}\left[1 + \frac{r}{2j\omega L}\right]$$

since $r/(\omega L)$ is a small quantity and $[r/(\omega L)]^2$, etc., can be neglected. Hence

$$\begin{aligned} n &= \frac{r}{2}\sqrt{\frac{C}{L}} + j\omega\sqrt{CL} \\ &= \alpha + j\beta \end{aligned} \quad (21)$$

and the velocity

$$v = \frac{\omega}{\beta} = \frac{1}{\sqrt{CL}} \cong c = 3 \times 10^{10} \text{ cm/sec} \quad (22)$$

¹ Convenient points are every other current antinode.

where C and L are the high-frequency capacitance and inductance per centimeter length of the line.

If the ordinary formulas for C and L for wires of $d_{(\text{cm})}$ diameter and spacing $a_{(\text{cm})}$ between centers are used, we have

$$\left. \begin{aligned} C &= \frac{1}{4 \times 9 \times 10^{11} \log_e \left[\frac{a + \sqrt{a^2 - d^2}}{d} \right]} \text{ farads} = \frac{1}{4c^2 \log_e \frac{1}{b}} \text{ sec}^2/\text{cm} \\ L &= \left[4 \log_e \frac{2a}{d} + 1 \right] 10^{-9} \text{ henries} = \left[4 \log_e \frac{2a}{d} + L_i \right] \text{ cm} \end{aligned} \right\} \quad (23)$$

where the expressions to the right are given in e.m.c.g.s. units and

$$b = \frac{d/a}{1 + \sqrt{1 - (d/a)^2}} \quad (24)$$

$c = 2.9982 \times 10^{10}$ cm/sec and L_i denotes that portion of the inductance which may be considered as due to the internal field of the wires. The capacitance formula holds even for the highest frequencies used in radio. The inductance formula holds for commercial alternating currents, that is, for lower frequencies where the current is uniformly distributed over the cross section of the wire. Since practically a cylindrical current field exists for high-frequency currents, the inductance L_i due to the flux within the conductors can be neglected, which leads to the approximate formula for higher frequencies

$$L \cong 4 \times 10^{-9} \log_e \frac{2a}{d} \text{ henries} \quad (25)$$

If the spacing between the wires is not chosen too small, so that the diameter d of the wires is small compared with the spacing a , the capacitance formula simplifies to

$$C \cong \frac{1}{4 \times 10^{-9} c^2 \log_e (2a/d)} \text{ farads} \quad (26)$$

With such assumptions we obtain from (22), (25), and (26) the phase velocity $v = c$. For very accurate work, however, it should be remembered that (25) is not accurate enough since the high-frequency inductance L is a function of the frequency, the resistance, and the dimensions of the wire system. According to C. Snow of the Bureau of Standards, the formula

$$\left. \begin{aligned} L^{(\text{cm})} &= 4 \log_e \frac{1}{b} + D \\ D &= \sqrt{\frac{r_0}{\omega[1 - (d/a)^2]}} \quad \text{and} \quad b = \frac{d/a}{1 + \sqrt{1 - (d/a)^2}} \end{aligned} \right\} \quad (27)$$

holds up to the highest frequencies used in radio. All units are in the e.m.c.g.s. system and r_0 denotes the direct-current resistance per centimeter length in centimeters per second.

The high-frequency resistance r per centimeter length of the parallel wires is

$$r = \sqrt{\frac{r_0 \omega}{1 - (d/a)^2}} \quad (28)$$

If the small quantity D in (27) were neglected, we should again obtain the result $v = c$, although the assumptions are somewhat different, since nothing needs to be omitted in the capacitance formula. By taking D into account, we find from the capacitance formulas of (23) and (27)

$$CL = \frac{D + 4 \log_e (1/b)}{4c^2 \log_e (1/b)}$$

Inserting this in (22) yields¹

$$v = c \sqrt{\frac{1}{1 + \frac{D}{4 \log_e (1/b)}}} = c \sqrt{\frac{1}{1 + 2\Delta}} \cong c[1 - \Delta] \quad (29)$$

for

$$\Delta = \frac{\sqrt{r_0}}{8 \log_e (1/b) \sqrt{\omega[1 - (d/a)^2]}} \quad (29a)$$

Introducing the high-frequency resistance r from (28) in the expression for Δ , we find, from (29),

$$v = c \left[1 - \frac{r}{8\omega \log_e (1/b)} \right] \quad (30)$$

or

$$\Delta \cong \frac{r}{2\omega L} \quad (31)$$

155. Current and Voltage Distribution along Lines and Antennas and Possible Modes.—Figure 233 gives the voltage and current distribution for the open-ended parallel-wire system for three successive modes. The upper representation shows how the potential difference V and current I change during the cycle at any place on a line of length $l = \lambda/4$. Figure 234 gives the case for a long horizontal antenna.

There are two ways for producing successive modes of predominating standing waves. One is to keep the frequency ($f = f_1$) constant and

¹ For details, see *Bur, Standards, Sci. Paper* 491 (Fig. 5), which shows, for instance, that the phase velocity v between 16×10^8 kc/sec and 34×10^8 kc varies from 2.99415×10^{10} to 2.99542×10^{10} cm/sec for a spacing $a = 4.2$ cm and copper wires of $d = 0.145$ cm diameter.

to choose the length l , as for the short-circuited double line of Fig. 235, equal to $\lambda/2$ or any other integral multiple of it. For each case, a decided maximum current is noted at the short-circuited end, and even very little shortening of the line decreases the reading considerably. The actual length l of the line becomes longer for the higher modes of stationary waves because a larger portion of the wave length due to the

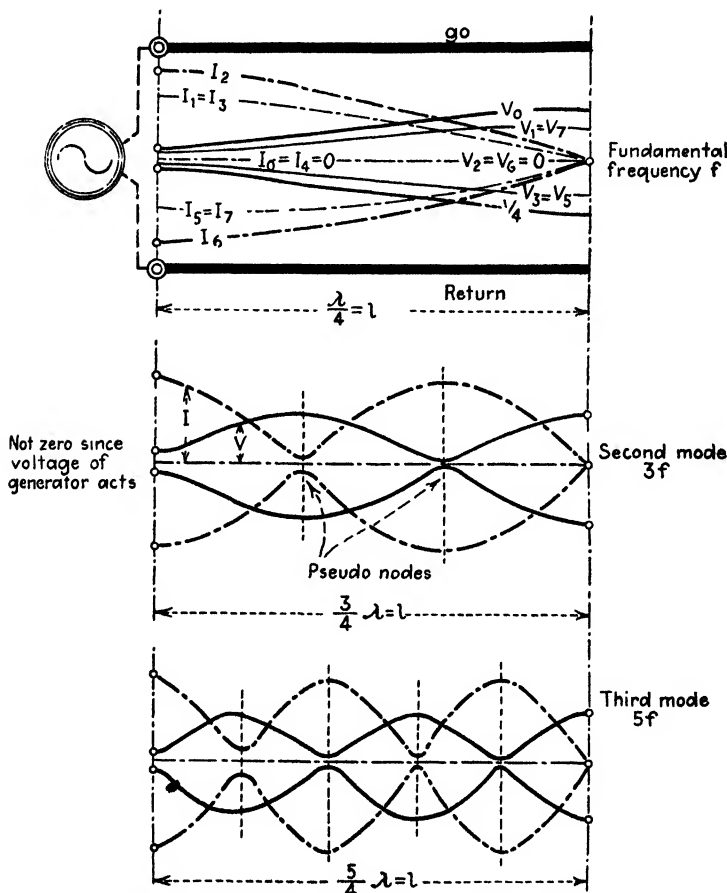


FIG. 233.—Wave development along an open-ended parallel-wire system.

impressed frequency f_1 is developed. The second way is to maintain the physical length fixed as in Fig. 236. The frequency $f = f_1$ of the exciting current is then changed to the values as indicated in this figure. Figure 237 shows the distribution on a vertical wire for which the standing waves are excited either at the ground side (for $\lambda/4, 3\lambda/4, 5\lambda/4$ etc., distributions) or at the mid-point in case of a free wire and for $l = \lambda/2$. For Franklin antennas, a beam effect is produced by properly exciting

the antenna, but the effect decreases beyond $l = \lambda/2$ since the phase reverses in the upper part of the vertical wire as is indicated in diagram *e*. But we can add one-half wave-length aerials (diagram *i*) by means of phasing coils (diagram *f*) or by exciting inphase distributions as shown in *g* and *h*. A parallel-wire system is used as lead-in in order to have feeders without appreciable antenna effects. The equations for the

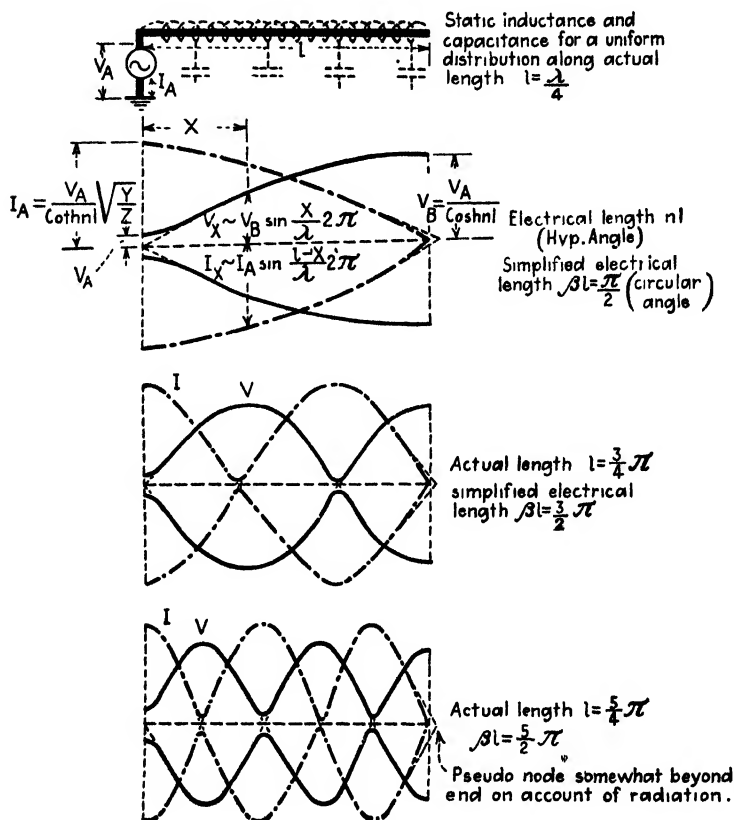


FIG. 234.—Wave development along a horizontal wire.

distribution for standing waves are given in (8) and (9). The electrical length $n x$ for the actual length l is $(\alpha + j\beta)x$ in which α can often be neglected for conductors which develop a considerable portion of the wave length. We can change the hyperbolic functions to circular functions since

$$\sinh j\beta x = j \sin \beta x; \quad \cosh j\beta x = \cos \beta x; \quad \tanh j\beta x = j \tan \beta x; \\ \cotanh j\beta x = -j \cotan \beta x$$

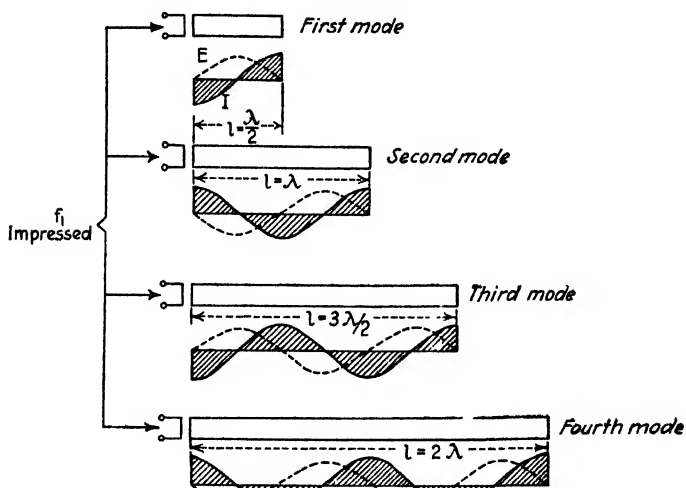


FIG. 235.—Modes of predominating standing waves with frequency f_1 of exciting current constant.

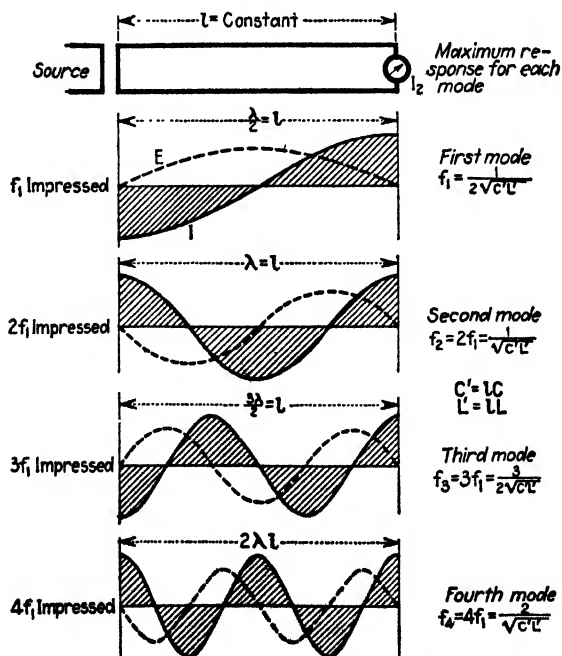


FIG. 236.—Modes of predominating standing waves with frequency adjusted to $f_1, 2f_1, 3f_1$, etc.

We have, therefore, for the open-ended parallel-wire system (Fig. 233) and the corresponding case of a grounded antenna with quarter-wave-length distributions (Figs. 234 and 237, *a*, *b*, *c*, and *d*), sinusoidal and cosinusoidal distributions as indicated. Whether the distribution follows a sine or a cosine law depends upon the point of reference. For instance, if the effective potential V_x at any place a distance x from the potential node is a sine function, we have $V_x = V \sin (2\pi x/\lambda)$ if V denotes the effective value at the potential loop. If we reckon x with respect to

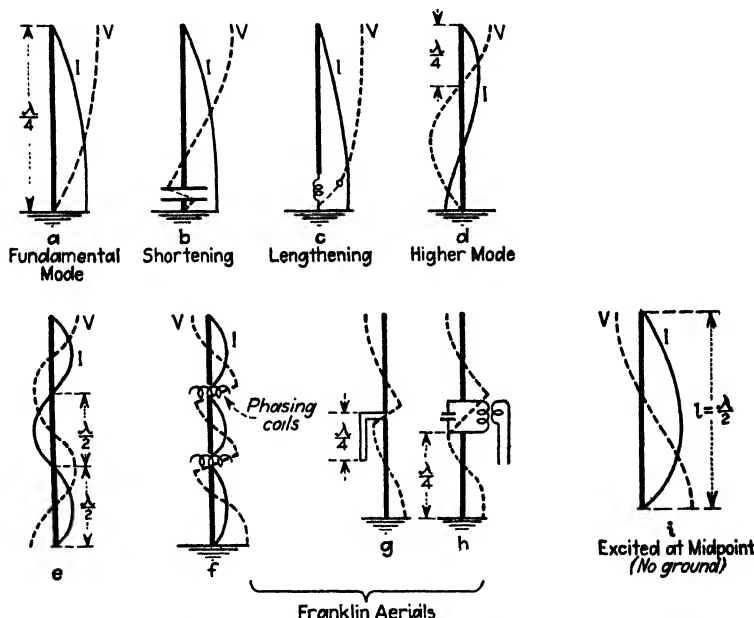


FIG. 237.—Potential (V) and current (I) distributions along aeriels.

the open end, that is, with respect to the potential loop, we have a cosine function.

According to (10), we have, for the impedance of the open-ended line and, with a good degree of approximation, also for an antenna which is excited at the ground side,

$$Z_1 = Z_0 \coth \Omega = \sqrt{\frac{z}{y}} \coth nl = \sqrt{\frac{z}{y}} \coth l\sqrt{yz}$$

But $z = r + j\omega L$ and $y = g + j\omega C$ and, by neglecting r in comparison with ωL and the g in comparison with ωC , the reactance $Z_1 = X_1$ experienced at the input side is

$$X_1 = -j\sqrt{\frac{L}{C}} \cotan \omega l\sqrt{CL} \quad (32)$$

The generator current I_1 at the beginning of the line is

$$I_1 = \frac{E_1}{X_1} = E_1 \sqrt{\frac{L}{C}} \tan \omega l \sqrt{CL} = E_1 \sqrt{\frac{L}{C}} \tan \omega \sqrt{C_A L_A} \quad (33)$$

if $lC = C_A$ and $lL = L_A$ denote the total static capacitance and inductance of the antenna or parallel-wire system, respectively, for uniform distribution along the length l cm. By means of (32) as well as (33), we can find the conditions for which natural oscillations occur since I_1 must become a maximum when X_1 vanishes. Hence the different possible modes occur for all values that make $\cotan \omega l \sqrt{CL} = 0$, that is, for¹

$$\omega l \sqrt{CL} = \frac{\omega l}{c} = \frac{2\pi f l}{c} = \frac{2\pi l}{\lambda}$$

equal to $\pi/2$, $3\pi/2$, $5\pi/2$, etc. But $2\pi l/\lambda = \pi/2$ gives $l = \lambda/4$ and $2\pi l/\lambda = 3\pi/2$ gives $l = 3\lambda/4$, etc. Hence the fundamental mode corresponds to a quarter-wave-length distribution and the possible modes are odd multiples of $\lambda/4$. Since for the fundamental mode $\lambda_1 = 4l$, we find for the fundamental frequency

$$f_1 = \frac{c}{\lambda_1} = \frac{c}{4l} = \frac{1}{4l\sqrt{CL}} = \frac{1}{4\sqrt{C_A L_A}} \quad (34)$$

in contrast to the effective antenna constants C_e and L_e which give

$$f_1 = \frac{1}{2\pi\sqrt{C_e L_e}} \quad (35)$$

For the second possible mode we find $f_2 = 3f_1$, for the third mode $f_3 = 5f_1$, and so on. By checking these results against the actual distribution, it will be found that they hold fairly well for the parallel-wire system and the long horizontal antenna which is not too close to ground. According to A. Meissner, we have, for ordinary antennas, the values of Table XVIII.

TABLE XVIII

Kind of Antenna	Fundamental Wave Length in Terms of the Actual Length l
Vertical wire.....	$\lambda = 4l$ to $4.1l$
Straight wire inclined to ground.....	$\lambda = 4.2l$
Horizontal wire 1 m above ground.....	$\lambda = 5l$
T antenna with small, flat top.....	$\lambda = 4.5l$ to $5l$
T antenna with wide, flat top.....	$\lambda = 5l$ to $7l$
T antenna (b = width of flat top and height $h = b/2$ to $b/3$).....	$\lambda = 9l$ to $10l$
Umbrella antenna according to the number of wires....	$\lambda = 6l$ to $8l$
Umbrella antenna with maximum number of wires....	$\lambda = 8l$ to $10l$

¹ From (22); $c = 1/\sqrt{CL}$.

For antennas with more branches, l denotes the longest current path to ground. The factor k in $\lambda = kl$ becomes larger the larger the ratio of antenna capacitance to antenna inductance, that is, the larger the top of the antenna. Such discrepancies may be expected since in reality the C and L per unit length cannot be the same everywhere even for a single vertical wire. In spite of this, the actual value of $k = 4$ to 4.1 for the vertical wire comes surprisingly close to the theoretical value 4.

For a more accurate¹ theory, C and L cannot be considered constant but as functions of the position, that is, functions of x . But the functions are chosen such that CL remains constant in order to fulfill the condition of constant phase velocity $v = 1/\sqrt{CL}$. The solution no longer is of the form given here but uses cylindrical harmonics with Bessel functions. The constancy of v is obtained by choosing

$$L = L_0 x^p \quad \text{and} \quad C = \frac{C_0}{x^p} \quad (36)$$

and (1) and (2) read, for ri and ge neglected,

$$\frac{\partial e}{\partial x} = L \frac{\partial i}{\partial t} \quad \text{and} \quad \frac{\partial i}{\partial x} = C \frac{\partial e}{\partial t}$$

Utilizing (36) gives the Bessel equation

$$\left. \begin{aligned} \frac{\partial^2 e}{\partial x^2} - \frac{p}{x} \frac{\partial e}{\partial x} &= C_0 L_0 \frac{\partial^2 e}{\partial t^2} \\ \frac{\partial^2 i}{\partial x^2} + \frac{p}{x} \frac{\partial i}{\partial x} &= C_0 L_0 \frac{\partial^2 i}{\partial t^2} \end{aligned} \right\} \quad (37)$$

which for $m = (p - 1)/2$ gives the following solution for the current:

$$i = \frac{I_m(qx)}{x^m} A + \frac{I_{-m}(qx)}{x^m} B \quad (38)$$

for

$$\left. \begin{aligned} \frac{I_m(qx)}{x^m} &= \frac{(q/2)^m}{0!m!} + \frac{(q/2)^{m+2}x^2}{1!(m+1)!} + \frac{(q/2)^{m+4}x^4}{2!(m+2)!} + \dots \\ \frac{I_{-m}(qx)}{x^m} &= \frac{(q/2)^{-m}x^{-m}}{0!(-m)!} + \frac{(q/2)^{-m+2}x^{-m+2}}{1!(-m+1)!} + \frac{(q/2)^{-m+4}x^{-m+4}}{2!(-m+2)!} + \dots \end{aligned} \right\} \quad (39)$$

Assuming a vertical wire of height l and $x = 0$ at the grounded end, we have $i = I$ for $x = 0$, and $i = 0$ for $x = l$. We find the constants

$$A = \frac{0!m!}{(q/2)^m} I \quad \text{and} \quad B = -\frac{I_m(ql)}{I_{-m}(ql)} A \dots \quad (40)$$

which, inserted in (38), give the final solution.

Moreover, the fact that the length of the line permits stationary waves does not necessarily mean that these waves are of much value.

¹ O. Heaviside, "Electromagnetic Theory," Vol. II, London, 1899, pp. 239, 240, 244, has given a solution for such a condition for the cable. J. Stone-Stone, *Elec. Rev.*, Oct. 15, 1904, has applied it to an oscillator; A. Press, *Proc. I.R.E.*, 6, 317, 1918, to a vertical antenna.

For instance, the distributions shown in Fig. 238 are correct. The current, however, is theoretically zero at the input side, that is, at a place where it should be a maximum in order to transfer much power into the line. The line then behaves practically like an infinite reactance against the source since, according to (32), for the simplified electrical length

$$\beta l = \frac{\omega}{v} l = \omega l \sqrt{CL} = \frac{2\pi}{\lambda} l$$

$$X_1 = \sqrt{\frac{L}{C}} \cotan \frac{2\pi}{\lambda} l = \sqrt{\frac{L}{C}} \cotan 2\pi = \infty$$

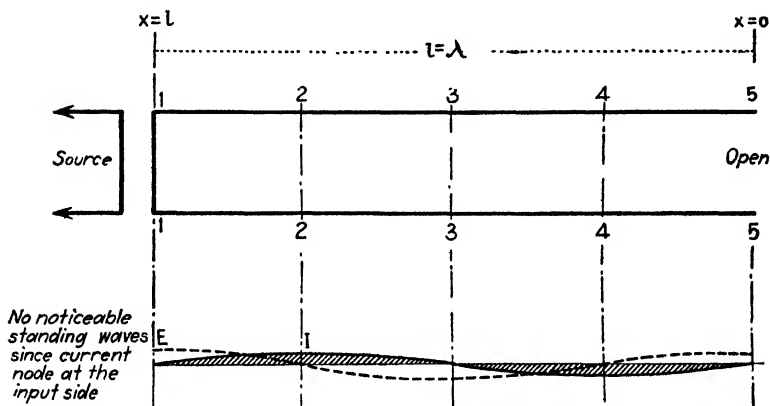


FIG. 238.—Full-wave-length distribution for the open-ended double line.

But if the line is short-circuited either at 5-5 or 3-3, very strong oscillations are set up for this condition and we have, according to (9),

$$X_1 = \sqrt{\frac{L}{C}} \tan \frac{2\pi}{\lambda} l = \sqrt{\frac{L}{C}} \tan 2\pi = 0$$

The *full-wave-length* distribution, however, can be greatly excited if the e.m.f. is induced at a place where a large current flow is possible.

The impedance offered by the open-ended line at the input end is, according to (8),

$$Z_1 = \sqrt{\frac{z}{y}} \cotanh nl = \sqrt{\frac{z}{y}} \left[\frac{1}{nl} + \frac{1}{3} nl + \dots \right]$$

When, for instance, an *audio* current excites a high-frequency antenna, it is sufficiently accurate to retain the first two terms of the series only, and we find, for $n = \sqrt{yz}$,

$$Z_1 = \frac{1}{yl} + \frac{zl}{3} = \frac{1}{y_A} + \frac{z_A}{3} \quad (41)$$

where y_A is the total admittance across the line and z_A the total impedance along it. This expression shows that, if a radio aerial is excited at an audio frequency, the voltage distribution is essentially constant but the current decreases linearly toward the open end. In Eq. (41) we have $y_A = g_A + j\omega C_A$ and $z_A = r_A + j\omega L_A$. Hence the measurement of these quantities with *audio-frequency* currents is a way of determining the static value of the total line or antenna capacitance C_A and the fractions $L_A/3$ and $r_A/3$ of the total static inductance L_A and resistance r_A .

156. Effective Antenna Reactance for the Loaded and Unloaded Antenna.—For the vertical antenna, the theoretically possible natural modes correspond fairly well with the actual case and also for the long horizontal antenna which is not too close to ground. The reactance formula of Eq. (32) can, therefore, be used for finding the condition of such antennas. For other antennas, the formula holds only approximately. The customary ways of exciting an antenna are (1) by having a loading coil at the input side, (2) a loading condenser, (3) a condenser and a coil in series, and (4) a coil and a condenser in parallel.

Case A.—When a high-frequency e.m.f. is impressed at the ground side and the effective reactance is due to the antenna only, according to (32).

$$X_e = -j\sqrt{\frac{L}{C}} \cotan \beta l = -j\sqrt{\frac{L}{C}} \cotan \Omega \quad (42)$$

where $\Omega = \beta l = \omega l \sqrt{CL} = 2\pi l/\lambda$ denotes the simplified electrical length of the antenna of actual length l cm. The imaginary unit j indicates a reactance and has no value in the numerical calculation. The reactance follows a cotangent law and a graphical solution ($\cotan \Omega$ plotted against Ω) will show that the fundamental mode gives a frequency determined by the electrical length $\Omega_1 = \pi/2$, the second mode occurs when $\Omega_2 = 3\pi/2$, and so on, and that, for $\Omega = \pi, 2\pi, 3\pi$, etc., no current could be forced into the antenna when excited at the ground side.¹

Case B.—When a loading inductance L_0 is inserted at the ground side, the natural frequency of the system is lowered since, for the unloaded antenna with the effective constants C_e and L_e , the fundamental frequency

$$f_1 = \frac{1}{2\pi\sqrt{C_e L_e}} \quad (43)$$

but, for coil loading² at the base,

$$f_1' = \frac{1}{2\pi\sqrt{C_e'[L_e' + L_0]}} \quad (44)$$

¹ For other details see "High Frequency Measurements," McGraw-Hill Book Company, Inc., New York, 1933, pp. 395-396.

² The effective antenna constants C_e , L_e , and R_e change with the loading to C_e' , L_e' , and R_e' .

This can also be seen from the formula for the effective reactance

$$X_e' = j\omega L_0 - j\sqrt{\frac{L}{C}} \cotan \Omega = j\left[\omega L_0 - \sqrt{\frac{L}{C}} \cotan \Omega\right] \\ = j\sqrt{\frac{L_A}{C_A}} \left\{ \frac{L_0}{C_A} \Omega - \cotan \Omega \right\}$$

which can likewise be solved graphically.¹

For the fundamental and all higher modes, the ratio of the load inductance to the static antenna inductance is

$$\frac{L_0}{L_A} = \frac{\cotan \Omega_1'}{\Omega_1'} = \frac{\cotan \Omega_2'}{\Omega_2'} = \frac{\cotan \Omega_3'}{\Omega_3'} = \tan \theta \quad (45)$$

since $X_e = 0$ and L_0 denotes another loading inductance for each mode. The static antenna inductance can therefore be calculated from either the electric length $\Omega' = \beta'l$ or the corresponding wave length λ' . For the fundamental mode, we find

$$L_A = L_0 \Omega_1' \tan \Omega_1' = L_0 \frac{2\pi}{\lambda_1'} l \tan \frac{2\pi}{\lambda_1'} l \quad (46)$$

The frequency in cycles per second for the fundamental mode becomes

$$f_1' = \frac{\Omega_1'}{2\pi\sqrt{C_A^{(\text{farad})} \cdot L_A^{(\text{henry})}}} \quad (47)$$

The natural modes occur for $X_e' = 0$, that is, for

$$\cotan \Omega = \frac{L_0}{L_A} \Omega = \Omega \tan \theta \quad (48)$$

which is a transcendental equation. The successive solutions Ω_1' , Ω_2' , Ω_3' , Ω_4' , etc., for the possible modes is therefore obtained by plotting the cotangent curves

$$y = \cotan \Omega$$

and the inclined line

$$y = \frac{L_0}{L_A} \Omega = \frac{L_0}{L_A} \omega \sqrt{C_A L_A} = \omega L_0 \sqrt{\frac{C_A}{L_A}} = \frac{\omega L_0}{Z_0}$$

Hence if we determine the intersections of the cotangent curves with the inclined line (at the angle θ), we note that the electrical lengths Ω_1' , Ω_2' , Ω_3' , Ω_4' , etc., are no longer integral multiples of the fundamental electrical length Ω_1' as for the unloaded aerial. Also the possible resonance frequencies are no longer integral multiples of the fundamental frequency, and we find, for instance, for the scaled-off electrical lengths

¹L. Cohen has proposed such a solution for coil-loaded antennas (*Elec. World*, 65, 286, 1915).

which are given below, $f_2 = 3.49f_1$ instead of $3f_1$ and $f_3 = 6.53f_1$ instead of $5f_1$. The electrical lengths are

$$\left. \begin{aligned} \Omega_1' &= 0.314\pi = 0.986 \\ \Omega_2' &= 1.094\pi = 3.44 \\ \Omega_3' &= 2.05\pi = 6.44 \end{aligned} \right\} \begin{array}{l} \text{with the} \\ \text{corresponding} \\ \text{angles} \end{array} \left\{ \begin{array}{l} 56.5^\circ \\ 180^\circ + 17^\circ \\ 360^\circ + 90^\circ \end{array} \right\} \text{ and } \left\{ \begin{array}{l} \tan \Omega_1' = 1.5 \\ \tan \Omega_2' = 1.05 \\ \tan \Omega_3' = 1.02 \end{array} \right\}$$

Case C.—When a loading condenser C_0 is inserted at the ground side, the natural frequency of the system is increased since the effective antenna constants C_e'' and L_e'' for the fundamental mode give

$$f_1'' = \frac{1}{2\pi \sqrt{\frac{C_e'' C_0}{C_e'' + C_0} L_e''}} \quad (49)$$

The effective reactance of the condenser loaded antenna becomes

$$\begin{aligned} X_e'' &= \frac{1}{j\omega C_0} - j\sqrt{\frac{L}{C}} \cotan \Omega = -j \left[\frac{1}{\omega C_0} + \sqrt{\frac{L}{C}} \cotan \Omega \right] \\ &= -j\sqrt{\frac{L_A}{C_A}} \left\{ \frac{C_A}{C_0} \frac{1}{\Omega} + \cotan \Omega \right\} \quad (50) \end{aligned}$$

For the fundamental and all higher modes, $X_e'' = 0$ and the static antenna capacity C_A becomes

$$\begin{aligned} C_A &= C_0 \Omega_1'' \cotan \Omega_1'' \\ &= C_0 \Omega_2'' \cotan \Omega_2'' \\ &= C_0 \Omega_3'' \cotan \Omega_3'' \\ &= \text{etc.} \end{aligned} \quad (51)$$

since C_0 denotes another loading capacity for each mode. In this case, the angle θ of the slant line is given by

$$\tan \theta = \frac{C_0}{C_A} \quad (52)$$

and the frequency for the fundamental mode is

$$f_1'' = \frac{\Omega_1''}{2\pi \sqrt{C_A L_A}} \quad (53)$$

According to (50), the natural modes occur for $X_e'' = 0$, that is, whenever

$$\cotan \Omega = -\frac{C_A}{\Omega C_0} \quad (54)$$

The graphic solution simplifies when we put it in the form

$$\tan \Omega = -\frac{C_0}{C_A} \Omega = -\Omega \tan \theta \quad (55)$$

Then it is only necessary to draw the tangent curves ($y = \tan \Omega$) and the inclined line for these solutions. Because of the minus sign the inclined line due to C_0 is drawn downward at the angle θ given by (52).

Case D.—Often a loading coil L_0 and a loading condenser C_0 are used in series in order to adjust for the proper frequency and produce favorable distributions. The fundamental frequency is given by

$$f_1^{\text{III}} = \frac{1}{2\pi\sqrt{\frac{\bar{C}_e^{\text{III}}C_0}{\bar{C}_e^{\text{III}} + C_0}[L_e^{\text{III}} + L_0]}} \quad (56)$$

The effective reactance becomes

$$\begin{aligned} X_e^{\text{III}} &= j\omega L_0 + \frac{1}{j\omega C_0} - j\sqrt{\frac{L}{C}} \cotan \Omega = j\left[\omega L_0 - \frac{1}{\omega C_0} - \sqrt{\frac{L}{C}} \cotan \Omega\right] \\ &= j\sqrt{\frac{L_A}{C_A}} \left\{ \frac{L_0}{L_A} \Omega - \frac{C_A}{C_0 \Omega} - \cotan \Omega \right\} \end{aligned} \quad (57)$$

The frequency of the fundamental mode is

$$f_1^{\text{III}} = \frac{\Omega_1^{\text{III}}}{2\pi\sqrt{C_A L_A}} \quad (58)$$

and, for the fundamental and higher modes, we have the relation

$$\begin{aligned} (X_e^{\text{III}} = 0) \\ \cotan \Omega &= \frac{L_0}{L_A} \Omega - \frac{C_A}{C_0 \Omega} \\ &= \Omega \tan \theta - \frac{C_A}{C_0 \Omega} \end{aligned} \quad (59)$$

In the graphical solution we draw $y = \cotan \Omega$; and

$$y = \Omega \tan \theta - \frac{C_A}{C_0 \Omega}$$

which is a hyperbola with the y -axis and the inclined line (at the angle θ) as asymptotes.

Case E.—In another case the antenna loading consists of a loading coil L_0 parallel to a loading condenser C_0 as in Fig. 239. The fundamental frequency for the effective antenna constants C_e^{IV} and L_e^{IV} is

$$f_1^{\text{IV}} = \frac{1}{2\pi\sqrt{[C_e^{\text{IV}} + C_0][L_e^{\text{IV}} + L_0]}} = \frac{\Omega_1^{\text{IV}}}{2\pi\sqrt{C_A L_A}} \quad (60)$$

and the effective reactance is

$$X_e^{\text{IV}} = j\left[\frac{\omega L_0}{1 - \omega^2 C_0 L_0} - \sqrt{\frac{L_A}{C_A}} \cotan \Omega\right] \quad (61)$$

The graphical solution is based on the $y = \sqrt{L_A/C_A} \cotan \Omega$ and $y = \omega L_0/(1 - \omega^2 C_0 L_0)$ curves, the intersections of which again give the electrical lengths Ω_1^{IV} , Ω_2^{IV} , Ω_3^{IV} , etc., for the possible modes.

The frequency equation ($X_c^{IV} = 0$) is conveniently written in the form

$$\tan \Omega = \omega C_0 \sqrt{\frac{L_A}{C_A}} \left[\frac{1}{\omega^2 C_0 L_0} - 1 \right] = \sqrt{\frac{L_A}{C_A}} \left[\frac{1}{\omega L_0} - \omega C_0 \right] \quad (62)$$

and the intersections of the curves

$$y_1 = \tan \Omega \quad \text{and} \quad y_2 = \sqrt{\frac{L_A}{C_A}} \left[\frac{1}{\omega L_0} - \omega C_0 \right]$$

give the consecutive electrical lengths Ω_1 , Ω_2 , Ω_3 , etc., where, for simplicity, the indices IV are omitted. These lengths correspond to the possi-

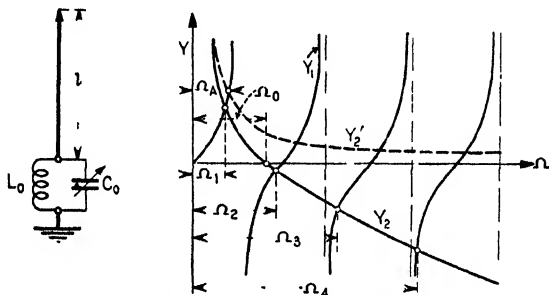


FIG. 239.—Graphical solution for a loading $L_0 C_0$ of an aerial.

ble frequencies f_1, f_2, f_3 , etc. The intersection of the hyperbola y_2 with the abscissa gives the electrical length Ω_0 which corresponds to the natural frequency f_0 of the loading circuit. Hence the corresponding coupling frequencies f_1 and f_2 are lower and higher than the natural loading frequency f_0 . It is therefore of interest to know the natural frequency f_A of the antenna without coupling. This can be obtained by putting in (62) the quantity $C_0 = 0$, which gives

$$y_2^I = \frac{1}{\omega L_0} \sqrt{\frac{L_A}{C_A}}$$

The intersection of this curve with the tangent curves then gives the natural frequencies, which for the fundamental mode yields the electrical length Ω_A corresponding to frequency f_A . We have for the frequencies the relations

$$f_1 < f_A \leq f_0 < f_2$$

Hence the higher coupling frequency exceeds the higher of both natural frequencies. The lower coupling frequency is smaller than the smaller

natural frequency. We have therefore the same case as that for two closed coupled circuits.

It is possible to find the static inductance and capacitance of an aerial by the methods just described.

157. Apparent Effective and True Effective Antenna Constants.—As mentioned in the previous section, the effective antenna constants C_e and L_e depend upon the degree and kind of loading. The reason for this can be seen from Fig. 240 and the following derivations. An unloaded aerial has, for sinusoidal distributions, an electrical length $\Omega = \beta l$ for the fundamental. For a coil loading, a longer equivalent length l' must be taken into consideration and therefore also an equivalent electrical

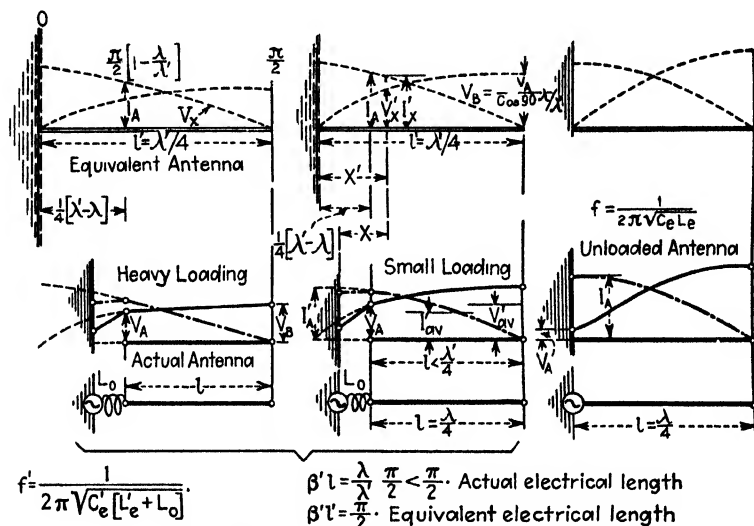


FIG. 240.—Effective potential and current for coil loading.

length $\beta'l'$ instead of the apparent electrical length $\beta'l$, and $\beta'l'$ becomes larger as the loading inductance L_0 is increased. If the effective potential along the aerial were uniform, the effective value of the antenna capacity would be equal to the true (static) value $C_A = lC$. A uniform current distribution along the line would make the static and dynamic values of antenna inductance and resistance identical since they depend upon the current distribution. This follows from the fact that the magnetic-field energy is $\frac{1}{2} \cdot lLI_A^2$, and the Joulean heat loss is equal to rII_A^2 . According to Fig. 240, the effective antenna current I_e at any distance x from the current source with a current of effective value I_A is

$$I_e = I_A \cos \frac{2\pi x}{\lambda}$$

and at a certain instant, for the fundamental mode ($l = \lambda/4$), the average value of the effective values along the line is

$$I_{av} = \frac{4}{\lambda} \int_{x=0}^{\lambda/4} I_A \cos \frac{2\pi x}{\lambda} dx = \frac{2}{\pi} I_A$$

But the definition

$$L_A = lL = \frac{\text{magnetic flux}}{I_{av}}$$

shows the *apparent effective* antenna inductance

$$L_e = 0.636L_A \quad (63)$$

that is, only 63.6 per cent of the static value. In a similar way the potential distribution is

$$V_x = V_B \sin \frac{2\pi x}{\lambda}$$

for an effective potential V_B at the free end with respect to ground. The average value along the antenna is

$$V_{av} = \frac{4}{\lambda} \int_0^{\frac{\lambda}{4}} V_B \sin \frac{2\pi x}{\lambda} dx = \frac{2}{\pi} V_B$$

But the true (static) antenna capacity according to definition is

$$lC = C_A = \frac{\text{charge}}{V_{av}}$$

Hence the *apparent effective* antenna capacitance

$$C_e = 0.636C_A \quad (64)$$

Since at any instant the effective value along the line is

$$I_e = \sqrt{\frac{4}{\lambda} \int_0^{\frac{\lambda}{4}} I_A^2 \cos^2 \frac{2\pi x}{\lambda} dx} = \frac{I_A}{\sqrt{2}}$$

and the heat loss in the entire line is

$$I_e^2(r \cdot l) = \frac{I_A^2 r_A}{2}$$

we have for the *apparent effective* antenna resistance

$$r_e = 0.5r_A \quad (65)$$

For a heavy coil loading, the current decreases toward the open end almost linearly, and the potential distribution is substantially uniform. Hence

$$I_{av} = \frac{I_A}{2}$$

$$I_e = \frac{I_A}{\sqrt{3}}$$

$$V_{av} = V_B \quad \text{Magnetic flux} = \frac{L_A I_A}{2}$$

$$\text{Heat loss} = \left(\frac{1}{3}\right) r_A I_A^2$$

$$\text{Electric charge} = V_B C_A, \text{ or}$$

$$C_e = C_A; \quad L_e = 0.5L_A; \quad r_e = 0.33r_A \quad (66)$$

The apparent effective antenna capacity changes therefore from 63.6 to 100 per cent of the static value, the inductance from 63.6 to 50 per cent, and the resistance from 50 to 33 per cent for unloaded antenna to heavy coil loading. Hence the resonance frequencies f for coil loading is smaller than for the unloaded aerial.

For condenser loading, we have the conditions illustrated in Fig. 241 which shows that the fundamental frequency f'' and the corresponding higher modes are greater with loading.

To find the apparent effective values for any degree of coil loading, we have, for example, for an inductance L_0 at the ground side, the equivalent electrical length $\beta'l'$ and the actual electrical length $\beta'l = (f'/f)(\pi/2) = (\lambda/\lambda')(\pi/2) < \pi/2$ since

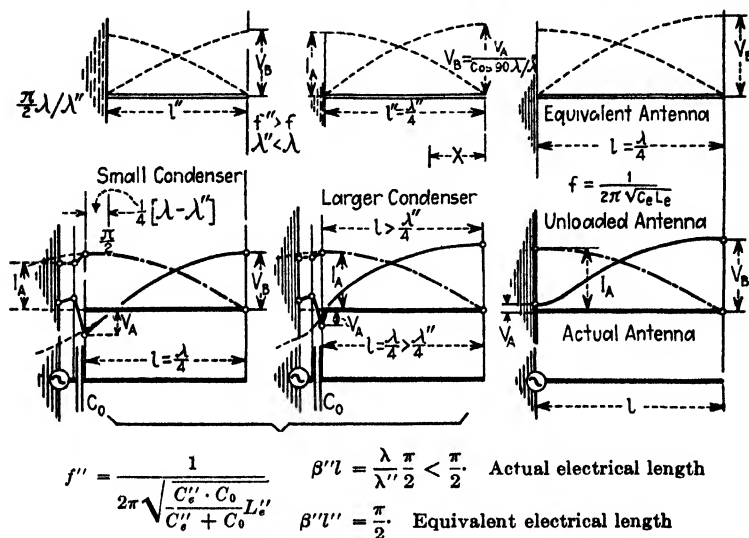


FIG. 241.—Condenser loading.

$\beta'l' < \beta'l$ and $\beta'l' = 2\pi f' \sqrt{CL} \lambda' / 4 = \pi/2$ because $1/f' = \lambda' \sqrt{CL}$. In this case potential and current for any actual distance x , that is, for an effective¹ distance x' from the ground, are

$$\left. \begin{aligned} V'_x &= V_B \sin \frac{2\pi x'}{\lambda'} = V_B \sin x' \\ I'_x &= I_A' \cos \frac{2\pi x'}{\lambda'} = \frac{I_A}{\sin \frac{\pi}{2} \frac{\lambda}{\lambda'}} \cos x' \end{aligned} \right\}$$

since

$$I_A = I_A' \cos \left\{ \frac{\pi}{2} \left[1 - \frac{\lambda}{\lambda'} \right] \right\} = I_A' \sin \left(\frac{\pi}{2} \frac{\lambda}{\lambda'} \right)$$

The average values of antenna potential and current for an electrical length

$$\frac{\pi}{2} - \frac{\pi}{2} \left(1 - \frac{\lambda}{\lambda'} \right) = \frac{\pi}{2} \frac{\lambda}{\lambda'} = \beta'l$$

¹ For such calculations it seems more logical to use the wave length λ instead of the frequency f in the derivations since we deal with distributions and use the frequency in the final result.

are

$$V'_{av} = \frac{2\lambda'}{\pi\lambda} V_B \int_{x'=\left(\frac{\pi}{2}\right)(1-\lambda/\lambda')}^{x'=\pi/2} \sin x' dx' = \frac{2\lambda'}{\pi\lambda} V_B \sin 90 \frac{\lambda}{\lambda'} = \frac{2f}{\pi f'} V_B \sin \left(90 \frac{f'}{f}\right) \quad (67)$$

and

$$I'_{av} = \frac{2\lambda'}{\pi\lambda} \frac{I_A}{\sin \frac{\pi}{x} \frac{\lambda}{\lambda'}} \int_{(\pi/2)(1-\lambda/\lambda')}^{\pi/2} \cos x' dx' = \frac{2\lambda'}{\pi\lambda} \frac{I_A}{\sin (90\lambda/\lambda')} \left[1 - \cos (90\lambda/\lambda') \right] =$$

$$\frac{2f I_A}{\pi f' \sin (90f'/f)} \left[1 - \cos \left(90 \frac{f'}{f}\right) \right] \quad (68)$$

where f denotes the resonance frequency for the unloaded antenna and f' the resonance frequency for a coil loading of any degree.

Since

$$\begin{aligned} \text{Charge} &= (\text{average voltage})(\text{static antenna capacitance}) \\ &= V'_{av} \cdot \mathcal{C} = \left\{ \frac{2\lambda'}{\pi\lambda} C_A \sin \left(90 \frac{\lambda}{\lambda'}\right) \right\} V_B \end{aligned}$$

the *apparent effective* capacity for any coil loading L_0 becomes

$$C'_e = \left\{ \frac{2f}{\pi f'} \sin \left(90 \frac{f'}{f}\right) \right\} C_A = A_2 C_A \quad (69)$$

Since

$$\begin{aligned} \text{Magnetic flux} &= (\text{average current})(\text{static inductance}) \\ &= I'_m \cdot \mathcal{L} = \frac{2\lambda' L_A}{\pi\lambda \sin \left(90 \frac{\lambda}{\lambda'}\right)} \left[1 - \cos \left(90 \frac{\lambda}{\lambda'}\right) \right] I_A \end{aligned}$$

the *apparent effective* inductance of the antenna for any coil loading is

$$L'_e = \frac{2f[1 - \cos 90(f'/f)]}{\pi f' \sin (f'/f) 90} L_A = B_2 L_A \quad (70)$$

Moreover, since the potential at the generator end with respect to ground is

$$V_A = V_B \sin \left\{ \frac{\pi}{2} \left[1 - \frac{\lambda}{\lambda'} \right] \right\} = V_B \cos \left(\frac{\pi}{2} \frac{\lambda}{\lambda'} \right)$$

we have for the unknown effective potential at the free end of the antenna

$$V_B = \frac{V_A}{\cos (f'/f) 90} \quad (71)$$

For any condenser loading C_0 (Fig. 241), we find for the electrical length

$$\beta'' l = \frac{2\pi \lambda}{\lambda''} \frac{1}{4} = \frac{\lambda}{\lambda''} \frac{\pi}{2} = \frac{f''}{f} \frac{\pi}{2} > \frac{\pi}{2}$$

Hence the electrical (space) angle is greater than 90 deg since $\lambda'' < \lambda$. The frequencies f and f'' denote the resonance frequencies for the unloaded and condenser-loaded aerial

We find for the average value of the effective voltage along the line

$$V_{av} = \frac{2\lambda'' V_B}{\pi\lambda} \int_0^{\frac{\lambda}{\lambda''} \frac{\pi}{2}} \cos x dx = \frac{2\lambda''}{\pi\lambda} V_B \sin \left(90 \frac{\lambda}{\lambda''} \right) = \frac{2f}{\pi f''} V_B \sin \left(90 \frac{f''}{f} \right) \quad (72)$$

and since

$$I_A = I_A'' \sin \left(\frac{\lambda}{\lambda'} \frac{\pi}{2} \right)$$

we find

$$I_{av}'' = \frac{2\lambda''}{\pi\lambda} \frac{I_A}{\sin \left(\frac{\lambda}{\lambda''} \frac{\pi}{2} \right)} \int_0^{\frac{\lambda}{\lambda''} \frac{\pi}{2}} \sin x dx = \frac{2\lambda'' I_A}{\pi\lambda \sin \left(90 \frac{\lambda}{\lambda''} \right)} \left[1 - \cos \left(90 \frac{\lambda}{\lambda''} \right) \right] =$$

$$= \frac{2f I_A}{\pi f'' \sin \left(90 \frac{f''}{f} \right)} \left[1 - \cos \left(90 \frac{f''}{f} \right) \right] \quad (73)$$

which leads to the *apparent effective* antenna constants

$$\left. \begin{aligned} C_e'' &= \left\{ \frac{2f}{\pi f''} \sin \left(90 \frac{f''}{f} \right) \right\} C_A \\ L_e'' &= \left\{ \frac{2f \left[1 - \cos \left(90 \frac{f''}{f} \right) \right]}{\pi f'' \sin \left(90 \frac{f''}{f} \right)} \right\} I_A \end{aligned} \right\} \quad (74)$$

Tables XIX and XX show the application of this method. For each case the fundamental frequency of the unloaded antenna was 438 kc/sec and $V_A = 10$ volts.

TABLE XIX

Measured values		Results		
Coil loading L_0 (henries)	Resonance frequency (fundamental mode) f' , kc/sec	V_B (volts)	Apparent effective values	
			C_e' per cent of C_A	L_e' per cent of L_A
0.000246	296	21.0	82.6	56.0
0.000279	284	19.1	83.5	54.8
0.000308	274	18.0	85.0	54.5
0.000345	265	17.3	85.6	54.2
0.000384	258	16.6	86.4	53.8
0.000422	252	16.2	86.6	53.6
0.000448	245	15.7	88.0	53.6

TABLE XX

Measured values		Results		
Loading capacity $C_0(\mu f)$	Resonance • frequency (fundamental mode) f'' , kc/sec	V_B (volts)	Apparent effective values	
			C_e'' per cent of C_A	L_e'' per cent of L_A
0.00241	535	29.2	48.8	74.3
0.00217	550	25.6	46.7	76.5
0.00192	560	23.6	45.0	78.0
0.00165	570	21.9	43.4	80.0
0.00141	582	20.3	41.5	82.2
0.00116	595	18.9	39.9	84.7
0.00092	615	16.9	36.4	89.6
0.00067	660	13.9	29.4	104.0
9.00042	740	11.3	17.6	151.0
0.00018	810	10.3	8.2	284.0

The derivation of the *true effective* antenna constants is based on the energy equation

$$W_h + \frac{\partial W_e}{\partial t} + \frac{\partial W_m}{\partial t} = 0$$

where W_h denotes the power consumed by heat losses and W_e and W_m the energy of the electric and magnetic field, respectively. This equation holds for lumped as well as for distributed circuit quantities. For the antenna of length l we have

$$W_h = \int_0^l r I^2 dx$$

$$W_e = \int_0^l \frac{1}{2} C V^2 dx$$

$$W_m = \int_0^l \frac{1}{2} L I^2 dx$$

which leads to the expression

$$\frac{\partial I}{\partial t} \int_0^l r \cos^2 \beta x dx + \frac{\partial^2 I}{\partial t^2} \int_0^l L \cos^2 \beta x dx + \frac{I}{\frac{\left[\int_0^l C \sin \beta x dx \right]^2}{\int_0^l C \sin^2 \beta x dx}} = 0 \quad (75)$$

when compared with

$$\frac{\partial I}{\partial t} r_e + \frac{\partial^2 I}{\partial t^2} L_e + \frac{1}{C_e} = 0 \quad (76)$$

Equation (75) shows that the effective capacitance and inductance of the line can be calculated from the expressions

$$\left. \begin{aligned} C_e &= \frac{1}{\beta l} \frac{\left[\int_0^l Cl \sin \beta x dx \right]^2}{\int_0^l Cl \sin^2 \beta x dx} \\ L_e &= \frac{1}{\beta l} \int_0^l Ll \cos^2 \beta x dx \end{aligned} \right\} \text{(for any electrical length) } \beta l \quad (77)$$

For the unloaded antenna, when (75) is written in another form, we have

$$r_e I + L_e \frac{\partial I}{\partial t} + \frac{1}{C_e} \int Idt = 0$$

for all natural modes. L_e , C_e , and r_e denote the *correct* effective constants since they confirm, in addition to the effective oscillation constant $C_e L_e$, the effective decrement $\delta_e = \pi r_e \sqrt{C_e/L_e}$ whereas the apparent effective constants, as a rule, confirm the oscillation constant only. This can be demonstrated with an artificial antenna circuit built up of the apparent effective constants and the correct effective constants, respectively, both circuits excited independently with impact excitation (damped wave trains of single frequency). The circuit with the apparent constants gives resonance at the correct frequency, but the resonance current is either smaller or larger than the true antenna current, depending upon whether the apparent effective antenna capacitance was too large or too small. The equivalent circuit with the correct constants gives, however, the correct resonance current of the antenna.

For the unloaded antenna, we find for the correct effective antenna resistance

$$r_e = r \int_0^{\frac{\lambda}{4}} \cos^2 \frac{2\pi x}{\lambda} dx = \frac{rl}{2} = 0.5r_A \quad (78)$$

$$L_e = 0.5L_A \quad (78a)$$

since, according to (75), the same distribution function holds for L_e as for r_e and

$$C_e = \frac{\left[\int_0^{\frac{\lambda}{4}} C \sin (2\pi x/\lambda) dx \right]^2}{\int_0^{\frac{\lambda}{4}} C \sin^2 (2\pi x/\lambda) dx} = \frac{8}{\pi^2} Cl = 0.81C_A \quad (79)$$

For heavy coil loading, the antenna current decreases almost linearly toward the open end; that is,

$$I_x = I_A \left[1 - \frac{x}{l} \right]$$

if x is the distance along the wire from any point of the antenna to the upper end of the loading inductance L_0 . The effective antenna potential remains substantially constant; hence

$$V_x = V_B$$

In these expressions I_A denotes the effective current at the foot of the antenna and V_B the potential of the far end to ground. The *correct effective* resistance of the antenna for heavy coil loading due to the distribution function

$$f(x) = 1 - \frac{x}{l}$$

becomes

$$r_e = \int_0^l r \left[1 - \frac{x}{l} \right]^2 dx = \frac{l \cdot r}{3} = 0.33r_A \quad (80)$$

as well as

$$L_e = \int_0^l L \left[1 - \frac{x}{l} \right]^2 dx = 0.33L_A \quad (81)$$

and the *correct effective* capacity because of the potential function $F(x) = 1$ becomes

$$C_e = \frac{\left[\int_0^l C dx \right]^2}{\int_0^l C dx} = lC = C_A \quad (82)$$

We see therefore that the *correct effective* constants vary from

$$\left. \begin{aligned} r_e &= (50 \text{ to } 33\%)r_A \\ L_e &= (50 \text{ to } 33\%)L_A \\ C_e &= (81 \text{ to } 100\%)C_A \end{aligned} \right\} \begin{array}{l} \text{(between unloaded antenna} \\ \text{and heavy coil loading)} \end{array} \quad (83)$$

For any coil loading L_0 , according to Fig. 240, the electrical length is $\beta' l = (f'/f)(\pi/2) = (\lambda/\lambda')(\pi/2)$. Since the effective potential V_x and the effective current at any place x are

$$V_x = V_B \sin x \quad \text{and} \quad I_x = \frac{\cos x}{\sin [(\lambda/\lambda')(\pi/2)]} I_A$$

the potential function is

$$F'(x) = \sin x$$

and the current function

$$F''(x) = \frac{\cos x}{\sin [(\lambda/\lambda')90^\circ]}$$

The effective electrical length over which the integration is to be taken is $\beta' l = \pi/2 - \pi/2(1 - \lambda/\lambda')$. Hence

$$C_e' = \frac{\left[\int_{\frac{\pi}{2}[1-(\lambda/\lambda')]}^{\pi/2} C \sin x dx \right]^2}{\int_{\frac{\pi}{2}[1-(\lambda/\lambda')]}^{\pi/2} C \sin^2 x dx} = C \frac{4 \cos^2 \{ \pi/2[1 - \lambda/\lambda'] \}}{\pi \lambda/\lambda' + \sin \{ \pi[1 - \lambda/\lambda'] \}}$$

But $C_A = lC$ along the actual length l of electrical length $(\pi/2)(\lambda/\lambda')$; hence for any coil loading L_0 ,

$$\begin{aligned} C_e' &= \frac{lC}{\frac{\pi}{2} \frac{\lambda}{\lambda'}} \cdot \frac{4 \cos^2 \left\{ \left(\frac{\pi}{2} \right) \left[1 - \frac{\lambda}{\lambda'} \right] \right\}}{\frac{\pi \lambda}{\lambda'} + \sin \left\{ \pi \left[1 - \frac{\lambda}{\lambda'} \right] \right\}} = \frac{8\lambda'}{\pi \lambda} \frac{C_A \sin^2 \left\{ \frac{\lambda}{\lambda'} 90 \right\}}{\frac{\lambda}{\lambda'} + \sin \left\{ 180 \left(1 - \frac{\lambda}{\lambda'} \right) \right\}} \\ &= \frac{8f}{\pi f'} \frac{C_A \sin^2 \left\{ \left(\frac{f'}{f} \right) 90 \right\}}{\pi \frac{f'}{f} + \sin \left\{ 180 \left(1 - \frac{f'}{f} \right) \right\}} = A_1 C_A \quad (84) \end{aligned}$$

which for $f = f'$ gives $\frac{8}{\pi^2} C_A = C_e$.

For the correct effective inductance L_e' for any coil loading, we find

$$\begin{aligned} L_e' &= \int_{\frac{\pi}{2}[1-(\lambda/\lambda')]}^{\pi/2} \frac{\cos^2 x}{\sin^2 \{ (\pi/2)(\lambda/\lambda') \}} dx = \frac{\lambda'}{2\pi \lambda} \frac{\pi(\lambda/\lambda') - \sin \{ 180[1 - (\lambda/\lambda')] \}}{\sin^2 \{ (\lambda/\lambda') 90 \}} L_A \\ &= \frac{f}{2\pi f'} \frac{\pi(f'/f) - \sin \{ 180[1 - (f'/f)] \}}{\sin^2 \{ (f/f') 90 \}} L_A = B_1 L_A \quad (85) \end{aligned}$$

which for $f = f'$ gives $L_e' = 0.5 \cdot L_A = L_e$. For the correct effective antenna resistance we have the same function as for L_e' ; hence

$$r_e' = B_1 r_A \quad (86)$$

Tables XXI and XXII show the application of these formulas.

Figure 242 illustrates the conditions of an antenna without loading. The static antenna constants C_A , L_A , and r_A can be calculated from standard formulas or determined by the graphical methods given in "High-frequency Measurements." In addition to these, the reactance equation

$$X_e' = \sqrt{\frac{L_A}{C_A}} \left\{ \frac{L_0}{L_A} \frac{2\pi}{\lambda'} l - \cotan \frac{2\pi}{\lambda'} l \right\}$$

for any coil loading L_0 gives, for cases of resonance ($X_e' = 0$),

$$\frac{L_0}{L_A} \frac{2\pi}{\lambda'} l = \cotan \frac{2\pi}{\lambda'} l$$

and for the fundamental mode $l = \lambda/4$, we find the static inductance of an antenna

$$\begin{aligned}
 L_A^{(\text{henries})} &= L_0^{(\text{henries})} \frac{\lambda}{\lambda'} \frac{\pi}{2} \tan \frac{\lambda}{\lambda'} 90^\circ \\
 &= L_0 \frac{f'}{f} \frac{\pi}{2} \tan \frac{f'}{f} 90^\circ
 \end{aligned}
 \quad (87)$$

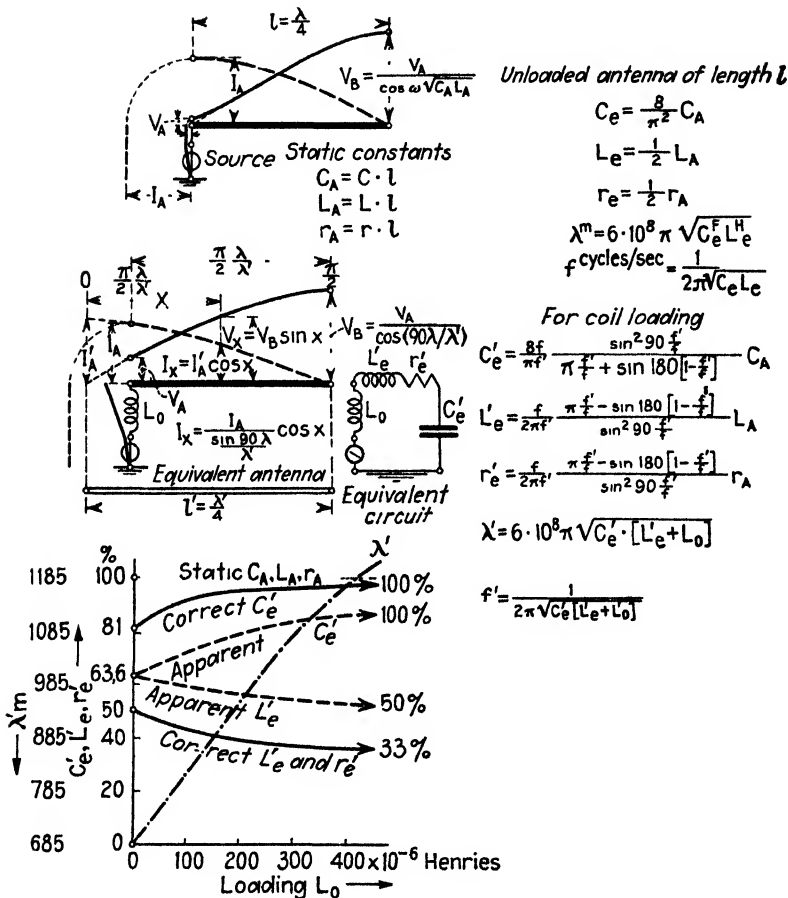


FIG. 242.—Curves and formulas for the correct effective aerial constants.

when f and f' denote the resonance frequencies of the antenna for no loading and loading L_0 , respectively. The static antenna capacity can be found from (87) and

$$f \approx \frac{1}{4\sqrt{C_A L_A}}$$

$$C_A^{(\mu f)} = \frac{1}{16f^2 L_A^{(\text{henries})}} \quad (88)$$

if the frequency f is expressed in kilocycles per second. Table XXIII gives an application.

TABLE XXII

Measured quantities		Calculated correct effective antenna constants in percentage of the corresponding static values		
Loading L_0 (henries)	Resonance frequency f , kc/sec	C_e same dimension as C_A	L_e same dimension as L_A	r_e same dimension as r_A
0. no loading	438	81.0	50 0	50 0
0.000246	296	96.7	39.3	39.3
0.000279	284	97.4	38.6	38.6
0.000308	274	97.9	38.1	38.1
0.000345	265	98.1	37 7	37.7
0.000384	258	98.2	37.6	37.6
0.000422	252	98.5	37.2	37.2
0.000448	245	98.9	31 1	31.1

General remarks: The measured frequency can be checked by for C_e' in farads and L_e' in henries.

$$f' = \frac{1}{2\pi\sqrt{C_e'[L_e' + L_0]}}$$

TABLE XXIII

Measured quantities		L_A , henries	Remarks
Loading inductance L_0 (henries)	Resonance frequency f , kc/sec		
0.000246	296	0.000466	For no loading, resonance frequency $f = 438$ kc/sec with the average value of $L_A = 0.000468$ henries $C_A = 0.00069 \mu f$
0.000279	284	0.000463	
0.000308	274	0.000454	
0.000345	265	0.000463	
0.000384	258	0.000474	
0.000422	252	0.000485	
0.000448	245	0.000474	

Another method for determining the static antenna constants can be obtained by comparing the expressions for the apparent effective and true effective constants. According to (84) and (85), the correct effective constants are

$$C_e = A_1 C_A \quad \text{and} \quad L_e = B_1 L_A$$

and, according to (69) and (70), the corresponding apparent effective currents are

$$C_{e_1} = A_2 C_A \quad \text{and} \quad L_{e_1} = B_2 L_A$$

for the distribution constants

$$\begin{aligned} A_1 &= \frac{8f}{\pi f^1} \frac{\sin^2 \{(f^1/f)90^\circ\}}{\pi(f^1/f) + \sin \{180[1 - (f^1/f)]\}} \\ B_1 &= \frac{f}{2\pi f^1} \frac{\pi(f^1/f) - \sin \{180[1 - (f^1/f)]\}}{\sin^2 \{90(f^1/f)\}} \\ A_2 &= \frac{2f}{\pi f^1} \sin \left\{ 90 \frac{f^1}{f} \right\} \\ B_2 &= \frac{2f}{\pi f^1} \frac{[1 - \cos \{90(f^1/f)\}]}{\sin \{90(f^1/f)\}} \end{aligned}$$

Since the oscillation constants of the apparent effective and true effective value for the same loading inductance L_0 are the same, we have

$$C_{e_1}[L_{e_1} + L_0] = C_{e_2}[L_{e_2} + L_0]$$

or

$$A_1 C_A [B_1 L_A + L_0] = A_2 C_A [B_2 L_A + L_0]$$

The static or true antenna inductance becomes

$$L_A^{(\text{henries})} = \frac{A_1 - A_2}{A_2 B_2 - A_1 B_1} L_0^{(\text{henries})} \quad (89)$$

and C_A as in (88), since

$$f = \frac{1}{2\pi \sqrt{(8/\pi^2) C_A \cdot (L_A/2)}} = \frac{1}{4\sqrt{C_A L_A}}$$

158. Transmission-line and High-frequency Equation.—If in Eqs. (1) and (2) the variable i is eliminated, we obtain the equation for the transmission line

$$\frac{\partial^2 e}{\partial x^2} = CL \frac{\partial^2 e}{\partial t^2} + [gL + Cr] \frac{\partial e}{\partial t} + gre \quad (90)$$

which is also known as the *telegraph equation*. The equation obtained by substituting i for the e in (90) is also true. Relation (90) is satisfied by the solution

$$e = \Sigma E \epsilon^{[pt + iqx]} = \Sigma E \epsilon^m$$

and leads to

$$-q^2 E \epsilon^m = p^2 CL E \epsilon^m + p[gL + Cr] E \epsilon^m + gr E \epsilon^m \quad (91)$$

or

$$CLp^2 + [gL + Cr]p + [gr + q^2] = 0$$

with the roots

$$p_1 = -\left[\frac{r}{2L} + \frac{g}{2C}\right] + j\sqrt{\frac{gr + q^2}{CL} - \left[\frac{r}{2L} + \frac{g}{2C}\right]^2}$$

$$= \alpha + j\omega$$

$$p_2 = \alpha - j\omega$$

for

$$\alpha^2 < \frac{gr + q^2}{CL}$$

The final expression is therefore

$$e = Ee^{-(r/2L) + (g/2C)t} \sin [qx \pm \omega t]$$

$$= Ee^{-(r/2L) + (g/2C)t} \sin \left[\frac{2\pi}{\lambda}x \pm \frac{2\pi}{\lambda}vt \right] \quad (92)$$

since the wave length $\lambda = 2\pi/q$ and the velocity of propagation $v = \omega/q = \omega\lambda/2\pi$. Hence a damped wave train Ee^{p_1t} passes toward the end of the line and a wave train of Ee^{p_2t} of the same form is reflected back with the same velocity v toward the source.

For the high-frequency line, the resistance r is small compared with the surge impedance (wave resistance) $Z_0 = \sqrt{L/C}$, and the leakance g is small compared with $\sqrt{C/L}$. For $r = 0$ and $g = 0$, (90) reduces to the high-frequency equation

$$\frac{\partial^2 e}{\partial x^2} = CL \frac{\partial^2 e}{\partial t^2} = \frac{1}{c^2} \frac{\partial^2 e}{\partial t^2} \quad (93)$$

This expression shows that, for high-frequency systems, the frequency of the impressed e.m.f. does not affect the velocity of propagation (since $v = c = 3 \times 10^{10}$ cm/sec) and that by means of the velocity c one can always calculate one of the antenna constants if the other is known (C_A or L_A). The solution of the high-frequency equation for $t = 0$ (space distribution) and for $n = \alpha + j\beta \cong j\beta = \pm j\omega\sqrt{CL}$ is

$$e = \sum_{+n}^{-n} \frac{E}{2} \epsilon^{nx} = \frac{E}{2} \{ \epsilon^{j\omega\sqrt{CL}x} + \epsilon^{-j\omega\sqrt{CL}x} \} = E \cos \omega\sqrt{CL}x$$

and for $x = 0$ (time distribution)

$$e = \sum_{+\omega}^{-\omega} \frac{E}{2} \epsilon^{j\omega t} = \frac{E}{2} \{ \epsilon^{j\omega t} + \epsilon^{-j\omega t} \}$$

$$= E \cos \omega t$$

These two results can be found directly by the universal solution

$$e = \sum \frac{E}{2} e^{i\omega t} e^{nx} = \sum \frac{E}{2} e^{j\beta[ct+x]} = E \cos \beta[ct+x] E \cos \omega[t + \sqrt{CL}x] \quad (94)$$

where

$$\left. \begin{aligned} \beta &= \frac{\omega}{c} = \frac{2\pi f}{c} = \frac{2\pi}{\lambda} = \omega \sqrt{CL} \\ \lambda &= \frac{2\pi}{\beta} = \frac{2\pi c}{\omega} = \frac{1}{f \sqrt{CL}} \\ c &= \frac{1}{\sqrt{CL}} = 3 \times 10^{10} \text{ cm/sec} \end{aligned} \right\} \quad (95)$$

From these relations, we note that, if an e.m.f. E is suddenly applied, this voltage will produce a current flow $I = E/Z_0$ (where $Z_0 = \sqrt{L/C}$) toward both sides of $x = 0$, since generally $I = \text{function}(t \pm x/v)$.

159. Theory for the Experimental Determination of the Propagation Constant and Surge Impedance of a Line.—According to (8) and (9) for the open and short-circuited line (at the free end),

$$\left. \begin{aligned} E_1 &= E_2 \cosh nl \\ I_1 &= \frac{E_2}{Z_0} \sinh nl \end{aligned} \right\} \quad (96)$$

and

$$\left. \begin{aligned} E_1 &= Z_0 I_2 \sinh nl \\ I_1 &= I_2 \cosh nl \end{aligned} \right\} \quad (97)$$

if E_1 and I_1 denote the maximum value of voltage and current, respectively, at the input end and E_2 and I_2 the values at the far end of the line. For the open line, the measurement of E_1 and I_1 gives the impedance

$$Z_{op} = Z_0 \cotanh \Omega \quad (98)$$

for the electrical length $\Omega = nl$ and for the short-circuited line, the value

$$Z_{sc} = Z_0 \tanh \Omega \quad (99)$$

From which the surge impedance becomes

$$Z_0 = \sqrt{Z_{op} \cdot Z_{sc}} \quad (100)$$

If a sinusoidal e.m.f. is impressed, E_1 and I_1 denote the measured effective values also. Since the generalized electrical length $nl = \Omega$ is the propagation constant times the length of line, we also have a means for finding $n = \Omega/l$ from

$$\tanh \Omega = \sqrt{\frac{Z_{sc}}{Z_{op}}} \quad (101)$$

which leads to

$$\Omega = \frac{1}{2} \log_e \frac{1 + \sqrt{Z_{sc}/Z_{op}}}{1 - \sqrt{Z_{sc}/Z_{op}}} \quad (102)$$

Equation (101) reduces

$$\tan \Omega = \sqrt{\frac{Z_{sc}}{Z_{op}}} \quad (103)$$

for the high-frequency line since $nl \cong j\beta l$.

The surge impedance is

$$Z_0 = \sqrt{\frac{z}{y}} = \sqrt{\frac{r + j\omega L}{g + j\omega C}} \quad (104)$$

which in many high-frequency cases can be simplified to

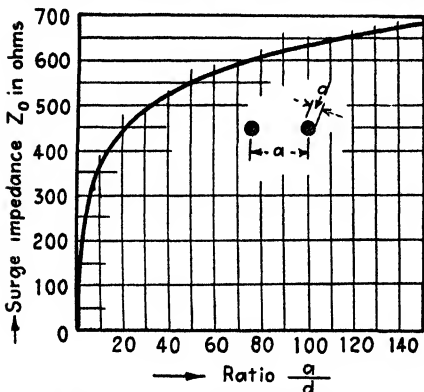


FIG. 243.—Surge (characteristic) impedance of parallel-wire system.

if a denotes the spacing between the centers of the wires and d the diameter of the copper wire. This formula is not correct for very small spacings since the proximity effect $(d/a)^2$ is neglected in comparison with unity as is the factor D in the strict high-frequency equation (27). Very small spacings, however, are impractical for this class of work. The neglect of D does not affect the result very much if the size of the parallel wires is not chosen unreasonably small. For example, $D = 0.03928$, $4 \log_e (1/b) = 16.236$ represents the most important portion in (27). Neglecting D gives 487 instead of 487.9 ohms.

Moreover, from Fig. 243 it is seen that the surge impedance Z_0 of a Lecher-wire system¹ can, with practical dimensions, not be made very

¹ In short-wave work, for instance below 10-m wave length, for aerial feeders the parallel-wire line is often made up as a transposed double line in order to obtain more symmetry and a better balance toward ground. Transposition insulators at equal distances along the double line are then required. A transposed line then consists of a Lecher-wire line for which the go and the return cross over at equal distances.

$$Z_0^{(\text{ohms})} = \sqrt{\frac{L^{(\text{henries})}}{C^{(\text{farads})}}} \quad (105)$$

Figure 243 gives the value of the surge impedance of a Lecher system for different sizes of copper wire and spacings. The curve is calculated by means of the ordinary L and C formulas (25) and (26) which lead to

$$\begin{aligned} Z_0^{(\text{ohms})} &= 120 \log_e \frac{2a}{d} \\ &= 276 \log_{10} \frac{2a}{d} \end{aligned} \quad (106)$$

low. This is a drawback when the line is to be used as feeder for transferring power from a high-frequency source to elevated Hertzian or other radiating systems. For instance, Fig. 243 shows that a surge impedance only as low as 150 ohms would require a very close spacing of the parallel wires. It would therefore not be possible to match suitably certain aeri-als¹ with such feeder lines. This can, however, be done readily with a concentric double-line feeder for which the surge impedance is

$$Z_0 = 138 \log_{10} \frac{d_1}{d_2} \text{ ohm} \quad (106a)$$

where d_1 is the inside diameter of the outer conductor and d_2 the outside diameter of the inner conductor.² Formula (106a) is again the outcome of $Z_0 = \sqrt{L/C}$ since for the concentric double line the capacitance C per centimeter length

$$C = \left[2 \log_e \frac{d_1}{d_2} \right]^{-1} \quad (106b)$$

in e.s. c.g.s. units and the inductance L per centimeter length

$$L = 2 \log_e \frac{d_1}{d_2} \quad (106c)$$

in e.m. c.g.s. units. According to A. Russell³ the high-frequency resistance of a concentric parallel line is

$$R = 2\sqrt{\mu\rho f} \left\{ \frac{1}{d_1} + \frac{1}{d_2} \right\} 10^{-9} \text{ ohm/cm} \quad (106d)$$

for the specific resistance ρ in e.m. c.g.s. units and the frequency f in cycles per second. The quantity μ denotes the magnetic permeability. The respective diameters d_1 and d_2 are expressed in centimeters. Equation (106a) shows that it is an easy matter to design concentric lines from about 10 to 150 ohms. The inner conductor of such lines may be either solid or made of a tube. For a ratio $d_1/d_2 = 3.44$ the value

¹ A Hertz aerial (one half-wave length distribution) has at any point along it a series impedance which behaves like a pure resistance, with a value of 74 ohms at the center and practically several thousand ohms near the ends. At any point a series resistance with a value of 74 divided by the square of the ratio of the current at that point to the current at the center exists.

² The power transferred by a concentric line is all confined to the inside since the outside sleeve acts as a shield. The line itself can not, therefore, radiate. The outside tubing can then be grounded at any point along it and even be buried in the ground with practically no losses. For this reason the outside tubing is generally connected to ground and the terminal of the inside wire moved along an aerial until proper matching occurs.

³ "Alternating Currents," vol. I., p. 222, Cambridge Press, 1914.

$Z_0 = 74$ ohms matches the feed at the center of a Hertzian dipole. Hence if a copper wire A.W.G. No. 4 is used for the axial inside wire of a $\frac{1}{32}$ -in. thick copper tubing with $\frac{3}{4}$ -in. outside diameter the central matching resistance of a Hertzian one half-wave length aerial is satisfied. The axial inside wire is kept in place by means of quartz pegs or pegs of hard rubber which has better dielectric properties at ultra-high frequencies than bakelite.

If the line is bridged at the far end through a resistance R , for the high-frequency equation [Eq. (93)], we have the solutions

$$\begin{aligned} e &= F(x + ct) + \Phi(x - ct) \\ i &= \frac{F(x + ct) - \Phi(x - ct)}{Z_0} \end{aligned}$$

which show that wavelike disturbances F and Φ move in opposite directions with the velocity $c = 1/\sqrt{CL}$. Since $e_2 = Ri_2$ and $x = 0$ at the far end

$$\begin{aligned} Ri_2 &= F(ct) + \Phi(-ct) \\ i_2 &= \frac{F(ct) - \Phi(-ct)}{Z_0} \end{aligned}$$

or

$$\Phi(-ct) = \frac{R - Z_0}{R + Z_0} F(ct) = \rho F(ct) \quad (107)$$

Hence at any point x

$$\begin{aligned} e &= F(x + ct) + \rho F(-x + ct) \\ i &= \frac{F(x + ct) - \rho F(-x + ct)}{Z_0} \end{aligned} \quad (108)$$

where ρ is the reflection factor caused by the resistance bridge. For $R > Z_0$, the factor ρ is positive and the reflected-wave disturbance will have decreased in height. Otherwise it would behave as though coming from an open line. For $R < Z_0$, the reflection factor becomes negative and a reflection similar to that of a short-circuited line is obtained, but the reflected wave starts out with a smaller amplitude. If $R = Z_0$, no reflection takes place since all the energy of the arriving wave is consumed by R . This gives, therefore, another method for experimentally finding the surge impedance of a line.

For a line of infinite length, the wavelike disturbance passes outward only, since no reflected wave can return and (5) and (6) reduce to

$$\begin{aligned} E &= ae^{nx} \\ I &= \frac{ae^{nx}}{Z_0} \end{aligned} \quad (109)$$

and the voltage at any place divided by the current at that place gives the surge impedance

$$Z_0 = \frac{E}{I} \quad (110)$$

which can also be considered as wave resistance for most high-frequency work. Hence the outgoing-voltage disturbance depends upon the generalized angular velocity $n = \alpha + j\beta$ given in Eq. (19). From it we note that, for the voltage E at the sending end, we have at any place x on the line

$$Ee^{-\alpha x} \sin(\omega t + \beta x + \varphi)$$

where β denotes the phase reduction for each unit length (1 cm).¹ The quantity α , the natural logarithm of the ratio of the voltages (or currents), measured a unit length apart, is also known as the "damping factor." The phase measure βx is of little importance for the transmission of speech over homogeneous lines but α , Z_0 and the length l play a part. The quantity α is a measure of the losses in the line and therefore becomes smaller as the resistance r per unit length and the leakance g per unit length become smaller. In order to transmit currents of all frequencies with the same velocity (no distortion),² we have the condition

$$\frac{r}{L} = \frac{g}{C} \quad (111)$$

Equation (21) gives the propagation constant

$$n = \frac{r}{2}\sqrt{\frac{C}{L}} + j\omega\sqrt{CL}$$

that is,

$$\alpha = \frac{r}{2}\sqrt{\frac{C}{L}} \quad \text{and} \quad \beta = \omega\sqrt{CL}$$

if the leakance g is neglected as is practically the case for the parallel-wire system (Lecher wires) used in high-frequency work. But for wired radio, in some cases, it is not permissible to neglect the leakance and we have the attenuation factor

$$\alpha = \frac{r}{2}\sqrt{\frac{C}{L}} + \frac{g}{2}\sqrt{\frac{L}{C}} \quad (112)$$

¹ For telephone and power lines, the unit length is either 1 km or 1 mile.

² The same can be obtained when loading coils (Heaviside, Pupin) with large ωL make $v = \omega/\beta$ as well as α independent of $\omega/2\pi$. In this case the damping constant is only half the value for the condition of (111).

since

$$\begin{aligned}
 n = \sqrt{yz} &= \sqrt{g + j\omega C} \sqrt{r + j\omega L} = j\omega \sqrt{CL} \sqrt{1 + \frac{g}{j\omega C}} \sqrt{1 + \frac{r}{j\omega L}} \\
 &= j\omega \sqrt{CL} \left[1 + \frac{g}{2j\omega C} \right] \left[1 + \frac{r}{2j\omega L} \right] \\
 &= \frac{1}{2} \left[r \sqrt{\frac{C}{L}} + g \sqrt{\frac{L}{C}} \right] + j \frac{4\omega^2 CL - 1}{4\omega \sqrt{CL}} \\
 &= \alpha + j\beta \quad (113)
 \end{aligned}$$

For the amplitude and the effective value of a current, only the damping term $\epsilon^{-\alpha x}$ is of importance. For the infinite line, we have

$$I_x = I \epsilon^{-\alpha x} \quad (114)$$

if I denotes the effective current at the beginning of the line, and I_x the current at a distance x . But $\log_e I/I_x = \alpha x$; and if x denotes a unit length, we have, for the damping factor,

$$\alpha = \frac{\log_{10} (I/I_x)}{0.4343} \quad (115)$$

For wired radio, using power lines, the line can be regarded practically as infinitely long since the carrier frequency may be of the order of 25 to 60 kc/sec. The sending-end impedance is therefore the surge impedance Z_0 and is practically a pure resistance to the high-frequency currents. The line can be imagined as a line which is bridged at the far end by a resistance¹ $R = Z_0 = \sqrt{L/C}$.

If we assume, therefore, that the resistance per unit length is small compared with the reactance per unit length and that g is negligible, as in some cases, then

$$\left. \begin{aligned} \alpha &= \frac{r}{2\sqrt{L}} \sqrt{\frac{C}{L}} \\ Z_0 &= \sqrt{\frac{L}{C}} \end{aligned} \right\}$$

Hence the resistance per unit length can be determined from

$$r = 2\alpha Z_0 \quad (116)$$

It is then only necessary to measure the input current I and the current I_x , 1 mile away or some other suitable distance, and calculate α from (115) which holds for the distance $x = 1$. The surge impedance is E/I , the voltage-current ratio at the input end. The surge impedance can also be calculated by means of formula (106) which for the loop mile as a unit distance gives

¹ Z_0 is in the neighborhood of 300 to 900 ohms.

$$Z_0^{(\text{ohms})} = 276 \log_{10} \frac{2a}{d} \quad (117)$$

since the capacitance and inductance per loop mile

$$\left. \begin{aligned} C^{(\mu f)} &= \frac{0.01941}{\log_{10} (2a/d)} \\ L^{(\text{henries})} &= 14.8 \times 10^{-4} \log_{10} \frac{2a}{d} \end{aligned} \right\} \quad (118)$$

for a diameter d of a copper conductor and a spacing a between centers of the conductors.

The velocity of propagation v is somewhat smaller than that of light but, if it is known, we have $v = 1/\sqrt{CL}$ and together with $Z_0 = \sqrt{L/C}$; this gives another means for finding the inductance and capacitance per unit length, namely,

$$\left. \begin{aligned} L &= \frac{Z_0}{v} \\ C &= \frac{1}{Z_0 v} \end{aligned} \right\} \quad (119)$$

and the static values of antenna inductance and capacity become

$$\left. \begin{aligned} L_A &= \frac{Z_0 l}{v} \\ C_A &= \frac{l}{Z_0 v} \end{aligned} \right\} \quad (120)$$

For some types of power lines, the effect due to leakance is not negligible. Then Eq. (112) must be used. The constants refer to the loop mile as the unit length. For such a condition, the attenuation factor becomes

$$\alpha = \frac{r}{2Z_0} + \frac{gZ_0}{2} \quad (121)$$

160. Theory of the Lecher System When Excited with a Harmonic E.M.F.—A wire arrangement can be used to calibrate frequency meters. A thermoelectric current indicator of low resistance (shunted by a No. 14 A.W.G. wire) is connected across the line and can be made to slide along the parallel wires. For a certain position, the indicator gives a pronounced deflection and again when the instrument has been moved to a position which is one half-wave length farther away. It is of interest to learn how close the wave length obtained by such a measurement checks the wave length which would be obtained in free ether and without the guiding effect of the wires. There can be no difference when the velocity of propagation along the wires is equal to $c = 2.9982 \times 10^{10}$ cm/sec.

Phase velocity has been dealt with in Sec. 154 and Eqs. (29), (30), and (31) hold. For the sake of simplicity, l cm is the distance between the indicator bridge and the input end and, according to (9), we have for the current through the bridge

$$I_2 = \frac{E_1}{Z_0 \sinh nl} \quad (122)$$

for $Z_0 = \sqrt{z/y} = n/y$; $y = j\omega C$; $g = 0$; $n = \alpha + j\beta$ and E_1 the voltage impressed at the input end. Since $v = \omega/\beta$, the indicator current becomes

$$I_2 = \frac{2yE_1}{n[\epsilon^{nl} - \epsilon^{-nl}]} = \frac{2vCE_1}{[1 - j(\alpha/\beta)][\epsilon^{\alpha l}\epsilon^{j\beta l} - \epsilon^{-\alpha l}\epsilon^{-j\beta l}]} \quad (123)$$

Substituting in the ratio α/β the values given by

$$n = \frac{r}{2}\sqrt{\frac{C}{L}} + j\omega\sqrt{CL} = \alpha + j\beta$$

and neglecting insignificant terms in the series for $\epsilon^{\pm\alpha l}$ leads to

$$\epsilon^{\pm\alpha l} = 1 \pm \alpha l$$

and

$$I_2 = \frac{vCE_1}{[1 - j\Delta][\alpha l \cos \beta l + j \sin \beta l]} \quad (124)$$

where, according to (31), $\Delta = r/(2\omega L)$, the correction term in the velocity of propagation

$$v = c(1 - \Delta) \quad (125)$$

Therefore, for the scalar values, we have

$$I_2 = \frac{vcE_1}{\sqrt{[1 + \Delta^2][(\alpha l)^2 \cos^2 \beta l - \sin^2 \beta l]}}$$

and for the current in the indicator bridge

$$I_2 = \frac{vcE_1}{\sqrt{(\alpha l)^2 \cos^2 \beta l + \sin^2 \beta l}} \quad (126)$$

since Δ^2 is very small compared with unity and the scalar value of the denominator is the same for positive and negative signs. The effective current which is actually measured follows, of course, the same relation as the maximum value I_2 . The current through the indicating instrument, therefore, becomes a maximum for all values of βl that render the function

$$\Psi(\beta l) = (\alpha l)^2 \cos^2 \beta l + \sin^2 \beta l$$

a minimum. This happens for¹

$$\begin{aligned} (\beta l)_m &= m\pi[1 - \Delta^2] \\ &\cong m\pi \end{aligned} \quad (127)$$

where $m = 1, 2, 3$, etc. The distance between two consecutive current maxima is therefore π corresponding to $\lambda/2$. This is, however, the wave length which is developed along the parallel-wire system. But, according to (125),

$$v = 2.9982 \times 10^{10}[1 - \Delta] \text{ cm/sec} \quad (128)$$

For $f = 26 \times 10^3$ kc/sec, we have, for example, for copper wires, diameter $d = 0.14$ cm; spacing $a = 4.2$ cm, $\Delta = 0.001088$. The scaled-off wave length is therefore $\frac{1}{10}$ per cent too short if we assume $v = c$, and the correct formula for the wave length in free ether is

$$\lambda_0^{(m)} = 2l^{(m)}(1 + \Delta)$$

The corresponding formula for the frequency in kilocycles per second when the distance l between consecutive maximum settings is measured in meters becomes

$$f = \frac{1.4991 \times 10^5}{l}[1 - \Delta] \quad (129)$$

Table XXIV is added in order to give an idea of the percentage error for different frequencies if the correction term Δ is neglected. The table also takes up the case for which a somewhat larger diameter ($d = 0.145$)

TABLE XXIV

f , kc/sec	Percentage error	$l^{(m)}$	True velocity $v = c(1 - \Delta)$, cm/sec	Percentage error	$l^{(m)}$	Percentage error
16×10^3	0.139	9.356	2.9940×10^{10}	0.135	9.356	0.131
18	0.131	8.317	2.9943	0.127	8.317	0.123
20	0.124	7.486	2.9945	0.121	7.486	0.118
22	0.118	6.806	2.9946	0.115	6.806	0.112
24	0.113	6.239	2.9948	0.110	6.239	0.107
26	0.109	5.759	2.9949	0.106	5.759	0.103
28	0.105	5.348	2.9950	0.102	5.348	0.099
30	0.101	4.992	2.9952	0.099	4.992	0.096
32	0.098	4.680	2.9953	0.096	4.680	0.093
34	0.095	4.405	2.99535	0.093	4.405	0.090
Diameter $d = 0.14$ cm				$d = 0.145$ cm		$d = 0.145$ cm $a = 4.7$ cm
Distance between wires $a = 4.2$ cm						

¹ The proof for this was given in *Bur. Standards, Sci. Paper* 491, 528, 1924.

is used. In each case it can be seen that the error is about $\frac{1}{10}$ per cent and any small changes in the diameter of the wire are negligible.

The space-resonance curves of Fig. 244 can also be interpreted theoretically since, according to (9), the impedance experienced at the input side of the parallel-wire system is

$$Z_1 = Z_0 \tanh nl = Z_0 \frac{\epsilon^{nl} - \epsilon^{-nl}}{\epsilon^{nl} + \epsilon^{-nl}} \quad (130)$$

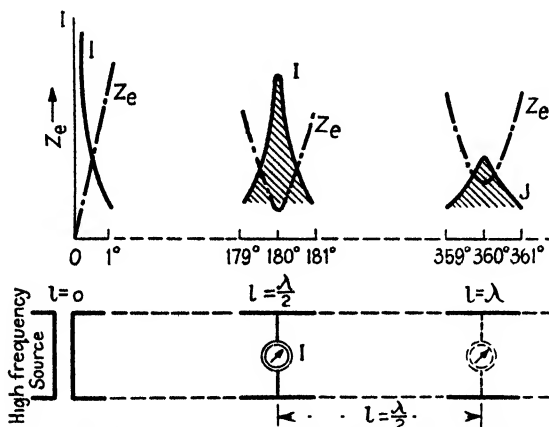


FIG. 244.—Space resonance curves of a parallel-wire system which is bridged over for a 20 megacycles/sec excitation (spacing between centers of conductors $a = 4.2$ cm, diameter of copper conductor $d = 0.145$ cm).

Since

$$Z_0 = \frac{1 - j\Delta}{vC}$$

we have

$$Z_1 = \frac{[1 - j\Delta][\alpha l \cos \beta l + j \sin \beta l]}{vC[\cos \beta l + j\alpha l \sin \beta l]}$$

when only the significant terms in the series for $\epsilon^{+\alpha l}$ are used. Since $\alpha l = \Delta \beta l$ and Δ^2 is very small compared with the unity, we find upon scalarizing for the effective impedance experienced at the input side that

$$Z_e = \frac{1}{vC} \sqrt{\frac{(\Delta \beta l)^2 \cos^2 \beta l + \sin^2 \beta l}{(\Delta \beta l)^2 \sin^2 \beta l + \cos^2 \beta l}} \quad (131)$$

Any minimum values of Z_e cause a maximum current flow into the parallel wires, and thus through the indicating instrument. Equation (131) shows that $Z_e \cong (\tan \beta l)/(vC)$. Current maxima then occur every half wave length. This is practically true since $\Delta^2(\beta l)^2$ is a small quantity. For the dimensions given in Table XXIV, for example, for $f = 20 \times 10^3$ kc/sec, we have $\Delta^2(\beta l)^2 = 5.779 \times 10^{-5}$. The minimum values for Z_e can be found by using the results $(\beta l)_m = m\pi$ of (127) and (131) for which

$$Z_{e_{\min}} = (-1)^m \frac{mrv}{4f} \quad \text{cm/sec} \quad (132)$$

since $\Delta = r/(2\omega L)$. All quantities are expressed in e.m.c.g.s. units. The final result, therefore, needs only to be multiplied by 10^{-9} in order to express the impedance in ohms. The maximum values $Z_{e_{\max}}$ are found by putting $(\beta l)_m = (2m - 1)(\pi/2)$; hence

$$Z_{e_{\max}} = \frac{2}{(2m - 1)\pi\Delta vC} = \frac{8c \log_e (1/b)}{(2m - 1)\pi\Delta} \quad (133)$$

since $c^2/v \cong c$ and $b = \frac{d/a}{1 + \sqrt{1 - (d/a)^2}}$, according to the capacitance expression of (23), and m stands for 1, 2, 3, 4, etc., corresponding to successive settings. By means of (131), the distribution curves of Fig. 244 were obtained. Plotting $1/Z_e$ gives the admittance curves, which, for a constant applied e.m.f. of constant frequency f , gives the shape of the space-resonance curve (I), that is, the effective current as a function of the displacement of the indicator bridge on each side of the resonance position. For the dimensions noted in the figure and $f = 20 \times 10^3$ kc/sec, a condition of 1 deg corresponds to a displacement of 41.35 mm, and a shift of 1 mm produces a noticeable effect. This is small when compared with the corresponding wave length $\lambda = 14,973$ mm. The calculation of the successive impedances for maximum values (133) $m = 1, 2, 3$, etc., shows that the first maximum value

$$Z_e = \frac{8c \log_e (1/b)}{\pi\Delta} 10^{-9} = P \text{ ohms,}$$

while the next is $P/3$ ohms. The successive maxima are therefore as 1:3:5:7, etc., and corresponding relatively large values since, for the dimensions of Fig. 244, $P = 2.56 \times 10^5 \Omega$. In a similar way we can show that the consecutive minimum values of (132) are for $\beta l = 0$, $Z_e = 0$, for $\beta l = \pi$ corresponding to $l = \lambda/2$, $Z_e = (rv/4f)10^{-9} = Q$ ohms, for $\beta l = 2\pi$ corresponding to $l = \lambda$, $Z_e = 2Q$, for $l = \frac{3}{2}\lambda$, $Z_e = 3Q$, etc. For the dimensions given in the figure, $Q = 1.85$ ohms. The successive minima differ more and more from a zero value, and the settings for maximum current farther out must therefore become less sharp. The successive space-resonance curves show that the decrement for settings farther out becomes larger; for this reason it is better to use only the first two maximum settings and to shorten the line by means of a condenser connected across it near the input terminals. The degree of moving the first current maximum $I-I$ in Fig. 245 can be treated graphically as with antenna loadings, but it should be remembered that in this case we have the transcendental equation

$$\Omega \frac{C_0}{C_t} = \cotan \Omega \quad (134)$$

since, according to Eq. (97) on page 441, the entrance impedance for a short-circuited line is

$$Z_1 = Z_0 \tanh nl \cong j\sqrt{\frac{L}{C}} \tan \beta l$$

With a condenser C_0 as in Fig. 245, the net impedance becomes

$$\begin{aligned} Z_e &= j\sqrt{\frac{L}{C}} \tan \beta l' + \frac{1}{j\omega C_0} \\ &= j\sqrt{\frac{L}{C}} \left\{ \tan \Omega - \frac{C_t}{C_0 \Omega} \right\} = 0 \end{aligned} \quad (135)$$

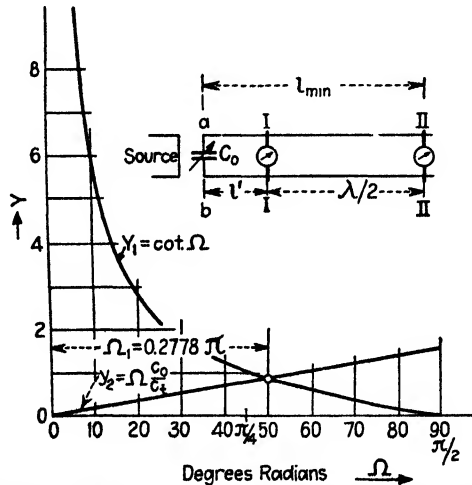


FIG. 245.—Graphical determination of line shortening produced by setting of C_0 .

if l' is the actual distance from the input end to a setting of the low resistance indicating instrument for maximum response,

$$\Omega = \beta l' = \omega l' \sqrt{CL}$$

and $C_t = l'C$ is the total static capacitance of the parallel-wire section of length l' . It is therefore only necessary to determine the intersections of $y_2 = \Omega C_0/C_t$ with $y_1 = \cotan \Omega$. Only the first intersection is of interest here since the distance $l' = \Omega_1/\beta$ gives the length to the first current maximum (position I-I). Since $\beta = 2\pi/\lambda$ we find that

$$l'_s = \frac{\Omega_1 \lambda}{2\pi} \quad (136)$$

and the entire minimum length of the parallel wires can be computed from the expression

$$l_{\min} = 0.5\lambda \left[1 + \frac{\Omega_1}{\pi} \right] \quad (137)$$

The graphical solution of Fig. 245 shows the case for the capacitance $C_0 = C_t$. In this case draw a cotangent curve from 0 to 90 deg corresponding to an electrical length $\Omega = \pi/2$. Since $C_0 = C_t$, the absolute value of $y = C_0\Omega/C_t$ must be equal to Ω itself. Hence draw the ascending line such that the ordinate of $\Omega = \pi/2$ is 1.57. The intersection of this line with the cotangent curve gives $\Omega_1 = 0.2778\pi$ and a minimum length for $\lambda = 10$ m of $l_{\min} = 5 \times 1.2778 = 6.389$ m instead of 10 m. The actual length l' to the first current response $I-I$ is therefore as short as 1.389 m. This can also be computed from (136). The percentage shortening S can be computed from the formula

$$S(\%) = 50 \left[1 - \frac{\Omega_1}{\pi} \right] \quad (138)$$

which for this example gives 36.11 per cent. Equation (137) can also be used in order to find the limiting conditions. One limit exists for a capacity C_0 so large as to form a short circuit. Then $C_0/C_t = \infty$ and, according to (134), the cotan $\Omega_1 = \infty$; that is, $\Omega_1 = 0$. This can be seen from the ascending line of Fig. 245 since, as C_0/C_t increases, the ascending line becomes steeper and, for $C_0/C_t = \infty$, it coincides with the ordinate through the origin. The intersection takes place at infinity corresponding to $\Omega = 0$. This value inserted in (137) gives $l_{\min} = \lambda/2$ and inserted in (138) gives 50 per cent shortening. Now, when $C_0/C_t = 0$ and the ascending line is horizontal, that is, when it coincides with the abscissa, then the intersection occurs at $\Omega_1 = \pi/2$ and from (137) we obtain $l_{\min} = 0.75\lambda$, which is a three-quarter-wave-length distribution. This is true since an infinitely small condenser C_0 means an open circuit.

CHAPTER XII

DIRECTIVE SYSTEMS¹

Directive aerial systems are desirable in many cases since the radiated power can be directed along certain space channels. It is thus possible to guide aeroplanes, etc., and to project radio signals to certain localities (beam radiation).

161. Theory of the Wave Antenna (Beverage Antenna).²—The simplest type of wave antenna is given in the upper diagram of Fig. 246. It consists of a long horizontal aerial which has a length at least equal to one wave length and which points toward the sender. The arriving electromagnetic wave moves with the velocity of light c along the horizontal wire and induces a current in it. Hence waves travel in the wire

¹ MACDONALD, H. M., Note on Horizontal Receivers and Transmitters in Wireless Telegraphy, *Electrician*, **63**, 312, 1909; E. BELLINI, Aerials for Directive Wireless Telegraphy, *Jahrb. drahtl.*, **2**, 381, 608, 1909; J. ZENNECK, Arrangement for Directive Telegraphy, *Jahrb. drahtl.*, **9**, 417, 1915; F. BRAUN, On the Substitution of Open Conductors by Closed Circuits, *Jahrb. drahtl.*, **8**, 1, 1914; An Absolute Determination of the Radiation Field at Strassburg Due to the Radiation from the Eiffel Tower, *Jahrb. drahtl.*, **8**, 132, 212, 1914; A. ESAU, The Frame Antenna Due to Braun, *Elektrotech. u. Maschinenbau*, **37**, 401, 1919; J. H. DELLINGER, *Bur. Standards, Sci. Paper* 354, 1919; H. R. TRAUBENBERG, On the Quantitative Determination of Radiation Fields, *Jahrb. drahtl.*, **14**, 569, 1919; M. ABRAHAM, Coil in the Radiation Field Compared with Antenna, *Jahrb. drahtl.*, **14**, 259, 1919; R. MESNY, On the Radiation of a Frame, *L'onde élec.*, **2**, 571, 1923; H. CHIREIX, Directive Antennas, *Radioélectricité*, **5**, 65, 1924; *L'onde élec.*, **54**, 262, 1926; L. BOUTHILLON, "Optic and Radioelectricity," *L'onde élec.*, 287, 1923; 577, 1926; A. ESAU, Direction Characteristics of Antenna Combinations, *Jahrb. drahtl.*, **27**, 142, 1926; **28**, 1, 147, 1926; E. GREEN, Directive Reception, *Exptl. Wireless*, **25**, 828, 1925; W. W. TATARINOFF, The Construction of the Radio Mirror, *Jahrb. drahtl.*, **28**, 117, 1926; K. STRECKER, "Hilfsbuch für die Elektrotechnik, Schwachstromausgabe," 10^{te} Auflage, Julius Springer, Berlin, 1928; E. GREEN, Calculation of Polar Curves of Extended Aerial Systems, *Exptl. Wireless*, **4**, 587, 1927; J. A. FLEMING, Approximate Theory of the Flat Projector (Franklin) Aerial Used in the Marconi Beam System, *Exptl. Wireless*, **4**, 387, 1927; W. BURSTYN, The Radiation and Direction Effect in Free Space, *Jahrb. drahtl.*, **13**, 362, 1918–1919; W. H. MURPHY, Space Characteristics, *J. Franklin Inst.*, **201**, 420, 1926; W. BURSTYN, Wireless Telegraphy in Space, *Jahrb. drahtl.*, **18**, 322, 1920; R. MESNY, Directive Transmission with Grid Antennas, *L'onde élec.*, **6**, 181, 1927; R. M. FOSTER, *Bell System Tech. J.*, **5**, 292, 1926; G. C. SOUTHWORTH, *Proc. I.R.E.*, **18**, 1502, 1930; H. DIAMOND, *Bur. Standards, J. Res.*, **10**, 7, 1933; F. G. KEAR, *Proc. I.R.E.*, **22**, 847, 1934.

² BEVERAGE, H. H., C. W. RICE, and G. W. KELLOG, *Trans. A.I.E.E.*, **90**, 258, 372, 510, 635, 728, 1923; H. BUSCH, *Jahrb. drahtl.*, **21**, 290, 374, 1923.

in opposite directions with a velocity v which is smaller than c . The current wave traveling toward the receiver increases as it passes on since the electromagnetic wave in space moving in the same direction (although with somewhat larger velocity) keeps on feeding into the line while the traveling wave toward the transmitter is thereby weakened. If the resistance R at the end toward the sender is adjusted to the value of the wave resistance $Z_0 = \sqrt{L/C}$ of the line, all wave trains traveling toward

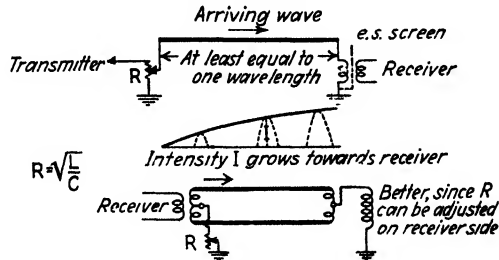


FIG. 246.—Wave antenna.

R will be completely absorbed by it and no reflections are possible at this end. The aerial then acts as an ordinary resistance and receives only in one direction. The direction effect becomes more pronounced as more wave lengths are developed on the antenna. Even if R is not exactly $= \sqrt{L/C}$, a certain direction effect is experienced for a long aerial since the reflected wave arrives with much diminished amplitude at the receiver side.

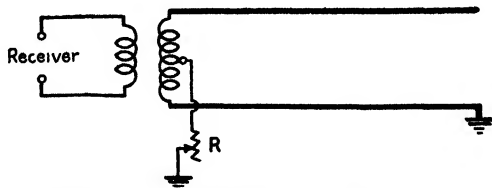


FIG. 247.—Open-ended parallel-wire system acting as wave antenna.

The lower diagram of Fig. 246 shows a wave antenna with two wires (a parallel-wire system). For this case, the wave resistance can be adjusted on the receiving end of the apparatus. The receiving set is on the end pointing toward the transmitter. The other end is closed through a transformer and both wires serve as return wires. This is evident from the following: When an electromagnetic wave comes from the left, that coil which is grounded at the right side returns the energy and the antenna acts like a parallel-wave system, which gives off the energy at the left end. When a wave arrives from the right, the corresponding currents in the two primary halves of the detector transformer cancel each other.

In Table XXV, the experimental constants for a single-wire and double-wire wave antenna are given. Figure 247 gives the case of an open-ended parallel-wire wave antenna.

TABLE XXV

Constant	Single-wire antenna	Double-wire antenna
L	2.31 mh/km	1.59 mh/km
C	0.006 μ f/km	0.0098 μ f/km
v/c	0.853	0.806
$Z_0 = \sqrt{\frac{L}{C}}$	592 ohms	384 ohms
α (see p. 446)	0.039	0.056

In order to have a picture of the respective currents I_1 and I_2 which pass to ground at each end, they are plotted in Fig. 248 to the same scale.

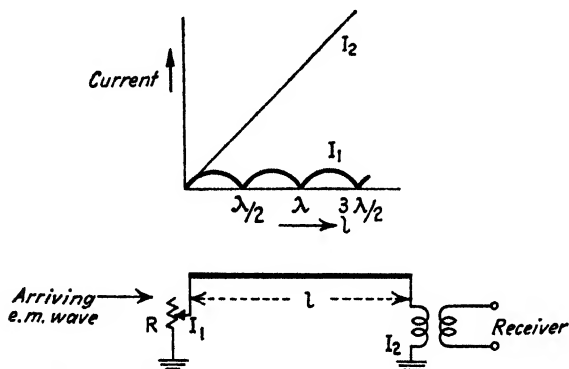


FIG. 248.—Currents at the two ends of a wave antenna for $v = c = 2.9982 \times 10^8$ km/sec.

The wave velocity along the aerial is for this case assumed equal to the velocity of an electromagnetic wave in free space. The theory shows that for such an assumption, that is, $p = v/c = 1$, the respective currents are

$$\begin{aligned} I_1 &= \frac{\varepsilon \lambda}{4\pi Z_0} \sin \frac{2\pi l}{\lambda} \\ I_2 &= \frac{\varepsilon \cdot l}{2Z_0} \end{aligned} \quad (1)$$

where ε denotes the electric gradient in volts per kilometer.

Example.—A wave antenna has a length $l = 2.5$ km, $\varepsilon = 0.0314$ volt/km, the wave resistance of the antenna $Z_0 = 500$ ohms, $v = c = 3 \times 10^8$ km/sec and wave length of the arriving electromagnetic wave $\lambda = 10$ km. Then

$$I_1 = \frac{0.0314 \times 10}{4\pi 500} = 5 \times 10^{-4} \text{ amp}$$

and

$$I_2 = \frac{0.0314 \times 2.5}{1000} = 7.85 \times 10^{-5} \text{ amp}$$

while, for $l = 7.5 \text{ km}$, $I_2 = 23.55 \times 10^{-5} \text{ amps}$, and since I_1 is as before, a pronounced directional effect occurs. For $l = \lambda/2, 3\lambda/2$, etc., I_1 for the ideal case ($v = c$) is equal to zero (Fig. 248). As Table XXV shows, the phase velocity along the aerial is smaller than c , often as small as $v = 0.8c$. This is due to the long wires which must be held by insulators and are only a short distance above ground. The electrical length is then no longer, as above, $\beta l = 2\pi l/\lambda$ but $\beta l = 2\pi l/(p\lambda)$ for $p = v/c$. The respective currents are

$$\begin{aligned} I_1 &= \frac{p\epsilon\lambda}{2\pi[1+p]Z_0} \sin \frac{l[1+p]\pi}{p\lambda} \\ I_2 &= \frac{p\epsilon\lambda}{2\pi[1-p]Z_0} \sin \frac{l[1-p]\pi}{p\lambda} \end{aligned} \quad (2)$$

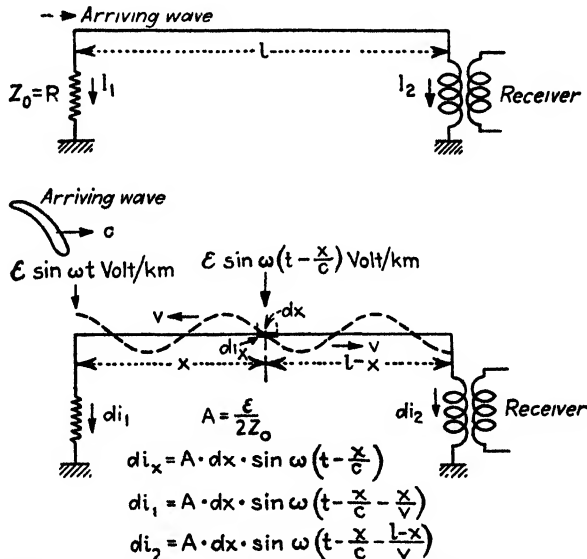


FIG. 249.—Building up of currents di_1 and di_2 at the respective ends of a wave antenna.

The proof of these formulas which hold generally, according to Fig. 249, is as follows: Imagine an infinitesimally small antenna element dx . The arriving electromagnetic wave following a sine law produces at the beginning of the line a gradient $\mathcal{E} \sin \omega t$ volts/km. Since the electromagnetic wave travels with a velocity c in the space near the line, it must take x/c seconds until the wave reaches the infinitesimal section dx of the line. Hence we have at this place the gradient $\mathcal{E} \sin \omega[t - x/c]$ volts/km. In the length dx an e.m.f. $e_x = \mathcal{E} dx \sin \omega[t - x/c]$ and a corresponding current di_x is induced. Since $R = \sqrt{L/C} = Z_0$, the induced current experiences a total resistance $2Z_0$ and is $di_x = e_x/2Z_0$. This causes a flow of current in both directions which is propagated with

the somewhat smaller velocity v . Hence the e.m.f. in dx produces the resulting currents di_1 and di_2 at the respective ends which lag behind the current di_x since it takes x/v sec. before the disturbance reaches the left end and $(l - x)/v$ sec. before it reaches the receiver coupling coil at the right end of the wave antenna.

The measured effective values of the respective currents is obtained by the integration of di_1 and di_2 between the limits $x = 0$ and $x = l$; that is,

$$\left. \begin{aligned} I_1 &= A \int_0^l \sin \omega[t - bx] dx \\ I_2 &= A \int_0^l \sin \omega \left[t - \frac{l}{v} + ax \right] dx \end{aligned} \right\}$$

for

$$A = \frac{\varepsilon}{2Z_0} \quad a = \frac{1}{v} - \frac{1}{c} \quad b = \frac{1}{v} + \frac{1}{c}$$

For $B = A/(\omega b)$, we obtain the solution for I_1

$$\begin{aligned} I_1 &= B \left[\cos \omega(t - bx) + \text{constant} \right]_0^l \\ &= B [\cos \omega t \cdot \cos \omega bl - \cos \omega t + \sin \omega t \sin \omega bl] \\ &= B \{ [\cos \omega bl - 1] \cos \omega t + \sin \omega bl \sin \omega t \} \\ &= B \left\{ -2 \sin \frac{\omega bl}{2} \sin \frac{\omega bl}{2} \cos \omega t + 2 \sin \frac{\omega bl}{2} \cos \frac{\omega bl}{2} \sin \omega t \right\} \\ &= 2B \sin \frac{\omega bl}{2} \left[\cos \frac{\omega bl}{2} \sin \omega t - \sin \frac{\omega bl}{2} \cos \omega t \right] \\ &= 2B \sin \frac{\omega bl}{2} \sin (\omega t - \varphi) \end{aligned} \quad (2a)$$

For $\varphi = \omega bl/2$. The factor $\sin (\omega t - \varphi)$ plays no part in the value of the measured effective current and we can write

$$\begin{aligned} I_1 &= 2B \sin \frac{\omega bl}{2} \\ &= \frac{2A}{\omega b} \sin \frac{\omega bl}{2} = \frac{\varepsilon}{\omega b Z_0} \sin \frac{\omega bl}{2} \end{aligned}$$

But

$$\omega b = \omega \left[\frac{1}{v} + \frac{1}{c} \right] = \frac{\omega}{v} [1 + p] = \beta [1 + p]$$

hence

$$I_1 = \frac{\varepsilon}{\beta [1 + p] Z_0} \sin \frac{1}{2} \beta [1 + p] l \quad (3)$$

which leads to the I_1 relation of (2) by putting $\beta = 2\pi/(\rho\lambda)$. If the integration is carried out in the same way for di_2 , we find an expression as (3) with the exception that $(-p)$ appears instead of p . Hence

$$I_2 = \frac{\varepsilon}{\beta[1 - p]Z_0} \sin \frac{1}{2}\beta[1 - p]l \quad (3a)$$

From the solutions given in (2), we can calculate for an actual case in which $v < c$. For instance, making the same assumptions as for the ideal wave antenna when $\varepsilon = 0.0314$ volt/km, $Z_0 = 500$ ohms $\lambda = 10$ km, $l = 7.5$ km, but $v = 0.8c$; that is, $p = 0.8$. Then

$$I_1 = \frac{0.8 \times 3.14 \times 10^{-2} \times 10}{2\pi \times 1.8 \times 500} \sin \frac{7.5 \times 1.8}{0.8 \times 10} 180^\circ = 25.8 \mu \text{ amp}$$

$$I_2 = \frac{0.8 \times 3.14 \times 10^{-2} \times 10}{2\pi \times 0.2 \times 500} \sin \frac{7.5 \times 0.2}{0.8 \times 10} 180^\circ = 222.5 \mu \text{ amp}$$

We have therefore a very good directional effect. For a wave antenna for which a full wave-length distribution ($l = \lambda$) exists, only the factor with the sine term changes; hence

$$I_1 = 44.4 \times 10^{-6} \sin \frac{1+p}{p} \pi = 31.4 \mu \text{ amp}$$

$$I_2 = 400 \times 10^{-6} \sin \frac{1-p}{p} \pi = 282.8 \mu \text{ amp}$$

According to the theory of the line, we have for the surge impedance

$$Z_0 = \sqrt{\frac{r^2 + \omega^2 L^2}{g^2 + \omega^2 C^2}} \cong \frac{\sqrt{r^2 + \omega^2 L^2}}{\omega C}$$

The wave resistance is therefore somewhat dependent on the frequency $\omega/2\pi$. If we also neglect r^2 in comparison with $\omega^2 L^2$, we have $Z_0 = \sqrt{L/C}$, a quantity which is apparently independent of the frequency. The high-frequency formulas for L and C show, however, that Z_0 is not exactly constant. But, for practical work, $\sqrt{L/C}$ may be regarded as an ohmic resistance since for such experiments the accuracy of the method is usually hardly better than 1 per cent. When the wave antenna is grounded through a resistance $R = Z_0$, or a parallel-wire system is closed at the end through Z_0 , the entire line is *aperiodic*; that is, it acts as though it did not possess any capacitance and inductance. This gives means for finding the wave resistance experimentally.

The wave antenna usually consists of a horizontal wire about 3 m above ground. For a construction of this kind, the vertical lead-in does not play a part in the direction effect. If the horizontal wire is brought closer to ground, the velocity v of propagation decreases. This velocity determines the maximum length l of the wave antenna, since, for instance, for a velocity $v < c$, the antenna wave falls back more and more behind the space wave, until points are reached for which counter-

phase effects (current decrease) occur. The maximum length l_{\max} can for $p = v/c$ be calculated from

$$l_{\max} = \frac{\lambda}{4[(1/p) - 1]} \quad (4)$$

Example: $\lambda = 500$ m, $v = 0.9$ c; that is, $p = 0.9$,

$$l_{\max} = \frac{500}{4[(10/9) - 1]} = 1125 \text{ m}$$

and the wave antenna can only be somewhat longer than 2λ .

Moreover, it can be shown that, for a wave antenna, the direction factor is given by

$$D = \cos \theta \sqrt{\frac{2e^{-\alpha l} \left\{ \cosh \alpha l - \cos \left[\frac{2\pi l}{p\lambda} [1 - p \cos \theta] \right] \right\}}{\alpha^2 + \left\{ \frac{2\pi l}{p\lambda} [1 - p \cos \theta] \right\}^2}} \\ = D_0 \cos \theta \quad (5)$$

since the arriving electromagnetic wave induces in each line element dx an e.m.f. proportional to the cosine of the angle of incidence of the wave with respect to the line. Hence the wave antenna is excited only when the arriving field is somewhat tilted so that the horizontal antenna wire cuts the lines of magnetic force. In other words, the wave antenna would *not show directive properties if the ground were a perfect conductor*. When the wave comes from the front, $\theta = 0^\circ$ and, when it comes from the rear, $\theta = 180^\circ$. Therefore if we neglect the damping ($\alpha = 0$), that is, put $\cosh \alpha l = 1$ and assume for simplicity that the velocity of propagation is equal to that in free space, then $v = c$, $p = 1$, and (5) reduces to

$$D = \frac{\cos \theta \sqrt{2 \left\{ 1 - \cos \frac{2\pi l}{\lambda} [1 - \cos \theta] \right\}}}{\frac{2\pi l}{\lambda} [1 - \cos \theta]} \quad (6)$$

Hence for a wave coming from the rear $\cos \theta = -1$, the value of

$$D' = \frac{\lambda \sqrt{2 \left[\cos \frac{4\pi l}{\lambda} - 1 \right]}}{4\pi l} \quad (6a)$$

should be zero. However, this is only the case when $\cos (4\pi l/\lambda) - 1 = 0$; that is, $\cos (2\pi l/\lambda) = 1$, which happens when the length l of the line is $\lambda/2$ or any integral multiple of $\lambda/2$. That this is more or less true can be seen from the diagrams of Fig. 250. When the length l is equal

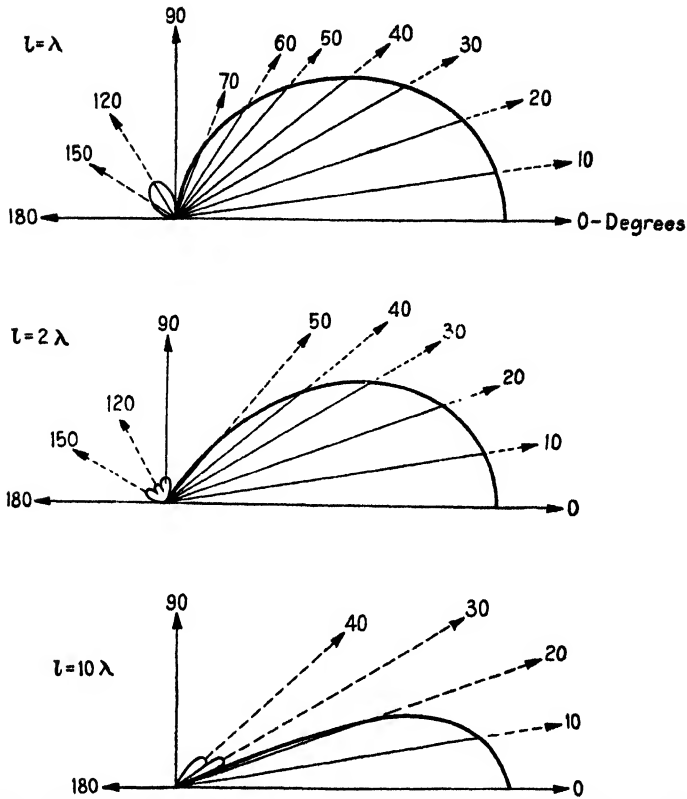


FIG. 250.—Direction effects of long aerials which develop from one to ten wave lengths.

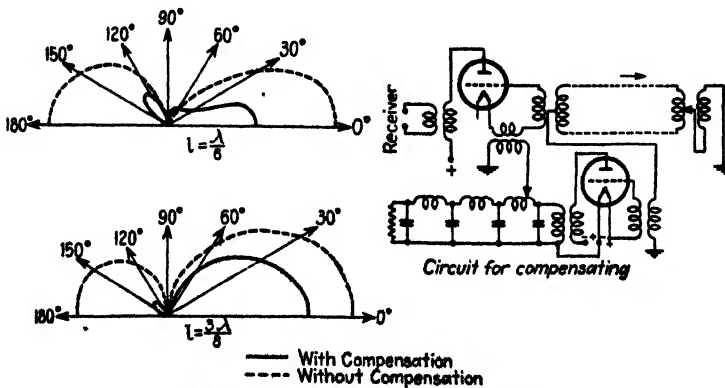


FIG. 251.—Direction characteristics.

to only one wave length, small components for the waves coming from the rear exist. For $l = 2\lambda$, the components are still less pronounced and, for $l = 10\lambda$, they disappear altogether. This, however, is not the case for the other wave-length distributions. For instance, for $l = \lambda/6$ and $l = \frac{3}{8}\lambda$, we obtain the dotted direction characteristics indicated in Fig. 251. The rear effect can, however, be greatly reduced (full-line characteristics) when a compensation due to Beverage is applied. The compensation is accomplished by means of a recurrent network similar to that used in filter circuits. The recurrent network of Fig. 251 acts as a phase changer so that the disturbing wave reaching the other end is again brought to the receiver circuit with such a phase and amplitude as to neutralize the effect of the disturbing wave reaching the receiver directly.

162. Sommerfeld-Pfrang Reciprocity Theorem,¹ the Carson Theorem, the Lorentz Theorem and Ballantine's Combined Lorentz-Carson Theorem.— A_1 and A_2 are two antennas located at O_1 and O_2 , respectively, with arbitrary orientations. Signals are first sent from A_1 and received by A_2 and then sent with the same average power from A_2 and received by A_1 . The intensity and phase of the electric field at the receiver A_1 will then be equal to that previously produced at A_2 regardless of the electrical properties and geometry of the intervening media and the form of the antennas.

If the Sommerfeld-Pfrang theorem is correct, it does not matter whether the equations for antennas of any kind are derived from the standpoint of the antenna as a sender or as a receiver. The theorem is based on the Lorentz reciprocal theorem which is as follows: If ξ_1 , H_1 are the field vectors of a wavelike disturbance from a source A_1 located at O_1 and ξ_2 , H_2 the corresponding field vectors of a wavelike disturbance originating in A_2 from a source at O_2 , then we have for vector products

$$\int \int_{1+2} [\xi_1 \times H_2] dS = \int \int_{1+2} [\xi_2 \times H_1] dS \quad (7)$$

or

$$\int \int_1 [\xi_1 \times H_2]_n dS_1 + \int \int_2 [\xi_1 \times H_2]_n dS_2 = \int \int_1 [\xi_2 \times H_1]_n dS_1 + \int \int_2 [\xi_2 \times H_1]_n dS_2$$

where the surface integrals are taken over the closed surfaces 1 and 2 surrounding the sources A_1 and A_2 , respectively. The Lorentz theorem can also be written in the form

$$\text{div} [\xi_1 \times H_2] = \text{div} [\xi_2 \times H_1] \quad (8)$$

¹ *Jahrb. drahtl.*, 26, 93, 1925 (this paper is reviewed in detail by S. Ballantine, *Proc. I.R.E.*, 16, 513, 1928); S. BALLANTINE, *Proc. I.R.E.*, 17, 929, 1929; J. R. CARSON, *Proc. I.R.E.*, 17, 952, 1929; R. M. WILMOTTE, *J. I.E.E.*, 17, 306, 1929.

The Carson theorem which is based on the Rayleigh reciprocal theorem (which holds for quasi-stationary systems only) is as follows: Let a distribution of impressed periodic electric intensity

$$\xi_1 e^{j\omega t} = \xi_1(x, y, z) e^{j\omega t}$$

produce a corresponding distribution of current density

$$I_1 e^{j\omega t} = I_1(x, y, z) e^{j\omega t}$$

and let a second distribution $\xi_2 e^{j\omega t}$ produce a second distribution $I_2 e^{j\omega t}$ of current density, then for the scalar product we have

$$\iiint [\xi_1 \cdot I_2] d\tau = \iiint [\xi_2 \cdot I_1] d\tau \quad (9)$$

The volume integration is extended over all conductive and dielectric media. The Carson theorem is therefore the generalized Rayleigh theorem. If there are any two circuits of insulated wire *A* and *B* and in their vicinity any combination of wire circuits or solid conductors in communication with condensers, a periodic e.m.f. in the circuit *A* will give rise to the same current in *B* as would be excited in *A* if the e.m.f. operated in *B*.

According to Carson's theorem, the only restriction is that the current (conduction plus polarization) must be a linear function of the electric-field intensity. The medium can vary arbitrarily from point to point. Transmitting and receiving aerials are unrestricted in their physical form and disposition with respect to other bodies. For short-wave problems, the Sommerfeld-Pfrang theorem as well as the Carson theorem fails since the waves are propagated partially through the ionized layer in which the earth's magnetic field has an appreciable effect on the conduction currents.

The main restrictions of the Sommerfeld-Pfrang theorem are the following: (a) The sending and the receiving aerials must not have arbitrary geometrical forms, but both must behave like simple electric or magnetic *dipoles*, as far as their radiation fields are concerned. (b) The sending and receiving aerials must be far enough away and isolated from other conducting bodies (including the earth) so as to make the reflected field due to induced currents and charges in such bodies negligible in the neighborhood of the sender antenna.

Restriction *a* can be readily understood from the proposition indicated in Fig. 252 which, according to S. Ballantine,¹ is the work of L. Hochgraf. Two equal antennas A_1 and A_2 are oriented such that one is in the equatorial plane of the other, and both are excited in the full-wave-length distribution. According to the Sommerfeld-Pfrang theorem, these antennas radiate equal average power since the received

¹ *Loc. cit.* and *Proc. I.R.E.*, 12, 838 and Fig. 3, 1924.

field strength at A_2 due to the radiation of a certain average power from A_1 is equal to that at A_1 with radiation of the same average power from A_2 . This is, however, not true when the aerial does not act as a dipole. The electric-field intensity at A_2 and due to source A_1 is finite, while that produced at A_1 due to source A_2 is zero for a large distance since antenna A_1 is in the equatorial plane of antenna A_2 .

Over the surface of integration 1 [Eq. (7)] enclosing the source A_1 , the vectors ξ_2 , H_2 are assumed constant, and similarly over the surface of integration 2 enclosing source A_2 the vectors ξ_1 , H_1 are taken as constant. The Sommerfeld-Pfrrang theorem, therefore, cannot be used to solve problems with extended antenna arrays and those involving wave antennas.

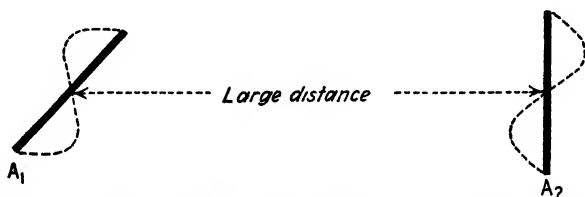


FIG. 252.—Two equal aeriels for which A_1 is in the equatorial plane of A_2 .

According to S. Ballantine,¹ the expressions of Lorentz [Eq. (7)], who surrounds all sources with a surface integral, and of Carson [Eq. (9)] who uses the volume integral over all space, assuming that all external influences could be accounted for by ponderomotive forces on the electricity can be combined and give

$$\iiint [\xi_1 \cdot I_2 - \xi_2 \cdot I_1] d\tau = \frac{c}{4\pi} \iint [\xi_1 \times H_2 - \xi_2 \times H_1]_n dS \quad (10)$$

where I_1 and I_2 denote the total current densities $\left[= \left(\sigma + \frac{\kappa}{4\pi} \right) \frac{\partial(\xi_{1,2} + \xi)}{\partial t} \right]$ resulting from the action of ξ_1 and ξ_2 , respectively, if all quantities vary as $e^{j\omega t}$ and if the properties of the medium μ , κ , σ are scalars and independent of ξ and H . This is evident since, for an impressed force, the field equations for the quasi-stationary state ($\partial/\partial t = j\omega$) are in Gaussian units

$$\begin{aligned} \xi_1 &= \frac{c \cdot \text{curl } H}{4\pi[\sigma + (j\omega\kappa/4\pi)]} - \xi \\ c \cdot \text{curl } \xi &= -j\omega\mu H \\ \text{div } \mu H &= 0 \\ \text{div } \kappa \xi &= 0 \end{aligned}$$

¹ Loc. cit.

Application.—A normally polarized wave¹ induces a certain distribution in a vertical receiver antenna, and the same antenna (Fig. 253) is excited by a generator. What is the condition for the same distribution, and what is the effective height? If I_x denotes the effective current through any current element dx , the effective height h_e is given by

$$\int_0^h I_x dx = Ih_e \quad (11)$$

where I denotes the maximum value measured at the base (Fig. 213, page 350). For the electric vector \mathcal{E} in terms of the magnetic vector H of an electromagnetic wave, we have

$$\mathcal{E} = cH$$

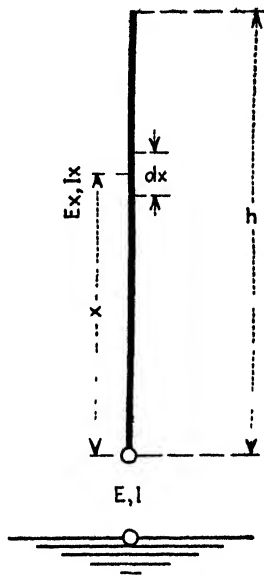
Hence each antenna element will be cut by the magnetic field $H\epsilon^{i\omega t}$ with a velocity c and an e.m.f. cHh_e will be induced between the ends of the vertical wire. Assume now that the vertical wire is excited by a harmonic e.m.f. $E\epsilon^{i\omega t}$ at the ground end so that the same current is produced at that point as by an incoming wave of strength $H\epsilon^{i\omega t}$. The problem is to find the value for the e.m.f. E to be inserted. The reciprocity theorem states that in any element dx the current I_x produced by E will be equal to the current at the point of application of E due to an equal voltage E_x impressed at dx . Here x denotes the distance along the vertical wire. But the effective height h_e is also defined as

$$h_e^{(m)} = \frac{E}{\mathcal{E}} \quad (12)$$

if E is the induced voltage in volts and \mathcal{E} the electric-field intensity in volts per meter. But, according to (11),

$$h_e = \frac{1}{I} \int_0^h I_x dx \quad (13)$$

¹ The direct wave of a sender is generally so propagated that, for good conducting ground (for instance, ocean), the electric vector ξ is perpendicular to it, but for ground of relatively poor conductivity it tilts forward by a few degrees (p. 352 and Table XIII) while the magnetic field *always* oscillates parallel to the surface of the earth. Such waves are said to be "normally polarized." The plane of polarization is formed by the direction of the electric vector and the direction of propagation and is perpendicular to the magnetic vector H .



and combining (12) and (13) shows that

$$\frac{E}{\varepsilon} = \frac{1}{I} \int_0^h I_x dx$$

or

$$EI = \int_0^h \varepsilon I_x dx \quad (14)$$

The same expression can also be obtained by integrating the relation $EI = E_x I_x$ for each line element dx if it is remembered that the impressed voltage acting upon the length dx in a receiving antenna is the component of the electric vector along the wire. The effective height can therefore be calculated from (13) if the current distribution is known. For a vertical antenna with no loading, according to Fig. 240, we have

$$I_x = I \cos \frac{2\pi}{\lambda} x$$

and thus obtain the effective height

$$\int_0^h \cos \frac{2\pi x}{\lambda} dx = 0.636h$$

since, for the fundamental, $h = \lambda/4$.

163. The Theory of the Loop Antenna as a Receiver with Special Reference to Field-intensity Measurements and the Determination of Effective Height.¹—A loop antenna is an antenna consisting of one or more complete turns of wire. This is also called a "coil antenna" or "frame antenna." According to the expression $\varepsilon = cH$, the relations for the coil antenna can be derived either by means of the magnetic flux² passing across the plane of the frame or by means of the electric-field intensity along the wire of the loop. A loop antenna as indicated in Fig. 254 possesses at first only a single turn enclosing the area $S = a \cdot h$ and is suspended so that its plane is perpendicular to relatively good-conducting ground and in such a way that it points to the transmitter. The arriving wave is normally polarized. The two vertical sides of the frame act as two vertical antennas for which the induced voltage $E^{(\text{volts})}$, according to (12), is

$$E = \varepsilon \cdot h_e$$

if the electric-field intensity is expressed in volts per meter and the effective height h_e in meters. The resulting voltage E_r is the *geometric* sum

¹ The derivation is for sinusoidal field vectors.

² The electric- and magnetic-field intensities ε and H are for space waves always in phase; that is, when ε has at any place a maximum value, the same is also true for H at that place. This is not true for stationary or standing waves since at times the energy can be entirely electric and at other times entirely magnetic.

of the voltages E_1 and E_2 since there is a certain phase difference θ between E_1 and E_2 equivalent to the time (t sec) required for the arriving wave to pass from the left side of the frame to the right side. The phase difference is

$$\theta = \frac{2\pi a}{\lambda} \quad (15)$$

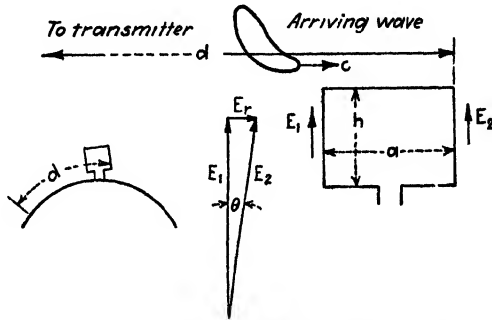


FIG. 254 —Induced voltages for frame aerial.

since the velocity of propagation $c = \lambda f = \lambda/T$; that is, $\lambda = cT$ and $a = ct$, and accordingly

$$\frac{a}{\lambda} = \frac{t}{T} = \frac{\theta}{2\pi}$$

According to the ordinary induction law, due to the magnetic flux $\Phi = \Phi_{\max} \sin \omega t$ which is interlinked with the loop, the instantaneous induced e.m.f. is

$$e = -\frac{d\Phi}{dt} = -\omega \Phi_{\max} \cos \omega t$$

with an effective value

$$E^{(\text{volts})} = \frac{\omega \Phi_{\max} 10^{-8}}{\sqrt{2}}$$

where $\omega = 2\pi f$. If $B_{\max} = \Phi_{\max}/S$, the flux density in gauss, that is, the number of magnetic lines of force per unit area of the area $S = a \cdot h$, for N turns, we have an induced voltage

$$E_r^{(\text{volts})} = \frac{\omega N B_{\max}^{(\text{gauss})} S^{(\text{cm}^2)}}{\sqrt{2}} 10^{-8} \quad (16)$$

According to $B = \mu H \approx H$ and $\epsilon = cH$, we have

$$\epsilon_{\max}^{(\text{abvolts/cm})} = c B_{\max}^{(\text{gauss})} = N f B_{\max} = \frac{\omega \lambda B_{\max}}{2\pi} \quad (17)$$

or

$$\omega B_{\max} \approx \frac{2\pi}{\lambda} \epsilon_{\max}$$

for the induced effective voltage we have

$$E_r^{(\text{volts})} = \frac{2\pi \varepsilon_{\max}^{(\text{volts/cm})} N S^{(\text{cm}^2)}}{\sqrt{2} \lambda^{(\text{cm})}} \quad (18)$$

The effective value of the magnetic-field strength, according to (16), is

$$H = \frac{E_r 10^5}{2\pi f N S}$$

if the frequency is expressed in kilocycles per second.

For measurements the frame is tuned and we find the effective resonance current I to be given by

$$E_r = I \cdot r$$

if r is the entire resistance of the loop antenna. The effective magnetic-field strength is then

$$H^{(\text{gilbert/cm})} = 159 \times 10^2 \frac{I^{(\text{amp})} r^{(\Omega)}}{f^{(\text{kc})} S^{(\text{cm}^2)} N} \quad (19)$$

which, because $\mu = 1$, also gives the effective flux density B in gauss. Because of the relation

$$\varepsilon^{(\text{volts/cm})} = 300 H^{(\text{gilbert/cm})} \quad (20)$$

for the effective electric-field intensity we have

$$\varepsilon^{(\text{volts/cm})} = 477 \times 10^4 \frac{I^{(\text{amp})} r^{(\Omega)}}{f^{(\text{kc})} S^{(\text{cm}^2)} N} \quad (21)$$

Since the effective height

$$h_e = \frac{E}{\varepsilon} = \frac{I \cdot r}{\varepsilon} \quad (22)$$

from (21), for the effective height of a loop antenna we obtain

$$h_e^{(\text{cm})} = 209 \times 10^{-9} f^{(\text{kc})} S^{(\text{cm}^2)} N \quad (23)$$

Since it is more common to express this quantity in meters, we find, from (21), that

$$\varepsilon^{(\mu\text{volts/m})} = 477 \times 10^8 \frac{I^{(\text{amp})} r^{(\Omega)}}{f^{(\text{kc})} a^{(\text{m})} h^{(\text{m})} N} \quad (24)$$

and the effective height

$$\begin{aligned} h_e^{(\text{m})} &= 209 \times 10^{-7} f^{(\text{kc})} a^{(\text{m})} h^{(\text{m})} N \\ &= \frac{6.28 a^{(\text{m})} h^{(\text{m})} N}{\lambda^{(\text{m})}} = 6.28 \frac{(\text{area of frame})(\text{number of turns})}{\text{wave length}} \end{aligned} \quad (24a)$$

The form factor of a loop antenna is therefore

$$F = 209 \times 10^{-7} f^{(\text{kc})} a^{(\text{m})} N \quad (25)$$

a quantity which can be readily calculated from the dimensions and the frequency, but only approximately estimated for open antennas.¹ For this reason, the loop antenna can be used for determining the effective height of other antennas. According to Eq. (64) on page 359, the electric-field strength at a distance d from an open antenna is

$$E(\mu\text{volts/m}) = 1.256 \frac{h_{e_s}^{(m)} I_s^{(amp)} f^{(kc)}}{d^{(km)}} \quad (26)$$

When a loop antenna is placed in the radiation field at a distance of about 10 wave lengths, the absorption factor can be neglected and the foregoing formula holds. Pointing the loop antenna toward the sender and tuning it to resonance gives the induced voltage

$$E_r = E h_{e_r} = I_r \cdot r$$

if r denotes the total effective resistance of the loop and I_r the received current, and

$$E(\mu\text{volts/m}) = \frac{I_r \cdot r 10^6}{h_{e_r}} \quad (26a)$$

Equating (26) and (26a) leads to the formula for the effective height of the sender antenna,

$$h_{e_s}^{(m)} = 796 \times 10^3 \frac{d^{(km)} r^{(\Omega)} I_r^{(amp)}}{h_{e_r}^{(m)} f^{(kc)} I_s^{(amp)}} \quad (27)$$

where h_{e_r} is given by (24). Solving this expression for I_r gives

$$I_r^{(\mu amp)} = 1.256 \frac{h_{e_s}^{(m)} h_{e_r}^{(m)} f^{(kc)} I_s^{(amp)}}{d^{(km)} r^{(\Omega)}} \quad (28)$$

a check on the received resonance current in microamperes when the effective height of the sender is already known. The same can be determined with the method of (27) and then used for other distances as in (28).

Substituting in (28) the value for h_{e_r} from (24) gives

$$I_r^{(\mu amp)} = 264 \times 10^{-7} \frac{h_{e_s}^{(m)} S^{(m^2)} I_s^{(amp)} [f^{(kc)}]^2}{d^{(km)} r^{(\Omega)}} \quad (29)$$

where S is the area of the frame in square meters.

This expression shows that the received current increases with the square of the frequency and is proportional to the area of the loop *irrespective of its shape*. This is, of course, self-evident from the induction

¹ $h_e = Fh = \frac{I_{av} \cdot h}{I_{max}} = \frac{1}{I_{max}} \int_0^h Idh$; I_{av} denotes the average effective current along the aerial of length h and I_{max} the value at the current loop.

law. It has a great bearing on waves that are not normally polarized. For instance, let us consider again plane-polarized waves but such that they have a forward tilt or are indirect rays. The loop (Fig. 255) is again pointed so that maximum current is received. We note that, for an elevation γ with the horizon, the resultant field intensity \mathcal{E} can be split into the components \mathcal{E}_1 and \mathcal{E}_2 and as such will produce circuital voltages in the same direction. Whereas, for a normal polarized wave, only the vertical sides of the loop act as antennas, in this case all four sides act in producing currents. This is different with a vertical antenna

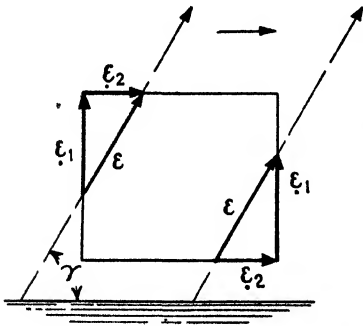


FIG. 255.—The electric vectors \mathcal{E}_1 and \mathcal{E}_2 show that only the area and not the shape of the frame aerial plays a part.

for which the component \mathcal{E}_2 is lost and only the \mathcal{E}_1 component is active. This can also be understood from the lines of magnetic force since the *loop cuts* just as many *lines* irrespective of the tilt. This is, of course, strictly true only when the loop is freely suspended and the effect of the ground is neglected.

It should be remembered that the preceding formulas hold only when the width a of the frame is smaller than about one-sixth of the wave length ($\lambda_{\min}/a > 6$) which is practically the case for most loop antennas as can be seen from Table XXVI dealing with loops of customary dimensions. When the width a is relatively large, the phase difference $\theta = 2\pi a/\lambda$ can no longer be expressed in the circular measure ($\theta = \sin \theta$ as for a small angle) but must be used in the formulas as a sine function. The effective height of a loop antenna then becomes

$$h_e^{(m)} = 2Nh^{(m)} \sin \frac{\pi a^{(m)}}{\lambda^{(m)}} = 2Nh^{(m)} \sin (1.045 \times 10^{-5} a^{(m)} f^{(kc)}) \quad (30)$$

since, according to Fig. 254, for 1 turn

$$E_r = 2E_1 \sin \frac{\theta}{2} = 2\mathcal{E}h \sin \frac{\theta}{2} = \left[2h \sin \frac{\pi a}{\lambda} \right] \mathcal{E} = h_e \mathcal{E}$$

instead of

$$E_r = E_1 \theta = \frac{2\pi a}{\lambda} E_1 = \left[\frac{2\pi a}{\lambda} h \right] \mathcal{E} = h_e \mathcal{E}$$

164. The Loop Aerial as Transmitter and Its Radiation Energy Compared with That of an Open Antenna.—If the sender current is of the form

$$i_s = I_{\max} \sin \omega t$$

TABLE XXVI

$\frac{\lambda_{\min}}{a}$	Construction of loop antenna				Electrical Quantities				
	Dimensions $a = h$ (Fig. 254)		Number of turns	Spacing of turns, inches	Induc- tance, μh	Frequency, kc/sec, with a variable condenser $C_{\min} = 5 \times 10^{-6} \mu f$; $C_{\max} = 5 \times 10^{-4} \mu f$		Wave length, m	
	Inches	Meters				f_{\max}	f_{\min}	λ_{\min}	λ_{\max}
16.6	10	0.254	4	0.25	10	7120	2252	42.11	133.3
15.7	10	0.254	4	0.5	9	7500	2375	39.98	126.3
14.75	10	0.254	4	0.75	8	7960	2520	37.67	119.0
13.9	10	0.254	4	1.0	7	8510	2695	35.23	111.3
29.3	10	0.254	8	0.25	31	4030	1280	74.40	234.2
25.8	10	0.254	8	0.5	24	4580	1456	65.46	206.1
23.5	10	0.254	8	0.75	20	5025	1593	59.60	187.8
21.6	10	0.254	8	1.0	17	5460	1726	54.91	173.8
15.8	12	0.305	4	0.25	13	6240	1978	48.05	159.5
14.5	12	0.305	4	0.5	11	6780	2150	44.22	139.5
13.8	12	0.305	4	0.75	10	7120	2252	42.11	133.3
13.1	12	0.305	4	1.0	9	7500	2375	39.98	126.3
13.1	20	0.508	4	0.25	25	4500	1426	66.63	211.0
12.2	20	0.508	4	0.5	22	4800	1522	62.46	197.2
11.7	20	0.508	4	0.75	20	5030	1592	59.61	188.6
11.4	20	0.508	4	1.0	19	5170	1635	57.99	183.3
12.4	24	0.61	4	0.25	32	3980	1260	75.33	238.0
22.2	24	0.61	8	0.25	103	2215	703	135.4	427.0
10.5	36	0.915	4	0.25	52	3120	988	96.10	303.1
19.3	36	0.915	8	0.25	173	1710	542	175.3	553.0
27.1	36	0.915	12	0.25	346	1210	383	247.8	783.0
41.5	36	0.915	20	0.25	809	792	250	379.0	1199.0

then its effect at a distance d is

$$i_d = I_{\max} \sin \omega \left[t - \frac{d}{c} \right]$$

since it takes the electromagnetic wave d/c sec to travel through the distance d . Consequently, we find the radiation effect for the loop antenna, as for the open antenna [pages 345 and 358], by means of the vector potential

$$\Lambda = \frac{\left[I_{\max} \sin \omega \left(t - \frac{d}{c} \right) \right] h}{d}$$

if, for simplicity, h denotes the effective height of a vertical wire, since the instantaneous value of the magnetic-field intensity is $H_i = 0.1(\partial \Lambda / \partial d)$. Hence in the direction of the plane of the frame (Fig. 256), we have to find the instantaneous electric-field intensities for a distance d and a distance $d - a$ which give the components

$$\begin{aligned}\mathcal{E}_{t_1}(\text{volts/cm}) &= 300H_{t_1} = \frac{30h\omega I_{\max}}{cd} \cos \left\{ \omega \left[t - \frac{d}{c} \right] \right\} \\ \mathcal{E}_{t_2} &= \frac{30h\omega I_{\max}}{cd} \cos \left\{ \omega \left[t - \frac{d-a}{c} \right] \right\}\end{aligned}$$

if we take the distance d large enough so that only radiation components exist. The term $(d-a)$ is practically equal to d in the denominator. But this approximation cannot be made in the cosine term since we are

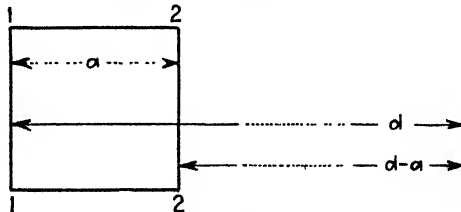


FIG. 256.—Width effect of frame aerial.

there concerned with phase differences. The instantaneous value of the resulting field strength is therefore

$$\mathcal{E}_t(\text{volts/cm}) = \frac{60h\omega I_{\max}}{cd} \sin \left\{ \omega \left[t - \frac{d - (a/2)}{c} \right] \right\} \sin \frac{\theta}{2}$$

since

$$\theta = \frac{a\omega}{c} = \frac{2\pi a}{\lambda}$$

The effective electric-field strength is then

$$\mathcal{E}(\text{volts/cm}) = \frac{60h\omega I}{cd} \frac{\theta}{2} = \frac{30a h \omega^2 I}{c^2 d}$$

or for a frame of N turns

$$\mathcal{E}(\mu\text{volts/m}) = 1315 \times 10^{-4} \frac{a^{(m)} h^{(m)} N I^{(\text{amp})} [f^{(\text{kc})}]^2}{d^{(\text{km})}} \quad (31)$$

According to Eqs. (50) and (50a) of page 350, we have, in the equatorial plane, for the effective intensity of the sinusoidal field

$$H = \frac{2\pi I d h}{\lambda \cdot d} \text{ c.g.s.}$$

while for a grounded antenna of effective height h_e , the corresponding amplitude values are

$$\left. \begin{aligned} H_{\max} &= \frac{4\pi I_{\max} h_e}{\lambda \cdot r} \text{ c.g.s.} \\ \mathcal{E}_{\max} &= \frac{4\pi c h_e I_{\max}}{\lambda \cdot d} \text{ c.g.s.} = 1.256 \frac{h_e^{(m)} I_{\max}^{(\text{amp})} f^{(\text{kc})}}{d^{(\text{km})}} \mu \text{ volts/m} \end{aligned} \right\} \quad (32)$$

if $I = I_{\max}/\sqrt{2}$ denotes the effective current measured at the base of the aerial. We find, therefore, at a distance large enough so that the radia-

tion term predominates, but not so large that the absorption factor must be taken into account, that the total direct-radiation energy passing through the hemisphere of radius d is

$$W_r^{(\text{ergs})} = \frac{c}{6} H_{\text{max}}^2 [d^{(\text{cm})}]^2$$

OR

$$\begin{aligned} W_r^{(\text{watts})} &= 5 \times 10^{15} H_{\text{max}}^2 [d^{(\text{km})}]^2 \\ &= 1579 \left[\frac{h_e}{\lambda} \right]^2 [I^{(\text{amp})}]^2 = R_r I^2 \\ &= 1754 \times 10^{-10} [h_e^{(\text{m})} f^{(\text{kc})} I^{(\text{amp})}]^2 \end{aligned} \quad (33)$$

The radiation energy can also be expressed in terms of the electric-field intensity and we find that

$$W_r^{(\text{watts})} = 111 \times 10^{-10} [d^{(\text{km})} \mathcal{E}^{(\mu \text{ volts/m})}]^2 \quad (34)$$

\mathcal{E} would in this case be the field strength which is determined for a loop antenna by means of (31). It is assumed in this procedure that the wave propagation between the antenna and the loop is not affected by attenuation. The radiation ability of an aerial can also be expressed by the product of the effective sender current at the current antinode and the effective height of the sender. This product is called the *meterampere* and, according to (33), is

$$\text{Meterampere} = I \cdot h_e = h_e \sqrt{\frac{W_r}{R_r}} \quad (35)$$

where R_r , according to (48) on page 349, is the radiation resistance. The effective height can, according to (32), be calculated from

$$h_e^{(\text{m})} = 796 \times 10^{-3} \frac{\mathcal{E}^{(\mu \text{ volts/m})} d^{(\text{km})}}{I^{(\text{amp})} f^{(\text{kc})}} \quad (36)$$

The radiation resistance of a loop antenna can be calculated from

$$R_r = 80\pi^2 \left[\frac{h}{\lambda} \right]^2 \quad (37)$$

since the Hertzian dipole¹ must be used for this case and not the Abraham

¹ For the Hertzian dipole, which is free in air, the radiation energy is

$$W_r = [80\pi^2 (h^2/\lambda^2)] I^2,$$

while for the Abraham dipole [Fig. 213 on p. 350] $h' = h/2$ (half of the dipole, the image is just as much below the ground as the antenna is above it)

$$W_r = [40\pi^2 (h^2/\lambda^2)] I^2.$$

Here the radiation occurs in the upper hemisphere only; hence

$$R_r = 40\pi^2 (h^2/\lambda^2) = 160\pi^2 (h'^2/\lambda^2)$$

where h' is the actual height of the elementary antenna.

dipole. This equation holds for any effective height h_e of the loop antenna and, according to (24), gives

$$R_r^{(\text{ohms})} = 80\pi^2 \left[\frac{h_e}{\lambda} \right]^2 = \frac{320\pi^4 N^2 S^2}{\lambda^4} \quad (38)$$

where the wave length is expressed in the same unit as the two dimensions a and h of the loop. This holds for a loop of any shape¹ since the loop radiates equally well in all directions in its plane. Therefore, for any loop of N turns and area S , the radiation resistance becomes

$$R_r^{(\text{ohms})} = 387 \times 10^{-20} [NS(\text{m}^2)]^2 \cdot [f(\text{kc})]^4 \quad (39)$$

165. Directional Effects of Linear and Coil Antennas.—We must distinguish between the directional effects of an antenna in the horizontal

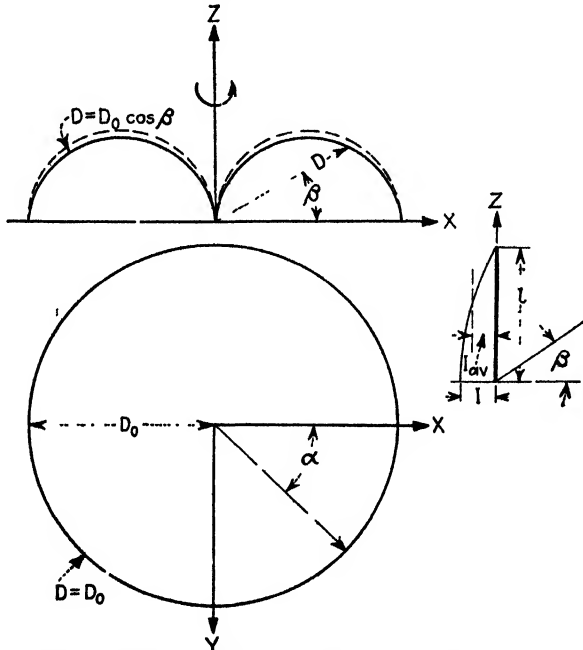


Fig. 257.—Direction characteristic for vertical antenna (antenna is axis of rotation).

plane and its space characteristics. The latter play a part in receiving and sending from aeroplanes and also for receiving indirect rays. For instance, a vertical antenna (Fig. 257) for normal polarized waves receives equally well waves coming in any horizontal direction (for any value α in the XY plane) but follows a cosine law in the XZ and any other plane

¹ For details see p. 470 in which it must be assumed that the loop is far enough from ground.

perpendicular to the surface of the earth. Theoretically, the vertical-wire antenna cannot send direct waves to a station directly above it. We see, therefore, that the directional effects in the equatorial plane and any plane perpendicular to it are

$$\left. \begin{aligned} D &= D_0 \\ D &= D_0 \cos \beta \end{aligned} \right\} \quad (40)$$

where D_0 denotes the radius of the polar diagram in the XY plane, and β denotes the elevation above ground. This is evident because the radiated field in the equatorial plane is proportional to the average effective current I_{av} along the wire times its length; that is,

$$\begin{aligned} D &= kI_{av}l \\ &= \frac{2}{\pi}kIl = D_0 \end{aligned}$$

while for any elevation β we have to multiply D_0 with $\cos \beta$. The quantity I denotes the effective current at the current antinode.

For the inverted L antenna, the characteristic in the horizontal plane is indicated in Fig. 258. The fields due to the height h and the flat top $(l - h)$ are no longer proportional to their lengths since the average values of the effective current along these parts are different. For the vertical portion, we have

$$I_{1_{av}} = \frac{1}{h} \int_0^h I \cos \left(\frac{\pi}{2l} z \right) dz = \frac{2lI}{\pi h} \sin \frac{\pi h}{2l}$$

and for the horizontal portion

$$I_{2_{av}} = \frac{1}{l-h} \int_h^l I \cos \left(\frac{\pi}{2l} z \right) dz = \frac{2lI}{[l-h]\pi} \left[1 - \sin \frac{\pi h}{2l} \right]$$

We have, therefore, the directional effect due to the vertical portion

$$D_1 = kI_{1_{av}}h = \frac{2klI}{\pi} \sin \frac{\pi h}{2l}$$

and the directional effect due to the horizontal portion

$$D_2 = kI_{2_{av}}(l-h) = \frac{2klI}{\pi} \left[1 - \sin \frac{\pi h}{2l} \right]$$

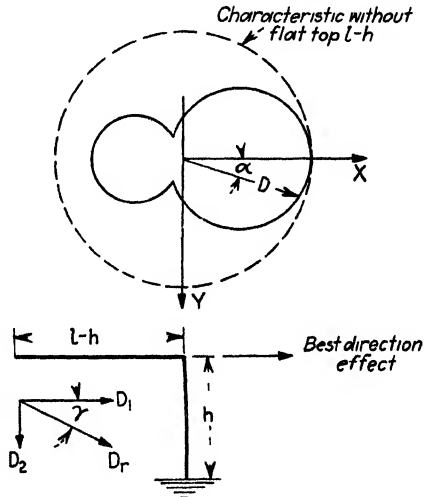


FIG. 258 —Direction effect of inverted L antenna compared with uniform radiation effect of vertical antenna

Hence the resultant field is inclined to the surface of the earth by an angle γ given by

$$\tan \gamma = \frac{D_2 [1 - \sin (\pi h/2l)]}{D_1 \sin (\pi h/2l)} \quad (41)$$

In this case we have absorption in the ground. For $l = 3h$, the fields due to the vertical and horizontal portion are equal since $\gamma = 45^\circ$.

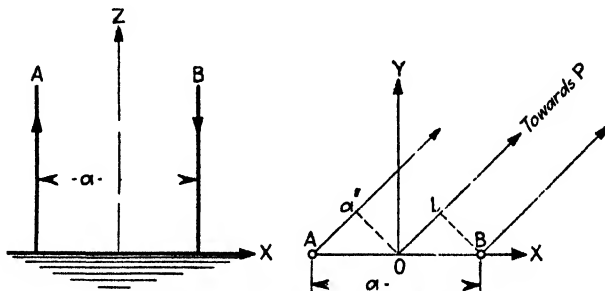


FIG. 259.—Distance action of two vertical aerials *A* and *B*.

In Fig. 259, two vertical antennas *A* and *B* are shown a distance *a* from each other. The antenna currents have equal amplitudes but a phase difference φ so that

$$\begin{aligned} i_A &= I \sin \omega t \\ i_B &= I \sin [\omega t + \varphi] \end{aligned}$$

Besides this, the waves traveling out to some distant point *P* will have a phase displacement ψ because of their path difference with respect to *O*.

The difference in path is *Ob*; hence $\frac{a}{2} \cos \alpha = \frac{t}{T} = \frac{\psi}{2\pi}$

or

$$\psi = \frac{\pi a}{\lambda} \cos \alpha = \frac{\omega a}{2c} \cos \alpha$$

At *P* we have, at any instant, the directional effects of the antennas *A* and *B*,

$$\left. \begin{aligned} d_A &= D_0 \sin \left[\omega t + \frac{\omega a}{2c} \cos \alpha \right] \\ d_B &= D_0 \sin \left[\omega t - \frac{\omega a}{2c} \cos \alpha + \varphi \right] \end{aligned} \right\} \quad (42)$$

For d_B , the phase displacement is negative because the wave due to *B* lags by $Ob = -\psi$, while the wave due to *A* is ahead by the same amount ($Ob = +\psi$). For the total field, we have then

$$d = 2D_0 \cos \left[\frac{\omega a}{2c} \cos \alpha - \frac{\varphi}{2} \right] \sin \left[\omega t + \frac{\varphi}{2} \right]$$

The amplitude value in any direction is

$$D = 2D_0 \cos \left[\frac{\omega a}{2c} \cos \alpha - \frac{\varphi}{2} \right] \quad (43)$$

An application of this is illustrated by the loop antenna for which the sender current as well as the resultant received current circulates around the loop. Hence the currents in *A* and *B* (Fig. 259) are 180 deg out of

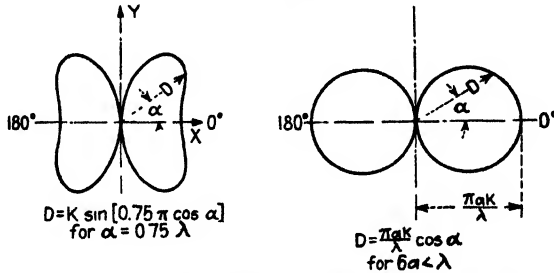


FIG. 260.—Direction characteristics of loop aerial in horizontal plane.

phase; that is, $\varphi/2 = 90^\circ$ and the directional effect of the loop antenna becomes

$$\begin{aligned} D &= 2D_0 \sin \left[\frac{\pi a}{\lambda} \cos \alpha \right] \\ &= K \frac{\pi a}{\lambda} \cos \alpha \end{aligned} \quad (44)$$

Since the width a is small compared with the wave length ($a < \lambda/6$) we have $\sin (\pi a/\lambda) = \pi a/\lambda$. The constant K is equal to $2D_0$. The directional characteristic of a loop antenna in the horizontal plane is a cosine function of the departure angle; that is,

$$D = F(\cos \alpha) \quad (45)$$

which gives two equal adjacent circles as in Fig. 260. The loop antenna has therefore a directional effect along the plane of the loop. As far as measurements with a loop antenna and with an ordinary open antenna are concerned, we obtain, for a loop antenna having the effective constants r , C , L , the differential equation

$$ri + L \frac{di}{dt} + \frac{c^2}{C} \int i dt = A \frac{dH}{dt} \cos \alpha \quad (46)$$

and, for an ordinary antenna,

$$ri' + L \frac{di'}{dt} + \frac{c^2}{C} \int i' dt = h_e \mathcal{E} \quad (47)$$

Equation (46) contains H and (47) contains \mathcal{E} itself, and since $\mathcal{E} = cH$ it is evident that the *exterior force* that acts on the loop is *different in phase* from the force that affects the open antenna. This can also be seen from (42) and (43) since the trigonometric function changes from a sine to a cosine term. For a single vertical wire as transmitter, the received current at any point P in the equatorial plane would be proportional to $\sin \omega[t - (d/c)]$.

The change in *intensity* for a change in frequency and in *damping* also varies *differently* for a loop from that for an open antenna. Thus, if the frequency or the damping is increased, the current increases more in the loop than in the open antenna. This explains why a loop receiver is less affected by static. These formulas can also be derived when a loop acts as a

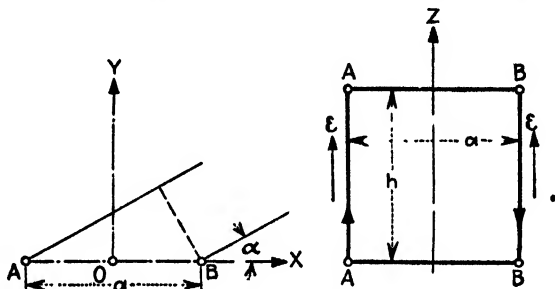


FIG. 261.—Loop aerial as receiver.

receiver. The induced e.m.f. in the vertical sides of the loop indicated in Fig. 261 is proportional to the height h and has a phase difference $(a\omega/c) \cos \alpha$ since the arriving wave $\mathcal{E} \sin \omega t$ makes an angle α with the plane of the loop. The resultant current flows as indicated in the figure. For N turns, the resultant e.m.f. is

$$\begin{aligned}
 E_r &= Nh\mathcal{E} \left[\sin \omega \left(t - \frac{d}{2c} \cos \alpha \right) - \sin \omega \left(t + \frac{d}{2c} \cos \alpha \right) \right] \\
 &= 2Nh\mathcal{E} \cos \omega t \sin \left(\frac{\pi d}{\lambda} \cos \alpha \right) \\
 &\cong \frac{2\pi ahN}{\lambda} \cos \alpha \cos \omega t \\
 &= \mathcal{E} h_e \cos \alpha \cos \omega t
 \end{aligned} \tag{48}$$

where h_e is the effective height of the loop. For an open antenna of an effective height h_e , we had $\mathcal{E} h_e \sin \omega t$. The same result is therefore obtained as for the loop as a transmitter.

166. Antenna Effect, Width Effect, and One-sided Loop System.—

If the capacity effect of the loop with respect to ground and other dissymmetries are not neglected, the directional characteristics of the loop are not as shown in Fig. 260. This loop antenna effect gives rise to

bearing errors since, for the effective height h_e of the loop and the fictitious height h_e' of the antenna, the resultant induced voltage, according to (48), becomes

$$E_r = \varepsilon \{ h_e \cos \alpha \cos \omega t + h_e' \sin \alpha t \} \quad (49)$$

if the condenser effects to ground are symmetrical. Otherwise these two effects are not exactly 90 deg out of phase. A current due to the antenna effect is therefore superimposed on the true induced loop current. This current can be decomposed into a component in phase with the true loop current and a component 90 deg out of phase. The latter is usually the most prominent term (because of the $\sin \omega t$ term in $h_e' \sin \omega t$) unless

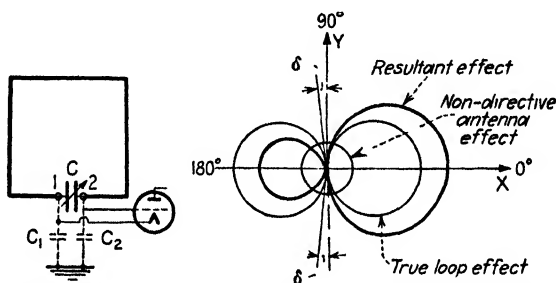


FIG. 262.—Bearing error for unsymmetrical antenna effects.

the parasitic antenna circuit is tuned to the arriving wave. The component 90 deg out of phase causes a small current for the positions $\alpha = 90^\circ$ and $\alpha = 270^\circ$ but does not shift the bearing. It only blurs the minimum positions. The component in phase with the true loop current causes a resultant current in the detector that is larger in one maximum position of the loop than when the loop is turned by 180 deg to obtain another maximum current response. But, for measurements, the minimum positions of the loop are more convenient positions for locating a sender direction. The plane of the loop is then perpendicular to the direction of propagation. With unsymmetrical antenna effects, the minimum positions are no longer 180 deg out of phase but make an angle of $(180 - 2\delta)$ only, as can be seen in Fig. 262. Terminal 1 of the tuning condenser sends more displacement current toward ground because it is connected with the batteries of the filament of the detector tube, while terminal 2 has a smaller fictitious condenser C_2 . The arriving electric field induces a voltage in the loop which is independent of the position of the loop, and which causes a larger displacement current from terminal 1 to ground than from terminal 2. This causes a potential difference across the tuning condenser and affects the indication on the detector instrument.

Now, if the undirective antenna effect is \hat{D}_0 , its phase with the true loop effect $D_1 \cos \alpha$ is about $\gamma = 90^\circ$ and is determined by C_1 , C_2 , and C . The resultant effect is

$$D = \sqrt{D_0^2 + D_1^2 \cos^2 \alpha + 2D_0D_1 \cos \alpha \cos \gamma} \quad (50)$$

an equation which proves that two minima positions exist, at

$$\alpha = 90^\circ + \delta \quad \text{and} \quad \alpha = 270^\circ - \delta$$

where

$$\sin \delta = \frac{D_0}{D_1} \cos \gamma \quad (51)$$

These minima are flat and unequal. Such dissymmetries can be balanced out by condensers C_1 and C_2 as indicated in Fig. 262. A three-plate

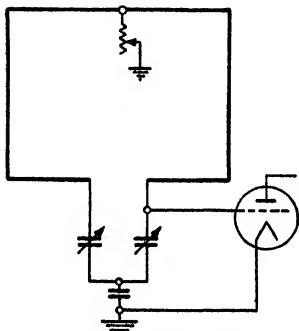


FIG. 263.—Capacitance potentiometer connection to receiver.

condenser could be used instead of C_1 and C_2 . The movable plates then connect to ground. Another way of avoiding the dissymmetry is due to Bellini and is shown in Fig. 263. The detector is coupled to a capacity potentiometer. The grid voltages due to the antenna effect and the loop effect are either in phase or in counterphase. By means of a variable resistance at the center of the loop, the magnitude of the antenna effect can be varied. The resultant direction effect is

$$D = D_0 \pm D_1 \cos \alpha \quad (52)$$

Another method is due to F. A. Kolster and F. W. Dunmore.¹ Two balancing condensers are used as in Fig. 262, together with a high-frequency transformer the primary of which is connected across C of Fig. 262 and the secondary across grid and filament. These portions of the apparatus are both within a grounded screen. From the direction diagram of Fig. 262 we note that the antenna effect makes the directional characteristic one-sided. It can therefore be used for sense finding. In addition to the loop antenna (Fig. 261) with the vertical sides $A-A$ and $B-B$, a vertical antenna OY can be used such that it is excited with an intensity twice that in $A-A$ and $B-B$ and in phase with $B-B$ and counterphase with $A-A$. Then obtain the cardioid of Fig. 264. We have therefore a system which is directive in only one direction and when turned by 180 deg cannot receive. The same characteristic is also found when the system is used as a sender and the field is measured at places where true radiation predominates (no induction field). According to Eq. (62) of page 358, the total effective magnetic field is

¹ *Bur. Standards, Sci. Paper 428.*

$$H = K \left[\underbrace{\frac{12.56}{\lambda d}}_{\text{causes radiation}} + \underbrace{\frac{2j}{d^2}}_{\text{causes induction field}} \right]$$

When the radiation and induction field are equal, the directional effect disappears. This happens for

$$\frac{12.56}{\lambda d} = \frac{2}{d^2}$$

since the j term expresses only that the second component is wattless as far as radiation is concerned. Hence, for $d = 0.1592$ and smaller distances from the sender, the receiving loop has no longer directive properties.

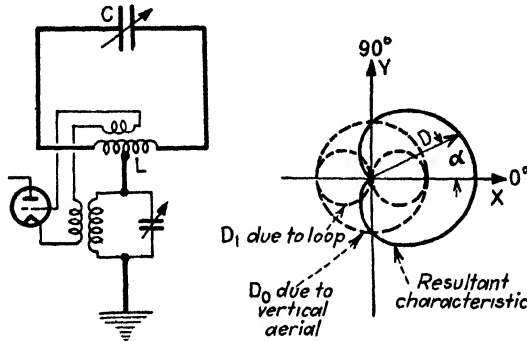


FIG. 264.—Loop and vertical aerial combined.

The cardioid can be obtained with the arrangement¹ to the left in Fig. 264. If the antenna again receives the amplitude D_0 and the loop the amplitude D_1 the corresponding induced voltages of which have a phase difference $\gamma = 90^\circ$, the directional effect, according to (50), becomes

$$D = \sqrt{D_0^2 + D_1^2 \cos^2 \alpha} \quad (53)$$

Hence, if the system in Fig. 264 is so adjusted that the antenna and loop effect are in phase,

$$D = D_0 + D_1 \cos \alpha \quad (54)$$

which, for an adjustment of equal amplitudes ($D_0 = D_1 = D'$), gives

$$D = D'[1 + \cos \alpha] \quad (55)$$

the equation of the cardioid.

¹ If C denotes the capacity of the tuning condenser, L the effective inductance inserted in the loop, and L_L the loop inductance, the natural frequency of the loop circuit is $f = \frac{1}{2\pi\sqrt{L_L \cdot L \cdot C / (L_L + L)}}$.

Reference is made to Fig. 265 for the width effect. In box loops of many turns the width b has to be taken into account since, for the minimum position (loop perpendicular to the direction of propagation), a certain voltage would be induced because the consecutive turns do not lie in the same plane and are therefore subjected to fields having different phase angles. For instance, for 2 turns a distance b apart, the time displacement between the 2 turns is $b \sin \alpha / c$ if α again denotes the angle of the plane of the loop with the direction of propagation. Hence, for $\alpha = 90^\circ$, this displacement is b/c and a displacement current passes across the turns, while, for $\alpha = 0$, no such effect is possible. Since these

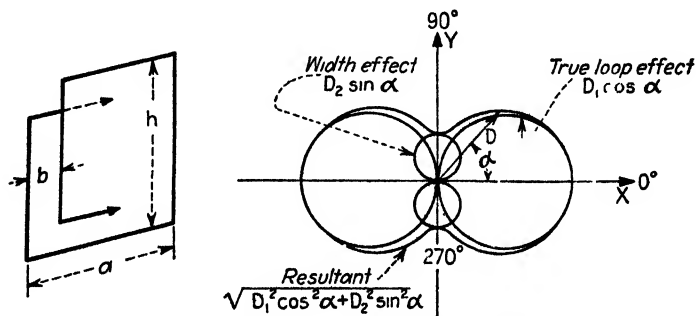


FIG. 265.—Direction effect with box frames.

fictitious circuits across the loop cannot be readily tuned, the displacement current will be about 90 deg out of phase with the true loop current. The width effect has therefore the directional characteristic

$$D_w = D_2 \sin \alpha \quad (56)$$

and the resulting characteristic for 90-deg displacement current is

$$D = \sqrt{D_1^2 \cos^2 \alpha + D_2^2 \sin^2 \alpha} \quad (57)$$

where D_1 is generally much larger than D_2 . The minima effects are flattened out (blurred) but not displaced from the 90- and 270-deg positions. Now if the width effect D is only about $\gamma = 90$ deg out of phase with respect to the true loop effect $D_1 \cos \alpha$, we obtain for the resultant effect

$$D = \sqrt{D_1^2 \cos^2 \alpha + D_2^2 \sin^2 \alpha + D_1 D_2 \sin 2\alpha \cos \gamma} \quad (58)$$

which for $\gamma = 90$ again gives the relation of Eq. (57). This formula shows that the two minima are again flattened out (blurred) and not exactly at 90 and 270 deg.

The width effect is only pronounced when box frames are used in which the width is relatively large. The pancake frame does away with the width effect but, because of increased capacitance to ground, is likely

to have a greater antenna effect. Also, its effective height is considerably smaller than for the box frame. When a box frame has not too much spacing between turns, the width effect is not important and can be readily compensated by an auxiliary antenna.

The combination of loop and antenna requires transmission lines for obtaining excitation or for carrying the induced currents to the detector. Assume again a coordinate system XYZ with XY as the horizontal plane and the origin O , a point of zero phase angle. A normal polarized wave $\mathcal{E} \sin \omega t$ arrives at an angle α . At any point P of the polar coordinates d and γ , a receiving antenna with the directional characteristic D equal to function of α is located. The induced voltage is

$$\begin{aligned} E &= D \sin \omega \left[t + \frac{d \cos (\alpha - \gamma)}{c} \right] \\ &= D \sin \left[\omega t + \frac{2\pi d}{\lambda} \cos (\alpha - \gamma) \right] \end{aligned} \quad (59)$$

If the effect is now transmitted to a detector by means of a line of length l with a phase velocity $v = p \cdot c$ which is normally $< c$ and an attenuation δ , we have, for the effect on the grid of the detector tube,

$$E = \mathcal{E} D e^{-\delta l} \sin \left[\omega t + \frac{2\pi d}{\lambda} \cos (\alpha - \gamma) - \frac{2\pi l}{p\lambda} \right] \quad (60)$$

and, for n such systems, the resultant effect is

$$D_r = \sum_n E \quad (61)$$

With this expression it is possible to study the case of multiple antenna arrays and the like as described on page 517.

167. Space Characteristics of Antennas and Loops and Effective Height in Any Direction.—The directional characteristics given so far refer to the XY plane only, that is, to the horizontal plane. But in receiving waves in aeroplanes or from them, the space characteristic must be taken into account. Assume again a vertical antenna, as in Fig. 257, which stands on relatively good conducting ground. For the various elevation angles β , we obtain in the XZ plane the characteristic shown. If I_z denotes the effective current at any distance z from the ground, we can calculate the effect of the element dz for any elevation. The resultant effect becomes

$$D = \cos \beta \int_0^l I_z \cos \left(\frac{2\pi z}{\lambda} \sin \beta \right) dz \quad (62)$$

which means that, for an elevation $\beta = 90$, no reception is possible. The resultant characteristic is almost two half circles, the dotted lines indicating the half circle.

In Fig. 266, AB denotes an antenna element the length of which is small compared with the wave length so that the effect of phase displacement is negligible. The distance d to the receiver point P , for simplicity, is unity and larger than λ , but not so large that the curvature of the earth need be considered. We call h_e' the effective length of the vertical wire for a certain direction of transmission. It is the length of the wire

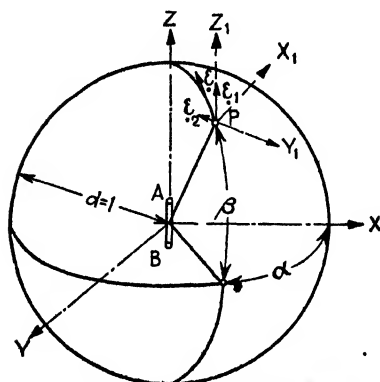


FIG. 266—Space effects.

corresponding to a dipole which would set up in the given direction in its equatorial plane a radiation field of the same magnitude as is set up in that direction by the vertical wire. If we plot h_e' as vectors for the corresponding directions, we obtain the directional characteristic. At large distances these vectors are proportional either to the electric- or to the magnetic-field intensity and the radiation density in that direction is proportional to $(h_e')^2$. Hence the energy W_r which the vertical antenna sends through a unit area at $d = 1$ is

$$W_r = k(h_e')^2 \quad (63)$$

If the dipole is drawn in the actual vertical wire, its extremities can be regarded as the radiation poles of the wire. The electric field is therefore along great circles which are perpendicular to the XY plane (Fig. 266). The effective height of the dipole is, for an elevation β ,

$$h_\beta = h_e \cos \beta \quad (64)$$

if h_e denotes the effective height in the equatorial plane, and the radiation density for elevation β is

$$W_\beta = kh_\beta = W \cos^2 \beta \quad (65)$$

The radiation energy which passes through the spherical zone belonging to $d\beta$ (Fig. 267) is

$$W_\beta \cdot 2\pi \cos \beta d\beta = 2\pi W \cos^3 \beta d\beta$$

Hence, for the total surface of the sphere,

$$W_t = 2\pi W \int_{-\pi/2}^{\pi/2} \cos^3 \beta d\beta = \frac{8\pi}{3} W \quad (66)$$

Dividing this by the surface ($= 4\pi$), we obtain the average radiation density

$$W_{av} = \frac{2}{3}W \quad (67)$$

where W denotes the radiation density at the equator. Correspondingly we obtain for the average effective height

$$h_{av} = h_e \sqrt{\frac{2}{3}} \quad (68)$$

Hence the average effective height of a dipole in all directions is 83 per cent of the maximum possible value which exists in the equatorial plane.

The result of (65) can also be derived as follows: Although the electric-field intensity directly above the dipole (Fig. 266) is zero, this is not true for a general location in space such as at a point P . The resultant field intensity at P is ξ and tangent to the meridian. Its value, according to Sec. 165, is proportional to the elevation for all planes perpendicular to the XY plane. Hence

$$\xi = \cos \beta$$

if the constant of proportionality is, for simplicity, taken as unity. This field intensity is now decomposed in the plane of the electric meridian passing through P and gives the components ξ_1 and ξ_2 along the new coordinate axes Z_1 and $-Y_1$. The vertical component ξ_1 is given by

$$\xi_1 = \cos^2 \beta \quad (69)$$

since for $\beta = 0^\circ$ it is ξ and for $\beta = 90^\circ$ it is zero. The other component becomes

$$\xi_2 = -\sin \beta \cos \beta \quad (70)$$

since $\xi_2 = -\xi \sin \beta$. There is no component along X_1 since the field lies in the Z_1Y_1 plane.

The resultant field at P therefore is

$$\xi = \xi_1 + \xi_2 = \cos \beta \sqrt{\sin^2 \beta + \cos^2 \beta} = \cos \beta \quad (71)$$

In Table XXVII are given the resultant¹ and component-field intensities of different antennas for a space point a distance d away which is large compared with the wave length.

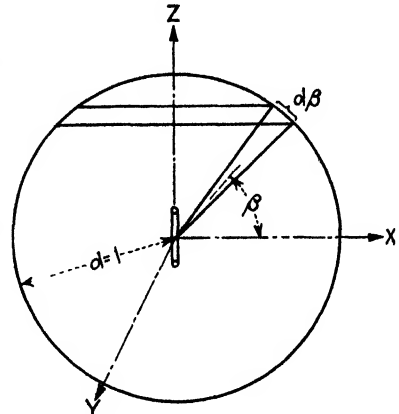


FIG. 267.—Radiation through spherical zone $d\beta$.

¹ MURPHY, W. H., *J. Franklin Inst.*, 201, 420, 1926.

TABLE XXVII

Kind of aerial.....	Field ξ_1 along Z-axis	Field ξ_2 along Y-axis	Field ξ_3 along X-axis	Resultant field $\xi = \xi_1 + \xi_2 + \xi_3$
Vertical antenna ...	$\cos^2 \beta$	$-\sin \beta \cos \beta$	0	$\cos \beta$
Horizontal antenna.	$-\cos \beta \sin \beta \cos \alpha$	$\sin^2 \beta \cos \alpha$	$\sin \alpha$	$\sqrt{\sin^2 \beta \cos^2 \alpha + \sin^2 \alpha}$
Inclined antenna, inclination θ against horizontal plane.....	$\cos \beta [\sin \theta \cos \beta - \cos \theta \sin \beta \cos \alpha]$	$\sin \beta [\cos \theta \sin \beta \cos \alpha - \sin \theta \cos \beta]$	$\cos \theta \sin \alpha$	$\sqrt{[\sin \theta \cos \beta - \cos \theta \sin \beta \cos \alpha]^2 + \cos^2 \theta \sin^2 \alpha}$
Vertical loop.....	$-\cos \beta \cos \alpha$	$\sin \beta \cos \alpha$	$\sin \beta \sin \alpha$	$\sqrt{\cos^2 \alpha + \sin^2 \alpha \sin^2 \beta}$
Horizontal loop....	0	0	$\cos \beta$	$\cos \beta$
Vertical loop and horizontal antenna.....	$-\cos \beta \cos \alpha [1 + \sin \beta]$	$\sin \beta \cos \alpha [1 + \sin \beta]$	$\sin \alpha [1 + \sin \theta]$	$1 + \sin \beta$
Vertical loop and vertical antenna...	$\cos \beta [\cos \beta - \cos \alpha]$	$\sin \beta [\cos \alpha - \cos \beta]$	$\sin \beta \sin \alpha$	$\cos \beta \cos \alpha - 1$
Horizontal loop and vertical antenna...	$\cos^2 \beta$	$-\sin \beta \cos \beta$	$\cos \beta$	$\cos \beta \sqrt{2}$
Remarks.....	α horizontal departure in (XY plane); β vertical elevation of field point; θ angle of antenna wire with horizon.			

The application of Table XXVII is as follows: The intensity of the radiated field at a distance d due to a vertical loop antenna is

$$\mathcal{E}_d = \frac{\mathcal{E}}{d} \sqrt{\cos^2 \alpha + \sin^2 \alpha \sin^2 \beta}$$

Hence along the ground ($\beta = 0$)

$$\mathcal{E}_d = \frac{\mathcal{E}}{d} \cos \alpha$$

which expresses the well-known cosine law giving the figure 8 in the horizontal (XY) plane, showing that the radiated field passes through zero

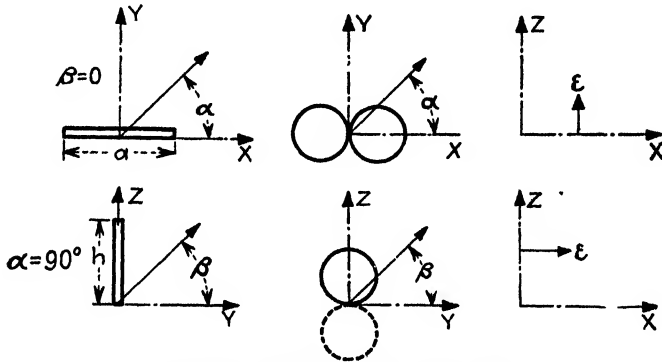


FIG. 268 —Radiated field of loop aerial

when $\alpha = 90, 270$, etc., that is, whenever the plane of the loop transmitter is perpendicular to the direction of the receiver. But when there exists a certain elevation β , the radiated field at such points can never pass through zero. Even when $\alpha = 90^\circ$, that is, when the loop is again perpendicular, we find that

$$\mathcal{E}_d = \frac{\mathcal{E}}{d} \sin \beta$$

The field of a loop antenna therefore increases from a zero value along the surface of the earth to a maximum value \mathcal{E}/d directly above the loop. Although the waves radiated from a loop antenna are plane polarized, the plane of polarization varies according to the values of the horizontal departure α and the elevation β . Along the ground ($\beta = 0$), the waves are *vertically* polarized since the electric intensity \mathcal{E}_d is in the vertical plane of propagation. In the plane $\alpha = 90^\circ$, they are *horizontally* polarized so that the electric force \mathcal{E}_d is horizontal for all values of β . This is shown in Fig. 268.

The case of a double dipole is indicated in Fig. 269. The dipoles are a distance a apart and carry currents of equal strength and opposite

phase. The effective height in any direction is equal to twice the effective height h_e' of one dipole times the interference factor $\sin \frac{\pi d}{\lambda}$ where d denotes the projection of the distance a on a ray in the desired

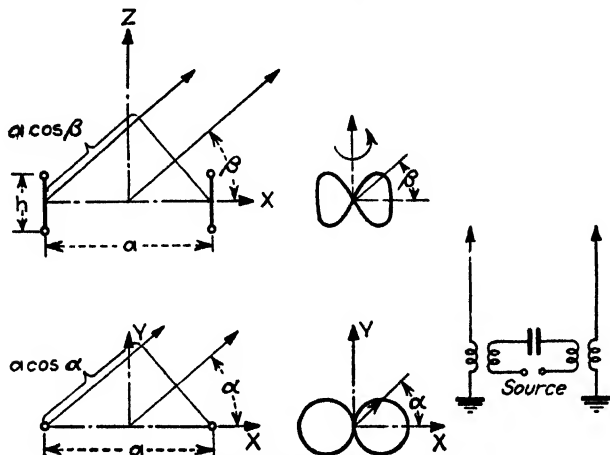


FIG. 269.—Radiation characteristics of double dipole.

direction. For the distance a small compared with the wave length λ , ($a < \lambda/6$), the interference factor again reduces to $\pi d/\lambda$ and the effective height in the X direction becomes

$$h_x = 2h_e \frac{\pi a}{\lambda} = \frac{2\pi a h}{\lambda} = \frac{\omega}{c} a h \quad (72)$$

and in the XY plane in any direction α

$$h_\alpha = 2h_x \cos \alpha \quad (73)$$

In the XZ plane it becomes, in any direction β

$$\begin{aligned} h_\beta &= 2h \cos \beta \frac{\pi a \cos \beta}{\lambda} \\ &= h_x \cos^2 \beta \end{aligned} \quad (74)$$

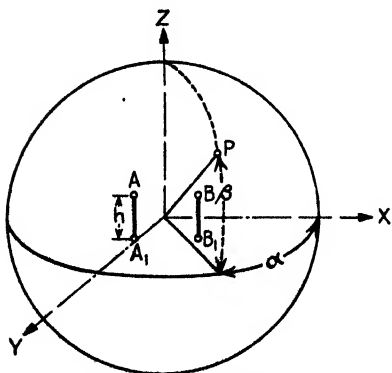


FIG. 270.—Double dipole.

According to Fig. 270, we find, for any direction α, β in space,

$$d = a \cos \alpha \cos \beta$$

and

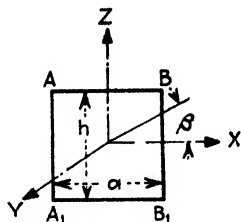
$$\begin{aligned} h_{\alpha, \beta} &= \frac{2h\pi d}{\lambda} \cos \beta = \frac{2\pi a h \cos \alpha \cos^2 \beta}{\lambda} \\ &= h_x \cos \alpha \cdot \cos^2 \beta \end{aligned} \quad (75)$$

The case of a double dipole leads to that of a rectangular loop as shown in Fig. 271 for which it is again assumed that a and h are smaller than $\lambda/6$. The radiation conditions in any direction within the plane of the loop can again be found by finding the effective height in any direction β . We have here two double dipoles, AA_1 , BB_1 and AB , A_1B_1 . For the first set, we have the effective height in any direction β

$$h_h = [2h \cos \beta] \frac{\pi a \cos \beta}{\lambda} \quad (76)$$

and for the other set

$$h_a = [2a \cos (90 - \beta)] \frac{\pi h \cos (90 - \beta)}{\lambda} \quad (77)$$



These two effective heights act in the same sense and have the same phase; hence the effective height of the rectangular loop in any direction β becomes

$$h_\beta = h_a + h_h = \frac{2\pi ah}{\lambda} [\sin^2 \beta + \cos^2 \beta] = \frac{\omega S}{c} \quad (78)$$

and, for N turns,

$$h_\beta^{(m)} = 209 \times 10^{-7} f^{(ke)} S^{(m^2)} N \quad (79)$$

which is the same expression as found in (24a). The radiation is therefore the same in any direction of the plane of the loop, and whatever its shape.

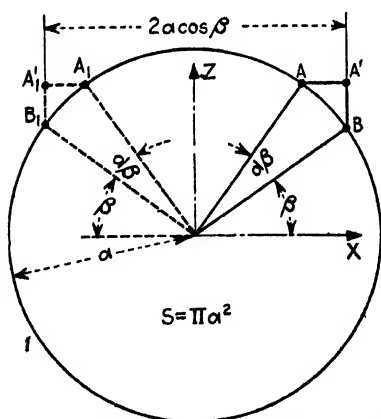


FIG. 272.—Proves that radiation is independent of shape of loop aerial.

In a direction perpendicular to the loop, no radiation takes place and the radiation in the XY plane is proportional to $\cos \alpha$ because in this plane the field due to the double dipole AA_1 and BB_1 is everywhere zero and that due to AB and A_1B_1 decreases according to the cosine of the departure [Eq. (73)]. In the YZ plane, the field also changes with the cosine law.

That the radiation in any direction of the XZ plane is independent of the shape of the loop can be proved as follows: Suppose the loop now forms

a circle of radius a as shown in Fig. 272. An element $AB = a(d\beta)$ forms a dipole $A'B = AB \cdot \cos \beta$ of effective length $a(d\beta) \cos \beta$ in the X direction and, together with a symmetrically situated dipole $A_1'B_1 = A_1B_1 \cos \beta$, forms a double dipole of effective length

$$dh_a = 2a(d\beta) \cdot \cos \beta \sin \frac{2\pi a \cos \beta}{\lambda}$$

in the X direction. The effective length of the entire loop in the X direction is therefore

$$h_x = 2a \int_{-\pi/2}^{\pi/2} \left[\cos \beta \sin \frac{2\pi a \cos \beta}{\lambda} \right] d\beta$$

Developing the sine term up to and including the second term, we find that

$$\begin{aligned} h_\beta = h_x &= \frac{2\pi^2 a^2}{\lambda} \left[1 - \frac{\pi^2 a^2}{2\lambda^2} \right] \\ &\cong \frac{2\pi^2 a^2}{\lambda} = \frac{2\pi S}{\lambda} = \frac{\omega S}{c} \end{aligned} \quad (80)$$

since, for symmetry, the effective height h_x of the freely suspended loop must be the same in any direction β of the XZ plane. The result is again the same as found in Eq. (78) for the rectangular loop.

168. Application to Airplane and Airship Guiding.¹—The orientation of airplanes and the like, for relatively small distances to the beacon stations compared with the height above ground, gives rise to bearing errors which are due to the directional effect of the airship antenna. If, for instance, the airship sends out a wave and the airship antenna is not perpendicular to the surface of the earth, the waves arrive at an angle to the antenna on the ground and become again reflected by the ground. The vertical component of the resulting magnetic-field intensity is then zero, for ground of relatively good conductivity, while the horizontal component of H is doubled. If a vertical loop antenna is used for the orientation of the sender, only the horizontal component of H is of importance. Hence, if as in Fig. 273 the quantity β is the angle at which the airship flies above the horizontal plane, α the angle between the receiving loop antenna and the vertical plane through the airship and the receiver, and δ the angle between the airship antenna and the horizontal plane, we have for the bearing error γ

$$\tan \gamma = \frac{\sin \alpha}{\cos \alpha - (\tan \delta / \tan \beta)} \quad (81)$$

The bearing error vanishes when the airship flies either toward ($\alpha = 0$) the receiver or away ($\alpha = 180$) from it. This can readily be understood from Fig. 273. It is assumed that the airplane wings are horizontal. The projection of its mid-point on the horizon is C and LC is the true direction of the loop toward the vertical plane through the center of the aeroplane. DE denotes the direction of the antenna of the plane. The loop gives a minimum effect when the magnetic lines of force at L are

¹ See also W. BURSTYN, *loc. cit.*; R. BALDUS and E. BUCHWALD, *Jahrb. drahtl.*, 15, 214, 1920.

parallel to the area of the loop. But, since the airplane antenna is along DE , the magnetic lines of force must be perpendicular to the area DEL , that is, along LG . The loop must be perpendicular to ground and along LG . The plane of the loop then cuts the ground along LH instead of along LK . Hence γ is the bearing error. From this we note also that no bearing error occurs when the airplane antenna is along DC , that is, perpendicular to ground.

A more detailed study is as follows: We again treat the antennas as dipoles or double dipoles where loop antennas are concerned. According to the radiation law, the received current I in the antenna on the ground is inversely proportional to the distance d between the sending and receiving dipoles, proportional to the sine of the angle φ which the direc-

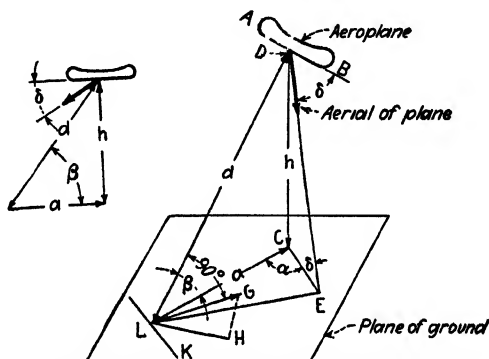


FIG. 273.—Bearing error for airplane aerial.

tion of radiation makes with the axis of the transmitting dipole and proportional to the sine of the angle ψ which the arriving electric intensity makes with the axis of the receiving dipole. Hence

$$I = \frac{k \sin \varphi \sin \psi}{d}$$

where it is understood that the electric lines of force are the meridians of a sphere (Fig. 266) with the dipole at the center and along the polar axis. Now, according to Fig. 273,

$$\begin{aligned} d &= \frac{a}{\cos \beta} \\ \cos \varphi &= \sin \delta \sin \beta + \cos \delta \cos \beta \cos \alpha \\ \sin \psi &= \frac{\sin \delta - \cos \varphi \sin \beta}{\sin \varphi} \end{aligned}$$

hence

$$I = \frac{k \cos^2 \beta}{a} [\sin \alpha - \cos \delta \cos \varphi \tan \beta] \quad (82)$$

for any position of the airplane. Thus when the airplane travels parallel with the surface of the earth,

$$a = \frac{h}{\tan \beta}$$

and

$$I = \frac{k \sin \beta \cos \beta}{h} [\sin \delta \cos \beta - \cos \delta \sin \beta \cos \alpha] \quad (83)$$

and, when the plane passes directly over the receiving station, $\alpha = 0$ and

$$I = \frac{k}{2h} \sin 2\beta \sin (\delta \mp \beta) \quad (83a)$$

where the positive sign is for the arriving plane and the negative sign for the leaving plane. When the plane travels near the receiving station,

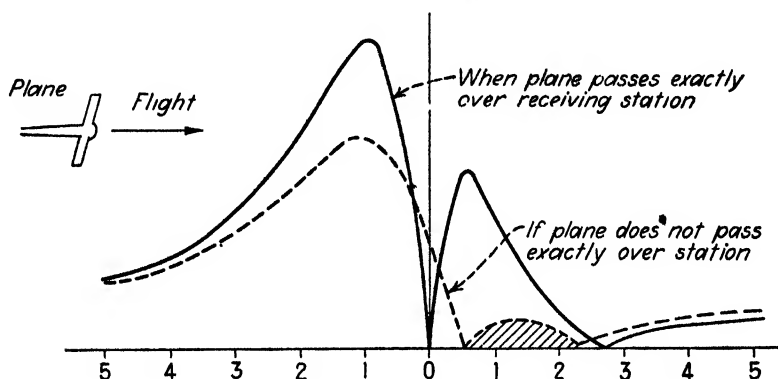


FIG. 274.—Calculated intensity curves.

the received current goes through zero (Fig. 274, dotted curve) twice at places

$$\sin 2\alpha = \frac{2d_0}{h} \tan \delta \quad (84)$$

where d_0 denotes the shortest horizontal distance between the grounded receiving antenna and the sender antenna of the plane. These two minima vanish and the small maximum between them becomes a minimum for $h/d_0 \geq 2 \tan \delta$, that is, when $\delta = 21^\circ$ does not exceed the angle $\beta = 37.5^\circ$. The largest maximum always occurs when a plane starts. When traveling over a station and away, three or two maxima occur depending upon the position of the plane. In each case minima are distinct since the received current experiences a phase change and the shaded area should be drawn below the abscissa axis.

169. The Goniometer (Inclined Double-loop Antenna).—The Bellini and Tosi goniometer (Fig. 275) consists of two directive antennas in which there are currents I_1 and I_2 with planes perpendicular to each other.

The coupling to a third coil L_3 is by means of the split coils L_1, L_1 and L_2, L_2 which are stationary and perpendicular to each other, as is the antenna system, while L_3 can be turned through 360 deg. The split coils are used to obtain a uniform magnetic field in which the movable coil is located. The mutual inductances M_{31} and M_{32} , between the coil L_3 and coils L_1, L_1 and L_2, L_2 , respectively, are such that

$$M_{31} = L \cos \theta$$

$$M_{32} = L \sin \theta$$

or

$$\frac{M_{32}}{M_{31}} = \tan \theta$$

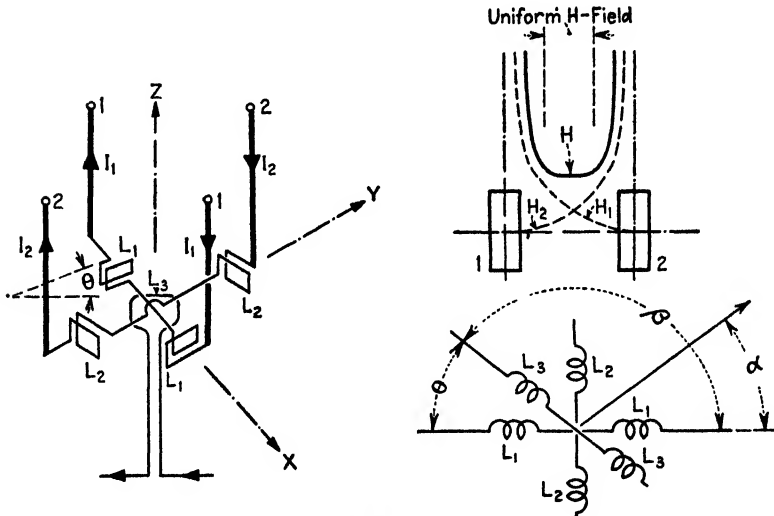


FIG. 275.—Action in goniometer.

where θ denotes the angle which the coil¹ L_3 makes with the split coil L_1, L_1 . In the modified Bellini and Tosi goniometer, two perpendicular loop antennas are used, which means that the points 1, 1 and the points 2, 2, in Fig. 275 are connected together. Single-turn triangular loops are used² in order to simplify the construction. If an arriving electromagnetic wave makes in the XY plane an angle α with the X -axis, the induced voltages in the two loops 1 and 2 are, according to Eq. (44), respectively proportional to the cosine and the sine of this angle; that is,

$$E_1 = k \cos \alpha$$

$$E_2 = k \sin \alpha$$

¹ When the goniometer is used as a receiver, L_3 is known as the "search coil."

² For instance, the experimental beacon station of the Bureau of Standards at College Park, Md.

and the magnetic fields of the corresponding currents I_1 and I_2 also follow such laws; that is,

$$\begin{aligned}H_1 &= K \cos \alpha \\H_2 &= K \sin \alpha\end{aligned}$$

Then the corresponding voltages induced in the search coil L_3 are

$$\begin{aligned}E_1' &= K_1 \cos \alpha \cos \theta \\E_2' &= K_1 \sin \alpha \sin \theta\end{aligned}$$

The resultant voltage in the coil L_3 for the tuned aerial system becomes

$$E_3 = E_1' + E_2' = K_1 \cos (\alpha - \theta) \quad (85)$$

Therefore the horizontal direction characteristic of the goniometer is the same as that of the double antenna or that of the loop antenna since for the latter

$$D = D_0 \cos \alpha$$

and for the goniometer

$$D = D_0 \cos (\alpha - \theta) \quad (86)$$

Since the direction of the receiver to the sender station is displaced by the angle θ , the directional characteristic of the goniometer can be turned into any position by turning the search coil L_3 . Where no e.m.f. is noted across L_3 , we have $\alpha = \theta$, the true angle of the arriving wave with the 1-1 plane. The advantage of the goniometer over that of the ordinary loop antenna is that the antenna system is fixed and can be of any suitable size since only the small coil L_3 is movable. The directional effect, however, is identical with that of the ordinary loop for normal polarized waves (H field parallel to the surface of the earth). The goniometer can give rise to undefined minimum settings when the loops have unequal high-frequency resistance. The effects of both loops are then somewhat out of phase and produce a revolving field which blurs the minima positions. Such phase displacement can be overcome by tuning both loops. When the amplitudes of both loop currents are unequal (may be due to unequal loops or unequal goniometer coils), a bearing error occurs because the minimum positions are shifted and are dependent on the angle α of the arriving wave. For unequal amplitudes, the error can be determined from

$$E_3 = K_1 \cos \alpha \cos \theta + K_2 \sin \alpha \sin \theta \quad (87)$$

Putting $\theta = 90 + \gamma$, since the direction of the incident wave is perpendicular to the minimum setting of the goniometer, we have, for the error γ ,

$$\sin (\gamma - \alpha) = \frac{[K_2 - K_1] \sin 2\alpha}{2\sqrt{K_1^2 \cos^2 \alpha + K_2^2 \sin^2 \alpha}} \quad (88)$$

The goniometer today plays an important part in unidirectional radio-beacon work for aircraft.¹ Figure 276 illustrates the principle. A master oscillator supplies power at a high frequency F to two power amplifier tubes which operate alternately with an audio-frequency plate supply of frequency f . The audio frequency serves at the same time as modulation. The stator coils are in the anode branches. The secondary coils are in series with the respective triangular loops which are at right angles and mounted together.² The resultant signal, according to the foregoing theory, can be shifted by rotating either pair of goniometer coils. With this arrangement there are four directions from the sender in which a signal modulated at frequency $2f$ can be heard (Fig. 277). These are the directions in which the radiation from the two loops is received with equal intensity. Theoretically these directions are lines, but practically they have a small width. In all other directions, the modulation will be f cycles/sec only. By means of the goniometer these four directions which are 90 deg apart can be turned around in space together and used to indicate a desired direction to an airplane.

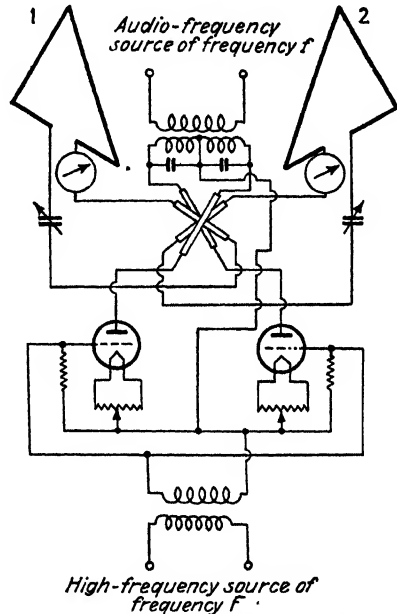


FIG. 276.—Goniometer with modulation.

The space characteristic can be explained by means of Fig. 277. Each of the two loops radiates according to a figure-8 pattern. Two loops sending alternately, therefore, radiate two "figures of 8" inclined to one another by the angle between the loops. This angle can be adjusted by the goniometer coils. Since the modulating frequency f is sufficiently high (for instance, 500 cycles/sec), the detecting device cannot follow the alternations from one loop to another and the two fields overlap and give the horizontal space characteristics. A much sharper indication is obtained when vibrating reeds are used to indicate the positions of the course. One loop then radiates a high-frequency current of carrier

¹ KIRBITZ, F., New Experiments with Scheller's Directional Transmitter, *Jahrb. drahtl.*, 15, 299, 1920; F. W. DUNMORE and F. H. ENGEL, *Bur. Standards, Sci. Paper* 469, 1923; E. Z. STOWELL, *Bur. Standards, Research Paper* 35; J. H. DELLINGER and H. PRATT, *Proc. I.R.E.*, 16, 890, 1928.

² For the sake of symmetry, they are drawn separate in the figure.

frequency F and modulation frequency f_1 , and the other loop radiates a current of the same carrier frequency but modulation frequency f_2 (for instance, $f_1 = 65$ volts/sec and $f_2 = 85$ volts/sec). When the plane travels along the course (equisignal zone $\xi_1 = \xi_2$), the two vibrating

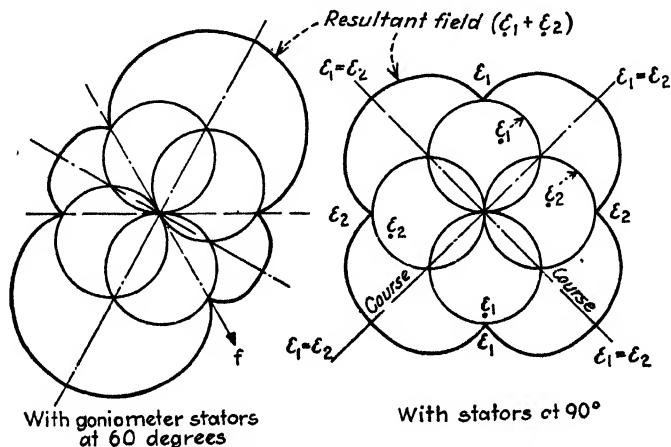


FIG. 277.—Course pattern for airplane guiding.

reeds give the same deflection; if it goes off the course, one reed shows less vibration amplitude.

170. Theory of the Double-loop and the Adcock System.—In about 1918, R. A. Weagant suggested the double-loop system indicated in Fig. 278. The two loops are in a vertical plane, one-half wave length

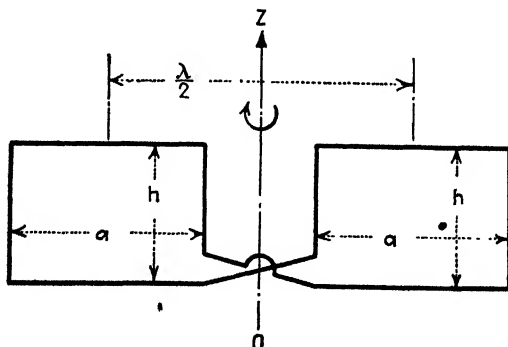


FIG. 278.—Double-loop system.

apart and each can be rotated about the Z -axis. The purpose of this scheme is to eliminate the night effects due to the rays which come down from the ionized layer. The induced currents of the horizontal portion are eliminated since the indirect waves of the layer will cause currents in

the horizontal portions which will be balanced out because of the differential connection. The induced currents in the vertical portions will be out of phase and will be received as with an ordinary loop.

The double-loop system was also used by T. L. Eckersley in 1921 and by H. T. Friis¹ in 1925 for a selective directive receiving system. With respect to the direction characteristic in the horizontal plane XY , reference is made to Fig. 279 where the two differential loops are spaced a distance $2l$ apart between centers. P again denotes any point in the

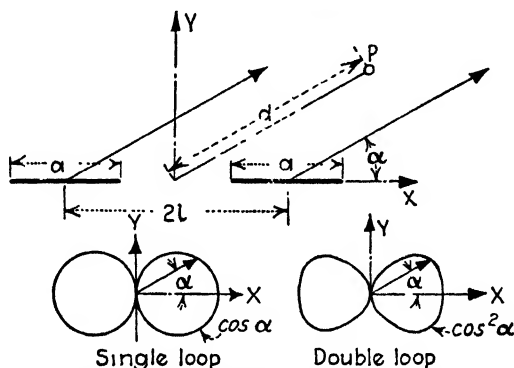


FIG. 279.—Characteristic for double loop.

horizontal plane which is at a distance d large compared with the wavelength. The electric-field intensity at P is therefore, for any angle α ,

$$\mathcal{E}_\alpha = k \cos \alpha \left[\frac{\sin(\omega t - \psi)}{d - l \cos \alpha} - \frac{\sin(\omega t + \psi)}{d + l \cos \alpha} \right] \quad (89)$$

when the phase angle is

$$\psi = \frac{2\pi l \cos \alpha}{\lambda} \quad (90)$$

since we can apply the loop law. For a place in the true radiation field (when the double loop acts as a sender), l is negligibly small compared with d and, for $2k/d = K$, we have

$$\mathcal{E}_\alpha = K \cos \alpha \cos \omega t \sin \psi \quad (91)$$

Hence as the double-loop system rotates about the Z -axis, the electric-field intensity becomes zero for values of $\alpha = 90^\circ$ and $\alpha = 270^\circ$, which is the same as for the single loop. But it should be noted that, for other values of α , the double loop behaves differently from the single loop since it follows a $\cos^2 \alpha$ -law as indicated in Fig. 279. This is, of course, a disadvantage when observing the orientation of another station by means

¹ ECKERSLEY, T. L., *Radio Rev.* 2, 61 and 231, 1921; H. T. FRIIS, *Proc. I.R.E.*, 13, 685, 1925; R. SMITH ROSE, *J.I.E.E.*, 68, 270, 1928.

of the minimum settings (theoretical zero settings) since the rate of change for the single loop is $\partial(\cos \alpha)/\partial \alpha$ which gives a $\sin \alpha$ -function, that is, a maximum change at $\alpha = 90^\circ$ and $\alpha = 270^\circ$. For the differential double loop, the rate of change is $\partial(\cos^2 \alpha)/\partial \alpha = 2 \cos \alpha \sin \alpha$. When the point P is not in the horizontal plane but is somewhere in space, according to Table XXVII on page 486, for the space characteristic of a vertical loop at any elevation β above the horizon for the field strength at a distance d , we have

$$\mathcal{E}_d = \frac{\mathcal{E}}{d} \sqrt{\cos^2 \alpha + \sin^2 \alpha \sin^2 \beta} \quad (92)$$

and for the double-loop system

$$\mathcal{E}_d = K \cos \omega t \sin \psi \sqrt{\cos^2 \alpha + \sin^2 \alpha \sin^2 \beta} \quad (93)$$

where $K = 2\mathcal{E}/d$. Hence in the direction $\alpha = 90^\circ$, we have $\psi = 0$ and $\mathcal{E}_d = 0$ whatever the value of β . The double-loop system can therefore

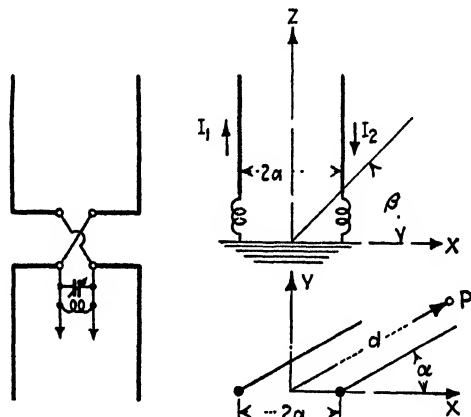


FIG. 280.—Adcock aerials.

radiate nothing perpendicular to its plane. This is not true for the single-loop sender since in a plane perpendicular to the loop the field intensity disappears only for $\beta = 0$ (in the horizontal plane) but owing to (92) passes through only a minimum value $(\mathcal{E} \sin \beta)/d$ in the plane $\alpha = 90^\circ$. For the receiving of indirect waves (from the ionized layer), a bearing error can, however, occur as for the single-loop system as is proved in the next paragraph.

The Adcock system¹ consists of two vertical antennas as indicated in Fig. 280. The currents I_1 and I_2 are in antiphase. According to Eq. (71), the space characteristic gives an electric-field intensity \mathcal{E}_d when the system is acting as a sender

¹ Adcock, F., British Patent No. 130490.

$$\begin{aligned}\varepsilon_d &= k \cos \beta \left[\frac{\sin (\omega t - \psi)}{d - l \cos \alpha} - \frac{\sin (\omega t + \psi)}{d + l \cos \alpha} \right] \\ &\cong K \cos \beta \cos \omega t \sin \psi\end{aligned}\quad (94)$$

for $K = 2k/d$ and $l \ll d$. Hence, when $\alpha = 90^\circ$ or $\alpha = 270^\circ$, the radiated field intensity $\varepsilon_d = 0$ for all elevations β , and no radiation exists for any elevation in the plane perpendicular to the plane of the two aerials.

171. Direct and Indirect Waves, Bearing Error¹ with Loops, and Goniometer Systems.—Bearing errors from airplane antennas and goniometers have been treated in Secs. 168 and 169. Equation (70) of page 401 and Fig. 230 indicate that the arriving electric field can be due to both the direct and the indirect rays and that the indirect wave is generally elliptically polarized. The coil receiver must therefore give rise to a bearing error since we no longer have the case of vertically

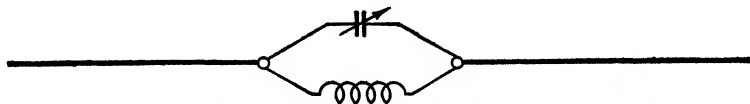


Fig. 281.—Hertzian dipole for polarization measurements.

polarized electromagnetic waves. The ratio of $\varepsilon_y/\varepsilon_z$ in Fig. 230 and in Eq. (70) of page 401 can be computed as well as measured with a Hertzian dipole,² as indicated in Fig. 281. The dipole can be rotated in any position at O (Fig. 230).

Case A.—When the receiver is far enough away so that the direct ray AB does not exist and we assume at first that the downcoming rays are circularly polarized, we have in Eq. (70) of page 401

$$\xi_z = \xi_z' - \xi_z''$$

since, according to Fresnel, the component of the electric-field intensity which is perpendicular to the surface of reflection of *perfect* conductivity does not undergo a change in phase, while the component along the surface changes its phase by 180 deg. The effective value of the horizontal component becomes

$$\begin{aligned}\varepsilon_z &= \sqrt{\frac{1}{2\pi} \int_0^{2\pi} [\varepsilon \sin \Omega - \varepsilon \sin (\Omega + \varphi)]^2 d\Omega} \\ &= \varepsilon \sqrt{1 - \cos \varphi}\end{aligned}\quad (95)$$

¹ SMITH ROSE, R. L., *J.I.E.E.*, **66**, 270, 1928; R. L. SMITH ROSE and R. H. BARFIELD, *Proc. Roy. Soc. (London)*, **110A**, 580, 1926; R. L. SMITH ROSE, *Proc. I.R.E.*, **17**, 425, 1929; E. O. HULBURT, *J. Franklin Inst.*, **201**, 597, 1926; E. V. APPLETON and M. A. F. BARNETT, *Proc. Roy. Soc. (London)*, (A), **109**, 621, 1925.

² Such experiments were carried on by G. W. Pickard, *Proc. I.R.E.*, **14**, 4, 1926, for short waves and compared theoretically by E. O. Hulburt (*loc. cit.*).

if φ denotes the phase difference at point O , due to the different lengths of the ray path EDO and CO and if $\Omega = \omega t$. The phase difference in radians can be calculated from

$$\varphi = \frac{4\pi h \cos \theta}{\lambda} \quad (96)$$

where θ is the angle of incidence of the downcoming rays and h the height of field point above the ground. Similarly, we find, for the vertical component in the case of *perfect ground* and circular polarization,

$$\begin{aligned} \varepsilon_z &= [\varepsilon_s' + \varepsilon_s''] \sin \theta \\ &= \sin \theta \sqrt{\frac{1}{2\pi} \int_0^{2\pi} [\varepsilon \sin \Omega + \varepsilon \sin (\Omega + \varphi)]^2 d\Omega} \\ &= \varepsilon \sqrt{1 + \cos \varphi} \sin \theta \end{aligned} \quad (97)$$

which gives the ratio of the horizontal to the vertical component

$$\frac{\varepsilon_x}{\varepsilon_z} = \frac{1}{\sin \theta} \sqrt{\frac{1 - \cos \varphi}{1 + \cos \varphi}} \quad (98)$$

Case B.—When the ground is considered a *perfectly transparent* dielectric with the index of refraction $n = \sqrt{\kappa}$ and θ and δ the angle of incidence and refraction, respectively, we have

$$n \sin \theta = \sin \delta$$

and for

$$m = \frac{\sin (\theta - \delta)}{\sin (\theta + \delta)} \quad \text{and} \quad p = \frac{\tan (\theta - \delta)}{\tan (\theta + \delta)}$$

the horizontal and vertical components become

$$\left. \begin{aligned} \varepsilon_x &= \varepsilon \sqrt{\frac{1}{2\pi} \int_0^{2\pi} [\sin \Omega - m \sin (\Omega + \varphi)]^2 d\Omega} \\ &= \varepsilon \sqrt{0.5[1 + m^2 - 2m \cos \varphi]} \\ \varepsilon_z &= \varepsilon \sin \theta \sqrt{\frac{1}{2\pi} \int_0^{2\pi} [\sin \Omega - p \sin (\Omega + \varphi)]^2 d\Omega} \\ &= \varepsilon \sin \theta \sqrt{0.5[1 + p^2 - 2p \cos \varphi]} \end{aligned} \right\} \quad (99)$$

and the ratio of these components

$$\frac{\varepsilon_x}{\varepsilon_z} = \frac{1}{\sin \theta} \sqrt{\frac{1 + m^2 - 2m \cos \varphi}{1 + p^2 - 2p \cos \varphi}} \quad (100)$$

In the actual case, the downcoming ray is elliptically polarized and the ε_x and ε_y components are different. Also, the ground is neither a perfect

conductor nor a perfect dielectric but possesses conductivity σ and a dielectric constant κ so that the effective dielectric constant

$$\kappa_e = \kappa - (2j\sigma/f)$$

and the index of refraction $n = \sqrt{\kappa_e}$. At the surface of the ground, we have to satisfy the boundary conditions, that is, that the tangential forces in the two media (air and ground, respectively) are equal and that the normal components are equal.

Case C.—A vertically polarized wave of intensity \mathcal{E} comes down from the ionized layer as in Fig. 282. The wave arrives in the ZX plane with

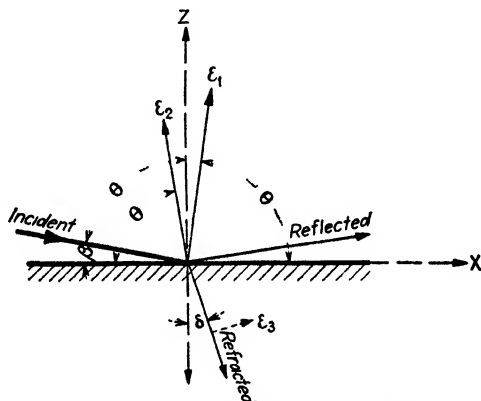


FIG. 282.—Vertically polarized electromagnetic wave.

an angle of incidence θ . The angle of refraction is δ . Since vertical polarization exists in the X direction,

$$\mathcal{E}_y = 0; \quad H_x = H_z = 0$$

and, because of the boundary conditions,

$$\begin{aligned} \mathcal{E}_x &= \mathcal{E}_x'; & \mathcal{E}_z &= \kappa_e \mathcal{E}_z'; & H_y &= H_y' \\ n &= \sqrt{\kappa_e} = \frac{\sin \theta}{\sin \delta} \end{aligned}$$

where \mathcal{E}_x' , \mathcal{E}_z' and H_y' are the components in ground at the boundary. Hence¹

$$\frac{\mathcal{E}_x}{\mathcal{E}_z} = \frac{\mathcal{E}_x'}{\kappa_e \mathcal{E}_z'} = \frac{\cotan \delta}{\kappa_e} \quad (101)$$

or

$$\frac{\mathcal{E}_x}{\mathcal{E}_z} = \frac{\sqrt{1 - (\sin^2 \theta / \kappa_e)}}{\sin \theta \sqrt{\kappa_e}} \cong \frac{1}{\sin \theta \sqrt{\kappa_e}} \quad (102)$$

¹ When the indirect wave is not taken into consideration, we obtain for the ground or direct wave $\mathcal{E}_x/\mathcal{E}_z = \cotan \theta$ which gives the wave tilt relation (page 353).

According to Fig. 282, we have, for the components,

$$\left. \begin{aligned} \varepsilon_x &= \varepsilon_1 \cos \theta - \varepsilon_2 \cos \theta = \varepsilon_1 \left[1 - \frac{\varepsilon_2}{\varepsilon_1} \right] \cos \theta = \varepsilon_1 [1 - \rho_v] \cos \theta \\ \varepsilon_z &= [1 + \rho_v] \sin \theta \\ H_y &= [1 + \rho_v] \end{aligned} \right\} \quad (103)$$

where ρ_v is the coefficient of reflection of the ground for *vertically* polarized waves. The ratio

$$\frac{\varepsilon_z}{H_y} = \sin \theta \quad (104)$$

can be measured with an alternate loop-aerial system. This gives a means for finding the angle of incidence.

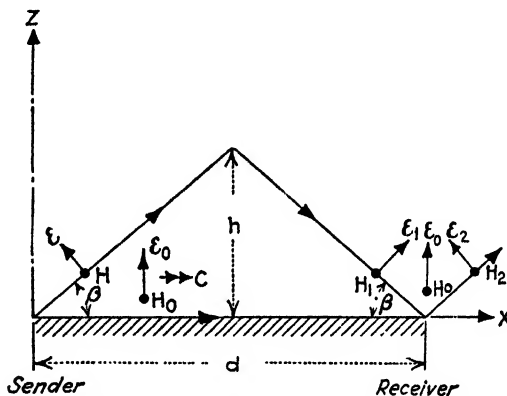


FIG. 283.—Electric- and magnetic-field components before and after reflection.

Example.—In Fig. 283 the direct wave ε_0 , H_0 of the broadcast range travels through a distance d and the indirect wave ε , H (assuming for simplicity equivalent reflection at the ionized layer) through the distance $2\sqrt{(d^2/4) + h^2}$. The magnetic vectors are perpendicular to the paper and the electrical vectors as indicated in the case of *vertically* polarized waves. The sender is at first a loop transmitter. The direct wave has a field intensity

$$\varepsilon_0 = K_1 \cos \omega t \cos \alpha \quad (105)$$

since it always remains perpendicular to the XY (horizontal) plane. This is, however, not the case for the indirect waves. For the arriving components ε_1 , H_1 , we must utilize the space characteristics for the sender loop given in Table XXVII of page 486 and account for the difference in path of the direct and indirect waves. Hence

$$\varepsilon_1 = K_2 \cos (\omega t + \varphi) \sqrt{\cos^2 \alpha + \sin^2 \alpha \sin^2 \beta} \quad (106)$$

The constants are

$$K_1 = \frac{k_1}{d} \quad \text{and} \quad K_2 = \frac{k_2}{2\sqrt{(d^2/4) + h^2}}$$

where k_1 and k_2 account for the amplitude of the electric vector at the sender and the different kinds of attenuations. For the component reflected at the ground, we have

$$\mathcal{E}_2 = \rho_v \mathcal{E}_1$$

where the vertical reflection coefficient ρ_v is for waves within the broadcast range and is in the neighborhood of 0.9. The angle of incidence is now $(90 - \beta)$. A vertical receiving antenna will therefore indicate the vertical components of the resultant electric field \mathcal{E}_z ; that is, according to (103),

$$\begin{aligned} \mathcal{E}_z &= \mathcal{E}_0 + \mathcal{E}_1[1 + \rho_v] \cos \beta \\ &= K_1 \cos \omega t \cos \alpha + K_2[1 + \rho_v] \cos \beta \cos(\omega t + \varphi) \sqrt{\cos^2 \alpha + \sin^2 \alpha \sin^2 \beta} \quad (107) \end{aligned}$$

During the day, waves in the broadcast range can hardly be transmitted through indirect waves, so the second term of (107) vanishes and $\mathcal{E}_z = \mathcal{E}_0$. When the vertical

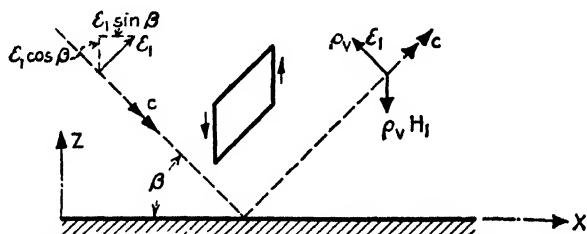


FIG. 284.—Downcoming sky wave vertically polarized.

plane of the loop sender is perpendicular to the direction between sender and receiver, no signal can be received since $\alpha = 90^\circ$ and $\mathcal{E}_z = 0$, and the bearing is correct. When the night effects prevail, for which the second part of (107) is also to be taken into account, the received signal is only a minimum since, for $\alpha = 90^\circ$,

$$\mathcal{E}_z = 2K_2[1 + \rho_v] \sin 2\beta \cos(\omega t + \varphi) \quad (108)$$

There is, however, a condition for which this expression becomes zero. This happens when the phases due to the direct and indirect waves are exactly in opposition, that is, $\varphi = \pi$. Equation (107) leads to

$$K_1 \cos \alpha = K_2[1 + \rho_v] \cos \beta \sqrt{\cos^2 \alpha + \sin^2 \alpha \sin^2 \beta}$$

which gives the expression

$$\tan \alpha = \frac{2\sqrt{1 - P^2 \cos^2 \beta}}{P \sin 2\beta} \quad \text{for} \quad P = \frac{K_2}{K_1}[1 + \rho_v] \quad (109)$$

For a correct bearing, α should be 90 deg which is not the case according to the result of (108). Hence α must be some smaller angle and $(90 - \alpha) = \gamma$ is the bearing error which can be calculated from

$$\tan \gamma = \frac{P \sin 2\beta}{2\sqrt{1 - P^2 \cos^2 \beta}} \quad (110)$$

The elevation β can be estimated from measurements, the reflection factor ρ_v is about 0.9 for the broadcast range, and K_2/K_1 is the ratio of the mean field intensities of the indirect and direct waves. The last quantity can also be estimated from measurements.

The bearing error can be of considerable magnitude, and during sunset periods it becomes erratic and variable since the plane of polarization rotates. When a loop antenna is used for receiving, we have, for the indirect wave,¹ no bearing error in the case indicated in Fig. 284 since, for the vertical loop perpendicular to the direction of the sender station, the voltages induced in the vertical portions of the loop are equal and in opposite phase (same distance to sender) and no voltages are induced in the horizontal portions for this position of the loop ($\alpha = 90^\circ$).

Example.—A Hertzian rod may be used to investigate the arriving electric field of Fig. 284. We then measure the resultant field ϵ_r as indicated in Fig. 285, that is,

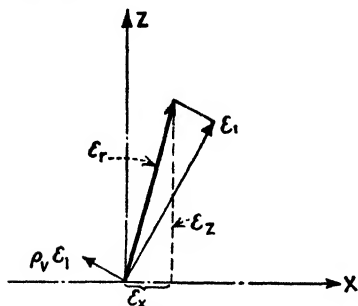


FIG. 285.—Vector diagram of measured resulting vector ϵ_r .

the direction of the rod, as it is rotated about the origin and in the ZX plane for maximum response, gives the forward tilt t of the wave which can be expressed by the components ϵ_x and ϵ_y as

$$\tan t = \frac{\epsilon_x}{\epsilon_y} = \frac{1}{n \cos \beta} \quad (111)$$

Here $(90 - \beta)$ is the angle of incidence of the indirect ray, β the angle which the indirect ray makes with the ground, and $n = \sqrt{\kappa_e}$ the index of refraction of the ground. Equation (111) holds for vertically polarized waves coming from above. But the rod will also measure the effect of the direct wave ϵ_0 passing along the

surface of the earth. During the day it measures the tilt t_0 according to

$$\tan t_0 = \frac{\epsilon_{0x}}{\epsilon_{0y}} \quad (112)$$

Therefore when, during the night hours, the indirect wave also acts upon the receiver and the vertical and horizontal components are measured with the Hertzian rod or a tilting loop, we have for the resultant effect

$$\begin{cases} \epsilon_{xr} = \epsilon_x - \epsilon_{0x} \\ \epsilon_{yr} = \epsilon_y - \epsilon_{0y} \end{cases} \quad \frac{\epsilon_{xr}}{\epsilon_{yr}} = \frac{1}{n \cos \beta}$$

and

$$\cos \beta = \frac{\epsilon_x - \epsilon_{0x}}{n[\epsilon_x \tan t - \epsilon_{0x} \tan t_0]} \quad (113)$$

and hence a means for finding the direction of the indirect ray and the apparent height of the layer.

Case D.—Direct and indirect waves arrive at a vertical aerial from a double-loop sender. According to (91) and (93) for the vertical component of the arriving electric intensity of both the direct and the indirect wave, we have

$$\epsilon = K_1 \cos \alpha \cos \omega t \sin \psi + K_2 [1 + \rho_e] \cos \beta \cos (\omega t + \varphi) \sin \psi \sqrt{\cos^2 \alpha + \sin^2 \alpha \sin^2 \beta} \quad (114)$$

Since, according to (90), the term ψ is proportional to $\cos \alpha$, there can be no field ϵ when $\alpha = 90^\circ, 270^\circ$, etc., that is, when the plane of the

¹ Direct wave neglected.

double-loop transmitter is perpendicular to the direction toward the receiving antenna. Hence the bearing is correct despite the conditions of the night effect.

But, as for the single-loop sender, we also obtain zero field intensity $\mathcal{E} = 0$ when the phases of the direct and indirect waves are exactly opposite ($\varphi = 180^\circ$) for which

$$K_1 \cos \alpha = K_2[1 + \rho_v] \cos \beta \sqrt{\cos^2 \alpha + \sin^2 \alpha \sin^2 \beta} \quad (115)$$

gives exactly the same relation as for the single-loop transmitter and a bearing error γ for the additional minimum position as given by Eq. (110).

Case E.—When an Adcock antenna is used as a sender and a vertical wire as receiver, according to Eq. (94), we have, for the vertical intensity at the receiving antenna due to the direct and the indirect wave,

$$\mathcal{E} = K_1 \cos \omega t \sin \psi + K_2[1 + \rho_v] \cos^2 \beta \cos(\omega t + \varphi) \sin \psi \quad (116)$$

where ψ is again proportional to $\cos \alpha$, that is, for $\alpha = 90^\circ, 270^\circ$, etc., or when the plane of the two sending aerials is perpendicular to the direction of the receiving antenna, there can be no radiation and no bearing error. When with such a sender system the direct and the indirect waves are again in opposite phase ($\varphi = 180^\circ$), we obtain the condition for zero field intensity ($\mathcal{E} = 0$)

$$\frac{K_1}{K_2[1 + \rho_v]} = \cos^2 \beta \quad (117)$$

that is, a condition which depends upon the elevation of the indirect ray only and not upon the sidewise departure since α is not contained in this expression. We have therefore only obtained an equation (117) which expresses fading. Hence the Adcock sending system has no bearing error even when night effects occur. The same is also true when the system is used as a receiver as is shown on page 498.

Case F.—A horizontally polarized wave comes down from the ionized layer as is indicated in Fig. 286. In this case it is more convenient to draw the magnetic vectors. H_1 then denotes the magnetic vector of the incident wave, $H_2 = \rho_h H_1$ the vector of the reflected wave, and H_3 the intensity of the refracted wave. The factor ρ_h now denotes the reflection factor for horizontally polarized waves. In this case we have

$$\mathcal{E}_x = \mathcal{E}_z = 0 \quad \text{and} \quad H_y = 0$$

and the boundary conditions require that

$$\mathcal{E}_x = \mathcal{E}_x'; \quad H_x = H_x' \quad \text{and} \quad H_z = H_z'$$

where \mathcal{E}_x' , H_x' , and H_z' again denote the field vectors in the ground at the boundary. Hence

$$\tan \delta = \frac{H_z'}{H_x'} = \frac{H_z}{H_x} \quad (118)$$

where H_z and H_x are the vertical and horizontal components at the boundary of the resultant vector $H_1 + H_2$ when drawn in the proper direction. The angle δ is therefore measured by a tilting loop which can be rotated about a horizontal axis with its direction perpendicular to the direction of the sender. We have therefore a method which measures the angle of refraction and a method for finding the index of refraction and the effective dielectric constant of the ground when the angle of

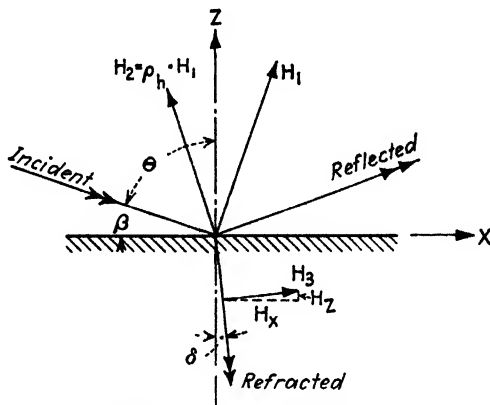


FIG. 286.—Horizontally polarized electromagnetic wave.

incidence is known. The relation between the dielectric constant κ_e , the index of refraction n , and this angle of tilt $t = \delta$ is

$$\tan \delta = \frac{\sin \theta}{\sqrt{\kappa_e - \sin^2 \theta}} = \frac{\sin \theta}{\sqrt{n^2 - \sin^2 \theta}} \quad (119)$$

But, for ground, $n = \sqrt{\kappa_e} \gg 1$ and the foregoing relation reduces to

$$\tan \delta \cong \frac{\sin \theta}{\sqrt{\kappa_e}} = \frac{\sin \theta}{n} \quad (120)$$

The bearing error of horizontally polarized waves can be derived as in (110) and becomes

$$\begin{aligned} \tan \gamma &= \frac{K_2}{K_1} [1 + \rho_h] \cos \theta \\ &= \frac{K_2}{K_1} [1 + \rho_h] \sin \beta \end{aligned} \quad (120a)$$

where the elevation β of the outgoing sky wave can again be estimated from the measurements, ρ_h in the reflection coefficient at the surface of the

earth for the horizontally polarized wave (about 0.9 for ordinary ground and unity for ocean), and K_2/K_1 the ratio of the mean field intensities of indirect and direct waves. It should be noted that γ denotes the

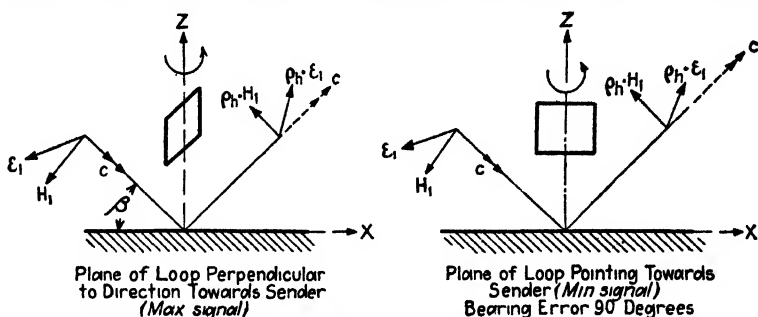


FIG. 287.—Downcoming electromagnetic wave horizontally polarized.

bearing error when the loop is used as a sender and a vertical antenna as a receiver. The error is generally only a few degrees (about 2 deg) for transmission over sea but may be considerable over land.

For a receiving loop and horizontally polarized waves arriving from the sky, we have the case indicated in Fig. 287. For maximum signal

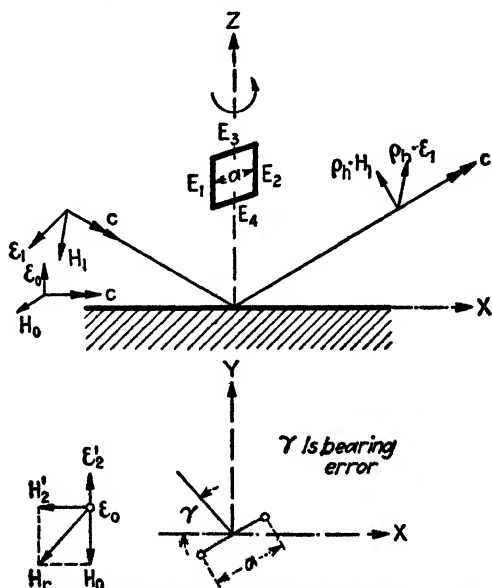


FIG. 288.—Direct vertically polarized electromagnetic wave (E_0 , H_0) and reflected horizontally polarized wave (E_1 , H_1 and $\rho_h \cdot E_1$, $\rho_h \cdot H_1$) affect loop.

intensity, the vertical sides of the loop do not produce current but the horizontal branches cause the current flow. For the loop in minimum position, theoretically none of the sides can give rise to a current flow.

When the receiving loop is close enough to the sender so that both the direct *vertically* polarized wave and an indirect *horizontally* polarized wave arrive, we obtain a bearing error γ as indicated in Fig. 288. The loop current vanishes when the induced voltages $E_1 - E_2 = E_3 - E_4$. The bearing error can be calculated from (120a) on account of the Sommerfeld-Pfrang*reciprocity theorem.

Case G.—A downcoming wave is generally not polarized in any particular plane since it does not travel over a conducting surface which would attenuate, by absorption, any components of the magnetic field which were not parallel to it. The descending wave (Fig. 289), which is generally elliptically¹ polarized, is therefore decomposed into a normal

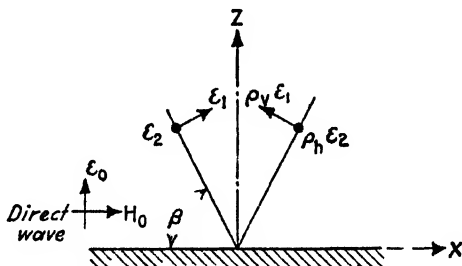


FIG. 289 —Horizontal and vertical polarization of downcoming electromagnetic wave.

component E_1 and an *abnormal* (horizontal) component E_2 (perpendicular to the paper). The first produces the usual directional effects, while the latter does not induce currents in a vertical antenna but does in a loop. However, according to the foregoing considerations, the bearing errors experienced with loop direction finders are due to the action of the horizontally polarized component of the descending indirect waves when it is assumed that the waves do not deviate laterally from the great circle between the sender and the receiver. This is a permissible assumption except for very short waves (below 80 m). The bearing error γ can be understood from the representation of Fig. 290. Any receiving system such as the Adcock antenna and the like which is unaffected by a horizontal component of the electric intensity does away with the night

¹ The most general case is that in which the electric field is resolved into three components: one vertical and two horizontal components which are perpendicular to each other. In that case a position of zero current in a loop receiver is never possible. The relative values of these components depend upon the angle β and the degree of twist of the plane of polarization. The plane of polarization can rotate erratically and produce fluctuations in the received current (fading) and may account for the swinging of the bearing of loop receivers. For more details, reference is made to G. W. Pickard, The Polarization of Radio Waves, *Proc. I.R.E.*, 14, 205, 1926; J. Hollingworth, The Polarization of Radio Waves, *Proc. Roy. Soc. (London)*, (A), 119, 444, 1928.

errors even though the vertically polarized indirect wave still produces fading effects.

When $(90 - \beta)$ denotes the angle of incidence of the indirect wave, ϵ_{0x} , ϵ_{0y} , ϵ_{0z} the components of the direct wave, ϵ_0 and ϵ_{1x} , ϵ_{1y} , ϵ_{1z} the components of the resultant field ϵ_1 produced by the descending wave together with the reflected wave, we have

$$\left. \begin{aligned} \frac{\epsilon_{0z}}{\epsilon_{0x}} = n = \sqrt{\kappa_e}; \quad \frac{\epsilon_{1z}}{\epsilon_{1x}} = n \cos \beta; \quad \frac{\epsilon_{0z}}{H_{0y}} = 1; \\ \frac{\epsilon_{1z}}{H_{1y}} = \cos \beta; \quad \frac{H_{1z}}{H_{1x}} = \frac{\cos \beta}{n}; \end{aligned} \right\} \text{and } \left. \begin{aligned} \epsilon_x &= \epsilon_{0x} + \epsilon_{1x} \\ \epsilon_y &= \epsilon_{0y} + \epsilon_{1y} \\ H_x &= H_{0x} + H_{1x} \\ H_y &= H_{0y} + H_{1y} \end{aligned} \right\} \quad (121)$$

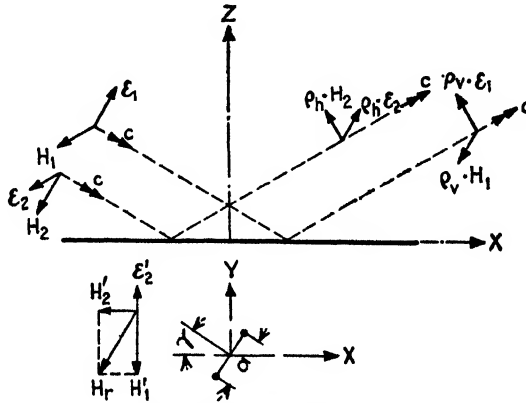


FIG. 290.—Bearing error γ .

and the angle β which the descending wave makes with the surface of the group can be found from

$$\cos \beta = \left. \begin{aligned} &\frac{1}{n} \left[\frac{\epsilon_x - \epsilon_{0x}}{\epsilon_x - \epsilon_{0x}} \right] \text{ (with Hertzian rod)} \\ &n \left[\frac{H_x - H_{0x}}{H_x - H_{0x}} \right] = n \frac{H_x}{H_x} \text{ (with tilting loop)} \\ &\frac{\epsilon_x - \epsilon_{0x}}{H_y - H_{0y}} \text{ (with loop and vertical aerial)} \end{aligned} \right\} \quad (122)$$

These relations hold, however, only when the descending waves have travelled through the upper region of the atmosphere *without deviating laterally* from the great circle plane through the transmitter and receiver.

For the *vertically polarized* components,

$$\epsilon_1 = \frac{\epsilon_{1z}}{[1 + \rho_z] \cos \beta} \quad \text{and} \quad \epsilon_0 \cong \epsilon_{0z}$$

and the ratio of the relative intensities of the indirect and direct waves becomes

$$\frac{\varepsilon_1}{\varepsilon_0} = \frac{\varepsilon_z - \varepsilon_{0z}}{\varepsilon_{0z}[1 + \rho_v] \cos \beta} \quad (123)$$

For the *horizontally polarized* components, we have

$$\begin{aligned} H_{1x} &= H_1[1 + \rho_h] \sin \beta = \varepsilon_1[1 + \rho_h] \sin \beta \\ \varepsilon_0 &= \varepsilon_{0z} = H_{0y} \end{aligned}$$

and the relative intensities of indirect and direct waves are given by

$$\frac{\varepsilon_1}{\varepsilon_0} = \frac{H_{1x}}{\varepsilon_{0z}[1 + \rho_h] \sin \beta} \quad (124)$$

The reflection factors ρ_i and ρ_h for an angle of incidence $\theta = (90 - \beta)$ and an angle of refraction δ (Figs. 282 and 286) are

$$\left. \begin{aligned} \rho_v &= \frac{\tan(\theta - \delta)}{\tan(\theta + \delta)} \\ \rho_h &= \frac{\sin(\theta - \delta)}{\sin(\theta + \delta)} \end{aligned} \right\} \quad \text{where} \quad n = \frac{\sin \theta}{\sin \rho} \quad (125)$$

172. Day¹ and Night Effects on Vertical Antennas and Loops When Used as a Receiver and Austin's Barrage Circuit Method. *a. The Vertical Antenna.*—Since the downcoming wave is generally elliptically polarized, we can split it into two components, one of which, ε_1 , is *normally* polarized in the vertical plane through the direction of propagation, and an *abnormally* polarized component the maximum value of which, ε_z , is perpendicular to the plane above (perpendicular to paper; hence horizontal). The ground acts as a perfect reflector (case A, page 499, which is about the case for waves > 300 m) so that the reflection factor $\rho = 1$ and there is neither amplitude nor phase change. The electric vector ε_0 of the normally polarized ground wave which reaches the vertical antenna is in the direction of the Z-axis, and the corresponding magnetic vector is perpendicular to the plane of the paper, that is, along the Y-axis. If d_0 denotes the path of the direct wave and d_1 that of the indirect wave (assuming, for simplicity, equivalent reflection at the ionized layer which is especially justified for long waves), we have the two fields

$$\varepsilon_0 \sin \omega \left[t_0 - \frac{d_0}{c} \right] \quad \text{and} \quad 2\varepsilon_1 \sin \omega \left[t_0 - \frac{d_1}{c} \right]$$

¹ APPLETON, E. V., and M. A. F. BARNETT, On Some Direct Evidence for Downward Atmospheric Reflection of Electric Rays, *Proc. Roy. Soc. (London)*, **109**, 621, 1925; E. V. APPLETON and J. A. RATCLIFFE, On the Nature of Wireless Signal Variations, *Proc. Roy. Soc. (London)*, (A), **115**, 291, 1927; L. W. AUSTIN, Experiments in Recording Radio Signal Intensity, *Proc. I.R.E.*, **17**, 1192, 1929.

at the receiving vertical antenna, which for

$$(-\varphi) = \frac{\omega d}{c} = \frac{2\pi d}{\lambda} = \frac{2\pi}{\lambda}[d_1 - d_0] \quad \text{and} \quad t = t_0 - \frac{d_0}{c}$$

gives the two fields

$$\mathcal{E}_0 \sin \omega t \quad \text{and} \quad 2\mathcal{E}_1 \sin [\omega t + \varphi]$$

Since, for the vertical antenna, only the electric component in its direction can induce an e.m.f., we have

$$\mathcal{E}_z = \mathcal{E}_0 \sin \omega t + 2\mathcal{E}_1 \cos \beta \sin [\omega t + \varphi]$$

or

$$\mathcal{E}_z = \sqrt{\mathcal{E}_0^2 + 4\mathcal{E}_0\mathcal{E}_1 \cos \beta \cos \varphi + 4\mathcal{E}_1^2 \cos^2 \beta \sin [\omega t + \psi]} \quad (126)$$

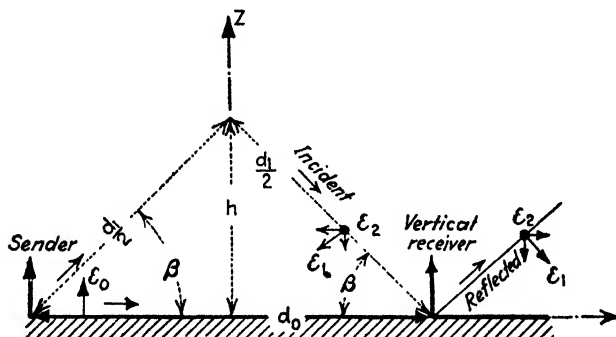


FIG. 291.—Vertical aerial reception.

and the resultant voltage induced in the antenna for an effective height h_e is

$$E = h_e \mathcal{E}_z$$

The current induced in the vertical antenna during the night is therefore different from that induced during the day since, for most waves, the absorption in the upper atmosphere during the day is so pronounced that the indirect waves are not returned. Whether the nighttime value of \mathcal{E}_z is greater or smaller than the daytime value depends upon the phase of the direct and indirect waves. When the distance is not too great, marked differences can occur, while, for longer distances, the ground wave no longer contributes since it is too attenuated.

b. The Single Loop.—If in place of the vertical antenna (Fig. 291) a loop receiver is employed, we have the case indicated in Fig. 292. Both the horizontal and vertical components of \mathcal{E}_1 contribute to the induced current, while the abnormal component \mathcal{E}_2 (perpendicular to the paper) cannot induce currents when the loop points to the sender. The resultant induced voltage here is *independent* of the angle β at which the wave strikes the loop since the effective height of the loop, according to (78), is

$$h_e = \frac{[2\pi \text{ times frequency}][\text{effective area of loop}]}{\text{velocity of propagation}}$$

that is, the same for all directions in the plane of the loop.¹ The loop current may be considered as due to the difference in phase $2\pi s/\lambda$ of the wave between the points where it enters and leaves the loop. The quantity s denotes the distance from front to back of the loop in the direction of propagation. The phase of the horizontal component is shifted 180 deg by reflection and, as the reflected wave passes the loop from below, the resulting voltage induced in the loop by the reflected wave is in the same direction as when due to the descending wave, and the sum is $2h_e\epsilon_1$.

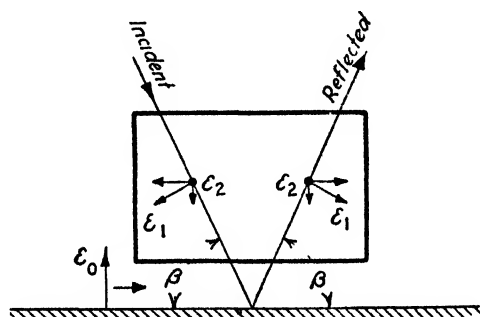


FIG. 292.—Loop receiver.

When the voltage across the terminals of the tuning condenser of the loop pointing toward the station (maximum effect) is linearly amplified and rectified by a detector following a square law, the direct current I measured by the indicator, according to the intensities $\epsilon_0 \sin \omega t$ and $2\epsilon_1 \sin [\omega t + \varphi]$ of the direct and indirect wave, is

$$I = k[\epsilon_0^2 + 4\epsilon_0\epsilon_1 \cos \varphi + 4\epsilon_1^2] \quad (127)$$

Assuming again that, for most wave lengths, the indirect ray does not exist during the day, that the effect of the ground wave at the receiver is the same during day and night, and that $I_D = k\epsilon_0^2$ is the current measured during the day and that I_N is the current noted during the night, we have

$$\frac{I_N}{I_D} = 1 + 4\frac{\epsilon_1}{\epsilon_0} \cos \varphi + 4\left[\frac{\epsilon_1}{\epsilon_0}\right]^2 \quad (128)$$

since, according to the preceding definition, (127) denotes the night value. When, therefore, the frequency of the sender is changed through a small amount Δf , the phase $\varphi = 2\pi f d/c$ changes, since the difference in path between the indirect and the direct waves for such a small change is

¹ Effective area is the area of the loop times the number of turns.

practically the same. When the direct and indirect intensities are in phase, we have a maximum and, when they are in antiphase, we note a minimum current indication. If p is the number of current maxima (or minima) while the frequency is changing from f_1 to f_2 for the corresponding phase angles φ_1 and φ_2 , we have

$$p = \frac{\varphi_1 - \varphi_2}{2\pi} = \frac{f_1 d}{c} - \frac{f_2 d}{c} \quad (129)$$

Hence a maximum value in the current produced in such a way shows that φ is 0; 2π ; 4π , etc., and a minimum value in I indicates that $\varphi = \pi$; 3π ; 5π ; etc.

c. Loop and Vertical Antenna as Receiver.—Let E_D be the resonance voltage of the vertical antenna when measured with a tube voltmeter during daytime, and E_N the voltage during nighttime, and E_D' , E_N' the corresponding voltages for the loop when pointing toward the sender, then

$$\left. \begin{aligned} E_D &= K\varepsilon_0 \\ E_N &= K\varepsilon_z = K\sqrt{\varepsilon_0^2 + 4\varepsilon_0\varepsilon_1 \cos \beta \cos \varphi + 4\varepsilon_1^2 \cos^2 \beta} \\ E_D' &= K'\varepsilon_0 \\ E_N' &= K'\varepsilon_1 = K'\sqrt{\varepsilon_0^2 + 4\varepsilon_0\varepsilon_1 \cos \varphi + 4\varepsilon_1^2} \end{aligned} \right\} \quad (130)$$

Hence, for the vertical antenna, we have for

$$P = \frac{2\varepsilon_1}{\varepsilon_0} \quad (131)$$

the ratio

$$\frac{E_N}{E_D} = \sqrt{1 + 2P \cos \beta \cos \varphi + P^2 \cos^2 \beta} \quad (132)$$

and for the loop

$$\frac{E_N'}{E_D'} = \sqrt{1 + 2P \cos \varphi + P^2} \quad (133)$$

Thus we have three equations and can solve for the unknowns P , β , and φ . When the ground and indirect waves are in phase, we have maximum values for the night indications and also for the ratio of night-to-day value. This inphase condition occurs when $\cos \varphi = 1$ and gives the ratios

$$\left. \begin{aligned} \frac{E_N}{E_D} &= 1 + P \cos \beta \\ \frac{E_N'}{E_D'} &= 1 + P \end{aligned} \right\} \quad (134)$$

From this, the relative intensity $P = 2\varepsilon_1/\varepsilon_0$ of the indirect and direct waves as well as the angle β of the descending wave with the horizon can

be calculated from the four measurements E_N , E_N' , E_D , and E_D' . Since the distance d_0 along the ground is known, we can find the apparent height of the ionized layer, according to Fig. 291, from

$$h = 0.5d_0 \tan \beta \quad (135)$$

The inphase condition is established by varying the frequency f of the sender current by a small amount Δf (Fig. 293) and, if the receiving antenna is, for each frequency, tuned for constant sender output, the induced voltages during the night will go through maxima M and minima m . The maxima correspond to inphase and the minima to antiphase adjustments.

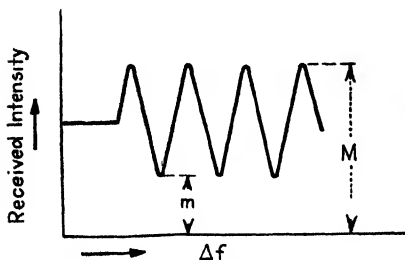


FIG. 293.—Intensity variation if frequency of sender current is varied.

Equations (132) and (133) can also be simplified by measuring the field intensities closer to the sender; for this condition the ratio ϵ_1/ϵ_0 is

small compared with unity since the direct wave is most important. We then obtain

$$\left. \begin{aligned} \frac{E_N}{E_D} &= 1 + P \cos \beta \cos \varphi \\ \frac{E_N'}{E_D'} &= 1 + P \cos \varphi \end{aligned} \right\} \quad (136)$$

Hence the variations due to fading are larger in the loop than in the aerial. For the angle β , we find

$$\cos \beta = \frac{[E_N - E_D]E_D'}{[E_N' - E_D']E_D} \quad (137)$$

Generally we have, for the vertical antenna, the field intensities $\epsilon_D = \epsilon_0$ and $\epsilon_N = \epsilon_0 + 2K\epsilon_1 \cos \beta$ and for the loop as a receiver $\epsilon_D' = \epsilon_0$ and $\epsilon_N' = \epsilon_0 + 2K\epsilon_1$. This gives the difference in night and day field intensities $\epsilon_N - \epsilon_D = 2K\epsilon_1 \cos \beta$ and $\epsilon_N' - \epsilon_D' = 2K\epsilon_1$. Hence

$$\cos \beta = \frac{\epsilon_N - \epsilon_D}{\epsilon_N' - \epsilon_D'}$$

where it should be remembered that K is a factor depending upon the integral phase between ϵ_0 and ϵ_1 which is brought out in Fig. 294.

According to L. W. Austin, the measurement can be conveniently carried out by means of the barrage circuit for which a vertical aerial with a coil L couples to a coil L_1 connected in a tuned loop. The loop is again turned about its vertical axis so that its plane points toward the

sender but is so coupled to the antenna that the reception from the given direction on the loop opposes that on the antenna. The coupling between L and L_1 is adjusted so that in the middle of the day, when it is assumed that only the vertical ground wave \mathcal{E}_0 is present, the two receptions balance and no deflection on the indicator of the detector circuit is noted.

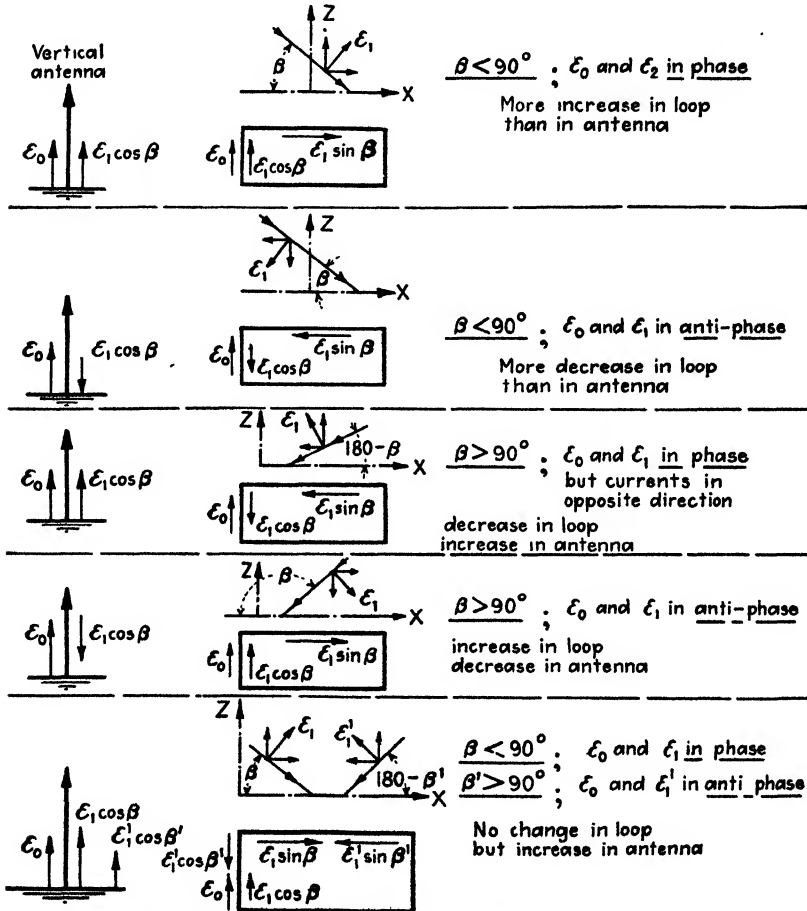


FIG. 294.—Vertical antenna compared with loop aerial.

But during the night descending waves appear, and deflections will be produced because their horizontal components destroy the balance. Since the effect of an antenna on the receiver is proportional to

$$\mathcal{E}_0 + k\mathcal{E}_1 \cos \beta$$

for $k = 2K$ and that of the loop is $\mathcal{E}_0 + k'\mathcal{E}_1$ for $k' = 2K$, and the loop produces equal and opposite effects on the antenna, for the resultant effect on the detector when downcoming waves occur, we have

$$\begin{aligned}
 E &= k_1[\varepsilon_0 + k'\varepsilon_1 - \varepsilon_0 - k\varepsilon_1 \cos \beta] \\
 &= k_1\varepsilon_1[k' - k \cos \beta]
 \end{aligned}
 \tag{138}$$

where k_1 is a constant and k' and k depend upon the effective height of the loop and antenna, respectively, and include the phase difference between the direct and indirect wave.

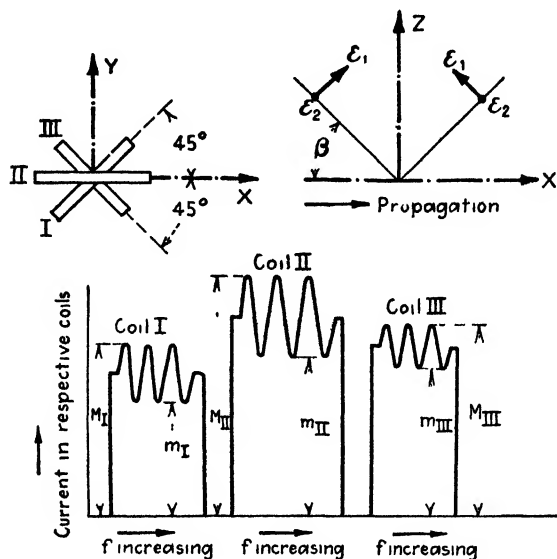


FIG. 295.—Three-loop method.

d. Three-loop System.—Three vertical loops I, II, III are used one at a time and in the orientation indicated in Fig. 295. The voltages induced in the three loops are

$$\left. \begin{aligned}
 E_I &= k[\varepsilon_0 \sin \omega t + 2\varepsilon_1 \sin [\omega t + \varphi_1] - 2\varepsilon_2 \sin \beta \sin [\omega t + \varphi_2]] \\
 E_{II} &= k\sqrt{2}\{\varepsilon_0 \sin \omega t + 2\varepsilon_1 \sin [\omega t + \varphi_1]\} \\
 E_{III} &= k[\varepsilon_0 \sin \omega t + 2\varepsilon_1 \sin [\omega t + \varphi_1] + 2\varepsilon_2 \sin \beta \sin [\omega t + \varphi_2]]
 \end{aligned} \right\}
 \tag{139}$$

since the abnormal component ε_2 which is perpendicular to the paper plays a part when the loop is not pointing toward the sender. Putting

$$\left. \begin{aligned}
 P &= \frac{2\varepsilon_1}{\varepsilon_0}; & Q &= \frac{2\varepsilon_2}{\varepsilon_0} \sin \beta; & \varphi &= \varphi_2 - \varphi_1 \\
 \tan \Psi_1 &= -\frac{Q \sin \varphi}{P - Q \cos \varphi} \\
 \tan \Psi_2 &= \frac{Q \sin \varphi}{P + Q \cos \varphi}
 \end{aligned} \right\}
 \tag{140}$$

we find

$$\left. \begin{aligned} E_I &= k\varepsilon_0[\sin \omega t + \sqrt{P^2 - 2PQ \cos \varphi + Q^2} \sin (\omega t + \varphi_1 + \Psi_1)] \\ E_{II} &= k\sqrt{2}\varepsilon_0[\sin \omega t + P \sin (\omega t + \varphi_1)] \\ E_{III} &= k\varepsilon_0[\sin \omega t + \sqrt{P^2 + 2PQ \cos \varphi + Q^2} \sin (\omega t + \varphi_1 + \Psi_2)] \end{aligned} \right\} \quad (141)$$

The frequency f of the sender is again varied by a small amount Δf in order to produce successive maxima and minima in the voltage of the tuned loop system in use at the time. The change is so small that amplitudes of ε and the phase displacement $\varphi = \varphi_2 - \varphi_1$ between the normal (ε_1) and the abnormal (ε_2) polarized wave are practically independent of Δf . The three readings E_I , E_{II} , and E_{III} are taken in rapid succession. The indicated currents pass again through successive maxima (M) and minima (m) and yield

$$\left. \begin{aligned} \frac{M_I - m_I}{M_I + m_I} &= \sqrt{P^2 - 2PQ \cos \varphi + Q^2} \\ \frac{M_{II} - m_{II}}{M_{II} + m_{II}} &= P \\ \frac{M_{III} - m_{III}}{M_{III} + m_{III}} &= \sqrt{P^2 + 2PQ \cos \varphi + Q^2} \end{aligned} \right\} \quad (142)$$

The left side of these three expressions is known from measurements; and the unknowns P , Q , and φ can be calculated. When β is determined by one of the foregoing methods, we find the ratio of the abnormal indirect wave to the direct wave, according to (140), to be

$$\frac{\varepsilon_2}{\varepsilon_0} = 0.5Q \sin \beta \quad (143)$$

while that of the direct wave becomes

$$\frac{\varepsilon_1}{\varepsilon_0} = 0.5P$$

173. Directive Antenna Arrays.¹—The arrangements to be described are of use for comparatively short waves only; otherwise the antenna systems would have to be of very large physical dimensions.

If we have n equal vertical antennas (strictly dipoles) the same distance a apart along a straight line and connected through parallel-wire systems of equal electrical length to the detector (when acting as a

¹ CHIREIX, H., *Radioélectricité*, 5, 65, 1924; R. MESNY, *L'onde élec.*, 6, 181, 1927; J. A. FLEMING, *Exptl. Wireless*, 4, 387, 1927; E. GREEN, *Exptl. Wireless*, 4, 587, 1927; S. BALLANTINE, *Proc. I.R.E.*, 16, 1261, 1928; H. YAGI and S. UDA, *Proc. I.R.E.*, 16, 715, 1928. For other details, see F. OLLENDORFF, "Die Grundlagen der Hochfrequenztechnik," Julius Springer, Berlin, 1926, p. 590.

receiver system) or to the generator (when acting as a sender), then, according to Eqs. 59, 60, and 61 for the horizontal characteristic, we have $D = D_0$; $\gamma = 0$; $l = \text{constant}$ and may be equated to zero. Equation (61) yields the direction characteristic

$$D_r = D_0 \frac{\sin [n(\pi a/\lambda) \cos \alpha]}{\sin [(\pi a/\lambda) \cos \alpha]} \quad (144)$$

Hence, if we have two vertical antennas ($n = 2$) a distance $a = \lambda/2$ apart, we have

$$D_r = D_0 \frac{\sin [\pi \cos \alpha]}{\sin [(\pi/2) \cos \alpha]}$$

which is the characteristic shown in Fig. 296. Figure 297 illustrates the case of three vertical antennas with the spacings as indicated. The quantity α , for example, denotes the angle which an incident wave makes with the X -axis. The theory of such an antenna array is, according to Fig. 298, as follows.

P is again a point in the true radiation field and far enough away so that the width $p\lambda$ of the aerial system of the n vertical antennas is very

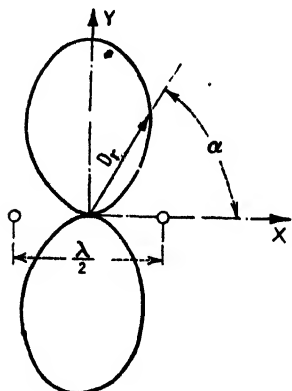


FIG. 296.—Direction characteristic for $a = 0.5\lambda$.

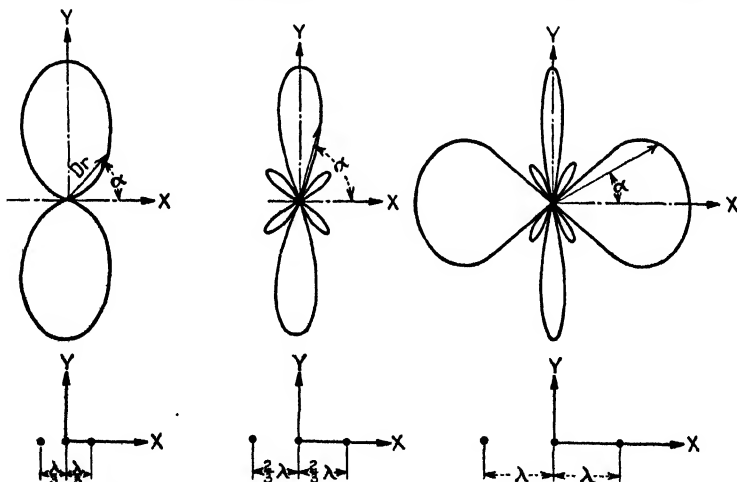


FIG. 297.—Direction characteristics for two vertical wires spaced $\lambda/3$, $2\lambda/3$ and λ .

small compared with the distance d of the right antenna to P . The distances of the other aerials are $d + a \cos \alpha$; $d + 2a \cos \alpha$; . . .

$$d + (n - 1)a \cos \alpha = d + p\lambda \cos \alpha$$

where p is simply the factor by which the operating wave length is multiplied in order to give the entire width of the system. These dis-

tances affect only as the phase angle of the effect of each antenna at P ; the distance d is so much greater than $(n - 1)a \cos \alpha$ that the intensities at P due to each sending antenna are all equal. Hence, instead of the expressions

$$\frac{\varepsilon}{d} \sin \left[\omega t - \frac{2\pi}{\lambda} d \right]; \quad \frac{\varepsilon}{d - a \cos \alpha} \sin \left[\omega t - \frac{2\pi}{\lambda} (d - a \cos \alpha) \right];$$

$$\frac{\varepsilon}{d - 2a \cos \alpha} \sin \left[\omega t - \frac{2\pi}{\lambda} (d - 2a \cos \alpha) \right]; \text{ etc.}$$

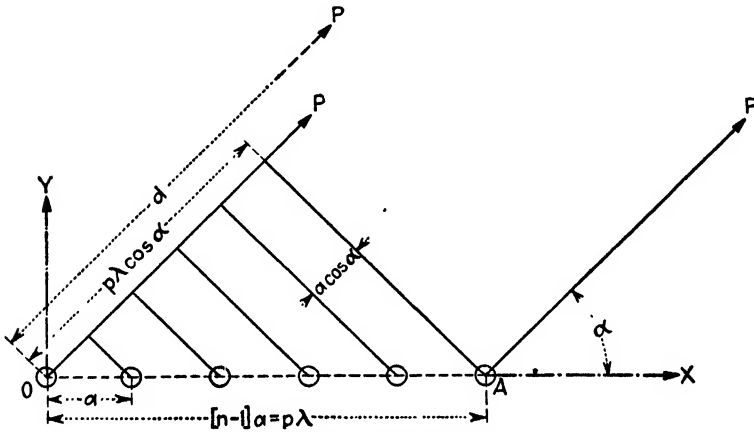


FIG. 298.—Antenna array.

we can write for the resultant field at P

$$\begin{aligned} \varepsilon_r &= \frac{\varepsilon}{d} \left\{ \sin \left[\omega t - \frac{2\pi}{\lambda} d \right] + \sin \left[\omega t - \frac{2\pi}{\lambda} (d - a \cos \alpha) \right] + \right. \\ &\quad \sin \left[\omega t - \frac{2\pi}{\lambda} (d - 2a \cos \alpha) \right] + \\ &\quad \left. + \dots + \sin \left[\omega t - \frac{2\pi}{\lambda} [d - p\lambda \cos \alpha] \right] \right\} \\ &= k \left\{ \sin \gamma + \sin [\gamma + \delta] + \sin [\gamma + 2\delta] + \dots + \sin \left[\gamma + \frac{p\lambda}{a} \delta \right] \right\} \\ &= k \sin \left[\gamma + (n-1) \frac{\delta}{2} \right] \frac{\sin (n\delta/2)}{\sin (\delta/2)} \end{aligned} \quad (145)$$

since $p\lambda/a = (n - 1)$; $\gamma = \omega t - (2\pi/\lambda)d$ and $\delta = (2\pi/\lambda)a \cos \alpha$. The directional characteristic is therefore as in (144) since

$$D_0 = k \sin [\gamma + (n - 1)\delta/2]$$

and

$$\frac{\sin (n\delta/2)}{\sin (\delta/2)} = \frac{\sin [(n\pi a/\lambda) \cos \alpha]}{\sin [(\pi a/\lambda) \cos \alpha]}$$

If we had had a great number of vertical antennas lined up and excited from the same source by means of parallel lines of the same electrical length, the antenna currents would have the same amplitude and phase. The field at a point P along the Y -axis ($\alpha = 90^\circ$), according to Fig. 298, would be due to component fields which are also in phase and of the same strength. But, for any angle α smaller or larger than 90 and 270 deg, the phase effect due to $a \cos \alpha$, $2a \cos \alpha$, etc., must be taken into account and each consecutive vector due to a consecutive antenna of the array has the same phase displacement with respect to the preceding

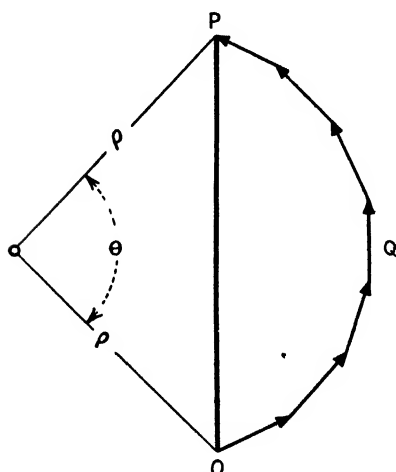


FIG. 299.—Vectorial addition for several vertical antennas.

one. The vectors along the path OQP of Fig. 299 then give the resultant vector, forming the straight line OP . For a great number of vertical antennas along the distance $p\lambda$ (Fig. 298), the component vectors along the path OQP (Fig. 299) are practically part of a circle of radius ρ and the arc OPQ subtends an angle θ which is a function of the direction toward P , that is, of the angle α . We have, therefore, another means for finding the magnitude of the resultant vector at P for any angle α . From Fig. 298, we note that at P the vector of the antenna O and the vector of the antenna A have a phase difference $p\lambda \cos \alpha$ which, according to Fig. 299, corresponds to an angle θ . But when the difference of path from O to P and A to P is exactly one wave length (λ), the angle θ is 360 deg, that is, corresponds to 2π radians. Hence

$$\theta = \frac{2\pi p\lambda \cos \alpha}{\lambda} = 2\pi p \cos \alpha \quad (146)$$

Now the resultant vector $OP = 2\rho \sin (\theta/2)$, is a measure of the field intensity at P for any angle α , while the arc $OQP = \rho\theta$ radians is a measure of the field intensity in the direction OY , that is, for ($\alpha = 90^\circ$). The directional characteristic in the XY plane with these assumptions becomes

$$D_r = \frac{OP}{OQP} = \frac{\sin (\theta/2)}{\theta/2} = \frac{\sin [\pi p \cos \alpha]}{\pi p \cos \alpha} \quad (147)$$

Figure 300 gives the characteristics for $p = 2$ and $p = 10$, that is, a vertical antenna array which is 2λ and 10λ wide. The positions of the maxima, according to (146), are

$$\frac{d\left[\frac{\sin \theta/2}{\theta/2}\right]}{d[\theta/2]} = \frac{\cos \theta/2}{\theta/2} - \frac{\sin \theta/2}{[\theta/2]^2} = 0$$

or for

$$\tan \frac{\theta}{2} = \frac{\theta}{2} \quad (148)$$

which yields the angles $\theta/2 = 1.43\pi$; 2.45π ; 3.47π , etc. For $p = 2$, according to (146), the first side maximum occurs at $\alpha = 44^\circ 40'$.

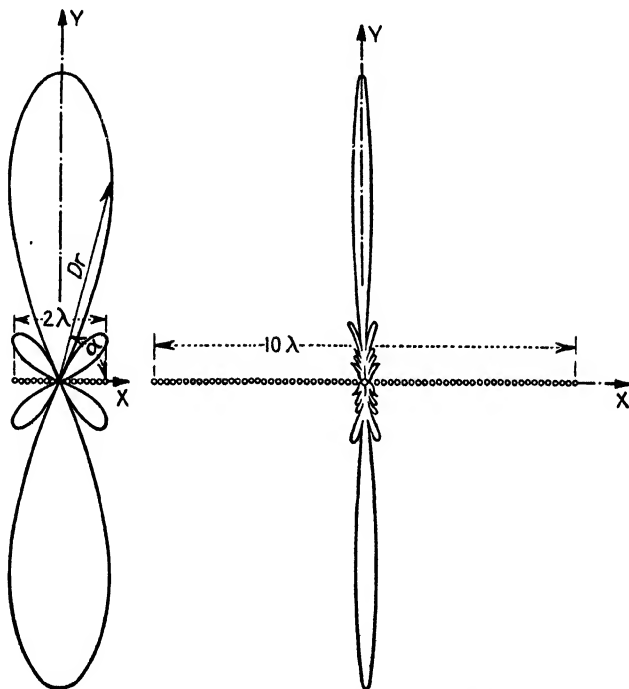


FIG. 300.—Direction characteristics.

Figure 301 illustrates the system used to excite an antenna array for which the antennas are spaced $\lambda/2$ apart and are in phase. Figure 302 shows the Mesny system for exciting an antenna array with the proper phase and amplitude. The dotted lines indicate the current distributions. The currents along the vertical Z -axis are all in phase and produce a two-sided beam along the horizontal Y -axis since the currents in the horizontal portions of the wire along the X -axis are in phase opposition and their effects cancel. The excitation of the wire can be applied either at the middle or at the ends by means of separate generators with synchronized currents. The Chireix system shown below is a half-wave-length zigzag arrangement.

Figure 303 shows the case for $\lambda/2$ spacing and eight vertical dipoles but arranged so that in one case the currents are in phase while for the other case they are out of phase by the angle 180 deg. This angle corre-

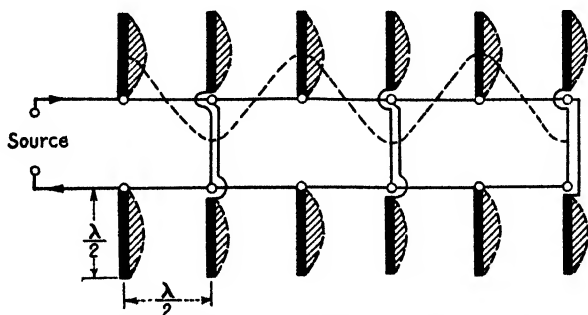


FIG. 301.—Excitation of half-wave-length aerials.

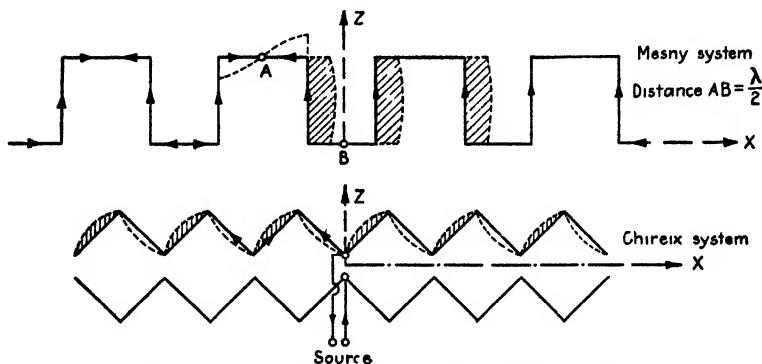


FIG. 302.—Dotted curves are current distributions.

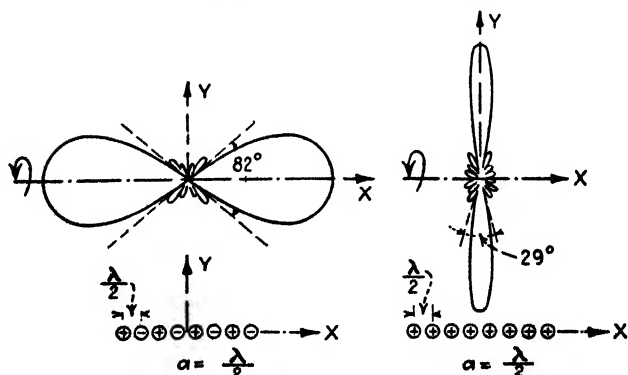


FIG. 303.—Beam radiation for eight vertical dipoles.

sponds to the constant angle of the separation $a = \lambda/2$ and is $\varphi = 2\pi a/\lambda$. It will be noted that, for the inphase excitation, the radiation is essentially along the Y -axis, that is, perpendicular to the alignment of the

vertical dipoles, while, for the consecutive antiphase conditions, the main radiation is along the X-axis, that is, in the direction of alignment, and the beam is not so sharp. When the distance between the vertical antennas is chosen $a = \lambda/4$, the current in the adjacent wires must be in quadrature ($\varphi = \pi/2$). The beam is then largely in the direction of the antenna alignment and a practically *one-sided* directive characteristic is obtained, as is shown in Fig. 304. For the inphase case of Fig. 303, we note that an advantage is the sharpness of the beam and a disadvantage is that the beam is propagated along both the positive and the negative direction of the Y-axis. The advantage of the system indicated in Fig. 304 is that the

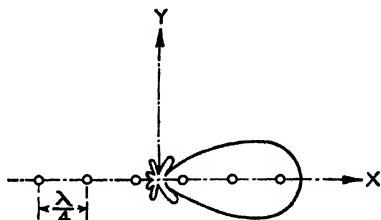


FIG. 304.—Quarter-wave-length spacing gives *one-sided* beam transmission.

beam is largely in one direction, although less concentration is obtained. Combining both cases leads to the C. S. Franklin system using wave reflectors at a distance $\lambda/4$ behind the exciting antenna array as is shown in Fig. 305. The field of the reflector is equal to that of the corresponding exciter antenna but is 90 deg ahead in time phase. The magnitudes of the side maxima decrease as the number of vertical wires is increased for a given total length of the array.

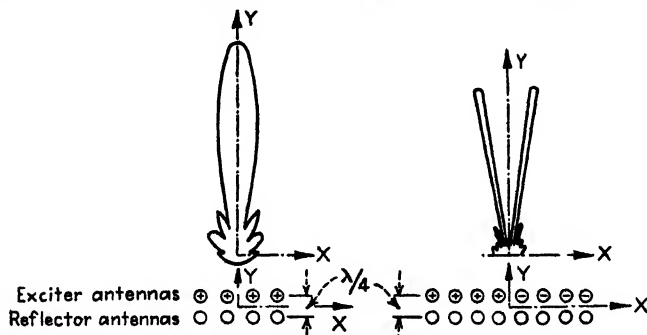


FIG. 305.—One-sided beam transmission by means of reflector arrays.

The beam can be made narrower by choosing the length of the array as large as possible. The field at P due to all reflector wires (Fig. 306) can be found by realizing that the distance of the reflector wire A to P is $d + (\lambda/4) \sin \alpha$, that of B is less distant by $a \cos \alpha$, that of C less distant by $2a \cos \alpha$, etc. The field at P due to the reflector wire A is

$$\frac{\mathcal{E}_A}{d + (\lambda/4) \sin \alpha} \sin \left[\omega \left(t - \frac{T}{4} \right) - \frac{2\pi}{\lambda} \left(d + \frac{\lambda}{4} \sin \alpha \right) \right]$$

$$= \sin \left[\omega t - \frac{2\pi}{\lambda} d - \frac{\pi}{2} \sin \alpha - \frac{\pi}{2} \right]$$

which, for $\varphi = 90^\circ$, gives $\varphi/2 = \pi/4$ and, for a spacing $a = \lambda/4$,

$$D_e' = k \cos \frac{\pi}{4} [\cos \alpha - 1] \quad (151)$$

Combining the characteristic of the alignment of the vertical antennas (147) with the elementary characteristic (151) by means of the relation

$$D_t = D_e \cdot D_r \quad (152)$$

we obtain the total directional characteristic in the horizontal (XY) plane

$$D_t = \frac{\sin [\pi p \cos \alpha]}{\pi p \cos \alpha} \cos \left[\frac{\pi}{4} (\cos \alpha - 1) \right] \quad (153)$$

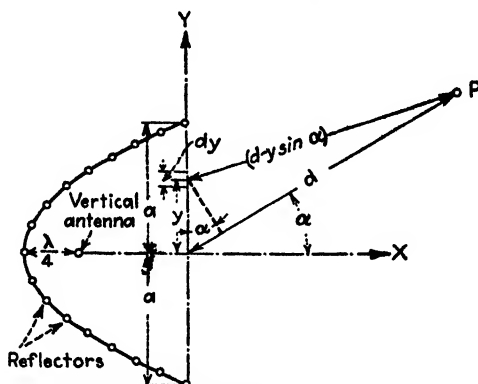


FIG. 307.—Parabolic reflector antenna arrangement.

where, for simplicity, k is taken equal to unity, and $p = [(n-1)a]/\lambda$ denotes the factor by means of which the operating wave length must be multiplied in order to give the length of the aerial alignment (Fig. 306).

The theory of the parabolic reflector, according to Fig. 307, can be established by means of Huygens' principle for which the radiation can be imagined as being due to fictitious radiators which lie in the front face of the reflector. It is assumed that, in the front face of width a and height z , a current of density $i = i_{\max} \sin \omega t$ flows in the Z direction. Everywhere in the face, the current has the same amplitude and phase. We have, for the surface element of width dy , a current

$$dI = idy$$

and a total current, for the width $2a$,

$$I = \int_{-a}^{+a} idy = 2ai$$

The ratio of the average current I_{av} along the actual antenna to the foregoing value gives the mirror factor

$$F = \frac{I_{av}}{I} \quad (154)$$

The field intensity $d\varepsilon$ at P due to the current dI is

$$\begin{aligned} d\varepsilon &= \frac{k}{d} \cos \omega \left[t - \frac{d - y \sin \alpha}{c} \right] i_{\max} dy \\ &= K \left[\cos \omega t' \cos \frac{y \omega \sin \alpha}{c} - \sin \omega t' \sin \frac{y \omega \sin \alpha}{c} \right] i_{\max} dy \end{aligned}$$

for $K = -\omega k/d$ and $\omega t' = \omega[t - (d/a)]$.

The resultant field strength at P becomes

$$\begin{aligned} \varepsilon &= \int_{-a}^{+a} d\varepsilon = K i_{\max} \cos \omega t' \cdot \frac{2}{(\omega \sin \alpha)/c} \cdot \sin \frac{\omega a \sin \alpha}{c} \\ &= K i_{\max} \frac{2\pi c}{\lambda} \cdot \frac{2}{\sin \alpha} \cdot \sin \left[\frac{2\pi}{\lambda} a \sin \alpha \right] \end{aligned} \quad (155)$$

for $K_1 = cK/\omega$. The directional characteristic of a vertical antenna with a parabolic reflector is

$$D = D_0 \frac{\sin [(2\pi/\lambda) a \sin \alpha]}{\sin \alpha} \quad (156)$$

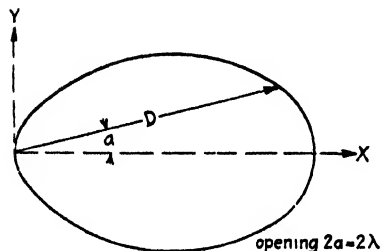


FIG. 308.—Direction characteristics with reflectors along a parabola and vertical radiator about at the focus.

The acuity of the beam in the horizontal plane largely depends upon the opening $2a$ of the mirror. Figure 308 gives the directional characteristics for the openings 2λ and 6λ . It is essential that the reflector wires be of exactly the same size as the antenna and tuned to it. The equation for the directional characteristic can also be obtained by means of Eqs. (60) and (61).

With reference to the distance s between the reflector element and the antenna, it should be remembered that the phase displacement consists of two parts: one part, $\psi_1 = 2\pi s/\lambda$, due to the distance between the reflector and the sender antenna and part ψ_2 due to the reflection caused by coupling which is about 180 deg. It is strictly 180 deg only when $s = 0$ and decreases with s and approaches asymptotically $\psi_2 = 90^\circ$. Hence

$$\psi = \text{function}(s) + \frac{2\pi s}{\lambda}$$

and $\lambda/4$ is no longer the best focal distance. From experimental results, the value 0.27λ seems better.

174. Elementary and Group Characteristics.—From the representations of Figs. 257 and 269, we note that the directional characteristics in any horizontal plane (parallel or in XY plane) can be obtained from the surface characteristic found by the rotation of the characteristic of the ZX plane about the Z -axis.

The total characteristic expressed by Eq. (153) was obtained by multiplying the elementary characteristic D , by the group characteristic D_r of the antenna array without the reflector wires.

Generally, when $F_1(\alpha)$ characterizes the rotation surface of the characteristic in the XY plane about the group axis X (Fig. 309) and $F_2(\beta)$ characterizes the function of the rotation surface of the elementary

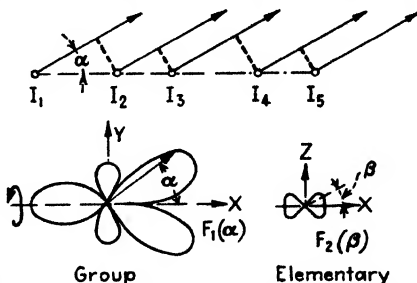


FIG. 309.—Elementary and group characteristic.

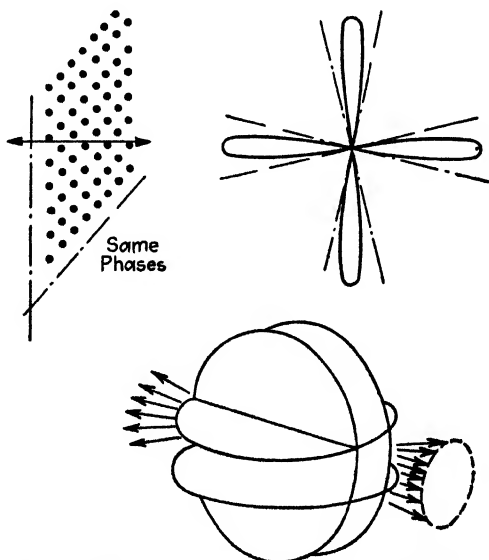


FIG. 310.—Space angle 29 deg. for 8×8 elements.

characteristic in the ZX plane about the axis (Z) of the element, then for the total characteristic we have

$$F(\alpha, \beta) = F_1(\alpha) \cdot F_2(\beta) \quad (157)$$

In the example of this figure, $F_1(\alpha)$ denotes the group characteristic of several dipoles perpendicular to the XY plane along the X -axis, such that the currents have different amplitude and phase. By suitable choice of the two characteristics $F_1(\alpha)$ and $F_2(\beta)$, the concentration of a beam can be adjusted in any direction.

The system of grouping elementary antennas along a line has been described above. If they are grouped in a plane, we obtain the case indicated in Fig. 310, where 8×8 dipoles are arranged to be perpendicular to a certain plane and then produce beams of about 29 deg opening. If 16×16 elements are used, the acuteness of the beam can be brought to 14 deg. When enough antennas are used in the array, the values of the elementary characteristics in the space of the beam become practically constant so that a single antenna has little effect on the shape of the beam.

175. Space Radiation by Means of Higher Modes of Distributions along Aerials.—For studying the ionized layer and other problems, it is of interest to send off beams at a certain elevation β with respect to the surface of the earth. This is made possible by the use of vertical antennas on which more than a quarter wave length is developed and for which the directional characteristic is given by Eq. (62). It leads to the function

$$D_\beta = \frac{1}{\cos \beta} \cos \left[\frac{2\pi}{\lambda} h \sin \beta \right] \quad (158)$$

for the characteristic in any vertical plane through the antenna wire of height h . For the fundamental mode $h = \lambda/4$, we find

$$D_\beta = \frac{1}{\cos \beta} \cos \left[\frac{\pi}{2} \sin \beta \right] \quad (159)$$

The space characteristic (Fig. 311) is then the rotation surface of the upper characteristic in the ZX plane rotated about the vertical antenna (Z -axis). If the antenna were a dipole, the characteristic in the ZX plane would be two semicircles. We note that no radiation is possible along the antenna axis, and maximum radiation occurs along the equatorial plane (XY plane). When the antenna is excited in the third odd mode, that is, in the five-fourths-wave-length distribution,

$$D_\beta = \frac{1}{\cos \beta} \cos \left[\frac{5\pi}{2} \sin \beta \right] \quad (160)$$

for which relation $(5\pi/2) \sin \beta = \pi/2; 3\pi/2; 5\pi/2$; we find $\sin \beta = 0.2; 0.6$; and 1. Hence along elevations $\beta = 11.5^\circ, 37^\circ$, and 90° no radiation takes place. The rotational symmetry about the Z -axis does not hold when several $\lambda/4$ -wave-length antennas are combined and the directional

surface becomes more complicated. It can be calculated for any elevation β and horizontal departure α , according to (60) and (62). The diagrams of Fig. 312 illustrate the case for a full-wave-length and a three-fourths-wave-length distribution. The case for the full-wave-length

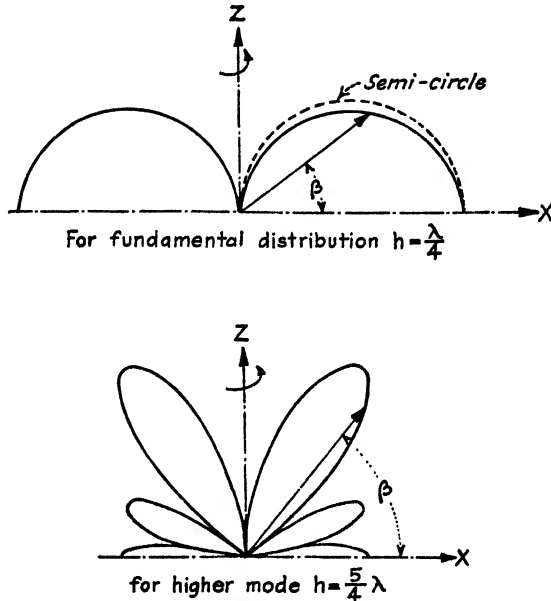


FIG. 311.—For odd $\lambda/4$ distributions along a vertical antenna.

distribution $h = \lambda$ is of especial interest since the *effects along the ground cancel* each other because the elementary currents in the upper and lower half are symmetrically in phase opposition. The effects along the Z

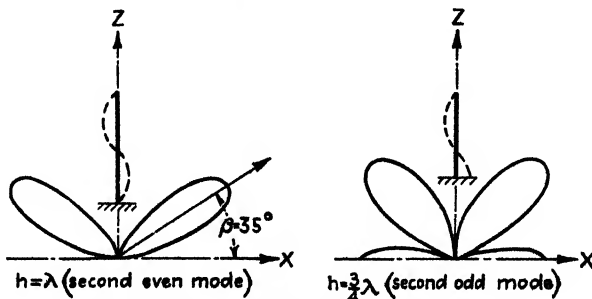


FIG. 312.—Beam projection toward the sky.

direction must always be zero and the maximum radiation is along an elevation angle of about 35 deg. With such an arrangement we can therefore project any radio beam toward the ionized layer without horizontal radiation.

When we use vertical heights smaller than $\lambda/4$, the space phase of the elementary currents in the real aerial and its image will not be sufficiently different to cause cancellation of radiation in non-horizontal directions. But, as h is increased to $\lambda/2$, the maximum current in the vertical wire is at a distance $\lambda/2$ (corresponding to 180-deg phase displacement) from the maximum image current, and there will be considerable cancellation of radiations at high angles of elevation. But the effect of still higher

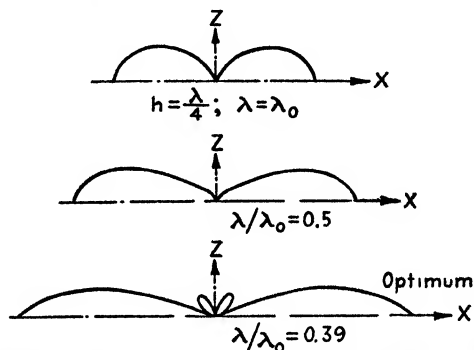


FIG. 313.—Wave distributions for obtaining beam transmission essentially along the ground.

aerials decreases beyond $\lambda/2$ because the phase reverses in the upper part of the vertical wire. This can be corrected by adding $\lambda/2$ -wavelength aerials as in the Franklin system (Fig. 237), which uses phasing coils or other means for avoiding phase reversals. The cancellation of the radiation effect will be still more pronounced in all directions except the horizontal. Figure 313 shows how the beam is more and more concentrated along the surface of the earth as the ratio of the operating wave length λ to the natural wave length λ_0 of the vertical antenna is decreased.

According to S. Ballantine,¹ the case $0.39\lambda_0$ corresponds to the optimum condition.

¹ See p. 356.

CHAPTER XIII

THEORY OF RECURRENT NETWORKS

Combinations of resistance, capacitance, and inductance are employed in order to have compact equivalent circuits for laboratory and other work instead of actual lines of considerable length. Arrangements of this kind can also be used to determine the amplification of receiving and sending apparatus, to produce artificial attenuation, to determine very small currents, and to suppress currents of a certain frequency band¹ with a fairly good over-all efficiency.

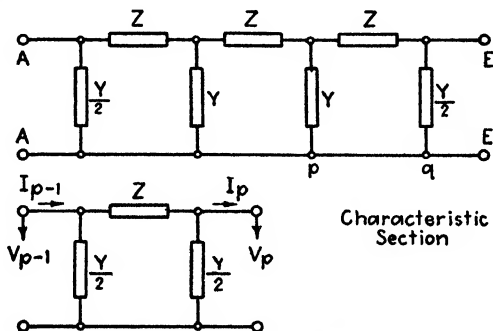


FIG. 314.—Filter with π sections.

176. Artificial Lines.—Figure 314 represents an artificial line made up of π sections, and Fig. 315 an artificial line consisting of T sections. Sections of this type are usually employed although in some cases L sections and H sections are preferred. The quantity Z stands for any impedance along the line, and Y for any admittance across it. The characteristic term indicated below makes up the recurrent network shown above it. There are as many sections as there are admittances

¹ CAMPBELL, G. A., *Trans. A.I.E.E.*, **30**, Part II, 885; 1911; *Bell System Tech. J.*, November, 1922; K. W. WAGNER, *Arch. Elektrotek.*, **3**, 315, 1915; **8**, 61, 1919; O. J. ZOBEL, *Bell System Tech. J.*, January, 1923; October, 1924; J. R. CARSON and O. J. ZOBEL, *Bell System Tech. J.*, July, 1923; L. COHEN, *J. Franklin Inst.*, **5**, 641, 1923; L. J. PETERS, *J. A.I.E.E.*, **42**, 445, 1923; K. KUFFMUELLER, *E.N.T.*, **141**, 1924; K. S. JOHNSON, and T. E. SHEA, *Bell System Tech. J.*, January, 1925; K. P. TURNER, *Exp. Wireless*, August, 1925, 673, 821, October, 1925; PH. LE CORBEILLER, and CHARLES LANGE, *L'onde élec.*, **560**, 1923; P. DAVID, *L'onde élec.*, January, February, 1926; "Les filtres électriques," Gauthier-Villars et Cie., Paris, 1926. For a general theory on wave filters see W. CAUER, *Physics*, **2**, 242, 1932. On magnetostriction filter, H. H. HALL, *Proc. I.E.E.*, **21**, 1328, 1933.

(Y). The terminals A - A signify the beginning and E - E the end of the artificial line. If these networks are to be equivalent to an actual line, Z and Y must have definite values.

The arrangement of Fig. 316 is often used for filters. For simplicity, the admittance Y is expressed by the reciprocal of the corresponding impedance Z_1 , the quantity Z_2 denotes the series impedance along the

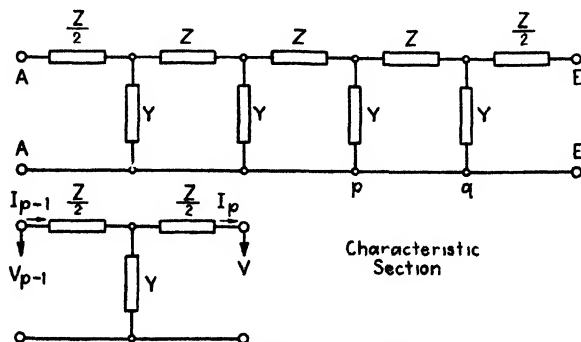


FIG. 315.—Filter with T sections.

line, and Z_E the impedance of the load. According to the theory of the parallel-wire system (pages 444–445), the effective currents at the end and beginning of the line must satisfy the relation

$$\frac{I_E}{I_A} = e^{-\theta}$$

The quantity θ corresponds to the generalized electrical length nl . Moreover, the equivalent impedance Z_E at the generator end must be

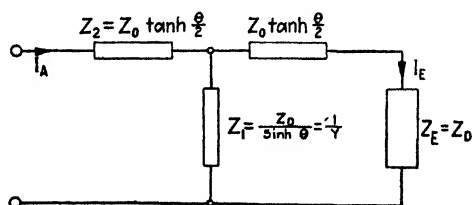


FIG. 316.—Equivalent T line (useful for the design of attenuation box).

equal to the surge impedance Z_0 of the line ($Z_E = Z_0$) since for this condition no reflections take place. Hence

$$Z_E = Z_0 = Z_2 + \frac{Z_1[Z_2 + Z_0]}{Z_1 + Z_2 + Z_0} \quad (1)$$

The current delivered to the load becomes

$$I_E = \frac{I_A Z_1}{Z_1 + Z_2 + Z_0}$$

and the current ratio

$$\frac{I_E}{I_A} = \frac{Z_1}{Z_1 + Z_2 + Z_0} = \epsilon^{-\theta} \quad (2)$$

From (1) and (2) we find, for $K = \epsilon^\theta - 1$, the quadratic equation

$$[2 + K]Z_2^2 + 2Z_0Z_2 - KZ_0^2 = 0$$

giving

$$Z_2 = Z_0 \tanh \frac{\theta}{2} \quad (3)$$

and

$$Z_1 = \frac{Z_0}{\sinh \theta} \quad (4)$$

The surge impedance, according to (1), is

$$Z_0 = \sqrt{Z_2^2 + 2Z_1Z_2} \quad (5)$$

For the π circuit of Fig. 317, we find

$$\frac{I_E}{I_A} = \frac{Z_1^2}{Z_1^2 + 2Z_0Z_1 + Z_0Z_2 + Z_1Z_2} = \epsilon^{-\theta} \quad (6)$$

and

$$Z_0 = Z_1 \sqrt{\frac{Z_2}{Z_2 + 2Z_1}} \quad (7)$$

When an attenuation network is needed for merely matching an internal generator impedance Z_g with a load impedance Z_l , an L pad is the simplest coupling device. Hence if Z_1 denotes the shunt and Z_2 the series impedance of it we have for $P = \sqrt{Z_g(Z_g + Z_l)}$ the design formulas

$$Z_1 = Z_g Z_l / P \quad \text{and} \quad Z_2 = P \quad (7a)$$

for the generator impedance larger than that of the load.

177. Application of Artificial Lines for the Determination of Amplification and the Measurement of Small Currents (Theory of the Attenuation

Box).—The amplification of an amplifier can be compensated by a device of known variable damping. An artificial line can be used for this purpose if sections of the same surge impedance are connected in series with a load $R = Z_0$. The small current at the end of the artificial line is

$$I_E = I_A \epsilon^{-\theta}$$

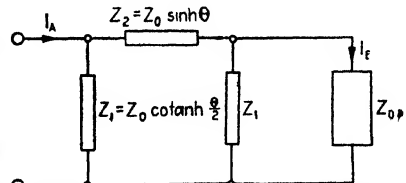


Fig. 317.—Equivalent π line (useful for design of attenuation box).

The quantity θ can be computed from (2) and (6), according to whether T or π sections are used. Such networks are used often in communication as well as high-frequency measurements. When a small receiving current in a frame antenna is to be determined by means of an auxiliary generator, the process is as follows:

A current taken from a local generator is made to produce, by means of a 1-ohm resistance inserted at the middle of a receiving loop, the same effect as the signal current. This current is usually much too small to be read off directly. By using the artificial line indicated in Fig. 318 with pure resistance along and across the line, a variable attenuation is obtained which is independent of the frequency. This is practically

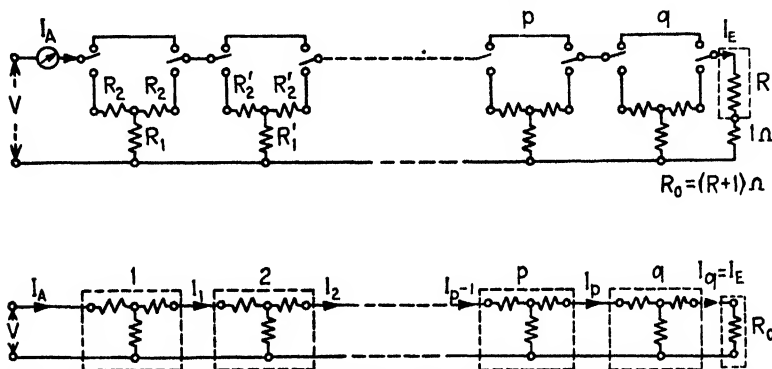


FIG. 318.—Network with variable attenuation (I_A measurable current, I_E very small high-frequency current)

true up to frequencies of about 500 kc/sec. The recurrent network consists of q sections which are so arranged that any number of sections can be switched in series in any order. In order to avoid reflections at the end of the attenuation box, a resistance $R = (R_0 - 1)$ ohms must be inserted at this end to satisfy the value of the wave resistance R_0 of any section for which the box is designed.

Since

$$\frac{I_1}{I_A} = \frac{I_2}{I_1} = \dots = \frac{I_p}{I_{p-1}} = \frac{I_q}{I_p} = \epsilon^{-\theta} \quad (8)$$

and T sections are used, according to (2), we have

$$\frac{R_1}{R_1 + R_2 + R_0} = \frac{R'_1}{R'_1 + R'_2 + R_0} = \frac{R''_1}{R''_1 + R''_2 + R_0}, \text{ etc.} \quad (9)$$

and, according to (5) for the wave resistance, the formula

$$R_0 = \sqrt{R_2^2 + 2R_1R_2} \quad (10)$$

Choosing $R_0 = 600\Omega$, then $R = 599\Omega$. For $R_1 = 2730\Omega$, according to (10), we have $R_2 = 65.15\Omega$ and, according to (8) and (9),

$$\frac{I_A}{I_1} = \frac{R_1 + R_2 + R_0}{R_1} = 1.244$$

For $R_1' = 1802\Omega$, we have $R_2' = 97.25\Omega$ and

$$\frac{I_1}{I_2} = \frac{R_1' + R_2' + R_0}{R_1'} = 1.387$$

Connecting both sections 1 and 2 in series gives

$$\frac{I_A}{I_1} \frac{I_1}{I_2} = \frac{I_A}{I_2} = 1.244 \times 1.387 = 1.725$$

The current I_2 at the end of the second section is therefore only $0.58I_A$. In order to obtain larger attenuation, we need either many sections of

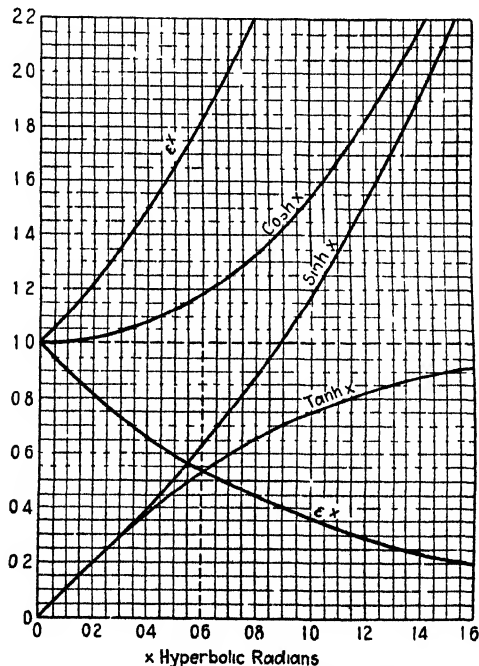


FIG 319.—Hyperbolic functions

this type or a section with a relatively small resistance R_1 and a correspondingly large series resistance R_2 . For instance, for $R_1 = 15.32\Omega$ and $R_2 = 584.9\Omega$, the current at the end of the section is only $1/78.33$ th of the value at the beginning of it. Therefore, using two sections in series makes the entering current about 6140 times greater than the current leaving the second section. When two such sections are connected in series with the two sections mentioned above, the input current

I_A is 10,600 times larger than the output current. Such a series combination facilitates the adjustment of the desired attenuation.

The computation of the *attenuation box* for T sections is based upon the *formulas*

$$R_1 = \frac{R_0}{\sinh \theta}; \quad R_2 = R_0 \tanh \frac{\theta}{2} \quad (11)$$

since, in place of the impedances, pure resistances are used. It can be seen that the resistance R_1 is proportional to the reciprocal value of the hyperbolic sine function of the attenuation constant and the series resistance R_2 is never larger than the wave (or load) resistance R_0 since the hyperbolic tangent function approaches unity (Fig. 319). Table XXVIII gives the computations for an attenuation box up to give a maximum attenuation constant of 10.

TABLE XXVIII.—CALCULATION OF AN ATTENUATION BOX FOR A TERMINATING LOAD
RESISTANCE OF $R_0 = 600$ OHMS

Numerical $\frac{I_E}{I_A} = e^{-\theta}$	Radians (damping) θ	Ohms $R_1 = \frac{R_0}{\sinh \theta}$	Ohms $R_2 = R_0 \tanh \frac{\theta}{2}$
1	0	∞	0
0 905	0 1	6000	30
0 819	0 2	2990	59 5
0 741	0 3	1995	90 5
0 670	0 4	1462	118
0 606	0 5	1150	147
0 549	0 6	942	174
0 497	0 7	795	202
0 449	0 8	674	228
0 407	0 9	585	254
0 368	1 0	513	267
0 223	1 5	281	380
0 135	2 0	166	457
0 082	2 5	100	508
0 050	3	60	542
0 0183	4	22	578
0 0067	5	8 1	594
0.00248	6	2 98	598
0 000912	7	1 105	600
0.000335	8	0 403	600
0.000123	9	0 148	600
0 0000454	10	0 0545	600

It will be evident that the series resistance R_2 remains almost constant for $\theta > 5$ (practically $= R_0$). Formulas (11) could also be obtained from filter formula (56) on page 548. The damping can also be expressed

by the transmission unit (TU) which corresponds to 1 mile (M) of standard cable.¹ The number of miles is given by

$$M = 21.12 \log_{10} \frac{I_A}{I_E} \quad (12)$$

where $I_A/I_E = \epsilon^\theta$. The decimal logarithmic unit is the decibel. We then have

$$1 \text{ db} = 1 \text{ TU} = 0.115 \text{ neper}; \quad 1 \text{ neper} = 8.686 \text{ TU} = 8.686 \text{ db.}$$

With respect to the decibel (db) unit² it must be borne in mind that it is a *relative* unit since the number of decibels

$$\text{db} = 10 \log_{10} \frac{P_1}{P_2}$$

is a logarithm of a *ratio* between *two* powers P_1 and P_2 . Hence when two voltages E_1 and E_2 or two currents I_1 and I_2 act in the *same* or *equal* impedances Z

$$\left. \begin{aligned} \text{db} &= 20 \log_{10} \frac{E_1}{E_2} \\ \text{db} &= 20 \log_{10} \frac{I_1}{I_2} \end{aligned} \right\}$$

For unequal impedances Z_1 and Z_2 with the respective power factors p_1 and p_2 we have for the number of decibels

$$\left. \begin{aligned} \text{db} &= 20 \log_{10} \frac{E_1}{E_2} + 10 \log_{10} \frac{Z_2}{Z_1} + 10 \log_{10} \frac{p_2}{p_1} \\ \text{db} &= 20 \log_{10} \frac{I_1}{I_2} + 10 \log_{10} \frac{Z_1}{Z_2} + 10 \log_{10} \frac{p_1}{p_2} \end{aligned} \right\}$$

From this it can be seen that a power ratio $P_1/P_2 = 10$ corresponds to 10 db, and $P_1/P_2 = 100, 1000, 10,000$, etc., to 20, 30, 40, etc., db. In a similar way the *negative* values $-10, -20, -30$, and -40 db correspond to the power ratios $P_1/P_2 = 0.1, 0.01, 0.001$, and 0.0001 which are *less* than unity.

Inasmuch as a change of 3 db for composite sinusoids is about just noticeable, it is evident that not much would be gained if, for instance, the power of a modulated high-frequency source was doubled since this would be just noticeable. It is therefore customary to increase the power for a gain of 10 db, that is, choose a tenfold power. Hence, if the power of a 10-watt transmitter is not sufficient, the transmitter is designed for 100 watts.

For sound work as used in broadcasting $P_2 = 12.5$ and for recording, $P_2 = 6$ milliwatts is used as the *reference* level. Hence 0 db stands then for $P_1 = 6$ milliwatts since P_1/P_2 must be unity in this case. An indication of -5 db would then correspond to a power ratio P_1/P_2 of 0.3162 with a value P_1 of 0.0018975 watt. For (-10 db) indication we have $P_1/P_2 = 0.1$ and $P_1 = 0.0006$ watt, while for $(+10 \text{ db})$ indicates on account of $P_1/P_2 = 10$ the available power $P_1 = 0.06$ watt.

¹ Uses No. 19 A.W.G. and refers to 796 cycles/sec, for which $\omega = 2\pi f = 5000$. A current with an amplification of 25 miles would therefore require 25 miles of standard cable to reduce the amplified current to the original value.

² For other details "High-Frequency Measurements," pp. 90-91, 300, 444-448. McGraw Hill Book Company, Inc., New York, 1933.

For noise measurements, it seems more practical to calibrate a meter *above* zero level, that is, only in positive values of decibels. It is then customary to use as reference level $P_2 = 10^{-16}$ watt of sound energy per square centimeter. In air for standard conditions of pressure and temperature this corresponds to 0.207 millibar of sound pressure.

For practical work, decibel tables do not have to be carried on very far, for instance, only up to 10 db. A 48-db reading is then brought within the reach of the table by subtracting 20 db successively which gives $48 \text{ db} - 20 \text{ db} - 20 \text{ db} = 8 \text{ db}$, which is within the reach of a 10-db table. Since the table gives for 8 db a power ratio of 6.31 and a gain of 20 db corresponds to a hundred-fold power and 20 db had to be *twice* subtracted to get it within the table, we find that 48 db corresponds to a power ratio $P_1/P_2 = 100 \times 100 \times 6.31 = 631 \times 10^2$. For the case of the voltage ratio E_1/E_2 and the corresponding current ratio I_1/I_2 , a gain of 20 db corresponds only to tenfold voltage and 8 db corresponds only to 2.512 fold voltage. Hence, 48 db corresponds to a voltage or a current ratio of only $10 \times 10 \times 2.512 = 251.2$.

When an L pad with a shunt resistance R_1 ohms and series resistance R_2 ohms is used for matching a source of internal resistance R_g with a load resistance R_l , formulas (7a) apply when the impedances are substituted by these resistances. The loss in decibels due to the matching device then is

$$\text{db} = 20 \log_{10} [\sqrt{\rho} + \sqrt{\rho - 1}]$$

if $\rho = (R_g/R_l) > 1$.

178. Theory of Filters with T and π Sections.—According to page 532, the equivalent recurrent T section is made up of a series impedance $Z_2 = Z_0 \tanh \theta/2$, and a shunt impedance $Z_1 = Z_0/\sinh \theta$ (Fig. 316). When these results are compared with the generalized circuit (Fig. 315), we note that the admittance

$$Y = \frac{1}{Z_1} = \frac{\sinh \theta}{Z_0} \quad (13)$$

and that the half-series impedance of the equivalent T section

$$\frac{Z}{2} = Z_2 = Z_0 \tanh \frac{\theta}{2} \quad (14)$$

The surge impedance of the artificial line is

$$Z_0 = \frac{Z}{2 \tanh (\theta/2)} \quad (15)$$

where θ is given by

$$\sinh \frac{\theta}{2} = \pm \sqrt{YZ} \quad (16)$$

since

$$\sinh \theta = 2 \sinh \frac{\theta}{2} \cosh \frac{\theta}{2}$$

For the homogeneous line (page 408), the propagation constant is

$$n = \pm \sqrt{YZ} \quad (17)$$

where Y and Z denoted the admittance across the line and Z the impedance along it per unit length. This also holds for recurrent networks, that is, for solution (16), since for p sections we obtain the attenuation constant

$$\theta = n \cdot p$$

This corresponds, for a homogeneous line of length l , to the quantity $\theta = nl$. The homogeneous line would be identical with a recurrent network of an infinite number of sections, since then

$$\sinh \frac{\theta}{2} = \tanh \frac{\theta}{2} = \frac{\theta}{2}$$

Hence, for a recurrent network for each section ($p = 1$), we have the surge impedance

$$Z_0 = \frac{Z}{2 \tanh (n/2)} \quad (18)$$

and, for the propagation constant n , the expression

$$\pm \sqrt{YZ} = 2 \sinh \frac{n}{2} \quad (19)$$

For the π section, the same expression for \sqrt{YZ} is obtained as in (16) and (19) since, according to Figs. 314 and 317,

$$\left. \begin{aligned} Z &= Z_2 = Z_0 \sinh \theta \\ Y &= \frac{2}{Z_1} = \frac{2}{Z_0 \coth (\theta/2)} \end{aligned} \right\} \quad (20)$$

that is, the surge impedance of a π section is

$$Z_0 = \frac{2 \tanh (n/2)}{Y} \quad (21)$$

The same results can also be found by means of difference equations.

For the recurrent network (Fig. 314) for the p th section,

$$\left. \begin{aligned} V_{p-1} - V_p &= Z \left[I_{p-1} - \frac{Y}{2} V_{p-1} \right] \\ I_{p-1} - I_p &= \frac{Y}{2} [V_p + V_{p-1}] \end{aligned} \right\} \quad (22)$$

where the voltages V and current I are vectors. By means of

$$\left. \begin{aligned} V_p &= \sum_{-n}^{+n} V e^{np} \\ I_p &= \sum_{-n}^{+n} I e^{np} \end{aligned} \right\} \quad (23)$$

Eq. (22) gives

$$\left. \begin{aligned} IZ &= V \left[1 - \epsilon^n + \frac{YZ}{2} \right] \\ I[1 - \epsilon^n] &= \frac{Y}{2} V [1 + \epsilon^n] \end{aligned} \right\} \quad (24)$$

By dividing these equations into each other, V and I are eliminated and give

$$[1 - \epsilon]^2 = YZ\epsilon^n$$

or

$$1 - \epsilon = \pm \epsilon^{\frac{n}{2}} \sqrt{YZ}$$

or

$$\epsilon^{-\frac{n}{2}} - \epsilon^{+\frac{n}{2}} = \pm \sqrt{YZ} \quad (25)$$

which gives the same result as (19). In order to find the expression for the surge impedance Z_0 , in the last equation we solve for the ratio V/I and obtain

$$Z_0 = \frac{V}{I} = -\frac{2}{Y} \frac{\epsilon^n - 1}{\epsilon^n + 1} = -\frac{2}{Y} \tanh \frac{n}{2}$$

which confirms the result of (21). In the same way the expression (18) for the surge impedance of a T section can be confirmed.

It can, therefore, be seen that the surge impedance of a T section differs from that of a π section, but the propagation constant (19) is the same for both sections. Equation (19) is *basic for filter calculations* since the propagation constant n includes the series and shunt impedances of the recurrent network.

179. Recurrent Network in a Circuit.—Figure 320 illustrates the case in which q sections of a recurrent network are energized by a source with an internal impedance Z_a and a terminal voltage V_a . The end of the network is connected to a load impedance Z_c . Since, according to (19), we have to deal with two values $\pm n$, Eqs. (23) yield

$$\left. \begin{aligned} V_p &= V_1 \epsilon^{np} + V_2 \epsilon^{-np} \\ I_p &= \frac{1}{Z_0} [-V_1 \epsilon^{np} + V_2 \epsilon^{-np}] \end{aligned} \right\} \quad (26)$$

The expressions¹ resemble those for the homogeneous line and the constants V_1 and V_2 are determined in a similar way by means of the boundary conditions.

At the beginning of the recurrent network, $p = 0$, and the voltage and current equal V_a and I_a , respectively. Hence

$$\left. \begin{aligned} V_a &= V_1 + V_2 \\ I_a Z_0 &= -V_1 + V_2 \end{aligned} \right\}$$

¹ The complete solution is $V_p = (-1)^p [V_1 \epsilon^{np} + V_2 \epsilon^{-np}]$, since a phase change of 180 deg takes place for each filter section.

where Z_0 is the surge impedance of the filter section (T or π section). The constants are

$$\left. \begin{aligned} V_1 &= \frac{V_a - I_a Z_0}{2} \\ V_2 &= \frac{V_a + I_a Z_0}{2} \end{aligned} \right\} \quad (27)$$

For the p th section

$$\left. \begin{aligned} V_p &= V_a \cosh np - Z_0 I_a \sinh np \\ I_p &= I_a \cosh np - \frac{V_a}{Z_0} \sinh np \end{aligned} \right\} \quad (28)$$

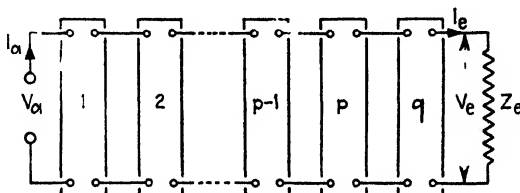


FIG. 320.—Recurrent network in a circuit.

The preceding solutions have the form

$$\left. \begin{aligned} V_p &= A_p V_a - B_p I_a \\ I_p &= A_p I_a - D_p V_a \end{aligned} \right\} \quad (29)$$

for

$$\left. \begin{aligned} A_p &= \cosh np \\ B_p &= Z_0 \sinh np \\ D_p &= \frac{\sinh np}{Z_0} \end{aligned} \right\} \quad (30)$$

Since for a recurrent network the end section ($p = q$) is of importance, we find, adopting the abbreviations

$$\left. \begin{aligned} A &= \cosh nq \\ B &= Z_0 \sinh nq \\ D &= \frac{\sinh nq}{Z_0} \end{aligned} \right\} \quad (31)$$

that

$$\left. \begin{aligned} V_e &= A V_a - B I_a \\ I_e &= A I_a - D V_a \end{aligned} \right\} \quad (32)$$

and

$$\left. \begin{aligned} V_a &= A V_e + B I_e \\ I_a &= A I_e + D V_e \end{aligned} \right\} \quad (33)$$

since $\cosh^2 x - \sinh^2 x = 1$ and, according to (31),

$$A^2 - BD = 1$$

180. Equations for Any Alternating-current Network.—Expressions as obtained in (33) also hold for the parallel-wire system and generally for any alternating-current network when the complex constant A in the V_a equation has a different value from the constant A in the I_a equation. We have, for any network which has an e.m.f. V_a impressed at a place a and sends a current I_a into the network, the voltage and current, at a place e , V_e and I_e

$$\begin{cases} V_e = A_1 V_a + B I_a \\ I_e = A_2 I_a + D V_a \end{cases} \quad (34)$$

where

$$A_1 A_2 - BD = 1$$

When the input and output places are interchanged, the currents flow in the opposite direction; that is, I_a gives $-I_a$, and I_e gives $-I_e$. Hence

$$\begin{cases} V_e = A_2 V_a + B I_a \\ I_e = A_1 I_a + D V_a \end{cases} \quad (35)$$

The constants A_1 , A_2 , B , and D , can be determined from the voltage and current readings taken at the input end for open and short-circuited output terminals. When this is done for the condition corresponding to (34), we have

$$\begin{cases} Z_{oc} = \frac{V_a}{I_a} = \frac{A_1}{D} \\ Z_{sc} = \frac{V_a}{I_a} = \frac{B}{A_2} \end{cases} \quad (36)$$

and similarly for (35)

$$\begin{cases} Z'_{oc} = \frac{V_e}{I_e} = \frac{A_2}{D} \\ Z'_{sc} = \frac{V_e}{I_e} = \frac{B}{A_1} \end{cases} \quad (37)$$

By means of these results certain networks (for example, transformers) can be matched to a line or to a filter impedance.

181. Filter Impedance and Effective Voltages at the End of a Recurrent Network.—The load impedance Z_e is of great importance for the calculation of filters. It is

$$Z_e = \frac{V_e}{I_e} \quad (38)$$

If, as in Fig. 320, V_a is the voltage impressed on a recurrent network and I_e the current flowing to the load, Eqs. (32), (33), and (38) give, for the filter impedance,

$$Z_F = \frac{V_a}{I_e} = \frac{AV_e + BI_e}{I_e} = AZ_e + B = Z_e \cosh nq + Z_0 \sinh nq \quad (39)$$

The filter impedance can also be expressed by means of the admittance instead of the surge impedance Z_0 of the recurrent network. We then have

$$Z_F = Z_e \cosh nq + \frac{\sinh n \sinh nq}{Y} = AZ_e + \frac{G}{Y} \quad (40)$$

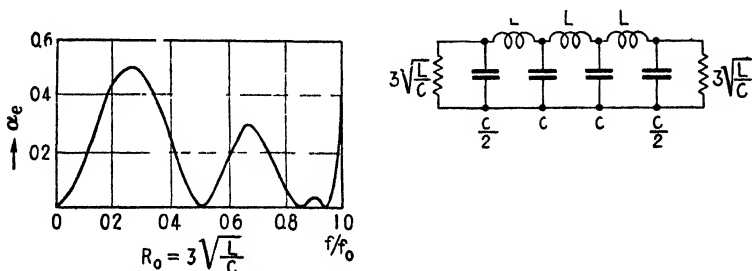


FIG. 321.- Effective damping α_e (filter "under" matched).

for $G = \sinh n \sinh nq$, since, for a π section,

$$Z_0 = \frac{-Z}{2 \tanh (n/2)} = \frac{-\cosh (n/2)}{2 \sinh (n/2)} Z$$

$$\sinh n = 2 \sinh \frac{n}{2} \cosh \frac{n}{2}$$

and therefore

$$Z_0 = \frac{-\sinh n}{4 \sinh^2 (n/2)} Z = \frac{-Z}{YZ} \sinh n = -\frac{\sinh n}{Y}$$

The portion of the voltage impressed on the filter which reaches the load is given by

$$Q = \frac{Z_F}{Z_e} = A + \frac{B}{Z_e} = \cosh nq - \frac{Z_0}{Z_e} \sinh nq$$

$$= \cosh nq - \frac{\sinh n \sinh nq}{YZ_e}$$

$$= A - \frac{G}{YZ_e} \quad (41)$$

This result gives a means for computing the attenuation of currents of any frequency passing through a recurrent network of q sections for any loading Z_e . It can be seen that the voltage Q delivered at the load oscillates between Z_0/Z_e and unity, and that the number of oscillations

depends upon the number of recurrent sections. If the load Z_e is chosen equal to the characteristic impedance Z_0 , we have

$$Q' = \frac{Z_r}{Z_e} = \cosh nq - \sinh nq = \epsilon^{-nq} = \epsilon^{-\alpha q} \epsilon^{-i\beta q} \quad (42)$$

where the real part α of the propagation constant n is a measure of the attenuation, and the imaginary part βq determines the phase.

Figure 321 illustrates the case of a recurrent network of three sections connected between two ohmic resistances R_0 equal to $3\sqrt{L/C}$. The effective attenuation is calculated by means of Eq. (55) of page 548.

182. Propagation Constant and Characteristic (Surge) Impedance of a Recurrent Network.—The propagation constant n , according to considerations in a previous section, is given by the same expression whether T or π sections are used, namely, by

$$\sinh \frac{n}{2} = \pm \frac{1}{2} \sqrt{YZ}$$

But

$$\sinh \frac{n}{2} = \sqrt{\frac{1}{2} [\cosh n - 1]}$$

and we have the *basic filter expression*

$$\cosh n = 1 + \frac{YZ}{2} \quad (43)$$

The characteristic impedance, according to (15) and (21), differs for T and π sections. If we make the following substitutions in these equations,

$$\begin{aligned} \tanh \frac{n}{2} &= \frac{\sinh (n/2)}{\cosh (n/2)} \\ \cosh \frac{n}{2} &= \sqrt{\frac{1}{2} [\cosh n + 1]} \end{aligned}$$

we find, for the *characteristic impedance of the T section*

$$Z_T = \sqrt{\frac{Z}{Y}} \sqrt{1 + \frac{YZ}{4}} \quad (44)$$

and for the *π section*

$$Z_\pi = \frac{\sqrt{(Z/Y)}}{\sqrt{1 + (YZ/4)}} \quad (45)$$

where $\sqrt{Z/Y}$ indicates the surge impedance of a homogeneous line. Since the product YZ is a negative quantity for filter sections, the characteristic impedance increases with the frequency in one case and decreases with it in the other case.

If the damping factor α and the phase factor β are introduced in (43), we find that

$$\cosh n = \cosh (\alpha + j\beta) = a + jb \quad (46)$$

and since

$$\cosh n = \underbrace{\cosh \alpha \cos \beta}_a + j \underbrace{\sinh \alpha \sin \beta}_b$$

we find for the damping factor α

$$\sinh^2 \alpha = -F + H \quad (47)$$

or

$$\cosh \alpha = 0.5\{\sqrt{1 + a^2 - 2a + b^2} + \sqrt{1 + a^2 + 2a + b^2}\} \quad (48)$$

and for the phase factor β

$$\sin^2 \beta = F + H \quad (49)$$

where

$$\left. \begin{aligned} F &= \frac{1 - a^2 - b^2}{2} \\ H &= \sqrt{b^2 + F^2} \end{aligned} \right\} \quad (50)$$

By means of (47) it is, for instance, possible to calculate filter losses over the entire frequency band. For q equal sections in series, the total attenuation¹ of a properly terminated filter is $q\alpha$ and the number of decibels of attenuation can be computed from the voltage ratio

(voltage applied to the filter)/(voltage given off by the filter).

It is

$$\text{db} = 20 \log_{10} \frac{V_1}{V_2} = 20 \log_{10} e^{q\alpha} = \frac{20}{2.303} q\alpha$$

For $\alpha = 0.2303$, this would give 2 db per filter section.

Theoretically, a recurrent network has two regions (Fig. 322). For one, currents of a definite frequency band are transmitted unhindered along the network, and for the other frequency band the currents experience considerable attenuation and are practically reduced to zero.

a. For the *pass region*, the attenuation must vanish; that is, $\alpha = 0$, and (43) and (46) reduce to

$$\cosh j\beta = \cos \beta = 1 + \frac{YZ}{2} \quad (51)$$

Since all values of the cosine are between ± 1 , the currents of that frequency band must pass *without attenuation* which satisfies

¹ This holds when input and output impedances are the same.

$$-1 \leq \frac{YZ}{4} \leq 0 \quad (52)$$

That is, for the pass region, the impedance $1/Y$ must have the opposite sign to that of the series impedance Z , and the effective impedance can

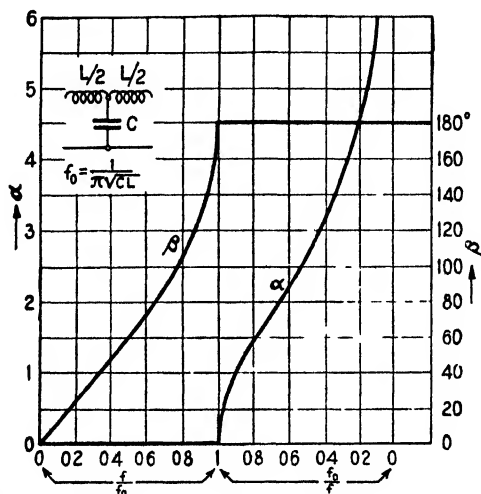


FIG. 322.—Phase (β) and attenuation (α) constants of a low-pass filter.

never exceed the value $4/Y$. It is therefore possible to read off the pass region on curves which give Z and $4/Y$ as functions of the frequency. This can also be done by means of curves YZ as functions of f/f_0 , if f

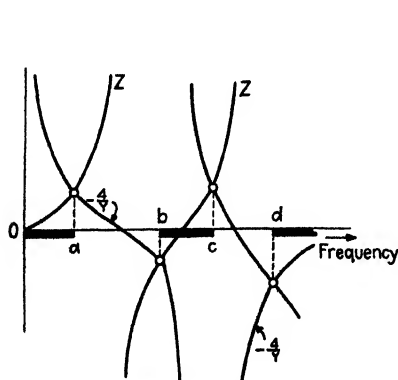


FIG. 323.—Pass regions 0 to a ; b to c ; etc.

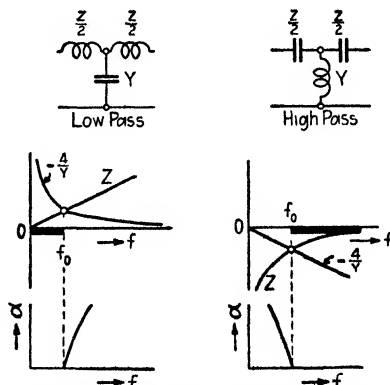


FIG. 324.—Pass region for *low pass* from 0 to f_0 ; for *high pass* from f_0 to ∞ .

denotes any frequency and f_0 the cutoff frequency beyond which attenuation takes place. Figure 323 gives an example of the graphical solution, and Fig. 324 an illustration of the low- and high-pass filters. Assuming pure reactances Z and $1/Y$, we note from (18) and (21) that, for the pass

region, the characteristic impedance Z_0 is real; hence for each frequency there is a certain load resistance $Z_0 = R_0$ which is real. Figure 325 shows how the critical frequencies can be found from the $YZ/4$ curves. The proof is given on pages 557 and 558.

When the pure load resistance R is chosen very different from Z_0 , the filter can actually attenuate in the pass region. We therefore have to

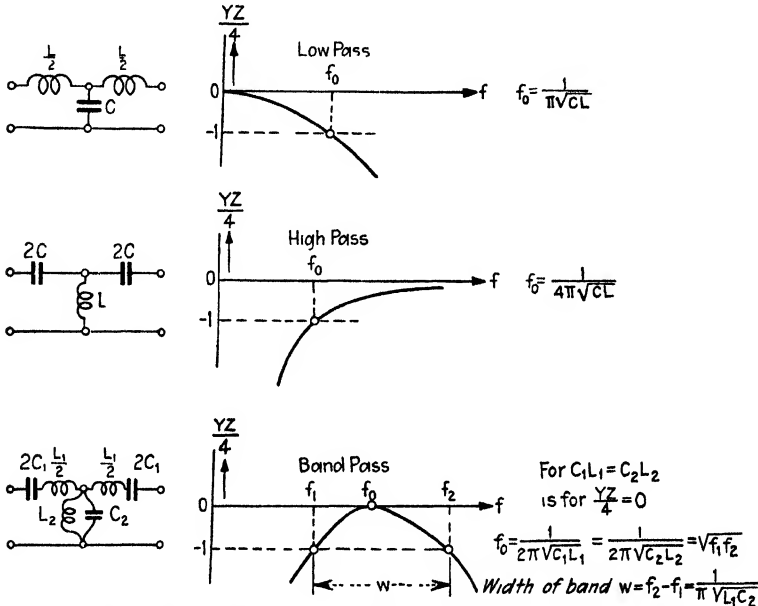


FIG. 325.—Critical frequencies obtained from $YZ/4$ curves.

deal with an effective attenuation α_e . If jX_{sc} is the short-circuit and jX_{oc} the open-circuit reactance of the recurrent network, we have

$$Z_0 = \sqrt{jX_{sc} \cdot jX_{oc}} \quad (53)$$

Since Z_0 is real in the pass region, X_{sc} and X_{oc} must be of opposite sign. The apparent resistance of the recurrent network is

$$R_a = jX_{oc} \frac{jX_{sc} + R}{jX_{oc} + R} \cong \frac{jX_{oc} \cdot jX_{sc}}{R} \cong \frac{Z_0^2}{R} \quad (54)$$

since R is negligible compared with jX_{sc} which becomes infinitely great, and jX_{oc} vanishes in comparison with R . The current I_a which flows toward filter resistance R_a and load resistance R is for an impressed voltage V_a given by

$$I_a = \frac{V_a}{R_a + R} = \frac{V_a}{(Z_0^2/R) + R}$$

From the Joulean heat losses without and within the recurrent network,

$$W_1 = \frac{V_a^2}{4R}; \quad W_2 = \left[\frac{V_a}{(Z_0^2/R) + R} \right]^2 R$$

we find the effective attenuation

$$\alpha_e = \log_e \left[\frac{1 + (Z_0/R)^2}{2Z_0/R} \right] \quad (55)$$

b. In the *attenuation region*, the recurrent network produces only attenuation α but no phase displacement. The quantity β in (43) and (46) must therefore vanish and we find

$$\cosh \alpha = 1 + \frac{YZ}{2} \quad (56)$$

This formula can also be used for designing the attenuation box. If we take, for instance, the value $\theta = \alpha = 2$ from Table XXVIII on page 536, the corresponding series resistance per section is $2R_2 = Z = 2 \times 457 \Omega$ and the admittance per section $Y = 1/R_1 = (1/166)$ mhos. Hence $1 + YZ/2 = 3.762 = \cosh \alpha = \cosh \theta = \cosh 2$. Moreover, in this region the characteristic impedance Z_0 is purely imaginary. For the cutoff frequency f_0 , the characteristic impedance is either zero or infinite.

183. Action of Parallel and Series Impedances in Networks.—An inductance represents a small impedance for low frequencies and a high impedance for high frequencies. The opposite is true of capacitance. When inductances and condensers are connected up as in Fig. 326 and their magnitudes chosen properly, the current I , leaving the section is about as indicated in the figure. Therefore, when inductances are connected along, and capacities across, the network as in Fig. 326a, direct currents can flow freely along the network, and alternating currents of very low frequency experience very small impedance. But as the frequency becomes higher, the network impedes more and more until, for frequencies above a critical frequency f_0 (limiting frequency), pronounced attenuation of the current takes place. The lower diagram of Fig. 326a indicates that the characteristic section of the filter indicated above it is of T form.

When condensers are used along the network and the inductances across the network (case *b* in the figure), we have to deal with a high-pass filter which can never pass a direct current but only alternating currents above a certain critical frequency f_0 .

The diagrams under *c* and *d* show the case of a band-pass and band-suppression filter. The former passes only currents of a certain frequency band, while the latter passes currents of lower and higher frequencies but suppresses currents of medium frequencies. Such actions could also be produced by a low- and a high-pass filter in series or in

parallel. The series case corresponds to the band-pass filter. Experience shows, however, that sharper cutoffs are obtained for band-pass and band-suppression filters with networks as indicated in diagrams *c* and *d* of Fig. 326 and with coupled-circuit filters as in Fig. 327 than with a low- and high-pass filter in cascade.

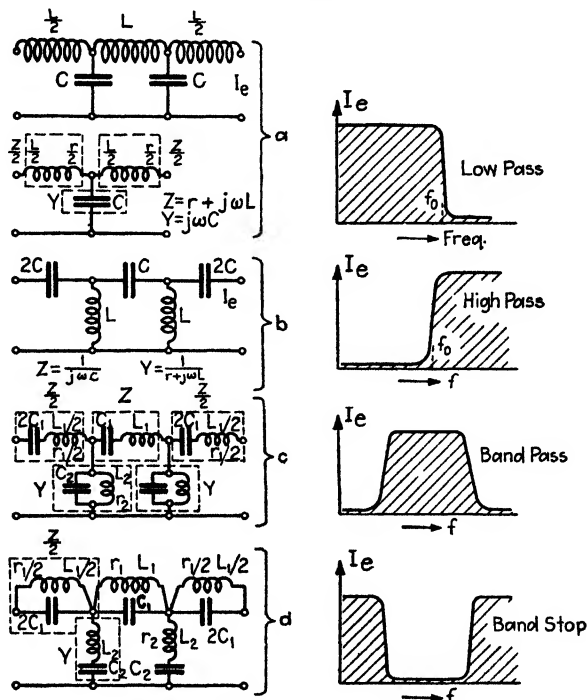


FIG. 326.—The four kinds of filters.

184. Theory of the Low-pass Filter with Inductance along and Capacitance across the Section.—The simplest low-pass filter consists of inductances along the recurrent network and capacities across the same. We find for the arrangement shown in Fig. 326*a*, for the series impedance Z per section,

$$Z = r + j\omega L$$

and the admittance across a section

$$Y = j\omega C$$

Introducing these values into Eq. (43) gives

$$\begin{aligned} \cosh n &= 1 + \frac{YZ}{2} = a + jb \\ &= 1 - \frac{\omega^2 CL}{2} + j\frac{\omega r C}{2} \end{aligned} \quad (57)$$

where $\omega/2\pi = f$ denotes the frequency of a voltage applied to the filter. We then have

$$\left. \begin{aligned} a &= 1 - \omega^2 \frac{CL}{2} = 1 - 2 \left[\frac{f}{f_0} \right]^2 \\ b &= \frac{\omega r C}{2} = r \sqrt{\frac{C}{L}} \frac{f}{f_0} \end{aligned} \right\} \quad (58)$$

where f_0 is the critical frequency at which attenuation just begins. The natural or critical frequency f_0 can also be obtained from Eq. (44), the expression for the characteristic impedance of the network, since for negligible resistance the value of Z must vanish; that is,

$$Z_T = \sqrt{\frac{r + j\omega L}{j\omega C}} \sqrt{1 + \frac{1}{4}j\omega C|r + j\omega L|} = 0$$

or

$$1 - \frac{1}{4}\omega^2 CL + \frac{1}{4}j\omega Cr = 0$$

or

$$\omega = \omega_0 = \frac{2}{\sqrt{CL}} \quad (59)$$

giving the critical frequency

$$f_0 = \frac{1}{\pi\sqrt{CL}} \quad (60)$$

or a value which is only one-half as large as in the case of an ordinary resonant circuit. If the resistance is neglected as compared with the reactance, $Z = j\omega L$ and $Y = j\omega C$. Equation (44) then yields

$$Z_T = \sqrt{\frac{L}{C}} \sqrt{1 - \left[\frac{f}{f_0} \right]^2} = Z_0 \sqrt{1 - \left[\frac{f}{f_0} \right]^2} \quad (61)$$

For the π section, we find

$$Z_\pi = \frac{Z_0}{\sqrt{1 - [f/f_0]^2}} \quad (62)$$

Z_T therefore begins with a value $Z_0 = \sqrt{L/C}$ and decreases as f/f_0 becomes larger until, at the critical frequency $f = f_0$, the characteristic impedance Z_T becomes zero, while Z_π starts with a value Z_0 and increases with increasing ratio f/f_0 until, at $f = f_0$, it becomes infinite. This variation of the characteristic impedance with the frequency is a drawback in filter design but can roughly be overcome by proper terminating devices.

It can be seen that, for pure reactances along and across the filter section, the ratio

$$\frac{Z}{Y} = \frac{L}{C} = Z_0^2 = R_0^2$$

is a constant and

$$R_0 = \sqrt{\frac{L}{C}} = \sqrt{\frac{Z}{Y}},$$

which resembles the surge impedance of a parallel-wire system and is a pure resistance. The equality $R_0 = Z_T = Z_\pi$ occurs for the T section when at its maximum value, and for the π section when at its minimum value. This is true with all inverse network filter sections and the

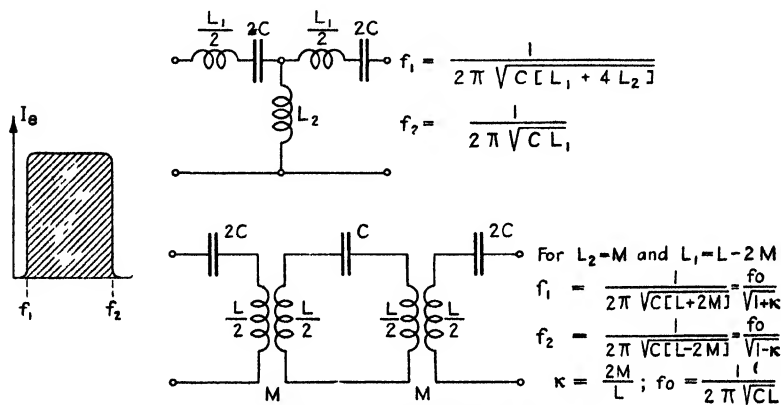


FIG. 327.—Band-pass filters.

value R_0 can be used in the design of the network. Writing (44) and (45) in terms of R_0 , we find that

$$Z_T = \sqrt{\frac{Z}{Y} + \frac{Z^2}{4}} = \sqrt{R_0^2 + \frac{Z^2}{4}} \quad (63)$$

$$Z_\pi = \frac{R_0^2}{\sqrt{R_0^2 + (Z^2/4)}} \quad (64)$$

which shows that R_0 occurs for a frequency f which makes the impedance Z along the section equal to 0. This happens for the low-pass filter of Fig. 326a at zero frequency since $Z = \omega L$.

Figure 322 gives the attenuation α and phase measure β of each T section of a low-pass filter as a function of the ratio f/f_0 . If the ohmic resistance of the coil were taken into account, it would have but little influence on many filter coils. Only the corner of the β curve, where $\beta = 180^\circ$ and the corner of the α curve, where α becomes zero for $f/f_0 = 1$, would be more rounded. These curves were computed by means of Eqs. (47) and (49). It can be seen that, for smaller frequencies ($f < f_0$), the phase β at first increases almost proportionally with f . Then a more rapid increase takes place until a phase displacement of 180 deg is reached. During the entire process no damping α exists. Any section

of a recurrent network then acts as a *phase changer* and theoretically passes currents of frequencies $f < f_0$ without any attenuation. But, as the frequency f is only slightly increased above f_0 , attenuation α takes place which increases at first very rapidly with f while the phase β undergoes no change. These are the characteristic properties of low-pass filters. Moreover, since in Eq. (46)

$$\left. \begin{aligned} a &= \cosh \alpha \cos \beta \\ b &= \sinh \alpha \sin \beta \end{aligned} \right\} \quad \text{and} \quad \cosh n = a + jb$$

that is, for a section of negligible coil resistance,

$$\cosh n = 1 + \frac{1}{2}YZ = 1 - \frac{\omega^2 CL}{2} = 1 - 2\left[\frac{f}{f_0}\right]^2$$

we have

$$\left. \begin{aligned} a &= 1 - 2\left[\frac{f}{f_0}\right]^2 = \cosh \alpha \cos \beta \\ \sinh \alpha \sin \beta &= 0 \end{aligned} \right\}$$

For values of $f < f_0$, we have (as shown in Fig. 322) $\alpha = 0$ and $\cosh \alpha = 1$ or

$$\cos \beta = a = 1 - \left[\frac{f}{f_0}\right]^2 \quad (65)$$

or

$$\sin \frac{\beta}{2} = \frac{f}{f_0} \quad (66)$$

For $f > f_0$, $\beta = 180^\circ$, that is, $\cos \beta = -1$ or

$$\cosh \alpha = -a = \left[\frac{f}{f_0}\right]^2 - 1 \quad (67)$$

and

$$\cosh \frac{\alpha}{2} = \frac{f}{f_0} \quad (68)$$

By means of (66) and (68), the curves of Fig. 322 can be checked. The inversion of the sign of α and that of β indicate that currents are reflected toward the source for frequencies f above the critical frequency f_0 , and that the *filter action of such a recurrent network can take place with small losses*. The portion of the impressed filter voltage which is obtained at the output end does not undergo any changes (reflections) if, as in Eq. (42), the load impedance Z_L is made equal to the characteristic impedance of the network. The term e^{α} in Eq. (42) gives a measure for the filter action. Figure 328 illustrates cases of 1, 2, 3, and 10 recurrent filter sections. It is noted that damping begins right after the

critical frequency $f_0 = 1/(\pi\sqrt{CL})$ is exceeded. Even for small excesses of f over f_0 , the damping is very pronounced when 10 recurrent sections are used. Such a large number of sections would, however, lead to expensive filters. Figure 329 gives the damping effect of three sections over a larger frequency band. It is noted that, for such a uniform filter, three sections give good action. It is well to assume the critical frequency f_0 somewhat lower. When doing this we note that, for three sections, the amplitude of currents of frequencies 50 per cent more than the critical frequency is practically zero. If, therefore, a low-pass filter

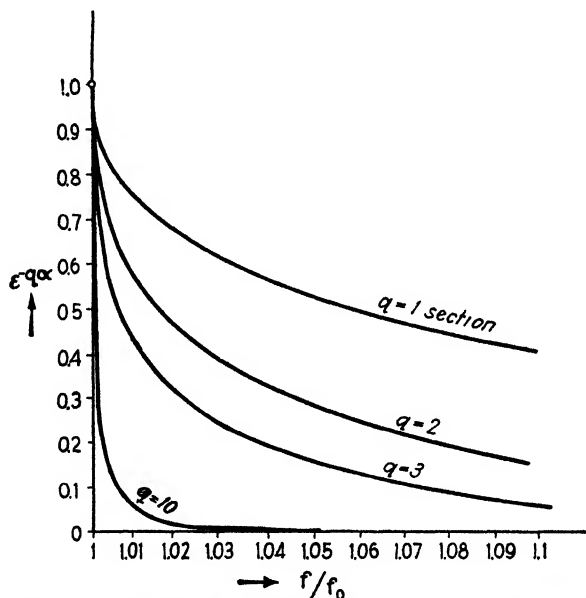


FIG. 328.—Damping curves (indicate effect of number of filter sections).

is to be designed for a B eliminator to cut off alternating-current hum of 60 cycles/sec, it is well to assume the critical frequency f_0 somewhat lower, say about 40 cycles/sec.

When π sections are used, the critical frequency f_0 is obtained for $Z_\pi = \infty$ which yields the same expression as for the T section.

The calculation of the simple low-pass filter is, therefore, based upon a choice of C and L according to Eqs. (60) and (61) or (62). If Z_e is the load for a T-section filter without reflections, we find that

$$\left. \begin{aligned} Z_e = Z_\pi = P\sqrt{\frac{L}{C}} = PZ_0 \\ f_0 = \frac{1}{\pi\sqrt{CL}}; \quad P = \sqrt{1 - \left[\frac{f}{f_0}\right]^2} \end{aligned} \right\} \quad (69)$$

and

$$C^{(\mu f)} = \frac{P \times 10^6}{\pi f_0 Z_e} \quad L^{(\text{henry})} = \frac{Z_e}{\pi f_0 P} \quad (70)$$

For the π -section filter

$$Z_e = Z_\pi = \frac{Z_0}{P} \quad (71)$$

and f_0 is as before; hence

$$C^{(\mu f)} = \frac{10^6}{\pi f_0 Z_0 P} \quad L^{(\text{henry})} = \frac{P Z_0}{\pi f_0} \quad (72)$$

where the critical (cutoff) frequency is in cycles per second, and the characteristic impedances Z_T and Z_π are in ohms. These apparently

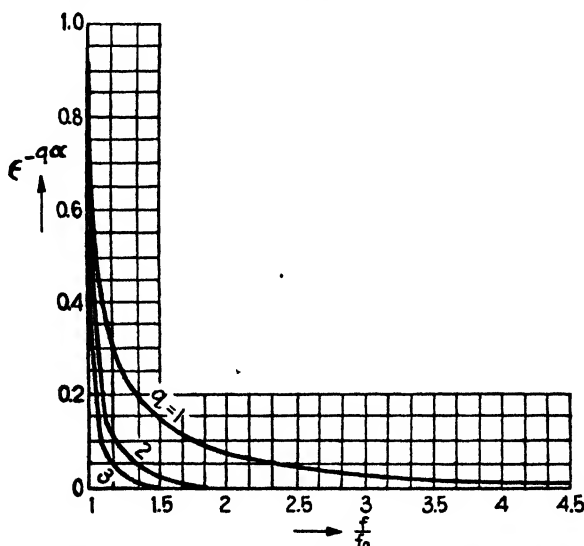


FIG. 329.—Damping curves for one, two, and three sections.

simple expressions have the disadvantage of having the term P appear in the formulas for C and L . We have, therefore, a factor involved which depends upon the frequency. This factor actually belongs to the characteristic impedance of the filter and shows that the load should change with the frequency. Figure 321 shows the case in which $P = \frac{1}{3}$ is assumed. We have then to deal with a recurrent network which is "underfiltered." The effective damping α_e varies for any characteristic impedance Z_0 of a recurrent network, as in Fig. 330, where R denotes the terminating resistance load. In many cases it is sufficient to choose $P = 1$; that is, the resistance load $R_0 = Z_T = Z_\pi = Z_0 = \sqrt{L/C}$ as would be the case for a homogeneous line. The formulas in Fig. 331

make such assumptions. In some cases $P = 0.6$ gives better results. When composite filters are used with terminating half sections and a resistance load, a much better regularity in the pass region can be obtained as is shown in Sec. 197.

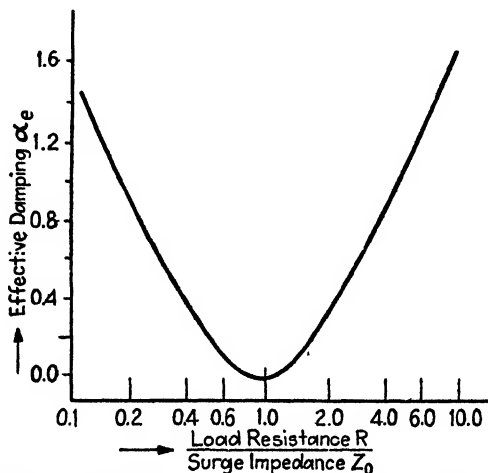


FIG. 330.—Effect of matching load resistance with characteristic impedance.

185. Design of a Low-pass Filter.—Suppose a filter is to be designed to pass currents equally well below 2000 cycles/sec, but to act as a pronounced impedance to currents above this frequency. The filter is to work into a load of 50 ohms. A low-pass filter as shown in Fig. 331 can be used for this purpose. The recurrent network is to be made up of

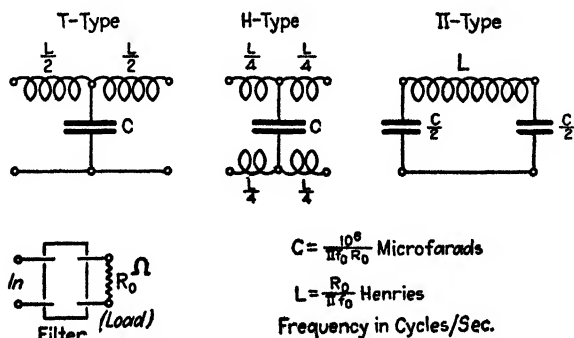


FIG. 331.—Low-pass filter.

π sections. We find by means of the formulas given in Fig. 331 or more quickly by means of the curves in Fig. 332 that, for $R_0 = 50$ ohms and $f_0 = 2000$ cycles/sec, $C = 3.185\mu\text{f}$ and $L = 7.96$ mh. The capacitance on each side of the section would then be $1.5925\mu\text{f}$. Such a capaci-

tance can be obtained by means of several condensers in parallel. However, it seems more practical to use $1.5\mu\text{f}$ on each side and compensate the error by changing either R_0 or f_0 . Figure 332 shows that for

$$C = 2 \times 1.5\mu\text{f},$$

we have $L = 8.5 \times 10^{-3}$ henries and $R_0 = 53.2$ ohms. We have therefore only to increase the load by 3.2 ohms and still satisfy $f_0 = 2000$ cycles/sec.

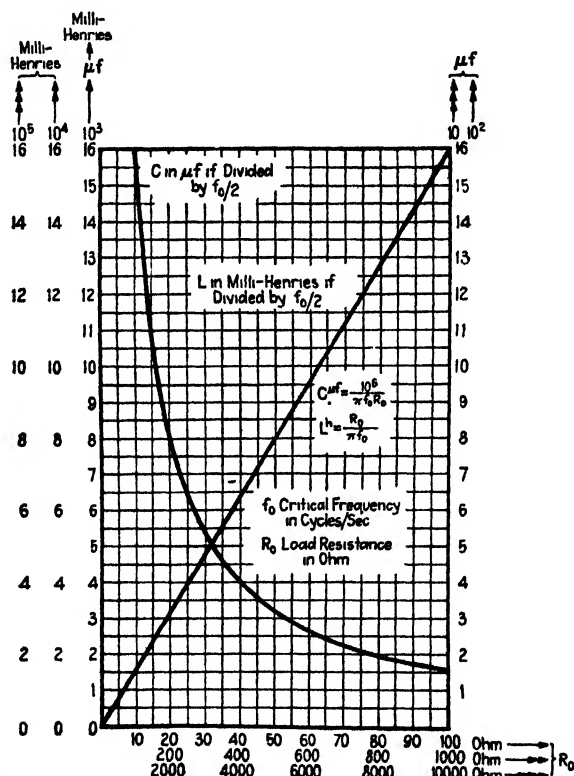


FIG. 332.—Curves for the calculation of a low-pass filter for resistance loads up to 10,000 ohms.

For T sections, we have the case in Fig. 326a and may use 4.25×15^{-3} henries at the ends of the section and $C = 3\mu\text{f}$.

The performance of such a filter can be examined by Eq. (41) since the ratio $Q = Z_F/Z_c$ gives that portion of the impressed filter voltage which exists at the output end. For one filter section $q = 1$, for two sections $q = 2$, etc. Using the complete solution (footnote 1, page 540), Eq. (41) yields

$$\begin{aligned}
 Q &= \frac{Z_f}{Z_e} = (-1)^q \left[A + \frac{B}{Z_e} \right] \\
 &= (-1)^q \left[\cosh nq + \frac{Z_0}{Z_e} \sinh nq \right] = (-1)^q \left[\cosh nq - \frac{\sinh n \sinh nq}{YZ_e} \right] \\
 &= (-1)^q \left\{ A - \frac{G}{YZ_e} \right\} \quad (73)
 \end{aligned}$$

These formulas show that the quotient Q for one section ($q = 1$)

$$Q_1 = \frac{G_1}{YZ_e} - A_1 \quad (74)$$

For two and three sections ($q = 2, q = 3$), it is

$$\begin{aligned}
 Q_2 &= A_2 - \frac{G_2}{YZ_e} \\
 Q_3 &= \frac{G_3}{YZ_e} - A_3
 \end{aligned} \quad (75)$$

where

$$\begin{aligned}
 A &= (-1)^q \cosh nq \\
 &= (-1)^q \cos mq \\
 G &= (-1)^q \sinh n \sinh nq \\
 &= -(-1)^q \sin m \sin mq \\
 n &= jm
 \end{aligned} \quad (76)$$

The relation $n = jm$ can be used to advantage for the pass region ($f/f_0 < 1$).

TABLE XXIX.—COMPUTATION OF THE FILTER EFFECT [Eq. (73)]

For any other filter (band pass), band suppression, etc., use column YZ instead of f/f_0 , since f/f_0 refers to low-pass filters only

f/f_0	YZ	A_1	A_2	A_3	G_1	G_2	G_3
0.2	-0.16	-0.92	+ 0.695	- 0.358	- 0.152	+ 0.282	- 0.366
0.4	-0.64	-0.68	- 0.076	+ 0.783	- 0.536	+ 0.730	- 0.456
0.6	-1.44	-0.28	- 0.842	+ 0.755	- 0.918	+ 0.518	+ 0.63
0.7	-1.96	-0.02	- 0.999	+ 0.06	- 0.995	+ 0.0522	+ 0.996
0.8	-2.56	+0.28	- 0.845	- 0.749	- 0.92	- 0.514	+ 0.637
0.9	-3.24	+0.62	- 0.231	- 0.906	- 0.615	- 0.763	- 0.331
1.0	-4.00	+1.0	+ 1.0	+ 1.0	0	0	0
1.1	-4.84	+1.42	+ 3.032	+ 7.19	+ 1.01	+ 2.88	+ 7.17
1.2	-5.76	+1.88	+ 6.072	+ 20.85	+ 2.53	+ 9.54	+ 33.15
1.3	-6.76	+2.38	+10.37	+ 46.85	+ 4.66	+22.3	+101.2
1.4	-7.84	+2.92	+16.08	+ 90.64	+ 7.5	+44.1	+248.5
1.5	-9.0	+3.5	+23.51	+160.27	+11.24	+78.8	+538.0

For a low-pass filter as in this example, it is of advantage to also add the column f/f_0 in order to know A and G as functions of the deviation

TABLE XXX.—EXAMINATION OF A FILTER

f/f_0	$1/(YZ_0) = -j\epsilon_0/(2\beta)$	$G_1/(YZ_0)$	$G_2/(YZ_0)$	$(G_2/(YZ_0))$	Q_1 (for one section)	Q_2 (for two sections)	Q_3 (for three sections)
0.2	-2.5 <i>j</i>	+0.38 <i>j</i>	-0.705 <i>j</i>	+0.913 <i>j</i>	+ (0.38 <i>j</i> + 0.92) = +0.995	+ (0.695 + 0.705 <i>j</i>) = + 0.99	+ (0.913 <i>j</i> + 0.358) = + 0.98
0.4	-1.25 <i>j</i>	+0.67 <i>j</i>	-0.913 <i>j</i>	+0.57 <i>j</i>	+ (0.67 <i>j</i> + 0.68) = +0.955	+ (-0.076 + 0.913 <i>j</i>) = + 0.916	+ (0.57 <i>j</i> - 0.783) = + 0.968
0.6	-0.833 <i>j</i>	+0.765 <i>j</i>	-0.432 <i>j</i>	-0.525 <i>j</i>	+ (0.765 <i>j</i> + 0.28) = +0.815	+ (-0.842 + 0.432 <i>j</i>) = + 0.946	+ (0.525 <i>j</i> + 0.755) = - 0.919
0.7	-0.714 <i>j</i>	+0.71 <i>j</i>	-0.037 <i>j</i>	-0.711 <i>j</i>	+ (0.71 <i>j</i> + 0.02) = +0.71	+ (-0.999 + 0.0373 <i>j</i>) = + 0.99	+ (0.711 <i>j</i> + 0.06) = - 0.713
0.8	-0.625 <i>j</i>	+0.576 <i>j</i>	+0.321 <i>j</i>	-0.398 <i>j</i>	+ (0.576 <i>j</i> - 0.28) = +0.64	- (0.845 + 0.321 <i>j</i>) = - 0.904	+ (0.398 <i>j</i> + 0.749) = + 0.848
0.9	-0.555 <i>j</i>	+0.341 <i>j</i>	+0.423 <i>j</i>	+0.184 <i>j</i>	+ (0.341 <i>j</i> - 0.62) = +0.708	- (0.231 + 0.423 <i>j</i>) = - 0.482	+ (0.184 <i>j</i> + 0.906) = + 0.925
1.0	-0.5 <i>j</i>	0	0	0	- 1	+ 1.0	- 1
1.1	-0.4646 <i>j</i>	-0.459 <i>j</i>	+1.31 <i>j</i>	-3.26 <i>j</i>	- (0.459 <i>j</i> + 1.42) = -1.49	+ (3.032 - 1.31 <i>j</i>) = + 3.32	+ (3.26 <i>j</i> + 7.19) = - 7.9
1.2	-0.4165 <i>j</i>	-1.055 <i>j</i>	-3.975 <i>j</i>	-13.81 <i>j</i>	- (1.055 <i>j</i> + 1.88) = -2.15	+ (6.072 - 3.9752 <i>j</i>) = + 7.25	+ (13.81 <i>j</i> + 20.85) = - 25.0
1.3	-0.3845 <i>j</i>	-1.791 <i>j</i>	-8.57 <i>j</i>	-38.9 <i>j</i>	- (1.791 <i>j</i> + 2.38) = -2.98	+ (10.37 - 8.57 <i>j</i>) = +13.5	+ (38.9 <i>j</i> + 46.85) = - 60.9
1.4	-0.357 <i>j</i>	-2.68 <i>j</i>	-15.76 <i>j</i>	-88.7 <i>j</i>	- (2.68 <i>j</i> + 2.92) = -3.96	+ (16.08 - 15.76 <i>j</i>) = +22.5	+ (88.7 <i>j</i> + 90.64) = -127.0
1.5	-0.333 <i>j</i>	-3.745 <i>j</i>	-26.25 <i>j</i>	-179 <i>j</i>	- (3.745 <i>j</i> + 3.5) = -5.15	+ (23.51 - 26.25 <i>j</i>) = +35.2	+ (179 <i>j</i> + 160.27) = -240.0

from the cutoff frequency. Since any other filter (high pass, band pass, band suppression) has different values for the first column, it is best to work out the computation by means of column YZ . With this in mind, Table XXIX can be used for computing the action of any filter. For coupled-circuit filters, a similar table can be employed as is suggested on page 576. Table XXX is used to find the final values. The term $1/(YZ_e)$ may be simplified since in the calculation of C and L it is assumed that $R_0 = Z_e = Z_0\sqrt{L/C}$; that is,

$$\frac{1}{YZ_e} = \frac{1}{j\omega CR_0} = \frac{-j}{\omega\sqrt{CL}} = \frac{-j\omega_0}{2\omega} = -j\frac{f_0}{2f}$$

Moreover,

$$YZ = j\omega C \cdot j\omega L = -\omega^2 CL = -\left(\frac{2f}{f_0}\right)^2$$

It can be seen that, for the attenuation region $f/f_0 > 1$, the damping is not very great when only one section is used. For two sections, the quotient Q_2 gives a much better voltage ratio between the input and output ends, and for three sections the values for Q_3 show that the filter acts quite well. For instance, for $f/f_0 = 1.1$, that is, at 2200 cycles/sec instead of 2000 cycles/sec, the voltage at the load is $1/Q_3 = 1/7.9$ th of the voltage impressed to the filter. For 2400 cycles/sec ($f/f_0 = 1.2$), only one-twenty-fifth of the impressed voltage acts across the load. Therefore, the attenuation increases rapidly with f as soon as $f > f_0$. By plotting Q_1 , Q_2 , Q_3 , as functions of f/f_0 , and generally as functions of YZ , the action of the number of sections can be studied. In the pass region ($f/f_0 < 1$ for low-pass filters, $YZ = 0$ to $YZ = -4$ for any filter), we note that the filter impedance varies from positive to negative values, the number of cycles depending upon the number of sections. The impedances experienced in this region are relatively small and show a fairly good pass region (for the filters examined).

We note from this table and Eq. (73) that, for a pure inductive and a pure capacitive load, respectively,

$$Z_e = j\omega L_e \quad \text{and} \quad Z_e = \frac{1}{j\omega C_e}$$

we have

$$\frac{1}{YZ_e} = -\frac{1}{\omega^2 CL_e}$$

and

$$\frac{1}{YZ_e} = \frac{C_e}{C}$$

Hence the effect of the frequency f is eliminated for a capacity load.

186. Design of a Low-pass Filter Which Also Completely Suppresses Currents of a Definite Frequency.—A low-pass filter as just described produces attenuation as soon as $-YZ > 4$. The attenuation increases rapidly but in practical cases never reaches an infinite value. However, for certain types of work it may be necessary, in addition to a pronounced pass and attenuation region, to have the filter completely suppress currents of a particular frequency. For instance, this is the case in the design of battery eliminators. The desired operation could be approximated if many sections of the low-pass filter shown in Fig. 326a were used. This is, however, an expensive method. The same charac-

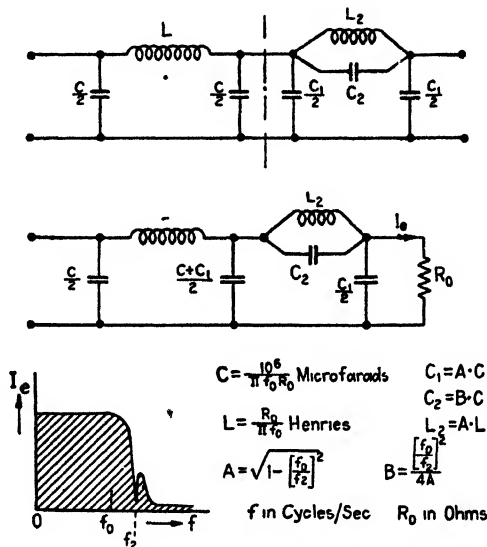


FIG. 333.—Low-pass filter with selective absorption.

teristics could be attained more economically by the use of a composite filter, as shown in Fig. 333, with only two sections, since a frequency trap $C_2 L_2$ is used for eliminating the undesired frequency f_2 . The first section represents an ordinary π section of the simple low-pass type. The formulas given in Fig. 333 are based on $f_0 = [\pi\sqrt{CL}]^{-1}$ and $f_2 = [2\pi\sqrt{C_2 L_2}]^{-1}$ since, above the frequency f_0 , attenuation must exist for either section, and currents of frequency f_2 must meet a reactance of infinite value along the line.

For the first section, we have

$$Y_1 = j\omega C \quad \text{and} \quad Z_1 = j\omega L$$

and, for the second section,

$$Y_2 = j\omega C_1$$

$$Z_2 = \frac{j\omega L_2}{1 - \omega^2 C_2 L_2} = j \frac{\omega L_2}{1 - (f/f_2)^2}$$

For the natural frequency of the first section (reactance along the closed loop must vanish for this frequency),

$$j\omega_0 L + \frac{4}{j\omega_0 C} = 0 \quad \text{or} \quad \omega_0 = \frac{2}{\sqrt{CL}} = 2\pi f_0$$

and in a similar way, for the second section,

$$\frac{j\omega L_2}{1 - \omega^2 C_2 L_2} + \frac{4}{j\omega C_1} = 0 \quad \text{or} \quad \omega = \frac{2}{\sqrt{C_1 L_2 + 4C_2 L_2}} = 2\pi f$$

Inserting the values for C_1 , C_2 , and L_2 leads to

$$C_1 L_2 + 4C_2 L_2 = CL[A^2 + 4AB] = CL$$

that is,

$$\omega = \omega_0 \quad \text{or} \quad f = f_0$$

since

$$4AB = \left[\frac{f_0}{f_2} \right]^2 \quad \text{and} \quad A^2 = 1 - \left[\frac{f_0}{f_2} \right]^2$$

The correctness of the formulas given in Fig. 333 can also be seen from the expression for the propagation constant

$$\cosh n = 1 + \frac{1}{2}YZ$$

which shows that, for a symmetrical network, this constant depends on the product YZ . If this is done for both sections, we find, when $Y_1 Z_1 = 0$, that $Y_2 Z_2 = 0$, and, when $Y_1 Z_1 = -4$, that $Y_2 Z_2 = -4$. The section with the trap impedance has therefore the same cutoff as has the simple section ahead of it.

Currents of frequency f_2 can also be suppressed by means of voltage resonance (condenser and coil in series, and across sections). However, this has the disadvantage that, for a constant voltage impressed on the filter, considerable resonance currents of frequency f_2 pass across the filter and back to the source. A derived low-pass filter of this type is described on page 583.

Example.—A low-pass filter is to be designed to suppress the superimposed alternating currents flowing in a full-wave rectifier. The power is to be supplied from an alternating-current network of $f = 60$ cycles/sec. The rectified current is to feed through the filter into two transmitter tubes of 1000 volts rated anode voltage, and 100 ma anode current. The load resistance is

$$R_0 = \frac{1000}{2 \times 100 \times 10^{-3}} = 5000 \Omega$$

Since, for full-wave rectification, $2 \times 60 = 120$ cycles/sec gives the fundamental frequency of the variable components in the rectified branch, it is particularly essential to suppress currents of this frequency. Choosing the cutoff frequency as

$$f_0 = 40 \text{ volts/sec,}$$

according to Fig. 333,

$$C = \frac{10^6}{\pi \times 40 \times 5000} = 1.59 \mu\text{f}; \quad L = \frac{5000}{40\pi} = 39.8 \text{ henries};$$

$$A = \sqrt{1 - \left[\frac{40}{120}\right]^2} = 0.94; \quad B = \frac{[\frac{40}{120}]^2}{4 \times 0.94} = 0.0295$$

$$C_1 = 0.94 \times 1.59 = 1.495 \mu\text{f}$$

$$C_2 = 0.0295 \times 1.59 = 0.047 \mu\text{f}$$

$$L_2 = 0.94 \times 39.8 = 37.4 \text{ henries}$$

187. Theory of the High-pass Filter with Capacitance along and Inductance across the Section.—Case *b*, in Fig. 326, and Fig. 334 show recurrent networks for which neither direct currents nor currents of the

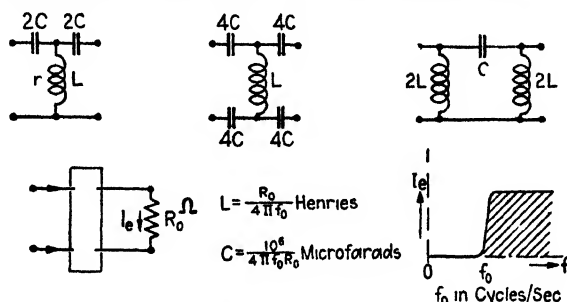


FIG. 334.—High-pass filter of the *T*, *H*, and π type.

lower frequency range (zero frequency up to cutoff frequency f_0) can flow. We have

$$Z = \frac{1}{j\omega C} \quad \text{and} \quad Y = \frac{1}{r + j\omega L}$$

If these values are introduced into the expression for the propagation constant n and r is neglected, we find that

$$\cosh n = 1 + \frac{YZ}{2} = 1 - \frac{1}{2} \frac{1}{\omega^2 CL}$$

The critical cutoff frequency $f_0 = \omega_0/2\pi$, below which appreciable attenuation exists, is found by putting $\cosh n = \pm 1$. For $\cosh n = -1$,

$$\omega_0 = \frac{1}{2\sqrt{CL}}$$

$$f_0 = \frac{1}{4\pi\sqrt{CL}} \quad (77)$$

For the characteristic impedance, according to (44) and (45), we have

$$Z_r = \sqrt{\frac{Z}{Y}} \sqrt{1 + \frac{1}{4}YZ} = \sqrt{\frac{L}{C}} \sqrt{1 - \frac{1}{4\omega^2 CL}}$$

$$= Z_0 \sqrt{1 - \left[\frac{f_0}{f}\right]^2} \quad (78)$$

and, for a π section,

$$Z_{\pi} = \frac{Z_0}{\sqrt{1 - [f_0/f]^2}} \quad (78a)$$

When comparing this with expressions (61) and (62) for the low-pass filter, we note that, in place of $(f/f_0)^2$, we have here the reciprocal value. By means of these results, we can derive the design formulas given in Fig. 334. The load R_0 must be equal either to Z_T or to Z_{π} , depending on the section used, and we have

$$\omega_0 = \frac{1}{2\sqrt{CL}}; \quad R_0 = P_1 Z_0; \quad P_1 = \sqrt{1 - \left[\frac{f_0}{f}\right]^2}; \quad Z_0 = \sqrt{\frac{L}{C}}$$

or

$$\left. \begin{aligned} C^{(\mu f)} &= \frac{10^6 P_1}{4\pi f_0 R_0} \\ L^{(\text{henry})} &= \frac{R_0}{4\pi f_0 P_1} \end{aligned} \right\} \text{(for T section)} \quad (79)$$

and

$$\left. \begin{aligned} C^{(\mu f)} &= \frac{10^6}{4\pi f_0 R_0 P_1} \\ L^{(\text{henry})} &= \frac{R_0 P_1}{4\pi f_0} \end{aligned} \right\} \text{(for } \pi \text{ section)} \quad (80)$$

Again in these formulas a factor P_1 appears which depends upon the frequency f , which means that, for an ideal filter action, the load R_0 must change correspondingly with f_0/f . However, for some filters, it is possible to assume $P_1 = 1$ and arrive at the formulas given in Fig. 334. For other cases, different values are assumed and the filter action examined by means of Tables XXIX and XXX of pages 557 and 558. It is then only necessary to find a good value for $1/(YZ_e)$ where Z_e can be an ohmic resistance for coils of negligible resistance. The formulas given in Fig. 334 can be plotted similarly to the case shown in Fig. 332, which holds for the simple type of low-pass filter. To obtain a better match with the load, half sections can also be used at the terminations as described in Sec. 196.

188. Notes on Symmetrical Recurrent Networks Which Use Capacitance and Inductance Combinations along and across a Section (Band-pass and Band-suppression Filters).—When dealing with filter sections as in Fig. 335, it is convenient to distinguish between cutoff frequencies (f_1 and f_2) and natural frequencies (f_{01} and f_{02}) of certain branches. The resonance frequencies of the series impedance Z and crosswise admittance Y are

$$\left. \begin{aligned} f_{01} &= \frac{1}{2\pi\sqrt{C_1L_1}} \\ f_{02} &= \frac{1}{2\pi\sqrt{C_2L_2}} \end{aligned} \right\} \quad (81)$$

and are generally not identical with the cutoff frequencies f_1 and f_2 which can be found from

$$\cosh n = -1 = 1 + \frac{\omega^2 C_1 L_2}{2[1 - \omega^2 C_2 L_2][\omega^2 C_1 L_1 - 1]}$$

The attenuation region is between f_1 and f_2 . From the curves for $\cosh n$ and for the attenuation α , we note that a minimum attenuation exists

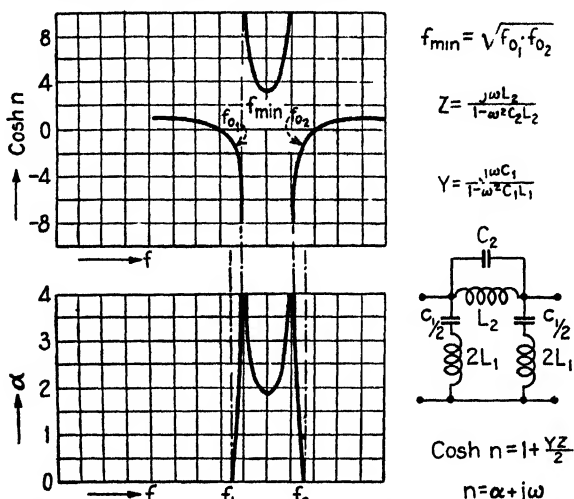


FIG. 335.—Propagation constant and attenuation constant of a section with capacitance and inductance along and across the section.

for f_{\min} in the attenuation region. This is a disadvantage since currents within the band $f_2 - f_1$ are supposed to experience pronounced attenuation everywhere. Therefore, it is of interest to know f_{\min} and α for the suppression band. We find f_{\min} from

$$\frac{d[\cosh n]}{df} = 0$$

as

$$f_{\min} = \sqrt{f_{01} \cdot f_{02}} \quad (82)$$

Inserting this value in the expression for $\cosh n$ yields

$$\begin{aligned} \cosh n &= [\cosh n]_{\min} = 1 + \frac{4\pi^2 f_{01} f_{02} C_1 C_2}{2[1 - (f_{01}/f_{02})][(f_{02}/f_{01}) - 1]} \\ &= 1 + \frac{L_2}{2L_1[1 - (f_{01}/f_{02})]^2} \end{aligned} \quad (83)$$

which expresses that the smallest attenuation α in the suppression region depends upon the ratio L_2/L_1 and f_{01}/f_{02} . When f_{01}/f_{02} deviates from unity, the minimum attenuation is smaller. Therefore, a good filter action depends upon the proper choice of the cutoff frequencies. The more the natural frequencies f_{01} and f_{02} approach each other, the more effective is the attenuation (the larger the minimum damping in the suppression region), but the cutoff frequencies f_1 and f_2 are different from the corresponding natural frequencies. The attenuation α_{\min} can also be increased by choosing a larger ratio of L_2/L_1 . In many cases it is customary to let the natural and the corresponding cutoff frequencies be almost the same, which is permissible for a small ratio of L_2/L_1 (about

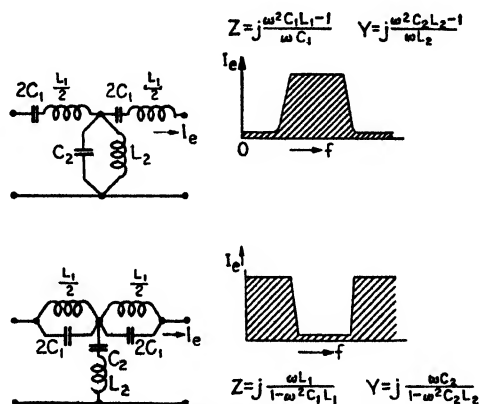


FIG. 336.—Basic formulas for band-pass and band-stop filter.

0.1). The minimum attenuation α_{\min} is then increased by the use of several filter sections.

Table XXIX on page 557 can be used to examine the filter effect. The pass region is for values $YZ = 0$ to $YZ = -4$. For values from $YZ = -4$ to values which are still more negative, pronounced filter impedances exist, since we are in the attenuation region. The column f/f_0 of Table XXIX refers to low-pass filters of the simple type only.

For the arrangements shown in Fig. 336, the constants can be found by the following method: In the upper arrangement, which represents a *band-pass* section, we find, for the characteristic product,

$$YZ = -\frac{[\omega^2 C_1 L_1 - 1][\omega^2 C_2 L_2 - 1]}{\omega^2 C_1 L_2}$$

If $C_1 = C_2 = C$ and $L_1 = L_2 = L$, then

$$YZ = -\frac{[\omega^2 CL - 1]^2}{\omega^2 CL} = -\left[\frac{f}{f_0} - \frac{f_0}{f}\right]^2 \quad (84)$$

for the natural frequency $f_0 = 1/(2\pi\sqrt{CL})$ of the Z and the Y branches. This frequency is not to be confused with the cutoff frequency of low- and high-pass filters.

These simplifications give a means for computing the cutoff frequencies of the band-pass filter more quickly. In order to do this, (84) is used as a starting formula, and in the course of the calculation C_1 , C_2 , L_1 , and L_2 are assumed such that

$$C_1 L_1 = C_2 L_2 = CL$$

Hence we assume that both natural frequencies are equal. By a proper choice of L_1/L_2 , the width $w = f_2 - f_1$ of the pass band can be changed. By doing this we arrive at the formulas

$$\left. \begin{aligned} L_1 &= mL_2 \\ C_1 &= \frac{C_2}{m} \end{aligned} \right\}$$

Hence, for values of $m > 1$, the width of the pass band becomes smaller. Equation (84) then leads to

$$YZ = -m \left[\frac{f}{f_0} - \frac{f_0}{f} \right]^2 \quad (85)$$

When YZ of (84) gives the same value as in (85), the two cutoff frequencies f_1 and f_2 can be found. This common value must be $-YZ > 4$, and the choice of m is also given. For instance, for $f/f_0 = 2.1415$, we have $f_0/f = 0.415$, and

$$\left[\frac{f}{f_0} - \frac{f_0}{f} \right]^2 = 4$$

Putting this in (84) gives $YZ = -4$. Assuming $f = 0.415 f_0$ again gives $YZ = -4$, and therefore the filter passes currents of all frequencies between $0.415f_0$ and $2.415f_0$.

Example.—Suppose a filter is to be designed to pass currents between 400 and 600 kc/sec. The impedances at 400 kc/sec are to give a value $-YZ$ which is somewhat larger than 4

Solution.—For $f = 400 \times 10^3$, we obtain $f/f_0 = 0.8$ since $f_0 = 500 \times 10^3$. We have $f_0/f = 1.25$, and (84) gives $YZ = -0.202$. Assuming in (85) the value

$$YZ = -4.2$$

gives $m = 21$; that is, $C_1 = C_2/21$ and $L_1 = 21L_2$.

In the same way for the band-suppression filter shown in the lower diagram of Fig. 336, we find

$$\star \quad YZ = -\frac{1}{\left[\frac{f}{f_0} - \frac{f_0}{f} \right]^2} \quad (86)$$

where $C_1 = C_2 = C$, and $L_1 = L_2 = L$, and

$$YZ = -\frac{m}{[(f/f_0) - (f_0/f)]^2} \quad (87)$$

for $C_1 L_1 = C_2 L_2 = CL$.

189. Theory and Design Formulas of Uniform Band-pass Filters.—All electrical constants are expressed in practical units, that is, in cycles per second, farads, henries, and ohms from now on. With reference to the cutoff frequencies f_1 and f_2 , it is immaterial whether we deal with

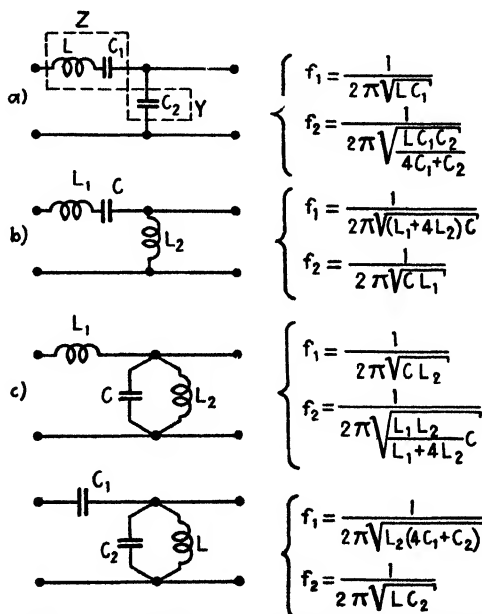


FIG. 337.—Band-pass filters (f_1 lower and f_2 upper cutoff frequency).

a T, π , H, or any other section, since only the product YZ will enter our calculations. The possible networks of simple types of band-pass filters are therefore drawn in Fig. 337 in the form of an inverted L section with Z and Y along and across the section as for the foregoing symmetrical networks. According to Eq. (52), currents will pass for frequencies which satisfy $(-1) \leq YZ/4 \leq 0$, which means that the *cutoff* frequencies f_1 and f_2 are given by the conditions,

$$\left. \begin{aligned} YZ &= 0 \\ YZ &= -4 \end{aligned} \right\} \quad (87a)$$

These expressions lead to the frequencies given in Fig. 337.

Referring to the T section shown in Fig. 338, according to Eq. (87a), we find the cutoff frequencies f_1 and f_2 and the width

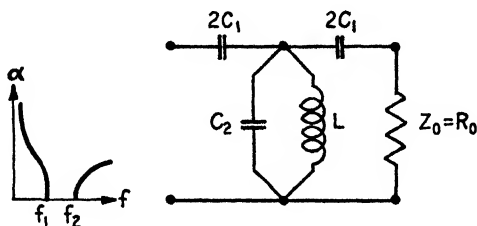
$$w = f_2 - f_1$$

for the pass band. For the impedance along and the admittance across the section, we have

$$\left. \begin{aligned} Z &= -\frac{j}{\omega C_1} \\ Y &= j \frac{\omega^2 C_2 L - 1}{\omega L} \end{aligned} \right\}$$

and for

$$YZ = \frac{\omega^2 C_2 L - 1}{\omega^2 C_1 L}$$



$$f_1 = \frac{1}{2\pi\sqrt{L_2(4C_1 + C_2)}}, \quad f_2 = \frac{1}{2\pi\sqrt{C_2 L}}$$

FIG. 338.—Loaded band-pass filter.

which for the value (-4) corresponding to the lower cutoff frequency f_1 gives

$$\frac{4\pi f_1^2 C_2 L - 1}{4\pi f_1^2 C_1 L} = -4 \quad (88)$$

and, for the zero value corresponding to the upper cutoff frequency f_2 , gives

$$\omega^2 C_2 L = 4\pi^2 f_2^2 C_2 L = 0 \quad (89)$$

Putting the characteristic impedance of the T section

$$Z_s = Z_T = \sqrt{\frac{Z}{Y}} \sqrt{1 + \frac{YZ}{4}} = Z_0$$

for the mean frequency $f_m = \sqrt{f_1 \cdot f_2}$, we find

$$Z_0 = \sqrt{\frac{L}{C_1[1 - 4\pi^2 f_1 f_2 C_2 L]} - \frac{1}{4\pi^2 f_1 f_2 C_1^2}} \quad (90)$$

Combining these expressions, we find that, for $Z_0 = R_0$,

$$\begin{aligned} C_1 &= \frac{1}{4\pi f_1 R_0} \\ C_2 &= \frac{f_1}{\pi[f_2^2 - f_1^2]R_0} \end{aligned} \quad L = \frac{[f_2^2 - f_1^2]R_0}{4\pi f_1 f_2} \quad (91)$$

Using π sections, which are more expensive to build than T sections, we have the surge impedance

$$Z_s = Z_\pi = \frac{\sqrt{Z/Y}}{\sqrt{1 + YZ/4}} \quad (92)$$

Employing again the value $Z_s = Z_0 = R_0$ which holds for $f_m = \sqrt{f_1 f_2}$, we have

$$\left. \begin{aligned} C_1 &= \frac{f_1 + f_2}{4\pi f_1 f_2 R_0} \\ C_2 &= \frac{f_1}{\pi f_1 [f_2 - f_1] R_0} \\ L &= \frac{[f_2 - f_1] R_0}{4\pi f_1 f_2} \end{aligned} \right\} \quad (93)$$

a. The π section shown in Fig. 339 leads to the formulas

$$\begin{aligned} L_1 &= \frac{f_1 R_0}{\pi[f_2^2 - f_1^2]} \\ L_2 &= \frac{R_0}{4\pi f_1} \\ C &= \frac{f_2^2 - f_1^2}{4\pi f_1 f_2^2 R_0} \end{aligned} \quad (94)$$

and the π section shown in Fig. 340 with a condenser across the section gives

$$\begin{aligned} C_1 &= \frac{f_2^2 - f_1^2}{4\pi f_1^2 f_2 R_0} \\ C_2 &= \frac{1}{\pi f_2 R_0} \end{aligned} \quad L = \frac{f_2 R_0}{\pi[f_2^2 - f_1^2]} \quad (95)$$

The T section shown in Fig. 341 gives similar attenuation characteristics and leads to

$$\begin{aligned} L_1 &= \frac{R_0}{\pi f_2} \\ L_2 &= \frac{[f_2^2 - f_1^2] R_0}{4\pi f_1^2 f_2} \end{aligned} \quad C = \frac{f_2}{\pi[f_2^2 - f_1^2] R_0} \quad (96)$$

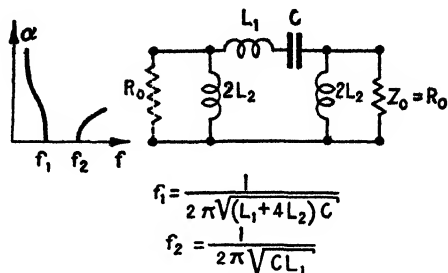


FIG. 339.—Loaded band-pass filter.

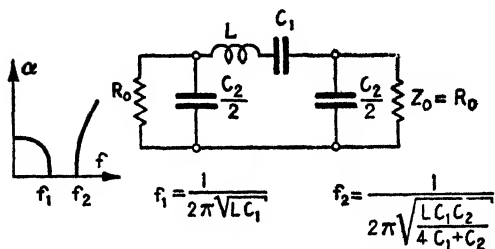


FIG. 340.—Loaded band pass.

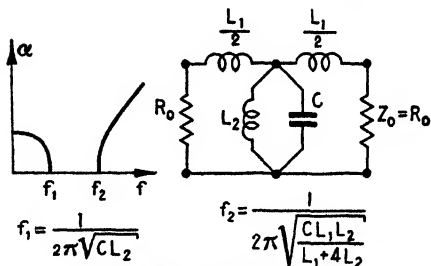


FIG. 341.—Loaded band pass.

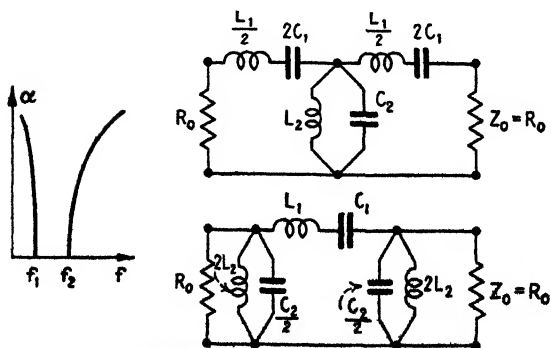


FIG. 342.—Loaded band pass.

b. Figure 342 shows a band-pass filter for T and π sections. Both are of the inverse network type for which Z/Y is equal to a constant. From the relations

$$\left. \begin{aligned} \omega_1 L_1 - \frac{1}{\omega_1 C_1} &= -2Z_0 \\ \omega_2 L_1 - \frac{1}{\omega_2 C_1} &= +2Z_0 \end{aligned} \right\} \quad (97)$$

we obtain for the T as well as for the π section, for $Z_0 = R_0$,

$$\left. \begin{aligned} L_1 &= \frac{R_0}{\pi[f_2 - f_1]} & C_1 &= \frac{f_2 - f_1}{4\pi f_1 f_2 R_0} \\ L_2 &= \frac{[f_2 - f_1]R_0}{4\pi f_1 f_2} & C_2 &= \frac{1}{\pi[f_2 - f_1]R_0} \end{aligned} \right\} \quad (98)$$

The derivation of these formulas is based on the relations

$$\left. \begin{aligned} \frac{Z}{Y} &= \text{constant} = Z_0^2 = R_0^2 \\ Z_T Z_\pi &= \frac{Z}{Y} \end{aligned} \right\} \quad (99)$$

The latter relation is the outcome of the general equations of (44) and (45). Although it is not possible to make a fixed load $Z_0 = R_0$ equal to either Z_T or Z_π for the entire range of frequencies in the pass band, this condition can be approximated since the mean value

$\sqrt{Z/Y}$ is approximately preserved for a good portion of the band $[f_2 - f_1]$ (Fig. 343). This mean value corresponds to a frequency $f_m = \sqrt{f_1 f_2}$. Owing to the first relation of (99) expressing the inverse character of the filter section shown in Fig. 342, the derivation of formulas (98) is simplified. Combining relations

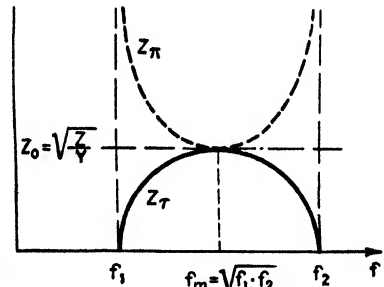


FIG. 343.—Characteristic impedance for T and π sections.

$$YZ = -4 \quad \text{and} \quad Z_0 = \sqrt{\frac{Z}{Y}}$$

which, according to Fig. 343, hold for both T and π sections, leads to Eq. (97) when Y is eliminated. It is also possible to eliminate Z instead of Y in order to find (98) from the expressions of the admittance branch Y .

An application of formula (98) is as follows: The band-pass filter is terminated at each side by a resistance $R_0 = 600$ ohms. The lower cutoff frequency is 120, and the upper 123 kc/sec. The width of the band is 3000 cycles/sec, and

$$L_1 = \frac{600}{3000\pi} = 6.37 \times 10^{-8} \text{ henries; } C_1 = \frac{3000}{4\pi \times 120 \times 123 \times 600 \times 10^6} = 2.7 \times 10^{-11} \text{ farads}$$

$$L_2 = \frac{3000 \times 600}{4\pi \times 120 \times 123 \times 10^6} = 9.7 \times 10^{-8} \text{ henries; } C_2 = \frac{1}{3000\pi \times 600} = 1.77 \times 10^{-7} \text{ farads}$$

190. The Coupled-circuit Filter.—The coupled-circuit filter shown in Fig. 327 has a pass range which is dependent upon the coupling between successive resonance circuits and a main frequency equal to the resonance frequency of each circuit. It is a most suitable band-pass filter for high-frequency work. If Z_1 , in Fig. 344, is the impedance of each coupled

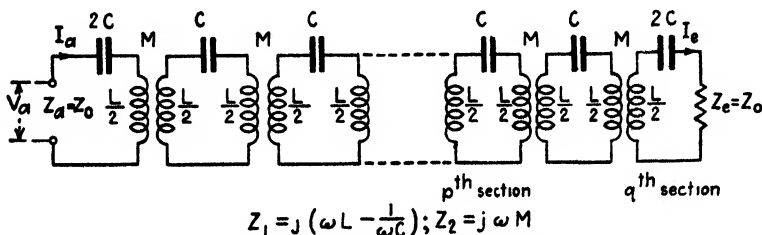


FIG. 344.—Coupled-circuit filter.

circuit when acting independently, and Z_2 the mutual or transfer impedance along the system of coupled circuits, we have, for the p th circuit,

$$Z_2 I_{p-1} + Z_1 I_p + Z_2 I_{p+1} = 0 \quad (100)$$

All other circuits except the two terminating circuits are satisfied by the solution

$$I_p = I' \epsilon^{np} + I'' \epsilon^{-np} \quad (101)$$

which, when substituted in (100), yields

$$Z_1 [I' \epsilon^{np} + I'' \epsilon^{-np}] + Z_2 [I' \epsilon^{n(p-1)} + I'' \epsilon^{-n(p-1)} + I' \epsilon^{n(p+1)} + I'' \epsilon^{-n(p+1)}] = 0$$

or

$$I' \epsilon^{np} [Z_1 + Z_2 (\epsilon^n + \epsilon^{-n})] + I'' \epsilon^{-np} [Z_1 + Z_2 (\epsilon^n + \epsilon^{-n})] = 0$$

and the equations for all coupled circuits are satisfied if the propagation constant n has a value which makes

$$Z_1 + Z_2 (\epsilon^n + \epsilon^{-n}) = 0$$

Therefore, we find the fundamental equation for the coupled-circuit filter

$$\cosh n = -\frac{Z_1}{2Z_2} = -\frac{a + jb}{2} \quad (102)$$

where Z_1 denotes any circuit impedance, and Z_2 any transfer impedance. For the simple case, shown in Fig. 344, all circuits are alike and the terminating branches may be considered as half circuits working into either the generator or load, respectively, of the same iterative impedance Z_0 . Assuming the resistance negligible, we have

$$\left. \begin{aligned} Z_1 &= j \left[\omega L - \frac{1}{\omega C} \right] \\ Z_2 &= j \omega M \end{aligned} \right\}$$

$$\kappa = \frac{M}{\sqrt{(L/2)(L/2)}}$$

and

$$\cosh n = \cosh (\alpha + j\beta) = \frac{\omega L - \frac{1}{\omega C}}{\omega \kappa L} = -\frac{b}{2} \quad (103)$$

where κ denotes the coefficient of coupling between consecutive circuits. Equations (102) and (103) show that Z_1/Z_2 is a function of the frequency f .

a. For the pass region, the attenuation α must vanish, and we obtain

$$\cos \beta = -\frac{Z_1}{2Z_2} \quad (104)$$

and, since all cosine values are between the limits ± 1 , corresponding to a phase shift of $\beta = 180^\circ$, currents of all frequencies must be *passed* on *unattenuated* which satisfy the condition

$$-2 < \frac{Z_1}{Z_2} < 2 \quad (105)$$

or Z_1/Z_2 must have values between -2 and $+2$. Thus the values

$$\left. \begin{aligned} \frac{Z_1}{Z_2} &= 2 \\ \frac{Z_1}{Z_2} &= -2 \end{aligned} \right\} \quad (106)$$

determine the lower (f_1) and upper (f_2) *cutoff frequencies*. We find for the arrangement in Fig. 344

$$\frac{Z_1}{Z_2} = \frac{\omega L - \frac{1}{\omega C}}{\omega M} = \frac{2[\omega L - (1/\omega C)]}{\omega \kappa L}$$

where the coupling coefficient is always smaller than unity and is usually between 20 to 70 per cent for filters. We find the cutoff frequencies of this band-pass filter to be

$$f_1 = \frac{f_0}{\sqrt{1 + \kappa}}$$

$$f_2 = \frac{f_0}{\sqrt{1 - \kappa}}$$
(107)

if $f_0 = 1/(2\pi\sqrt{CL})$ denotes the natural frequency of each coupled circuit when acting independently. These formulas are the same as for the

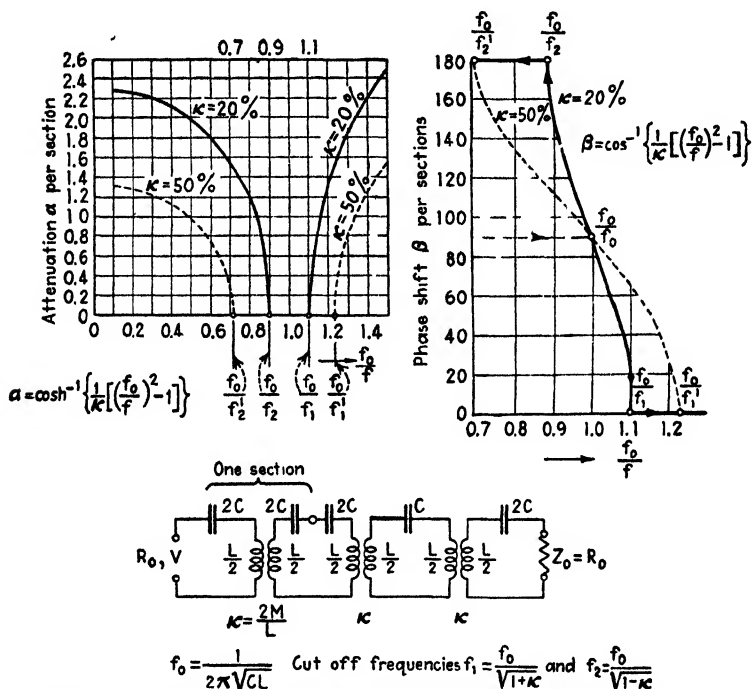


FIG. 345.—Attenuation and phase shift characteristics of coupled-circuit filter.

coupling frequencies of two coupled circuits of the foregoing kind. It may be of interest to note that, for an ideal coupling $\kappa = 1$, $f_2 = \infty$, we arrive at the characteristics of a high-pass filter.

b. For the attenuation region, the coupled-circuit filter produces attenuation but no phase shift, since

$$\cosh n = \cosh \alpha = -\frac{Z_1}{2Z_2} = -\frac{a}{2}$$
(108)

and the attenuation α outside¹ the pass band can be computed from the formula

¹ For negligible coil and condenser losses and properly terminated filter, $\alpha = 0$ within the pass band.

$$\cosh \alpha = \frac{[f_0/f]^2 - 1}{\kappa} \quad (109)$$

since

$$-\frac{Z_1}{2Z_2} = \frac{\omega^2 CL - 1}{\kappa \omega^2 CL} = \frac{[\omega/\omega_0]^2 - 1}{[\omega/\omega_0]^2 \kappa} = \frac{\omega^2 - \omega_0^2}{\kappa \omega^2}$$

Figure 345 gives the attenuation and phase-shift characteristics of the coupled-circuit filter. It can be seen that, for $f = 0$, $\alpha = \infty$ and, for $f = \infty$, $\alpha = \cosh^{-1} [1/\kappa]$.

191. Characteristic Impedance of Coupled-circuit Filter.—Inserting the solutions for I_p and I_{p-1} in the expression

$$V_p + Z_2 I_{p-1} + \frac{Z_1}{2} I_p = 0$$

for the p th coupled circuit shown in Fig. 344 yields

$$V_p = -Z_2 \sinh n [I' \epsilon^{np} - I'' \epsilon^{-np}] \quad (110)$$

According to (102),

$$\sinh n = \sqrt{\left[\frac{Z_1}{2Z_2} \right]^2 - 1}$$

and

$$V_p = Z_0 [-I' \epsilon^{np} + I'' \epsilon^{-np}] \quad (111)$$

where

$$Z_0 = \sqrt{\frac{Z_1^2}{4} - Z_2^2} \quad (112)$$

denotes the characteristic or surge impedance of the filter. Terminating the filter into a load $Z_e = Z_0$, we have again the conditions indicated in Fig. 320 and, according to Eqs. (101) and (111), the relations

$$\left. \begin{aligned} V_p &= Z_0 [-I' \epsilon^{np} + I'' \epsilon^{-np}] \\ I_p &= I' \epsilon^{np} + I'' \epsilon^{-np} \end{aligned} \right\} \quad (113)$$

At the generator end $p = 0$, and the voltage and current $V_p = V_a$ and $I_p = I_a$, respectively, and

$$\left. \begin{aligned} \frac{V_a}{Z_0} &= -I' + I'' \\ I_a &= I' + I'' \end{aligned} \right\}$$

that is,

$$\left. \begin{aligned} I' &= \frac{I_a - (V_a/Z_0)}{2} \\ I'' &= \frac{(V_a/Z_0) + I_a}{2} \end{aligned} \right\} \quad (114)$$

Putting these values into (113) gives

$$\left. \begin{aligned} V_p &= V_a \cosh np - Z_0 I_a \sinh np \\ I_p &= I_a \cosh np - \frac{V_a}{Z_0} \sinh np \end{aligned} \right\} \quad (115)$$

which is exactly the same solution as found for ordinary filters in Eq. (28). The solutions of Eqs. (32) and (33), therefore, also hold for the coupled-circuit filter.

For an open-ended, coupled-circuit chain, since $I_e = 0$ according to (33), we find the input impedance

$$Z_a' = \frac{V_a'}{I_a'} = \frac{AV_e}{DV_e}$$

and, for the chain short-circuited at the end, $V_e = 0$ and

$$Z_a'' = \frac{V_a''}{I_a''} = \frac{BI_e}{AI_e}$$

The characteristic impedance Z_0 of the chain can therefore be computed from the measured input values V_a' , V_a'' , I_a' , I_a'' since

$$Z_0 = \sqrt{Z_a' \cdot Z_a''} \quad (116)$$

because, according to Eq. (31), for q -coupled sections

$$Z_a' \cdot Z_a'' = \frac{B}{D} = \frac{Z_0 \sinh(nq)}{[\sinh(nq)]/Z_0} = Z_0^2$$

192. Filter Impedance and Effective Voltages at the End of a Coupled-circuit Filter.—It is evident from the preceding results that the general solutions given on page 557 also hold for the coupled-circuit chain. It is only necessary to insert the value $\sqrt{\frac{Z_1^2}{4} - Z_2^2}$ for Z_0 . By doing this, we find for the filter impedance of q circuits

$$\begin{aligned} Z_f &= \frac{\text{voltage impressed on filter}}{\text{current leaving filter}} = Z_e \cosh nq + Z_0 \sinh nq \\ &= Z_e \cosh nq + \sqrt{\frac{Z_1^2}{4} - Z_2^2} \sinh nq \end{aligned} \quad (117)$$

and, for the portion of the impressed filter voltage which reaches the load impedance Z_e ,

$$Q = \frac{Z_f}{Z_e} = (-1)^q \left[\cosh nq + \frac{\sqrt{Z_1^2 - 4Z_2^2}}{2Z_e} \sinh nq \right] \quad (118)$$

This equation is a criterion for the filter action for the entire range (pass and attenuated range) and plotting Q for $q = 1$, $q = 2$, $q = 3$, etc., gives a means¹ of estimating the number of sections which are needed and the best load. We find for one section $q = 1$

$$Q_1 = - \left[\cosh n + \frac{\sqrt{Z_1^2 - 4Z_2^2}}{2Z_e} \sinh n \right] \quad (119)$$

where $\cosh n = -Z_1/2Z_2$.

For two ($q = 2$) and three ($q = 3$) sections,

$$\left. \begin{aligned} Q_2 &= \cosh 2n + \frac{\sqrt{Z_1^2 - 4Z_2^2}}{2Z_e} \sinh 2n \\ Q_3 &= - \left[\cosh 3n + \frac{\sqrt{Z_1^2 - 4Z_2^2}}{2Z_e} \sinh 3n \right] \end{aligned} \right\} \quad (120)$$

In this case it is well to tabulate the various factors of (118), (119), and (120) with respect to f/f_0 , where f denotes any frequency either within or

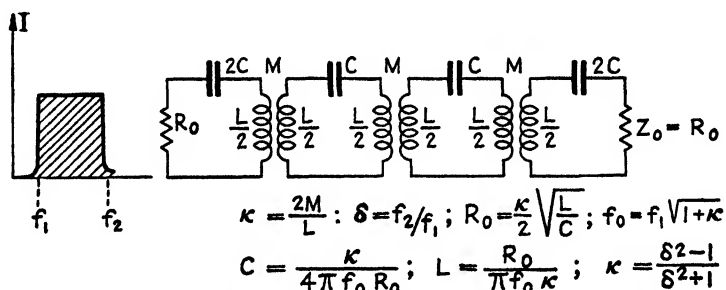


FIG. 346.—Design formulas for coupled-circuit band pass.

without the pass band, and $f_0 = 1/(2\pi\sqrt{CL})$. The pass band is between the values of f/f_0 which are $1/\sqrt{1+\kappa}$ and $1/\sqrt{1-\kappa}$, since κ determines the width of the band. The process of examining the coupled-circuit filters is then as for ordinary filters and shown in Tables XXIX and XXX on pages 557 and 558. These tables can be used directly when, for the coupled-circuit filter, the constants of the equivalent network are used.

193. Design of a Band-pass Filter Consisting of Coupled Circuits.—The surge impedance Z_0 is a function of the frequency as in the case of ordinary filters; and if the load is to be a fixed resistance, certain assumptions must be made. They are as follows:

1. The value Z_0 of the surge impedance for the frequency $f_0 = 1/(2\pi\sqrt{CL})$ is chosen as the reference value since the pass band $[(f_0/\sqrt{1-\kappa}) - (f_0/\sqrt{1+\kappa})] = f_2 - f_1$ is determined by the resonance frequency $f_0 = 1/(2\pi\sqrt{CL})$ of each coupled circuit when acting independently.

¹ Two coupled circuits correspond to one section ($q = 1$), three coupled circuits to two sections ($q = 2$). For one circuit, only the frequency f_0 would exist.

2. A resistance $R_0 = Z_0$ then denotes the load.
3. The degree of coupling determines the width of the pass band.

According to Fig. 346 and Eq. (112) for negligible coil and condenser losses (since $Z_1 = j\left[\omega L - \frac{1}{\omega C}\right]$ and $Z_2 = j\omega M = \frac{j\omega\kappa}{2}$), we find the value of the square of the surge impedance for any frequency to be

$$\begin{aligned} Z_s^2 &= \frac{[Z_1 + 2Z_2][Z_1 - 2Z_2]}{4} = -\frac{[\omega L(1 + \kappa) - (1/\omega C)][\omega L(1 - \kappa) - (1/\omega C)]}{4} \\ &= -\frac{[\omega^2 CL(1 + \kappa) - 1][\omega^2 CL(1 - \kappa) - 1]}{4\omega^2 C^2} \\ &= -\frac{\left[\frac{f^2}{f_0^2}(1 + \kappa) - 1\right]\left[\frac{f^2}{f_0^2}(1 - \kappa) - 1\right]}{4\omega^2 C^2} \quad (121) \end{aligned}$$

Therefore, the surge impedance Z_s at the resonance frequency f_0 has the value

$$Z_0 = \frac{\kappa}{2\omega_0 C} = \frac{\kappa}{2}\sqrt{\frac{L}{C}} = R_0 \quad (122)$$

since, for $f = f_0$,

$$Z_s^2 = Z_0^2 = \frac{\kappa^2}{4\omega_0^2 C^2}$$

and (121) reads in terms of Z_0

$$Z_s = Z_0 \sqrt{\frac{f^2}{f_0^2} - \frac{[f/f_0 - f_0/f]^2}{\kappa^2}} \quad (123)$$

For the frequency $f = f_0$, the impedance Z_0 acts as a resistance R_0 which is used for terminating the network on each side, and for finding the design values for C and L .

From (122), we find the value of the capacity C in farads

$$C = \frac{\kappa}{4\pi f_0 R_0} \quad (124)$$

where the resonance frequency is expressed in cycles per second and the load resistance R_0 in ohms. For the inductance L in henries, we find from $f_0 = 1/(2\pi\sqrt{CL})$ and (124)

$$L = \frac{R_0}{\pi\kappa f_0} \quad (125)$$

The frequency f_0 and the coupling coefficient is determined from the width of the band ($f_2 - f_1$) and is given by the two relations

$$\left. \begin{aligned} f_1 &= \frac{f_0}{\sqrt{1 + \kappa}} \\ f_2 &= \frac{f_0}{\sqrt{1 - \kappa}} \end{aligned} \right\}$$

for $\delta = f_2/f_1$ as

$$\left. \begin{aligned} \kappa &= \frac{\delta^2 - 1}{\delta^2 + 1} \\ f_0 &= f_1 \sqrt{1 + \kappa} \end{aligned} \right\} \quad (126)$$

The process of designing such a filter is to find, for the given cutoff frequencies f_1 and f_2 , the ratio $\delta = f_2/f_1$, to calculate κ and f_0 by means of (126), and C and L from (124) and (125). After this is done, it is well to check the performance of the filter by means of Eq. (118) and, if the performance curve for the number of sections chosen is not satisfactory, to assume another load and try by means of curves to obtain the best filter action.

194. Notes on a Coupled-circuit Filter with Coil Losses.—When filters are to be designed for frequency ranges which require larger inductances, the resistances of the coils used must be taken into account. When R denotes the total effective coil resistance of each coupled circuit (Fig. 346), and $\tau = L/R$ the time constant, we find, from Eq. (102), that

$$\begin{aligned} \cosh n &= \cosh (\alpha + j\beta) = -\frac{R + j[\omega L - (1/\omega C)]}{j\omega \kappa L} \\ &= \frac{1}{\kappa} \left[\frac{f_0^2}{f^2} - 1 \right] + j \frac{R}{\kappa \omega L} \\ &= \frac{1}{\kappa} \left\{ \left[\frac{f_0^2}{f^2} - 1 \right] + \frac{j}{\omega \tau} \right\} = a + jb \quad (127) \end{aligned}$$

We now have a complex value $(a + jb)$ for $\cosh n$ where

$$\left. \begin{aligned} a &= \frac{1}{\kappa} \left[\frac{f_0^2}{f^2} - 1 \right] \\ b &= \frac{1}{\omega \kappa \tau} \end{aligned} \right\} \quad (128)$$

The attenuation α and the phase factor β can be computed by means of Eqs. (48), (49), and (50), and the filter loss in decibels for q sections becomes

$$\text{db} = 8.68 \alpha q \quad (129)$$

since $\text{db} = 20 \log_{10} (I_1/I_2) = 20 \log_{10} (V_1/V_2) = 20 \log_{10} e^{\alpha q}$

195. Filters with Unequal Sections (Composite Networks).—The filters described so far are made up of equal sections.¹ The total attenu-

¹ Except the case shown in Fig. 333.

ation and total phase shift are equal to the number of sections times the attenuation or the phase shift per section, respectively. For no reflections at the junction points of sections, and at the load, the filter must be terminated into a proper load which is equal to the surge impedance Z_0 for each section. The surge impedance Z_0 , however, is a function of the frequency, and a value $Z_0 = R_0$ must be assumed which gives, as nearly as possible, the desired operation in the pass band. As far as the attenuation region is concerned, R_0 need not have values equal to Z_0 since currents of this band are much attenuated and any reflections at the load R_0 due to an irregularity between Z_0 and R_0 are desirable because they tend to keep currents of the undesired frequencies out of the load branch.

Now, when inverse network sections ($Z/Y = \text{constant}$) are connected in series with sections whose surge impedances are equal to that of the inverse network, no reflections take place at the junction points, and the cutoff frequencies will be the same for all sections used. Nevertheless, it is possible to choose different attenuations $\alpha_1, \alpha_2, \alpha_3$ etc., as well as phase shifts $\beta_1, \beta_2, \beta_3$, etc., for the different sections so that the total filter attenuation and phase shift become

$$\left. \begin{aligned} \alpha &= \alpha_1 + \alpha_2 + \alpha_3 + \dots \\ \beta &= \beta_1 + \beta_2 + \beta_3 + \dots \end{aligned} \right\} \quad (130)$$

These statements show that all sections behave in the same way for the conditions

$$\left. \begin{aligned} YZ &= 0 \\ YZ &= -4 \end{aligned} \right\} \quad (131)$$

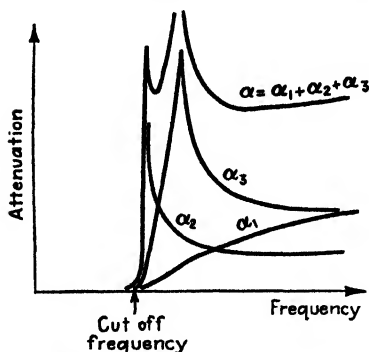


Fig. 347.—Superposition of attenuations.

but, within the pass band, the effective attenuation and phase shift may be different. This property can be used to advantage since more uniform transmission and attenuation characteristics can be obtained by properly cascading unequal sections of the foregoing type. For a filter of similar sections, any undesirable irregularities of the characteristics are emphasized with the number of sections, while, for instance, for a low-pass filter with three unequal sections of attenuations α_1, α_2 , and α_3 (Fig. 347), the resultant characteristic can be made desirable. We note that the resultant attenuation α is such that attenuation sets in rapidly after the cutoff frequency f_0 is reached and soon becomes almost constant over the remainder of the frequency range.

The composite filter is due to O. J. Zobel¹ and can also be used with half sections connected to the input and load, respectively, in order to

¹ *Loc. cit.*

obtain a more regular match with the terminal impedances within the pass band.

196. Theory of Zobel's Composite Filters.—The single or elementary type of low-pass filter (Fig. 326a) has a half T section as indicated in Fig. 348. For coils and condensers with no appreciable losses, we have practically the case of an inverse network since

$$\frac{Z}{Y} = \frac{L}{C} = Z_0^2 = R_0^2 = \text{constant}$$

The surge impedance Z_0 , according to (44), is

$$Z_0 = \sqrt{R_0^2 + \frac{Z^2}{4}} \quad (132)$$

If Z_1 is the impedance along, and Y_1 the admittance across, one section for the derived-type filter, we obtain for the same surge impedance

$$Z_0 = \sqrt{\frac{Z_1}{Y_1} + \frac{Z_1^2}{4}} \quad (133)$$

or

$$\frac{Z_1}{Y_1} + \frac{Z_1^2}{4} = R_0^2 + \frac{Z^2}{4} \quad (134)$$

a condition which must be satisfied by derived sections if they are to be connected in series with elementary sections to a load resistance R_0 . A more convenient form of (134) is

$$Y_1 = \frac{Z_1}{R_0^2 + \frac{1}{4}[Z^2 - Z_1^2]} \quad (135)$$

Since the surge impedance is also expressed by

$$Z_0 = \sqrt{Z_{oc} \cdot Z_{sc}} \quad (136)$$

where Z_{oc} denotes the open-circuit impedance at the input end of the filter for the load disconnected, and Z_{sc} the input impedance for the output of the filter short-circuited. The identity of Eqs. (132) and (133) require that for mZ_{sc} we must assume Z_{oc}/m where m denotes any factor by which the entrance impedance of the elementary-type filter section (for load terminals connected together) must be multiplied in order to give the same value as that of the derived-type filter of the same characteristic impedance Z_0 . For $m = 1$, the elementary section is obtained. Writing down the impedance values for the elementary- and derived-type half sections (indicated in full lines in Fig. 348), we obtain

$$\left. \begin{aligned} Z_{sc} &= \frac{Z}{2} \\ Z_{oc} &= \frac{Z}{2} + \frac{2}{Y} \end{aligned} \right\} \text{(elementary type)} \quad (137)$$

$$\left. \begin{aligned} Z'_{sc} &= mZ_{sc} = \frac{mZ}{2} \\ Z'_{oc} &= \frac{Z_{oc}}{m} = \frac{Z}{2m} + \frac{2}{mY} \end{aligned} \right\} \text{(derived type)} \quad (138)$$

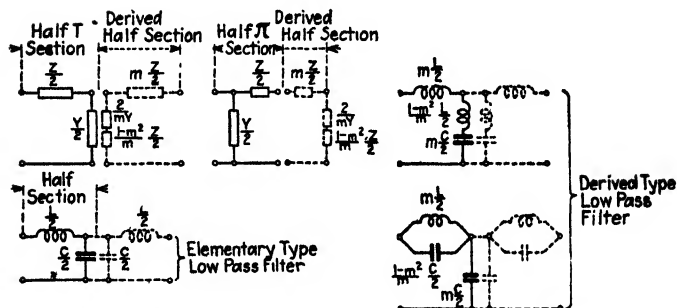


FIG. 348.—Elementary and derived half-filter sections.

Hence, for the elementary-type filter,

$$Z_{oc} - Z_{sc} = \frac{2}{Y} \quad (139)$$

and for the derived type

$$Z'_{oc} - Z'_{sc} = \frac{1}{m} \frac{2}{Y} + \left[\frac{1 - m^2}{m} \right] \frac{Z}{2} \quad (139a)$$

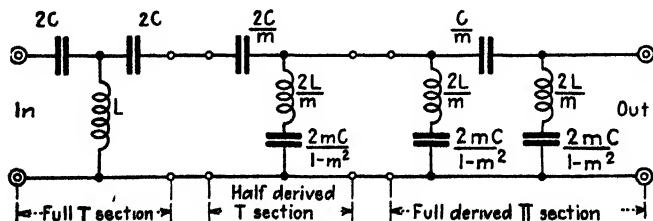


FIG. 349.—Composite high-pass filter.

The first expression of (137) and (138), respectively, shows that the half-section impedance Z_1 along a section of derived-type filter is

$$\frac{Z_1}{2} = \frac{mZ}{2} \quad (140)$$

and the comparison of (139) with (139a) shows that the half-section admittance across a section of a derived-type filter in terms of an elementary type of filter is

$$\frac{2}{Y_1} = \frac{2}{mY} + \left[\frac{1 - m^2}{m} \right] \frac{Z}{2} \quad (140a)$$

That is, a derived-type filter can be computed from formulas (140) and (140a) and treated as indicated in Fig. 348.

Figure 349 illustrates the case in which a high-pass elementary T section is combined with a derived π section through a half section. This is done in order to match the respective image impedances. The formulas given in Fig. 349 are based on the expressions given in Fig. 348 which lead to

$$\left. \begin{aligned} \frac{mZ}{2} &= \frac{m}{2\omega C} \text{ corresponding to } \frac{2C}{m} \\ \frac{2}{mY} &= \frac{2\omega L}{m} \text{ corresponding to } \frac{2L}{m} \\ \frac{1 - m^2}{m} \frac{Z}{2} &= \frac{1 - m^2}{2m} \frac{1}{\omega C} \text{ corresponding to } \frac{2mC}{1 - m^2} \end{aligned} \right\} \text{(for half section)}$$

$$\left. \begin{aligned} mZ &= \frac{m}{\omega C} \text{ corresponding to } \frac{C}{m} \\ \frac{2}{mY} \text{ as per half section} &= \frac{2L}{m} \\ \frac{1 - m^2}{2m} Z &= \frac{1 - m^2}{2m} \frac{1}{\omega C} \text{ corresponding to } \frac{2mC}{1 - m^2} \text{ (as for half section)} \end{aligned} \right\} \text{(for derived } \pi \text{ section)}$$

197. Design Formulas for Derived-type Filter Sections.—The general formulas are given in Fig. 348, and the process of application to a composite high-pass filter has just been illustrated. But, for practical work, it seems better to give expressions in terms of the load resistance R_0 for which the filter is to be designed.

a. The Low-pass Filter.—We found in Eqs. (61)' and (62) the expressions for the characteristic impedances of the T and π sections. For the cutoff frequency f_0 , we have the condition

$$YZ = -4$$

Applying this to the derived T section of Fig. 350, we find

$$\begin{aligned} Y &= j \left(\omega L_2 - \frac{1}{\omega C_2} \right) \\ Z &= j\omega L_1 \\ 2\pi f_0 L_1 &= 4 \left[\frac{1}{2\pi f_0 C_2} - 2\pi f_0 L_2 \right] \end{aligned}$$

The last expression gives

$$f_0 = \frac{1}{\pi \sqrt{L_1 C_2 + 4L_2 C_2}}$$

and must be the same as $f_0 = 1/(\pi\sqrt{CL})$ which holds for the elementary low-pass filter (Fig. 326a). For the elementary low-pass filter whose load $R_0 = \sqrt{L/C}$, we find that $L = R_0/(\pi f_0)$ when all quantities were expressed in practical units (henries, ohms, cycles per second, and farads). Hence the impedance Z of the elementary low-pass filter along the section is

$$Z = j\omega L = \frac{2jfR_0}{f_0}$$

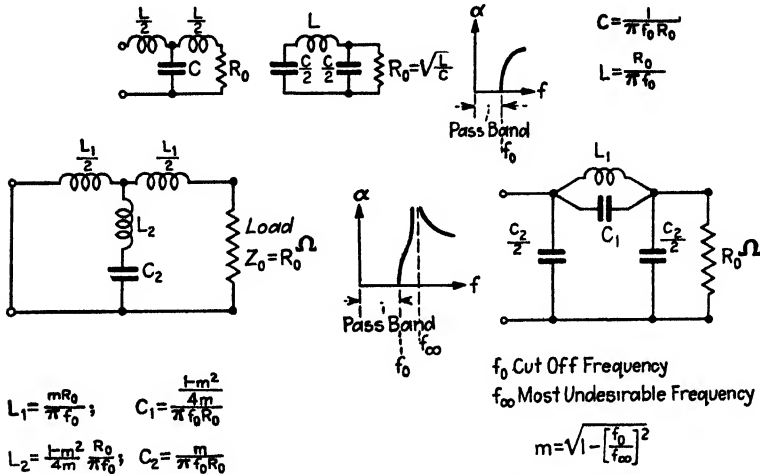


FIG. 350.—Elementary and derived T and π sections.

and for the derived section, according to Eq. (140), it is m times greater; that is,

$$Z_1 = 2jmR_0 \frac{f}{f_0} \quad (141)$$

and from Eq. (135), for the admittance Y_1 across the section, we find

$$\begin{aligned}
 Y_1 &= \frac{Z_1}{R_0^2 + \frac{1}{4}[1 - m^2]Z^2} \\
 &= \frac{2jmR_0(f/f_0)}{R_0^2 + [m^2 - 1] R_0^2 f^2 / f_0^2} \\
 &= \frac{2mf f_0}{R_0[f_0^2 + (m^2 - 1)f^2]} \quad (142)
 \end{aligned}$$

Hence, for resonance in the admittance branch, Y_1 must become ∞ ; that is,

$$f_0^2 + (m^2 - 1)f^2 = 0$$

and

$$m = \sqrt{1 - \left[\frac{f_0}{f_\infty}\right]^2} \quad (143)$$

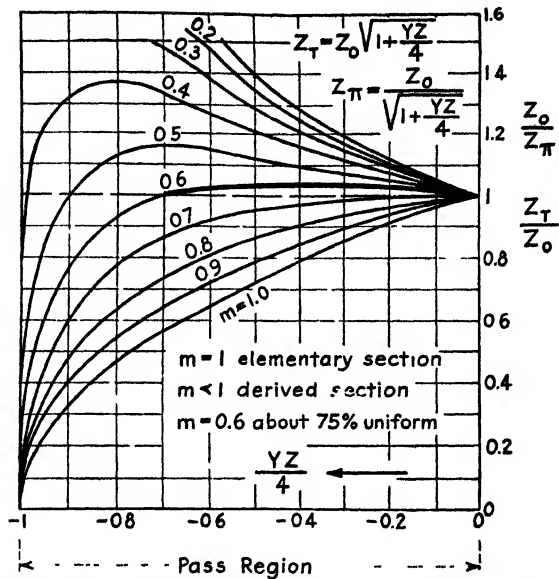


FIG. 351.—Curves for Z_0/Z_π and Z_T/Z_0 show that for $m = 0.6$ these ratios are essentially constant over quite a range of $YZ/4$.

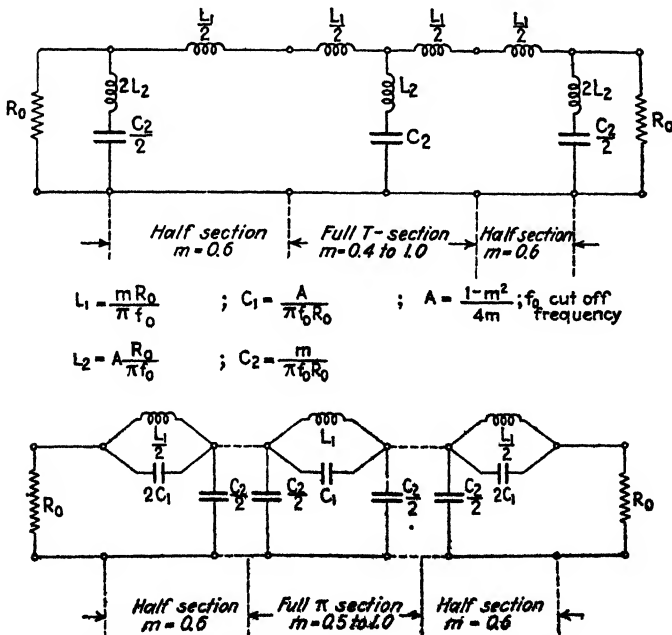


FIG. 352.—T and π filters with half section on each side.

By applying the formulas in Fig. 348 for the half sections, we obtain the expressions for the circuit constants as given in Fig. 350. From Eq. (143), it can be seen that the attenuation of the derived section can be readily changed by choosing another value for f_{∞} . The value of f_c cannot generally be altered since it is the desired cutoff frequency which is given by the constants of the elementary section. The attenuation α of the derived T network depends, therefore, upon the location of $f_{\infty} = 1/(2\pi\sqrt{C_2L_2})$ with respect to the cutoff frequency f_0 . It is desirable to choose a different value of f_{∞} for each section in order to make the resultant attenuation more nearly uniform. From Fig. 351, it can be

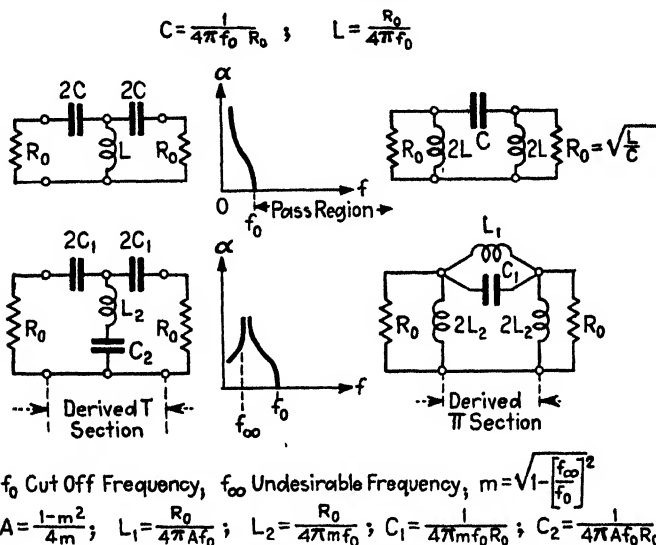


FIG. 353.—Design formulas for derived high-pass filter.

seen that, for the elementary section ($m = 1$), the surge impedance is not at all constant since the factor $Z_0 = \sqrt{Z/Y} = \sqrt{L/C} = R_0$ when divided by Z_r or the value Z_r/Z_0 varies greatly with $YZ/4$. However, it becomes fairly uniform over quite a range if $m = 0.6$. For this reason, it is sometimes customary to use half sections at each end of the filter and terminate the entire combination at each end into a resistance load $R_0 = Z_0$, as shown in Fig. 352, where about two full sections should be used between the half sections. In a similar way, the formulas for the derived-type high-pass filter given in Fig. 353 are obtained.

198. Notes on Coils and Condensers Used in Filter Circuits.—Good air condensers should always be used. In the lower frequency range where larger capacities are needed, high-grade mica condensers are suitable. Low-loss coils should be used for larger-wound air inductances. Honeycomb, universal-wound coils with Litz are recommended. When

the inductances must be so large that iron cores are needed, an air gap should be provided in the iron path. The inductance can be adjusted to the exact value by means of this air gap whose length should be within certain limits. For a large gap, too many turns are required to obtain the desired inductance and, for too small an air gap, distortion may take place and the filter action be thereby impaired. The flux density should not exceed about 30,000 lines per square inch, and the iron core should be magnetized by about 10 per cent of the ampere-turns. Generally for frequencies up to 1 kc/sec, and currents up to 1 ma, an air gap from 0.5 to 1 mm seems to be desirable. For still higher frequencies and current values, a larger air gap is needed.

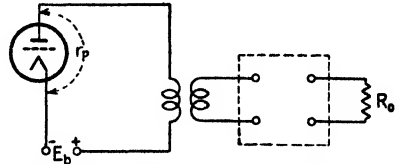


FIG. 354.—Transformer matching between tube and filter circuits.

199. Transformer as a Matching Device in Filter Circuits.—Suppose the filter is to be put in the output branch of a tube whose effective plate resistance is r_p . It is not always convenient to match a certain filter directly into the tube branch. However, the impedances may be matched by means of a transformer as shown in Fig. 354. If N is the ratio of transformation (secondary/primary), the characteristic filter

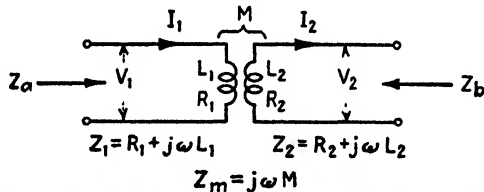


FIG. 355.—Effective impedances Z_a and Z_b when looking into input and output, respectively.

impedance $Z_0 = R_0$, which is also effective across the secondary of the transformer, acts across the primary of the transformer as an apparent resistance of value R_0/N^2 , and the ratio of transformation can be computed from the relation

$$N = \sqrt{\frac{r_p}{R_0}} \quad (144)$$

from which the transformer can be designed since r_p and R_0 are known.

If the case of an air-core transformer (Fig. 355), as much used in high-frequency work, is considered, we can prove that it behaves like a changer of surge impedance Z_0 since the impedance looking into the primary side is Z_a , and looking into the secondary side is Z_b . The proof is as follows:

$$\left. \begin{aligned} V_1 &= Z_1 I_1 - Z_m I_2 \\ Z_2 I_2 + V_2 - Z_m I_1 &= 0 \end{aligned} \right\}$$

or

$$\left. \begin{aligned} V_1 &= \frac{Z_1}{Z_m} V_2 + \frac{Z_1 Z_2 - Z_m^2}{Z_m} I_2 \\ I_1 &= \frac{1}{Z_m} V_2 + \frac{Z_2}{Z_m} I_2 \end{aligned} \right\} \quad (145)$$

This result is of the form as given in Eq. (34) for any alternating-current network and reads

$$\left. \begin{aligned} V_1 &= A_1 V_2 + B I_2 \\ I_1 &= D V_2 + A_2 I_2 \end{aligned} \right\} \quad (146)$$

Since the determinant of (146) gives

$$A_1 A_2 - BD = 1 \quad \text{or} \quad \frac{Z_1 Z_2}{Z_m^2} - \frac{Z_1 Z_2 - Z_m^2}{Z_m} = 1 \quad (147)$$

the transformer may be considered as an unsymmetrical network with a propagation constant n given by

$$\cosh n = \sqrt{\frac{Z_1 Z_2}{Z_m^2}} \quad (148)$$

For an open secondary, the input impedance is

$$Z_{oc} = \frac{A_1}{D} = Z_1$$

and, for a short-circuited secondary, it becomes

$$Z_{sc} = \frac{B}{A_2} = \frac{Z_1 Z_2 - Z_m^2}{Z_2}$$

that is, the characteristic impedance of the transformer, looking into the primary, becomes

$$Z_a = \sqrt{Z_{oc} \cdot Z_{sc}} = \sqrt{\frac{Z_1}{Z_2} [Z_1 Z_2 - Z_m^2]} \quad (149)$$

By writing down the expression for the output impedance for open and short-circuited primary, in the same way we find the characteristic impedance of the transformer looking into the secondary to be

$$Z_b = \sqrt{\frac{Z_2}{Z_1} [Z_1 Z_2 - Z_m^2]} \quad (150)$$

If the capacity effect of the coils is neglected, and tight coupling

$$(\kappa = 1 \quad \text{or} \quad M = \sqrt{L_1 L_2})$$

is assumed, we find that, for the time constants $\tau_1 = L_1/R = \tau$ and $\tau_2 = L_2/R_2 = \tau$ (which is approximately the case in practice),

$$\cosh n = \cosh (\alpha + j\beta) = 1 - \frac{j}{\omega\tau} = a - jb \quad (150a)$$

Using the approximation

$$\cosh (\alpha + j\beta) \cong 1 + \frac{[\alpha + j\beta]^2}{2}$$

we find the attenuation

$$\alpha = \sqrt{\frac{1}{\omega\tau}} \quad (151)$$

and the phase shift

$$\beta = -\sqrt{\frac{1}{\omega\tau}} \quad (152)$$

For a small attenuation, the time constant $\tau = L/R$ must be made large. In a similar way, for the characteristic impedances, we find

$$\left. \begin{aligned} Z_a &= \omega L_1 \sqrt{\frac{2j}{\omega\tau} + \frac{1}{\omega^2\tau^2}} = \omega L_1 P \\ Z_b &= \omega L_2 P \end{aligned} \right\} \quad (153)$$

For the ratio of the two characteristic impedances, we find

$$\frac{Z_a}{Z_b} = \frac{L_1}{L_2} = N^2 \quad (154)$$

where N denotes the ratio of the transformer since, for unity coupling, $L_1 = NM$, and $L_2 = M/N$. This relation shows that, for filters of characteristic impedance Z_a and Z_b connected to the respective sides of the transformer, the square of the transformer ratio must be satisfied. This result is employed in the formula given by Eq. (144).

For the product of Z_a and Z_b , we find the approximation

$$Z_a Z_b \cong \frac{2\omega L_1 L_2}{\tau} = \frac{2\omega M^2}{\tau}$$

that is, for M ,

$$M = \sqrt{\frac{Z_a Z_b \tau}{2\omega}} \quad (155)$$

and because of (154) and $L_1 = NM$, $L_2 = M/N$, $R_1 = L_1/\tau$, $R_2 = L_2/\tau$

$$\left. \begin{aligned} L_1 &= Z_a \sqrt{\frac{\tau}{2\omega}}; & R_1 &= \frac{Z_a}{\sqrt{2\omega\tau}} \\ L_2 &= Z_b \sqrt{\frac{\tau}{2\omega}}; & R_2 &= \frac{Z_b}{\sqrt{2\omega\tau}} \end{aligned} \right\} \quad (156)$$

201. Notes on Coupling Devices Employing Recurrent Networks.—

We may distinguish between recurrent networks with lumped circuit constants (artificial lines) and single and double lines for which more or less uniform distribution of circuit elements exists. The latter type is especially useful for supplying power to Hertzian¹ aerials, etc., in the ultra-high frequency band (20 to 300 megacycles/sec.). There will always be a certain loss in a coupling device used for transferring power from the impedance of the source to the impedance of the load. If the coupling device is used for matching certain terminating impedances, the loss can be made fixed or variable.² When stationary waves prevail along a parallel-wire coupling device, increased losses exist. This is, of course, also true for single-wire feeds. In many cases the double line as well as a single feeder is made aperiodic so that it behaves as a pure ohmic resistance³ over a wide frequency band. The transmission loss may be computed from the ratio of the power dissipated in the load to the power delivered by the generator. The coupling device may be called ideal if it transfers power in only one direction without reflections at the respective ends (generator end, load end). The transfer then occurs at a uniform voltage level and no standing waves can be developed along the coupling system. It happens when the load is a pure resistance and equal to the characteristic impedance of the coupling device. Hence it does not matter whether the coupling system is an actual line or an equivalent network with lumped constants.

For aerial feeds a single line in addition to a double line as a coupling device is preferable to an artificial network since it is an easy matter to match resistances from about 10 ohms up to several thousands of ohms. The lower resistance range from about 10 to 150 ohms can be readily obtained with a concentric⁴ parallel-wire feed and the range from 400 to 800 ohms with a Lecher wire and single-wire feeder system. All other useful ranges can be obtained with impedance transforming lines or with matching transformers. A line that develops a quarter-wave-length distribution along it can be used as a step-up as well as a step-down transformer, because the generator-end impedance Z_g and the load end impedance Z_l are connected with the characteristic impedance Z_0 of the line by

$$Z_0 = \sqrt{Z_g Z_l}$$

¹ "High-frequency Measurements," McGraw-Hill Book Company, Inc., New York, 1933, pp. 392-393; STERBA, E. J., and C. B. FELDMAN, *Proc. I.R.E.*, **20**, 1163, 1932; HARDIN, Jr., L. L., *QST*, February, 1935, p. 23; REINARTZ, J. L., *QST*, February, 1935, pp. 10-12; PORTER, W. S., and H. C. GOODMAN, *QST*, April, 1935, pp. 21-26; JONES, F. C., "5-Meter Radiotelephony," 2d ed., Pacific Radio Publishing Co., San Francisco, Calif., 1934, pp. 6-10; TIVUS, W. C., *Electronics*, **8**, 239, 1935.

² See pp. 409 and 538. ³ "High-frequency Measurements," p. 386. ⁴ See p. 443.

Hence if a line used as a coupling device is designed for a suitable value of Z_0 , any two real impedances Z_g and Z_l may be matched as long as the ratio Z_g/Z_l has no unreasonable value. This is brought out in Fig. 357 for the case of the quarter-wave-length distribution. The impedance Z_l looking into the open-ended double line will give a value $Z_l = Z_0^2/Z_g$. For a half-wave-length distribution the impedance Z_l' looking in the open-ended double line would measure the value Z_g' . Hence half-wave-length lines behave like a "one-to-one" matching device, while quarter-wave-

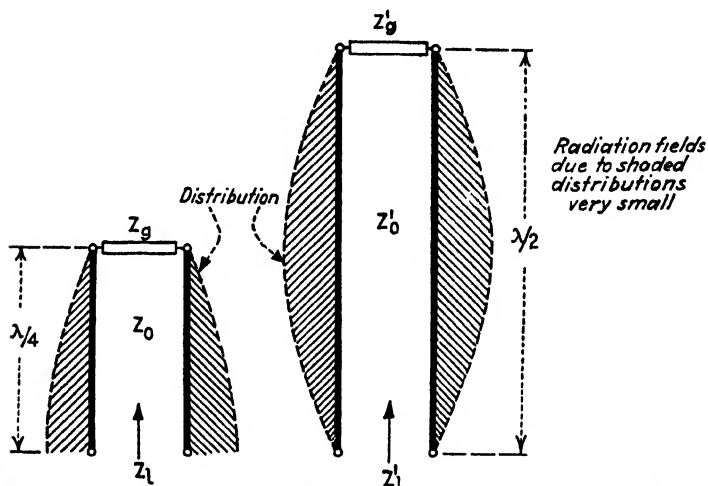


FIG. 357.—Impedances Z_l and Z_l' looking into the open end of a quarter- and half-wave-length parallel-wire system.

length distribution gives any desired ratio of impedance transformation. As far as the practical end is concerned, it is evident that for high-frequency work a line matching device is simpler than a transformer.

Now Hertzian radiators (half-wave-length aerials) have a radiation resistance of about 74 ohms. Hence if such an aerial is cut at the middle, the impedance measured across the cut would be also 74 ohms, if the half-wave-length aerial is freely suspended and well above ground. If the Hertzian aerial is not cut but the shunt impedance measured between any two points equally distant from the middle, a larger value than 74 ohms will be found. The closer the measuring points toward the open ends, the larger the value. A measurement across the end points gives a value of about 12,000 ohms. A matching device as indicated in Fig. 333 of "High-frequency Measurements"¹ can then be used in order to obtain a good power match. If a Hertzian half-wave aerial is 100 units long, points which are 24 units apart, that is, each point 12 units from the middle,

¹ *Op. cit.*, p. 392.

will give a 500-ohm resistance across these points. A parallel-wire line of 500 ohms will produce uniform current distribution along the parallel wires, that is, act aperiodically for a wide frequency range. A 500-ohm impedance exists according to Fig. 243 on page 442 for a ratio $(a/d) = 32.5$,

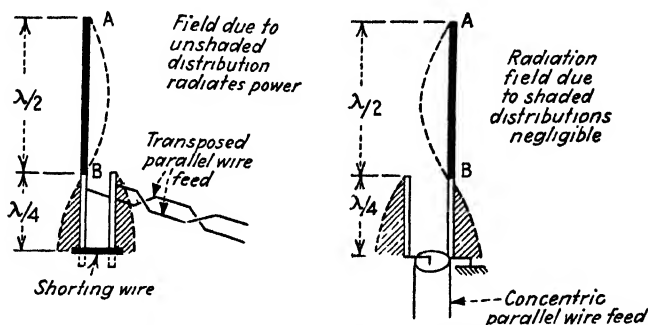


FIG. 358.—Impedance matching by means of quarter-wave-length section.

where a denotes the spacing between the centers of the two parallel wires and d the diameter of each wire.

From the above it is obvious that the impedance of a quarter-wave-length line closed at one end will increase from about 37 ohms to several thousand ohms (theoretically infinity) at the open end. Utilizing this we have the case to the left in Fig. 358. AB denotes a Hertzian aerial.

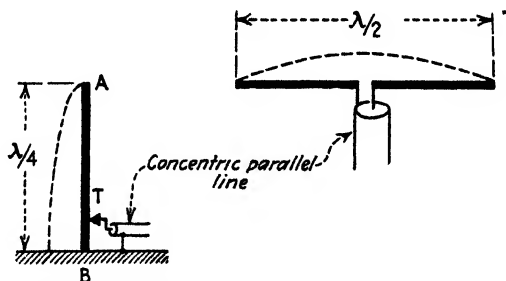


FIG. 359 —Shunt feed for a $\lambda/4$ and series feed for a $\lambda/2$ wave aerial.

The short-circuiting wire is used for adjusting to the quarter-wave-length distribution. The circuit with the grounded concentric-wire feed is used in combination with a quarter-wave-length section for matching an aerial resistance of several thousand ohms with about 75 ohms in order to terminate it into a concentric line feed that cannot radiate. Figure 359 shows how a concentric line feeds power into a vertical quarter-wave-length aerial and into a horizontal half-wave-length aerial. For the quarter-wave-length aerial the case of an adjustable shunt feed is indicated. The outside conductor of the concentric double line is grounded

and the tap T is moved along the vertical aerial until the resistance experienced across B and T is equal to the surge impedance of the concentric feeder. Inasmuch as the concentric line can be designed for very low values of resistance, there is no difficulty in using a series feed. For it the outside conductor of the concentric feeder is grounded and the inside wire of it connected directly to the foot of the vertical quarter-wave-length aerial. The concentric line must then have a characteristic impedance of $Z_0 = 37$ ohms, since it is about 74 ohms for the floating half-wave-length aerial in case of a central series feed.

APPENDIX

202. Electrostatic, Electromagnetic, Gaussian, Heaviside, and Practical Systems and Their Units.—The first two systems are based on the attraction and repulsion of electric and magnetic matters, respectively, and expressed in c.g.s. units. For the practical system such units as the ampere, volt, ohm, henry, and the farad are employed. In the electrostatic system the dielectric constant κ is numerical, that is, without dimension, and in the electromagnetic system the permeability μ has no dimension. For the Gaussian system the electrical quantities have the same dimensions as in the electrostatic system, and the magnetic quantities the same dimensions as in the electromagnetic system. Hence both μ and κ are numerical. The unit of the capacitance and inductance is then the centimeter. Table XXXI gives the units for the electrostatic and electromagnetic systems in terms of the practical units.

From the ohm (resistance of a mercury column 106.3 cm long and 1 mm² cross section at 0° C) and the ampère (this unit deposits 1.118 mg silver in a silver voltameter per second) the other international practical units become

1 coulomb	= ampere × second
1 volt	= ampere × ohm
1 watt	= ampere × volt
1 joule	= watt × second
1 farad	= coulomb × volt ⁻¹
1 henry	= volt × second × ampere ⁻¹

The most important relations are brought out in the columns for the practical units. From it we can see that for the inductance 1 cm = 10⁻⁹ henry if the change is made from the e.m. c.g.s. system, and 1 μ f = 9 × 10⁸ cm if the change is made from the practical system (1 μ f = 10⁻⁶ farad) to e.s. c.g.s. units. The column with the ratio e.m. c.g.s./e.s. c.g.s. is useful in writing down the electromagnetic-field equations. If this is done, for instance, with all the quantities expressed in the e.m. c.g.s. system, we arrive at Eq. (7) on page 329 whereas

$$\text{curl } H = 4\pi\sigma c \cdot \mathcal{E} + \frac{\kappa}{c} \frac{\partial \mathcal{E}}{\partial t}$$

is the expression when \mathcal{E} and κ are in e.s. units and H in e.m. units.

A clearer and more condensed form of units due to Heaviside is used by Hertz and is also found in the publications of H. A. Lorentz. By means of them most of such factors as 4π and $\sqrt{4\pi}$ can be avoided. The unit of electricity is then $\sqrt{4\pi}$ times smaller than the usual electrostatic unit. With this in mind we have at the same time fixed for every case the number by which the electric force is to be represented. As to the magnetic force, we assume by it a force acting on a pole of unit strength; the latter is likewise $\sqrt{4\pi}$ times smaller than the unit commonly used. The symbol used for the electric force can also be employed for the electric displacement because in the foregoing choice of units it has the same numerical magnitude as the electric force. Equation (6) on page 329 for the total current then simplifies to

$$I' = \sigma \mathcal{E} + \kappa \frac{\partial \mathcal{E}}{\partial t}$$

TABLE XXXI

 $(L = \text{length, cm; } M = \text{mass, g; } T = \text{time, sec})$

Physical quantity or property	Dimension		e.m. c.g.s. e.s. c.g.s.	Electro- magnetic c.g.s. unit =	Electrostatic c.g.s. unit =	Remarks
	Electromag- netic system, e.m. c.g.s.	Electrostatic system, e.s. c.g.s.				
Electric quantity (charge).....	$[L^{3/2} M^{1/2}]$	$[L^{3/2} M^{1/2} T^{-1}]$	$1/c$	10 coulombs	$10^{-9}/3$ coulomb	$c = 3 \times 10^{10}$ cm/sec
Magnetic quantity (mass).....	$[L^{3/2} M^{1/2} T^{-1}]$	$[L^{3/2} M^{1/2}]$	c			
Electric-field strength.....	$[L^{-1/2} M^{1/2} T^{-1}]$	$[L^{-3/2} M^{1/2} T^{-1}]$	c			
Magnetic-field strength.....	$[L^{-1/2} M^{1/2} T^{-1}]$	$[L^{1/2} M^{1/2} T^{-2}]$	$1/c$	gauss	$10^{-10}/3$ gauss	
Magnetic induction.....	$[L^{-1/2} M^{1/2} T^{-1}]$	$[L^{-3/2} M^{1/2}]$	c	10^{-8} volt maxwell	300 volts 3×10^{10} maxwell	
Electric potential.....	$[L^{3/2} M^{1/2} T^{-2}]$	$[L^{1/2} M^{1/2} T^{-1}]$	$1/c$		$10^{-9}/3$ amp.	
Magnetic flux.....	$[L^{3/2} M^{1/2} T^{-1}]$	$[L^{1/2} M^{1/2}]$	c		$10^{-9}/3$	
Dielectric displacement.....	$[L^{-3/2} M^{1/2}]$	$[L^{-1/2} M^{1/2} T^{-1}]$	$1/c$	10 amp.		
Current.....	$[L^{3/2} M^{1/2} T^{-1}]$	$[L^{3/2} M^{1/2} T^{-2}]$	$1/c$	10 amp./sq cm 10^{-9} ohm	amp./sq cm 9×10^{11} ohms	
Current density.....	$[L^{-1/2} M^{1/2} T^{-1}]$	$[L^{-3/2} M^{1/2} T^{-2}]$	$1/c$			
Resistance.....	$[L T^{-1}]$	$[L^{-1} T]$	c^2			
Specific conductivity.....	$[L^{-2} T]$	$[T^{-1}]$	$1/c^2$			
Capacitance.....	$[L^{-1} T^2]$	$[L]$	$1/c^2$			
Inductance.....	$[L]$	$[L^{-1} T^2]$	c^2	10^{-9} farad	$10^{-11}/9$ farad	
Electric energy.....	$[L^2 M T^{-2}]$	$[L^2 M T^{-2}]$	1	10^{-9} henry	9×10^{11} henries	
Permeability μ	Numerical (1)	$L^{-2} T^2/(1/c^2)$	c^2	10^{-7} watt	10^{-7} watt	
Dielectric constant ϵ	$L^{-2} T^2/(1/c^2)$	Numerical (1)	$1/c^2$			

and the curl equation (7) becomes

$$c \cdot \text{curl } H = I'$$

When the conditions of an electromagnetic field are expressed in Gaussian units and as formulated by H. A. Lorentz, we have for $n = \partial/\partial t$

$$\left. \begin{aligned} c \cdot \text{curl } \mathcal{E} &= -nH \\ c \cdot \text{curl } H &= n\mathcal{E} + 4\pi I \\ \text{div } \mathcal{E} &= 4\pi\rho \\ \text{div } H &= 0 \\ F &= q\mathcal{E} + q \frac{v \times H}{c} \end{aligned} \right\}$$

force acting in direction of electric field
force acting perpendicular to both direction of electron motion and magnetic field (exists *only* when electrons are in motion)

if ρ stands for the volume density of charge, I for the current density, v for the velocity of the electron, and F for the driving force acting on the electron of charge q .

USEFUL SOLUTIONS, FORMULAS, AND TABLES

203. Notes on Series.—If we have N terms in a series for which a constant difference d between adjacent terms exists, then we have an algebraic series whose sum is

$$\begin{aligned} S &= a + [a + d] + [a + 2d] + \cdots + [a + (N - 1)d] \\ &= \frac{N}{2}[2a + (N - 1)d] \end{aligned} \quad (\text{I})$$

hence the sum of all numbers from 1, 2, 3, up to 500 is $S = 250(2 + 499) = 125,250$.

If we have N terms and each one equal to the preceding one multiplied by a constant factor k , we have a geometric series whose sum is

$$\begin{aligned} \Sigma &= a + ka + k^2a + \cdots + k^{N-1}a \\ &= a \frac{k^N - 1}{k - 1} \quad \text{or} \quad = a \frac{1 - k^N}{1 - k} \end{aligned} \quad (\text{II})$$

For $k < 1$ it gives for an infinite number N

$$\sum_{\infty} = \frac{a}{1 - k} \quad (\text{IIa})$$

since $k^{\infty} = 0$. Hence $\sum_{\infty} = 1 + \frac{1}{3} + \frac{1}{9} + \frac{1}{27}$ gives $\frac{1}{1 - \frac{1}{3}} = 1.5$

THE BINOMIAL THEOREM

$$\begin{aligned} [a + b]^N &= a^N + Na^{N-1}b + \frac{N(N-1)}{2!}a^{N-2}b^2 + \frac{N(N-1)(N-2)}{3!}a^{N-3}b^3 + \cdots \\ &\quad + \frac{N!a^{N-k}b^k}{(N-k)!k!} \end{aligned} \quad (\text{III})$$

for $2! = 1 \times 2$ and $3! = 1 \times 2 \times 3$, etc., gives very useful expansions. This series is convergent for $b^2 < a^2$. Thus we have, for instance,

$$\begin{aligned}\sqrt{a+b} &= [a+b]^{\frac{1}{2}} = a^{\frac{1}{2}} + \frac{1}{2}a^{-\frac{1}{2}}b - \frac{1}{8}a^{-\frac{3}{2}}b^2 + \frac{1}{16}a^{-\frac{5}{2}}b^3 - \dots \\ &= \sqrt{a} \left[1 + \frac{b}{2a} - \frac{b^2}{8a^2} + \frac{b^3}{16a^3} - \dots \right]\end{aligned}\quad (\text{IIIa})$$

If b/a is a small fraction, then all terms after the second may be neglected and

$$\sqrt{a+b} \cong \sqrt{a} + \frac{b}{2\sqrt{a}} \quad (\text{IIIb})$$

Hence

$$\sqrt{144.2} = \sqrt{144 + \frac{1}{5}} = 12 + \frac{1/5}{2 \times 12} = 12.0083$$

We have

$$\sqrt{1+a} = 1 + \frac{a}{2} \quad (\text{IIIc})$$

for a small compared with unity.

Other series of this nature are

$$[a - bx]^{-1} = \frac{1}{a} \left[1 + \frac{bx}{a} + \frac{b^2x^2}{a^2} + \frac{b^3x^3}{a^3} + \dots \right] \quad (\text{IIIId})$$

which is convergent for $b^2x^2 < a^2$

$$\begin{aligned}[1 \pm x]^N &= 1 \pm Nx + \frac{N(N-1)}{2!}x^2 \pm \frac{N(N-1)(N-2)}{3!}x^3 + \dots \\ &\quad + \frac{(\pm 1)^k N! x^k}{(N-k)! k!}\end{aligned}\quad (\text{IIIe})$$

$$\begin{aligned}[1 \pm x]^{-N} &= 1 \mp Nx + \frac{N(N+1)}{2!}x^2 \mp \frac{N(N+1)(N+2)}{3!}x^3 + \dots \\ &\quad + \frac{(\pm 1)^k (N+k-1)! x^k}{(N-1)! k!}\end{aligned}\quad (\text{IIIf})$$

Both series as well as the following applications are convergent for $x^2 < 1$.

$$\sqrt{1 \pm x} = 1 \pm \frac{1}{2}x + \frac{1}{2 \cdot 4}x^2 + \frac{1 \cdot 3}{2 \cdot 4 \cdot 6}x^3 - \frac{1 \cdot 3 \cdot 5}{2 \cdot 4 \cdot 6 \cdot 8}x^4 \pm \dots \quad (\text{IIIg})$$

$$\frac{1}{\sqrt{1 \pm x}} = 1 \mp \frac{1}{2}x + \frac{3}{2 \cdot 4}x^2 \mp \frac{1 \cdot 3 \cdot 5}{2 \cdot 4 \cdot 6}x^3 + \frac{1 \cdot 3 \cdot 5 \cdot 7}{2 \cdot 4 \cdot 6 \cdot 8}x^4 \mp \dots \quad (\text{IIIh})$$

$$\sqrt[3]{1 \pm x} = 1 \pm \frac{1}{3}x - \frac{1 \cdot 2}{3 \cdot 6}x^2 \pm \frac{1 \cdot 2 \cdot 5}{3 \cdot 6 \cdot 9}x^3 - \frac{1 \cdot 2 \cdot 5 \cdot 8}{3 \cdot 6 \cdot 9 \cdot 12}x^4 \pm \dots \quad (\text{IIIi})$$

$$\frac{1}{\sqrt[3]{1 \pm x}} = 1 \mp \frac{1}{3}x + \frac{1 \cdot 4}{3 \cdot 6}x^2 \mp \frac{1 \cdot 4 \cdot 7}{3 \cdot 6 \cdot 9}x^3 + \frac{1 \cdot 4 \cdot 7 \cdot 10}{3 \cdot 6 \cdot 9 \cdot 12}x^4 \mp \dots \quad (\text{IIIk})$$

$$\frac{1}{1 \pm x} = 1 \mp x + x^2 \mp x^3 + x^4 \mp x^5 + \dots \quad (\text{IIIl})$$

$$(1 \pm x)^{\frac{3}{2}} = 1 \pm \frac{3}{2}x + \frac{3 \cdot 1}{2 \cdot 4}x^2 \mp \frac{3 \cdot 1 \cdot 1}{2 \cdot 4 \cdot 6}x^3 + \frac{3 \cdot 1 \cdot 1 \cdot 3}{2 \cdot 4 \cdot 6 \cdot 8}x^4 \mp \dots \quad (\text{III m})$$

The binomial theorem (III) can also be used to make series. We obtain, for instance,

$$a^x = 1 + \alpha x + \frac{\alpha^2}{2!}x^2 + \frac{\alpha^3}{3!}x^3 + \frac{\alpha^4}{4!}x^4 \quad (\text{IV})$$

for

$$\alpha = (a-1) - \frac{(a-1)^2}{2} + \frac{(a-1)^3}{3} - \frac{(a-1)^4}{4} + \dots$$

For $\alpha = 1$ we obtain $a = 2.71828 = e$, the base of the natural logarithms. Hence

$$e^x = 1 + x + \frac{x^2}{2!} + \frac{x^3}{3!} + \frac{x^4}{4!} + \dots \quad (\text{V})$$

which converges for $x^2 < \infty$. This series gives, for $x = 1$, $e^x = 2.71828$. Derived series of this type are

$$\left. \begin{aligned} e^{jx} &= 1 + jx - \frac{x^2}{2!} - \frac{jx^3}{3!} + \frac{x^4}{4!} + \frac{jx^5}{5!} \\ &= \left[1 - \frac{x^2}{2!} + \frac{x^4}{4!} - \dots \right] + j \left[x - \frac{x^3}{3!} + \frac{x^5}{5!} - \dots \right] = \cos x + j \sin x \\ \frac{e^x + e^{-x}}{2} &= 1 + \frac{x^2}{2!} + \frac{x^4}{4!} + \frac{x^6}{6!} + \dots \\ \frac{e^x - e^{-x}}{2} &= x + \frac{x^3}{3!} + \frac{x^5}{5!} + \frac{x^7}{7!} + \dots \end{aligned} \right\} \quad (\text{Va})$$

$$\left. \begin{aligned} \sin x &= x - \frac{x^3}{3!} + \frac{x^5}{5!} - \frac{x^7}{7!} + \dots \\ \cos x &= 1 - \frac{x^2}{2!} + \frac{x^4}{4!} - \frac{x^6}{6!} + \dots \end{aligned} \right\} \quad (\text{VI})$$

$$\left. \begin{aligned} \sinh x &= x + \frac{x^3}{3!} + \frac{x^5}{5!} + \frac{x^7}{7!} + \dots \\ \cosh x &= 1 + \frac{x^2}{2!} + \frac{x^4}{4!} + \frac{x^6}{6!} + \dots \end{aligned} \right\} \quad (\text{VII})$$

$$\begin{aligned} \tanh x &= x(1 - \frac{1}{3}x^2 + \frac{1}{45}x^4 - \frac{1}{945}x^6 + \dots) \\ \cotanh x &= \frac{1}{x} \left(1 + \frac{1}{3}x^2 - \frac{1}{45}x^4 + \frac{2}{945}x^6 - \dots \right) \end{aligned}$$

Figure 319 on page 535 and Table XXXII give the curves for the hyperbolic functions together with the e functions. Equations (VI) and (VII) are convergent for $x^2 < \infty$.

According to Maclaurin we have for any function $y = f(x)$ the series

$$y = f(0) + f'(0)x + \frac{f''(0)}{2!}x^2 + \frac{f'''(0)}{3!}x^3 + \dots \quad (\text{VIII})$$

where $f'(0)$, $f''(0)$, $f'''(0)$, etc., stand for consecutive differential quotients dy/dx , d^2y/dx^2 , d^3y/dx^3 , etc., for $x = 0$. With this progression we can find the series expansion of functions. For instance, if $y = \sin x$, we have

$$f(x) = \sin x; \quad f'(x) = \cos x; \quad f''(x) = -\sin x; \quad f'''(x) = -\cos x$$

which for $x = 0$ gives the values 0, 1, 0, -1, etc., and

$$\sin x = x - \frac{x^3}{3!} + \frac{x^5}{5!} - \dots$$

According to Taylor we have the series

$$f(x_0 + h) = f(x_0) + f'(x_0)h + \frac{f''(x_0)}{2!}h^2 + \frac{f'''(x_0)}{3!}h^3 + \dots \quad (\text{IX})$$

which plays a very important part in high-frequency problems. For instance, let the voltage applied between the grid and the filament of an amplifying tube be

$$e_s = e_0 + e_1 \sin \omega_1 t + e_2 \sin \omega_2 t$$

TABLE XXXII.— e AND HYPERBOLIC FUNCTIONS

x	e^x	e^{-x}	$\sinh x$	$\cosh x$
0.00	1.0000	1.0000	0.0000	1.0000
0.01	1.0100	0.9900	0.0100	1.0000
0.02	1.0202	0.9802	0.0200	1.0002
0.03	1.0305	0.9704	0.0300	1.0004
0.04	1.0408	0.9608	0.0400	1.0008
0.05	1.0513	0.9512	0.0500	1.0013
0.06	1.0618	0.9418	0.0600	1.0018
0.07	1.0725	0.9324	0.0701	1.0025
0.08	1.0833	0.9231	0.0801	1.0032
0.09	1.0942	0.9139	0.0901	1.0041
0.10	1.1052	0.9048	0.1002	1.0050
0.11	1.1163	0.8958	0.1102	1.0061
0.12	1.1275	0.8869	0.1203	1.0072
0.13	1.1388	0.8781	0.1304	1.0085
0.14	1.1503	0.8694	0.1405	1.0098
0.15	1.1618	0.8607	0.1506	1.0113
0.16	1.1735	0.8521	0.1607	1.0128
0.17	1.1853	0.8437	0.1708	1.0145
0.18	1.1973	0.8353	0.1810	1.0162
0.19	1.2092	0.8270	0.1911	1.0181
0.20	1.2214	0.8187	0.2013	1.0201
0.21	1.2337	0.8106	0.2115	1.0221
0.22	1.2461	0.8025	0.2218	1.0243
0.23	1.2586	0.7945	0.2320	1.0266
0.24	1.2712	0.7866	0.2423	1.0289
0.25	1.2840	0.7788	0.2526	1.0314
0.26	1.2969	0.7711	0.2629	1.0340
0.27	1.3100	0.7634	0.2733	1.0367
0.28	1.3231	0.7558	0.2837	1.0395
0.29	1.3364	0.7483	0.2941	1.0423
0.30	1.3499	0.7408	0.3045	1.0453
0.31	1.3634	0.7334	0.3150	1.0484
0.32	1.3771	0.7261	0.3255	1.0516
0.33	1.3910	0.7189	0.3360	1.0549
0.34	1.4049	0.7118	0.3466	1.0584
0.35	1.4191	0.7047	0.3572	1.0619
0.36	1.4333	0.6977	0.3678	1.0655
0.37	1.4477	0.6907	0.3785	1.0692
0.38	1.4623	0.6839	0.3892	1.0731
0.39	1.4770	0.6771	0.4000	1.0770
0.40	1.4918	0.6703	0.4108	1.0811
0.41	1.5068	0.6636	0.4216	1.0852
0.42	1.5220	0.6570	0.4325	1.0895
0.43	1.5373	0.6505	0.4434	1.0939
0.44	1.5527	0.6440	0.4543	1.0984
0.45	1.5683	0.6376	0.4653	1.1030
0.46	1.5841	0.6313	0.4764	1.1077
0.47	1.6000	0.6250	0.4875	1.1125
0.48	1.6161	0.6188	0.4986	1.1174
0.49	1.6323	0.6126	0.5098	1.1225
0.50	1.6487	0.6065	0.5211	1.1276

TABLE XXXII.— e^x AND HYPERBOLIC FUNCTIONS.—(Continued)

x	e^x	e^{-x}	$\sinh x$	$\cosh x$
0.50	1.6487	0.6065	0.5211	1.1276
0.51	1.6653	0.6005	0.5324	1.1329
0.52	1.6820	0.5945	0.5438	1.1383
0.53	1.6989	0.5886	0.5552	1.1438
0.54	1.7160	0.5827	0.5666	1.1494
0.55	1.7333	0.5770	0.5782	1.1551
0.56	1.7507	0.5712	0.5897	1.1609
0.57	1.7683	0.5655	0.6014	1.1669
0.58	1.7860	0.5599	0.6131	1.1730
0.59	1.8040	0.5543	0.6248	1.1792
0.60	1.8221	0.5488	0.6367	1.1855
0.61	1.8404	0.5433	0.6485	1.1919
0.62	1.8589	0.5379	0.6605	1.1984
0.63	1.8776	0.5326	0.6725	1.2051
0.64	1.8965	0.5273	0.6846	1.2119
0.65	1.9155	0.5220	0.6967	1.2188
0.66	1.9348	0.5169	0.7090	1.2258
0.67	1.9542	0.5117	0.7213	1.2330
0.68	1.9739	0.5066	0.7336	1.2402
0.69	1.9937	0.5016	0.7461	1.2476
0.70	2.0138	0.4966	0.7586	1.2552
0.71	2.0340	0.4916	0.7712	1.2628
0.72	2.0544	0.4867	0.7838	1.2706
0.73	2.0751	0.4819	0.7966	1.2785
0.74	2.0959	0.4771	0.8094	1.2865
0.75	2.1170	0.4724	0.8223	1.2947
0.76	2.1383	0.4677	0.8353	1.3030
0.77	2.1598	0.4630	0.8484	1.3114
0.78	2.1815	0.4584	0.8615	1.3199
0.79	2.2034	0.4538	0.8748	1.3286
0.80	2.2255	0.4493	0.8881	1.3374
0.81	2.2479	0.4449	0.9015	1.3464
0.82	2.2705	0.4404	0.9150	1.3555
0.83	2.2933	0.4360	0.9286	1.3647
0.84	2.3164	0.4317	0.9423	1.3740
0.85	2.3396	0.4274	0.9561	1.3835
0.86	2.3632	0.4232	0.9700	1.3932
0.87	2.3869	0.4190	0.9840	1.4029
0.88	2.4109	0.4148	0.9981	1.4128
0.89	2.4351	0.4107	1.0122	1.4229
0.90	2.4596	0.4066	1.0265	1.4331
0.91	2.4843	0.4025	1.0409	1.4434
0.92	2.5093	0.3985	1.0554	1.4539
0.93	2.5345	0.3946	1.0700	1.4645
0.94	2.5600	0.3906	1.0847	1.4753
0.95	2.5857	0.3867	1.0995	1.4862
0.96	2.6117	0.3829	1.1144	1.4973
0.97	2.6379	0.3791	1.1294	1.5085
0.98	2.6645	0.3753	1.1446	1.5199
0.99	2.6912	0.3716	1.1598	1.5314
1.00	2.7183	0.3679	1.1752	1.5431

For short-circuited anode circuit we have the anode current

$$i_p = f(e_c + e_1 \sin \omega_1 t + e_2 \sin \omega_2 t)$$

According to (IX)

$$i_p = f(e_c) + [e_1 \sin \omega_1 t + e_2 \sin \omega_2 t] f'(e_c) + \frac{[e_1 \sin \omega_1 t + e_2 \sin \omega_2 t]^2 f''(e_c)}{2!} + \dots$$

or

$$\begin{aligned} i_p = & f(e_c) + f''(e_c) \frac{1}{4} [e_1^2 + e_2^2] \\ & + f'(e_c) [e_1 \sin \omega_1 t + e_2 \sin \omega_2 t] \\ & - f''(e_c) \frac{1}{4} [e_1^2 \cos 2\omega_1 t + e_2^2 \cos 2\omega_2 t] \\ & + f''(e_c) e_1 e_2 \sin \omega_1 t \sin \omega_2 t \end{aligned}$$

hence superimposed on the direct-current component

$$f(e_c) + f''(e_c) \frac{1}{4} [e_1^2 + e_2^2]$$

are two currents which have the same frequencies $\omega_1/2\pi$ and $\omega_2/2\pi$ as applied to the grid as well as currents of twice these frequencies. For series of the Bessel functions reference is made to pages 337, 420 and to formula (XXa) of the appendix.

204. Trigonometric and Hyperbolic Functions.—The trigonometric functions expressed in terms of exponentials are

$$\left. \begin{aligned} \sin x &= \frac{e^{ix} - e^{-ix}}{2j} \\ \cos x &= \frac{e^{ix} + e^{-ix}}{2} \\ \tan x &= \frac{\sin x}{\cos x} = \frac{e^{ix} - e^{-ix}}{j[e^{ix} + e^{-ix}]} = \frac{1}{\cotan x} \end{aligned} \right\} \quad (\text{X})$$

and the corresponding hyperbolic functions are

$$\left. \begin{aligned} \sinh x &= \frac{e^x - e^{-x}}{2} \\ \cosh x &= \frac{e^x + e^{-x}}{2} \\ \tanh x &= \frac{e^x - e^{-x}}{e^x + e^{-x}} = \frac{1}{\cotanh x} \end{aligned} \right\} \quad (\text{XI})$$

The circular functions are therefore based on e^{ix} and e^{-ix} terms while the hyperbolic functions are based on e^x and e^{-x} terms. We have therefore

$$\left. \begin{aligned} e^{ix} &= \cos x + j \sin x \\ e^{-ix} &= \cos x - j \sin x \\ e^x &= \cosh x + \sinh x \\ e^{-x} &= \cosh x - \sinh x \end{aligned} \right\} \quad (\text{XII})$$

Moreover,

$$\begin{array}{ll} \sin jx = j \sinh x & \sinh jx = j \sin x \\ \cos jx = \cosh x & \cosh jx = \cos x \\ \tan jx = j \tanh x & \tanh jx = j \tan x \\ \cotan jx = -j \cotanh x & \cotanh jx = -j \cotan x \end{array} \quad \text{and} \quad (\text{XIII})$$

We have the corresponding operations

$\sin^2 x + \cos^2 x = 1$	$\cosh^2 x - \sinh^2 x = 1$	} (XIV)
$1 + \tan^2 x = \frac{1}{\cos^2 x}$	$1 + \tanh^2 x = \frac{1}{\cosh^2 x}$	
$1 + \cotan^2 x = \frac{1}{\sin^2 x}$	$1 + \cotanh^2 x = \frac{1}{\sinh^2 x}$	
$\sin(x \pm y) = \sin x \cos y \pm \cos x \sin y$	$\sinh(x \pm y) = \sinh x \cosh y \pm \cosh x \sinh y$	
$\cos(x \pm y) = \cos x \cos y \mp \sin x \sin y$	$\cosh(x \pm y) = \cosh x \cosh y \pm \sinh x \sinh y$	
$\tan(x \pm y) = [\tan x \pm \tan y]: [1 \mp \tan x \tan y]$	$\tanh(x \pm y) = [\tanh x \pm \tanh y]: [1 \pm \tanh x \tanh y]$	
$\sin \frac{x}{2} = \sqrt{\frac{1}{2}[1 - \cos x]}$	$\sinh \frac{x}{2} = \sqrt{\frac{1}{2}(\cosh x - 1)}$	
$\frac{d \sin x}{dx} = \cos x$	$\frac{d \sinh x}{dx} = \cosh x$	
$\frac{d \cos x}{dx} = -\sin x$	$\frac{d \cosh x}{dx} = \sinh x$	
$\frac{d \tan x}{dx} = \frac{1}{\cos^2 x}$	$\frac{d \tanh x}{dx} = \frac{1}{\cosh^2 x}$	
$\frac{d \cotan x}{dx} = -\frac{1}{\sin^2 x}$	$\frac{d \cotanh x}{dx} = -\frac{1}{\sinh^2 x}$	
$\int \sin x dx = -\cos x + C$	$\int \sinh x dx = \cosh x + C$	
$\int \cos x dx = \sin x + C$	$\int \cosh x dx = \sinh x + C$	
$\int \tan x dx = -\log_e \cos x + C$	$\int \tanh x dx = \log_e \cosh x + C$	
$\int \cotan x dx = \log_e \sin x + C$	$\int \cotanh x dx = \log_e \sinh x + C$	
$\frac{d^2 y}{dx^2} + a^2 y - b = 0$ is satisfied	$\frac{d^2 y}{dx^2} - a^2 y - b = 0$ is satisfied	
by $y = \sin ax + \frac{b^2}{a^2} = \cos ax + \frac{b^2}{a^2}$	by $y = \sinh ax - \frac{b^2}{a^2} = \cosh ax - \frac{b^2}{a^2}$	

$$n = \cosh [\log_e (n + \sqrt{n^2 - 1})] = \cosh^{-1} \left[\frac{e^n + e^{-n}}{2} \right] \quad (\text{XIVa})$$

205. Approximations in Formulas with Small Quantities.— α and β denote small quantities in comparison with unity and α , respectively. α and β are expressed in radians. If the exponent n is real in $[1 \pm \alpha]^n$, then

$$[1 \pm \alpha]^n = 1 \pm n\alpha \quad (\text{XV})$$

from which we obtain

$$\frac{1 \pm \alpha_1}{1 \pm \alpha_2} = 1 \pm \alpha_1 \mp \alpha_2 \quad \text{and} \quad [1 \pm \alpha_1][1 \pm \alpha_2] = 1 \pm \alpha_1 \pm \alpha_2 \quad (\text{XVa})$$

$$\sqrt{A[A + \alpha]} = 0.5\{A + [A + \alpha]\} \quad (\text{XVb})$$

For the angle functions we have the approximations

$\sin \beta = \beta - \frac{\beta^3}{6}$	$\sin(\alpha \pm \beta) = \sin \alpha \pm \beta \cos \alpha$	} (XVI)
$\cos \beta = 1 - \frac{\beta^2}{2}$	$\cos(\alpha \pm \beta) = \cos \alpha \mp \beta \sin \alpha$	
$\tan \beta = \beta + \frac{\beta^3}{3}$	$\tan(\alpha \pm \beta) = \tan \alpha \pm \frac{\beta}{\cos^2 \alpha}$	
$\cotan \beta = \frac{1}{\beta} - \frac{\beta}{3}$	$\cotan(\alpha \pm \beta) = \cotan \alpha \mp \beta[\cotan^2 \alpha + 1]$	

and for the logarithms

$$\left. \begin{aligned} A^a &= 1 + a \log_e A \\ \log_e [1 \pm a] &= \pm a - \frac{a^2}{2} \end{aligned} \right\} \quad (\text{XVII})$$

$$\left. \begin{aligned} \log_e \left[\frac{1+a}{1-a} \right] &= 2a \left[1 + \frac{a^2}{3} \right] \\ \log_e (1+a) &= a \quad \text{and} \quad \log_{10} (1+a) = 0.4343a \end{aligned} \right\} \quad (\text{XVIIa})$$

206. Solutions of Differential Equations Common for Electrical Networks.—
Differential equations which occur often are of the form

Equation	Solution	
$\frac{dy}{dx} + ny = 0$	$y = Ae^{-nx}$	
$\frac{d^2y}{dx^2} + n^2y = 0$	$y = Ae^{inx}$ or $y = A_1e^{-nx} + A_2e^{+nx}$	(XVIII)
$B\frac{d^m y}{dx^m} + C\frac{d^{m-1}y}{dx^{m-1}} + \dots + T\frac{dy}{dx} + Sy = 0$	$y = A_1e^{n_1x} + A_2e^{n_2x} + \dots$ $ = \Sigma Ae^{n_x}$	

Hence an equation with a time function of the form

$$\frac{d^2y}{dt^2} + B_1\frac{dy}{dt} + B_2y = 0 \quad (\text{XVIIIa})$$

has a solution

$$y = \sum_n Ae^{nt}$$

hence

$$\frac{dy}{dt} = nAe^{nt} \quad \frac{d^2y}{dt^2} = n^2Ae^{nt}$$

and

$$n^2Ae^{nt} + nB_1Ae^{nt} + B_2Ae^{nt} = 0$$

or

$$n^2 + B_1n + B_2 = 0$$

with the roots

$$n = \frac{-B_1 \pm \sqrt{B_1^2 - 4B_2}}{2}$$

Oscillations will occur when $4B_2 > B_1^2$; that is,

$$\left. \begin{aligned} n_1 &= \alpha + j\beta = -\frac{B_1}{2} + j\frac{\sqrt{4B_2 - B_1^2}}{2} \\ n_2 &= \alpha - j\beta \end{aligned} \right\} \quad (\text{XVIIIb})$$

where α is the damping factor and β the angular velocity. The solution is

$$y = A_1e^{n_1t} + A_2e^{n_2t} \quad (\text{XVIIIc})$$

For a third-order equation we find

$$\frac{d^3y}{dt^3} + B_1\frac{d^2y}{dt^2} + B_2\frac{dy}{dt} + B_3y = 0 \quad (\text{XVIIIId})$$

with the equation for the roots

$$n^3 + B_1 n^2 + B_2 n + B_3 = 0$$

When the system executes oscillations, we have the roots

$$\begin{aligned} n_1 &= \alpha_1 \\ n_2 &= \alpha + j\beta \\ n_3 &= \alpha - j\beta \end{aligned} \quad (\text{XVIII}e)$$

Here α_1 is the reciprocal of the time constant, α the damping factor, and β the angular velocity where n_2 and n_3 may be regarded as generalized angular velocities of which α corresponds to a hyperbolic angular velocity. If α is zero, then we have sustained oscillations for which

$$B_2 = \frac{B_3}{B_1} \quad (\text{XVIII}f)$$

since

$$\begin{aligned} B_1 &= -(n_1 + n_2 + n_3) \\ B_2 &= n_1 n_2 + n_2 n_3 + n_3 n_1 \\ B_3 &= -n_1 n_2 n_3 \end{aligned} \quad (\text{XVIII}g)$$

For the fourth-order equation, we have

$$\frac{d^4 y}{dt^4} + B_1 \frac{d^3 y}{dt^3} + B_2 \frac{d^2 y}{dt^2} + B_3 \frac{dy}{dt} + B_4 y = 0 \quad (\text{XVIII}h)$$

with the equation for the roots

$$n^4 + B_1 n^3 + B_2 n^2 + B_3 n + B_4 = 0$$

Normally the application of this expression is used for double periodic terms for which

$$\begin{aligned} n_1 &= \alpha_1 + j\beta_1 & n_3 &= \alpha_2 + j\beta_2 \\ n_2 &= \alpha_1 - j\beta_1 & n_4 &= \alpha_2 - j\beta_2 \end{aligned} \quad (\text{XVIII}i)$$

For the single periodic case we have

$$\begin{aligned} n_1 &= \alpha_1 + j\beta_1 & n_3 &= \alpha_2 \\ n_2 &= \alpha_1 - j\beta_1 & n_4 &= \alpha_2 \end{aligned} \quad (\text{XVIII}j)$$

Sustained oscillations exist when

$$\frac{B_1}{B_3} = \frac{2}{B_2 \pm \sqrt{B_2^2 - 4B_4}} \quad (\text{XVIII}k)$$

since

$$\left. \begin{aligned} B_1 &= -2[\alpha_1 + \alpha_2] \\ B_2 &= \alpha_1^2 + \beta_1^2 + 4\alpha_1\alpha_2 + \alpha_2^2 + \beta_2^2 \\ B_3 &= -2[\alpha_1(\alpha_2^2 + \beta_2^2) + \alpha_2(\alpha_1^2 + \beta_1^2)] \\ B_4 &= [\alpha_1^2 + \beta_1^2][\alpha_2^2 + \beta_2^2] \end{aligned} \right\} \quad (\text{XVIII}l)$$

A differential equation of the form

$$\frac{\partial^2 y}{\partial x^2} = \frac{1}{v^2} \frac{\partial^2 y}{\partial t^2} \quad (\text{XIX})$$

has the solution

$$y = f(x - vt) + f(x + vt) \quad (\text{XIX}a)$$

where $f(x \pm vt)$ stands for some curve moving with the velocity $\pm v$,

Another type of differential equation which occurs frequently is the Bessel equation

$$\frac{d^2y}{dx^2} + \frac{1}{x} \frac{dy}{dx} + a^2y = 0 \quad (\text{XX})$$

with the solution

$$y = J_0(ax) = 1 - \frac{(ax)^2}{2^2} + \frac{(ax)^4}{2^2 \cdot 4^2} - \frac{(ax)^6}{2^2 \cdot 4^2 \cdot 6^2} + \dots \quad (\text{XXa})$$

If the Bessel differential equation is written in the form

$$\frac{d^2y}{dx^2} + \frac{1}{x} \frac{dy}{dx} + \left[1 - \frac{m^2}{x^2}\right]y = 0 \quad (\text{XXI})$$

we have the general integral

$$Z_m(x) = c_1 J_m(x) + c_2 N_m(x) \quad (\text{XXII})$$

where $J_m(x)$ is the Bessel function of the first kind of the order m and $N_m(x)$ is the Bessel function of the second kind of the order m . We have

$$\left. \begin{aligned} J_0(x) &= 1 - \frac{(x/2)^2}{1!^2} + \frac{(x/2)^4}{2!^2} - \frac{(x/2)^6}{3!^2} + \dots \\ J_1(x) &= -\frac{dJ_0(x)}{dx} = \frac{x}{2} \left[1 - \frac{(x/2)^2}{1!2!} + \frac{(x/2)^4}{2!3!} - \frac{(x/2)^6}{3!4!} + \dots \right] \\ N_0(x) &= \frac{2}{\pi} \left[J_0(x) \log \epsilon \frac{\alpha x}{2} + \left(\frac{x}{2}\right)^2 - \left(1 + \frac{1}{2}\right) \frac{(x/2)^4}{2!^2} + \right. \\ &\quad \left. \left(1 + \frac{1}{2} + \frac{1}{3}\right) \frac{(x/2)^6}{3!^2} - \dots \right] \end{aligned} \right\} \quad (\text{XXIII})$$

where $\alpha = 1.7811$ and

$$\left. \begin{aligned} N_{m-1}(x)J_m(x) - N_m(x)J_{m-1}(x) &= \frac{2}{\pi x}; & Z_{m-1}(x) + Z_{m+1}(x) &= \frac{2m}{x}Z_m(x) \\ \frac{dZ_m(x)}{dx} &= Z_{m-1}(x) - \frac{m}{x}Z_m; & \frac{d}{dx}[x^m Z_m(x)] &= x^m Z_{m-1}(x) \end{aligned} \right\} \quad (\text{XXIV})$$

207. Vector Analysis.—The vectors of size A and B are expressed by \vec{A} and \vec{B} , respectively. Generally they form an angle α with one another. The inner product or scalar product of the vector is

$$\vec{A}\vec{B} = \vec{A} \cdot \vec{B} = AB \cos \alpha \quad (\text{XXV})$$

while the exterior or vector product is

$$\vec{A} \times \vec{B} = AB \sin \alpha \quad (\text{XXVI})$$

that is, equal to the area of the parallelogram formed by the two vectors. The inner product is numerical (scalar) and the exterior product is a vector of length $AB \sin \alpha$ perpendicular to the plane of \vec{A} and \vec{B} and in such a direction that a twist necessary to turn \vec{A} into the position \vec{B} is that of a corkscrew. For the scalar it is immaterial whether the first vector is multiplied by the second or the second by the first but for vector products a reversal of the order of the products reverses the sign of the product according to the corkscrew rule. Hence

$$\left. \begin{aligned} \vec{A} \cdot \vec{B} &= \vec{B} \cdot \vec{A} \\ \vec{A} \times \vec{B} &= -\vec{B} \times \vec{A} \end{aligned} \right\} \quad (\text{XXVII})$$

If \vec{A} is a vector of magnitude A and $\hat{i}, \hat{j}, \hat{k}$ unit vectors along the three coordinates x, y , and z , then

$$\left. \begin{aligned} A &= A_x + A_y + A_z = iA_x + jA_y + kA_z \\ A &= \sqrt{A_x^2 + A_y^2 + A_z^2} \end{aligned} \right\} \quad (\text{XXVIII})$$

if A_x , A_y , and A_z are the magnitudes of the component vectors A_x , A_y , and A_z . Since, according to the foregoing definitions (XXV) and (XXVI),

$$\left. \begin{aligned} i \cdot i &= j \cdot j = k \cdot k = 1 \\ i \times i &= j \times j = k \times k = 0 \end{aligned} \right\} \quad (\text{XXIX})$$

we have for two vectors A and B

$$\left. \begin{aligned} A \cdot B &= A_x B_x + A_y B_y + A_z B_z \\ A \times B &= i[A_y B_z - A_z B_y] + j[A_z B_x - A_x B_z] + k[A_x B_y - A_y B_x] \\ &= \begin{vmatrix} i & j & k \\ A_x & A_y & A_z \\ B_x & B_y & B_z \end{vmatrix} \end{aligned} \right\} \quad (\text{XXX})$$

since all other terms either simplify or vanish.

For differentials we have the rules

$$\left. \begin{aligned} dA \cdot B &= A \cdot dB + B \cdot dA \\ dA \times B &= A \times dB + dA \times B = A \times dB - B \times dA \end{aligned} \right\} \quad (\text{XXXI})$$

hence

$$\frac{dA \times B}{dt} = A \times \frac{dB}{dt} + \frac{dA}{dt} \times B$$

If $l = ix + jy + kz$, then $dl(i + j + k) = dx + dy + dz$, and

$$\left. \begin{aligned} \nabla &= i \frac{\partial}{\partial x} + j \frac{\partial}{\partial y} + k \frac{\partial}{\partial z} \\ \text{grad } V &= i \frac{\partial V}{\partial x} + j \frac{\partial V}{\partial y} + k \frac{\partial V}{\partial z} \end{aligned} \right\} \quad (\text{XXXII})$$

These expressions are applied throughout the text of electromagnetic theory (page 324). If l_1 , is the unit vector of l , then

$$dV = l_1 dl \text{ grad } V \quad (\text{XXXIII})$$

and if l_1 coincides with the direction of dl , we obtain

$$\frac{dV}{dl} = \text{grad } V \quad \text{and} \quad \int_1^2 \text{grad } V dl = V_2 - V_1 = \int_1^2 V dl \quad (\text{XXXIV})$$

Hence if dl denotes a very short straight path in an electric field connecting a point of potential V with a point of potential $V + dV$, then the work done in moving a unit charge along this path is $\oint \cdot dl$ if \oint denotes the vector of the electric force \oint . But $\oint = -\text{grad } V$; hence

$$\oint \cdot dl = -\text{grad } V \cdot dl = dV \quad (\text{XXXV})$$

For a closed path

$$\oint \oint \cdot dl = 0 \quad \text{div } A = \frac{\partial A_x}{\partial x} + \frac{\partial A_y}{\partial y} + \frac{\partial A_z}{\partial z} \quad (\text{XXXVI})$$

If V is again as above a function of the coordinates, then

$$\begin{aligned} dV &= \frac{\partial V}{\partial x} dx + \frac{\partial V}{\partial y} dy + \frac{\partial V}{\partial z} dz \\ &= \underbrace{\left(i \frac{\partial V}{\partial x} + j \frac{\partial V}{\partial y} + k \frac{\partial V}{\partial z} \right)}_{\nabla V \text{ [according to (XXXII)]}} \underbrace{(i dx + j dy + k dz)}_{dl} \end{aligned} \quad (\text{XXXVII})$$

Combining (XXXV) and (XXXVII) we have

$$\text{grad } V = \nabla V \quad (\text{XXXVIII})$$

The operator $\partial/\partial x + \partial/\partial y + \partial/\partial z$ in (XXXVI) or (XXXVII) is called the divergence (div) of A and V , respectively. It is the amount of A or V , respectively, which diverges or originates from each unit volume of space (for proof and applications, page 324).

The scalar product of

$$\nabla = i\frac{\partial}{\partial x} + j\frac{\partial}{\partial y} + k\frac{\partial}{\partial z}$$

and

$$A = iA_x + jA_y + kA_z$$

becomes

$$\nabla \cdot A = \text{div } A \quad (\text{XXXIX})$$

and the vector product according to (XXIX) is

$$\begin{aligned} \nabla \times A &= i\left(\frac{\partial A_z}{\partial y} - \frac{\partial A_y}{\partial z}\right) + j\left(\frac{\partial A_x}{\partial z} - \frac{\partial A_z}{\partial x}\right) + k\left(\frac{\partial A_y}{\partial x} - \frac{\partial A_x}{\partial y}\right) \\ &= iC_x + jC_y + kC_z = \text{curl } A \\ &= \begin{vmatrix} i & j & k \\ \frac{\partial}{\partial x} & \frac{\partial}{\partial y} & \frac{\partial}{\partial z} \\ A_x & A_y & A_z \end{vmatrix} \end{aligned} \quad (\text{XL})$$

Hence the curl¹ of a vector is again a vector and we find for the curl of a curl of a vector

$$\begin{aligned} \text{curl}^2 A &= i\left(\frac{\partial C_z}{\partial y} - \frac{\partial C_y}{\partial z}\right) + j\left(\frac{\partial C_x}{\partial z} - \frac{\partial C_z}{\partial x}\right) + k\left(\frac{\partial C_y}{\partial x} - \frac{\partial C_x}{\partial y}\right) \\ &= \begin{vmatrix} i & j & k \\ \frac{\partial}{\partial x} & \frac{\partial}{\partial y} & \frac{\partial}{\partial z} \\ C_x & C_y & C_z \end{vmatrix} \end{aligned} \quad (\text{XLI})$$

which for the values of the components C_x , C_y , and C_z gives

$$\text{curl}^2 A = \text{grad } (\text{div } A) - \nabla^2 A \quad (\text{XLII})$$

for

$$\nabla \cdot \nabla = \nabla^2$$

If τ is a portion of the space, S its surface, dS a surface element, η a unit vector (equal to 1 which goes outward perpendicularly from dS), and $d\vec{S} = \eta dS$ the vector of the surface element, then

$$\left. \begin{aligned} \text{grad } p &= \lim_{\tau \rightarrow 0} \frac{1}{\tau} \int_S p d\vec{S} \\ \text{div } A &= \lim_{\tau \rightarrow 0} \frac{1}{\tau} \int_S A \cdot d\vec{S} \\ \text{curl } A &= \lim_{\tau \rightarrow 0} \frac{1}{\tau} \int_S d\vec{S} \times A \end{aligned} \right\} \quad (\text{XLIII})$$

Here $\text{grad } p$ denotes a vector, whose component along any direction l represents the space derivative $\partial p / \partial l$ of the scalar quantity p along l . The quantity $\text{div } A$ is the

¹ Some writers use "rot" instead of "curl."

flux of vector \mathbf{A} which emanates from the infinitely small volume unity and therefore a measure for the \mathbf{A} lines of force which originate in each unit of volume. If \mathbf{A} denotes a force, then the component of curl along any direction expresses the mechanical work which is produced by \mathbf{A} when going once around an infinitely small unit of area perpendicular to the foregoing direction.

Other rules are

$$\left. \begin{aligned} \text{curl grad } p &= 0 \\ \text{div curl } \mathbf{A} &= 0 \\ \text{grad } \mathbf{A} \cdot \mathbf{B} &= (\mathbf{A} \text{ grad})\mathbf{B} + (\mathbf{B} \text{ grad})\mathbf{A} + \mathbf{A} \times \text{curl } \mathbf{B} + \mathbf{B} \times \text{curl } \mathbf{A} \\ \text{div } \mathbf{A} \times \mathbf{B} &= \mathbf{B} \cdot \text{curl } \mathbf{A} - \mathbf{A} \cdot \text{curl } \mathbf{B} \end{aligned} \right\} \quad (\text{XLIV})$$

$$\left. \begin{aligned} \text{curl } \mathbf{A} \times \mathbf{B} &= (\mathbf{A} \text{ grad})\mathbf{B} - (\mathbf{B} \text{ grad})\mathbf{A} + \mathbf{B} \cdot \text{div } \mathbf{A} - \mathbf{A} \cdot \text{div } \mathbf{B} \\ \text{div } \mathbf{A} \cdot \mathbf{p} &= \mathbf{A} \text{ grad } p + p \cdot \text{div } \mathbf{A} \\ \text{curl } \mathbf{A} \cdot \mathbf{p} &= -\mathbf{A} \times \text{grad } p + p \cdot \text{curl } \mathbf{A} \end{aligned} \right\} \quad (\text{XLV})$$

Moreover, we have the theorems

$$\left. \begin{aligned} \iint \mathbf{A} d\mathbf{S} &= \iiint \text{div } \mathbf{A} d\mathbf{t} \text{ (Gauss)} \\ \iint (\text{curl } \mathbf{A}) d\mathbf{S} &= \int \mathbf{A} \cdot d\mathbf{l} \text{ (Stokes)} \end{aligned} \right\} \quad (\text{XLVI})$$

INDEX

A

- A battery, 2, 65
- A-class amplifier, 194
- Abnormal ray, 400
- Abraham, M., on dipole, 473
 - on directive systems, 454
- Absolute temperature (Kelvin degrees), 3, 5-10, 48, 205-206, 279-281, 385
- Absorption, in atmosphere, 360, 362, 363
 - critical, 385, 394, 396, 560
 - in filter, 560
 - in ground, 333-335, 340, 352, 364-366
 - in ionized layer, 380, 385
 - in recurrent network, 560
 - selective, 385, 394, 396, 560
 - in tubes, 8-9
- Absorption factor of space waves, 360, 469
- Accelerated electron, 12, 18, 22, 23, 25, 33, 37, 38, 41, 272
- Accelerated ion, 271
- Accuracy, of frequency, 96-116, 118-125
 - of resonance curve, 104, 105, 108
- Acoustic currents, 56, 112-114, 124-125, 177-180, 183, 204, 220, 229-231
- Acoustic feedback, 122, 256
- Adcock aerial, 496, 498, 505, 508
- Adjustment effect on frequency, 96-116, 118-125
- Admittance, 407, 531
- Aerial, 418, 433, 454, 411
 - Adcock, 498
 - aperiodic, 459
 - artificial, 437
 - attenuation, 445
 - Beverage, 454
 - box, 482
 - capacitance, 437
 - constants, 437
 - coupling, 437, 591-594
 - current distribution, 414, 427, 437
 - directional properties, 454-530
 - directive, 454
 - Aerial, distinction between actual and effective height, 350
 - distinction between static and effective constants, 427, 437
 - distributions, 434
 - effective height, 350, 468
 - electric image, 350, 351, 357
 - energy relation, 432
 - feeder, 406, 409, 422, 442, 591-594
 - field close to it, 345, 358
 - field far from it, 345, 347, 358, 466
 - formulas, 437, 468ff.
 - frame (loop), 466
 - Franklin, 418, 523, 530
 - frequency (wave length), 422, 424
 - half wave length, 443
 - Hertz, 443, 591-594
 - horizontal, 416
 - inductance, 437
 - L type, 354, 356, 475
 - loading, 422, 443, 587-594
 - loop (frame), 466
 - compared with open aerial, 470, 477
 - matching, 409
 - open, effective height of, 350
 - operation on harmonics, 436
 - quarter wave length, 436
 - radiated power, 348, 349, 356, 357
 - radiation resistance, 354-357
 - reactance, 422
 - received current, 359
 - received field intensity, 359, 360
 - resistance, 437
 - space resonance curve, 450
 - surge impedance, 442
 - T type, 356
 - velocity of propagation, 449
 - vertical, 418
 - compared with loop aerial, 470, 477, 515
 - voltage distribution, 414, 427, 437
- Affinity of electron, 4, 6, 10-11
- Air pressure, in ionized regions of upper atmosphere, 383

- Airship guiding, 466-530**
Albersheim, W., on abrupt frequency changes in oscillators, 103
Alberti, E., and Leithauser, G., on trigger oscillator, 278
Alexanderson, E. F. W., on high-voltage transformer, 141
 on magnetic amplifier, 185
Alexanderson, E. F. W., and Fessenden R. A., alternator, 58, 59
 α quartz, 303
 α rays, 405
Alternating current, 56, 58-60, 159
Alternating-current constants 65-66, 187-189
Alternating-current network, 66, 73, 76, 84, 89, 90, 92, 119, 121, 122, 126, 207, 216, 222, 223, 226, 231, 233, 234, 236, 248, 252, 279
Alternator, 58-60
 inductor type, 58, 59
 reactor type, 59
Ammeter, for average value, 159-163, 167-168
 for direct current reading as a measure of effective current value, 166
 dynamometric, 159-163, 167-168
Ampère turns, 227
Ampère's law, 324, 328, 331
Amplification, action in telephone receiver, 282
 audio-frequency, 204, 206-232, 278-283
 class A, 194
 class B, 195
 class C, 195
 class D, 195
 definition, 185
 direct current, 206-207, 214
 without and with distortion, 192
 factor, 13-15, 187-202
 inverse, 94
 gain, 188, 190-191, 196, 198, 207, 210, 212, 216-218, 221, 224, 232-235, 239, 241-243, 245, 250, 253-254, 271-277
 in gaseous tubes, 271-277
 high frequency, 185-277
 magnetic, 185
 by negative resistance, 262-264
 power, 185, 191
 push-pull, 256
 regenerative, 239
 Amplification, superheterodyne, 255
 superregenerative, 246-248
 in telephone receiver, 282
 thermal, 278-282
 threshold, 45, 264-271
 trigger, 277
Amplifier, current, 185
 equivalent circuits, 66, 207, 216, 222, 223, 226, 231, 233, 234, 236, 248, 252, 279
 floating grid, 12
 interelectrode back-feed effect, 84-92, 203-205, 238-255
 loading, 192
 lumped-tube constants, 14, 200-202
 magnetic, 185
 neutralization, 250-252
 oscillation, 248
 power, 185, 191
 reactance coupled, 222-255, 258
 resistance capacitance coupled, 206-222
 resistance coupled, 203, 206-222
 space charge, 28
 stability, 246-256
 theory, 186-283
 transformer coupled, 222-235, 238-244, 247-258
 triode, 187
 tube noise, 255
 voltage, 185, 191
Amplitude, in amplifiers, 81, 192
 of crystal vibration, 311
 in detectors, 168, 177-180, 283
 of ionic oscillation, 386
 in oscillators, 81
 in telephone receivers, 282-283
 of voltage and current, 159-161, 163, 167, 183
Andrew, V. J., and Hoag, J. B., electro-magnetic echoes, 403
Angle, of ascent, 367, 390, 393
 Brewster, 366
 of incidence, 501-517
 limiting, for ionized layer, 393
 of phase (*see* Phase angle)
 of reflection, 501-517
 of refraction, 501-517
Anode, current, 2-3, 7, 12, 15, 25, 27-29, 32, 35, 66
 loss, 8-9
 rectification, 177-180

- Anode, resistance, 14, 66, 199
 split, 27, 138-139
 voltage, 2, 4, 6-8, 65, 193, 201, 208, 270
- Antenna, and loop (frame) compared, 470, 477, 515
 matching, 409, 591-594
 (*see also* Aerial)
- Aperiodic aerial, B eliminator, 454, 462
 input in B-eliminator circuits, 171
- Apparent constants, for line and aerials, 407
- Appleton, E. V., on automatic synchronization, 111
 on wave propagation, 368
- Appleton, E. V., and Barnett, M. A. F.,
 on wave propagation, 499, 510
- Appleton, E. V., and Ratcliffe, J. A., on
 nature of wireless signal variation, 510
- Arc, compared with spark, 45
 oscillations, 48, 58, 127
 rectifier, 1, 172, 176
- Ardenne, M. von, on resistance-coupled
 amplifier, 193, 215
- Argon gas, 42, 177, 267
- Armstrong, E. H., on superregeneration, 246
- Artificial aerial, 437
 (*see also* Equivalent aerial)
- Atmosphere, absorption, 360-363
 constituents, 383
 pressure, 383
 temperature, 383
- Atomic mean free path, 384
- Atoms, 42-49, 176-177, 180-182, 264-277
- Attenuation, along aerials and lines, 408, 456
 box, 531-538
 constant, 360, 407, 531-548, 574
 effective, 548
 factor, 445, 543
 in ground, 334, 352, 360, 363-366
 in ionized layer, 381, 385, 396
 loss, 335, 352, 360
 in low-pass filter, 537, 546
 in recurrent network, 531-548, 574
 region of, in filter, 546, 548, 574
 in space wave, due to losses, 352, 360, 363
 due to wave spread, 347
- Audio amplifier, 204, 206-232, 278-283
- Austin, L. W., barrage circuit, 514
 on damped wave-buzzer oscillator, 58
 on recording of field intensity, 510
- Austin, L. W., and Cohen, L., on transmission formula, 361, 365
- Austin, O., and Starke, H., on secondary electrons, 25
- Autodyne receiver, 277
- Autoheterodyne, 277
- Automatic synchronization, 111-116
- Autotransformer, 234*ff.*
- B**
- B battery, 3, 65
- B-class amplifier, 195
- B eliminator, 170-171, 182-184
- B-pack corrector, 170-171
- Back coupling (*see* Back feed)
- Back feed, 60, 61, 75, 76, 82-84, 89
- Back-feed factor, 82-84
- Back-feed phase, 75, 83
- Bailey, A., Dean, S. W., and Wintringham, W. T., on electric vector tilt for long waves, 353
- Baker, W. G., and Rice, C. W., on ionized layer, 368, 383
- Balance, of amplitude, 75
 of energy, 62-63, 72, 75
 of phase, 75
- Balanced amplifier, 256
- Balanced electron pressure, 3, 7
- Balanced network, 256
- Balancing current, 175, 257-258
- Balancing protective resistance, 269, 271
- Baldus, R., and Buchwald, E., on direction effects of airplane aerials, 490
- Ballantine, S., on directive aerials, 517, 530
 on internal back feed in amplifiers, 84
 on Lorentz theorem, 462, 463, 464
 on radiation resistance, 354, 356
- Baltruschat, M., and Starke, H., on secondary electrons, 25
- Band, frequency, 549, 551, 564, 565
 pass filter, 549, 551, 564, 565, 572
 suppress filter, 549, 565
- Barfield, R. H., on wave propagation, 363
- Barfield, R. H., and Munro, G. H., on energy absorption for electromagnetic waves, 366

- Barfield, R. H., and Smith Rose, R. L.,
on wave propagation, 363, 364, 499
- Barkhausen, H., and Kurz, K., on
oscillator, 18, 21, 35, 56-58, 63, 132,
134-137
- Barnett, M., A. F., and Appleton, E. V.,
on wave propagation, 499, 510
- Bartels, H., on optimum output and
distortion in output amplifiers, 193
- Battery, A, B, and C, 65
- Beam, electron, 146, 157
transmission, 347, 361, 496, 521,
525-527
wave spread, 347
- Bearing error, 478, 482, 490-517
- Beat frequency, 111-116, 170, 179, 255,
258, 283
heterodyne, 111-116, 170, 179, 255,
258, 283
- Beauvais, G., on short-wave oscillators,
132
- Bedeau, M. F., on piezo-electric phe-
nomena, 284
- Bell, bel (decibel), 537-538
- Bellini, E., on goniometers, 480
- Bellini, E., and Tosi, A., on goniometer,
492, 493
- Bending of electromagnetic waves, 342,
380, 389
- Ber and bei functions, 337
- Berkner, L. V., and Wells, H. W., on
ionized layer, 368, 370
- Bessel functions, 337, 420, 606
- β quartz, 303
- β rays, 405
- Bethenod, J., on frequency constancy of
tube oscillators, 94
- Beverage, H. H., Rice, C. W., and Kellog,
G. W., on ionized layer, 454
- Beverage antenna, 454, 462
- Bias, 12
- Bijl, H. J. Van der, tube equation, 63
- Biphase rectification (full wave), 109,
163, 174, 176, 183
- Birkland, Villard, and Stoermer, on
electromagnetic echoes, 369
- Black, K. C., on piezo crystals, 119
- Blattermann, A. S., on internal back
feed in amplifiers, 84
- Bley, H., and Seibt, G., on glow tubes,
272
- Bligh, N. R., on amplification, 237
- Blodgett, K. B., and Langmuir, I., on
tube actions, 265, 268
- Blondel, Guillaume, and Poincaré, on
ionized layer, 367
- Blue glow, 1, 42-45, 47, 270, 272
- Boltzmann constant, 5-7, 22-23, 279
- Boltzmann-Stefan law, 9
- Bombardment, ionic, 1, 42-49, 176-177,
180-182, 264-277
- Bontsch-Bruewitsch, M. A., on radiation
resistance, 354
- Bouthillon, M. L., on directive systems,
454
on surface waves, 365
- Bower, W. E., and Wheeler, L. P., on
piezo oscillator with acoustic back
feed, 122
- Bowman, J. L., on tube oscillator with
rectangular wave form, 128
- Box aerial, 482
- Brain, B. C., on output characteristics
of amplifiers, 193
- Braun, F., on cathode-ray tube, 1, 146,
157
on first loop aerial, 454
- Breakdown voltage, 42, 48, 270
- Breisig, F., on penetration of electro-
magnetic waves into ground, 353
- Breit, G., and Tuve, M. A., on ionized
layer, 368
- Brewster angle, 366
- Bridge, circuits, 144, 159, 174, 183,
257-258
- Brillouin, M. L., on radiation resistance,
354
- Brown, W. J., on amplifier loading, 192
- Buchwald, E., and Baldus, R., on direc-
tion effects of airplane aeriels, 490
- Building up of oscillations, 62
in wave aeriels, 457
- Bureau of Standards, 84, 118, 120, 233,
277, 286, 292, 298, 304, 313, 318,
368, 370, 402, 413, 414, 449, 454,
480, 493, 495, 510
- Burstyn, W., on direction effects of
airplane aeriels, 490
on directive systems, 454
- Busch, H., on directive systems, 454
- Bush, V., and Smith, C. G., on glow-tube
rectifiers, 32, 181, 182

- Butterworth, S., on equivalent circuit, 307
 Buzzer, 58
 By-pass condenser, 60, 62
- C**
- C battery, 12, 65
 C bias, 12 *ff.*
 C-class amplifier, 195
 Cable, concentric, 443, 591-594
 Cady, W. G., on piezo resonator, 118, 284, 290, 302, 307, 308, 310
 Caesium photo-cell, 51
 Calibration, for attenuation box, 533
 for Barkhausen-Kurz and Hollmann oscillations, 136
 of direct-current amplifier, 207-208
 for piezo crystals, from dimensions, 297-318
 for small high-frequency currents by means of direct current, 166
 Campbell, G. A., on filters, 531
 Canal rays, 271
 Candle power, 50
 Capacitance, aerial, 437
 of concentric cable, 443
 coupling, 61, 84, 207-209, 211, 233
 double line, 456
 equivalent across grid, 90, 203, 222
 filament-grid gap, 84, 90, 203, 222
 grid, 84
 grid filament, 84, 203, 222
 grid plate, 84, 203, 210, 222
 interelectrode, 84, 91, 203, 222
 ionic oscillations, 18, 21-24
 of Lecher-wire system, 413
 line, 456
 of parallel wires, 413, 443
 piezo-electric, 119, 121-122
 plate filament, 84, 203, 210, 222
 reactance, 424
 single wire, 456
 specific inductive, 363, 377
 tube, 84, 203, 210, 222
 Capacitive coupling, for amplifier, 84, 207-209, 211, 233
 for detector, 178
 for oscillator, 61
 Carborundum detector, 172-173
 Carrier, frequency, 406
 wave, 406
- Carson, J. R., on balanced tube circuits, 257
 on triode theory, 187
 Carson, J. R., and Zobel, O. J., on filters, 531
 Carson theorem, 462-464
 Cascade amplifier, 208, 209, 211, 216, 222, 223, 233, 235-236
 Cathode, amplifier, 278-282
 cold, 171-174, 180-182
 dark space, 43
 disintegration, 176
 drop, 43
 for gaseous tubes, 43
 glow, 43
 hot, 1-8 *ff.*
 indirectly heated, 29
 materials, 11
 mercury pool, 176
 oscillator, 278
 thermal, 278-282
 Cathode-ray tube, 1, 146, 157
 Cathode rays, 405
 Cauer, W., on a generalized method of designing filters, 531
 Cell, caesium, 51
 Karolus, 54
 Kerr, 54
 photoelectric, 1, 49
 potassium hydride, 51
 Chaffee, E. L., on Chaffee gap, 58
 Changer, current, 141, 159
 frequency, 150
 phase, 143
 voltage, 141
 Chapman, S., and Milne, E. A., on condition of upper atmosphere, 383
 Char, S. T., Mohammed, Aijar, and Verman, L. C., on ionized layer, 403
 Characteristic, for air gap and pressure effect, 305
 for α and β quartz, 303
 for amplification factor, 190
 for amplifier, 77, 190, 192, 194, 197, 200-201, 207, 279
 for antenna, 474
 for antenna and line constants, 437
 for attenuation box, 536
 for B eliminator, 183
 for band-pass filter, 549
 for band-suppress filter, 549
 for Barkhausen-Kurz oscillations, 136

- Characteristic, for beat production, 179
 for crystal detector, 159, 168, 173
 for cuprox, 174
 for current distribution, 336
 demodulation, 177
 dynamic tube, 64, 68, 70, 72, 113, 188, 190, 194, 197, 200
 dynatron, 25
 for elasticity of quartz crystal, 291
 for electron tubes, 3, 7, 12, 15, 25, 27, 29, 33, 35, 36, 40, 64, 67, 68, 70, 72, 76, 77, 79, 81, 82, 104, 105, 108, 110, 111, 114, 124, 127, 136, 138, 154, 157, 168, 177, 178, 180, 183, 190, 192, 194, 197, 199-201, 207, 240, 241, 257, 261
 for filter, 531-591
 for frequency changer, 150-158
 for glow tube, 43, 269
 for glow-tube amplifiers, 271-277
 for glow-tube rectifier, 180
 for grid rectification, 178
 for grid voltage-plate current, 12, 15 *ff.*
 for high-pass filter, 547, 549
 for Hollmann and Barkhausen-Kurz oscillator, 136
 for hyperbolic functions, 535
 impedance (surge), 408, 442, 443, 544
 of line, 407, 442, 443
 of recurrent network, 544
 for loaded amplifier, 192, 194, 197, 200-201, 207
 for low-pass filter, 546, 547, 549
 lumped, 14, 200
 for magnetic amplifier, 186
 for magnetic effects on electrons and ions, 33-36, 40
 magnetostriction, 124
 magnetron, 15, 36, 138
 for modulus of elasticity, 291
 mutual conductance, 190
 negative, 15
 negatron, 27
 oscillation, 81-83
 for oscillator, 64, 77, 104-111, 113-114
 for photoelectric cell, 49-51
 for piezo oscillations, 314, 319-320
 plate rectification, 177
 plate resistance, 190
 for plate voltage-plate current, 7, 67
 for potential distribution, in electron tubes, 328
- Characteristic, for potential distribution, in ion tubes, 326
 for push-pull amplifier, 257
 reactance, 248
 for rectifier, 159, 161, 163, 168, 173-174, 177-180, 183
 for recurrent network, 147, 183, 531
 for static tube, 3, 7, 12, 15, 25, 27, 29, 36, 49, 67, 127
 for thermal amplifier, 279
 for thyatron, compared with that for high-vacuum tube, 264
 for transmission in filters, 546, 547, 549
 for trigger oscillator, 277
 for triple-grid tube, 261
 tungar, 127
- Charge, electronic, 3, 16 *ff.*
 ionic, 16-24, 42-45
 space, 3, 5, 12, 13, 27, 43, 286, 318, 320, 324
 surface, 285, 314, 318
- Child, C. D., on space-charge equation, 5, 6, 16
- Chireix, H., on directive systems, 454, 517, 521
- Choke coil, for short waves, 130
- Cioffi, P. P., and McKeehan, L. W., on magnetostriction, 119
- Circuit, aperiodic, 171, 454, 462
 attenuation, 71 *ff.*, 334, 407, 533, 546 *ff.*
 closed, and its radiation effect, 346
 coupled, for recurrent networks, 572
 derived, 582
 elementary, 582
 equivalent (*see* Equivalent networks)
 open, 406
 parallel resonance, 69
 phase angle, 69, 70, 75, 80, 82, 83, 89, 96, 99, 114 *ff.*
 reactance, 71, 75, 84, 88, 89, 120, 418, 421 *ff.*
 recurrent, 147, 183, 531
- Circular field, 143, 144, 146, 157, 395
- Circular and hyperbolic functions, 416, 602
- Circular piezo disks, 119, 299
- Circular polarization, 395
- Class A amplifier, 194
- Class B amplifier, 195
- Class C amplifier, 195
- Class D amplifier, 195
- Clausius-Clapeyron relation for rate of evaporation, 5

- Clavier, A., and Podliasky, I., on distortionless amplification, 193
- Closed circuit, radiation, 346
- Coates, W. M., and Lawrence, E. O., on X-rays by impact of positive ions, 24
- Cobbold, G. W. N., and Underdown, A. E., on piezo-electric appliances, 118
- Coblentz, W. W., on light effects on molybdenum, 57
- Coefficient, of coupling, 104, 224-226
of reflection, 502-510
- Cohen, L., on aerial constants, 423
on filters, 531
- Cohen, L., and Austin, L. W., on transmission formula, 361, 365
- Coil, aerial, 466
with iron core, 227
line, 147
loading of aerial, 422-439
tilting, 509
- Cold cathode, 42-55, 172-174, 180, 264-277
- Colebrook, F. M., on amplification, 215
- Colley, A., on short-wave ions generation, 57
- Collision frequency, of ions, 384
- Colpitts, E. H., on oscillator, 61, 129, 130
- Compass, radio, 466-530
- Complex amplification factor, 66
- Complex dielectric constant, 16, 352, 377
- Complex plate current, 66
- Complex plate resistance, 66
- Complex refraction in ground, 352
- Composite filter, 581
- Compton, A. H., on Compton effect, 52
- Compton, K. T., on arc discharge, 48
- Concentration, electronic, 16, 21, 370, 382, 391, 396
ionic, 16, 21, 370, 382, 391, 396, 401
- Concentric line, 406, 443, 491-494
- Condenser, fictitious, ionic, 375
for ionic-tube oscillations, 21, 134
grid, 84-92, 203-205, 238-255
grid filament, 84-92, 203-205, 238-255
grid plate, 84-92, 203-205, 238-255
loading, 422
plate, 84-92, 203-205, 238-255
plate filament, 84-92, 203-205, 238-255
and resistance, time constant, 213-214
- Conductance, mutual, 12-15, 68, 70-72, 74, 81-82, 94, 113, 188, 190, 218
- Conductance, plate, 12-15, 30, 63, 188, 190
- Conductivity, due to ions, 331
- Conductor, aerial feed, 406, 443, 491-494
capacitance, 406
concentric cable, 406, 443, 491-494
high-frequency resistance, 335-338, 414
inductance, 406
natural frequency, 406
parallel wire (Lecher), 406
radiation effect, 345
- Constancy of frequency, 96, 103, 118, 119, 124, 284, 297-305, 313-318
- Constant, attenuation, 407
oscillation, 104
time, 579, 589
- Continuous electromagnetic waves, 56-58
- Control, of amplifier glow tube, 271
electrode, 271
of grid-glow tube, 268
- Coolidge, W. D., on X-ray tube, 2
- Copper—copper oxide rectifier (cuprox), 174
- Corona, 42, 45, 48
- Cosmic rays, 369
- Coupled circuits, 58, 61, 62, 63, 75, 76, 92, 96, 98, 99, 104, 123, 124, 129, 143-145, 148, 206, 208, 209, 211, 216, 222, 226, 235
- Coupling, coefficient (*see* Coefficient, of coupling)
condenser, 178, 206, 208, 209, 211, 216, 222
degree of, 223, 427, 574, 577, 579, 588
electronic, 103
frequency, of quartz elements, 299
for tube oscillations, 104
tapped, 61, 62, 91, 120, 122, 123, 128, 129, 131
transformer, 226
- Crookes (Hittorf) dark space, 43
- Crossley, A., on piezo oscillator, 118
- Crystal, contact rectifier, 172
piezo-electric, 119, 284-323
quartz, 119, 284-323
- Cunningham tube, 189
- Cuprox rectifier, 174
- Curie Brothers, on piezo electricity, 19, 284-288, 290-305, 315, 320
- Curie-cut crystal, 119, 284, 287, 291, 292, 294, 297-301

- Curie and Lippman, M. G., on piezo electricity, 286, 297
 Curie-Lippman law, 297
 Current, amplification, 185, 190, 198
 average, 159-170
 changer, 141, 159
 displacement, 329
 effective, 159-168
 electronic, 1 *ff.*
 and ionic, 16-24, 42-48, 127, 132-140, 176-177, 180, 264-277
 emission, 1 *ff.*
 grid, 15, 25, 28, 29, 32 *ff.*
 impulse registration with a single tube, 258
 impulses for frequency multiplication, 153-157
 inversion, 159, 170
 ionic contribution, 16, 330-332
 plate, 2-8, 12, 14, 63, 65 *ff.*
 complex, 66
 received, 359, 456, 469
 rectification, 159
 resonance, 69, 108
 saturation, 5 *ff.*
 transmitted, 469
 Curvature, of characteristics, 169
 of earth, 360, 364, 391, 484
 of ionized ray, 389, 399
 for potential distribution, of electron tubes, 326
 of ionic tubes, 326
 Cutoff frequency, 548-573
 Cutting, F., on radiation resistance, 354
 Cycloid electron path, 36
 Cylindrical electromagnetic waves, 361
- D**
- D-class amplifier, 195
 Damped-wave train, 56, 58
 Damping, degree of, 71
 as factor, 71, 74, 100, 102, 103, 110, 115, 116, 407, 422, 445, 447, 469
 for piezo crystal, 308, 313
 of filter, 543
 Darrow, K. K., on modern physics, 52
 David, P., on filters, 531
 David, P., and Mesny, R., push-pull oscillator, 132
 Davison C. J., and Germer, L. H., wave-like nature of electrons, 52, 53
 Day transmission, 372, 402, 403, 510
 Dead zones, 362, 367, 371
 Dean, S. W., Wintringham, W. T., and Bailey, A., on tilt of electric vector for long waves, 353
 Debye, P., on electrons, 4
 De Broglie, Louis, on De Broglie waves, 52, 53
 Decelerated, electrons, 12, 18
 Decelerated, ion, 271
 Decibel, 537, 545, 579
 Decrement, logarithmic, 100, 102, 103, 313, 433
 for lines and aerials, 433
 for piezo crystal, 313
 Deflection of cathode ray, 143, 146, 157
 De Forest, Lee, on grid in vacuum tube, 2, 12, 42
 Degree, of aerial coupling, 427
 of bending, 380, 389
 of coupling, 223, 427, 574, 577, 579, 588
 of vacuum in glow tubes, 42, 43, 176, 177, 180, 181, 267, 268, 272
 of vacuum for regions of the ionized layer of the upper atmosphere, 383
 Dellinger, J. H., on radiation of loop aerial, 454
 Dellinger, J. H., and Pratt, H., on guiding by electromagnetic waves, 495
 Δ connection, 531
 (See also π section)
 Demodulation, 168, 172, 177
 Density, electronic, 16, 21, 330, 375, 380, 384, 387
 of quartz, 298
 Depth penetration of electromagnetic waves, 333
 Derived filter, 582
 Descending electromagnetic wave, 352, 353, 362, 366-388, 390, 401, 484, 499, 501-517
 Design, of amplifier, 206-238
 Detection, anode, 177-178
 grid, 178
 Detector, 168, 172, 177
 Detuning, 96-116
 Deviation from direction of wave propagation, 479, 482, 491, 492
 Diamond, H., on directive system, 454
 Diamond, H., and Stowell, E. Z., effect of mutual capacitance in amplifiers, 233

- Dielectric, of ground, 363
- Dielectric, of ionized layer, 330
- Dielectric absorption constant, 363, 377
- Diode, electron tube, 2, 7, 33-42, 49, 138-140, 154-155, 157, 159, 161, 174, 175, 177, 183
 - ion tube, 23, 42, 49, 154-155, 180
- Dipole, 418, 443, 487, 499, 591, 593
- Direct current, from alternating current, 159
 - amplifier, 206
 - inversion, 159, 170
 - smoothing out, 160, 163, 183
- Direct electromagnetic wave, 362, 367, 370, 499
- Direction factor, 460
- Direction finder, 454
- Directional aeriads, 454
- Directional characteristics, 454
- Discharge tubes (glow), 21-24, 42-45, 176, 180, 264-277
- Discrete wave trains, 56, 58
- Dispersion in ionized layer, 382
- Displacement current, 329
- Dissipation, in ground, 364-366
 - in ionized layer, 380
 - in recurrent network, 543, 548, 553, 555, 574, 579
- Distance effect of electromagnetic wave, 344, 345, 347 *ff.*
- Distinction between stationary and moving electromagnetic waves with respect to phase difference between electric and magnetic vector, 466
- Distortion, amplifier, 191-200
 - of modulated waves, due to ionized layer of atmosphere, 382
- Distributed constants, line and aeriads, 407-453
 - recurrent networks, 531-594
- Distribution, capacitance, 407-453
 - of current, 407-453
 - inductance, 407-453
 - of potential, 407-453
 - resistance, 407-453
 - of voltage, 407-453
- Distribution law (Maxwell), 3, 7
- Dornig, W., on magnetic frequency multiplier, 153
- Double dipole, 487
- Double frequency, 150-158
- Double grid, 28-32, 123, 128, 251, 259
- Double layer, 370, 390
- Double line, capacitance, 407, 413, 443
 - concentric cable, 443, 591-594
 - inductance, 407, 413, 443
 - Lecher, 407, 413
 - surge impedance, 442, 443
 - transposed line, 442
- Double loop, 497
- Double plate, 26, 127, 138-139, 174
- Doubler, frequency, 150-158
- Dow, J. B., on oscillator, 94, 96, 103
- Downcoming sky wave, 361-363, 366, 367, 370, 390, 401, 470, 496, 499, 501-517
- Drawing effect in oscillations, 103-116
- Dreyer, J. F., on neutralization, 250
- Driving point, current, 409, 541-544
 - impedance, 409, 541-544
 - voltage, 409, 541-544
- Drude, P., on short waves, 57
- Dull, emitter, 4
- Dunmore, F. W., and Engel, F. H., on guiding by electromagnetic waves, 495
- Dunmore, F. W., and Kolster, F. A., on balancing condensers in loops, 480
- Dunoyer, L., and Toulon, P., on gaseous tubes, 264
- Duration of electron flight, 17, 32-42, 66, 132-140
- Dushman, S., on modified Richardson equation, 5
- Dushman, S., and von Raschevsky, on modified Richardson equation, 5, 9
- Dushman, S., Rowe, H. N., Ewald, J., and Kidner, C. A., on tube equation, 5
- Dye, D. W., on piezo resonator, 118, 307
- Dynamic characteristics, 64, 68, 70, 72, 113, 188, 190, 194, 197, 200
- Dynamic line constants, 406-453
- Dynamic permeability, 227
- Dynamic quartz vibration, compared with static linear change, 313
- Dynamic tube constants, 7, 14-15, 31, 65-70
- Dynamometric current indicator, 159-163, 167-168
- Dynatron, 25, 125

E

- Earth, curvature, 360, 364, 391, 484
 echoes, 403
 magnetic field, 394-400
 and wave propagation, 330, 394-400
 radius, 367
- Eccles, W. H., on ionized layer, 368, 369
 on tube analysis, 14
 on tube oscillators, 94
- Eccles, W. H., and Jordan, F. W.,
 originators of push-pull oscillators,
 57, 132
- Eccles, W. H., and Larmor, J., on ionized
 layer, 395
- Echo effect for electromagnetic wave,
 403
- Eckart, C., on modern physics, 52
- Eckersley, T. L., on double loop, 497
 on ionized layer, 402
- Eckhardt, E. A., and Karcher, J. C., on
 trigger oscillator, 277
- Edgeworth, J., on oscillators, 94, 96
- Edison effect, 2
- Effect, of ground on loop aerial, 470
 Lippman, 285, 286
- Effective current, 159-168
- Effective length, 350, 416-419, 427, 429
- Efficiency, for inversion, 170, 171
 for rectification, 162-166, 168, 171
 in tubes, 8-9, 162
- Eichhorn, G., buzzer exciter, 58
- Electric field, in cathode-ray tube, 143,
 146, 157
 close to a station, 345, 348, 349, 358
 of descending electromagnetic waves,
 366, 401, 470, 496, 499-517
 at a distance, 345, 347, 348, 483 *ff.*
 of electromagnetic waves, 345, 347,
 348 *ff.*
 at great distance, 342, 347-351, 359,
 360
 in ionized layer, 16, 331
 and magnetic action in ionized layer,
 17, 331
 in magnetron, 32-42, 138-139
 near surface of earth, 401
 relation to magnetic field, 342
 in tubes, 1-8, 12-43, 48, 49, 326
- Electrical length of line, 407, 416, 424,
 426, 427, 429
- Electrode, cold, 42-55, 172-174, 180,
 264-277
 hot, 1 *ff.*
- Electromagnetic field, close to aerial,
 345, 348, 349, 358
 at distance, 344, 345, 347-359
 energy in, 348, 349, 357, 365, 366, 473
 and loop, 466
 theory of, 324
- Electromotive force, induced in open
 aerial, 465
 in loop aerial, 467
- Electron, accelerated, 12, 18, 22, 23, 25,
 33, 37, 38, 41, 272, 370
 affected by magnetic and electric field,
 17, 32-42, 138-139, 331, 394-400
 affinity, 4, 6, 10-11
 beam, 146, 157
 cathode-ray tube, 1, 146, 157
 charge, 3, 16 *ff.*
 concentration, 16, 21, 384
 decelerated, 12, 18
 deflection by electric field, 143, 146, 157
 emission, 1 *ff.*
 lag, 18-24, 33-45, 66, 132-139
 mass, 3, 16 *ff.*
 mean free path, 384
 motion, 12, 16-24, 32-42, 132-139, 146,
 157, 330-332, 373-400
 oscillation, 16-24, 32-42, 132-139, 330-
 332, 373-400
 saturation, 1-8, 10, 15, 25, 27
 secondary, 24-26, 125, 261, 262
 total emission, 1-8, 10, 15, 25, 27
 velocity, 2, 7, 12, 16-26, 32 *ff.*
- Electron tubes, 2, 12, 20, 25, 27, 28, 32,
 34, 35, 43 *ff.*
 potential distribution, 326
- Electrostriction, 118-123, 284-323
- Elementary direction characteristic, 527
- Elementary electronic charge, 3, 16 *ff.*
- Elementary electronic mass, 3, 16 *ff.*
- Elementary section of recurrent network,
 531-533, 546, 547, 549, 551, 555, 562,
 564, 565, 567, 568, 570, 572, 582,
 584-586
- Elias, G., on ionized layer, 368
- Eller, K. B., on frequency constancy of
 oscillators, 94, 96
- Elliptical polarization, 395, 401
- Elster and Geitel, photoelectric effects, 49

- Emission, ability, 10
 - electron, 1 *ff.*
 - formulas, 5-8, 10, 14-16, 26, 30, 46
 - Energy, absorption in ground, 364-366
 - equation for line and aerial, 432
 - flux for radiation, 348, 349, 366, 473
 - level, 537-538
 - Engel, F. H., and Dunmore, F. W., on guiding by means of electromagnetic waves, 495
 - Epstein, P. S., on frequency multiplication, 151
 - on space-charge equation, 6
 - Equality of radiation and non-radiation fields, 358, 481
 - Equation of motion for ionized medium, 374
 - Equivalent aerial, 437
 - Equivalent constants, 427
 - Equivalent H sections, 555
 - Equivalent networks, 66, 73, 76, 84, 90, 92, 203, 207, 209, 222, 223, 226, 231, 233, 234, 236, 248, 252
 - Equivalent π section, 531, 533, 555
 - Equivalent resistance-coupled amplifier, 222
 - Equivalent space charge, 286, 319
 - Equivalent T section, 532, 555
 - Equivalent transformer-coupled amplifier, 222-334
 - Equivalent tube circuit, 66, 207, 231, 234
 - Error, bearing, 478, 482, 490-517
 - frequency, 94, 96, 103, 118
 - Esau, A., on loop aerials, 454
 - on short waves, 56, 131, 362
 - Euler, solution for spherical wave motion, 348
 - Ewald, J., on space-charge equation, 5
 - Exponentials, 535, 602
 - Extraordinary electromagnetic ray, 400
- F
- Factor, absorption, 360, 469
 - amplification, 13-15, 187-202
 - attenuation, 445
 - back feed, 81-84
 - direction, 460
 - form, 160, 468
 - peak, 160
 - reflection, 444, 502-510
 - for space absorption, 360
 - Fading, 399, 401, 402, 505, 514
 - Faraday, dark space, 43, 44
 - Faraday-Maxwell, induction law, 336
 - Faraday's law, 324, 332
 - Feedback, 60, 84, 250
 - factor, 81-84
 - in generators, 60-63, 70-84, 91-93, 98, 99, 104, 119-124, 238-255
 - within tubes, 84-91, 250-255
 - Feeder for aerials, 406, 409, 442, 443, 591-594
 - Feige, A., on magnetic modulator, 185
 - Feldman, C. B., and Sterba, E. J., on line feeders, 406, 591
 - Fessenden, R. A., on electrolytic detector, 172
 - Fessenden, R. A., and Alexanderson, L. F. W., alternator, 58-59
 - Field, electric, 16, 17, 331, 347-351, 358, 401
 - and magnetic, on ion, 16-24, 32-42, 331, 394-400
 - electromagnetic, 324
 - equality of induction and radiation field, 358, 481
 - equation, for glow tube, 23, 326, 330
 - for ionized medium, 330
 - for tube oscillations, 16-24, 132-137
 - induction, 345, 358, 481
 - intensity, 324, 328, 331, 332, 345, 347 *ff.*
 - magnetic, 325, 328, 331 *ff.*
 - radiation, 341, 345, 358, 481
 - revolving, circular, 143, 144, 146, 157, 398-401
 - elliptical, 395, 401
 - Filament, current amplifier, 278
 - current frequency doubler, 157
 - current oscillator, 278
 - emission, 1 *ff.*
 - magnetron effect, 40
 - magnetron effect applied, 138-139, 156-157
 - material, 11
 - power loss, 9
 - unequal current flow, 2-3
 - Filter, attenuation region, 545, 546, 548
 - band pass, 549
 - band suppress, 549
 - brute force, 183
 - characteristic, 546, 547, 549 *ff.*
 - equations, 539, 544, 548, 557

- Filter, characteristic, impedance, 538 *ff.*
 circuits, 540-586
 composite, 581
 coupled circuit, 572-579
 cutoff frequencies, 548, 549, 551, 562, 565, 567, 573 *ff.*
 damping (effective), 543
 damping region, 543, 546, 548
 derived section, 581-586
 design, 531-590
 elementary section, 531-533, 546-548, 551, 555, 562, 565, 567, 572, 577, 582
 H type, 555, 562
 half section, 582, 585
 high pass, 546, 547, 549
 hyperbolic relations, 416, 535
 compared with circular relations, 416
 impedance, 543
 input, 540-544
 with input choke, 184
 with input condenser, 184
 loss, 543, 555, 579
 low pass, 543, 546, 549-555
 M derived, 581-585
 matching, 543, 579, 581, 587, 590
 output, 540-544
 over-all characteristics, 543, 557, 576
 pass region, 545
 π type, 531, 538, 555, 562
 for rectified current, 183
 single-suppressed frequency, 560
 surge impedance, 538 *ff.*
 T type, 532, 538, 555, 562
 termination, 540-544
 "under" matched, 543
 use in amplifiers, 590
 Zobel composite filter, 555, 581
 Five-electrode tubes, 32, 260
 Fleming, J. A., on antenna arrays, 517
 on directive systems, 454
 Fleming valve, 2
 Flewelling circuit, 246, 247
 Flight of time for electrons, 2, 18-24, 33-45, 66, 132-139
 Forced amplification in oscillators, 111-116
 Form factor, for alternating current, 160
 for loop aerial, 468
 Formation of current and voltage distributions, 414-422
 Forstmann, A., and Schramm, E., on amplification, 193
 Foster, R. M., on directive systems, 454
 Four-electrode tubes, 27-29, 123, 127, 128, 251, 271-277
 Four-plate mounting of piezo crystal, 314, 315
 Frame aerial, effective height, 470
 and open antenna, effects compared, 470, 477, 515
 inductance, 471
 shape and radiation, 470, 489
 tuning, 471
 width, effect of, 482
 Franklin aerial, 415, 418, 454, 523, 530
 Frequency, alternator, 58
 beat, 111-116, 170, 179, 255, 258, 283
 changer, 150
 collision, of ions, 384
 constancy, 96, 103, 118, 119, 124, 284, 297-305, 313-318
 cutoff, 548-573
 doubler, 150-158
 electronic oscillations, 16, 17, 20-23, 36, 39, 132-139, 331, 373-400
 fundamental of line, 415-418, 427, 429, 437
 harmonic, 64, 77, 116
 higher modes on lines and aerials, 415-426
 ionic oscillations, 20-24, 331, 373-400
 jumps in oscillators, 103
 limiting, 57, 255
 M-fold, 150, 153-155
 for magnetostriction oscillator, 124
 for magnetron, 36, 39, 156
 mid-frequency in filters, 564, 571
 multiplier, 150
 natural, of aerials and lines, 415-420, 423-427
 for ionized layer, 17
 of piezo-electric elements, 119, 298-299, 301-302, 305, 308, 315, 317-318
 oscillator, 71, 73, 74, 90-93, 95-116
 regeneration, 18, 136
 resonance, 96-118
 six-fold, 153
 spectrum, 56
 tripler, 150-157
 wave-length relation, 19, 412, 419 *ff.*
 Fresnel law, 499

- Friis, H. T., on double loop, 497
 Fromy, E., on stability of tube oscillators, 96
 Fry, T. C., on limited use of tubes, 255
 Functions, Bessel, 337, 420, 606
 exponential, 535, 602
 hyperbolic, 535, 600
 in relation to circular, 416, 602
- G
- Gain amplifier, 188, 190-191, 196, 198, 207, 210, 212, 216-218, 221, 224, 232-235, 239, 241-243, 245, 250, 253-254, 271-277
 Galena rectifier, 172
 Gans, F., on refraction law applied to ionized layer, 390
 Gas, argon, 42, 177, 267
 for ionization, 42-45, 175-176, 180-182, 264-277
 for low cathode drop, 42
 neon, 42, 272
 nitrogen, 272
 phototubes, 49
 Gaseous conduction, 42-45, 175-176, 180-182, 264-277
 Gauss theorem, 324, 325
 Gaussian units, 329, 331, 332, 344, 351, 464
 Geiger, P. H., and Grondahl, L. O., on cuprox rectifier, 174
 Geiger, P. H., and Scheel, K., on arc discharge, 48
 Geissler tube, 42
 Geitel and Elster, photoelectricity, 49
 General Electric Research Laboratory, 2, 3, 5, 6, 9, 11, 17, 21, 25, 28, 40, 48, 59, 63, 125, 138, 141, 171, 175, 177, 186, 193, 252, 255, 263, 264, 326, 368, 454
 Generalized angular velocity, 70, 74, 93, 95, 98, 102, 106, 308, 309, 407
 Generalized electrical length of line and aerial, 441
 Generalized impedance, 106 *f*.
 Generalized reactance, 106 *f*.
 Generator, alternator, 58-60
 tube, 60-140
 Gerdien, H., on magnetic control in thermionic tubes, 32
 Germer, L. H., and Davisson, C. J., on wave-like behavior of electrons, 52
 Gerth, F., and Scheppmann, W., on short-wave propagation, 56, 362
 Giebe, E., on piezo resonator, 118
 Giebe, E., and Scheibe, A., on piezo resonator, 303, 313, 315, 318
 Gill, E. W. B., and Morrell, J. H., on ionic oscillations, 18, 56, 58, 135
 Gilliland, T. R., Kenrick, G. W., and Norton, K. A., on ionized layer, 368
 Glagolewa-Arkadiewa, A., on short waves, 57, 139
 Glasgow, R. S., on neutralization, 250
 Glow-discharge devices, 42-45, 180, 264-277
 glow amplifier, 271-277
 glow rectifier, 180
 grid-glow tube, 264-271
 oscillations, 23
 piezo crystals, 321
 potential distribution, 326
 Goldschmidt, R., reflection-type alternator, 58, 59, 151
 Goldstein, S., on ionized layer, 368
 Golz, J., on automatic synchronization, 111
 Goniometer, 492-496, 516
 Goodman, H. C., and Potter, W. S., on aerial feeders, 591
 Goyder, C. W., on piezo-electric apparatus, 118
 Gradient, 343, 345
 Great circle, 484
 Grechowa, M. T., on short waves, 57, 134
 Green, E., on antenna arrays, 517
 on directive systems, 454
 Grid, bias, 12 *f*.
 capacitance, 84, 90, 203, 222
 condenser, 84-92, 203-205, 238-255
 demodulation, 178
 effective capacitance, 84, 90, 203, 222
 filament capacitance, 84, 90, 203, 222
 leak, 61, 62, 119, 123, 129, 178, 203, 208, 210 *f*.
 plate capacitance, 84-92, 203-205, 238-255
 rectification, 177-180
 resistance, 209-215, 271 *f*.
 screen, 28 *f*.
 space charge, 28 *f*.

- Grid current, in gaseous tubes, 271-275
 in high-vacuum tubes, 12 *ff.*
 Grid-glow amplifier, 271-277
 Grid-glow tube, 264-271
 Grid voltage characteristic in gaseous tubes, 271-275 •
 Grondahl, L. O., and Geiger, P. H., on cuprox rectifier, 174
 Grosser, W., on stability of oscillations, 103
 Ground, absorption, 364, 365, 366
 conductivity, 330, 333, 335, 352, 353
 dielectric constant, 330, 333, 335, 352, 353, 363
 effect on loop, 470
 index of refraction, 352, 365
 influence on effective height of aerial, 470
 refracted waves, 352, 365
 resistance, 363
 wave, 352, 353
 Group directional characteristic, 517, 527
 Group velocity in electromagnetic waves, 16, 379
 Gugot, Lt., on short-wave propagation, 368
 Guillaume, Poincaré, and Blondel, on ionized layer, 367
 Güntherschulze, A., on rectifiers, 171
 Gutton, G., tube equation, 63, 64
 Gutton, G., and Pierret, E., on short waves, 57
 Gutton, G., and Touly, on short waves, 57
- H**
- H section in recurrent networks, 555, 562
 Habann, E., on magnetron oscillator, 32, 33, 38, 57, 138, 139
 Hahnemann, W., on short waves, 56, 362
 Half section, of filter, 582, 585
 Half-wave-length aerial, 418, 443, 499, 591, 593
 Hallwachs effect, 49
 Hals, J., on electromagnetic echoes, 404
 Hals-Stoermer electromagnetic echoes, 405
 Hamburger, F., on electronic oscillations in triple-grid tubes, 18
 Hanna, C. R., power-output tube, 193
 Hardin, L. L., Jr., on aerial feeder, 591
 Harmonic content, 64, 77, 116, 150-158, 163-167, 170, 183, 192
 Harmonic interference, 111-116, 255
 Harmonics, 64, 77, 116, 150-158, 163-167, 170, 183, 192
 Harms, F., on frequency jumps in oscillators, 103
 Harrison, J. R., on flexural piezo oscillations, 313
 on piezo apparatus, 118
 Hartley, R. V., on magnetic modulation, 185
 Hartley oscillator, 60, 61, 92, 124, 129
 Harvard University, 58, 118-120, 124, 172, 290, 304, 354, 356
 Hausrath, on detectors, 172
 Hazeltine, L. A. on neutralization, 250
 on tube oscillations, 71, 94
 Heaviside, O., on cable theory, 420
 Heaviside-Kennelly layer (conductivity and dielectric constant), 330, 367
 Heegner, K., on frequency jumps in oscillators, 103
 Height, effective, of *E* layer, 370, 390
 equivalent, 350
 of *F*₁ layer, 370, 390
 of *F*₂ layer, 370, 390
 of ionized layer, 362, 367, 369, 390
 and length of line and aerial, 407, 416, 417-419, 423, 424, 426-428
 of loop aerial, 470
 of open aerial, 350
 Heising, R. A., on tubes, 94
 Helium content in atmospheric ionized layer, 383
 Henney, K., on inversion, 171
 Hertz, H., aerial, 406, 444
 dipole, 418, 443, 499, 591, 593
 classical experiments and discovery, 56
 damped short waves, 139
 electromagnetic mirror, 57
 electromagnetic waves, 341, 342, 402, 403
 feeder, 406, 409, 422, 442, 443, 591-594
 photoelectric effect, 49
 radiation, 361, 364, 443
 rod, 499, 504, 509
 on theory of loading coils, 445
 Heterodyne, 111-116
 superheterodyne, 255
 Hewitt, P. C., on magnetic control in tubes, 32

High-frequency alternator, 56, 58-60
 High-frequency amplifier, 185
 High-frequency tube generators, 60-140
 High-pass filter, 546, 547, 549
 High-voltage production, 129, 141
 Hitchcock, R. C., on piezo apparatus, 118
 Hittorf (Crookes) dark space, 43
 Hoag, J. B., and Andrew, V. J., on electromagnetic echoes, 403
 Hochgraf L., on Sommerfeld-Pfrang theorem, 463
 Holborn, F., on push-pull oscillator, 57, 132, 135
 Hollingworth, J., on wave propagation, 402, 508
 Hollmann, H. E., on electronic oscillations, 56, 132, 134, 136, 137
 Hooke's law applied to piezo electricity, 285
 Horizontal aerial and line, 406-453
 (See also Hertz, H., aerial)
 Horton, J. W., on oscillator frequency, 96
 Horton, J. W., and Marrison, W. A., on piezo-electric frequency constancy, 119
 Howe, G. W. O., on penetration of electromagnetic waves into ground, 335
 Hulburt, E. O., on ionized layer, 368, 392 on short waves, 499
 Hulburt, E. O., and Taylor, A. H., ionized layer, 368
 Hull, A. W., on dynatron, 25, 125 on frequency constancy, 118 on magnetron, 32, 40, 138 on mercury-vapor tubes, 176 on screen-grid amplification, 252, 254, 262-265
 Hull, A. W., and Williams, N. H., on shield grid tubes, 2, 255
 Humphrey, W. J., on physics of the air, 383
 Huth-Kuehn oscillator, 91
 Huxford, W. C., on short-wave generator, 57, 130
 Huygens construction, 401 principle of, 525
 Hydrogen content in ionized layer, 383
 Hydrogen ion, 17, 375
 Hyperbolic functions, 416, 535, 600 and circular functions, 416, 602

I

Illumination characteristic, 50
 Image, aerial, 351, 357 integral of, 351
 Impact excitation (quenched spark gap), 433
 Impedance, generalized, 106 load, 66, 70-84 matching, 61, 120, 409, 443, 533, 555, 587-594 surge, 408
 Impedance characteristic, of magnetic amplifier, 186
 Impedance filter, 543, 544, 557, 576
 Impulse excitation, for frequency multiplication, 153 for high-frequency generators, 58, 152 for phase changers, 146, 153
 Inclined electric-field vector, 353
 Inclined loop, 509
 Inclined top aerial, 357
 Incremental permeability, 227
 Index of refraction, 342, 352, 365, 382 for ground, 352, 365 for ionized layer of upper atmosphere, 342, 380, 389-394, 398, 400
 Indirect electromagnetic waves, 362, 370, 393, 401, 404, 499-517
 Induced current, in loop aerial, 469 in open aerial, 359, 456, 466
 Induced voltage, in loop aerial, 466, 478, 479 in open aerial, 345, 350, 359, 465
 Inductance, aeriels and lines, 407-453 of concentric line, 443 fictitious, for ionic oscillations, 21, 134 in filters, 586 of Lecher wires, 407, 413 loading, 422-428, 431, 434 *ff.*
 Induction field of transmitter, 358
 Inductor-type alternator, 58-59
 Infinite line, compared with filter section, 539
 Input, of lines, 407-412, 415, 422 of recurrent networks, 531-544
 Intensity, of electric field, 342, 345, 347-353, 357, 359, 465-472, 485, 497-517 of illumination, 50 of magnetic field, 17, 32, 138, 325, 328, 330, 332, 334, 338, 342 *ff.*

Interaction between harmonics, 111-116, 255
 Interelectrode capacitance, 84, 91, 203, 222
 Interference beat note, 111-116, 255
 International Critical Tables, 310
 Interstage coupling, 207-209, 211, 216, 222, 223, 233-236
 Inversion (inverters), 159, 170-171
 Inverted L aerial, 356
 Ion sheath in glow tubes, 266
 Ionic bombardment, 1, 42-49, 176-177, 180-182, 264-277
 Ionic concentration, 16, 21, 267, 401
 of mercury ions in thyatron, 267
 Ionic oscillations, 16, 182, 330-332, 373-405
 Ionic recombination loss, 370
 Ionization, 1, 16, 42, 176, 180, 264-277
 secondary, 272
 voltages, 42
 Ionized absorption, 380
 Ionized layer, 361, 367
 multi-ionized layer, 390
 Ionized ray curvature, 389, 399
 Ionized space, 16, 42, 361, 367
 Ions, 266, 370, 374, 375, 397
 Iron-core inductance, 227
 Iron-core transformer, 222-232
 Ito, Yoji, on thermal amplifier and oscillator, 278

J

Jeans, J. H., on hydrogen content in air, 383
 Jelstrup, S. J., on electromagnetic echoes, 403
 Jen, C. K., and Kenrick, G. W., on ionized layer, 368
 Joffe, A. F., on physics of crystals, 284
 Johnson, J. B., on limitations with vacuum tubes, 255
 Johnson, K. S., and Shea, T. E., on filters, 531
 Johnson-Rabbe effect, 173
 Jolley, L. B., on rectifiers, 171
 Joly frequency doubler, 180-188
 Jones, D. E., on Hertz's classical experiments and discovery, 57
 Jones, F. C., on aerial feeder, 591
 Jones, T. V., on ionic oscillations, 135

Jordan, F. W., and Eccles, W. H., on original push-pull oscillator, 57, 132
 Jouaust, R., on piezo-electric frequency, 118

K

Kalinin, W. J., on short-wave oscillator, 132
 Kallitron, 264
 Karcher, J. C., and Eckhardt, E. A., on trigger relay, 277
 Karolus cell, 54, 55
 Karplus, E., on short-wave oscillators, 56
 Kear, F. G., on directive systems, 454
 Keith, C. R., on balanced tube circuits, 257
 Kellogg, G. W., on amplification, 193
 Kellogg, G. W., Beverage, H. H., and Rice, C. W., on Beverage antenna, 454
 Kelvin, Lord, on her and bei functions, 337
 Kennelly-Heaviside layer, 16, 361, 367
 Kenotron, 2-5, 8-9
 Kenrick, G. W., and Jen, C. K., on ionized layer, 368
 Kenrick, G. W., Norton, K. A., and Gilliland, T. R., on ionized layer, 368
 Kerr cell, 54, 55
 Kidner, C. A., on tube equation, 5
 Kiebitz, F., on guiding with electromagnetic waves, 495
 on short-wave oscillator, 132
 Kingdon, K. H., on suggestion to use mercury vapor for neutralization of space charge, 176
 Kingdon, K. H., and Koller, L. R., on constants of tube equation, 11
 Knowles, D. D., on glow tubes, 45
 Kohl, K., on electronic oscillators, 56, 132
 Kohlrausch, F., on thermal expansion coefficient of quartz, 303
 Koller, L. R., and Kingdon, K. H., on constants of tube equation, 11
 Kolster, F. A., and Dunmore, F. W., on balancing condensers for loop, 480
 Kozanowski, H. N., on electronic oscillators, 56, 135, 137
 Kramer, W., on Johnson-Rabbe effect, 173
 Kuehn, L., on magnetic modulation, 186

- Kuehn-Huth oscillator, 91
 Kundt, A., on dust patterns for noting vibrations, 300, 313
 Kupfmüller, K., on filter, 531
 Kurz, K., and Barkhausen, H., on electronic oscillations, 18, 35, 57, 132, 134-137
- L
- L-inverted antenna, 356
 Lack, F. R., on piezo-electric crystals, 296, 302
 Lag in electron tubes, 18-24, 33-42, 43-45, 66, 132-139
 Lamb, "Dynamic Theory of Sound," 307
 Lampa, A., on short-wave oscillators, 57, 139
 Lange, E. H., secondary electrons, 25
 Lange, E. H., and Myers, J. A., on magnetostriction, 119
 Langmuir, I., on phenomena in tubes, 2, 5, 6, 11, 45, 48, 63, 176, 264-267
 on space-charge law, 326
 Langmuir, I., and Blodgett, K. B., on physics in tubes, 265, 268
 Langmuir, I., and Mott-Smith, H. M., on phenomena in tubes, 264
 Langmuir, I., and Tonks, L., on ionic oscillations, 17, 21
 Laplace equation, 325
 Lardry, M., on ionized layer, 368
 Larmor, J., on ionized layer, 368
 Larmor, J., and Eccles, W. H., on ionized layer, 395
 Lassen, H., on ionized layer, 368, 369, 383, 392
 Latour, M., on alternator, 58, 59
 on tubes, 94
 Laue, M. von, on free potential energy per unit volume, 297, 307, 321
 on law for electron evaporation, 5
 Lawrence, E. O., and Coates, W. M., on X-rays by impact of positive ions, 24
 Laws, Ampère, 328, 331
 Child, 6
 Faraday, 332
 Gauss, 324
 Paschen, 49
 Snell, 390
 Layer, E layer, 370, 390
 F_1 layer, 370, 390
 Layer, F_2 layer, 370, 390
 ion sheath in glow tubes, 266
 ionized, 16, 361, 367
 Lazeref, W., on frequency constancy of tube oscillations, 96
 Leak resistance, 61, 62, 119, 123, 129, 178, 203, 208, 210 *ff.*
 Lebedew, P., on short-wave oscillators, 57, 139
 Lecher lines, 130, 133, 134, 136, 137, 139, 406, 409, 415, 421, 441, 447, 591
 Le Corbeiller, P., and Lange, Charles, on filter, 531
 Leithauser, G., and Alberti, E., on trigger circuit, 278
 Lenard, P., and Ramsauer, on ionization due to ultraviolet light, 388
 Lepel *etc.*, 58
 Lével, power, 537
 sound, 537-538
 Levin, S. A., and Young, C. J., on radiation resistance, 354
 Lewitsky, M., on short waves, 139
 Lieben, R. von, on magnetic-field control in tubes, 32
 von Lieben tube, 42
 Liebowitz, B., on rectification, 164
 Light effect on photoelectric cells, 50-52
 Limiting angle of sky ray, 371
 Limiting condenser for antenna and line loading, 453
 Limiting critical angle for ionized layer, 371, 393
 Lindemann-Dobson layer, 403
 Line, aperiodic, 459
 attenuation, 408, 456
 capacitance, 456
 coil, 147, 543
 concentric, 443, 591-594
 condenser, 546, 548
 constants, 407
 inductance, 408, 456
 infinite, 147, 406
 input, 406
 loaded, 408, 422, 453
 matching, 409, 591-594
 resistance, 407, 414, 428, 433, 437
 surge impedance, 408, 456
 transposed, 442
 velocity of propagation, 407, 411
 Linear wave propagation, 347, 361, 496, 521, 526, 527

- Lippman, M. G., on Lippman effect, 284-288
- Lippman, M. G., and Curie Brothers, on Lippman effect, 286
- Lippman-Curie law, 297
- Litz wire, 586
- Llewellyn, F. B., on tubes, 56, 94, 103, 187, 193, 255
- Loading, of amplifier, 192
of antenna, 422
of condenser, 422
- Logarithmic decrement, of circuit, 100, 102, 103, 313
for lines and aerials, 433
of piezo crystal, 313
- Long electrical line, 406
- Long-time radio echoes, 403
- Longhren, A. V., and Warner, J. C. on tube circuits, 193
- Longitudinal magnetic field, 124, 394
- Longitudinal vibration, in magneto-strictive rods, 124
in piezo crystals, 294-318
- Loop, double, 497
height of, effective, 470
and open aerial compared, 470, 477
- Loop aerial (see Frame aerial)
- Loose coupling in tube oscillators, 61, 89, 90, 98, 99, 113
- Lorentz, retarded potential, 351, 354
- Lorentz-Carson theorem, 462, 464
- Lorenz oscillator, 91, 131
- Losses in tubes, 8
- Low-frequency amplification, 204, 206-232, 278-283
- Low-pass filter, 543, 546, 549-555
- Lowell, P. D., on air and iron-core transformers in high-frequency range, 232
- Luebecke, Z., on continuously controlled arc discharge, 267
- Lumen, 50
- Luminous rod resonator, 303
- Lumped-tube constants, 14, 200
- M**
- M-derived filter, 581-585
- MacDonald, H. M., on horizontal aerials, 454
- McKeehan, L. W., and Cioffi, P. P., on magnetostriction, 119
- McNally, J. O., and Pidgeon, H. A., on loaded tube characteristics, 193
- Magnetic amplifier, 185
- Magnetic field, effect of, on electromagnetic wave propagation, 17, 331, 394-400
on ions, 17, 32-42, 331, 394-400
in rectifiers, 181
- Magnetic incremental permeability, 227
- Magnetostriction oscillator, 124
- Magnetron, 34, 138, 156
- de Mandrot, B. and Perrier, A., on α and β quartz, 296, 302, 303
- Marconi beam system, 454
- Marcus, A., on short-wave oscillators, 57, 130
- Marrison, W. A., and Horton, J. W., on piezo-electric frequency, 119
- Martyn, D. F., effect of grid current on frequency, 94, 96
- Maser, H. T., and Steiner, H. C., on mercury-vapor tubes, 176
- Mass, of electrons, 3, 16 *ff.*
of ions, 16, 20, 22, 23, 42, 45, 264-277
- Massachusetts Institute of Technology, 32, 181
- Matching, 409, 443, 533, 555, 587-594
of impedance, 61, 120, 409, 443, 533, 555, 587, 590, 591
- Materials for cathode, 11
- Matsumura, S., and Namba, S., on α and β quartz, 296, 302, 303, 313
- Maximum aerial current, 414, 439 *ff.*
- Maximum power transfer, 79, 120, 122, 160, 167, 190-200, 540, 545, 587-594
- Maxwell, displacement current, 329, 331, 374
distribution law, 3, 7
electromagnetic theory, 324
field equation, 332, 342
theory applied, 348, 363, 374
- Maxwell-Faraday induction law, 336
- Mayer, H. F., on amplifiers, 237
- Mean free path, of electrons, 369, 384
for molecules, 369, 384
- Measurement of field intensity, 466
- Meissner, A., on dust pattern of piezo crystal, 300
on natural wave lengths of aerials, 419
on piezo-electric appliances, 118
on tube oscillator, 60, 72, 98

- Melhuish, L. E., and Willis, F. C., on loaded tube characteristics, 193
- Mercury, ionic concentration in thyatron, 267
- pool rectifier, 175-176
- Mercury vapor, 20, 21, 23, 24, 139, 176, 267
- Mercury-vapor rectifier, 176
- Mercury-vapor trigger relay, 264
- Mesh of grid, 12, 27-32, 63-66, 188
- Mesny, R., on aerial arrays, 517, 521
- on directive system, 454
- on ionized layer, 368
- Mesny, R., and David, P., push-pull oscillators, 132
- Metastable orthohelium, 140
- Meter-ampere, 473
- Mid-frequency for filter, 564, 571
- Mie, G., on arc discharges, 48
- Miller, J. M., on interelectrode back feed, 84
- on piezo oscillator, 118, 120
- Milne, E. A., and Chapman, S., on physics of the air, 383
- Modes, of line oscillation, 415-426
- of piezo-electric oscillation, 297, 313
- Modulated wave distortion, due to ionized layer, 382
- Modulation, 179
- Moebius, W., on short-wave oscillators, 57, 139
- Moegel and Quaeck, long-time signals, 403
- Moeller, H. G., on oscillation characteristics, 81
- on short-wave oscillations, 132, 135
- on stability in tube oscillators, 96, 103, 111
- Mohammed, Aijar, Verman, L. C., and Char, S. T., on long-time signals, 403
- Molecular mean free path, 384
- Molybdenum, 5, 6
- Moon, distance of, from earth, 404
- electromagnetic echo effects, 405
- erratic travel path of, 405
- Moore, W. H., ionic oscillations, 18, 56, 134
- Morecroft, J. H., on grid-plate back feed, 84
- Morrell, J. H., and Gill, E. W. B., on ionic oscillations, 18, 56-58, 135
- Morrell, J. H., and Townsend, J. S., on ultra-high frequencies, 130
- Motion, equation of, for ionized medium, 374
- Motional diagram of oscillating piezo crystal, 312
- Mott-Smith, H. M., on physics in tubes, 48, 268
- Mott-Smith, H. M., and Langmuir, I., on physics in tubes, 264
- Moullin, E. B., on tube voltmeters, 179
- Multi-ionized layer, 390
- Multi-section, attenuation box, 531-538
- filter, 531-594
- Multiplier, frequency, 150-158
- phase, 143-149
- Munro, G. H., and Barnfield, R. H., on energy absorption of electromagnetic wave, 366
- Murphy, W. H., on space characteristics of aeriels, 454
- on space radiation characteristics, 485
- Mutual tube conductance, 12-15, 68, 70-74, 81, 82, 94, 113, 188, 190, 218
- Myers, J. A., and Lange, E. H., on magnetostriction, 119
- N
- Namba, S., and Matsumura, S., on α and β quartz, 296, 302, 303, 313
- Napierian (Neper) unit for transmission, 537
- National Physical Laboratory, 118, 307
- Natural frequency (wave length), of aeriels and lines, 415-437
- of electronic oscillations, 16, 17, 20-23, 36, 39, 132-139, 330-332, 373-405
- of ionic oscillations, 20-24, 132, 330-332, 373-405
- of ionized gas, 17, 20, 22, 23, 330-332, 373-405
- of magnetostriction rod, 124
- of piezo crystals, 119, 298, 299, 301, 302, 305, 308, 315, 317, 318
- (See also Wave length)
- Negative bias, 12 ff.
- Negative resistance, 34, 60, 125, 127, 138, 261-264
- action in magnetic-field tubes, 138
- amplifier, 262
- generator, 125, 127

- Neon, 42, 44, 272
 mass of positive neon ion compared with that of electron, 44
- Neper (Napier) unit of transmission, 537
- Nernst, W., on electrolytic rectifier, 172
- Nesper, E., on quenched oscillations, 58
- Nettelton, L., on short waves, 57
- Networks, equivalent lines, 416, 427, 428, 437, 531
 equivalent transformer, 222-234
 equivalent tube circuits, 66, 207, 231, 234
 recurrent, 147, 183-184, 531-594
 unsymmetrical, 490
 (*See also* Equivalent networks)
- Neutrodyne (neutralization), 250-252
- Nichols, E. F., and Tear, I. D., on ultra-short waves, 57, 139
- Nichols, H. W., on effect of interelectrode capacitance, 84
- Nichols, H. W., and Schelleng, I. C., on ionized layer, 368
- Nicol prism, 54
- Night effect on transmission, 369, 372, 510
- Nitrogen, 272, 383
 in ionized layer, 383
- Nixdorf, S. P., on magnetic amplification, 185
- Nodal points, on aeriels and lines, 415 *ff.*
 on high-frequency chokes, 130, 131
- Noises in tubes, 255
- Norton, K. A., on ionized layer, 368
- Norton, K. A., Gilliland, T. R., and Kenrick, G. W., on ionized layer, 368
- Number, of ions (electrons), 16, 21, 370, 382, 391, 396
 of molecules in atmosphere above ground, 384
- Ny Tai Ze, on piezo-electric saturation phenomena, 286, 288
- Nyquist, H., on limitations with tubes, 255
- O
- Ohm's law, in gaseous tubes, 42, 264
 in rectifiers, 159
 in thermionic tubes, 3, 7 *ff.*
- Okabe, K., on magnetron oscillations, 32, 39, 57, 138
- Okabe, K., and Yagi, H., on magnetron oscillations, 139
- Ollendorff, F., on direction characteristics, 517
- One-dimensional wave propagation, 347, 361, 496, 521, 526, 527
- Open circuit, condition for recurrent network, 532, 533, 540-542, 547, 588
- Open-circuit radiation, 345-361, 364 *ff.*
- Open-circuit radiators, compared with closed-circuit radiators, 477-478, 515
- Open-end effect, 416
- Open-ended aeriels and lines, 406-439 *ff.*
- Open-ended recurrent network as phase changer, 147, 531
- Optical system for Kerr cell, 54
- Ordinary electromagnetic ray, 400
- Oscillation, in amplifier, 238-255
 Barkhausen-Kurz, 18, 21, 35, 56-63, 132-137
 characteristic, 81-83
 constant, 104
 dynatron, 25, 125
 electronic, 16-24, 32-42, 132-139, 330-332, 373-405
 fundamental, 64, 116, 150-157, 159, 163-168, 305, 313, 314, 317, 414
 glow tube, 23, 271
 high-vacuum tube, 60-140
 higher mode, 305, 313, 314, 317, 414
 Hollmann, 136
 through internal back feed, 248
 ionic, 16, 20, 32, 330-332, 373-405
 in ionized layer, 16, 17, 22, 330-332, 373-405
 magnetostriction, 124
 magnetron, 34, 138
 Morrell-Gill, 18
 negatron, 127
 piezo-electric, 118, 284-323, 604-605
 tungan, 127
 Widdington, 18
- Oscillator, -characteristic, 64, 77, 81-83, 104-111, 113 *ff.*
 Colpitts, 61, 129, 130
 Hartley, 60, 61, 92, 124, 129
 line, 418, 443, 499, 591, 593
 tube, 18, 20, 23, 25, 34, 58, 60
- Output, amplifier, 187-199
 impedance, 66, 70, 84, 187-199, 587-590

Output, matching, 61, 91, 120, 409, 443, 533, 555, 587-594
 oscillator, 126
 resistance, 7, 65-69, 187-199
 termination in recurrent network, 531
 Owens, R. B., and Worrall, R. H., on piezo oscillators, 118
 Oxygen, 370, 383
 content in ionized layer, 383

P

Parabolic beam transmission, 525
 Parallel resonance, 61, 69 *ff.*
 Parallel-wire line, 406-453
 capacitance, 406-453
 characteristic impedance, 407, 409, 441, 442
 compared with concentric line, 443
 as feeder, 409, 422, 442, 443, 591-594
 inductance, 406-453
 Parhelium, 140
 Parkinson, T., on ionized layer, 402
 Paschen, law, 45, 49
 on metastable orthohelium, 140
 Pass band (region), 545
 Pass region, of filter, 545, 573
 Path, difference for direct and indirect electromagnetic waves, 370-373
 of sky wave, 362, 367
 Pauli, H., on abrupt frequency changes in oscillators, 103
 Peak factor, 160
 Penetration of electromagnetic waves, 333, 504-506
 Pentode, 32, 260
 Percival, W. S., on amplification, 237
 Period of oscillation, 17, 20, 21, 36, 64, 66, 155 *ff.*
 Permeability, incremental (dynamic), 227
 Perrier, A., and de Mandrot, B., on α and β quartz, 296, 302, 303
 Peters, L. J., on coupled circuit filters, 531
 Peuckert gap, 58
 Pfrang-Sommerfeld theorem, 462-464, 508
 Phase angle, 69, 70, 75, 80, 82, 83, 89, 96, 99, 114, 143-149, 160, 167, 180 *ff.*, 546, 551, 574
 Phase changers, 143-149, 546, 551, 574
 Phase constant (factor), 545, 546

Phase effect, on frequency, 1/8
 in oscillators, 74, 75, 89, 96
 Phase shift, 143-149, 545, 546, 551, 574
 Phase velocity, 378
 Phenomenon of Ny Tai Ze, 286
 Photoelectric effect, 49
 Photoelectric emission, 1, 49
 Photoelectric gas-filled cells, 49
 Photoelectric high-vacuum cells, 49
 Photoelectric sensitivity, 51
 Photoelectric work function, 51-52
Physikalische Technische Reichsanstalt, 57, 118, 303, 313, 315, 318
 π section, 531
 π -type characteristic impedance, 533
 π -type network, 531, 533, 555, 585, 586
 π -type propagation constant, 539
 compared with that of infinite line, 539
 Pickard, G. W., on experiments with Hertzian dipole, 499, 508
 Pidgeon, H. A., and McNally, J. O., on output power of tubes, 193
 Pierce, G. W., on contact detectors, 172
 on magnetostriction oscillator, 124
 on piezo oscillator, 118-120, 290
 on radiation resistance, 354-356
 on supersonic waves, 304
 Pierret, E., on short-wave generation, 132
 Pierret, E., and Gutton, G., on short-wave oscillations, 57
 Piezo crystals, equivalent, 119, 307
 Piezo-electric α quartz, 303
 Piezo-electric circular cut, 119, 299
 Piezo-electric Curie cut, 119, 284, 287, 291, 292, 294, 297-301
 Piezo-electric cuts, 284, 291, 297-304, 313-318
 Piezo-electric design formulas, 119, 297-318
 Piezo-electric dust pattern, 301
 Piezo-electric effect, along optical axis, 316-323
 application of, 119
 Piezo-electric equivalent constants, 119, 307
 Piezo-electric equivalent networks, 119, 307
 Piezo-electric frequency, 119, 297-318
 Piezo-electric higher modes, 297, 313-318, 320-323
 Piezo-electric holder (mounting) effect, 119, 305, 307

- Piezo-electric** longitudinal excitation, 294-318
Piezo-electric non-electric β quartz, 303
Piezo-electric oscillator, 119
Piezo-electric polar diagram for Young's modulus, 291
Piezo-electric pressure effect, 284-286, 295, 304
Piezo-electric resonator, 118, 297, 307
Piezo-electric temperature effect, 119, 296, 302
Piezo-electric theory, 284-323
Piezo-electric thirty-degree cut, 284, 291, 297-304
Piezo-electric vibrations, torsional, 297, 313
 transverse (flexural, bending), 297, 313
Pistolkors, A. A., on radiation resistance, 354
Pitch, of beat note, 111-116, 170, 179, 255, 258, 283
Planck, M., on Planck's constant, 9, 51, 52, 53
Plate capacitance, 84, 203, 210, 222
Plate current (*see* Anode, current)
Plate-filament capacitance, 84, 91, 203, 210, 222
Plate-grid capacitance, 84, 91, 203, 210, 222
Plate rectification, 177-180
Plate resistance, 7, 12, 14, 63-68, 71, 187-199
Pockels, F., on piezo electricity, 284, 317
Podliasky, I., and Clavier, A., on distortionless amplification, 193
Poincaré, Blondel, and Guillaume, on ionized layer, 367
Poisson's coefficient, 288
Poisson's equation, 22, 325-328
Polar diagram, directional aerial, Young's modulus for piezo crystals, 291
Polarization, circular, 395
 elliptical, 395
 of radio waves, 395, 400
Polarized cathode rays, 146, 157
Polarized electromagnetic waves, 395, 400
Polarized light, 54
Positive ionization, 1, 2, 20, 23, 42-48, 127, 176, 177, 180, 264-277
Potapenko, G., on short-wave generation, 132
Potassium cathode, 49
Potassium hydride cell, 51
Potential, distribution, along aerials and lines, 406-429
 for electron tubes, 326
 for ion tubes, 326
 energy per unit volume, 297
 gradient, 343, 345
 grid, 12, 14, 15 *ff.*
 lumped, 14, 200
 retarded, 342
 theory of, 342
 vector, 342, 358, 606
Potter, W. S., and Goodman, H. C., on aerial feeder, 591
Poulsen arc, 48, 56, 58, 138
Power, amplification, 185, 191
 dissipation in ground, 364-366
 equation, for line and aerial, 432
 radiation, 348-349, 356, 357, 366, 473
 transfer between circuits, 537-538, 540-542, 545, 587-594
Power amplifier, 185, 191
Power feed for aerials, 409
Power level, 537-538
Power oscillator, 80
Poynting's theorem, 348, 354
Pratt, H., and Dellinger, J. H., on guiding with electromagnetic waves, 495
Press, A., on non-uniform distribution of aerial constants, 420
Pressure, in tubes, 42, 176, 177, 272
 in upper atmosphere, 383
Prevention of self-oscillations in amplifiers, 248
Prince, D. C., on mercury-vapor tubes, 264
Prince, D. C., and Vogdes, F. B., on rectifiers, 171
Prism, nicol, 54
 quartz, 284
Propagation of electromagnetic waves, beam transmission, 347, 361, 496, 521, 526, 527
 cylindrical transmission, 347, 361
 fading, 399, 401, 402
 in ground, 330, 352, 353, 363, 365
 ground wave, 352, 353, 362, 364, 366, 371-373, 455, 502-517
 group velocity, 18, 379
 into interstellar space, 362, 371, 404
 in ionized layer, 361, 363, 367

- Propagation of electromagnetic waves,
 phase velocity, 378
 polarized wave, 371, 400, 501
 sky wave, 362, 367, 499
 space wave, 363
 spherical transmission, 347, 361
 surface wave, 363
 theory of, 338-530
 under upward angle, 362, 366-405,
 501-529
 along wires, 406
 around the world, 403
 Propagation constant, filter, 539, 544, 564
 along lines and aerials, 407, 411
 recurrent network, 536, 544
 Protective resistance in discharge tubes,
 269, 271
 Proximity effect, 442
 Pseudo-nodal points for line and aerial
 oscillations, 406, 415
 Pulling effect (drawing) in oscillator
 tubes 103-116
 Pungs, L., on magnetic modulator, 185
 Pupin, M., on electrolytic detector, 172
 on loading coils, 445
 Push-pull amplifier, 252, 257-258
 Push-pull detector, 32
 Push-pull oscillator, 123, 130, 132, 134,
 137, 138, 139
 Push-pull rectifier, 159, 163, 174, 176, 183
- Q
- Quaeck* and Moegel, long-time signals
 (round-the-world transmission), 403
 Quality amplifier, 187-203
 Quantum, 9, 51-53
 Quarter-wave-length distribution, 415 *ff.*
 Quartz crystal, 284
 longitudinal, 297, 298, 313
 torsional, 297, 313
 Quartz-crystal vibration, flexural (trans-
 verse or bending), 297, 313
 Quenching tube, 58
- R
- Rabbeek-Johnson effect, 173
 Radiated power, 343, 349, 356, 357, 473
 Radiation, near aerial, 345, 349, 358
 of closed circuit, 346
 Radiation, independent of shape of loop
 aerial, 470, 489
 of open circuit, 345
 Radiation field, 358
 Radiation resistance, 350, 354
 "Radio Amateur's Handbook," 371-372
 Radio compass, 493
 Radius of earth, 367
 Radt, W. P., on loaded amplifiers, 193,
 195
 Raman effect, 52
 Ramsauer and Lenard, on ionization by
 ultraviolet rays, 388
 Raschevsky, N. von, and Dushman, S.,
 on space charge, 5
 Ratcliffe, J. A., and Appleton, E. V., on
 nature of wireless signal variations,
 510
 Ratcliffe, J. A., and White, E. L. C., on
 ionized layer, 368
 Ratio, of current amplification, 190, 198
 of electronic charge to mass, 3, 7, 17 *ff.*
 of mv/q for cathode rays, α and β rays,
 405
 of power, 537
 of power amplification, 190, 198
 of voltage amplification, 190, 196, 198
 Ray, cathode, 1, 146, 157
 downward, 342, 361, 367, 370, 393, 401,
 499-517
 ground, 361, 363-366, 370, 499
 ordinary and extraordinary, 400
 Roentgen, 24, 80
 sky, 342, 361, 367, 370, 401, 499-517
 upward, 342, 361, 367, 370, 393, 401
 X-ray, 24, 80
 Rayleigh, Lord, on group and phase
 velocity, 379, 383
 Rayleigh reciprocal theorem, 463
 Reactance, of aerial, 418, 422
 of closed circuit, 69, 88, 120, 347, 547,
 555, 572, 587
 in filters, 547, 572
 of loaded aerial, 421, 422
 of open circuit, 418, 422
 Received current, 359, 456, 469
 Received field intensity, 345, 347, 358,
 359, 465, 467
 Received voltage, 359, 465, 466
 Receiver, Adcock aerial, 498
 autodyne, 277
 directive, 466-517

- Receiver**, loop aerial, 466
 superheterodyne, 255
 telephone, 282
 tilting loop, 509
 vertical wire, 465
- Rectification**, biphasic (full wave), 163, 174, 176, 183
 characteristics, 159
 effect, 160
 efficiency, 160
 full wave, 159-183
 grid, 178
 half wave, 159, 161, 163
 law, 168
 multiphase, 160
 plate (anode), 177
 single phase (*see* Rectification, half wave)
 six phase, 160
- Rectifier**, commutator, 171
 contact crystal, 172
 cuprox, 174
 electrolytic, 172
 glow tube, 180
 mercury pool (arc), 175
 mercury vapor, 176
 S tube, 181
 thermoelectric converter, 172
 tube, 175, 176, 177
 tungar, 177
 vibration, 171
- Recurrent network**, 531-594
 attenuation, 531-538, 543, 546 *ff.*
 and filter, 540-594
 for intensity measurement, 534
 as phase shifter, 147
 for wave antenna, 461-462
- Reference power level**, 537-538
- Reflected sky wave**, 362, 366, 367, 499-517
- Reflection**, of electromagnetic waves, 362, 366, 499-530
 factor for line and aerial, 444
 at ground, 502-510
 at layer, 362, 366, 367, 499-517
 principle in R. Goldsmidt alternator, 58, 59
 for wrong termination, 531, 552
- Reflection coefficient**, 502-510
- Reflector aerials**, 517-530
 aerial arrangement, 527
 linear arrangement, 518, 521-524
 Reflector aerials, parabolic arrangement, 525
- Refraction**, degree of, in ionized layer, 389, 398, 400
 of electromagnetic waves, 352, 389
 in ground, 352, 365
 in ionized medium, 389-394, 398, 400
- Refractive index**, 352, 365, 382
 for ground, 352, 365
 for ionized layer, 342, 389-394, 398, 400
- Regeneration**, frequency, 18, 136
 ionic, 272
 phase, 18, 66, 136
- Regenerative amplitude**, 238-243
- Regenerative circuits**, 61, 84, 119, 120, 238
- Reinartz**, J. L., on aerial feeder, 591
- Relation**, connecting electric- and magnetic-field vectors of electromagnetic waves, 345, 359
- Relaxation time** for electromagnetic disturbance, 340
- Relay**, glow tube, 264, 269
 oscillating-tube trigger, 277
 thyatron, 264
- Rentschler**, H. C., on photo cells, 51
- Resistance**, aerial, 437
 aperiodic, 171, 459
 of attenuation box, 534, 536
 balance, 175, 269, 271
 conductor, 338
 distributed along lines, 407
 dynamic, 7 *ff.*
 grid leak, 61, 62, 119 *ff.*
 ground, 363
 input of tubes, 84-89
 negative, 34, 60, 125, 127, 138, 261-264
 of parallel resonance system, 61, 69 *ff.*
 plate, 7, 12, 14, 63-68, 71, 187-199
 radiation, 350, 354
 static, tube, 17
- Resonance**, current, 108
 distribution along aerials and lines, 415-418, 426 *ff.*
 electronic, 17, 22, 36, 39, 382, 386, 396
 ionic, 17, 23, 396
 in ionized layer, 17, 382, 386, 396
 magneto-strictive rod, 124
 parallel, 69
 piezo crystal, 297-328
 in tubes, 18-24, 32-42
- Resonance curves**, 108

Resonator, crystal, 303, 307
 luminous rod, 303
 magneto-striction, 124
 Retarded vector, 342, 351, 354
 Retarded vector potential, 342
 Revolving, due to electric and magnetic actions, 32, 395-400
 Revolving (rotating) coil aerial, 466, 509, 516
 Revolving electric field, 146, 157
 Revolving goniometer, 493, 495
 Revolving Hertzian rod, 499, 509
 Revolving magnetic field, 144
 Rice, C. W., on neutralization, 250
 Rice, C. W., and Baker, W. G., on ionized layer, 368, 383
 Rice, C. W., Kellogg, G. W., and Beverage, H. H., on Beverage antenna, 454
 Richardson, O. W., space-charge equation, 4-6, 10, 32
 Richardson formula, 5
 Riecke, E., on piezo electricity, 317
 Riecke, E., and Voigt, W., on piezo electricity, 284
 Rod, Hertzian, 499, 504, 509
 luminous, 303
 magneto-striction, 124
 piezo rod, 307
 Roentgen rays, 52
 from positive ions, 24
 X-ray wave, 80
 Rogowski, W., on frequency changes in oscillators, 103
 Rossmaun, F., and Zenneck, J., on automatic synchronization, 111
 Rostagni, A., on ionic oscillations, 135
 Rotating generators, 58
 Rowe, H. N., on space charge, 5
 Rubidium cathode, 49
 Runge, W., on frequency changes in oscillators, 103
 Russell, A., high-frequency resistance of concentric cable, 443

S

S-tube rectifier, 181
 Saturation, current, 5 *ff.*
 electronic, 5 *ff.*
 magnetic, 150-151
 above magnetic, 151
 below magnetic, 151

Savart, T., on piezo electricity, 301
 Scheel, K., and Geiger, H., on discharges under high pressure, 48
 Scheibe, A., on piezo oscillators, 604-605
 on short waves, 57, 118, 134
 Scheibe, A., and Giebe, E., on piezo resonators, 303, 313, 315
 Schelleng, I. C., and Nichols, H. W., on ionized layer, 368
 Scheppmann, W., and Gerth, F., on short waves, 56, 362
 Schliephake, E., on short-wave generator, 131
 Schloemilch cell, 172
 Schmidt, K., on magnetic frequency multiplication, 58, 152
 Schottky, W., on emission formula, 5, 6
 on multigrid tubes, 2, 251, 259
 on shot effect, 255
 Schramm, E., and Forstmann, A., on loaded amplifier, 193
 Schroedinger, E., on wave mechanics, 52
 Schroeter, F., on Karolus cell, 54
 on transmission of short Hertzian and infrared waves, 56, 139
 Schultze, A., on magneto-striction, 119
 Scott-Taggart, I., on negatron, 26, 127
 Screen-grid tube, 28-32, 251
 Sea-water electrical constants, 330, 352, 364
 Search coil, goniometer, 492-496, 516
 in received field, 496
 Second harmonic content in current, 166
 Secondary electrons, 24-26, 125, 261, 262
 Secondary ionization, 272
 Section, attenuation box, 531-538
 filter, 531-591
 Seibt, G., and Bley, H., on electrons due to edge effect, 272
 Selective absorption, 385, 394, 396, 560
 Self-capacitance of tubes, 84, 91, 203, 222
 Self-excitation of oscillations, 62
 Self-heterodyne (autodyne), 277
 Self-inductance (*see* Inductance)
 Semiconductor, 341
 Sender current, 469
 field intensity farther out, 347, 358 *ff.*
 field intensity near aerial, 358
 radiation characteristic, 454
 Sense finding by electromagnetic waves, 466-530

- Sensitivity, of color, 51
 of telephone receiver, 282
 Series, arm in recurrent networks, 531
 Shape of loop aerial, no effect on radiation, 470, 489
 Shea, T. E., and Johnson, K. S., on filters, 531
 Shear oscillation, 302
 Shield grid tube, 28-32, 251
 Short-circuit impedance, 542
 Short-circuited line condition, 409
 Short-wave oscillators, 130-140
 Short-wave propagation, 361
 Shortened line, 417, 452
 Shunt arm, attenuation network, 531
 Signal strength, electric field, 345, 347, 348, 353, 359, 466
 magnetic field, 345, 348, 358, 359, 466
 received current, 465-470
 received voltage, 465-470
 ngle attenuation section, 531
 Single derived section, 582-587
 Single elementary section, 582-584
 Single filter section, 538
 Single frequency absorption in ionized layer, 17, 382, 386, 396
 in glow tube, 22
 piezo-electric resonator, 307
 in tank circuit, 69
 in thermionic tube, 103-116
 in tubes with magnetic control, 23, 36, 39
 Sixfold frequency, 153
 Skin effect, 336
 Skip distance, 362, 367, 371
 Sky wave, 362, 367, 370 *ff.*
 Slepian, J., on discharges under atmospheric pressure, 48
 Smith, C. G., and Bush, V., on magnetic effects in tube rectifiers, 32, 181, 182
 Smith Rose, R. L., on directive systems, 497, 499
 Smith Rose, R. L., and Barfield, R. H., on directive systems, 499
 on electromagnetic waves over ground, 363, 364
 Snell's law applied to ionic refraction, 390
 Snow, C., high-frequency inductance of
 double line, 418
 Sodium cathode, 49
 Sommerfeld, A., on numerical distance, 343, 365
 on surface and space waves, 352, 361, 363, 365, 402
 Sommerfeld-Pfarr theorem, 462-464, 508
 Sosman, R. B., on piezo electricity, 293
 Southworth, G. C., on directive systems, 454
 on short waves, 57, 130
 Space, absorption factor, 360
 attenuation, 360
 charge, 3, 5-8
 equivalent, 286, 318-323, 324
 charge tubes, 28, 29, 123, 324-326
 resonance curve, 450
 spread, 347
 wave, 402 *ff.*
 Spark, and arc, 45
 Spark-gap oscillations, 56-58
 Special generators, 58, 129-140
 Specific conductivity, 330
 Specific inductive capacitance, 363, 377
 Specific resistance, 335
 Spectrum, frequency, 56
 Speed of propagation, empty space, 329, 330, 332, 338 *ff.*
 group speed, 16, 379
 in ionized layer, 16, 379
 along lines, 411
 phase speed, 379
 Spherical wave propagation, 342, 347, 358, 360, 371
 Square wave shapes, 129
 Stability of tube oscillations, 96, 103
 Starke, H., and Austin, O., on secondary electrons, 25
 Starke, H., and Baltruschat, M., on secondary electrons, 25
 Static capacitance, 84, 86 *ff.*
 Static constants, for lines and aerials, 407
 for recurrent networks, 531
 for tubes, 7, 12, 63, 67, 86
 Static inductance, 407
 Static quartz elongation compared with dynamic amplitude, 313
 Static resistance, 7, 407
 Stationary waves along lines and aerials, 406
 Steady drift in ionic oscillation, 23
 Stefan-Boltzmann law, 9
 Steiner, H. C., and Maser, H. T., on mercury-vapor tubes, 176

- Sterba, E. J., and Feldman, C. B., on aerial feeder, 591
- Sterba, E. J., and Feldman, C. B., on lines, 406
- Stoermer, C., on electromagnetic echoes, 371, 403, 404
- Stoermer, Birkland, Villard, on electromagnetic echoes, 369
- Stoermer-Hals, on electromagnetic echoes, 405
- Stokes, G., on action of magnetic and electric forces on charged particles, 32
- Stokes law, 609
- Stone-Stone, J., on non-uniform distribution of line constants, 420
- Stowell, E. Z., on patterns for electromagnetic guiding, 495
- Stowell, E. Z., and Diamond, H., on amplification, 233
- Straight-line (beam) wave propagation, 347, 361, 362, 496, 521, 525-527
- Stratosphere, 383
- Strocker, K., on directive systems, 454
- Sun, distance from earth, 404
- Sunset and sunrise, effects on propagation, 367-370, 400-403
- Supersonic sound waves, 298, 305
- Supply voltages in tubes, 2, 3, 12, 65
- Suppression, of frequencies, 546, 548 *ff.* of one frequency, 560
- Suppressor grid tube, 32, 260
- Surface integral, 343, 348, 608
- Surface charge on piezo-electric elements, 318-323
- Surface waves, 363, 402
- Surge impedance, 408, 440, 441, 544 of concentric line, 443 of filter, 544 of Lecher wires, 442 of line and aerial, 408, 440, 441
- Sustained currents and waves, 56, 58
- Sutherland, L., on loaded amplifier, 193
- Swann, W. F. G., on ionization of air, 369
- Symmetrical amplifier, 252, 257-258
- Symmetrical detector, 32
- Symmetrical oscillator, 123, 130, 132, 134, 137, 138, 139
- Symmetrical rectifier, 159, 163, 174, 176, 183
- Synchronization, automatic, 111-116
- T**
- T aerial, 356
- T section, in recurrent network, 531
- Table, calculation of attenuation box, 536 characteristic factors of glow-amplifier tubes, 275 constants for loop (frame) aerial of different dimensions, 471 constants of Richardson equation, 5 correct effective antenna constants for coil loading, 438 different types of high-frequency sources, 58 effective input capacitance and grid resistance across grid-filament gap of a three-element tube, 204 electron affinity and thermionic work function, 6 examination of filters, 558 exponential and hyperbolic functions, 600-602 filter effect, 557 forward tilt of electric vector of electromagnetic waves passing over ocean and over dry ground, 352 gas content at different height of atmosphere, 383 grid resistance in terms of low negative and zero grid potentials, 206 high-frequency resistance in terms of direct-current resistance, 338 inductance, capacitance, and characteristic (surge) impedance for single and double line, 456 leakage reactance for different frequencies, 231 limiting angle of sky ray, 393 natural fundamental wave lengths of commercial antennas, 419 number of molecules, molecular mean free path, and electron collision frequency at different heights of atmosphere, 384 penetration of electromagnetic waves into ground, 335 possible natural mode of antenna oscillations and correct effective line constants, 436

- Table, potential at the far end and apparent effective line constants of a condenser-loaded aerial, 432
 potential at the far open end of aerials and apparent effective line constants for different degrees of coil loading, 431
 radiation for different kind of aerials, 486
 reflected impedance Z/N^2 for different frequencies, 229
 specific conductivity and dielectric constant for ground, river water, ocean, and ionized layer, 330
 static antenna constant for coil loading, 438
 table for units, 596
 velocity of propagation along lines, 449
 width of electron pockets for cathode, α and β rays, 405
 Young's modulus for Curie, 10-, 20- and 30-degree quartz cuts in different directions against optical axis, 292
- Taggart-Scott negatron, 26, 127
- Tank circuit, 69 ff.
- Tap, anode, 62, 91, 120, 122, 123, 128, 131
 transformer, 222, 587
- Tartarinoff, W. W., on directive systems, 454
- Tawil, E. P., on piezo-electric oscillations, 318
- Taylor, A. H., on short-wave propagation, 396
- Taylor, A. H., and Hulburt, E. O., on ionized layer, 368
- Taylor, J., on push-pull oscillator, 132
- Taylor and Young, long-time echoes, 403
- Taylor theorem, applied, 168, 202, 346
- Tear, I. D., and Nichols, E. F., on very short waves, 57
- Telegraph (telephone) equation, 439
- Telephone receiver, 282
- Tellegan, B. D. D. H., on putput amplification, 193
- Temperature, absolute (Kelvin degrees), 3, 5-10, 48, 205, 206, 279-281, 385
 cathode, 157, 178
 effect of, for multiplying frequency, 157
 in tubes, 3
 saturation, 3
- Temperature amplifier, 278
- Temperature coefficient (quartz), 303
- Temperature control on emission, 3, 157, 278
- Temperature oscillator, 278
- Termination, amplifier, 192
 attenuation box, 533
 Beverage aerial, 454
 filter, 541, 543, 550, 573, 585
- Terry, E. M., on theory of piezo oscillator, 118
- Tesla transformer, 141
- Tetrode (three-element tube), 12
- Thermal amplifier, 278
- Thermal expansion coefficient (quartz), 303
- Thermal frequency doubler, 157
- Thermal oscillator, 278
- Thermionic amplifier, 12, 187
- Thermionic demodulator, 177
- Thermionic detector, 177
- Thermionic emission, 1
 and positive ionization, 176, 177, 264
 for small negative plate potentials, 7
- Thermionic oscillator, 60
- Thermionic rectifiers, 168, 174
- Thermionic tubes, 2, 12, 20, 25, 27, 28, 32, 34, 35, 40
- Thermodynamic potential, 290
- Thirty-degree piezo-electric cut, 284, 291, 297-304
- Thomson, J. J., on arc discharges under atmospheric pressure, 48
 on Edison effect, 2
 on magnetic effect on ions, 32
 on physics of air, 383
- Thomson, W. (Lord Kelvin), oscillation formula, 134, 436
- Thoriated filament, 11
- Three-dimensional wave propagation, 347, 361
- Thunderstorm, effect on wave propagation, 370
- Thyratron, 264
- Tight coupling effect in oscillators, 108, 114
- Tilting, coil, 509
 of electric vector, 353
- Time, of echoes, 403
 of electron flight, 18-24, 33-42, 43-45, 66, 132-139
 of ion flight, 16, 32, 42, 264
- Time constant, 579, 589

- Time lag in electron tubes, 18-24, 33-42, 43-45, 66, 132-139
- Tinus, W. C., on aerial feeder, 591
on lines, 406
- Tonks, L., on ionic oscillations, 132
on ionized layer, 368
- Tonks, L., and Langmuir, I., on ionic oscillations, 17, 21
- Torsional piezo oscillations, 297, 313
- Tosi and Bellini goniometer, 492, 493
- Total electron emission, 5-8, 15, 25, 27, 29
- Toulon, P., on gaseous tubes, 264
- Toulon, P., and Dunoyer, L., on gaseous tubes, 264
- Touly and Gutton, G., on short waves, 57
- Townsend, J. S., on breakdown discharges, 48
on frequency changes in tube oscillators, 103
on ionic oscillations, 57
- Townsend, J. S., and Morrell, J. H., on short waves, 130
- Train, wave, 56, 58, 141
- Transformer, in amplifiers, 222
auto tuned and tapped, 91, 120, 122, 128, 232, 234
balanced, 174
iron core, 226
matched, 230, 587, 590
in tube circuits, 61, 62, 91, 98, 99, 104, 120, 130, 223, 232, 590
- Transmission, characteristic of filters, 531
of electromagnetic waves, 347, 361 *ff.*
(*See also* Propagation)
over power lines, 445-446
unit (decibel), 537
- Transoceanic waves, 352, 360, 361, 364, 365
- Transposed lines, 442
- Transverse magnetic-field effect, 33
- Transverse piezo-electric oscillations, 297, 313
- Trautenberg, H. R., on directive systems, 454
- Trigger circuits, 277
- Troposphere, 383
- Tube, amplifier, 187
double grid, 27
double plate, 26
gas-filled amplifier, 271
gas-filled oscillator, 127, 271
- Tube, gas-filled rectifier, 176, 177, 180
gas-filled trigger, 264
glow amplifier, 271
glow rectifier, 180
magnetically controlled, 181
grid glow, 264
magnetically controlled, 32, 138, 181
pentode, 32, 260
screen grid, 28
space charge, 28
thermionic general, 1
triple grid, 32, 260
- Tube noise, 255
- Tube oscillator, 60
- Tuned aerial, 416, 418 *ff.*
- Tuned amplifier, 232
- Tuned autotransformer, 232
- Tuned filter, 560, 564
- Tuned grid, 61
- Tuned grid plate, 61
- Tuned line, 414
- Tuned plate, 61
- Tuned transformer, 232
- Tungar oscillator, 127
- Tungar rectifier, 177
- Turner, K. P., on filter design, 531
- Turner, L. B., on Kallitron, 263
on trigger circuit, 277
- Tuve, M. A., and Breit, G., on ionized layer, 368
- Two-dimensional wave propagation, 347, 361
- Two-phase rectification, 159, 163, 174, 176, 183

U

- Uda, S., and Yagi, H., on antenna arrays, 517
- Ultraviolet rays, 370
- Underdown, A. E., and Cobbold, G. W. N., on piezo-electric application, 118
- Unequal sections, 534, 581, 590
- Uniform line distributions, 407
- Unilateral current conduction, 159
- Unilateral polar diagram for directive aeriels, 454
- Unilateral wave propagation, 347, 361, 496, 521, 526, 527
- Unipotential cathode, 29
- Units, decibel, 537
power level, 537

- Units, reference level, 537
 table for, 596
 University of California, 24
 Unsymmetrical network, 590
 Upp, C. B., on power-amplifier tube, 193
- V
- Vacuum, degree of, in glow tubes, 42, 43, 45, 176, 177, 180, 181, 267, 268, 272
 Vallauri, G., tube equation, 63, 64, 94
 Valve, Fleming, 2
 (See also Tube)
 Van der Bijl, H. J., tube equation, 63
 Van der Pol, B., on automatic synchronization, 111
 on electromagnetic echoes, 403, 404
 on radiation resistance, 354
 Van Dyke, K. S., on equivalent network of piezo resonator, 307
 on piezo resonator, 118
 Vapor, argon, 42, 177, 267
 helium, 42, 140, 267, 383
 hydrogen, 17, 20, 383, 388, 391, 396
 mercury, 20, 21, 23, 24, 139, 176, 267, 268
 neon, 42, 44, 45, 180, 181, 269, 272
 nitrogen, 272, 383, 388
 orthohelium, 140
 oxygen, 383
 parhelium, 140
 Vapor tubes, 42, 180, 264-277
 Vector, potential, 342, 358, 606
 Poynting, 354
 Velocity, angular in electron tubes, 2, 7, 8, 18-20, 23, 28, 34, 37, 38, 41
 generalized, 70, 74, 93, 95, 98, 102, 106, 308, 309
 hyperbolic, 70, 74, 93, 95, 98, 102, 106, 308, 309
 group, 16, 379
 phase, 378
 relativistic, 54
 of wave propagation, in free space, 329, 330, 332, 338 *ff.*
 in ionized layer, 16, 379
 along wires, 411
 Verman, L. C., Char, S. T., and Mohammed, Aijar, on electromagnetic echoes, 403
 Vertical aerial, 418
 Vibrations, in diaphragm of telephone receiver, 283
 Vibrations, electronic, 16-24, 32-42, 132-139, 330-332, 272-405
 flexural (piezo), 297, 313
 ionic, 16, 20, 32, 330-332, 373-405
 longitudinal (piezo), 294-318
 magneto-strictive, 124
 piezo-electric, 296, 317
 torsional (piezo), 297, 313
 transverse (piezo), 297, 313
 Villard, Stoermer, and Birkland, electro-magnetic echoes, 369
 Vincent, I. H., on automatic synchronization, 111
 on tube relations, 94
 Vogdes, F. B., and Prince, D. C., on rectifiers, 171
 Voigt, W., on classical piezo electricity, 284, 290, 293, 296, 297, 301, 317, 318, 322, 323
 Voigt, W., and Riecke, E., on classical piezo electricity, 284
 Voltage, amplification, 185, 191
 average value, 161, 427, 428 *ff.*
 changer, 141
 distribution along aeriads and lines, 407-453
 effective value, 159, 161, 162, 164 *ff.*
 lower critical, 42
 lumped, 14, 200
 peak value, 160
 upper critical, 42
 Von Laue, M. (see Laue, M. von)
 Von Lieben, R. (see Lieben, R. von)
 Von Raschevsky, N. (see Raschevsky, N. von)
 Vreeland, F. K., on magnetically controlled tubes, 32
- W
- Wagner, K: W., on filter design, 531
 Warner, J. C., and Longhren, A. V., on tube circuits, 193
 Watanabe, Y., on piezo-electric apparatus, 307
 on piezo-electric applications, 118
 Watson, G. N., on wave propagation, 360, 361, 368, 369
 Wattage, for starting glow discharge, 270
 Wave absorption, 333-335, 340, 352, 364-366
 Wave aerial, 457, 461-462

- Wave distortion, 382
 Wave filter, 531
 Wave-length aeriads, 454, 462
 Wave-length constant, 407
 Wave-length frequency relation, 19, 412, 419 *ff.*
 Waves, concave and convex front, 401
 front, 389, 400, 401
 in ground, 333-335, 340, 352, 364-366
 in ionized layer, 380, 385
 along lines, 406, 454, 462
 motion of, spherical, 358, 360, 371
 polarized, 395, 400
 propagation in empty space, 338
 resistance, 440
 sky, 362, 367, 370 *ff.*
 space, 347, 402
 spherical, 342, 371
 spread, 347, 363
 surface, 402
 in tubes, 16
 Weagant, R. A., on double-loop system, 496
 Weagant tube, 264
 Webster, W. L., on magneto-striction, 119
 Wegener tables, on physics of the air, 383
 Wehnelt, A., on Wehnelt cathode, 2, 4, 11
 Wells, H. W., and Berkner, L. V., on ionized layer, 368, 370
 Wesleyan University, Middletown, Connecticut, 118, 284, 302, 307
 Western Electric Company, 52, 53, 56, 57, 61, 63, 84, 94, 96, 119, 187, 193, 255, 257, 296, 353, 454, 462, 531, 580
 Westinghouse Electric Manufacturing Company, 45, 48, 51, 227, 269
 Wheeler, L. P., and Bower, W. E., on piezo oscillator with acoustic back feed, 122
 Whiddington, R., on ionic oscillator, 18, 20, 21, 56, 58
 White, E. L. C., and Ratcliffe, J. A., on ionized layer, 368
 White, W. C., on magnetron oscillator, 138
 Width, effect of, in frame aerial, 482
 of pass band in filter, 546, 547, 549, 551, 564, 565, 566 *ff.*
 Wien, M., on spark gap and quenching tubes, 58
 Wigge, H., on design of resistance-coupled amplifiers, 215
 Williams, N. H., and Hull, A. W., on shield-grid tubes, 2, 255
 Willis, F. C., and Melhuish, L. E., on loaded amplifier, 193
 Wilmotte, R. M., on aerial problems, 462
 Wilson, C. T. R., on ionized layer, 368
 Winter, W. F., on vapor tubes, 176
 Wintringham, W. T., Bailey, A., and Dean, S. W., on forward tilt of electric vector, 353
 Wired Radio, Inc., on glow-tube amplifiers and oscillators, 271
 Work function, photoelectric, 51-52
 thermionic, 6, 52
 Worrall, R. H., and Owens, R. B., on piezo-electric stabilization, 118
 Wright, J. W., on piezo-electric circuits, 118
 Wright, R. B., on piezo oscillations, 313
 Wunderlich, N. E., on symmetrical double-grid tube, 32
- X
- X-rays, 52
- Y
- Y network, 145, 146, 536
 (See also T section)
 Yagi, H., on magnetron, 32, 57, 138
 Yagi, H., and Okabe, K., on magnetron, 139
 Yagi, H., and Uda, S., on antenna arrays, 517
 Yale University, 32
 Young, C. J., and Levins, A., on radiation resistance, 354
 Young and Taylor, long-time sig., 33
 Young's modulus, 288, 290, 291, 298, 300, 308
- Z
- Zenneck, J., on detectors, 172
 on directive aeriads, 454
 on forward tilt of electric vector, 353
 Zenneck, J., and Rossmann, F., on synchronization in tube oscillators, 111
 Zenneck frequency multiplier, 150

Zero, absolute, 3

Zero-beat region, 111-116

voltage and current points along lines
and aeriels (nodes and pseudo-
nodes), 406, 415

Zero (apparent) level for decibel for-
mulas, 537-538

Zobel, O. J., on filters, 531, 580, 581

Zobel, O. J., and Carson, J. R., on filters.
531

**For Reference
Only.**